VASCULAR DISCOVERY: From Genes to Medicine
2018 Scientific Sessions

Abstract presentations

Oral Abstract Presentations

- **Abstracts 1-31 will be presented on Thursday**
- **Abstracts 32-59 will be presented on Friday**

Poster Abstract Presentations

- **Abstracts 88 – 290 will be presented on Thursday**
- **Abstracts 310-516 will be presented on Friday**
- **Abstracts 520 – 731 will be presented on Saturday**

1
Skap2 Regulates Atherosclerosis through Macrophage Polarization and Efferocytosis
Allison Schroeder, Danielle Hyatt, **Francis J Alenghat**, Univ of Chicago, Chicago, IL

BACKGROUND: Atherosclerosis causes more deaths than any other pathophysiologic process. It has a well-established inflammatory, macrophage-mediated component, but potentially protective intracellular macrophage processes in atherosclerosis remain enigmatic. Src Kinase-Associated Phosphoprotein 2 (Skap2) is a macrophage-predominant adaptor protein critical for cytoskeletal reorganization, and thereby, for macrophage migration and chemotaxis. The role of macrophage Skap2 in atherosclerosis is unknown and deserves exploration.
RESULTS: Human macrophages express Skap2, and in human arterial gene expression analysis, *Skap2* expression is enriched in macrophage-containing areas of human atheroma; the transcript level varies with plaque characteristics, with higher levels in more stable plaques. In *ApoE*$^{-/-}$ mice on a standard diet, deletion of *Skap2* accelerates atherosclerosis by threefold at 18 and 24 weeks. We find that Skap2 expression is switched on only as monocytes differentiate into adherent macrophages, so *Skap2*$^{-/-}$ monocytes do not have a defect in infiltrating the atheroma, as reflected by abundant macrophages in the Skap2$^{-/-}$ plaques. On the other hand, once they fully differentiate, Skap2-deficient macrophages cannot polarize efficiently into alternatively-activated, regulatory macrophages, and instead they preferentially polarize toward the classical pro-inflammatory phenotype both *ex vivo* and within the developing atheroma. This defect extends to polarized effector functions, as *ex vivo* analysis of macrophage phagocytosis of dying foam cells indicates that Skap2 is required for the regulatory process of efferocytosis. There are no differences in macrophage proliferation or apoptosis attributable to Skap2. Finally, Skap2 binds to Sirpα, whose interaction with CD47 has been shown to be important for efferocytosis, and we observe colocalization of actin, Sirpα, and CD47 at leading edges of macrophages in a Skap2-dependent manner.
Conclusions: Taken together, our findings support a model in which Skap2 drives a regulatory, efferocytic mode of behavior to quell atherosclerosis.
A. Schroeder: None. **D. Hyatt:** None. **F.J. Alenghat:** None.

This research has received full or partial funding support from the American Heart Association.

2
Resolvin D1 Limits Senescent Cells in Atherosclerosis
Sudeshna Sadhu, Nicholas Rymut, Justin Heinz, Gabrielle Fredman, Albany Medical Coll, Albany, NY

Non-resolving inflammation is the underpinning of several prevalent diseases including atherosclerosis. Understanding new mechanisms to promote the resolution of inflammation in atherosclerosis are of interest. Resolution is mediated by resolvins, including Resolvin D1 (RvD1). We recently showed that RvD1 prevents lesional necrosis in *Ldlr*$^{-/-}$ mice. However, the mechanisms underlying RvD1's protective actions remain unknown. In this regard, the accumulation of senescent cells (SCs) was recently shown to promote necrotic core formation in *Ldlr*$^{-/-}$ mice. SCs are harmful because they possess a pro-inflammatory and proteolytic phenotype called the senescence associated secretory phenotype (SASP). Because RvD1 decreased lesional necrosis, we questioned whether RvD1's actions were through limiting SCs in plaques. First, we found that human symptomatic plaques had significantly less RvD1 and significantly more SCs (quantified by positive p16^{INK4A} immunofluorescence staining) compared with asymptomatic plaques. To prove causation, we administered RvD1 to *Ldlr*$^{-/-}$ mice during advanced atherosclerosis and observed a significant decrease in lesional SCs and necrosis compared with vehicle controls. Mechanistically, we found that RvD1 significantly decreased the SASP as well as beta-galactosidase and p16^{INK4A} in WI-38 senescent cells. Importantly, a major component of the SASP is ADAM17, which is an enzyme that cleaves (and thus inactivates) a critical efferocytosis receptor on macrophages called MerTK. Because SCs are not cleared in plaques we questioned whether the SASP deranges efferocytosis mechanisms via their ability to cleave MerTK on macrophages. To investigate whether MerTK cleavage deranges SC clearance in plaques, we transplanted bone marrow from wild type (WT) or MerTK cleavage resistant (Mertk^{CR}) mice into Ldlr$^{-/-}$ mice, and quantified the levels of lesional p16^{INK4A} after 12 weeks of Western Diet feeding. Mertk^{CR} mice had significantly less p16^{INK4A} levels and smaller necrotic cores compared with WT controls. Overall, we identified new functions for RvD1 and uncovered, for the first time, an endogenous mechanism for SC clearance. Our findings may provide new therapeutic strategies to treat atherosclerosis.
S. Sadhu: None. **N. Rymut:** None. **J. Heinz:** None. **G. Fredman:** None.

3
The Impact of MHCII Loss in Myeloid Cells and Adipocytes on Atherosclerosis and Liver Fat Accumulation
Alecia Blaszczak, Valerie Wright, Joey Liu, The Ohio State Univ, Columbus, OH; Tuo Deng, Houston Methodist Weill Cornell Medical Coll, Houston, TX; David Bradley, Stephen Bergin, Willa Hsueh, The Ohio State Univ, Columbus, OH

The adipocyte is capable of functioning as an antigen presenting cell in the setting of diet induced obesity in both mouse models and humans; this adipocyte activity instigates adipose tissue (AT) inflammation. To determine the relative roles of adipocyte vs. myeloid adaptive immunity on obesity-associated complications, we investigated myeloid vs. adipocyte-specific knockout of a major histocompatibility II (MHCII) protein, H2Ab1, which in mice prevents antigen presentation. Loss of adipocyte, but not myeloid, MHCII led to improvements in insulin sensitivity, adipose tissue inflammation and inhibited the shift from anti to pro-inflammatory immune cells in adipose tissue during high fat diet feeding. Both models were placed on a pro-atherogenic background (LDLR -/-), then aged for one year to accelerate atherosclerosis and were fed a western diet high in cholesterol and fat for 12 weeks. Adipocyte specific, but not myeloid specific, loss of MHCII in LDLR -/- led to dramatic improvements in atherosclerosis development, liver fat accumulation and insulin sensitivity in conjunction with an increase in the adipose tissue Tregs and a decrease in the pro-inflammatory adipocyte cytokine gene expression with no differences noted in body weight or fat. Whereas in LDLR -/- with lack of myeloid MHCII compared to LDLR -/- , we saw no differences in liver fat accumulation, atherosclerosis development or insulin sensitivity with a decrease in the anti-inflammatory Tregs, a comparable increase in adipocyte pro-inflammatory cytokine expression, but a decrease in the pro-inflammatory M1 like macrophages. These studies highlight the importance of the adipocyte as a functional contributor to the development of obesity related complications and provide a potential targeted therapeutic avenue in the management of these metabolic diseases.
A. Blaszczak: None. **V. Wright:** None. **J. Liu:** None. **T. Deng:** None. **D. Bradley:** None. **S. Bergin:** None. **W. Hsueh:** Consultant/Advisory Board; Significant; Merck, Novo Nordisk.

4
Comprehensive Assessment of Immune Cells in Mouse and Human Atherosclerosis by Single-cell RNA-sequencing and Mass Cytometry
Holger Winkels, Erik Ehinger, Melanie Vassalo, Konrad Buscher, Huy Dinh, Kouji Kobiyama, Anouk Hamers, LJI, La Jolla, CA; Clement Cochain, Inst of Experimental Biomedicine, Wuerzburg, Germany; Ehsan Vafadarnejad, Antoine Emmanuel Saliba, Helmholtz Inst for RNA-based Infection Res, Wuerzburg, Germany; Alma Zernecke, Inst of Experimental Biomedicine, Wuerzburg, Germany; Pramod Akula Bala, Amlan Kanti Ghosh, LJI, La Jolla, CA; Nathaly Anto Michel, Natalie Hoppe, Ingo Hilgendorf, Andreas Zirlik, Dept of Cardiology and Angiology I, Univ Heart Ctr Freiburg, Freiburg, Germany; Catherine Hedrick, Klaus Ley, Dennis Wolf, LJI, La Jolla, CA

Atherosclerosis, an inflammatory disease of large arteries, is - through its clinical manifestations stroke and myocardial infarction - globally the leading cause of morbidity and mortality. The interplay of pro- and anti-inflammatory leukocytes in the aorta modulates and drives atherosclerosis. Although cells of the innate and adaptive immune system are found in atherosclerotic plaques, their phenotypic and functional diversity is poorly understood. Here, we applied single cell RNA-sequencing (scRNAseq) and mass cytometry (CyTOF) to assess leukocyte diversity in depth, thus defining an immune cell atlas in atherosclerosis. Single cell transcriptional profiling of aortic leukocytes from 20-week old chow (CD) and western diet (WD) fed *Apoe*$^{-/-}$ and *Ldlr*$^{-/-}$ mice revealed 11 phenotypically different leukocyte clusters. Atherosclerotic aortas exhibited enhanced leukocyte diversity, whilst WD further changed the abundance of leukocyte subpopulations. Gene set enrichment analysis of single cells established that multiple pathways, e.g. for lipid metabolism, proliferation, and cytokine secretion, pertained to particular leukocyte clusters. Applying a novel 35-marker CyTOF panel with metal-labelled antibodies confirmed the phenotypic diversity of aortic leukocytes. Among lymphocytes, we detected three principal B-cell subsets defined by scRNAseq, CyTOF, and flow cytometry. These B cell subsets harbor distinct surface marker expression, functional gene pathways, and *ex vivo* cytokine production. Finally, we used leukocyte cluster gene signatures to assess leukocyte frequencies in 121 human plaques by a transcriptomic deconvolution strategy. This approach revealed a similar immune cell complexity in human carotid plaques with a higher percentage of monocytes and macrophages. In addition, the frequency of genetically defined leukocyte populations in carotid plaques predicted cardiovascular events in patients. The definition of leukocyte diversity by high-dimensional analyses enables a fine-grained analysis of aortic leukocyte subsets, reveals new immunological mechanisms and cell-type specific pathways, and may result in novel diagnostic risk stratification tools.

H. Winkels: None. **E. Ehinger:** None. **M. Vassalo:** None. **K. Buscher:** None. **H. Dinh:** None. **K. Kobiyama:** None. **A. Hamers:** None. **C. Cochain:** None. **E. Vafadarnejad:** None. **A.E. Saliba:** None. **A. Zernecke:** None. **P.A. Bala:** None. **A.K. Ghosh:** None. **N.A. Michel:** None. **N. Hoppe:** None. **I. Hilgendorf:** None. **A. Zirlik:** None. **C. Hedrick:** None. **K. Ley:** None. **D. Wolf:** None.

5
An IL23-IL22 Axis Regulates Intestinal Microbial Homeostasis to Protect from Diet-induced Atherosclerosis
Aliia Fatkhullina, Iuliia Peshkova, Ekaterina Koltsova, Fox Chase Cancer Ctr, Philadelphia, PA; Giorgio Trinchieri, Amiran Dzutsev, Ctr for Cancer Res, Natl Cancer Inst, Natl Insts of Health, Bethesda, MD

Atherosclerosis is lipid-driven, chronic inflammatory disease of the arterial wall. While commensal microbiota is involved in the distal regulation of systemic immune responses, how this distant connection influences the development of atherosclerosis and what are the underlying mechanisms remains largely unknown. In a mouse model of atherosclerosis, we found, unexpectedly, that disease was augmented when expression of the otherwise inflammatory cytokine IL23 was ablated. IL23 and its immediate downstream target IL22 restrict atherosclerosis by preventing outgrowth of pro-atherogenic microbiota, as inactivation of IL23/IL22 signaling led to dysbiosis and expansion of bacteria with pro-atherogenic properties, due to defective production of antimicrobial peptides in the intestine. These pro-atherogenic bacteria contributed to elevated serum levels of several pro-atherogenic metabolites, which in turn induced osteopontin (OPN) expression by aortic macrophages. Microbiota transfer from IL23 deficient mice accelerated atherosclerosis, while microbial depletion or IL22 administration reduced aortic osteopontin expression and ameliorated the disease. Overall, our work uncovers IL23-IL22 signaling axis as a key regulator of atherosclerosis that controls diet-induced expansion of pro-atherogenic microbiota, and argues for informed usage of cytokine blockers with regard to cardiovascular side effects driven by microbiota and inflammation.

A. Fatkhullina: None. **I. Peshkova:** None. **E. Koltsova:** None. **G. Trinchieri:** None. **A. Dzutsev:** None.

6
Role of Endothelial YingYang1 in Controlling Angiogenetic Sprouting and Maturation
Shuya Zhang, Ji Young Kim, Suowen Suowen Xu, Marina Koroleva, Zhenggen Jin, Univ of Rochester, Rochester, NY

Angiogenesis is essential for growth and repair, and irregularity of angiogenesis contributes to numerous malignant, inflammatory and ischemic disorders. Transcription factors that regulate angiogenic gene expression are critical for proper vascular development and homeostasis. Here we show that YingYang1(YY1) is essential for vascular development both in embryonic and postnatal angiogenesis. We first found that endothelium-specific deletion of YY1 leads to embryonic lethality due to vascular defects. We further found inducible endothelial YY1 knockout (YY1$^{i\Delta EC}$) mice exhibited abnormality of sprouting angiogenesis with a blunted-end, aneurysm-like structure with fewer and dysmorphic filopodia in EC tip cells compared with those of wild-type mice. Similar results are also identified in vitro by using cultured HUVEC cells. Moreover, we found that endothelial deletion of YY1 also leads to severe impairments in retinal vessel remodeling and maturation. Mechanistically, we show that YY1 is a robust endogenous inhibitor of Notch1 signaling that controls explicitly endothelial cell fate. YY1 deficiency remarkably enhances Hey1 expression, resulting in impaired retinal sprouting angiogenesis, which can be rescued by the treatment of the Notch inhibitor. Furthermore, YY1 regulates Hey1 expression by binding to RBP-J via a highly conserved ankyrin (ANK) repeat domain, then inhibits the NICD-MAML1- RBPJ complex formation by competing with MAML1 binding to RBP-J, which attenuates expression of downstream target genes Hey1. Lastly, we found that tumor growth and angiogenesis is reduced significantly in YY1 $^{i\Delta EC}$ mice, suggesting that endothelial YY1 is required for pathological angiogenesis in mouse tumor models. Altogether, our study reveals a new role for YY1 as a central mediator of Notch signaling and an essential regulator in both physiologic and pathologic angiogenesis.

S. Zhang: None. **J. Kim:** None. **S. Suowen Xu:** None. **M. Koroleva:** None. **Z. Jin:** None.

This research has received full or partial funding support from the American Heart Association.

7
Athero-protective Flow Regulation of ITPR3: an Epigenetic Approach
Ming He, Tse-Shun Huang, Marcy Martin, Shu Chien, John Shyy, Univ of California, San Diego, La Jolla, CA

Background The topographic distribution of atherosclerosis in human vasculature underscores the role of shear stress in regulating gene expression and function in the endothelium. Recent advances in understanding of mechanotransduction reveal that epigenetic regulation is integral to shear stress-mediated gene expression. With the use of ChIP-seq and ATAC-seq, the current study aims to demonstrate the link between histone modifications and transcriptional regulation in endothelial cells (ECs) in response to shear stress.
Methods and Results We found that pulsatile shear (PS)- and oscillatory shear (OS)-induced differential H3K27ac enrichments were associated with adjacent gene expression in ECs, approximately 30% of which showed significant positive correlation (Pearson's correlation coefficient >0.7). *In silico* prediction revealed that Krüppel-like factor 4 (KLF4) binding motifs were enriched in the PS-enhanced H3K27ac regions. By integrating genes that are induced by PS, have the KLF4 binding loci, and contain PS-associated H3K27ac in their promoter regions, we identified 18 novel PS-upregulated genes. Validating these results in mouse ECs isolated from intima of the thoracic aorta vs aortic arch, lung ECs from EC-KLF4-TG vs EC-KLF4-KO mice, and atorvastatin-treated vs control ECs, we found that Inositol 1,4,5-trisphosphate receptor type 3 (ITPR3) had the most robust expression in multiple systems. Consistent with these findings, ATAC-seq and ChIP-qPCR demonstrated a specific locus in the promoter region of the ITPR3 gene that was essential for KLF4 binding, H3K27ac enrichment, chromatin accessibility, and ITPR3 transcription. Deletion of this KLF4 binding locus in ECs by using CRISPR-Cas9 resulted in blunted calcium influx, reduced eNOS expression, and diminished NO bioavailability. Furthermore, ITPR-KO mice fed an atherogenic diet resulted in exacerbated atherosclerosis compared to wildtype littermates.
Conclusions Using a multi-layer systems approach, we have demonstrated that KLF4 is crucial for the histone modifications that allow the transcriptional activation of ITPR3 in ECs. This novel mechanism contributes to $Ca2^{+}$-dependent eNOS activation and EC homeostasis by maintaining an athero-protective phenotype.
M. He: None. **T. Huang:** None. **M. Martin:** None. **S. Chien:** None. **J. Shyy:** None.

8
Perivascular Cell-specific Knockout of the Stem Cell Pluripotency Gene Oct4 Inhibits Angiogenesis in Part by Attenuating Perivascular and Endothelial Cell Migration
Daniel L Hess, Molly R Kelly-Goss, Olga Cherepanova, Anh T Nguyen, Brian H Annex, Shayn M Peirce, Gary K Owens, The Univ of Virginia, Charlottesville, VA

Objective: Angiogenesis requires coordinated migration of endothelial cells (EC) and perivascular cells, including smooth muscle cells and pericytes (SMC-P). Perivascular cell-specific mechanisms by which SMC-P migrate and invest EC remain largely unknown. Herein, we used Myh11-$CreER^{T2}$ SMC-P lineage tracing, combined with SMC-P specific knockout of the stem cell pluripotency gene Oct4, to test the hypothesis that SMC-P derived Oct4 regulates perivascular cell migration and recruitment necessary for angiogenesis. Methods and Results: Myh11-$CreER^{T2}$ ROSA floxed STOP eYFP $Oct4^{WT/WT}$ and Myh11-$CreER^{T2}$ ROSA floxed STOP eYFP $Oct4^{FL/FL}$ littermate mice were injected with tamoxifen from 6-8 weeks of age to permanently label Myh11-expressing cells with eYFP, without or with Oct4 KO, respectively. Mice were subjected to either corneal alkali burn or hindlimb ischemia (HLI), monitored by live confocal imaging and laser doppler perfusion respectively, and sacrificed for tissue analysis. SMC-P Oct4 KO resulted in markedly impaired eYFP+ (SMC-P derived) migration and increased vascular leak following corneal alkali burn. EC neovascular area and migration distance were also significantly decreased in SMC-P specific Oct4 KO mice. Following HLI, SMC-P Oct4 KO mice had impaired perfusion recovery and decreased capillary density. Slit3 was expressed in eYFP+ cells of the microvasculature in both cornea and muscle and was downregulated following Oct4 KO. RNA-seq and qRT-PCR analysis of cultured SMC revealed dysregulation of Slit3 as well as additional members of the Slit-Robo pathway of guidance genes, including downregulation of the receptors Robo1 and Robo2 and upregulation of Slit2 following loss of Oct4. Conclusions: Taken together, we demonstrate that SMC-P derived Oct4 is essential for angiogenesis in both corneal alkali burn and HLI models. These effects are at least partially due to Oct4-dependent regulation of the Slit-Robo pathway in SMC-P, with Oct4 KO resulting in dysregulated migration of both EC and SMC-P. To our knowledge, this is the first direct evidence that loss of a single gene exclusively in SMC-P impacts angiogenesis following injury.
D.L. Hess: None. **M.R. Kelly-Goss:** None. **O. Cherepanova:** None. **A.T. Nguyen:** None. **B.H. Annex:** None. **S.M. Peirce:** None. **G.K. Owens:** None.

This research has received full or partial funding support from the American Heart Association.

9
Ribosomal Profiling of Vascular Smooth Muscle Cells *in Vivo* Identifies Cell-type Specific Transcripts and Enrichment of Blood Pressure Associated Genes
Audrey C Cleuren, Martijn A van der Ent, Kristina L Hunker, Min-Lee Yang, Hui Jiang, David Ginsburg, Santhi K Ganesh, Univ of Michigan, Ann Arbor, MI

Background: Vascular smooth muscle cells (vSMCs) are essential for maintaining blood vessel tone and vascular remodeling. Although they play an important role in cardiovascular pathologies, studying peripheral artery vSMCs *in vivo* has been complicated given their interspersed anatomic distribution and technical difficulties with isolating vSMCs from arteries and arterioles while preserving transcriptome profiles.
Methods and Results: Combining the murine *Rpl22*^{fl} Ribotag model with a vSMC-specific Transgelin-Cre (*Tagln-Cre*) Recombinase knock-in, we performed translating ribosome affinity purification and isolation of mRNA derived specifically from *Cre*-expressing^{+} cells only. Subsequent high-throughput sequencing of both whole tissue mRNA and the vSMC-selected mRNA of the brain, kidney and liver was followed by differential expression analysis to identify genes enriched in the vSMC compartment. Genes significantly enriched in all three tissues (FDR <5%) included well known vSMC markers such as Smooth muscle actin (*Acta2*) and Calponin-1 (*Cnn1*) in addition to *Tagln.* Furthermore, transcripts involved in biological processes associated with extracellular matrix and structure organization were enriched and significant overrepresentation of these genes was also seen by gene ontology analysis. Genes with roles in blood pressure regulation, such as Regulator of G protein signaling 5 (*Rgs5*) and Sphingosine-1-phosphate receptor 3 (*S1pr3*) were also significantly enriched in the vSMC transcriptome, and the expression and vSMC-specific localization of these genes were confirmed by fluorescent single-molecule *in situ* hybridization assays. Further, we performed gene set enrichment analysis of genes associated with blood pressure and hypertension based on human genome-wide association studies, and a significant number of these genes (P=0.003) showed vSMC-specific expression patterns in our *in vivo* data.
Conclusion: Our data demonstrate the feasibility of profiling vSMC gene expression *in vivo.* Furthermore, we identified enrichment of blood pressure-associated genes in the vSMC transcriptome. This model has the potential to provide new

insights into the role of vSMCs in physiology and a variety of cardiovascular pathologies.
A.C.A. Cleuren: None. **M.A. van der Ent:** None. **K.L. Hunker:** None. **M. Yang:** None. **H. Jiang:** None. **D. Ginsburg:** None. **S.K. Ganesh:** None.

10
Similar Increases in Arterial Shear-rate Evoked by Handgrip Exercise Activate Autophagy and Enos to a Lesser Extent in Primary Endothelial Cells From Older vs. Adult Subjects
Seul Ki Park, D Taylor La Salle, James Cerbie, Jae Min Cho, Ashely Nelson, David E. Morgan, Joel D. Trinity, J David Symons, Univ of Utah, Salt Lake City, UT

We reported that genetic or pharmacological suppression of autophagy in bovine and human arterial endothelial cells (ECs) prevents shear-stress induced p-eNOS^{S1177} and NO generation (Bharath et al., *Arterioscler Thromb Vasc Biol*, 2017). To date, one human study indicates an aging-associated repression of EC autophagy is concurrent with arterial dysfunction (LaRocca et al., *J Physiol,* 2012). We tested the hypothesis that a physiological elevation of arterial shear-rate activates autophagy and p-eNOS^{S1177} to a lesser extent in primary ECs from older vs. adult participants. After familiarization with laboratory procedures, flow-mediated vasodilation (%FMD) was observed to be lower ($p<0.05$) in 4 older (68±5 yr; 3.9±1.3 %) vs. 5 adult (23±3 yr; 7.9±1.1 %) male subjects. Within 1-week, a catheter was placed into the radial artery (RA). ECs were collected 30-min later via j-wire from the RA. Next, subjects performed rhythmic handgrip exercise (RHE) for 60-min that elevated ($p<0.05$) arterial shear-rate similarly (2.6 ± 0.2-fold) between groups from pre-exercise values. Shear-rate [$8V_{mean}$/brachial artery (BA) diameter] was obtained by assessing BA diameter, BA blood flow velocity (V_{mean}), and BA blood flow [($V_{mean}\pi$ (vessel diameter / 2)^2 x 60)] at 5-10 min intervals using Doppler ultrasound. Compared to pre-exercise values, RHE did not alter heart rate, stroke volume, cardiac output, or arterial pressure (plethysmography) in either group. Immediately following RHE ECs were collected from the RA. Using quantitative immunofluorescence, primary ECs (75 ECs per endpoint per subject) were identified by positive co-staining for VE-cadherin and DAPI via confocal microscopy. Immortalized human arterial ECs processed and stained in parallel served as fluorescence intensity controls. Relative to pre-exercise, ECs from adult but not old subjects at 60-min displayed increased expression of microtubule associated protein light chain 3 ($p<0.04$), lysosomal associated membrane protein 2a ($p<0.01$), autophagy-related gene 3 ($p=0.06$), and p-eNOS^{S1177} ($p<0.02$), and decreased expression of the adaptor protein p62 ($p<0.02$). These data indicate aging limits shear-induced EC autophagy and eNOS activation in response to functional hyperemia.
S. Park: None. **D. La Salle:** None. **J. Cerbie:** None. **J. Cho:** None. **A. Nelson:** None. **D. Morgan:** None. **J. Trinity:** None. **J. Symons:** None.

This research has received full or partial funding support from the American Heart Association.

11
Cardiovascular Consequences of Cantu Syndrome and Response to Glibenclamide Treatment in Two Novel KATP Channel Mutant Mouse Models
Conor McClenaghan, Yan Huang, Theresa Harter, G. Schuyler Brown, Kristina Hinman, Carmen Halabi, Scot Matkovich, Robert P Mecham, Carla J Weinheimer, Attila Kovacs, Sarah England, Maria S Remedi, Colin G Nichols, Washington Univ in St Louis, Saint Louis, MO

The rare heritable disorder Cantú syndrome (CS) arises from gain-of-function mutations in the genes encoding the cardiovascular KATP channel subunits Kir6.1 and SUR2 (*KCNJ8* and *ABCC9,* respectively). CS is characterized by diverse features including hypertrichosis, osteochondrodysplasia and craniofacial dysmorphology. Multiple cardiovascular abnormalities are also reported in CS including vascular dilation and tortuosity, dramatic cardiomegaly, pulmonary hypertension and low systemic blood pressure. We have developed and characterized two novel mouse models of Cantu Syndrome in which disease causing amino acid substitutions have been engineered into either Kir6.1 (p.V65M) or SUR2 (p.A478V) using CRISPR/Cas9 genome editing. Electrophysiological assessment of isolated vascular smooth muscle cells (VSMCs) showed that both mutations result in increased basal activity of VSM KATP channels. Mutant mice also exhibit vascular dilation, low blood pressure, and pulmonary hypertension. In addition, mutant mice exhibited hypertrophic, hyper-contractile hearts. The latter findings are not trivially predictable as a consequence of KATP gain-of-function, but also recapitulates key clinical features of CS. The severity of pathophysiological remodeling correlated with the molecular effects of the substitution. These models provide novel insights to the cardiovascular consequences of KATP over-activity. Little is known about the long-term effects of human CS, nor reversibility of pathophysiological consequences. Chronic administration of the sulfonylurea KATP inhibitor glibenclamide (glyburide) by slow-release pellets implanted under the skin resulted in normalization of vascular consequences and reversal of cardiac hypertrophy in SUR2(A478V) mice over 3 weeks. Kir6.1(V65M) mice are less sensitive to glibenclamide treatment, as predicted from studies of recombinant channels. These results suggest that glibenclamide represents a promising pharmacotherapy for CS (but that sensitivity may be patient- and mutation-dependent), and perhaps for diverse cardiovascular conditions arising from decreased smooth muscle excitability in general.
C. McClenaghan: None. **Y. Huang:** None. **T. Harter:** None. **G. Brown:** None. **K. Hinman:** None. **C. Halabi:** None. **S. Matkovich:** None. **R.P. Mecham:** None. **C.J. Weinheimer:** None. **A. Kovacs:** None. **S. England:** None. **M.S. Remedi:** None. **C.G. Nichols:** None.

12
Aorta-on-a-chip: a Tool to Gain Molecular and Translational Insight Into Vascular Diseases
Valentina Paloschi, Claudio Rolli, Benedikt Buchmann, Technical Univ Munich, Munich, Germany; Sandro Meucci, Micronit Microtechnologies, Enschede, Netherlands; Felix Rogowitz, Fluigent Deutschland GmbH, Jena, Germany; Andreas Bausch, Lars Maegdefessel, Technical Univ Munich, Munich, Germany

Vascular cell biology research is focused on understanding how endothelial cells and smooth muscle cells react to relevant biological, chemical and physical stimuli. Importantly, *in vivo*, dynamic conditions are present: vascular endothelial cells (ECs) are constantly subjected to shear stress and smooth muscle cells (SMCs) are stretched due to pulsation during the cardiac cycle. A three-dimensional network composed of extracellular matrix proteins maintains the homeostasis of the cells. The aim of this project is to realize an *in vitro* model of the human aorta (*aorta-on-a-chip*), an innovative tool that by resembling the *in vivo* structure of the aorta allows us to study how cells layers and matrix are sensing and responding to a pro-atherogenic environment (i.e. low shear stress) and to gain insight in the pathological remodeling occurring during progression of vascular diseases. The device consists of two re-sealable glass slides, assembled with a membrane suspended in between them, which creates two separate flow chambers. After coating both sides of the membrane with fibronectin, ECs and SMCs are seeded sequentially, in order to obtain a confluent ECs-SMCs co-culture, mimicking the intima-media interface of the aortic wall. The co-culture device is connected to a microfluidic pump system where ECs are exposed to physiologically relevant shear stress (8-12

dyne/cm^2). The SMCs flow-chamber is exposed to a low shear stress (0.0042 dyne/cm^2) to ensure physiological turnover of influx of nutrients and efflux of waste. Molecular and phenotypic evaluation of the cells is performed by measuring gene expression changes (RNA sequencing) and protein analyses (immunofluorescence for cell markers), respectively. For translational purposes, cells deriving from patients with aortic diseases (compared to un-diseased organ donor controls) can be implemented and tested with the chip.

V. Paloschi: None. **C. Rolli:** None. **B. Buchmann:** None. **S. Meucci:** None. **F. Rogowitz:** None. **A. Bausch:** None. **L. Maegdefessel:** None.

13

Genotype to Phenotype: Function of Rare Coding Variants in *ANGPTL3*

Xiao Wang, Univ of Pennsylvania, Philadelphia, PA; A. Christina Vourakis, Alexandra E Sperry, Harvard Univ, Cambridge, MA; Alexandra C Chadwick, Wenjun Li, Wenjian Lv, Kiran Musunuru, Univ of Pennsylvania, Philadelphia, PA

Angiopoietin-like 3 (*ANGPTL3*) associates strongly with blood lipid phenotypes in human genetics studies and has thus emerged as promising therapeutic target for plasma lipids. We examined the coding regions of *ANGPTL3* and identified 82 rare variants in individuals from separate human cohorts. In light of the seemingly favorable clinical consequences of *ANGPTL3* deficiency, we established an experimental framework to determine the functional consequences of rare *ANGPTL3* missense mutations *in vivo*. We generated an *Angptl3* knockout mouse, which exhibited decreased triglyceride (TG) (61%, P < 0.001) and decreased total cholesterol (31%, P < 0.002). We attempted to rescue this phenotype using adenoviruses expressing either wild-type or missense variant of *ANGPTL3*. To date, all 82 rare missense variants have been assessed, of which 25 were validated in terms of loss-of-function as severe (conferring <25% of wild-type activity as assessed by either TG or cholesterol levels), 18 were moderate (25-50%), 18 were mild (50-75%), and 20 were benign (75-125%) while 1 was gain-of-function (>125%), underscoring the need for functional characterization of variants of uncertain significance. Furthermore, we noticed that 4 variants (H343R, S86L, E129G and T256K) were loss-of-function on triglyceride levels, while benign on cholesterol levels. On the other hand, 7 variants (L75F, C408R, Y350H, K387Q, Q293E, D455E and M259R) were loss-of-function on cholesterol while benign on TG. ANGPTL3 has been implicated in regulating TG and cholesterol through different mechanisms. Therefore, we studied the potential mechanisms by knocking in variants into induced pluripotent stem cells (iPSCs) *in vitro*. We next differentiated edited cells into hepatocyte-like cells (HLCs). We observed no cleaved N-terminal fragment of ANGPTL3 in HLCs with the E129G variant while the expression level of full-length ANGPTL3 was unaffected. It has been reported that N-terminal fragment is sufficient to inhibit lipoprotein lipase activity which is the primary mechanism by which triglyceride-rich lipoproteins are cleared from the circulation. These results indicate that variant E129G could not be cleaved and this might be the mechanism by which it only affects TG, not cholesterol levels.

X. Wang: None. **A. Vourakis:** None. **A.E. Sperry:** None. **A.C. Chadwick:** None. **W. Li:** None. **W. Lv:** None. **K. Musunuru:** None.

14

Interferon-induced Transmembrane 3 (IFITM3) on Megakaryocytes and Platelets Regulates Fibrinogen Endocytosis and Thrombosis During Inflammation

Robert A Campbell, Bhanu K Manne, Samantha Saperstein, Lauren Page, Hansjorg Schwertz, Jesse W Rowley, Andrew S Weyrich, Matthew T Rondina, Univ of Utah, Salt Lake Cty, UT

Introduction: IFITM3, an interferon (IFN) responsive gene, restricts pathogen replication through vesicular trafficking mechanisms. IFITM3 in megakaryocytes (MKs) and platelets has not been examined. We hypothesized that in MKs and platelets, IFITM3 regulates the endocytosis of pro-coagulant proteins, aggregation, and thrombosis. Methods: the regulation of IFITM3 gene expression was determined in MKs and platelets under inflammatory stimuli. Fibrinogen (Fgn) endocytosis, a clathrin-mediated event requiring αIIbβ3, and transferrin endocytosis, a clathrin-mediated, αIIbβ3-independent event, were examined in stimulated MKs and platelets from wild type (WT) and Ifitm$^{-/-}$ mice (KO). Integrin αIIbβ3 activation, platelet aggregation, and thrombosis was determined in WT and Ifitm$^{-/-}$ mice upon IFNα-stimulation. Co-immunoprecipitation identified interaction partners for IFITM3. To establish human relevance, IFITM3 expression, Fgn content, and aggregation was measured in platelets from septic patients, where systemic IFNs are increased. Results: IFNs significantly induced IFITM3 expression in MKs and platelets ($p<0.001$). Upregulation of IFITM3 by IFNs increased Fgn and transferrin endocytosis in MKs (2-fold vs. NT, $p<0.05$). Co-IP demonstrated a specific IFITM3 interaction between clathrin and αIIb. Upon IFN stimulation, IFITM3, clathrin, and αIIb shifted into lipid rafts. Increased Fgn endocytosis by IFNs enhanced platelet aggregation and accelerated death (~2-fold increased) due to platelet-dependent thrombosis ($p<0.05$ for all comparisons). In KO mice, enhanced Fgn endocytosis, platelet aggregation, and thrombosis to IFNs was completely prevented, demonstrating the necessity of IFITMs for these functional responses. Platelets from septic patients mirrored findings in mice with a ~20-fold increase in IFITM3 protein expression, with shifts into lipid rafts, compared to healthy controls ($p<0.0001$). Increased platelet IFITM3 expression was associated with greater platelet Fgn content and significant increases in platelet aggregation (20% increase, $p<0.05$). Conclusions: Our data identify IFITM3 as a previously unknown regulator of MK and platelet endocytosis and thrombosis under inflammatory stimuli in humans and mice.

R.A. Campbell: None. **B.K. Manne:** None. **S. Saperstein:** None. **L. Page:** None. **H. Schwertz:** None. **J.W. Rowley:** None. **A.S. Weyrich:** None. **M.T. Rondina:** None.

15

PAR4 Ala120Thr Variant Alters PAR4 Desensitization, Sensitivity to Platelet Antagonists and Risk of Large Vessel Stroke

Michael Whitley, Thomas Jefferson Univ, Philadelphia, PA; David Henke, Lukas Simon, Baylor Coll of Med, Houston, TX; Joanne Vesci, Thomas Jefferson Univ, Philadelphia, PA; Michael Holinstat, Univ Of Michigan, Ann Arbor, MI; Marvin Nieman, Case Western Reserve Univ, Cleveland, OH; Chad Shaw, Baylor Coll of Med, Houston, TX; Paul Bray, Univ of Utah, Salt Lake City, UT; **Leonard Edelstein**, Thomas Jefferson Univ, Philadelphia, PA

F2RL3 encodes protease-activated receptor 4 (PAR4) and harbors a A/G SNP (rs773902) with racially dimorphic allelic frequencies. This SNP mediates an alanine to threonine substitution at residue 120 that alters platelet PAR4 activation by the artificial PAR4-activation peptide (PAR4-AP), AYPGKF, which does not occur in vivo. Platelet function studies from healthy human donors demonstrated that compared to rs773902 GG donors, platelets from rs773902 AA donors had increased aggregation to low

concentrations (<1 nM) of thrombin, increased Ca^{2+} signaling, increased granule secretion and decreased PAR4 desensitization. The increased thrombin sensitivity of rs773902 AA platelets required both PAR4 and PAR1. Whereas receptor cleavage, dimerization, or lipid raft localization were not different between platelets from the two *F2RL3* genotypes, rs773902 AA platelets required more than 3-fold amounts of PAR4-AP for receptor desensitization. PAR4-AP stimulation of PAR4-transfected COS-7 cells *increased* PAR4 levels on the cell surface. Thrombin-stimulated platelets from rs773902 AA donors displayed reduced inhibition by P2Y12 and PAR1 blockers, but not aspirin. Finally, the association of rs773902 alleles with stroke was assessed using the Stroke Genetics Network (SiGN) study. Patients carrying at least one copy of the rs773902 A allele had an increased risk of both large vessel stroke and diabetes in the SiGN dataset. In summary, both PAR4 and PAR1 are required for platelet activation to sub-nanomolar thrombin concentrations. Compared to rs773902 GG platelets, rs773902 AA platelets have a lower EC50 for thrombin and are relatively resistant to receptor desensitization, perhaps due to anterograde trafficking of internal PAR4 to the plasma membrane post-stimulation. The association of the rs773902 A variant with large vessel stroke, diabetes and partial resistance to PAR1 and P2Y12 inhibition must be considered for development of personalized anti-platelet agents.

M. Whitley: None. **D. Henke:** None. **L. Simon:** None. **J. Vesci:** None. **M. Holinstat:** None. **M. Nieman:** None. **C. Shaw:** None. **P. Bray:** None. **L. Edelstein:** None.

16

Glucose Metabolism is Required for Platelet Hyperactivation in a Murine Model of Type 1 Diabetes Mellitus

Trevor P Fidler, Columbia Univ, New York, NY; Alex P Marti 52240, Katelyn Gerth, Univ of Iowa, Iowa City, IA; Matthew T Rondina, Andrew S. Weyrich, Univ of Utah, Salt Lake City, UT; Evan D Abel, Univ of Iowa, Iowa City, IA

Patients with type 1 diabetes mellitus (T1DM) have increased thrombosis and platelet activation. The mechanisms for platelet hyperactivation in diabetes are incompletely understood. T1DM is accompanied by hyperglycemia, hyperlipidemia, increased inflammation, and an alternated hormonal milieu. In vitro analysis of platelets demonstrates that low glucose reduces platelet activation while hyperglycemic conditions increase platelet activation. We therefore hypothesized that hyperglycemia increases platelet glucose utilization, which directly increases platelet activation to promote thrombosis. To test this hypothesis platelets were isolated from mice treated with streptozotocin (STZ), to induce T1DM and revealed increased glucose uptake and glycolysis along with induction of glucose transporter 3 (GLUT3). Functionally, platelets from STZ-treated mice exhibited increased activation following administration of PAR4 peptide and convulxin. In contrast, platelets isolated from platelet specific (glucose transporter 1 (GLUT1 and GLUT3) double knockout (DKO) mice, which lack the ability to utilize glucose, failed to increase activation in hyperglycemic mice. In addition, diabetic mice displayed decreased survival in a collagen/epinephrine induced pulmonary embolism model relative to non-diabetic controls. In contrast, survival following pulmonary embolism was increased in diabetic DKO mice, relative to non-diabetic controls. Together these data reveal that in a model of T1DM hyperglycemia increases platelet GLUT3 protein expression, glucose metabolism, platelet activation and thrombosis.

T.P. Fidler: None. **A.P. Marti:** None. **K. Gerth:** None. **M.T. Rondina:** None. **A.S. Weyrich:** None. **E.D. Abel:** None.

17

Platelet TLRs Mediate Complement C3 Release During the Initial Neutrophil Response to Pathogens

Milka Koupenova, Heather A Corkrey, Evelyn A. Kurt-Jones, Jane E Freedman, Univ of MA Medical Sch, Worcester, MA

The initial response to invading pathogens involves the Toll-like receptor (TLR) and complement systems and is mediated by neutrophils and platelets. Neutrophil activation by TLRs requires sensitization, yet the mechanism by which this activation occurs is not completely understood. We sought to determine how platelets regulate the neutrophil TLR response to pathogens, specifically, in initiating netosis. Here we demonstrate that, in human blood, both TLR7 and TLR2 mediate endothelial-free netosis and platelet-TLR7 is required for this response. In vivo activation in murine models lacking TLR2 or TLR7 confirms TLR specificity for netosis in blood. TLR-stimulation leads to secretion of complement C3 (C3) from platelets, C3-mediated DNA release from neutrophils and formation of large netting neutrophil aggregates. Neutrophil signaling resulting from platelet-TLR7 stimulation causes granulocyte-macrophage colony-stimulating factor (GM-CSF) secretion from platelets, leading to reduction in C3-initiated netosis. TLR-mediated release of antimicrobial myeloperoxidase (MPO) from neutrophils occurs only in the presence of platelets. These findings demonstrate that the initial intrinsic defense to pathogens is mediated by multifactorial platelet-neutrophil cross-communication tightly regulating the TLR and complement responses of the host.

M. Koupenova: None. **H.A. Corkrey:** None. **E.A. Kurt-Jones:** None. **J.E. Freedman:** None.

This research has received full or partial funding support from the American Heart Association.

18

TET2 Loss of Function-driven Clonal Hematopoiesis Promotes Age-related Vascular and Systemic Inflammation and Metabolic Dysfunction in Mice

Jose J Fuster, Univ of Virginia Sch of Med., Charlottesville, VA; Maria A. Zuriaga, Maya Polackal, Kenneth Walsh, Boston Univ, Boston, MA

BACKGROUND: Acquired mutations in the hematopoietic system and subsequent clonal hematopoiesis are emerging as potential new drivers of atherosclerotic cardiovascular disease. TET2 was the first gene reported to exhibit acquired mutations in blood cells of cancer-free elderly individuals and we recently reported that the clonal expansion of TET2-mutant hematopoietic cells accelerates atherogenesis in mouse models by exacerbating inflammatory responses in the atherosclerotic plaque. The objective of this study was to examine whether TET2 loss of function-driven clonal hematopoiesis also has systemic effects on age-related inflammation and metabolic function beyond its direct actions on the plaque. METHODS: An adoptive transfer technique was used to introduce a small percentage of Tet2-/- hematopoietic cells in non-irradiated C57Bl/6J mice, which were monitored for 16 months following transfer. Flow cytometry techniques were used to follow the expansion of Tet2-/- cells in the blood. RESULTS: Tet2-/- hematopoietic cells expanded progressively over time after adoptive transfer, with a mild myeloid bias. This was paralleled by increased expression of the pro-inflammatory cytokines IL-1β and IL-6 in the white adipose tissue and the aortic wall, as well as by increased serum levels of IL-6. Tet2-/- expansion also led to exacerbated systemic insulin resistance, as revealed by insulin tolerance tests. CONCLUSION: TET2-deficient hematopoietic cell expansion promotes vascular and systemic inflammation, as well as metabolic dysfunction in aging mice. These results support a causal role for TET2 mutation-driven clonal hematopoiesis in age-related cardiometabolic disease, and suggest that

somatic TET2 mutations may contribute to atherosclerosis by promoting inflammation both systemically and locally in the atherosclerotic plaque.
J.J. Fuster: None. **M.A. Zuriaga:** None. **M. Polackal:** None. **K. Walsh:** None.

This research has received full or partial funding support from the American Heart Association.

19
Anti-MicroRNA-144 Therapy Attenuates Progression and Promotes Regression of Atherosclerosis
Elizabeth J Tarling, Joan Cheng, Angela Cheng, UCLA, Los Angeles, CA; Nathalie Pamir, Oregon Health and Science Univ, Portland, OR; Tamer Sallam, Thomas Q de Aguiar Vallim, UCLA, Los Angeles, CA

Rationale: Removal of cholesterol from atherosclerotic lesions remains an unmet therapeutic need. The ATP Binding Cassette Transporter A1 (ABCA1) plays a key role in the efflux of cholesterol from macrophages, therefore strategies that increase macrophage ABCA1 levels are likely to be atheroprotective.
Objective: To determine the potential of miR-144 antagonism as an interventional therapeutic in high-fat, high-cholesterol-fed low-density lipoprotein receptor null ($Ldlr^{-/-}$) mice.
Methods: $Ldlr^{-/-}$ mice were treated with saline, control anti-miR, or anti-miR-144 oligonucleotides once a week for 16 weeks to assess the efficacy of long-term silencing of miR-144 on atherosclerosis progression. Second, $Ldlr^{-/-}$ mice with established atherosclerotic plaques were treated with anti-miR-144 for 4 weeks, in a model of atherosclerosis regression. All anti-miR-144-treated mice showed increased circulating high-density lipoprotein (HDL) levels. Anti-miR-144-treated mice also showed enhanced reverse cholesterol transport to the plasma, liver, and feces in the regression model. Consistent with these observations, all anti-miR-144-treated mice showed reductions in atherosclerotic burden. Notably, miR-144 antagonism also significantly remodeled the HDL particle proteome in both progression and regression models of atherosclerosis.
Conclusions: These studies suggest anti-miR-144 treatment may be a promising interventional therapeutic strategy to treat atherosclerotic disease.
E.J. Tarling: None. **J. Cheng:** None. **A. Cheng:** None. **N. Pamir:** None. **T. Sallam:** None. **T.Q. de Aguiar Vallim:** None.

This research has received full or partial funding support from the American Heart Association.

20
Regression of Atherosclerosis Through Manipulation of Vascular Macrophages; a Novel Gene-therapy Approach
Courtney Howard, Azzadine Ammi, Paul Muelle, Katherine Huynh, Federico Moccetti, Yllka Latifi, Jonathan Nelson, Aris Xie, Jonathan R Lindner, **Hagai Tavori**, Oregon Health & Science Univ, Portland, OR

Aggressive lipid lowering halts atherosclerotic plaque progression but does not lead to bulk plaque regression in humans. We have previously reported that gene transfection of the HDL protein apoAI into macrophages (MΦ-apoAI) decrease the rate of plaque development in atherosclerosis-prone mice. In this study, we hypothesized that MΦ-apoAI can promote regression of atherosclerosis synergistically with lipid-lowering.
Atherogenic mice ($LDLR^{-/-}$ and $LDLR^{-/-}$/MΦ-apoAI) were fed a high-fat diet to promote stage II/III atherosclerotic lesions (as baseline comparator), and then switched to an extreme lipid-lowering intervention (chow with MTTP inhibitor). After 3 weeks on the lipid-lowering diet, both groups showed reduced systemic and lesion inflammation, and reduced macrophage content on histology when compared to baseline. Upon lipid-lowering, vascular ultrasound showed that $LDLR^{-/-}$/MΦ-apoAI mice has 21% improvement in aortic pulse transit time, and a 37.1% improvement in instantaneous aortic compliance (a surrogate marker for arterial elastic modulus), compared to $LDLR^{-/-}$ mice. Histologic evidence showed that $LDLR^{-/-}$/MΦ-apoAI mice on lipid-lowering diet also had reduced lesion size (-24%), reduced macrophage content (-27.5%), increased M2/M1 ratio (+51%) and reduced necrotic core area (-28.6%), compared to $LDLR^{-/-}$ mice. Using transplantation of bone marrow cells from MΦ-apoAI mice into recipient mice with established lesions, we show that newly recruited cells are not major contributors to the regression afforded by MΦ-apoAI. Thus, to study the kinetics of pre-existing cells in the lesion during regression, we developed a contrast ultrasound-mediated gene delivery system to tag and trace lesion cells in $LDLR^{-/-}$ mice, which revealed that lesion macrophages expressing apoAI specifically migrate to mediastinal LN in a CCR7-dependent manner during regression.
Expression of apoAI in pre-existing lesion macrophages, promotes regression of atherosclerosis beyond lipid-lowering alone, and increases CCR7-dependent egress of macrophages to adjacent lymph nodes. Ultrasound-mediated gene delivery can be a useful device to study the kinetics of cell in the artery wall and also represent a novel approach with application to human therapy.
C. Howard: None. **A. Ammi:** None. **P. Muelle:** None. **K. Huynh:** None. **F. Moccetti:** None. **Y. Latifi:** None. **J. Nelson:** None. **A. Xie:** None. **J.R. Lindner:** None. **H. Tavori:** None.

This research has received full or partial funding support from the American Heart Association.

21
ARHGEF26 is a Novel Genetic Risk Factor for Vascular Inflammation and Coronary Artery Disease
Qiuyu M Zhu, Broad Inst, Cambridge, MA; Derek Klarin, Connor A Emdin, Massachusetts General Hosp, Boston, MA; Mark Chaffin, Steven Horner, Brian McMillan, Alison Leed, Broad Inst, Cambridge, MA; Michael E Weale, Chris C Spencer, Genomics plc, Oxford, United Kingdom; François Aguet, Ayellet V Segrè, Kristin G Ardlie, Broad Inst, Cambridge, MA; Amit V Khera, Massachusetts General Hosp, Boston, MA; Virendar K Kaushik, Broad Inst, Cambridge, MA; Pradeep Natarajan, Massachusetts General Hosp, Boston, MA; CARDIoGRAMplusC4D Consortium; Sekar Kathiresan, Massachusetts General Hosp, Boston, MA

Vascular inflammation drives the initiation and progression of coronary artery disease (CAD). However, the underlying genetic factors are not well understood. We performed a genome-wide association study in UK Biobank testing 9 million DNA variants for association with CAD (4,831 cases, 115,455 controls), followed by a meta-analysis with previous results. We identified *ARHGEF26* (Rho guanine nucleotide exchange factor 26) as a novel locus significantly associated with CAD (combined OR=1.08, 95% CI 1.06-1.11, $P=1.02 \times 10^{-9}$). We hypothesized that ARHGEF26 regulates vascular inflammation by affecting the function of vascular cells. Focusing on the haplotype tagged by the lead variant rs12493885 (ARHGEF26 p.Val29Leu), we performed eQTL and allele-specific expression analyses. There is no significant *ARHGEF26* transcription alteration or allelic imbalance associated with the risk allele in human coronary artery samples. Promoter luciferase assay showed no significant difference between the reference and alternative haplotypes. In contrast, expression of exogenous Leu29 mutant after depletion of endogenous ARHGEF26 led to rescued phenotypes consistently exceeding those observed with overexpression of wild-type ARHGEF26, including increased leukocyte transendothelial migration, leukocyte adhesion on endothelial cells, and smooth muscle cell

proliferation. These data suggest that the CAD-risk allele (Leu29) may lead to a gain of protein function in vascular cells. To identify the molecular mechanism, we compared the nucleotide-exchange activity between the wild-type and mutant proteins and found no significant difference. Evaluation of ARHGEF26 protein stability by cycloheximide chase showed the Leu29 mutant displayed longer half-life than wild-type ARHGEF26, suggesting the gain-of-function phenotypes of Leu29 in cells may be secondary to its resistance to degradation. Quantitative proteomics revealed differential protein interaction between the wild-type and Leu29 ARHGEF26 in endothelial cells, highlighting critical inflammatory pathways impacted by the CAD-risk allele. In summary, our work identified a novel genetic risk factor for CAD, and enabled discovery of novel CAD-causing pathways in vascular inflammation.

Q.M. Zhu: None. **D. Klarin:** None. **C.A. Emdin:** None. **M. Chaffin:** None. **S. Horner:** None. **B. McMillan:** None. **A. Leed:** None. **M.E. Weale:** None. **C.C.A. Spencer:** None. **F. Aguet:** None. **A.V. Segrè:** None. **K.G. Ardlie:** None. **A.V. Khera:** None. **V.K. Kaushik:** None. **P. Natarajan:** None. **S. Kathiresan:** None.

22

Hepatic Sortilin Regulates Apolipoprotein B Secretion only Under Conditions of Secretory StressDependent of the Presence of Secretory Stress

Donna M Conlon, Amrith Rodrigues, Kathy Guo, Nicholas Hand, Daniel Rader, Univ of Pennsylvania, Philadelphia, PA

SORT1 is strongly associated with plasma lipid traits and coronary artery disease. The protein it encodes, sortilin is a multi-ligand receptor involved in trafficking of proteins from the Golgi to the lysosome. Hepatic sortilin overexpression reduces VLDL secretion, but the effects of loss of sortilin function on apolipoprotein B100 (apoB) and VLDL secretion have been contradictory and perplexing. Conflicting studies have variously reported increased and decreased apoB/VLDL secretion in response to loss of sortilin, but used a variety of different models and methods of ablating sortilin function. To resolve this, we first measured VLDL secretion in Sort1 knockout (KO) mice on a chow diet and observed no differences in either apoB or TG secretion. ApoB secretion was similarly unaffected in Sort1 KO primary hepatocytes or in McA-RH7777 cells treated with siRNA to knockdown sortilin. We concluded that in a basal secretory state, loss of sortilin alone does not impact apoB secretion, leading us to test if differences in secretory state might explain the discrepancies in published results. We found that when hAPOB was overexpressed, Sort1 knockdown further increased its secretion. The reports of increased VLDL secretion with Sort1 knockout occurred with apoB overexpression, or on high fat diet (HFD); consistent with our hypothesis that secretory overload or metabolic stress are required to uncover the deficiency phenotype. We placed Sort1 KO mice on a 45% HFD for 12 weeks and observed a significant increase in VLDL secretion compared to controls. In addition, when we lipid-loaded hepatocytes with oleic acid or palmitic acid, apoB secretion was increased, and Sort1 knockdown further increased this compared to control. We treated cells with Tunicamycin to induce ER stress, and found that apoB secretion was decreased in the control group was observed, but not in the absence of Sort1, suggesting that sortilin regulates apoB secretion the cell is stressed. Based on these data, we propose that hepatic sortilin regulates the post-ER fate of apoB for either degradation or export; thereby coordinating intracellular apoB metabolism in response to the number and quality of apoB particles that reach the Golgi, and the level of post-ER pre-secretory proteolysis activity.

D.M. Conlon: None. **A. Rodrigues:** None. **K. Guo:** None. **N. Hand:** None. **D. Rader:** None.

23

Clearance of ApoC-III Glycoforms Associated With Triglyceride Metabolism

Hussein Yassine, Natalie Kegulian, Univ of Southern California, Los Angeles, CA; Bastian Ramms, Univ of California San Diego, San Diego, CA; Steven Horton, Univ of Southern California, Los Angeles, CA; Olgica Trenchevska, Dobrin Nedelkov, Arizona State Univ, Tempe, AZ; Mark J Graham, Ionis Pharmaceuticals, Carlsbad, CA; Philip L. Gordts, Univ of California San Diego, San Diego, CA

Background: We previously reported an association between higher abundance of disialylated (apoC-III_2) over monosialylated (apoC-III_1) apoC-III and lower plasma triglyceride (TG) concentrations in three independent studies. **Methods:** The goal of this study was to get mechanistic insights in the metabolism of apoC-III_1 and apoC-III_2. First, the relative abundances of human triglyceride-rich lipoproteins (TRL)-associated apoC-III glycoforms in plasma were assessed by mass spectrometric immunoassay (MSIA) over time after injecting human TRL in wild-type mice, mice lacking hepatic heparan sulfate proteoglycans (HSPG), and mice deficient for both low-density lipoprotein receptor (LDLR) and LDLR-Related Protein 1 (LRP-1). Secondly, the relative abundance of plasma apoC-III glycoforms was assessed by MSIA in 11 participants randomized to volanesorsen (apoC-III antisense drug; n=11) or placebo (n=6) treatment for 13 weeks. **Results:** Kinetic studies revealed that half of TRL-associated apoC-III (total) was rapidly cleared via LDLR and LRP1 ($t_{1/2}$= 16.5 min), and the remaining half via the much slower but higher capacity HSPGs ($t_{1/2}$= 55.5 min). After injection, a significant increase in the relative abundance of apoC-III_2 was observed in HSPG-deficient mice , while no increase in mice lacking LDLR and LRP-1. Clinically, the relative abundance of apoC-III_2 significantly increased (42% increase compared to placebo, p=0.05) and that of apoC-III_1 significantly decreased (15% decrease compared to placebo, p=0.007) in participants randomized to volanesorsen. The decrease in the relative abundance of apoC-III_1 after volanesorsen treatment was strongly correlated with the decrease in TG levels (r=0.63, p=0.006). **Conclusions:** Our results indicate slower clearance of apoC-III -containing particles through HSPGs, which preferentially clear apoC-III_2. In contrast, apoC-III_2 is less effectively cleared by LDLR/LRP-1 compared to apoC-III_1. Clinically, the increase in the apoC-III_2/apoC-III_1 ratio upon antisense lowering of apoC-III might reflect faster clearance of apoC-III_1 as it associates with improved TG levels.

H. Yassine: Consultant/Advisory Board; Modest; Akcea. **N. Kegulian:** None. **B. Ramms:** None. **S. Horton:** None. **O. Trenchevska:** None. **D. Nedelkov:** None. **M.J. Graham:** Ownership Interest; Significant; Ionis Pharmaceuticals. **P.L. Gordts:** None.

This research has received full or partial funding support from the American Heart Association.

24

Association of APOL1 Risk Alleles with Coronary Heart Disease in Million Veteran Program

Alexander G Bick, Massachusetts General Hosp, Boston, MA; Themistocles L Assimes, Stanford Univ Sch of Med, Stanford, CA; Ayush Giri, Vanderbilt Univ, Nashville, TN; Derek Klarin, Massachusetts General Hosp, Boston, MA; Julie Lynch, Salt Lake City VA Health Care System, Salt Lake City, UT; Cassieanne Robisson-Cohen, Vanderbilt Univ, Nashville, TN; Jennifer E Huffman, Boston VA Healthcare System, Boston, MA; Yan V Sun, Emory Univ, Atlanta, GA; Kyong-Mi Chang, Corporal Michael Crescenz VA Med Cntr, Philadelphia, PA; Donald R Miller, Boston Univ, Boston, MA; Kelly Cho, Boston VA Healthcare System, Boston, MA; Todd Edwards, Vanderbilt Univ, Nashville, TN; Chris O'Donnell, Boston VA Healthcare System, Boston, MA; Philip S Tsao, Palo Alto VA Health Care System, Palo Alto,

CA; Peter W Wilson, Atlanta VA Medical Ctr, Atlanta, GA; Sekar Kathiresan, Massachusetts General Hosp, Boston, MA; Daniel J Rader, Univ of Pennsylvania, Philadelphia, PA; Adriana M Hung, Vanderbilt Univ, Nashville, TN; Scott M Damrauer, Univ of Pennsylvania, Philadelphia, PA

Background: Approximately 13% of African-Americans carry 2 copies of the *APOL1* risk alleles G1 or G2, which are associated with increased risk of CKD. There have been conflicting reports as to whether an association also exists between *APOL1* and cardiovascular disease.
Objective: Determine the association between *APOL1* and CAD in African Americans genotyped in the Million Veteran Program (MVP)
Methods and Results: *APOL1* risk alleles were genotyped in 64,792 African American MVP participants. 7,987 (12%) of the participants carried the high-risk genotype comprised of 2 risk alleles. Of the high-risk carriers, 36% were G1 homozygotes, 49% were G1/G2 compound heterozygotes, and 15% were G2 homozygotes. We first confirmed the known association of the *APOL1* risk genotype with end stage renal disease (OR 2.75, $P=1.8 \times 10^{-66}$). We then considered the association between the high-risk *APOL1* genotype and prevalent CAD. Based on electronic health record data, 11,902 (19.4%) of the participants had CAD. Individuals with 2 risk alleles trended toward increased rates of CAD compared to those with no risk alleles (OR 1.075, p=0.03). The strength of the association varied by the nature of composition of the high-risk genotype: G1/G1 carriers had increased rates of CAD (OR 1.19, p=0.002), G1/G2 carriers had a trend towards increased CAD (OR 1.08, p=0.1), and G2/G2 carriers had no differences in CAD rates (OR 0.99, p=0.9) than controls. Adjusting for traditional CAD risk factors and kidney disease in multivariable regression models attenuated the significance of the association between *APOL1* and CAD.
Conclusions: *APOL1* variant contribution to CAD risk is genotype dependent and likely mediated by the known *APOL1* association with CKD. The modest effect of *APOL1* on CVD, the differential presence of CKD, and the relative proportion of G1 and G2 alleles may explain the conflicting findings in the published literature.
A.G. Bick: None. **T.L. Assimes:** None. **A. Giri:** None. **D. Klarin:** None. **J. Lynch:** None. **C. Robisson-Cohen:** None. **J.E. Huffman:** None. **Y.V. Sun:** None. **K. Chang:** None. **D.R. Miller:** None. **K. Cho:** None. **T. Edwards:** None. **C. O'Donnell:** None. **P.S. Tsao:** None. **P.W.F. Wilson:** None. **S. Kathiresan:** None. **D.J. Rader:** None. **A.M. Hung:** None. **S.M. Damrauer:** None.

25
Anti-Apolipoprotein A-I Antibody Profiles Predict Cardiovascular Disease Outcomes in Patients and in a Mouse Model of Atherosclerosis

Robert H. Kline IV, David Henson, **Vincent J Venditto**, Univ of Kentucky, Lexington, KY

Apolipoprotein A-I (ApoA-I) is the target of antibody induction in patients suffering from chronic inflammation associated with obesity, autoimmunity and cardiovascular disease (CVD). Anti-ApoA-I antibodies are considered serum markers for CVD, but the exact immunologic stimuli and role of these antibodies in disease progression are poorly understood. Our efforts in characterizing the anti-ApoA-I antibody profiles in 375 patients with coronary artery disease resulted in a hazard ratio of 1.52 (95% CI: 1.03-2.18; p = 0.02) when adjusted for 12 traditional markers of cardiovascular disease. We then aimed to recapitulate these findings in mice using an immunostimulatory liposomal formulation decorated with peptides derived from ApoA-I to induce epitope-specific antibody responses in mice. Intriguingly, acute inflammation associated with adjuvant exposure and high fat diet alone induced an anti-ApoA-I antibody response in mice. Immunization shifted the antibody profile to a pro-atherogenic phenotype, which accelerated atherosclerosis as measured by *en face* lesion area. Protective antibody profiles were also observed in mice, which recapitulate the phenotype observed in patients protected from major adverse cardiovascular events. Comparison of mice exhibiting a pro-atherogenic antibody profile with mice exhibiting an anti-inflammatory antibody profile result in lesion areas of 20% and 5% (p = 0.005), respectively. Continued evaluation of the immunologic mechanisms that lead to pro-atherogenic and anti-atherogenic antibody responses and the immunologic sequelae associated with specific antibody profiles will promote novel therapeutic strategies and guide interventions to improve patient outcomes.
R.H. Kline: None. **D. Henson:** None. **V.J. Venditto:** None.

This research has received full or partial funding support from the American Heart Association.

26
Apolipoprotein A-I Helical Registry Modulates Lecithin:cholesterol Acyl Transferase Activity

Allison L Cooke, Jamie C Morris, John T Melchior, Univ of Cincinnati, Cincinnati, OH; W. Gray Jerome, Vanderbilt Univ, Nashville, TN; Scott E Street, Thomas B Thompson, Univ of Cincinnati, Cincinnati, OH; Loren E Smith, Vanderbilt Univ, Nashville, TN; Amy S Shah, Andrew Herr, Cincinnati Children's Hosp Medical Ctr, Cincinnati, OH; Jere P Segrest, Vanderbilt Univ, Nashville, TN; Jay W Heinecke, Univ of Washington, Seattle, WA; W Sean Davidson, Univ of Cincinnati, Cincinnati, OH

The structure of apolipoprotein (APOA1), the major protein of high density lipoproteins (HDL), can modulate protein interactions affecting the cardioprotective functions of HDL particles. APOA1 on nascent discoidal HDL is composed of ten, tandem, α-helical repeats arranged in an anti-parallel, stacked ring-structure that encapsulates a lipid bilayer. Previous chemical cross-linking studies suggested that these APOA1 rings may adopt two different orientations, or registries, with respect to each other. These orientations include one where the bulk of APOA1 orients with the 5th helix of one molecule opposing the 5th helix of the other (5/5 helical registry), and another orientation adopting a 5/2 helical registry. Engineered HDL particles locked in both 5/5 and 5/2 registries, or rotamers, equally promoted cholesterol efflux from macrophages, indicating functional particles. However, the ability of lecithin:cholesterol acyl transferase (LCAT) to esterify cholesterol was increased over WT in the 5/5 rotamer, and dramatically impaired in the 5/2 rotamer (*p<0.001*), despite surface plasmon resonance studies showing that LCAT bound equally to both. Cross-linking experiments indicated that LCAT activity requires a hybrid epitope composed of helices 5-7 on one APOA1 molecule and 3-4 on the other. Thus, the reciprocating nature of APOA1's structure may represent a thumbwheel mechanism that influences the activity of HDL remodeling factors in plasma.
A.L. Cooke: None. **J.C. Morris:** None. **J.T. Melchior:** None. **W.G. Jerome:** None. **S.E. Street:** None. **T.B. Thompson:** None. **L.E. Smith:** None. **A.S. Shah:** None. **A. Herr:** None. **J.P. Segrest:** None. **J.W. Heinecke:** None. **W.S. Davidson:** None.

This research has received full or partial funding support from the American Heart Association.

27

A Micropeptide Concealed in a Putative Long Non-coding RNA Directs Inflammation

Coen van Solingen, Monika Sharma, New York Univ Langone Health, New York, NY; Roel Bijkerk, Leiden Univ Medical Ctr, Leiden, Netherlands; Milessa S Afonso, Graeme J Koelwyn, Kaitlyn R. Scacalossi, New York Univ Langone Health, New York, NY; Anton Jan van Zonneveld, Leiden Univ Medical Ctr, Leiden, Netherlands; Kathryn J Moore, New York Univ Langone Health, New York, NY

Long non-coding RNAs (lncRNAs), once considered 'genomic junk', have been found to regulate diverse biological processes and their study continues to reveal novel insights into lncRNA functions. Recent studies revealed that some lncRNAs may harbor small open reading frames (ORFs) that code for functional micropeptides. While investigating an unannotated primate-specific lncRNA, lncVLDLR, that is altered in patients with type II diabetes and cardiovascular disease, we discovered a previously unrecognized ORF encoding a 44 amino acid micropeptide. *In vitro* transcription and translation of the IMP coding sequence in the presence of ^{35}S-methionine produced a single 8 kDa peptide, which we have named Inflammation-modulating MicroPeptide (IMP). To dissect IMP function, we focused on its amino acid sequence and putative structure. These analyses revealed high sequence homology between IMP and transcription factors such as NFκB, c-myb and zinc finger proteins, and the presence of a hydrophobic region with an LxxLL motif often found in transcriptional regulators. Circular dichroism spectroscopy of synthesized IMP predicted an intrinsically disordered peptide, which is a common characteristic of transcriptional coactivators. To investigate a potential role of IMP in regulating gene transcription, we cloned a MYC-epitope tag in-frame with IMP within the full-length transcript of lncVLDLR and expressed it in HEK293 cells. Immunofluorescence staining, and cell fractionation combined with western blotting, confirmed nuclear localization of IMP. RNA-seq analysis of THP1 macrophages overexpressing IMP revealed an increase in inflammatory genes, including cytokines and chemokines. Moreover, analysis of upstream regulators of these genes suggests that IMP may interact with KIX domain-containing transcriptional coactivators to regulate inflammatory gene expression. Together our data identify a novel human micropeptide, encoded within a putative lncRNA that is dysregulated in diabetes and cardiovascular disease, that regulates inflammatory gene transcription. Further characterization of IMP and its regulatory network may uncover novel opportunities for therapeutic intervention in cardiovascular and other inflammatory diseases.

C. van Solingen: None. **M. Sharma:** None. **R. Bijkerk:** None. **M.S. Afonso:** None. **G.J. Koelwyn:** None. **K.R. Scacalossi:** None. **A. van Zonneveld:** None. **K.J. Moore:** None.

28

Neutrophils Aged Under Oxidative Stress Impede Vascular Repair

Derick Okwan-Duodu, Wenxue Liu, Kai xu, Eric Shin, Raymundo A Quintana, Giji Joseph, Laura Hansen, Hassan Sellak, Rebecca Levit, David Archer, W Robert Taylor, Emory Univ, Atlanta, GA

Objectives: The link between chronic inflammation and poor cardiovascular outcomes has long been appreciated, but the regulation of immune cellular targets to improve cardiovascular health remains a challenge. Mounting evidence suggests that neutrophils, previously considered acute first responder cells, play critical role in chronic inflammation. Following systemic surveillance of tissues, patrolling neutrophils age in the circulation and traffic to the bone marrow, where they undergo macrophage-mediated clearance. Here, we assessed how chronic inflammation and oxidative stress modify neutrophil trafficking and function during ischemia. **Methods**: Neutrophils from the Townes humanized sickle cell (SS) mice - surrogate for chronic inflammation and oxidative stress - were compared to neutrophils from MerTK deficient mice (MerKO), which age in the circulation owing to defective efferocytosis. Hind limb ischemia (HLI) was used as model of vascular injury. LASER Doppler perfusion imaging (LDPI) measured perfusion recovery after HLI. **Results:** The proportion of $CXCR4^{Hi}CD62L^{lo}$ aged neutrophils in circulation was markedly elevated in the SS (34 ± 4%) and MerKO mice (38 ± 4%) when compared to wild-type mice (7 ± 1.2%). However, in contrast with MerKO neutrophils, aged neutrophils from SS showed impaired phagocytosis, increased capacity to produce reactive oxygen species, and pronounced release of extracellular traps (NETs). In response to HLI, neutrophils accumulated in the MerKO and SS mice, but perfusion recovery on LDPI was only impaired in the SS mice, suggesting differential role of neutrophils aged by oxidative stress. Importantly, the phenotype of SS mice was reversed by treatment with the anti-oxidant N-acetyl cysteine (NAC), which had no impact on perfusion recovery in MerKO mice. **Conclusion**: Although SS and MerKO mice demonstrated elevated numbers of aged neutrophils, our data suggest that chronic inflammation and oxidative stress modifies the function of aged $CXCR4^{Hi}CD62L^{lo}$ neutrophils to impede vascular repair after ischemia. This specialized subset of neutrophils may be targeted to improve vascular health without compromising overall anti-microbial host defenses

D. Okwan-Duodu: None. **W. Liu:** None. **K. xu:** None. **E. Shin:** None. **R.A. Quintana:** None. **G. Joseph:** None. **L. Hansen:** None. **H. Sellak:** None. **R. Levit:** None. **D. Archer:** None. **W. Taylor:** None.

This research has received full or partial funding support from the American Heart Association.

29

Interleukin-35 Suppresses Endothelial Activation by Inhibiting Mitochondrial Reactive Oxygen Species Mediated Site-specific Acetylation of Histone 3 Lysine 14

Xinyuan Li, Ying Shao, Xiaojin Sha, Pu Fang, Lewis Katz Sch of Med, Philadelphia, PA; Yin-Ming Kuo, Andrew J. Andrews, Fox Chase Cancer Ctr, Temple Univ Health System, Philadelphia, PA; Ya-feng Li, William Y. Yang, Lewis Katz Sch of Med, Philadelphia, PA; Massimo Maddaloni, David W. Pascual, Univ of Florida, Gainesville, FL; Jin J. Luo, Xiaohua Jiang, Hong Wang, **Xiao-feng Yang**, Lewis Katz Sch of Med, Philadelphia, PA

Recently we reported that IL-35 is an inflammation-induced ant-inflammatory cytokine; thus, function as a HAMP (homeostasis associated molecular patterns). However, whether IL-35 affects endothelial cell activation and subsequent development of atherosclerosis is not known. Hence, we studied the expression of IL-35 during early atherosclerosis; and its roles and mechanisms in suppressing EC activation. Initially, we analyzed whether endogenous IL-35 levels and its receptor expression was increased in early atherosclerosis. Our data revealed that IL-35 level was significantly increased in the plasma of hyperlipidemic patients and apolipoprotein E (ApoE-/-) deficient mice. Further, the expression of IL-35 receptor components were increased in ApoE-/- mouse aortas. IL-35 inhibited monocyte recruitment on to human aortic endothelial cells (EC) activated by pro-atherogenic lysophosphatidylcholine (LPC). Furthermore, our RNA-Seq analysis showed that IL-35 selectively inhibited ICAM-1 expression that mediates EC activation. Further analysis by flowcytometry and electron spin resonance analysis revealed that IL-35 blocked LPC-mediated mitochondrial-reactive oxygen species (mtROS) production. The subsequent mass spectrometry, ChIP-Seq analysis and EMSA showed that LPC-mediated mtROS promotes acetylation of histone 3 lysine 14 (H3K14). Acetylation of histones facilitate the

transcription of EC activation-related genes. We found that acetylated H3K14 increased the binding of pro-inflammatory transcription factor Ap-1 on to ICAM-1 promoter region and induction of ICAM-1 gene transcription. IL-35 mediated Inhibition of mtROS attenuated H3K14 acetylation, inhibited AP-1 binding to ICAM-1 promoter and suppressed ICAM-1 transcription. Finally, IL-35 cytokine treatment inhibited the progression and development of atherosclerosis in ApoE-/- mice. Our study concluded that IL-35 is induced during atherosclerosis and plays an anti-atherogenic role by suppressing EC activation through mtROS and H3K14 acetylation dependent mechanism.

X. Li: None. **Y. Shao:** None. **X. Sha:** None. **P. Fang:** None. **Y. Kuo:** None. **A.J. Andrews:** None. **Y. Li:** None. **W.Y. Yang:** None. **M. Maddaloni:** None. **D.W. Pascual:** None. **J.J. Luo:** None. **X. Jiang:** None. **H. Wang:** None. **X. Yang:** None.

30

IL-17A Induces Vascular Dysfunction via Downregulation of eNOS Expression

Rebecca Schueler, Susanne Karbach, Katrin Schaefer, Sabine Kossmann, Matthias Oelze, Venkata Garlapati, Juak Huppert, Andrew Croxford, Andreas Daiber, Thomas Muenzel, Ari Waisman, Philip Wenzel, Univ Medical Ctr Mainz, Mainz, Germany

Introduction: Interleukin-17A is important in the development of vascular dysfunction. However, the mechanism behind is still not completely understood. The aim of our study was to investigate if IL-17A overexpression in T cells induces vascular dysfunction mainly via inflammatory cell recruitment to the vessel wall or if there are other mechanisms behind. **Methods:** We used a mouse model of T cell specific IL-17A overexpression (CD4-IL-17A$^{ind/+}$ mice) and a model of ubiquitous IL-17 receptor A knockout (IL-17RA^{del} mice). Vascular dysfunction was induced via Angiotensin-II (Ang-II, 1mg/kg/day, 1 week). Aortic relaxation was determined using isometric tension studies. Blood pressure measurements were performed with tail-cuff method and ROS/RNS detection in whole blood was accomplished using L-012 ECL. Flow cytometric and histological analysis of aorta and perivascular adipose tissue (PVAT) were performed. Aortic NO$^{\bullet}$ formation was detected by electron paramagnetic resonance spectroscopy (EPR). **Results:** The continuous overexpression of IL-17A in T cells indeed led to the development of vascular dysfunction accompanied by increased ROS/RNS formation under Angiotensin-II treatment compared to wildtype mice. These results go in line with an elevated blood pressure and a reduction of the left-ventricular ejection fraction in CD4-IL-17A$^{ind/+}$ mice. Although IL-17A plays an important role in neutrophil recruitment, chronic T cell specific overexpression of IL-17A did not lead to strongly elevated myeloid cells in the aortic vessel wall. Interestingly, IL-17A overexpression reduced NO$^{\bullet}$ formation in aortas and decreased eNOS expression in PVAT. In contrast, the attenuation of IL-17A signaling in IL-17RA^{del} mice significantly reduced the development of Ang-II induced vascular dysfunction as well as Ang-II induced aortic inflammation and peripheral ROS/RNS formation. **Conclusions:** Blockade of IL-17A signaling in IL-17RA^{del} mice partially protects from Ang-II induced vascular dysfunction and inflammation. IL-17A overexpression in T cells led to vascular dysfunction. This was independent from inflammatory cell infiltration to the aortic vessel wall and associated with a reduction of NO-release and a down-regulation of eNOS expression PVAT.

R. Schueler: None. **S. Karbach:** None. **K. Schaefer:** None. **S. Kossmann:** None. **M. Oelze:** None. **V. Garlapati:** None. **J. Huppert:** None. **A. Croxford:** None. **A. Daiber:** None. **T. Muenzel:** None. **A. Waisman:** None. **P. Wenzel:** None.

31

A Ligand-specific Blockade of the Integrin Mac-1 Selectively Targets Pathologic Vascular Inflammation While Maintaining Protective Host-defense

Dennis Wolf, Nathaly Anto Michel, Univ Heart Ctr Freiburg, Freiburg, Germany; Konrad Buscher, Klaus Ley, La Jolla Inst, La Jolla, CA; Peter Libby, Harvard Medical Sch, Boston, MA; Christoph Bode, Univ Heart Ctr Freiburg, Freiburg, Germany; Karlheinz Peter, Baker Heart Inst, Melbourne, Australia; Andreas Zirlik, Univ Heart Ctr Freiburg, Freiburg, Germany

Background: Integrins, such as Mac-1 (alphaMbeta2, CD11b/CD18), drive myeloid cell recruitment and inflammation in cardiovascular disease. Although integrins have generated interest as therapeutic targets in acute and chronic inflammation, they also contribute to host defense, regeneration, and haemostasis. To overcome these limitations, we have designed a novel antibody that targets a distinct region within the Mac-1 major ligand-binding (I-) domain required for binding of its ligand CD40L. Here, we describe the consequences of a ligand-specific inhibition and its efficacy in mice.
Methods and Results: To generate an antibody specifically targeting the interaction of Mac-1 with CD40L, mice were immunized with a peptide containing the CD40L-binding motif EQLKKSKTL. Antibody clones were screened and tested for specificity. One clone, termed anti-M7, showed specific peptide binding and blocked the binding of the activated, open conformation of Mac-1 to CD40L, but not to alternative Mac-1 ligands suggesting ligand specificity. Anti-M7 highly effectively limited leukocyte recruitment in vitro and to the mesentery and the omentum in intravital confocal microscopy. While conventional anti-Mac-1 antibodies induced outside-in activation of the integrin, anti-M7 did not provoke MAP-kinase dependent activation and expression of inflammatory cytokines in macrophages. Following cecal-ligation and puncture (CLP) sepsis in mice, a conventional anti-Mac-1 antibody inhibited leukocyte accumulation, but potentiated bacteremia and limited overall survival. In contrast, anti-M7 limited peritoneal leukocyte accumulation, reduced bacterial titers, and improved survival during CLP.
Conclusion: We present proof-of-concept demonstrating selective inhibition of the interaction between the leukocyte integrin Mac-1 and CD40L by a novel monoclonal antibody. This antibody shows several advantages over conventional anti-integrin therapy, and prevented inflammation and sepsis-related mortality in mice. This novel approach gives new insight into ligand-specific integrin pathways and merits further evaluation as a selective anti-inflammatory therapy in cardiovascular disease.

D. Wolf: None. **N. Anto Michel:** None. **K. Buscher:** None. **K. Ley:** None. **P. Libby:** None. **C. Bode:** None. **K. Peter:** None. **A. Zirlik:** None.

32

Somatic Editing of *Ldlr* with AAV-CRISPR for Atherosclerosis Studies

Kelsey E Jarrett, Alexandria M Doerfler, Ayrea Hurley, Rachel H Hsu, Marco De Giorgi, Baylor Coll Med, Houston, TX; Ang Li, Rice Univ, Houston, TX; Henry J Pownall, Houston Methodist Res Inst, Houston, TX; Ciaran Lee, Gang Bao, Rice Univ, Houston, TX; **William R Lagor**, Baylor Coll Med, Houston, TX

Background: Current methods to study genetic contributions to atherosclerosis are time-consuming and expensive. The *Ldlr* and *Apoe* knockout (KO) models are currently the gold-standard, but require extensive backcrossing to homozygosity and congenic status on the C57BL6/J background. More rapid and efficient methods are needed to investigate the ever-growing list of candidate genes identified through human genetics.The Clustered Regularly-Interspaced Short Palindromic Repeats/Cas9 (CRISPR/Cas9) genome editing system is a powerful new

tool for gene disruption. **Hypothesis:** Liver-directed somatic disruption of *Ldlr* using an all-in-one AAV-CRISPR vector can generate atherosclerotic lesions in adult mice, thereby avoiding the need to cross to *Ldlr* KO mice. **Methods:** An Adeno-Associated Viral (AAV) vector based on serotype 8 was used to deliver *Staphylococcus aureus* Cas9 (SaCas9) and small guide RNA (gRNA) targeting the *Ldlr* gene (AAV-CRISPR). This vector was compared head-to-head with AAV-mediated overexpression of a human gain-of-function variant of *PCSK9*, a recent model that mimics *Ldlr* KO through promoting degradation of the Ldlr protein. Adult C57BL6/J mice received either: *1)* saline, *2)* AAV-CRISPR, or *3)* AAV-hPCSK9, versus *4)* germline *Ldlr* KO mice. Animals were placed on a Western diet for twenty weeks and followed for changes in plasma lipids, atherosclerotic lesion burden, and editing efficiency. **Results and Conclusion:** Disruption of *Ldlr* with AAV-CRISPR vector was robust, resulting in severe hypercholesterolemia and atherosclerosis on a standard western diet. AAV-hPCSK9 also produced atherosclerotic lesions as expected from previous reports. Lesion burden was slightly lower with AAV-CRISPR and AAV-hPCSK9 relative to germline *Ldlr* KO mice. Unexpected sexual dimorphism was also observed with AAV-CRISPR, with the greatest effects seen in male mice. In summary, our all-in-one AAV-CRISPR vector is a rapid and efficient alternative to the use of *Ldlr* KO mice to study atherosclerosis.
K.E. Jarrett: None. **A.M. Doerfler:** None. **A. Hurley:** None. **R.H. Hsu:** None. **M. De Giorgi:** None. **A. Li:** None. **H.J. Pownall:** None. **C. Lee:** None. **G. Bao:** None. **W.R. Lagor:** None.

This research has received full or partial funding support from the American Heart Association.

33
Differential Effects of Proprotein Convertase Subtilisin/Kexin Type 9 (PCSK9) Production and Function on Microsomal Triglyceride Transfer Protein
Cecilia Huang, Joshua Miles, Hagai Tavori, Oregon Health and Science Univ, Portland, OR; Peter P Toth, Peter P Toth, CGH Medical Ctr, Sterling, IL; Sergio Fazio, Oregon Health and Science Univ, Portland, OR

Proprotein convertase subtilisin/kexin type 9 (PCSK9) is a circulating protein that plays a key role in the regulation of plasma low-density lipoprotein (LDL) cholesterol levels. PCSK9 binding to the LDL receptor (LDLR) leads to receptor-mediated endocytosis and lysosomal degradation of LDLR. Prior studies have shown that PCSK9 increases production of triglyceride-rich apoB-lipoproteins via up-regulation of lipogenic genes, and that PCSK9 inhibition reduces plasma triglyceride levels. However, the effect of PCSK9 inhibition on hepatic lipogenic genes expression remain unclear.
Using a human hepatocellular carcinoma cell line (HepG2) we show that overexpression of PCSK9 upregulated the expression of several lipogenic genes, including a 1.5-fold increase in ATP citrate lyase (ACLY), a 1.2-fold increase in Fatty Acid Synthase (FAS), a 1.2-fold increase in HMG-CoA-reductase, and a 1.8-fold increase in microsomal triglyceride transfer protein (MTTP), when compared with untransfected HepG2 cells. Overexpression of a gain-of-function mutant of PCSK9 (PCSK9-D374Y) had stronger effects in the same direction: a 2.3-fold increase in ACLY, a 1.8-fold increase in FAS, a 1.6-fold increase in HMG-CoA-reductase, and a 2.1-fold increase in MTTP. In HepG2 cells overexpressing either normal PCSK9 or PCSK9-D374Y, inhibition of PCSK9 function using a monoclonal antibody blocked PCSK9-mediated degradation of LDLR, and reduced expression of SREBP-dependent genes (ACLY, FAS and HMG-CoA-reductase) to levels of untransfected HepG2 cells. Interestingly, while inhibition of PCSK9 function via monoclonal antibody did not affect MTTP gene expression in these cells, inhibition of PCSK9 production via RNA interference reduced MTTP gene expression by 66%.
We conclude that inhibition of PCSK9 production decreases MTTP gene expression, whereas blockade of PCSK9 function (and cellular re-entry) only decreases SREBP-dependent genes expression, but does not affect MTTP gene expression. This study shows that while PCSK9 exerts an influence on genes related to both lipogenesis and lipoprotein assembly, any inhibition of PCSK9 controls SREPB-dependent genes but only inhibiting PCSK9 production controls MTTP gene expression.
C. Huang: None. **J. Miles:** None. **H. Tavori:** None. **P.P. Toth:** None. **P.P. Toth:** None. **S. Fazio:** None.

34
Leveraging Mouse Liver Co-expression Networks and Human Lipid Gwas Data to Identify Cholesterol Metabolism Genes
Zhonggang Li, Jenny Nguyen, Sabrina Belisle, Sophia Ly, Fernanda Leyva Jaimes, **Brian W Parks**, Univ of Wisconsin-Madison, Madison, WI

Genetic factors play an important role in contributing to variation in plasma lipid levels across the human population. Large genome-wide association studies (GWAS) in humans have identified more than 100 loci significantly associated with plasma levels of low-density lipoprotein (LDL) cholesterol, high-density lipoprotein (HDL) cholesterol, total cholesterol (TC), and triglycerides. To prioritize genes that are involved in cholesterol metabolism, we developed a systematic approach to leverage genome-wide liver transcriptomic and proteomic data from multiple mouse reference populations along with human lipid GWAS data. We constructed global co-expression networks from twelve distinct mouse liver datasets, encompassing more than 800 unique mice and identified a conserved module of genes highly enriched for cholesterol biosynthesis. Based on replication across datasets and presence in transcript and protein, we prioritized 112 unique genes. Intersection of these 112 prioritized genes with human GWAS data for LDL, HDL, TC, and triglycerides identified 54 genes to be within 100 kilobases of a significant or suggestive significant single nucleotide polymorphism (SNP). Out of the 54 identified genes that overlap with human GWAS data, 29 have well documented biological roles in cholesterol metabolism, such as *LDLR*, *PCSK9*, and *INSIG1*. With the 25 identified genes with no described role in cholesterol metabolism, we tested for transcriptional regulation to cholesterol and performed a functional screen by siRNA knockdown. From this analysis, we identified twelve genes that show transcriptional regulation to cholesterol levels and nine genes that are able to modulate cholesterol metabolism when targeted *in vitro* with siRNA. Five genes out of the 25 prioritized genes show both transcriptional regulation to cholesterol and ability to modulate cholesterol metabolism in vitro. One of these genes, *Sestrin1*, we validate *in vivo* and *in vitro* as a modulator of cholesterol metabolism. Collectively, through a systematic approach we have identified 25 highly prioritized genes that have no documented role in cholesterol metabolism, five genes are transcriptionally regulated by cholesterol and influence cholesterol metabolism.
Z. Li: None. **J. Nguyen:** None. **S. Belisle:** None. **S. Ly:** None. **F. Leyva Jaimes:** None. **B.W. Parks:** None.

35
Recombinant LCAT Restores Defective HDL mediated Endothelial Protection in Acute Coronary Syndrome
Alice Ossoli, Sara Simonelli, Univ degli Studi di Milano, Milano, Italy; Marisa Varrenti, Nuccia Morici, Fabrizio Oliva, Miriam Stucchi, ASST Grande Ospedale Metropolitano Niguarda, Milano, Italy; Monica Gomaraschi, Lorenzo Arnaboldi, Alberto Corsini, Univ degli Studi di Milano, Milano, Italy; Michael Thomas, Medical Coll of Wisconsin, Milwaukee, WI; Sotirios Karathanasis, MedImmune, Gaithersburg, MD; Fabrizio Veglia, Monzino Cardiologic Inst,

Milano, Italy; Laura Calabresi, Univ degli Studi di Milano, Milano, Italy

Recent evidence suggests that the vasoprotective effects of HDL are impaired in patients during an acute coronary syndrome (ACS). In particular, HDL from ACS patients are defective in promoting nitric oxide (NO) release from cultured endothelial cells (ECs). Lecithin:cholesterol acyltransferase (LCAT) plays a key role in HDL maturation and remodeling, and it is the enzyme responsible for cholesterol esterification in plasma. Very few studies have suggested that LCAT activity is decreased during an acute myocardial infarction, but the possible link between LCAT mass/activity and the HDL dysfunction observed in ACS has never been tested. To test this hypothesis, plasma from 30 STEMI patients was collected at admission, 48 and 72 hours and 30 days after event. LCAT concentration and activity significantly decreased 48 hours after event (-0.49±0.11 µg/ml, P<0.001, and -3.15±1.05 nmol/ml/h, P=0.006) and remained reduced at 72 hours. HDL isolated from STEMI patients lose the capacity to promote NO production in ECs (-0.13 ± 0.06 fold, P=0.04) and the reduction is significantly correlated to decreased LCAT activity (R= 0.52, P=0.003). *In vitro* studies were performed in which STEMI patients' plasma was added with rhLCAT and HDL vasoprotective activity assessed by measuring NO production in ECs. *In vitro* incubation of STEMI patients' plasma with rhLCAT remodels phospholipids and protein content in HDL and restores HDL ability to promote endothelial NO production (+25%, P=0.03). Impairment of cholesterol esterification may be a major factor in the HDL dysfunction observed during ACS. rhLCAT is able to restore HDL-mediated NO production in vitro, suggesting LCAT as potential therapeutic target for restoring HDL functionality in ACS.

A. Ossoli: None. **S. Simonelli:** None. **M. Varrenti:** None. **N. Morici:** None. **F. Oliva:** None. **M. Stucchi:** None. **M. Gomaraschi:** None. **L. Arnaboldi:** None. **A. Corsini:** None. **M. Thomas:** None. **S. Karathanasis:** Employment; Significant; MedImmune. **F. Veglia:** None. **L. Calabresi:** Research Grant; Significant; MedImmune.

36

Functionalized Nanoparticle Based "Two-pronged" Approach to Attenuate/regress Atherosclerosis by Simultaneous Knock Down OfSR-A and LXR-mediated Stimulation of Macrophage Cholesterol Efflux

Hongliang He, Jing Wang, Virginia Commonwealth Univ, Richmond, VA; Paul Yannie, Hunter McGuire VA Medical Ctr, Richmond, VA; Hu Yang, Shobha Ghosh, Virginia Commonwealth Univ, Richmond, VA

Imbalance between lipoprotein uptake and cholesterol efflux from macrophages underlies the formation of foam cells and development of fatty streaks, a process that starts early in life. While currently available lipid lowering interventions attenuate the progression of atherosclerotic plaques, no targeted therapy is presently available for reduction of existing plaques, a process dependent not only on limiting further accumulation of cholesterol but also on stimulation of cholesterol efflux. We earlier reported the development of a mannose functionalized dendrimeric nanoparticles (mDNP)-based platform for targeted delivery of therapeutics to arterial plaque associated macrophages. In this study, we used the optimized mDNP platform to simultaneously deliver SR-A siRNA (to knock down SR-A and limit modified LDL uptake) and LXR ligand (LXR-L, to stimulate macrophage cholesterol efflux by inducing expression of ABCA1/G1) - a "***Two Pronged***" approach. Compared to non-specific NS-siRNA, mDNP mediated delivery of SR-A siRNA led to significant reduction in expression of SR-A (A&B) with a corresponding decrease in uptake of DiI-labeled oxLDL (C). Delivery of LXR-L increased expression of ABCA1/G1 (D) as well as cholesterol efflux (E) and simultaneous delivery of SR-A siRNA did not alter these LXR-L effects. However, combined delivery of siRNA and LXR-L led to significantly higher decrease in macrophage cholesterol content compared to either treatment alone (F). Administration of this *in vitro* optimized formulation of mDNP complexed with SR-A siRNA and LXR-L to atherosclerotic LDLR-/- mice fed western diet (TD88137) led to a dramatic reduction in lesion area compared to single treatment alone (G). In conclusion, targeted delivery of multiple therapeutics using mDNP platform represents a novel strategy to not only reduce lesion size but it can also be used to simultaneously alter many lesion characteristics such as reducing inflammation or enhancing efferocytosis.

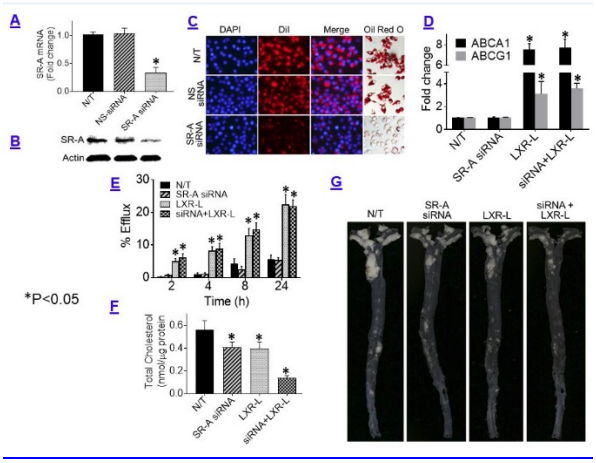

H. He: None. **J. Wang:** None. **P. Yannie:** None. **H. Yang:** None. **S. Ghosh:** None.

This research has received full or partial funding support from the American Heart Association.

37

Coagulation Factor XII Promotes Platelet Consumption in the Presence of Microbial Polyphosphate Under Shear Flow

Jevgenia Zilberman-Rudenko, Oregon Health & Science Univ, portland, OR; Stephanie E Reitsma, Oregon Health & Science Universit, Portland, OR; Cristina Puy, Oregon Health & Science Univ, Portland, OR; Stephanie A Smith, Univ of Michigan Medical Sch, Ann Arbor, MI; Chantal P Wiesenekker, Erik I Tucker, Oregon Health & Science Univ, Portland, OR; Richard J Travers, Univ of Michigan Medical Sch, Ann Arbor, MI; Coen Maas, Rolf T Urbanus, Univ Medical Ctr Utrecht, Utrecht, Netherlands; David Gailani, Vanderbilt Univ Sch of Med, Nashville, TN; Alvin H Schmaier, Case Western Reserve Univ, Cleveland, OH; Florea Lupu, Oklahoma Medical Res Fndn, Oklahoma City, OK; James H Morrissey, Univ of Michigan Medical Sch, Ann Arbor, MI; Andras Gruber, Owen J McCarty, Oregon Health & Science Univ, Portland, OR

Background: Terminal complications of bacterial sepsis include development of disseminated intravascular consumptive coagulopathy. Bacterial constituents, including long-chain polyphosphates (polyP), have been shown to activate the contact pathway of coagulation in plasma. Recent work shows that activation of the contact pathway in flowing whole blood can promote thrombin generation and platelet activation and consumption distal to thrombus formation *ex vivo* and *in vivo*.
Aim: Determine whether presence of long-chain polyP in the bloodstream promotes platelet activation and consumption in a coagulation factor (F)XII-dependent manner.
Methods/Results: The addition of long-chain polyP to human whole blood promoted platelet P-selectin expression, microaggregate formation and platelet consumption in the bloodstream under shear in a FXII-dependent manner. Moreover, long-chain polyP accelerated thrombus formation on immobilized collagen surfaces under shear flow in a thrombin generation-dependent manner. Distal to the site of thrombus formation, platelet consumption was dramatically

enhanced in the presence of long-chain polyP in the bloodstream. Inhibiting contact activation of coagulation using established and novel agents reduced fibrin formation on collagen as well as platelet consumption in the bloodstream distal to the site of thrombus formation. *In vivo*, FXII deficiency was protective against long-chain polyP occlusive lung thrombus formation in mice. Lastly, in a non-human primate model of sepsis, pretreatment of animals with an antibody blocking FXI activation by FXIIa (14E11) diminished LD_{100} *S. aureus*-induced platelet and fibrinogen consumption.
Conclusions: This study demonstrates that bacterial-type long-chain polyP promotes FXII-mediated thrombin generation and platelet activation in the flowing blood and could contribute to sepsis-associated thrombotic processes, consumptive coagulopathy and thrombocytopenia.
J. Zilberman-Rudenko: None. **S.E. Reitsma:** None. **C. Puy:** None. **S.A. Smith:** None. **C.P. Wiesenekker:** None. **E.I. Tucker:** None. **R.J. Travers:** None. **C. Maas:** None. **R.T. Urbanus:** None. **D. Gailani:** None. **A.H. Schmaier:** None. **F. Lupu:** None. **J.H. Morrissey:** None. **A. Gruber:** None. **O.J.T. McCarty:** None.

This research has received full or partial funding support from the American Heart Association.

38
Inflammasome Activation Triggers Blood Coagulation Through Pyroptosis
Congqing Wu, Yinan Wei, Zhenyu Li, Univ of Kentucky, Lexington, KY

Background Disseminated intravascular coagulation (DIC) is a frequent and fatal complication of sepsis. The presence of bacterial virulence factors can induce blood coagulation, yet the molecular events linking bacteria sensing to initiation of the coagulation cascade remain largely unknown. Inflammasome is the large sensory protein complex in the cytosol that alerts host to bacterial infection. The role of inflammasome in sepsis remains unclear.
Methods and Results We used *E. coli* type III secretion system (T3SS) inner rod protein EprJ and LPS to investigate the role of canonical and noncanonical inflammasome activation in sepsis, respectively. For efficient cytosolic delivery, EprJ was fused to the cytosolic translocation domain of anthrax lethal factor (LFn). Binding with LFn, anthrax protein protective agent (PA) delivers the LFn-EprJ fusion protein into the cytoplasma through receptor-mediated endocytosis. We found that EprJ, the inner rod protein, activated caspase-1 and induced systemic coagulation, while lipopolysaccharide (LPS) produced similar effects via caspase-11 activation. We also identified gasdermin D (Gsdmd) driven macrophage pyroptosis as a mechanism for the release of tissue factor, an essential initiator of coagulation cascades. Genetic deficiency of Gsdmd abolishes inflammasome-mediated coagulation.
Conclusion Inflammasome activation is a trigger for coagulation induced by Gram-negative bacterial products, connecting inflammation and thrombosis.
C. Wu: None. **Y. Wei:** None. **Z. Li:** None.

This research has received full or partial funding support from the American Heart Association.

39
A Small Fragment Derived from von Willebrand Factor Improves Survival in a Mouse Model of Endotoxemia-Induced Disseminated Intravascular Coagulation
Christian Valladolid, Sonya Cirlos, Marina Martinez-Vargas, Bobby Guillory, Miguel A. Cruz, Baylor Coll of Med, Houston, TX

Introduction: Disseminated intravascular coagulation (DIC) is a life-threatening condition that results in wide-spread clot formation and organ failure. Sepsis-induced DIC is associated with a high mortality rate, prompting the need for an effective therapeutic intervention. Our lab has identified the A2 domain of the von Willebrand factor (VWF) protein as a potent treatment for sepsis-induced DIC. Historically, VWF has only been described as a contributor of clot formation; however, our lab has demonstrated that purified recombinant full length A2 domain of the VWF protein can dampen fibrin-rich microthrombi formation in mice with endotoxin. The mode of action appears to be via the interaction with the cell-surface expressed vimentin on endothelium, inhibiting VWF strings formation and thus, platelet adhesion.
Goal: Since the VWF protein is naturally cleaved in circulation by the enzyme ADAMTS-13 via the A2 domain, one can argue whether the beneficial effect observed with full len gth A2 domain is terminated by the cleavage of ADAMTS-13. We produced recombinant proteins encompassing the sequences of the two proteolytic products of the A2 domain; the A2Nt and A2Ct proteins. I will identify which fragment retains the mode of action of the full length A2 domain in a mouse model of endotoxin-induced DIC.
Methods: The recombinant A2 and vimentin proteins were produced using the bacterial expression system. Protein: protein interactions were determined by optical interferometry. The endotoxin-induced DIC model was achieved by injecting C57B/6 mice with lipopolysaccharide (LPS). Treatment with A2 or its fragments was started approximately 2 hours after LPS insult.
Results: The A2N t protein has a higher affinity for vimentin than the A2Ct. Treatment of A2Nt in a LPS-induced DIC mouse model was effective in maintaining survival in males, a comparable finding that mimics treatment of mice with full-length recombinant A2. Interestingly, A2Nt showed less survival than full length A2 in females. These findings highlight the potential differences in therapy responses between genders, an occurrence that some studies have described to also occur in humans.
C. Valladolid: None. **S. Cirlos:** None. **M. Martinez-Vargas:** None. **B. Guillory:** None. **M.A. Cruz:** None.

40
Accelerated Atherosclerosis and Thrombosis in Jak2v617f Mice
Wei Wang, Columbia Univ, New York, NY; Wenli Liu, Tianjin Medical Univ, Tianjin, China; Ying Wang, Yang Tang, Columbia Univ, New York, NY; Brittany Woods, Memorial Sloan Kettering Cancer Ctr, New York, NY; Carrie Welch, Bishuang Cai, Columbia Univ, New York, NY; Ding Ai, Tianjin Medical Univ, Tianjin, China; Yong-Guang Yang, Columbia Univ, New York, NY; Carlos Silvestre, Oliver Soehnlein, Ludwig Maximilian Univ of Munich, Munich, Germany; Ira Tabas, Columbia Univ, New York, NY; Ross L. Levine, Memorial Sloan Kettering Cancer Ctr, New York, NY; Alan R. Tall, **Nan Wang**, Columbia Univ, New York, NY

The mechanisms driving increased athero-thrombotic risk in individuals with JAK2V617F positive clonal hematopoiesis or myeloproliferative neoplasms are poorly understood. This study was to assess atherosclerosis and thrombosis and associated mechanisms in hypercholesterolemic mice with hematopoietic JAK2V617F expression.
Irradiated *Ldlr*$^{-/-}$ mice were transplanted with bone marrow from WT or JAK2V617F mice and fed a high fat high cholesterol diet (WD). After 7 weeks of WD *JAK2V617F* mice showed increased hematopoiesis, platelet activation, accelerated thrombosis and increased atherosclerosis. Early atherosclerotic lesions showed increased neutrophils, correlating with lesion size and in association with increased rolling and adhesion of neutrophils on endothelial cells in carotid artery. After 12 weeks of WD JAK2V617F lesions were slightly larger than controls but showed additional complexity, with increased necrotic core area, prominent iron deposition and co-staining of erythrocytes and macrophages suggesting erythrophagocytosis. JAK2V617F erythrocytes were more susceptible to phagocytosis by WT macrophages

and showed decreased surface expression of CD47, a “don’t eat me” signal. Human JAK2V617F erythrocytes were also more susceptible to erythrophagocytosis. JAK2V617F macrophages displayed increased expression of pro-inflammatory cytokines and chemokines, increased p38 map kinase signaling and increased cleavage and reduced levels of MerTK, a key molecule mediating phagocytosis of apoptotic cells (efferocytosis) in atherosclerotic lesions. Erythrophagocytosis also suppressed efferocytosis. As a result, JAK2V617F lesional efferocytosis was reduced in advanced lesions.
In conclusion, JAK2V617F promotes early lesion formation, arterial thrombosis and increased complexity in advanced atherosclerosis. In addition to increasing hematopoiesis and neutrophil infiltration in early lesions, JAK2V617F caused cellular defects in erythrocytes and macrophages, leading to increased erythrophagocytosis but defective efferocytosis. These changes appear to promote accumulation of iron and increased necrotic core formation which, together with exacerbated pro-inflammatory responses, may contribute to plaque instability.
W. Wang: None. **W. Liu:** None. **Y. Wang:** None. **Y. Tang:** None. **B. Woods:** None. **C. Welch:** None. **B. Cai:** None. **D. Ai:** None. **Y. Yang:** None. **C. Silvestre:** None. **O. Soehnlein:** None. **I. Tabas:** None. **R.L. Levine:** None. **A.R. Tall:** None. **N. Wang:** None.

41
Neutrophil Extracellular Traps Enhance Venous Thrombosis in Mice Bearing Human Pancreatic Tumors
Yohei Hisada, Reaves Houston, Anaum Maqsood, Univ of North Carolina at Chapel Hill, Chapel Hill, NC; Charlotte Thalin, Karolinska Instt, Stockholm, Sweden; Denis F Noubouossie, Univ of North Carolina at Chapel Hill, Chapel Hill, NC; Hakan Wallen, Karolinska Instt, Stockholm, Sweden; Krasimir Kolev, Semmelweis Univ, Budapest, Hungary; Brian C Cooley, Nigel S Key, Nigel Mackman, Univ of North Carolina at Chapel Hill, Chapel Hill, NC

Introduction: Cancer patients have an increased risk of venous thromboembolism (VTE) compared with healthy individuals. Pancreatic cancer has one of the highest rates of VTE. We are interested in elucidating the pathways that contribute to cancer-associated thrombosis (CAT) particularly in pancreatic cancer. A recent study reported an association between plasma levels of citrullinated histone H3, a marker of neutrophil extracellular traps (NETs), and VTE in a population of patients with a variety of cancer-types. Importantly, subgroup analysis showed that increased levels of H3Cit are associate with VTE in patients with pancreatic and lung cancer but not in patients with other types of cancer. We use mouse models to investigate the role of different pathways in CAT.
Aim: To test the hypothesis that NETs enhance thrombosis in mice bearing human pancreatic tumors.
Methods: We recently established a CAT model in which venous thrombosis is induced by infrarenal vena cava (IVC) stasis in nude mice bearing human pancreatic tumors (BxPc-3). **Results:** We found that tumor-bearing mice had increased levels of plasma granulocyte-colony stimulating factor and neutrophilia. In addition, levels of plasma cell-free DNA are increased, which is used as a marker of NET formation. Tumor-bearing mice also had larger thrombi in an IVC stasis model compared with controls. Thrombi from tumor-bearing mice had increased levels of neutrophils and decreased levels of red blood cells compared with thrombi from control mice. Importantly, administration of DNAse I reduced thrombus size in tumor-bearing mice but not in control mice.
Conclusions: Our study indicates that the presence of human pancreatic tumors in mice induces neutrophilia and increases NET formation that enhances venous thrombosis. These results suggest that neutrophils and/or NETs represent new targets to prevent VTE in pancreatic cancer patients.
Y. Hisada: None. **R. Houston:** None. **A. Maqsood:** None. **C. Thalin:** None. **D.F. Noubouossie:** None. **H. Wallen:** None. **K. Kolev:** None. **B.C. Cooley:** None. **N.S. Key:** None. **N. Mackman:** None.

42
Activation of RIP1 Promotes Inflammation in Atherosclerosis and Obesity: a Novel Target for Cardiometabolic Diseases
Denuja Karunakaran, Adam Turner, My Anh Nguyen, Joshua Kandiah, David Smyth, Univ of Ottawa Heart Inst, Ottawa, ON, Canada; Calvin Pan, Univ of California Los Angeles, Los Angeles, CA; Michele Geoffrion, Zachary Lister, Majid Nikpay, Hailey Wyatt, Ella deKemp, Univ of Ottawa Heart Inst, Ottawa, ON, Canada; Richard Lee, Ionis Pharmaceuticals, Carlsbad, CA; Ludovic Boytard, Bhama Ramkhelawon, New York Univ Sch of Med, New York, NY; Mary-Ellen Harper, Univ of Ottawa, Ottawa, ON, Canada; Aldons Lusis, Univ of California Los Angeles, Los Angeles, CA; Ruth McPherson, Katey Rayner, Univ of Ottawa Heart Inst, Ottawa, ON, Canada

Introduction: Chronic activation of the innate immune system drives inflammation and contributes directly to obesity, insulin resistance and atherosclerosis. Previously we showed that pro-inflammatory necroptotic death drives advanced atherosclerosis via activation of RIP3 and MLKL. We sought to determine upstream regulators of necroptosis in atherosclerosis and metabolic disease, and **hypothesized** that RIP1, a key regulatory kinase upstream of NFκB activation, apoptosis and necroptosis, drives macrophage inflammation in cardiometabolic diseases. **Methods:** Two unique RIP1 anti-sense oligonucleotides (ASOs) were used to reduce RIP1 gene expression in 2 mouse models: i) atherosclerotic model [$ApoE^{-/-}$ mice fed a western diet for 8wks] and ii) diet-induced obesity (DIO) model [C57Bl/6 male mice fed a high fat diet for 24 wks]. Mice were given weekly injections of RIP1 ASOs (50 or 100mg/kg) or non-targeting control ASO. **Results:** RIP1 ASO treated $ApoE^{-/-}$ mice had a marked reduction in aortic sinus and *en face* lesions (47.2% or 58.8% decrease relative to control, $p<0.01$) and plasma inflammatory cytokines (IL-1α, IL-17A, $p<0.05$). RIP1 knockdown in macrophages decreased inflammatory gene expression (NFκB, TNFα, IL-1α) and *in vivo* LPS- or diet-induced NFκB activation. In obese mice, RIP1 ASOs strikingly decreased body weight (25% decrease versus control $p<0.001$) and total fat mass (50-65% decrease versus control, $p<0.001$). Further, insulin resistance was improved in RIP1 ASO treated mice (fasted blood glucose: 10.9mM in control versus 8.5±mM in RIP1 ASO, $p<0.001$; GTT and ITT both $p<0.001$). In humans, we identified 8 novel SNPs in strong linkage disequilibrium in or nearby RIP1 gene exon 5. Notably, in a cohort of >1,800 people, individuals carrying the minor allele of these RIP1 SNPs have a 75-89% increase in the risk of developing obesity (adjusted odds ratios: 1.75-1.89, $p<10^{-4}$) and a significant increase in RIP1 mRNA expression in adipose tissue (eQTL association in METSIM cohort, $p=10^{-23}$). Minor allele variation in one of these SNPs disrupts E4BP4, a repressor of RIP1 transcription, promoting increased RIP1 expression in adipose tissue. **Conclusions**: We have identified RIP1 as central a driver of insulin resistance, obesity, and atherosclerosis and demonstrate the potential of RIP1 as a novel therapeutic target.
D. Karunakaran: None. **A. Turner:** None. **M. Nguyen:** None. **J. Kandiah:** None. **D. Smyth:** None. **C. Pan:** None. **M. Geoffrion:** None. **Z. Lister:** None. **M. Nikpay:** None. **H. Wyatt:** None. **E. deKemp:** None. **R. Lee:** Employment; Modest; Ionis Pharmaceuticals Inc. **L. Boytard:** None. **B. Ramkhelawon:** None. **M. Harper:** None. **A. Lusis:** None. **R. McPherson:** None. **K. Rayner:** None.

43
Endothelial Adenosine Kinase Deficiency Ameliorates Diet-induced Insulin Resistance
Jiean Xu, Qiuhua Yang, Xiaoyu Zhang, Peiking Univ, Beijing, China; Zhiping Liu, Augusta Univ, Augusta, GA; Yapeng Cao, Lina Wang, Yaqi Zhou, Xianqiu Zeng, Min Zhang, Qian Ma, Peiking Univ, Beijing, China; Yiming Xu, Guangzhou Medical Univ, Guangzhou, China; Yong Wang, Chengdu Univ of Traditional Chinese Med, Chengdu, China; Zsolt Bagi, David J. Fulton, Augusta Univ, Augusta, GA; Mei Hong, Peiking Univ, Beijing, China; Yuqing Huo, Augusta Univ, Augusta, GA

Background: Obesity is associated with endothelial dysfunction characterized by reduced bioavailability of nitric oxide (NO). It is well known that adenosine regulates endothelial nitric oxide release and vasodilation. However, it is unclear whether intracellular adenosine is able to modulate endothelial nitric oxide production and diet-induced metabolic disorders. This study is to investigate the effect of elevated intracellular adenosine caused by adenosine kinase (ADK) deletion or knockdown on endothelial nitric oxide production and diet-induced insulin resistance as well as the pathways associated to this effect. **Methods and results**: Endothelial-specific ADK knockout mice fed a high-fat diet show decreased fasting blood glucose and insulin, suppressed adipose tissue inflammation and hepatic steatosis, increased skeletal muscle arteriole vasodilation in an eNOS dependent manner. Mechanistically, ADK knockdown in Human Umbilical Vein Endothelial Cells (HUVECs) with adenoviral ADK shRNA elevated both intracellular and extracellular adenosine, and consequently increased endothelial nitric oxide synthase (eNOS) expression and activation, resulting in an increase in NO production, insulin uptake and vasodilatory-stimulated phosphoprotein (VASP) phosphorylation. Treatment of HUVECs with adenosine A2b receptor antagonist MRS 1754 abolished ADK-knockdown induced eNOS expression. eNOS phosphorylation in ADK-knockdown HUVECs were not interfered with adenosine receptors antagonists. **Conclusion**: ADK knockdown-mediated elevation of intracellular adenosine in endothelial cells ameliorates diet-induced insulin resistance and metabolic disorders. This is attributed to an enhancement of NO production caused by increased eNOS activation and expression, the latter is regulated via endothelial adenosine A2b receptor.

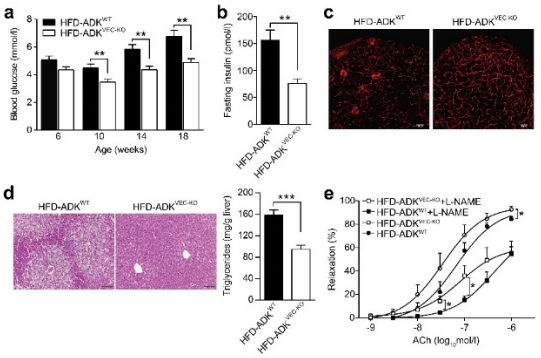

Figure: Effect of endothelial-specific ADK deletion on high fat diet induced metabolic disorders. A: Fasting blood glucose levels. B: Fasting serum insulin levels. C: Adipose vessel density and adipogenic/angiogenic cell clusters. D: Histology of liver and triglycerides contents in liver. E: Skeletal muscle arteriole relaxation in response to acetylcholine (ACh) with or without NOS inhibitor L-NAME. All images shown are representative, and data are the mean ± SEM (n=5-10 per group). *P<0.05, **P<0.01 and ***P<0.001 for HFD-ADK^{WT} vs HFD-ADK^{VEC-KO}.

J. Xu: None. **Q. Yang:** None. **X. Zhang:** None. **Z. Liu:** None. **Y. Cao:** None. **L. Wang:** None. **Y. Zhou:** None. **X. Zeng:** None. **M. Zhang:** None. **Q. Ma:** None. **Y. Xu:** None. **Y. Wang:** None. **Z. Bagi:** None. **D. Fulton:** None. **M. Hong:** None. **Y. Huo:** None.

44
Platelet-Endothelial Interactions in Atherosclerosis-Prone Arteries in a Non-Human Primate Model of Obesity and Insulin Resistance
Eran I Brown, J. Todd Belcik, James M Hodovan, Federico Moccetti, Koya Ozawa, Lindsay A Bader, Paul Kievit, Jonathan R Lindner, Oregon Health & Science Univ, Portland, OR

BACKGROUND: Platelet interactions with the vascular endothelium contribute to early atherogenesis, and occur in part from oxidative stress and secondary dysregulation of endothelial-associated von Willebrand factor (VWF). We used in vivo contrast enhanced ultrasound (CEU) molecular imaging of the carotid endothelium in a non-human primate model of diet-induced obesity to test whether platelet adhesion is present in atherosclerosis-susceptible arteries prior to plaque development, and whether it can be modified through NADPH-oxidase (Nox) inhibition.
METHODS: Six adult rhesus macaques fed a high-fat diet (HFD), with 30% of calories from fat, for >2 years were studied at baseline and after 8 weeks of therapy with the Nox inhibitor apocynin (50 mg/kg/d). Six lean chow-fed controls were also studied. Intravenous glucose tolerance tests (IVGTT) and body composition were assessed at each interval. CEU molecular imaging of VCAM-1 and platelet GPIbα of the carotid arteries bilaterally was used to assess endothelial activation and platelet adhesion. Carotid intimal thickening (IMT) and brachial flow-mediated dilation (FMD) were assessed by ultrasound.
RESULTS: Before therapy, animals on HFD compared to controls were obese (16.0 vs 9.3 kg, p=0.003), had increased visceral adiposity (49% vs 25% truncal fat, p=0.002), and were insulin resistant (4-fold higher insulin AUC on IVGTT, p=0.002). FMD and IMT were similar between cohorts, although mild plaque was seen in the carotid bulb in 3 HFD macaques. HFD animals had greater (p<0.01 vs. controls) carotid CEU signal for VCAM-1 (20.0 vs -2.7 IU) and GPIbα (12.7 vs -0.4 IU). There was a linear correlation between VCAM-1 and GP1ba signal (r^2=0.50, p=0.0001). Apocynin significantly reduced (p<0.01 vs pre-treatment) signal for VCAM-1 (3.96 IU) and GPIbα (0.19 IU); but did not alter IMT, FMD, visceral adiposity, or insulin resistance on IVGTT.
CONCLUSIONS: Platelet- endothelial interactions occur early in atherosclerosis-prone carotid arteries of obese and insulin resistant non-human primates, and correlates with the degree of endothelial adhesion molecule expression. Inhibition of Nox suppresses platelet adhesion and reduces VCAM-1 expression independent of any effects on insulin resistance and obesity.

E.I. Brown: None. **J. Belcik:** None. **J.M. Hodovan:** None. **F. Moccetti:** None. **K. Ozawa:** None. **L.A. Bader:** None. **P. Kievit:** Other Research Support; Significant; Novo Nordisk A/S and Janssen Pharmaceuticals. **J.R. Lindner:** Research Grant; Significant; Grant Support from Pfizer and GE Healthcare.

45
SR-BI and PCPE2 Modulate Lipid Trafficking in Adipocytes
Hao Xu, Sushma Kaul, Sarah Proudfoot, Rebecca L. Schill, Kaniz Fatema, Michael J. Thomas, Rachel Kallinger, Medical Coll Wisconsin, Milwaukee, WI; Mete Civelek, Univ of Virginia, Charlottesville, VA; Rebecca A. Haeusler, Columbia Univ, New York, NY; Alan T. Remaley, Edward B. Neufeld, Daniela A. Malide, Natl Heart, Lung, and Blood Inst, Translational Vascular Med Branch, Bethesda, MD; Daisy Sahoo, Mary G. Sorci-Thomas, Medical Coll Wisconsin, Milwaukee, WI

Adipose tissue undergoes distinct structural remodeling in response to increases in fat mass, as in obesity. During this process, the extracellular matrix (ECM) plays a pivotal role with respect to both adipocyte receptor signaling and structural remodeling. One ECM protein, procollagen

endopeptidase enhancer 2 (PCPE2), has been shown by our lab to work in partnership with the scavenger receptor class B type I (SR-BI) to regulate adipocyte cholesterol homeostasis. To investigate the functional impact of the partnership between SR-BI and PCPE2, we studied mature adipocytes differentiated from murine embryonic fibroblasts (MEF) and compared to our adipose specific PCPE2 knockout mice. Our studies showed the presence of an SR-BI-PCPE2 protein complex based on the co-immunoprecipitation of PCPE2 with SR-BI in both differentiated MEFs and mouse adipose tissue. Furthermore, stimulated emission depletion (STED) microscopy showed SR-BI and PCPE2 localized on the lipid droplet surface separated by distances ranging from 24 – 90 nm, suggesting that the SR-BI-PCPE2 complex may contain other proteins. Most significantly, a loss of SR-BI function was shown in PCPE2-deficient adipocytes by the SR-BI mediated HDL binding and cholesteryl ester (CE) uptake assays. Compared to differentiated MEFs from *Ldlr*$^{-/-}$ mice, binding of HDL to differentiated MEFs from *Ldlr*$^{-/-}$*Pcpe2*$^{-/-}$ mice was reduced by 75%, and HDL cholesteryl oleyl ether uptake was reduced by 50%. Disruption of adipocyte SR-BI function in the absence of PCPE2 also reduced free cholesterol efflux indicating substantial disruption to intracellular cholesterol homeostasis. Moreover, analysis of RNAseq from several human clinical studies show that PCPE2 mRNA expression is positively correlated with fat mass in specific adipose depots, while negatively correlated with plasma insulin, glucose and triglyceride levels, with the latter two more robust in type 2 diabetic populations (FDR < 0.004). Overall, these results suggest that the partnership between SR-BI and PCPE2 in adipocytes plays an important role in cholesterol trafficking and homeostasis which influences fat mass expansion, glucose tolerance and insulin resistance.
H. Xu: None. **S. Kaul:** None. **S. Proudfoot:** None. **R.L. Schill:** None. **K. Fatema:** None. **M.J. Thomas:** None. **R. Kallinger:** None. **M. Civelek:** None. **R.A. Haeusler:** None. **A.T. Remaley:** None. **E.B. Neufeld:** None. **D.A. Malide:** None. **D. Sahoo:** None. **M.G. Sorci-Thomas:** None.

46
Obesity-induced Oxidative Stress in Hematopoietic Stem and Progenitor Cells Allows a Sustained Myelopoiesis and Persistent Inflammation in Mouse Peripheral Artery Disease
Pijus Barman, Milie Fang, Giamila Fantuzzi, Timothy J Koh, **Norifumi Urao**, Univ Illinois Chicago, Chicago, IL

Peripheral artery disease (PAD) is linked with obesity-induced complications. Obesity induced by a high-fat diet (HFD) modulates myelopoiesis of hematopoietic stem and progenitor cells (HSPCs) and innate immune responses in a long-term. Here we show that, in a mouse hindlimb ischemia, normal mice transplanted HSPCs from HFD mice exhibit persistent inflammation and impaired healing using three-dimensional magnetic resonance images, compared to mice transplanted HSPCs from mice fed a normal diet (ND). Bone marrow cell population analysis revealed HFD induces expansion of myeloid progenitor cells in steady state and prolonged activity of more primitive HSPCs following hindlimb ischemia. Ex vivo culture of HSPCs revealed that HFD increases monocyte generation by damage-associated toll-like receptor stimulation, suggesting that HFD promotes myelopoiesis in a HSPC-intrinsic manner. This notion was confirmed by adoptive transfer of HSPCs from HFD mice in a mouse after hindlimb ischemia that contribute to monocyte generation in vivo. Mechanistically, HFD-induced oxidative stress is associated with increased histone-3 lysine-4 trimethylation (H3K4me3), an activating histone methylation, in HSPCs potentially through KDM5 histone demethylase, as a reduction of oxidative stress by cyclosporine A or MitoTEMPO decreased H3K4me3 and increased KDM5 activity in HSPCs. In myeloid progeny of HSPCs from HFD mice, we found enhanced gene expressions of inflammatory Tnfa and Il6, and increased H3K4me3-marks in KDM5 targets, compared to those from ND mice. Our results suggest that HFD-induced oxidative stress in HSPCs modulates their myelopoiesis and phenotype of their progeny via epigenetic reprogramming that, in turn, persistent inflammatory monocyte/macrophage response in an acute ischemic event of PAD.
P. Barman: None. **M. Fang:** None. **G. Fantuzzi:** None. **T.J. Koh:** None. **N. Urao:** None.

This research has received full or partial funding support from the American Heart Association.

47
The Signaling Adapter Tumor-Necrosis Receptor Associated Factor 1 (TRAF-1) Regulates Thrombosis and Haemostasis in Mice
Nathaly Anto Michel, Christoph Bode, Andreas Zirlik, **Dennis Wolf**, Univ Heart Ctr Freiburg, Freiburg, Germany

Background: The signaling pathways linking inflammatory and thrombotic circuits in platelets are only poorly understood. Here, we tested the role of the inflammatory signaling adapter TRAF-1, which bundles TNF-, TLR, and IL1-signaling, in platelets.
Methods and Results: To establish a role for platelet expressed TRAF-1, we verified its expression in *in vitro* generated mouse thrombi in immunohistochemistry and western blot. Blood clots generated from blood of *Traf1*-deficient mice were smaller, suggestive of a defective plasmatic coagulation. In accord, tail bleeding time was increased by ~4-fold in *Traf1*$^{-/-}$ mice. Genetically chimeric mice generated by bone marrow transplantations with a selective deficiency of *Traf1* in bone-marrow-derived leukocytes showed no changes in bleeding time, suggesting that the prolonged bleeding time in *Traf1*$^{-/-}$ mice was regulated by vascular/stromal cells. In a gene expression array of *Traf1*$^{-/-}$ endothelial cells, several factors that regulate coagulation, including fibrinogen, tumor-homing peptide (F3), and Von Willebrand factor (vWF) were reduced. In addition to this vascular phenotype, expression of P-selectin and the activation epitope Jon/A induced by *in vitro* ADP and thrombin stimulation was reduced in TRAF-1-deficient platelets. As a consequence, *in vivo* thrombus-generation in the mesenterium was delayed with an enhanced rate of emboli in *Traf1*$^{-/-}$ mice – an effect that was confirmed in mice transferred with *TRAF1*$^{-/-}$ platelets, and in mice with a selective deficiency of *Traf1* in bone-marrow-derived cells. Finally, we demonstrate TRAF-1 protein expression in human coronary thrombi and the presence of *TRAF1*-transcripts in RNA-sequencing of human platelets. *TRAF1*-mRNA expression was down-regulated in collagen and TRAP stimulated human platelets and correlated with the gene expression of several upstream platelet-receptors, including *EDA2R*, *RELT*, and *CD137.*
Conclusion: We present the novel finding that the pro-inflammatory signaling adapter TRAF-1 is expressed in mouse and human thrombi and participates in coagulation and thrombosis by vascular and platelet-mediated pathways. These findings emphasize the connection of inflammatory signaling and haemostasis.
N. Anto Michel: None. **C. Bode:** None. **A. Zirlik:** None. **D. Wolf:** None.

48
Platelets Amplify Monocyte and Macrophage Inflammation Propagating Atherosclerosis Progression
Tessa J Barrett, Felix Zhou, Mike Gorenchtein, Edward A Fisher, Jeffrey S Berger, NYU Sch of Med, New York, NY

Objective: Platelet-leukocyte interactions are recognized to play a central role in the initiation of atherosclerosis and are hypothesized to propagate lesion inflammation. Clinical studies have found that platelet activity is associated with atherosclerosis; however, how they contribute to sustained lesion development remains to be fully elucidated. In this

study, we sought to understand the effect of platelets on monocyte and macrophage (Mθ) inflammatory phenotype and trafficking during plaque development. **Methods and Results:** *Ldlr*$^{-/-}$ mice were fed a western diet for 7 weeks prior to platelet depletion (α-CD42b) for 2 weeks. Platelet depletion had no significant effect on monocyte count, yet, resulted in a significant reduction to the: (1) ratio of Ly6^{hi}:Ly6C^{lo} circulating monocytes, (2) monocyte surface expression of CD11b, and (3) expression of proinflammatory transcripts (*Ccl2*, *iL-1β*, *Cd11b*). Morphometric and immunohistological analysis of plaques demonstrated that platelet deficient mice have significantly reduced lesion area (31% reduction, p=0.03) and reduced Mθ content (38% reduction, p=0.01), compared to platelet competent mice. *In vivo* cell trafficking assays revealed that platelets play a critical role in the recruitment of circulating monocytes to lesions (58% reduction of recruitment in platelet deficient mice, p=0.04), but do not alter plaque macrophage egress. Furthermore, platelets do not alter the proliferative capacity of plaque Mθs, yet, do promote Mθ survival as assessed by cleaved caspase-3 staining, and skew them towards a proinflammatory phenotype (decreased plaque collagen and mannose receptor content, p=0.03 and p=0.05) that have a reduced capacity for efferocytosis. **Conclusion:**This study highlights for the first time novel roles of platelets to immunomodulate monocytes and Mθs, key cell types central to atherogenesis. We find that platelets are critical mediators of circulating monocyte inflammation and subsequent plaque Mθ inflammation and trafficking. The capacity of platelets to skew leukocytes towards a proinflammatory phenotype represents a significant driver of unresolved plaque inflammation, thereby contributing to atherosclerosis progression.

T.J. Barrett: None. **F. Zhou:** None. **M. Gorenchtein:** None. **E.A. Fisher:** None. **J.S. Berger:** None.

49

Novel Tirofiban Conjugate for the *in vivo* Detection of Activated Platelets

Khanh Q. Ha, Xiaoxin Zheng, Chase Kessinger, Farouc Jaffer, Jason McCarthy, Massachusetts General Hosp, Boston, MA

Background — Current intracoronary imaging approaches such as intravascular ultrasound and optical coherence tomographic imaging do not specifically detect activated platelets, a key cell that drives stent thrombosis, a life-threatening condition following percutaneous coronary intervention (PCI). Glycoprotein IIb/IIIa (GPIIb/IIIa) is the key receptor involved in platelet activation and is a validated target for both
therapeutic approaches and diagnostic imaging. A GPIIb/IIIa-targeted fluorescent imaging agent, used in conjunction with a catheter-based NIR fluorescence imaging system may provide powerful tool to detect thrombus prone stents.
Methods — A NIRF conjugate of tirofiban (Tf), a clinical IIb/IIIa antagonist, was synthesized via the chemical modification of the sulfonamide fragment of the molecule with a benzoic acid moiety and subsequent addition of the PEG-modified fluorophore, CyAl5.5 (ex/em 675/695nm). The efficacy of the conjugate was validated *in vivo* in the $FeCl_3$-induced model of femoral thrombosis, and compared to the free dye or blocking with the parent drug Tf. After injection, serial intravital fluorescence microscopy (IVFM) was carried out for one hour, followed by histological examination of binding.
Results — A NIR fluorescent conjugate of Tf was successfully synthesized via an optimized multi-step synthesis, with the identity and purity of the agent fully characterized after the final HPLC-based purification. IVFM characterization of conjugate efficacy showed an increase in NIRF signal in the thrombus over the initial 30 minutes, followed by a slow decrease until the endpoint of the experiment (1 h). The NIRF signal was 92% ablated by preinjection of excess Tf. Free dye did not display any localization to the thrombus. Histological analysis showed significant accumulation within the thrombus that co-localized with GPIIb/IIIa expression.
Conclusions — A novel NIR fluorescent Tf conjugate has been developed that specifically binds to GPIIb/IIIa, and could be used for the detection of activated platelets in experimental thrombi *in vivo*. This novel agent should permit assessment of GPIIb/IIIa activation in a broad range of biological processes and may also aid in the detection of thrombosis-prone stents.

K.Q. Ha: None. **X. Zheng:** None. **C. Kessinger:** None. **F. Jaffer:** None. **J. McCarthy:** None.

This research has received full or partial funding support from the American Heart Association.

50

The Vascular Ecto-enzyme, CD39 Protects from Venous Thrombogenesis by inhibiting Innate Immune Activation

Yogendra Kanthi, Benjamin N Jacobs, Liguo Chi, Vinita Yadav, Raymond Zhao, Alison Banka, Jason S Knight, David J Pinsky, Univ of Michigan, Ann Arbor, MI

Background: Venous thrombosis (DVT) is a serious health concern, with growing incidence in an aging, comorbid population. DVT is marked by sterile inflammation and innate immune activation. Early participants in DVT include platelets, and neutrophils (PMN) which extrude their DNA to form thrombus-potentiating extracellular traps (NETs). To identify improved therapeutic targets at the nexus of inflammation and coagulation, we focused on the vascular ectonucleotidase CD39, found on leukocytes and the endothelium. CD39 dissipates extracellular ATP & ADP, thrombo-inflammatory “danger” signals. We hypothesized that CD39 is a critical enzyme in venous homeostasis, restraining unchecked inflammation and thrombosis in DVT.
Methods: DVT was induced in *Cd39*$^{+/-}$ and WT control mice using a “flow-restriction” model of inferior vena cava (IVC) stenosis. Thrombus frequency and size were assessed 48h after DVT induction. A novel flow cytometry method, immunoblot, immunostaining were used to examine thrombus cellular content, fibrin, NETs, and inflammasome activation. **Results:** *Cd39*$^{+/-}$ mice had a significantly higher thrombus frequency (2.5-fold) and clot size (3-fold), with more fibrin content by immunoblot. Flow cytometry revealed exaggerated PMN recruitment to the growing thrombus in *Cd39*$^{+/-}$ mice, with more NETs *in vitro*, and within DVT compared with WT mice. *Cd39*$^{+/-}$ mice also had amplified DVT inflammasome activity *in vivo*, measured by increased NFkB phosphorylation and mature IL-1 beta compared with WT DVT. Flow cytometry of the thrombus revealed an increase in activated platelet-PMN heteroaggregates within *Cd39*$^{+/-}$ DVTs, indicating enhanced innate-coagulation system crosstalk. **Conclusion**: CD39 is a critical vasculoprotective ecto-enzyme in venous thrombogenesis. *Cd39*$^{+/-}$ mice have increased DVT burden, fibrin deposition, activated platelet-PMN interactions, and exaggerated inflammasome activation compared with WT mice. By enrolling NET formation and inflammasome activation, CD39 posits a previously unexplored link between venous inflammation and thrombosis. Studies are underway to modulate inflammasome activation in *Cd39*$^{+/-}$ mice, and to delineate the relative contributions of leukocyte/endothelial CD39 in venous thrombosis.

Y. Kanthi: Consultant/Advisory Board; Modest; Wells Fargo. **B.N. Jacobs:** None. **L. Chi:** None. **V. Yadav:** None. **R. Zhao:** None. **A. Banka:** None. **J.S. Knight:** None. **D.J. Pinsky:** Ownership Interest; Modest; Proteris.

51
A New Model of Murine Stasis Pulmonary Thromboembolism in vivo With Assessment by Noninvasive Multimodal Molecular-Structural Imaging
Chase W Kessinger, Farouc A Jaffer, Massachusetts General Hosp/Harvard Medical Sch, Boston, MA

OBJECTIVE: Pulmonary embolism (PE) is a life-threatening cardiovascular disease that urgently requires improved diagnostic, prognostic and therapeutic options. Here we established and investigated a novel murine PE model based on embolization of a stasis-induced venous thrombus (VT). We further utilized in vivo molecular-structural imaging of fibrin accessibility to assess the healing status of the PE. METHODS: Stasis VT was induced in the femoral veins of donor C57BL6 mice. VT was resected 24 hours (h) after induction and then intravenously injected into recipient mice to create PE. Pulse-wave Doppler of pulmonary artery flow was utilized to evaluate the pulmonary arterial pressure (PAP) before and 24h after embolization. One day after embolization, the fibrin-specific probe FTP11-CyAm7 (750/767nm ex/em, 150 nmoles/kg i.v.) assessed the FTP binding and spatial localization of PE via integrated fluorescence-mediated tomography and computed tomography (FMT-CT) pulmonary angiography. Mice were sacrificed 1, 4, 8, or 21 days following stasis-VT embolization, and underwent histological analysis of the PE. RESULTS: Femoral vein stasis-VT exhibited similar temporal inflammatory neutrophil and monocyte/macrophage infiltration and FTP11 binding (fibrin accessibility) kinetics compared to inferior vena cava stasis-VT models. The mean VT width and length were 2.4±0.2mm and 0.65±0.02mm, respectively (n=29 thrombi). Noninvasive ultrasound assessment of the mouse PAP, assessed via the pulmonary acceleration time (PAT), showed a 22% decrease (p=0.03) in pre-to-post-PE PAT times, consistent with increased PAP due to PE. FMT-CT imaging using FTP11 demonstrated accessible fibrin in day 1 PE and visualized PE confined to the lungs, primarily (91%) in the right lung. Ex vivo fluorescence reflectance imaging and histological analysis verified the location PE reported by FMT-CT. CONCLUSIONS: These data validate the first in vivo model of PE based on stasis VT formed in vivo. The model reproducibly generates a survival PE that harbors accessible fibrin in recent stasis VT lodged in the lung, and acute increases PAP. This new clinically relevant model of PE is anticipated to facilitate research of acute PE and chronic thromboembolic pulmonary hypertension.
C.W. Kessinger: None. **F.A. Jaffer:** None.

52
Clinical and Genetic Determinants of Varicose Veins: a Prospective, Community-Based Study of ~500,000 Individuals
Alyssa M Flores, Eri Fukaya, Stanford Univ Sch of Med, Stanford, CA; Daniel Lindholm, Stefan Gustafsson, Uppsala Univ, Uppsala, Sweden; Daniela Zanetti, Erik Ingelsson, Nicholas J. Leeper, Stanford Univ Sch of Med, Stanford, CA

Background: Varicose veins are a common problem with no approved medical therapies. While it is believed that varicose vein pathogenesis is multifactorial, there is a limited understanding of the genetic and environmental factors that contribute to their formation. Large-scale studies of risk factors for varicose veins may highlight important aspects of pathophysiology and identify groups at increased risk for disease.
Methods: We applied machine learning to agnostically search for risk factors of varicose veins in 493,519 individuals in the UK Biobank. Predictors were further studied using univariable and multivariable Cox regression analysis. A genome-wide association study (GWAS) of varicose veins was also performed among 337,536 individuals (9,577 cases) of white British descent, followed by eQTL and pathway analyses. Because height emerged as a new candidate predictor, we used LD score regression to estimate the genetic correlation between height and varicose veins. Finally, we performed Mendelian randomization analyses to assess for a causal role for height in varicose vein disease.
Results: Machine learning confirmed several known (age, gender, obesity, pregnancy, history of deep vein thrombosis) and identified several new risk factors for varicose vein disease. The most important novel predictors were leg bioimpedance (HR: 0.44, 95% CI: 0.39-0.50, $P < 0.0001$) and height (HR: 1.74; 95% CI: 1.51-2.01, $P < 0.0001$), which both remained independently associated with varicose veins after adjusting for traditional risk factors in Cox regression. A GWAS identified 30 new genome-wide significant loci, identifying pathways involved in vascular development and skeletal/limb biology. Mendelian randomization analysis provided evidence that increased height is causally related to varicose veins (IVW: beta = 0.266, $P = 1.28 \times 10^{-16}$).
Conclusions: Using data from nearly half a million individuals, we identified novel clinical and genetic risk factors which provide pathophysiological insights and could help future improvements of treatment of varicose vein disease.
A.M. Flores: None. **E. Fukaya:** None. **D. Lindholm:** None. **S. Gustafsson:** None. **D. Zanetti:** None. **E. Ingelsson:** None. **N.J. Leeper:** None.

53
Differential Effects of LRP1 in AngII-induced Ascending Aortic PathologiesBetween Male and Female Mice: Lack of Association With Elastin Fragmentation
Bradley Christopher Wright, Hisashi Sawada, Jessica J Moorleghen, Deborah A Howatt, Debra L Rateri, Mark W Majesky, Alan Daugherty, Univ of Kentucky, Lexington, KY

Objective: Low-density lipoprotein receptor-related protein 1 (LRP1), a transmembrane protein, is important in maintaining elastin fiber integrity of the aortic wall. Smooth muscle cells (SMCs) of the ascending aorta are composed of the inner medial layers from the cardiac neural crest and the outer layers from the second heart field (SHF). LRP1 depletion in SMCs of male mice augments angiotensin II (AngII)-induced ascending aortic dilation and rupture attributed specifically to SMCs of SHF origin. The purpose of this study was to determine whether depletion of LRP1 in SHF-derived SMCs (SHF-SMC LRP1) has differential effects on AngII-induced aortic dilation, rupture, and elastin fragmentation between male and female mice.
Methods and Results: Female LRP1 floxed mice were bred to male LRP1 floxed mice with Mef2c-Cre transgene to generate SHF-SMC LRP1 +/+ and -/- mice. Male and female mice at 12-14 weeks of age were infused with either saline or AngII (1,000 ng/kg/min) for 28 days (n = 12-31). Ascending aortic diameter (AoD) was measured by ultrasound, rupture was determined by necropsy, and elastin fragmentation was assessed by Movat's staining. In male mice of both genotypes, AoD and elastin breaks were increased by AngII infusion, and AoD was positively correlated with elastin fragmentation ($r^2 = 0.48$, $p < 0.001$). SHF-SMC LRP1 deletion augmented aortic dilation, rupture rate, and elastin fragmentation in AngII-infused male mice. In females, AngII infusion increased AoD in SHF-SMC LRP1 -/- mice, but not in their wild type controls. AngII-induced elastin fragmentation did not differ between SHF-SMC LRP1 +/+ and -/- female mice, and no correlation between AoD and elastin fragmentation was detected ($r^2 = 0.01$, $p = 0.88$). Despite the extent of AngII-induced elastin fragmentation that was equivalent to that in males, aortic rupture is lower in female than in male LRP1 deleted mice (9 vs 38%, $p = 0.02$).
Conclusion: In male mice, AngII infusion promotes dilation and rupture of ascending aorta that is augmented in SHF-SMC LRP1-/- mice and positively associated with elastin fragmentation. However, AngII only promotes ascending aortic dilation in female mice with SHF-SMC LRP1 deletion,

despite elastin fragmentation being equivalent between SHF-SMC LRP1 +/+ and -/- mice.
B.C. Wright: None. **H. Sawada:** None. **J.J. Moorleghen:** None. **D.A. Howatt:** None. **D.L. Rateri:** None. **M.W. Majesky:** None. **A. Daugherty:** None.

54
Genetic Deficiency in Nox2-containing NADPH Oxidase Decreases Susceptibility to Venous Thrombosis in Mice
Vijay K Sonkar, Rahul Kumar, Sean Gu, Prakash Doddapattar, Steven R Lentz, Sanjana Dayal, Univ of Iowa Health Care, Iowa City, IA

Activated neutrophils release neutrophil extracellular traps (NETs) via a pathway dependent on reactive oxygen species (ROS). NETs are enriched in extracellular DNA and histones, and contribute to venous thrombosis. Nox2-containing NADPH oxidase is a major upstream mediator of ROS-dependent release of NETs. Neutrophils from mice deficient in Nox2 or patients with X-linked chronic granulomatous disease due to Nox2 deficiency do not produce NETs, suggesting a role for Nox2 in venous thrombosis. We hypothesized that mice genetically deficient in Nox2 are protected from venous thrombosis. We studied male and female mice deficient in Nox2 (Nox2-KO) and their wild type (WT) littermates at 10-14 weeks of age (n=7-13/group). Using electron spin resonance and H2C-DCFH-DA staining, we confirmed that neutrophils from Nox2-KO mice do not produce ROS at baseline or upon PMA-activation. Neutrophils from WT mice displayed a dose-dependent release of NETs upon PMA-stimulation (SYTOX green staining using fluorescence microscopy), whereas Nox2-KO mice did not produce NETs. We next examined susceptibility to venous thrombosis in a stasis model of inferior vena cava (IVC) ligation. After 48 hours of ligation, both male and female Nox2-KO mice developed significantly smaller thrombi compared with WT mice ($P<0.05$). Markers for NETs were measured in plasma (nucleosome levels using ELISA) and venous thrombi (staining for citrullinated histones, Cit-H3). Levels of nucleosomes in the mice that did not develop thrombi were similar to those in baseline samples collected before IVC ligation. All of the mice that developed thrombi had significant elevation of plasma nucleosome levels compared with mice that did not develop thrombi ($P<0.05$), but nucleosome levels did not differ between WT and Nox2-KO mice. Likewise, the heterogeneous pattern of NET formation within thrombi detected by Cit-H3 staining was similar in WT and Nox2-KO mice. These findings suggest that Nox2 is an important determinant of thrombus size during IVC ligation. Interestingly, our study also provides evidence for Nox2-independent pathways for NET release during venous thrombosis.
V.K. Sonkar: None. **R. Kumar:** None. **S. Gu:** None. **P. Doddapattar:** None. **S.R. Lentz:** None. **S. Dayal:** None.

55
TRAIL Protects Against Endothelial Dysfunction in vivo and Inhibits Angiotensin-II Induced Oxidative Stress in Vascular Endothelial Cells *in vitro*
Pradeep Manuneedhi Cholan, Sian Cartland, Benjamin Rayner, Scott Genner, Heart Res Inst, Sydney, Australia; Lei Dang, Shane Thomas, Univ of New South Wales, Sydney, Australia; Mary Kavurma, Heart Res Inst, Sydney, Australia

The vascular endothelium is critical for maintenance of cardiovascular homeostasis and vascular oxidative stress is a primary cause of endothelial dysfunction. TNF-related apoptosis-inducing ligand (TRAIL) is increasingly recognised to play a protective role in atherosclerosis, however the molecular mechanisms by which it exerts its beneficial effects are unclear. Our aim was to identify whether TRAIL could protect against atherosclerosis by reducing vascular oxidative stress and improve endothelial cell (EC) function. *In vivo*, 12 w high fat diet (HFD)-fed *Trail*$^{-/-}$*Apoe*$^{-/-}$ mice had more severe atherosclerosis, with significant impairment in vasorelaxation in response to acetylcholine, but not sodium nitroprusside. HFD *Trail*$^{-/-}$*Apoe*$^{-/-}$ vessels also had increased vascular reactive oxygen species (ROS) as evident by dihydroethidium (DHE) staining compared to HFD *Apoe*$^{-/-}$ mice. Following injection of Evan's blue dye, blood vessels from highly vascularised organs of *Trail*$^{-/-}$ mice demonstrated increased vascular permeability compared to *Trail*$^{+/+}$ organs, and altered expression of adhesion molecule and tight junction proteins. *In vitro*, AngII (50 ng/ml) increased DHE and mitosox staining in ECs within 2 h, which was inhibited by apocynin, rotenone and L-Name, suggesting that NADPH oxidases (NOXs), the mitochondria and eNOS are major producers of ROS. siRNA targeting NOX-4, but not NOX-1, -2, or -5 reduced AngII-induced DHE, whereas siRNA targeting eNOS significantly augmented DHE staining. Importantly, pre-treatment of TRAIL at 1 ng/ml inhibited AngII-inducible DHE and mitosox staining. Functionally, TRAIL reduced eNOS monomer expression and monocyte recruitment in response to AngII. Furthermore, AngII reduced VCAM-1 and PECAM-1 mRNA was no rescued with TRAIL treatment. These findings demonstrate for the first time that TRAIL protects against endothelial dysfunction via its ability to modulate oxidative stress. Understanding the role TRAIL plays in normal physiology and disease, may lead to potential new therapies to improve endothelial function and atherosclerosis.
P. Manuneedhi Cholan: None. **S. Cartland:** None. **B. Rayner:** None. **S. Genner:** None. **L. Dang:** None. **S. Thomas:** None. **M. Kavurma:** None.

56
Endothelial 6-Phosphofructo-2-Kinase/Fructose-2,6-Bisphosphatase, Isoform 3 (PFKFB3) Deficiency Inhibits Hypoxia-Induced Pulmonary Hypertension in Mice
Yapeng Cao, Qiuhua Yang, Lina Wang, Jiean Xu, Peking Univ Shenzhen Graduate Sch, Shenzhen, China; Zhiping Liu, Augusta Univ, Augusta, GA; Yiming Xu, Guangzhou Medical Univ, Guangzhou, China; Yong Wang, Chengdu Univ of Traditional Chinese Med, Chengdu, China; David J Fulton, Neal L Weintraub, Augusta Univ, Augusta, GA; Chaodong Wu, Texas A&M Univ, College Station,, TX; Qinkai Li, Peking Univ Shenzhen Graduate Sch, Shenzhen, China; Yunchao Su, Augusta Univ, Augusta, GA; Mei Hong, Peking Univ Shenzhen Graduate Sch, Shenzhen, China; Yuqing Huo, Augusta Univ, Augusta, GA

Background: Pulmonary artery hypertension (PAH) is a severe proliferative disease characterized by the remodeling of small pulmonary arteries leading to a progressive increase in pulmonary vascular resistance and ultimately to right ventricular failure and death. Many studies have indicated that endothelial dysfunction is a key element in the pathogenesis of this disease. In this study, we investigated whether endothelial glycolysis plays a critical role in the development of hypoxia-induced PAH by knocking down endothelial PFKFB3 (encoding 6-phosphofructo-2-kinase/fructose-2,6-bisphosphatase, isoform 3), a critical regulator of glycolysis.
Methods and Results: Immunostaining results showed that pulmonary artery endothelial PFKFB3 was increased in the lung of PAH patients. Mice deficient in endothelial *Pfkfb3* showed decreased right ventricular systolic pressure, attenuated right ventricular hypertrophy and normal morphology of distal pulmonary arteries after four weeks of hypoxia compared with control mice. Furthermore, PFKFB3-deficient pulmonary arterial ECs secreted less growth factors, which ameliorated the proliferation of pulmonary artery smooth muscle cells. Additionally, the levels of endothelial derived inflammatory cytokines were also decreased. Besides, the inhibitory effect of endothelial *Pfkfb3* supression on PAH formation were demonstrated in Sugen 5416/hypoxia rat pulmonary hypertension model with 3PO, a specific PFKFB3 inhibitor. Mechanistically, genetic

deletion of *PFKFB3* or 3PO treatment decreased the TNF-α induced NLRP3 inflammasome activation in pulmonary arterial ECs.
Conclusions: Endothelial PFKFB3 inhibition is able to ameliorate the development of hypoxia-induced pulmonary hypertension.
Y. Cao: None. **Q. Yang:** None. **L. Wang:** None. **J. Xu:** None. **Z. Liu:** None. **Y. Xu:** None. **Y. Wang:** None. **D. Fulton:** None. **N. Weintraub:** None. **C. Wu:** None. **Q. Li:** None. **Y. Su:** None. **M. Hong:** None. **Y. Huo:** None.

57
Adenosine Kinase Epigenetically Regulates Abdominal Aortic Aneurysm Formation
Zhiping Liu, Augusta Univ, Augusta, GA; Jiean Xu, Peking Univ, Shenzhen, China; Jiaojiao Wang, Augusta Univ, Augusta, GA; Yiming Xu, Sch of Basic Medical Sciences, Guangzhou Medical Univ, Guangzhou, China; Yong Wang, Coll of Basic Med, Chengdu Univ of Traditional Chinese Med, Chengdu, China; Lina Wang, Yapeng Cao, Qiuhua Yang, Peking Univ, Shenzhen, China; Ha Won Kim, Neal L Weintraub, Yuqing Huo, Augusta Univ, Augusta, GA

Objectives: Abdominal aortic aneurysm (AAA) is a major cause of morbidity and mortality worldwide; however, the molecular mechanisms involved in AAA formation are not well understood. The nucleoside adenosine plays important roles in modulating vascular homeostasis. In this study, we sought to determine whether adenosine kinase (ADK), the adenosine-metabolizing enzyme, modulates AAA formation via control of intracellular adenosine level and investigate the involvement of ADK-mediated epigenetic mechanism in this aortic disease. **Methods and results:** ADK expression and activity were increased in murine AAA models, including calcium chloride-stimulated AAA and angiotensin II-induced AAA. Using a loss-of-function genetic mouse model, we demonstrated that genetic ADK knockout mice led to increased Intracellular adenosine level in macrophages and vascular cells and developed significantly smaller aortic expansion when subjected to AAA inductions. Notably, knockout of ADK alleviated arterial inflammation and diminished infiltration of macrophages, as well as suppressed arterial extracellular matrix degradation, which was associated with down-regulation of CXCL12, MMP2/9 and adhesion molecule expression. Mechanistically, elevation of intracellular adenosine by genetic inactivation of ADK or exogenous adenosine reduces activation of the transmethylation pathway via inactivation of SAH hydrolase (SAHH) and histone H3K4 methyltransferase (HMT), thus down-regulating expression and signaling of mitogen-activated protein kinases in activated macrophages and vascular cells with pro-inflammatory stimuli. Blocking of the H3K4 transmethylation pathway by knockdown of WDR5, a core subunit of HMT complex, abrogated the beneficial effects of ADK inactivation. **Conclusions:** Our findings reveal a previously unrecognized role of ADK mediated epigenetic pathways in the pathogenesis of AAA and provides a therapeutic target for the prevention of AAA.

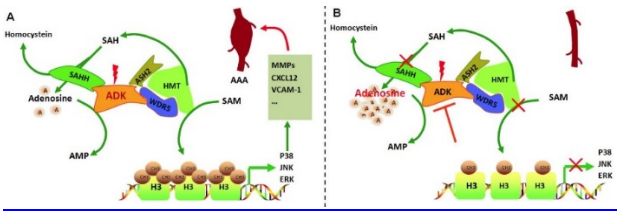

Z. Liu: None. **J. Xu:** None. **J. Wang:** None. **Y. Xu:** None. **Y. Wang:** None. **L. Wang:** None. **Y. Cao:** None. **Q. Yang:** None. **H. Kim:** None. **N.L. Weintraub:** None. **Y. Huo:** None.

This research has received full or partial funding support from the American Heart Association.

58
Efficacy and Mechanisms of Metformin Therapy in Established Experimental Abdominal Aortic Aneurysms
Baohui Xu, Gang Li, Fanru Shen, Trevor Weden, Anna Cabot, Hongping Deng, Stanford Univ Sch of Med, Stanford, CA; Xiaofeng Chen, Whenzhou Medical Univ Taizhou Hosp, Linhai, China; Ronald L Dalman, Stanford Univ Sch of Med, Stanford, CA

Objective: Diabetes reduces the risk for abdominal aortic aneurysm (AAA) disease. In prior work in rodent models, pre-treatment with metformin was protective against experimental AAA initiation and progression. This study examined the influence of metformin therapy on progression of existing experimental AAAs. **Methods:** AAAs were created in 10-12 week old male C57BL/6J mice via transient intra-aortic infusion of porcine pancreatic elastase (PPE). Mice were treated with metformin (250 mg/kg via oral gavage), metformin plus AMPK inhibitor Compound C (the later via 10 mg/kg intraperitoneal injection) or vehicle alone for 10 days starting on day 4 following AAA creation. Outcomes were assessed by serial transabdominal ultrasonographic assessment of aortic diameter during treatment, as well as histological examination at sacrifice. **Results:** The principal findings are summarized in the Figure. Vehicle-treated mice experienced progressive, time-dependent aortic enlargement from day 3 to 14 following PPE infusion. Metformin treatment substantially attenuated further enlargement of existing AAAs. Treatment with Compound C partially rescued the AAA phenotype in metformin-treated mice. Histologically, characteristic aneurysmal pathologic changes, including medial elastin degradation, smooth muscle cell (SMC) depletion, mural leukocyte accumulation and neoangiogenesis (assessed by CD31 staining), present in PPE-infused, vehicle-treated mice, were substantially attenuated with metformin treatment. Co-treatment with Compound C abrogated the effects of metformin on media elastin degradation, SMC depletion and mural macrophage infiltration, with less influence on mural angiogenesis. **Conclusion:** Metformin therapy suppresses further expansion of existing experimental AAAs. This effect is abrogated by co-treatment with Compound C. These findings further justify performance of a clinical trial of metformin for medical management of AAA disease.

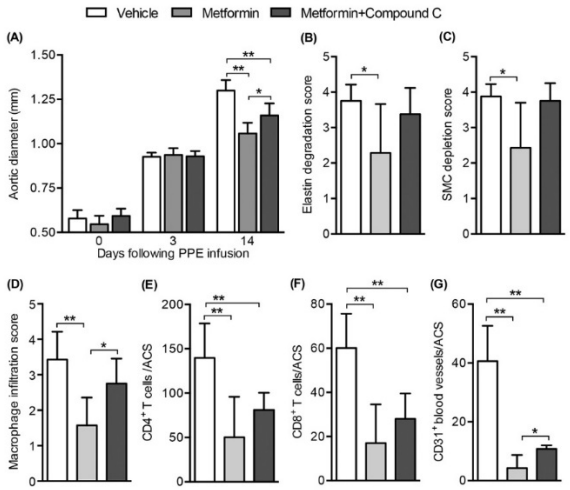

Figure. Metformin treatment limits the progression of established experimental AAAs. Male C57BL/6 mice were daily treated with given vehicle (n=7), metformin (250 mg/kg via oral gavage) (n=6), or metformin plus AMPK inhibitor compound C (10 mg/kg ip) (n=8) starting day 4 following PPE infusion. **(A):** Mean and SD of aortic diameters. Two-way ANOVA followed by two sample comparison, *P<0.05 and **P<0.01 between two group. (B-G): Quantification of medial elastin degradation, SMC depletion, leukocyte infiltration (macrophages and T cell subsets) and angiogenesis (CD31). Nonparametric Mann Whitney test, *P<0.05 and **P<0.01 between two groups.

B. Xu: None. **G. Li:** None. **F. Shen:** None. **T. Weden:** None. **A. Cabot:** None. **H. Deng:** None. **X. Chen:** None. **R.L. Dalman:** None.

59

Defining the Mechanisms of Autologous Bone Marrow Cell Therapy in Critical Limb Ischemia

Bianca Kenyon, Ashley Gutwein, S. Keisin Wang, Linden Green, Michael Murphy, Indiana Univ Sch of Med, Indianapolis, IN

Introduction. Here we present a composite of proteomic, cellular, and radiological analyses that define the mechanisms by which autologous concentrated bone marrow mononuclear cells (cBMNC) promote limb preservation in patients with critical limb ischemia. Methods. $CD45^+$, $CD34^+$, $CD105^+$, and $VEGFR\text{-}2^+$ cells were enumerated using fluorescent activated cell sorting (FACS) from aliquots of the cBMNC from each patient enrolled in the Phase III MOBILE TRIAL. Direct limb perfusion was measured with Positron Emission Tomography/Computed Tomography (PET/CT) with radiolabeled water ($^{15}H20$). Anterior tibialis muscle (ATM) into which cBMNC was injected prior to below knee amputation in the Phase I CHAMP trial were collected for capillary density and proteomic analyses. Results. There were no differences in the number of $CD45^+$ (636 ± 388 vs. 868 ± 699 x 10^6, p= 0.279), $VEGFR\text{-}2^+$ (0.4 ± 0.8 vs. 0.3 ± 0.6 x10^6, p=0.757) and $CD34^+$ (21 ± 13 vs. 35 ± 30 x 10^6, p= 0.156) cells in the cBMNC product injected in those patients undergoing amputation and those with a preserved limb (n=90). There was a significant association between $CD105^+$ (7 ± 4 vs. 16 ± 13 x 10^6, p= 0.05) cells in patients and freedom from amputation. A Blood Perfusion Index (*BPI*) was calculated by comparing the ratio of $H2O^{15}$ peak tracer uptake level of the untreated: treated leg with an increase from 0.38 at baseline to 0.54 (42%) at 12 weeks (n=4, p< 0.05). There was an increase in $CD31^+$ capillaries in the ATM after injection of cBMNC. ATM specimen also showed increases in VEGF-A, angiopoietin-2, and MMP-9 compared to the untreated specimen. Conclusion. This first in man analyses provides conclusive evidence that cBMNC improves limb perfusion via capillary formation. This study suggests that bone marrow cell mediated angiogenesis may be dependent on $CD105^+$ mesenchymal progenitor cells.

Characteristic of cBMNC	No Event (n=95)	Event (n=24)	*p*-value
Mononuclear cells, x10^6	868 ± 699 (n=65)	636 ± 388 (n=21)	0.279
CD34+ cells, x10^6	35 ± 30 (n=33)	21 ± 13 (n=11)	0.156
CD105+ cells, x10^6	16 ± 13 (n=33)	7 ± 4 (n=11)	0.048
VEGFR-2+ cells, x10^6	0.3 ± 0.6 (n=34)	0.4 ± 0.8 (n=13)	0.757
Cell viability, %	84 ± 18 (n=78)	90 ± 10 (n=22)	0.624

cBMNC = concentrated Bone Marrow Nucleated Cells
Data reported as mean ± standard deviation
VEGFR-2: vascular endothelial growth factor receptor-2

B. Kenyon: None. **A. Gutwein:** None. **S. Wang:** None. **L. Green:** None. **M. Murphy:** None.

88
Fibronectin Promotes EphA2 Expression through RGD Integrin Signaling in Vascular Smooth Muscle Cells
Alexandra C Finney, Jonette M Green, James G Traylor, A. Wayne Orr, LSU Health Sciences Ctr.-Shreveport, Shreveport, LA
Vascular smooth muscle cells undergo a phenotypic shift to a "synthetic" phenotype during atherosclerosis characterized by downregulation of contractile markers and augmented proliferation, migration, and deposition of extracellular matrix. While absent in contractile, medial vascular smooth muscle, the receptor tyrosine kinase EphA2 is detectable in vascular smooth muscle within the plaque and in synthetic vascular smooth muscle cells *in vitro*, and deletion of EphA2 in ApoE knockout mice attenuates plaque size and progression characterized by a loss of smooth muscle and fibrous tissue content. However, the mechanisms driving EphA2 expression in vascular smooth muscle remains unknown. Both serum treatment and plating on provisional extracellular matrix proteins (e.g. fibronectin) are sufficient to induce EphA2 protein expression and transcriptional activation of the EphA2 promoter. While multiple factors in serum could contribute to EphA2 expression, treating vascular smooth muscle cells with individual growth factors (PDGF, FGF, EGF) or insulin failed to recapitulate the increase in EphA2 expression. However, depleting fibronectin from the serum significantly attenuated expression of EphA2, suggesting fibronectin may critically regulate smooth muscle EphA2 expression. This reduction in serum-induced EphA2 expression upon fibronectin depletion was further enhanced by siRNA knockdown of smooth muscle fibronectin expression, suggesting that both serum fibronectin and smooth muscle-derived fibronectin contribute to the enhanced EphA2 expression. Fibronectin binds to a distinct subset of RGD-binding integrins, and blocking fibronectin-integrin interactions or inhibiting specific fibronectin-binding integrins both attenuate EphA2 expression. Together these data identify a novel role for fibronectin-dependent integrin signaling in the induction of smooth muscle EphA2 expression during phenotypic transition.
A.C. Finney: None. **J.M. Green:** None. **J.G. Traylor:** None. **A. Orr:** None.

This research has received full or partial funding support from the American Heart Association.

89
Role of LncRNA *Snhg18* in Diabetes Induced Macrophage Dysfunction and Atherosclerosis
Rituparna Ganguly, Marpadga A Reddy, Zhuo Chen, Vishnu Amaram, Anita Bansal, Linda Lanting, Rama Natarajan, Beckman Res Inst of the City of Hope, Duarte, CA

Atherosclerotic vascular disease is the major cause of mortality in diabetic patients. Evidence from our laboratory and others showed that long non-coding RNAs (lncRNAs) play important roles in diabetic vascular complications. Here we investigated role of lncRNAs in hyperglycemia-induced macrophage dysfunction and accelerated atherosclerosis in diabetes. Hyperglycemia (~300-400 mg/dl) was induced in atherosclerosis-prone ApoE$^{-/-}$ mice by low dose Streptozotocin injections (50mg/kg/day i.p., 5 days) and were sacrificed at 20 weeks' post diabetes. Aortic root F4/80 immunohistochemistry and morphometric analysis showed increased macrophage infiltration and enhanced atherosclerosis respectively in diabetic vs non-diabetic ApoE$^{-/-}$ mice. RNA-seq analysis identified ~45 up-regulated lncRNAs in bone marrow macrophages (BMM) from diabetic versus non-diabetic ApoE$^{-/-}$ mice. Among these, one of the robustly induced (~7.5 $\log_2$fold) lncRNA candidate was small nucleolar RNA host gene 18 (*Snhg18)* located on mouse chromosome 15. Gene expression analysis by RT-qPCR validated *Snhg18* upregulation in BMM from diabetic ApoE$^{-/-}$ mice and in peritoneal macrophages from type 2 diabetic db/db vs control db/+ mice. Moreover, diabetic-ApoE$^{-/-}$ aortic tissue also demonstrated increased expression of *Snhg18 as* compared to non-diabetic ApoE$^{-/-}$*s.* Additionally, *Snhg18* was significantly increased in high glucose (HG) (25mM) treated RAW mouse macrophages *in vitro.* A human ortholog, *SNHG18*, located on chromosome 5 was also significantly increased in HG treated human THP1 monocytes. Cellular fractionation of RAW macrophages demonstrated that *Snhg18* was localized in both cytoplasmic and nuclear compartments. Overexpression of *Snhg18* in RAW macrophages significantly increased expression of proinflammatory (*Il1b*, *Il6*, and *Tnf)* and proatherogenic (*Thbs1*) genes but downregulated a nearby gene, *Semaphorin 5A* (*Sema5a).* These results suggest that diabetes induced lncRNA *Snhg18* upregulates macrophage inflammatory phenotype to modulate diabetes induced accelerated macrophage dysfunction and atherosclerosis development.
R. Ganguly: None. **M. Reddy:** None. **Z. Chen:** None. **V. Amaram:** None. **A. Bansal:** None. **L. Lanting:** None. **R. Natarajan:** None.

90
Slc44a2 Deficient Mice Exhibit Less Severity of Thrombosis in a Stenosis Model of Deep Vein Thrombosis
Chrissta X Maracle, Julia Tilburg, Leiden Univ Medical Ctr, Leiden, Netherlands; Gaia Zirka, Aix-Marseille Univ, INSERM, Marseille, France; Lieke van den Heijkant, Leiden Univ Medical Ctr, Leiden, Netherlands; Pierre E Morange, Aix-Marseille Univ, INSERM & APHM, CHU de la Timone, Marseille, France; Bart J van Vlijmen, Leiden Univ Medical Ctr, Leiden, Netherlands; Grace M Thomas, Aix-Marseille Univ, INSERM, Marseille, France

Background/Objective: Recent genome wide association studies identified *SLC44A2* as a novel susceptibility locus for venous thromboembolism (VTE), a region encoding the solute carrier family 44 member 2 protein (SLC44A2). Here we utilize *Slc44a2* deficient mice (KO) to determine the importance of SLC44A2 in thrombotic disease. **Methods:** Mice lacking *Slc44a2* were included in two models of venous thrombosis: 1) a spontaneous thrombosis model using siRNA targeting anti-coagulants *Serpinc1* and *Proc* and 2) a model of deep vein thrombosis (DVT) induced by flow restriction (stenosis) of the inferior vena cava (IVC). **Results:** In the model of spontaneous thrombosis, *Slc44a2* deficiency did not affect incidence as occurrence of thrombotic phenotype reached 100% in both wild type (WT; 12/12) and KO (12/12) mice 32 hours after siRNA injection. Platelet counts and fibrin deposition in the liver were also comparable. However, levels of circulating neutrophils were significantly higher ($p=0.0017$) in KO mice along with substantially lower amounts of plasma VWF antigen ($p<0.0001$). As these findings suggested a link between SLC44A2 and neutrophil function, a DVT model previously determined to be neutrophil dependent, was also employed. After 48 hours of IVC stenosis, 100% of the WT mice developed an occlusive thrombus (10/10) whereas 80% of the mice lacking *Slc44a2* did (12/15). Thrombus length was significantly reduced in KO animals ($p=0.0184$), as was thrombus weight ($p=0.0413$). Immunhistochemical staining of the thrombi revealed different repartitions in the "white" (platelet-rich) over the "red" (RBC-rich) parts of the thrombi depending on the mouse genotype. This observation suggests a different blood cell mobilization at the site of stenosis depending of the genotype. Plasma VWF levels were correlated with thrombus weight in WT ($p=0.0175$), but not in KO mice ($p=0.3266$), and had been previously confirmed to be lower in KO mice. **Conclusion**: These

findings corroborate the original GWAS data, indicating a role for SLC44A2 in thrombotic disease. We have observed that SLC44A2 was not involved in a platelet-dependent model of thrombosis whereas it is involved in a thrombosis model where neutrophils and VWF have been shown to play a crucial role.
C.X. Maracle: None. **J. Tilburg:** None. **G. Zirka:** None. **L. van den Heijkant:** None. **P.E. Morange:** None. **B.J.M. van Vlijmen:** None. **G.M. Thomas:** None.

95
Comparison of Various Anthropometric Indices for the Identification of a Predictor of Incident Hypertension
Jung Ran Choi, Yonsei Univ, Wonju, Korea, Republic of

We compared the predictive capability of weight, waist circumference (WC), waist-to-height ratio (WHtR), waist-to-hip ratio (WHR), body mass index (BMI), body roundness index (BRI), and a body shape index (ABSI) to identify incident hypertension, and to determine whether any of these indices may be used as a better single predictor of incident hypertension. A total of 1,718 populations aged 39-72 years were collected in a longitudinal study. Logistic regression models were used to evaluate various anthropometric indices as significant predictors of hypertension. During 2.8 years of follow-up, 185 new cases of hypertension (10.8%) were reported. The BRI and ABSI were significantly higher in the participants who had developed hypertension than in those who had not (4.15±1.01 vs. 3.57±1.03, 0.80±0.04 vs. 0.78±0.05; respectively, p<0.001). After adjusting for confounding variables, logistic regression analysis indicated that participants within the highest quartile of WC and WHtR were 4.79 and 4.51 times more likely to have hypertension than those within the lowest quartile (OR 4.79, 95% CI 2.49-9.20 vs. OR 4.51, 95% CI 2.41-8.43, respectively, p<0.0001); in contrast, no such correlation was found for BMI, WHR, BRI, and ABSI. WC (AUC: 0.672) showed a more powerful predictive ability for hypertension (p<0.0001) than BMI (AUC: 0.623), and an equal predictive power for hypertension as WHtR (AUC: 0.662) and BRI (AUC: 0.662) in the general population. We concluded that WC and/or WHtR but not BMI, showed superior prediction capability compared to WHR, BRI and ABSI, for determining the incidence of hypertension in a community-based prospective study.
J. Choi: None.

96
Comparison of Different Metabolic Syndrome Definitions for the Risks of Arterial Stiffness and Diabetes
Sung-Sheng Tsai, **Pao Hsien Chu**, Chang Gung Memorial Hosp, Taipei, Taiwan

Context. The reported clinical outcomes of the metabolic syndrome (MetS), including cardiovascular disease and diabetes, vary according to the definitions used. *Objective.* To compare the performance of the Adult Treatment Panel III/ American Heart Association/National Heart, Lung, and Blood Institute (ATP III/AHA/NHLBI) and International Diabetes Federation (IDF) criteria for the risks of arterial stiffness and diabetes. *Design, Setting, Participants, and Outcome Measures.* In this Chinese population-based cross-sectional study, we screened subjects from a Health Examination Program from 1999-2015. The MetS scores were determined according to the ATP III/AHA/NHLBI and IDF criteria. A brachial-ankle pulse wave velocity (baPWV) ≧1400 cm/s indicated more severe arterial stiffness, and a high fasting glucose level ≧6.99 mmol/L or postprandial glucose level ≧11.10 mmol/L indicated diabetic-level hyperglycemia. Comparisons of the areas under receiver operating characteristic curves (AUC-ROC) for both MetS scores to predict a higher baPWV and diabetic-level hyperglycemia were evaluated. *Results.* Among the 26735 enrolled subjects (mean age 55 ± 12 years), 6633 (24.8%) and 7388 (27.6%) were classified as having MetS according to the ATP III/AHA/NHLBI and IDF criteria, respectively. The AUC-ROC for the ATP III/AHA/NHLBI-MetS score were higher than those for the IDF-MetS score (0.685 vs. 0.595 to predict a higher baPWV, P < 0.001; 0.791 vs. 0.665 to predict diabetic-level hyperglycemia, P < 0.001). *Conclusions.* To the best of our knowledge, this is the first study to show that through a holistic approach, the predictive performance of the ATP III/AHA/NHLBI-MetS score for the risks of arterial stiffness and diabetes was superior to the IDF-MetS score.
S. Tsai: None. **P. Chu:** None.

97
Diagnosis of Atherosclerotic Coronary Heart Disease using Plasma Extracellular Vesicle Proteins
Dominique P de Kleijn, Farahnaz Waissi, Mirthe Dekker, Ingrid Bank, UMC Utrecht, Vascular Surgery, Utrecht, Netherlands; Arjan Schoneveld, UMC Utrecht, Experimental Cardiology, Utrecht, Netherlands; Arend Mosterd, Meander MC, Amersfoort, Netherlands; Leo Timmers, UMC Utrecht, Cardiology, Utrecht, Netherlands

Atherosclerosis is the underlying syndrome of Cardiovascular Disease (CVD). Ischemic Heart Disease and Stroke are cardiovascular events both due to atherosclerosis that are the number 1 and 2 cause of death in the world and expect to increase especially in Asia.
Ischemic heart disease (IHD) comprises 3 entities: stable coronary artery disease (SCAD), unstable angina (UA) and myocardial infarction (MI). Despite its large numbers, diagnosis IHD is challenging, as many patients present with atypical symptoms with women have a different symptom sensation than men. Troponins are the main diagnostic tool for detection of MI. Blood biomarkers for SCAD (typically causing stable angina) and UA, however, are not available. These diagnoses frequently require hospital visits/admissions for time-consuming and costly (non)invasive tests.
Extracellular vesicles are composed of a lipid bilayer containing cytosolic, membrane and nuclear molecules derived from the cell and cell compartments of origin and released by the cell into extracellular biofluids. Using proteomics, we identified a plasma extracellular vesicle protein signature of inflammatory and coagulation proteins in different plasma vesicle subpopulations that can identify UA and SCAD patients. This signature was verified for UA in 60 acute chest pain patients (AUC 0.93), and for SCAD in 60 chest pain patients scheduled for heart perfusion imaging (AUC 0.86).
This shows that plasma extracellular vesicle proteins can be used for early diagnosis of SCAD and UA and underlines the biological role for extracellular vesicles in atherosclerosis.
D.P.V. de Kleijn: None. **F. Waissi:** None. **M. Dekker:** None. **I. Bank:** None. **A. Schoneveld:** None. **A. Mosterd:** None. **L. Timmers:** None.

98
Next Generation MicroRNA Sequencing to Identify Coronary Artery Disease Patients at Risk of Recurrent Myocardial Infarction
Sri Harsha Kanuri, Joseph Ipe, Kameel Kassab, Todd C Skaar, Howard J. Edenberg, Yunlong Liu, Hongyu Gao, Rolf Peter Kreutz, Indianapolis Sch of Med, Indianapolis, IN

Background: Circulating miRNA have the potential to become reliable biomarkers for risk stratification and early detection of cardiovascular events.
Methods: In a single center cohort study, whole blood was collected from 437 subjects undergoing cardiac catheterization, who were followed for recurrent cardiovascular events during a mean follow up of 1.5 years. We selected a case cohort (n=22) with recurrent thrombotic events on standard medical therapy (stent thrombosis (n=6) or spontaneous myocardial infarction (MI) (n=16)) and a matched cohort with CAD, but uneventful clinical follow up (n=26), as well as a control group with cardiovascular risk

factors, but without angiographic CAD (n=24). We performed complete miRNA next generation sequencing of RNA extracted from whole blood samples (including leukocytes and platelets).
Results: Differential pattern of miRNA expression was demonstrated between controls, CAD patients with no events, and CAD patients with recurrent events (figure). MiRNA that have been previously associated with MI, CAD, endothelial function, vascular smooth muscle cells, platelets, angiogenesis, heart failure, cardiac hypertrophy, arrhythmia, and stroke were replicated in our CAD case-control cohorts. Twenty miRNA (FDR<0.05) were linked with risk of recurrent myocardial infarction and stent thrombosis, as compared to CAD patients with uneventful follow up.
Conclusions: MiRNA next generation sequencing demonstrates altered fingerprint profile of whole blood miRNA expression among subjects with subsequent recurrent coronary thrombotic events on standard medical therapy ('non-responders'), as compared to subjects with no recurrent cardiovascular events. MiRNA profiling may identify high risk subjects and provide additional insights into disease mechanisms not currently attenuated with standard medical therapy used in treatment of CAD.

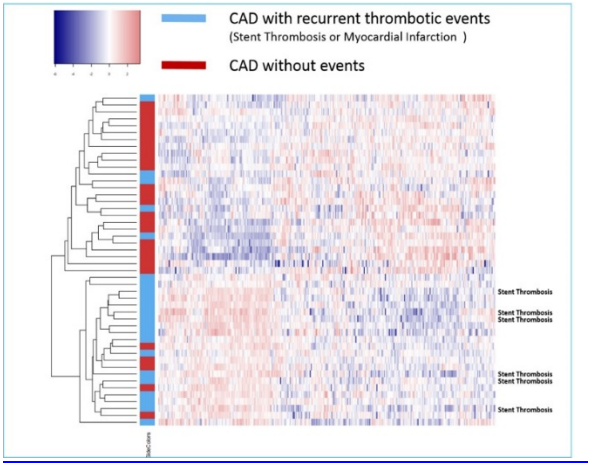

S. Kanuri: None. **J. Ipe:** None. **K. Kassab:** None. **T. Skaar:** None. **H. Edenberg:** None. **Y. Liu:** None. **H. Gao:** None. **R. Kreutz:** None.

99
Anti-atherosclerotic Effect of Il-1beta Blocker *in vitro*
Bo Rahm Kim, Seoul Natl Univ Bundang Hosp, Seongnam, Korea, Republic of; Eu Jeong Ku, Chungbuk Natl Univ Hosp, Cheongju, Korea, Republic of; Hye Li Lim, Tae jung Oh, Sung Hee Choi, Seoul Natl Univ Bundang Hosp, Seongnam, Korea, Republic of

Anakinra, an IL-1beta receptor antagonist, is a drug used to treat rheumatoid arthritis. To investigate the anti-atherosclerotic effect of anakinra, we plan to examine an anti-inflammatory effect of anakinra in various cell types including Human Umbilical Vein Endothelial Cells (HUVEC) and rat aortic smooth muscle cells (RaoSMC). To induce the inflammation, differentiated THP-1 cells from monocytes to macrophage with PMA treatment were stimulated by LPS and TNFα. Conditioned medium of THP-1 cells were treated to HUVEC and RAoSMC with or without anakinra. Inflammatory gene expeessions were analyzed by quantitative real-time polymerase chain reaction (qRT-PCR) and protein expressions were analyzed by western blot.In results, anakinra treatment significantly reduced the expression of inflammatory genes such as IL-1beta, IL-18 and NLRP3 in HUVEC and RaoSMC. Also, phosphorylation of p65 and jNK were decreased in Rao SMC.These results suggest that anakinra improves anti-inflammatory effects in HUVEC and RAoSMC.

B. Kim: None. **E. Ku:** None. **H. Lim:** None. **T. Oh:** None. **S. Choi:** None.

100
High-throughput Screening of FDA-approved Drugs Identifies Novel Inhibitors of Macropinocytosis
Hui-Ping Lin, Pushpankur Ghoshal, Bhupesh Singla, Jessica L Faulkner, Mary C Shaw, Paul M O'Connor, Jin-Xiong She, Eric J Belin de Chantemele, Gábor Csányi, Augusta Univ, Augusta, GA

Aims: Macropinocytosis has been implicated in atherosclerosis, cancer, allergic disorders, and other pathologies. Unfortunately, most currently available pharmacological inhibitors of macropinocytosis interrupt other endocytic processes and have non-specific endocytosis-independent effects. The goal of the present study was to perform a high-throughput screen (HTS) of FDA-approved drugs to identify new, clinically relevant inhibitors of macropinocytosis. Methods: In the present study, 640 FDA-approved compounds were tested for their ability to inhibit macropinocytosis. A series of secondary assays were performed to confirm inhibitory activity, determine IC_{50} values, and investigate cell toxicity. The ability of identified hits to inhibit phagocytosis, clathrin- and caveolin-mediated endocytosis was also investigated. Scanning electron microscopy and molecular biology techniques were utilized to investigate the mechanisms by which selected compounds inhibit macropinocytosis. Results: The HTS campaign identified 14 compounds that at ~10 µM concentration inhibit >95% of macropinocytotic solute internalization. Our results demonstrated that three lead compounds, namely imipramine, phenoxybenzamine, and vinblastine, potently inhibit ($IC_{50} \leq 130$ nM) macropinocytosis without exerting cytotoxic effects or inhibiting other endocytic pathways. Mechanistically, we found that imipramine inhibits translocation of ADP-ribosylation factor 6 to the plasma membrane and prevents membrane ruffle formation, a critical early step leading to macropinocytosis. Imipramine inhibited macropinocytosis in multiple cell types, including cancer cells, dendritic cells, and macrophages. Finally, incubation of macrophages with imipramine inhibited nLDL macropinocytosis and foam cell formation *in vitro*. Innovation and Conclusion: The identified macropinocytosis inhibitors may prove useful as new pharmacological tools to more fully discern the role of macropinocytosis in pathological processes and as therapeutic agents in various disorders involving macropinocytosis.
H. Lin: None. **P. Ghoshal:** None. **B. Singla:** None. **J.L. Faulkner:** None. **M.C. Shaw:** None. **P.M. O'Connor:** None. **J. She:** None. **E.J. Belin de Chantemele:** None. **G. Csányi:** None.

101
Noninvasive Venous Waveform Analysis (NIVA) for Volume Assessment
Reid McCallister, VoluMetrix, Nashville, TN; Bret Alvis, Susan Eagle, Vanderbilt Univ Medical Ctr, Nashville, TN; Kyle Hocking, VoluMetrix, Nashville, TN; Colleen Brophy, Vanderbilt Univ Medical Ctr, Nashville, TN

Background Current approaches to determine changes in intravascular volume are invasive, expensive, and of limited accuracy. Non-Invasive Venous Waveform Analysis (NIVA) uses a unique physiologic signal (the venous waveform) to obtain real-time measurement of intravascular blood volume. A prototype NIVA device was developed to assess blood volume in a porcine hemorrhage/resuscitation model. *Methods* The NIVA device was placed on a branch of the femoral vein of anesthetized pigs. Swan ganz catheters obtained pulmonary capillary wedge pressure (PCWP) and cardiac output (CO). Pigs were hemorrhaged in 100 mL increments to a total blood loss of 400mL, blood was re-infused and crystalloid was administered in 1 L increments to "over" resuscitate. Fast Fourier transformation and a

proprietary weighted algorithm was used to derive a NIVA score (LabChart, ADInstruments, Colorado Springs, CO). Statistical analyses (linear regressions) were performed using GraphPad Prism (GraphPad Software Inc, La Jolla, CA). *Results* NIVA correlated with absolute PCWP in experimental hemorrhage and over resuscitation in the porcine model (R=0.76, n=10, Figure 1). The correlations of *change* in NIVA and *change* in PCWP with volume changes were higher than the correlation of change in cardiac output with volume change (Table 1). *Conclusions* NIVA correlated with PCWP, and represents a novel physiologic signal to interrogate for non-invasive assessment of volume status, that may be useful for perioperative management. This study provides proof of concept for the NIVA prototype device and algorithm in measurement of intravascular volume.

Figure 1. Correlation between NIVA score and PCWP in a porcine hemorrhage and overload resuscitation model

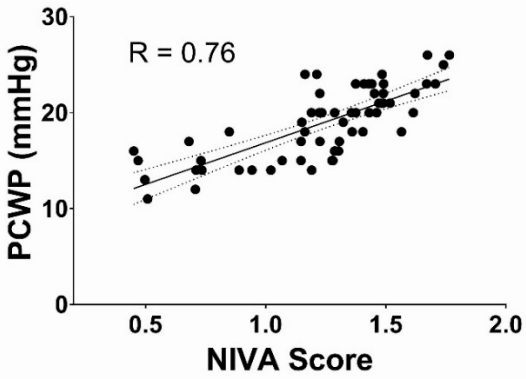

Table 1. Correlation (R Value) of change in NIVA score and change in central hemodynamic parameters with volume change in a porcine hemodynamic model

	Δ CO	Δ PCWP	Δ NIVA
Δ Volume	0.59	0.91	0.68

R. McCallister: Employment; Significant; VoluMetrix. **B. Alvis:** None. **S. Eagle:** Ownership Interest; Significant; VoluMetrix. **K. Hocking:** Ownership Interest; Significant; VoluMetrix. **C. Brophy:** Ownership Interest; Significant; VoluMetrix.

102
Semi-Automatic Measurement of External and Luminal Diameter Predicts the Four-Year Prognosis of Small Abdominal Aortic Aneurysms
Marko Bogdanovic, Moritz Lindquist Liljeqvist, Rebecka Hultgren, Karolinska Instt, Stockholm, Sweden; Christian Gasser, Royal Inst of Technology, Stockholm, Sweden; Joy Roy, Karolinska Instt, Stockholm, Sweden

OBJECTIVE: Predicting which abdominal aortic aneurysms (AAA) will require surgery and which may remain stable remains a challenge. We set out to evaluate whether semi-automatic diameter measurements and finite element analysis (FEA) might predict the four-year prognosis of AAAs more precisely than standard diameter measurements. METHODS: From a retrospective dataset of 97 patients with aneurysm baseline diameter of 40-50 mm, 39 AAAs remained below 55 mm in diameter for four years whilst 58 expanded beyond 54 mm within four years, or were treated surgically. Standard diameters, measured by radiologists or vascular surgeons, were recorded at baseline and at follow-up. Maximal external and luminal diameters as well as total and luminal volume were semi-automatically re-measured from 3D models based on CT images. FEA, estimating the peak wall rupture index (PWRI), was subsequently performed. Further, in 94 patients from the dataset, standard diameter growth rates between baseline and follow-up were calculated. RESULTS: Aneurysms that would require surgery within four years were identified with 100% specificity by semi-automatic diameter, n=13 (22%), luminal diameter, n=14 (24%), PWRI, n=7 (12%), and luminal volume, n=5 (8.6%). Neither standard diameter nor total volume could reach 100% specificity. AAA diameter growth rate correlated with baseline semi-automatic diameter (r=0.39, p=9.2e-5), luminal diameter (r=0.29, p=0.005) and luminal volume (r=0.23, p=0.027) but not with PWRI (r=0.17, p=0.094), total volume (r=0.16, p=0.13), nor standard diameter (r=0.14, p=0.17). CONCLUSION: In AAAs with small diameters, precise, semiautomatic measurement of the maximal external and luminal diameter is able to specifically identify aneurysms requiring surgery within four years.
M. Bogdanovic: None. **M. Lindquist Liljeqvist:** None. **R. Hultgren:** None. **C. Gasser:** Ownership Interest; Significant; Shareholder and scientific advisor of VASCOPS GmbH. **J. Roy:** None.

103
Local Mir-29b Inhibition Using Drug-eluting Balloons Blocks Abdominal Aortic Aneurysm Expansion in Atherosclerotic Ldlr-/- Mini-pigs
Albert Busch, Lars Maegdefessel, Dept for Vascular and Endovascular Surgery, Munich, Germany

Introduction: Abdominal aortic aneurysm (AAA) is a major challenge in vascular surgery practice due to high morbidity and mortality, especially in case of rupture. Despite open surgery or endovascular stent implantation, no therapeutic option remains to clinicians. Micro-RNAs (miR) have emerged as novel therapeutic targets in the cardiovascular field. For translational research, animal models mimicking human disease are crucial, however, most often a compromise between size, cost and features similar to human disease limits the translational value.
Material and Methods: We used the homozygote low-density lipoprotein receptor (LDLR) knockout (KO) Yucatan mini-pig to create a human-relevant animal model for AAA. Local application of porcine pancreatic elastase was applied to the infrarenal aorta for aneurysm inductions. Vascular ultrasound and CT was used for follow-up examination. 8 days after induction, catheter-guided anti-miR-29b coated balloon angioplasty was performed. Animals were sacrificed after 30 days. PCR and immunohistochemistry were used for further characterization of the model.
Results: The LDLR KO is hypercholesterolemic and shows severe atherosclerosis in the infrarenal aorta. Aneurysms can be induced by local elastase application for 10 minutes and the aortic diameter increases by 60% over the course of four weeks. Despite atherosclerosis, the aneurysmatic vessel wall shows many features of human disease such as inflammation, extracellular matrix remodeling, angiogenesis and vascular smooth muscle cell phenotype switch. Targeted delivery by balloon angioplasty is feasible and anti-miR-29b penetrates through all layers of the aortic wall, eventually inducing local matrix remodeling. Anti-miR-29b treated animals had significantly smaller AAAs, while not showing any signs of off-target effects.
Conclusion: Elastase perfusion in atherosclerosis-prone pigs is a feasible pre-clinical AAA model with many features similar to human disease. Locally balloon-delivered anti-miR-29b induces a pro-fibrotic response, halting aneurysm growth.
A. Busch: None. **L. Maegdefessel:** None.

104
Aortic Dilation and Elasticity in Thoracic Aortic Aneurysm in a Marfan Model is Sexually Dimorphic
Jeff Z Chen, Hisashi Sawada, Jessica Moorleghen, Alan Daugherty, Univ of Kentucky, Lexington, KY

Objective: Meta-analysis of data derived from Marfan patients in the Genetically-Triggered Thoracic Aortic Aneurysms and Cardiovascular Conditions (GenTAC) consortium revealed that thoracic aortic aneurysms occur more frequently in men than in women. To determine the characteristics of sexual dimorphism in experimental thoracic aortic aneurysms of a Marfan model, we determined ascending aortic and aortic root morphology in male and female fibrillin-1 haploinsufficent (FBN1 C1041G/+) mice using ultrasonography.
Method and Results: Aortas from 4 to 6 week old male and female FBN1 C1041G/+ mice and their wild type littermates were assessed by high frequency ultrasonography. Mice were anesthetized and maintained at a heart rate of 450-550 beats per minute. Ultrasound images were captured using a Vevo 3100 instrument with a 40 MHz tranducer. The maximal luminal diameter of ascending aortic between the sinotubular junction and the innominate artery, and the aortic root diameter at the sinus of valsalva, were measured in mid-systole and end-diastole by two independent observers who were blinded to mice identity. FBN1 C1041G/+ mice demonstrated greater ascending aortic dilation in male mice compared to female mice, whereas no difference in aortic root diameter were detected between male and female wild type littermates. In addition, modest ascending aortic dilation was detected before aortic root dilation in FBN1 C1041G/+ mice. Ascending aortas from FBN1 C1041G/+ mice also demonstrated loss of elasticity as evidenced by reduced expansion in systole. Interestingly, this difference was detected much earlier than expected.
Conclusion: The fibrillin-1 haploinsufficent model of Marfan syndrome associated thoracic aortic aneurysm demonstrate sexual dimorphism in ascending aortic dilation. Loss of elasticity in the ascending aorta is also an early manifestation in this thoracic aortic aneurysm model.
J.Z. Chen: None. **H. Sawada:** None. **J. Moorleghen:** None. **A. Daugherty:** None.

105
Increased Circulating Trimethylamine N-oxide (TMAO) Augments the Incidence of Abdominal Aortic Aneurysm in Low Penetrant C57BL/6J Mice
Kelsey Conrad, Shannon Jones, Robert Helsley, Rebecca Schugar, Zeneng Wang, Stanley Hazen, Mark Brown, A. Phillip Owens III, Univ of Cincinnati, Cincinnati, OH

Background: The gut microbiota is a metabolically active endocrine organ critical to the maintenance of cardiovascular health. Dietary sources of choline are metabolized by microbial enzymes to form trimethylamine (TMA). Metabolism by the host hepatic enzyme flavin-containing monooxygenase 3 (FMO3) converts TMA to the pro-inflammatory molecule trimethylamine N-oxide (TMAO). Human clinical trials have correlated high levels of circulating TMAO to an increased risk of cardiometabolic diseases. However, this meta-organismal pathway has not been evaluated in the context of abdominal aortic aneurysm (AAA). The objective of this study was to determine the effects of a high choline diet on the development of AAA. Methods: C57BL/6J male (n=20) and female (n=20) mice were fed either a standard chow control diet (n = 10 each sex) or a choline-rich diet (1%; n = 10 each sex) for 5 weeks. After 1 week of diet, basal abdominal ultrasounds were performed and angiotensin II (AngII; 1,000 ng/kg/min) was infused for 28 days via implantation of osmotic minipumps. Termination ultrasounds were performed on day 27 and mice were sacrificed on day 28. Aortas were harvested for evaluation of aneurysm progression and plasma was analyzed for the metabolites TMA, TMAO, and choline. To determine whether TMAO was elevated in human patients with AAA, plasma samples from participants with fast growing AAAs (n = 85), slow growing AAAs (n = 84), and normal (non-aneurysmal) aortas (n = 115) were analyzed for plasma TMAO levels via liquid chromatography tandem mass spectrometry (LC-MS/MS). Results: Administration of a choline-rich diet augmented the incidence ($P < 0.02$) and aortic diameter ($P < 0.001$) of AAAs in both male and female mice versus placebo-fed mice. Plasma levels of TMA, TMAO, and choline were significantly elevated in choline-fed mice versus normal chow ($P < 0.05$). Importantly, circulating levels of plasma TMAO were significantly elevated in a step-wise fashion with the rate of aneurysm growth versus non-aneurysmal control patients (fast growing > slow growing > normal patients; $P < 0.001$). Conclusions: Our results indicate increases in circulating TMAO augments the growth status of aneurysms in human patients and the incidence of AAA in a low penetrant C57BL/6J mouse model.
K. Conrad: None. **S. Jones:** None. **R. Helsley:** None. **R. Schugar:** None. **Z. Wang:** None. **S. Hazen:** None. **M. Brown:** None. **A. Owens III:** None.

106
Young *Tgfbr2*$^{G357W/+}$ Mice Have Decreased Expression of TGF-β Ligands and Receptors in the Proximal Aorta, Aortic Root Dilation, and Aortic Elongation
Jie H Hu, Stoyan N Angelov, Jay Zhu, Maxwell Weil, Alexandra Smith, David A Dichek, Univ Washington, Seattle, WA

Introduction *Tgfbr2*$^{G357W/+}$ mice have a loss-of-function *Tgfbr2* allele (*G357W*) that is orthologous to an allele found in humans with Loeys-Dietz syndrome (LDS). *Tgfbr2*$^{G357W/+}$ mice have kyphosis, aortic dilation and elongation, and die suddenly from aortic rupture. Elevations of mRNA encoding TGF-β ligands in cultured vascular smooth muscle cells from *Tgfbr2*$^{G357W/+}$ mice and LDS patients—as well as increased expression of *Tgfb1* and *Col1a1* and elevation of both P-Smad2 and P-ERK1/2 in aortic roots of older (24-36-week) *Tgfbr2*$^{G357W/+}$ mice—suggest that paradoxically increased TGF-β signaling might be responsible for aortic pathology in LDS. **Hypothesis** We hypothesized that downregulation of TGF-β signaling components accompanies the development of aortic pathology in young *Tgfbr2*$^{G357W/+}$ mice. **Methods** We performed anatomic and gene-expression studies on 8- and 12-wk-old *Tgfbr2*$^{G357W/+}$ mice and wild type (WT) littermates. For anatomic studies, mice were perfusion-fixed with formalin, and aortic length was measured in situ. Aortic roots as well as ascending (ASA), descending thoracic (DTA) and abdominal aortas (AA) were then embedded in OCT. Frozen sections were stained with H & E. External and internal elastic lamina lengths, aortic wall thickness and medial areas were measured. For gene expression studies, mice were saline-perfused, and the aortic root, ASA, and arch were snap frozen en bloc. RNA was extracted and TGF-β ligand and receptor mRNA were measured. **Results** LDS mice (12 wk old; n = 7-9 vs 12 WT) had elongated ASA, arch, and DTA (~20%; P≤0.02), their aortic roots were dilated (20%; P<0.001), and their DTA wall thickness and medial areas were decreased (15%; P<0.01). No aortic wall hematomas were observed, and Prussian Blue staining was absent in aortic sections. mRNA encoding *Tgfb1*, *Tgfb2*, *Tgfbr1, Tgfbr3, Serpine1,* and *LoxL1* were decreased in LDS mouse aortas (20-34%; P<0.05 for all; n=9-10). LDS mice (8 wk old; n = 10 vs 12 WT) had only borderline decreased aortic *Tgfbr1* mRNA. **Conclusions** In *Tgfbr2*$^{G357W/+}$ mice, development of aortic pathology is accompanied by decreased expression of several TGF-β signaling pathway components. These data suggest that the *G357W* loss-of-function allele causes aortopathy via an early reduction of aortic TGF-β signaling.
J.H. Hu: None. **S.N. Angelov:** None. **J. Zhu:** None. **M. Weil:** None. **A. Smith:** None. **D.A. Dichek:** None.

107
High Plasma Levels of Low-density Lipoprotein-cholesterol Accelerate Dissecting Aortic Aneurysms in Angiotensin II-induced Mice
Yasunori Iida, Dept of Cardiovascular Surgery, Keio Univ Sch of Med, Tokyo, Japan; Hiroki Tanaka, Dept of Medical Physiology, Hamamatsu Univ Sch of Med, Hamamatsu, Japan; Shigeharu Sawa, Dept of Cardiovascular Surgery, Ogikubo Hosp, Tokyo, Japan; Hideyuki Shimizu, Dept of Cardiovascular Surgery, Keio Univ Sch of Med, Tokyo, Japan

Background—Plasma low-density lipoprotein (LDL)-cholesterol is implicated in aortic aneurysm (AA) and dissection (AD); however, its role in the pathogenesis of AA and AD, a disease with a high mortality rate, remains unknown. The existing animal models of aortic AA and AD do not reproduce all aspects of disease, including elevated LDL-cholesterol and spontaneous atheroma formation; therefore, a more reliable in vivo model is required. In this study, we show that mice with combined deficiency of the LDL-receptor and the catalytic component of the apolipoprotein B-edisome complex (*Ldlr*$^{-/-}$*/Apobec1*$^{-/-}$) induced with angiotensin II are a useful model to study the pathophysiology of AA and AD associated with human type IIa dyslipidemia. **Methods**—AAs and ADs were created in 18-22-week-old male *Apoe*$^{-/-}$ and *Ldlr*$^{-/-}$*/Apobec1*$^{-/-}$ mice by subcutaneous angiotensin II infusion. Immunostaining allowed assessment of smooth muscle cells and mural monocytes/macrophages. **Results—***Ldlr*$^{-/-}$*/Apobec1*$^{-/-}$ mice had elevated LDL-cholesterol levels characteristic for human type IIa dyslipidemia, resulting in atherogenesis, which promoted mortality, AA formation, and AD development. Interestingly, variations in the distribution of atheroma and inflammatory sites between *Apoe*$^{-/-}$ and *Ldlr*$^{-/-}$*/Apobec1*$^{-/-}$ mice depending on lipid profiles resulted in differences in AA formation and AD occurrence in the thoracic aorta. **Conclusions—**Our results indicate the presence of a pathogenic pathway involving serum lipid composition that plays a key role in AA formation and AD occurrence in angiotensin II-induced mice.

Y. Iida: None. **H. Tanaka:** None. **S. Sawa:** None. **H. Shimizu:** None.

108
Lipopolysaccharide Fails to Augment Development of Angiotensin II-induced Abdominal Aortic Aneurysms in Mice
Shayan Mohammadmoradi, Deborah A. Howatt, Jessica J Moorleghen, Hong Lu, Alan Daugherty, Saha Cardiovascular Res Ctr, Univ of Kentucky, Lexington, KY

Background and objective: Our previous study demonstrated that deficiency of toll-like receptor 4 (TLR4) reduced angiotensin II (AngII)-induced abdominal aortic aneurysms (AAAs) in hypercholesterolemic mice. Lipopolysaccharide (LPS) is a well-known agonist of TLR4. Interaction of LPS and TLR4 promotes inflammation and augments hypercholesterolemia-induced atherosclerosis. The purpose of this study was to determine whether LPS augments AngII-induced AAAs. **Methods and Results:** Low-density lipoprotein (LDL) receptor -/- mice fed a Western diet develop hypercholesterolemia and have augmentation of AngII-induced AAAs. We found that LDL receptor -/- mice fed Western diet had increased LPS concentrations, as quantified by a *Limulus Amebocyte* lysate chromogenic endotoxin quantitation kit, compared to the same mice prior to Western diet feeding. To determine whether LPS plays a role on AngII-induced AAAs, 4 groups of male C57BL/6J mice, 10-week-old, were infused subcutaneously with: (1) Vehicle (N=5), (2) LPS (250 μ g/kg/day; N=10), (3) AngII (1,000 ng/kg/min; N=10), or (4) both AngII and LPS (N=10) through Alzet mini osmotic pumps for 28 days. Abdominal aortic expansion was monitored serially at 2 and 4 weeks of infusion using high frequency ultrasonography (Vevo 3100 system; FUJIFILM). Continuous luminal expansion was detected in both AngII-infused mice and mice co-infused with both AngII and LPS. These results were confirmed by *ex vivo* measurements of maximal outer diameters of suprarenal aortas after termination showing AngII infusion led to significant increase of abdominal aortic dilation, compared to vehicle or LPS infused mice. However, co-infusion of LPS with AngII did not augment AngII-induced AAAs. **Conclusion:** LPS has no effects on AngII-induced AAAs in normolipidemic mice.

S. Mohammadmoradi: None. **D.A. Howatt:** None. **J.J. Moorleghen:** None. **H. Lu:** None. **A. Daugherty:** None.

This research has received full or partial funding support from the American Heart Association.

109
Exosomes from Mesenchymal Stem Cells Suppress Aortic Elastin Induced Inflammation in Macrophages
Adam Oskowitz, Michael Conte, UCSF, San Francisco, CA

Introduction: Mesenchymal Stem Cells (MSCs) from bone marrow have been shown to attenuate aortic aneurysm formation in a variety of rodent models. These effects appear to rely on modulation of systemic inflammation, including the attenuation of macrophage mediated inflammation. Elastin appears to play a significant role in inducing this inflammation and stimulating macrophages to express an M1 phenotype. Here we evaluate the effects human elastin and elastin break down products on macrophage phenotype. We also evaluate the role of human exosomes derived from MSCs on modulating the effect of elastin on macrophage phenotype.
Methods: Human peripheral blood monocytes were collected and cultured for six days to isolate human macrophages. The cells were then treated with digested elastin from human aortic tissue or the human peptide VGVAPG in combination with human MSCs or exosomes derived from human MSCs. The phenotype of the macrophages was then analyzed using enzyme linked immune sandwich assays for tumor necrosis factor alpha (TNF-a) secretion, quantitative real time PCR and flow-cytometry for cellular proteins.
Results: Macrophages cultured with digested elastin from aortic tissue showed a significant dose response increase in TNF-a production and cell surface markers consistent with an M1 phenotype. In addition, transcripts for pro-inflammatory cytokines significantly increased after exposure to digested elastin. Similar results were obtained using the elastin peptide sequence VGVAPG. Co-culture with MSCs significantly attenuated elastin induced macrophage TNF-a production, production of pro-inflammatory transcripts and M1 related proteins. When MSC derived exosomes were cultured with macrophages, pro-inflammatory markers and TNF-a production was reduced below baseline levels, even after stimulation with elastin peptide.
Conclusions: Macrophages develop an M1 phenotype in response to digested aortic elastin and elastin derived peptides. This response is significantly attenuated by exosomes derived from human MSCs

A. Oskowitz: None. **M. Conte:** None.

110
Exogenous Vasohibin-2 Does Not Influence Angiotensin II-induced Abdominal Aortic Aneurysms Formation in Either Normolipidemic or Apolipoprotein E-Deficient Mice
Nozomu Otaka, Haruhito Adam Uchida, Yoshiko Hada, Hidemi Takeuchi, Yuki Kakio, Dept of Nephrology, Rheumatology, Endocrinology and Metabolism, Okayama Univ Graduate Sch of Med, Dentistry, and Pharmaceutical Science, Okayama, Japan; MIchihiro Okuyama, Dept of Cardiovascular Surgery, Okayama Univ Hosp, Okayama, Japan; Ryoko Umebayashi, Katsuyuki Tanabe, Dept of Nephrology, Rheumatology, Endocrinology and Metabolism, Okayama Univ Graduate Sch of Med, Dentistry, and Pharmaceutical Science, Okayama, Japan; Yasufumi Sato, Dept of Vascular Biology, Inst of Development, Aging and

Cancer, Tohoku Univ, Miyagi, Japan; Jun Wada, Dept of Nephrology, Rheumatology, Endocrinology and Metabolism, Okayama Univ Graduate Sch of Med, Dentistry, and Pharmaceutical Science, Okayama, Japan

Objective: Chronic angiotensin II (AngII) infusion promotes both ascending (TAAs) and abdominal aortic aneurysms (AAAs) in mice. Previously, we demonstrated that exogenous vasohibin-2 (VASH-2) exacerbated AngII-induced TAAs in normolipidemic mice. The purpose of this study was to examine whether exogenous VASH-2 influenced AngII-induced AAAs in mice. **Methods and Results:** In the initial study, male C57BL/6J mice (10 weeks old) were injected with VASH2 or LacZ expressing adenovirus (Ad; 7.5 x 109 vp/100 μ L) via tail vein at 2 week intervals. One week after the first injection, subcutaneous infusion of AngII (1,000 ng/kg/min) by mini osmotic pumps was initiated for 3 weeks. Consequently, mice were divided into 2 groups: AngII + Ad VASH2 in C57BL/6J mice (n=22) and AngII + Ad LacZ in C57BL/6J mice (n=21). VASH-2 overexpression had no effect on systolic blood pressure, heart rate, body weight, or serum total cholesterol concentrations. Exogenous VASH-2 did not affect *ex vivo* measurements of maximal diameters of abdominal aortas (AngII + Ad VASH2; 1.36 ± 0.39 mm, AngII + LacZ 1.34 ± 0.24 mm, n.s.) in AngII-infused mice. In a subsequent study, male apolipoprotein E-deficient (apoE-/-) mice (9 to 13 weeks old) were injected with VASH2 or LacZ as described for C57BL/6J mice. Consequently, mice were divided into 2 groups: AngII + Ad VASH2 in apoE-/- mice (n=14) and AngII + Ad LacZ in apoE-/- mice (n=14). Similarly, overexpression of VASH-2 had no effect on systolic blood pressure, heart rate, body weight, or serum total cholesterol concentrations in apoE-/- mice. Furthermore, exogenous VASH-2 did not affect *ex vivo* measurement of maximal diameter of abdominal aorta (AngII + Ad VASH2; 1.70 ± 0.61 mm, AngII + Ad LacZ; 1.61 ± 0.43 mm, n.s.) in AngII-infused apoE-/- mice. **Conclusion:** Despite our previous demonstration of the effects on TAA, exogenous VASH-2 did not influence AngII-induced AAA formation in either normolipidemic or apoE-/- mice.
N. Otaka: None. **H.A. Uchida:** None. **Y. Hada:** None. **H. Takeuchi:** None. **Y. Kakio:** None. **M. Okuyama:** None. **R. Umebayashi:** None. **K. Tanabe:** None. **Y. Sato:** None. **J. Wada:** None.

112
IL-27 Receptor Signaling Potentiates Angiotensin II Induced Myelopoiesis and Promotes Abdominal Aortic Aneurysm
Iuliia Peshkova, **Iuliia Peshkova**, Turan Aghayev, Aliia Fatkhullina, Petr Makhov, Stephen Sykes, Ekaterina Koltsova, Fox Chase Cancer Ctr, Philadelphia, PA

Abdominal Aortic Aneurysm (AAA) is a vascular disease, where aortic wall degradation is mediated by accumulated immune cells. Several cytokines have been suggested to play role in AAA, however the role of cytokines in immune cell accumulation and AAA progression remains poorly defined. Here we report an unexpected role of IL-27R signaling in the development of AAA. We found that in an animal model of AAA, prolonged infusion of Angiotensin (Ang) II robustly induced AAA formation in hyperlipidemic *Apoe*$^{-/-}$ and *Apoe*$^{-/-}$*Il27ra*$^{+/-}$ mice but failed to do so in *Apoe*$^{-/-}$ *Il27ra*$^{-/-}$ mice. This mitigation of AAA formation in *Apoe*$^{-/-}$ *Il27ra*$^{-/-}$ mice was associated with a blunted accumulation of pathogenic myeloid cells in suprarenal aortas resulting from a reduction in Ang II-induced hematopoietic stem and progenitor cell (HSPCs) expansion. We found that in the absence of IL-27R signaling HSPCs were unable to fully downregulate p21 expression in response to Ang II, which impeded the ability of *Apoe*$^{-/-}$*Il27ra*$^{-/-}$ HSPCs to proliferate. Collectively, these data demonstrate that IL-27R signaling influences AAA development by activating emergency hematopoiesis in response to elevated Ang II. Further, they provide new insights into how the immunoregulatory cytokine IL-27 drives a prominent lethal vascular disease by distant regulation of stress/emergency hematopoiesis.
I. Peshkova: None. **I. Peshkova:** None. **T. Aghayev:** None. **A. Fatkhullina:** None. **P. Makhov:** None. **S. Sykes:** None. **E. Koltsova:** None.

113
Thoracic Aortic Aneurysms Associated With Bicuspid Aortic Valve Have Altered MicroRNA Expression
Stefanie S Portelli, Elizabeth N Robertson, The Univ of Sydney, Sydney, Australia; Ratnasari Padang, Royal Prince Alfred Hosp, Sydney, Australia; Murat Kekic, Donna Lai, Paul G Bannon, Brett D Hambly, Richmond W Jeremy, The Univ of Sydney, Sydney, Australia

Bicuspid aortic valve (BAV) is the most common congenital heart malformation, affecting 1-2% of the population. BAV is caused by fusion of two of the three aortic valve leaflets in the heart during foetal development. Progressive dilatation of the thoracic aorta, resulting in aneurysm (TAA), develops in approximately 50% of individuals with BAV, and can be fatal. The cause of BAV-TAA is undetermined, however, current understanding suggests that it is a complex interplay between genetic susceptibility and the abnormal haemodynamic stress generated by the malformed valve. Changes in the expression of post-transcriptional genetic modifiers, such as microRNA (miRNA), can alter protein expression and disrupt normal tissue function, contributing to disease. miRNA are also viable therapeutic targets with demonstrated success in disease treatment. We hypothesised that there is altered expression of miRNA in BAV-TAA tissue that contributes to TAA development. Total RNA was isolated from aortic tissue of 11 patients with BAV-TAA (Age 54 ± 12 years; M:F 10:1), and 6 normal controls with no aortic disease (Age 35 ± 18 years; M:F 4:2). RNA was reverse transcribed with primers for 818 different miRNA and qPCR was performed using Taqman® OpenArray® Human miRNA Panels. A significant difference in miRNA expression was defined as a >±2 fold change ($p<0.05$) compared to control. In BAV-TAA tissue, miR-214, miR-497, miR-22, miR-151-3p and miR-24 were significantly decreased. These miRNA have been previously implicated in the regulation of biological pathways relevant to BAV-TAA, including vascular smooth muscle cell (VSMC) injury and apoptosis, oxidative and shear stress, vascular relaxation, VSMC phenotype and TGF-beta signalling. Therefore, these miRNA may contribute to BAV-TAA pathogenesis, either as part of a compromised genetic background, or in relation to haemodynamic stress arising from BAV. This study has identified a novel expression profile of miRNA in BAV-TAA, and provides promising candidates for further exploration and treatment.
S.S. Portelli: None. **E.N. Robertson:** None. **R. Padang:** None. **M. Kekic:** None. **D. Lai:** None. **P.G. Bannon:** None. **B.D. Hambly:** None. **R.W. Jeremy:** None.

114
Smooth Muscle Origin-specific Effects of LRP1 Deletion on Angiotensin II-induced Ascending Aortic Aneurysm
Hisashi Sawada, Debra L Rateri, Bradley C Wright, Jessica J Moorleghen, Deborah A Howatt, Univ of Kentucky, Lexington, KY; Mark W Majesky, Univ of Washington Sch of Med, Seattle, WA; Alan Daugherty, Univ of Kentucky, Lexington, KY

Objective: Low-density lipoprotein receptor-related protein 1 (LRP1) plays a critical role in maintaining aortic wall integrity. LRP1 deletion in smooth muscle cells (SMCs) augments angiotensin II (AngII)-induced ascending aortic aneurysms. SMCs in the ascending aorta originate from both the second heart field (SHF) and cardiac neural crest (CNC). The purpose of this study was to determine whether LRP1 depletion in these two SMC origins has differential effects on AngII-induced ascending aortic aneurysm.
Methods and Results: Mef2c-Cre was used to delete LRP1 in SMCs of SHF origin; while Wnt-1-Cre was utilized to

delete LRP1 in SMCs of CNC origin in mice. Saline or AngII (1,000 ng/kg/min) was infused for 28 days into 12 - 14 week-old male mice with LRP1 depletion in either SHF or CNC origin as well as their wild type littermates. No mice died in saline-infused groups of either genotype. In the AngII-infused mouse group, LRP1 depletion in SMCs of SHF origin led to 38% death due to ascending aortic rupture, compared to a 4% rupture rate in wild type littermates ($p = 0.002$). In the survivors of AngII-infused group, LRP1 deletion in SMCs of SHF origin resulted in larger ascending aortic diameter compared to wild type littermates (1.6 ± 0.1 vs 2.0 ± 0.1 mm, $p < 0.05$), as measured by ultrasonography. In contrast to the increases of aortic rupture and luminal dilation in mice with LRP1 depletion in SMCs of SHF origin, LRP1 deletion in SMCs of CNC origin did not affect AngII-induced aortic rupture rate or luminal dilation, compared to wild type littermates. To explore potential signaling mechanisms on how LRP1 depletion in SMCs of SHF origin augments AngII-induced ascending aortic aneurysm, mice were infused with either saline or AngII for 24 hours, and ascending aortic tissues were harvested for Western blot analyses. Aortic LRP1 protein abundance was decreased in mice with LRP1 depletion in SMCs of SHF origin regardless of infusion. Although SMAD2 and ERK signaling contribute to aortic wall integrity, this short interval of AngII infusion did not change these activities in the aorta of SHF-SMC specific LRP1 deleted mice.
Conclusion: LRP1 expression in SHF, but not in CNC, -derived SMCs exerts a critical role in the augmentation of AngII-induced ascending aortic aneurysm.
H. Sawada: None. **D.L. Rateri:** None. **B.C. Wright:** None. **J.J. Moorleghen:** None. **D.A. Howatt:** None. **M.W. Majesky:** None. **A. Daugherty:** None.

115
AT2 Receptor Regulates Ascending Aortic Dilation during AT1 Receptor Blockade in Transverse Aortic Constriction Mouse Model
Zhen Zhou, Andrew M Peters, Shanzhi Wang, Jiyuan Chen, Erin Arthur, Dianna M Milewicz, UT Health Science Ctr at Houston, Houston, TX

Introduction: The angiotensin II (Ang II) type 1 receptor (AT1R) antagonist losartan can slow aortic enlargement in mouse models and patients with Marfan syndrome. We have previously shown that losartan attenuates aortic enlargement and remodeling induced by thoracic aortic constriction (TAC).
Objective: We investigated the role of the Ang II type 2 receptor (AT2R) in an acute hypertensive remodeling of the ascending aorta induced by TAC.
Methods: 160 male C57BL/6J mice were subjected to TAC surgeries with 27-gauge needle or sham surgery. Echocardiography measurements were performed 2 weeks post-operation using the Vevo 3100 imaging system. Blood pressure was measured in the ascending aorta using a Millar catheter introduced through the right common carotid artery.
Results: TAC induced significant enlargement in aortic root and ascending aorta two weeks after surgery. The angiotensin converting enzyme inhibitor, captopril, decreased intraluminal systolic blood pressure (SBP) to the same degree as losartan, but did not prevent the increased aortic dilation, adventitial inflammation, medial elastin breakage, or *Mmp9* expression compared with TAC mice. Captopril plus an AT2R agonist, compound 21 (C21) attenuated TAC-indcued aortic dilation, elastin break numbers and *Mmp9* expression similar to losartan, despite an increase in SBP compared with captopril-treated TAC mice. Consistent with these results, treatment with losartan and an AT2R antagonist, PD123319, reversed the protective effects of losartan on TAC-induced aortic enlargement and remodeling. Note that treating with captopril and a Mas receptor agonist AVE0991 did not prevent TAC-induced aortic enlargement. Importantly, treating with C21 alone did not prevent TAC-induced aortic dilation, elastin breakage or *Mmp9* expression despite significantly decreased SBP.
Conclusions: These data indicate signaling through both AT1R and AT2R are key modulators in aortic dilation and remodeling with acute increases in biomechanical forces induced by TAC and these protective effects are independent of alterations in blood pressure.
Z. Zhou: None. **A. Peters:** None. **S. Wang:** None. **J. Chen:** None. **E. Arthur:** None. **D. Milewicz:** None.

116
A Novel Mediator of Heart Failure Development and Progression- Role of Manganese Superoxide Dismutase
Sumitra Miriyala, Timothy Labrie, Mini Chandra, Benjamin Maxey, Wayne Orr, Smiriy@lsuhsc.edu Bhuiyan, Kevin McCarthy, Manikandan Panchatcharam, LSUHSC-Shreveport, Shreveport, LA

Manganese Superoxide Dismutase (MnSOD), an antioxidant enzyme that catalyzes the conversion of superoxide radicals ($O_2^{\bullet-}$) in mitochondria. Constitutive activation mitochondrial reactive oxygen species (ROS) has been implicated in both the pathogenesis and the progression of cardiovascular disease. Absence of SOD2 (gene that encodes MnSOD) is found to be embryonic lethal in animal models due to impairment of mitochondrial function, most noticeably in the heart. In our earlier investigation, we have shown that the MnSOD mimetic, MnTnBuOE-2-PyP^{5+} distributes 3-fold more in mitochondria than in cytosol. The exceptional ability of MnTnBuOE-2-PyP^{5+} to dismute $O_2^{\bullet-}$ parallels its ability to reduce ONOO− and CO3−. Based on our earlier reports, we have generated mice that specifically lack MnSOD in cardiomyocytes (Myh6-SOD2$^{\Delta}$). These mice showed early mortality ~4 months due to cardiac mitochondrial dysfunction. Oxidative phosphorylation (OXPHOS) in mitochondria is the predominant mode for O_2 consumption in cells, and the mitochondria are the primary source of ROS in cells due to leaked electrons. FACS analyses using Mito-Tracker Green indicated that the mass of mitochondria per cell was slightly decreased in the Myh6-SOD2$^{\Delta}$ to the wild type. We then examined OXPHOS levels in Myh6-SOD2$^{\Delta}$ v.s. Wild type using a Seahorse XF analyzer. The rate of oxygen consumption per cells was significantly lower in Myh6-SOD2$^{\Delta}$ cardiomyocytes than that in wild type. The most noticeable difference in the O_2 consumption was found in the presence of FCCP (H^+ ionophore / uncoupler). FCCP is an inner membrane pore opener which resets the proton gradient between the mitochondrial matrix and the interspace, resulting in continuous transport of protons and consuming O_2 at the maximum potential. Remarkably, while the FCCP treatment increased O_2 consumption in wild type, the treatment showed no effect on the O_2 consumption in the Myh6-SOD2$^{\Delta}$ cardiomyocytes. The result indicated that the low basal OXPHOS activity in Myh6-SOD2$^{\Delta}$ was due to unusually low OXPHOS potential. We examined glycolysis in these cells by measuring extracellular acidification (ECAR) and the pattern exactly opposite to that of oxygen consumption rate (OCR) was observed for glycolysis rates between Myh6-SOD2$^{\Delta}$ and Wild type.
S. Miriyala: None. **T. Labrie:** None. **M. Chandra:** None. **B. Maxey:** None. **W. Orr:** None. **S. Bhuiyan:** None. **K. McCarthy:** None. **M. Panchatcharam:** None.

120
Short-term Oral Supplementation with a Novel Marine Oil Fraction Alters Resolution Phenotype in Healthy Subjects and Patients with Peripheral Arterial Disease
Melinda S Schaller, Mian Chen, UCSF, San Francisco, CA; Romain A Colas, William Harvey Res Inst, Queen Mary Univ, London, United Kingdom; Thomas A Sorrentino, S Marlene Grenon, UCSF, San Francisco, CA; Jesmond Dalli, William Harvey Res Inst, Queen Mary Univ, London, United Kingdom; Michael S Conte, UCSF, San Francisco, CA

Objectives: Peripheral arterial disease (PAD) is a chronic disease characterized by systemic inflammation. Recent work suggests that the resolution of inflammation is orchestrated by specialized pro-resolving lipid mediators

(SPM), largely derived from n-3 PUFA. We hypothesize that PAD is associated with defective resolution, and is modifiable via oral intake of marine lipid fractions enriched for SPM.
Methods: In an oral dose finding study, 10 PAD subjects and 10 healthy subjects received three escalating doses (1.25, 2.5, and 5 g/d) of a novel marine lipid supplement for 5-day periods over 1 month. The RBC content of n-3 PUFA, the omega-3 index (O3I), was measured. We profiled plasma lipid mediators, phagocytic activity of PMN and monocytes (Mo) to E.coli, Mo surface markers, and Mo-derived macrophage (MDM) gene expression.
Results: Compared to baseline, all subjects had an increase in the ratios of n-3 PUFA:arachidonic acid (P<0.00005) and SPM:prostaglandins (P=0.08) in plasma, an increase in the DPA-derived maresins (P=0.001), and an increase in the O3I (24%; P<0.0001). In the PAD cohort, there was an increase in the DHA-derived resolvins (P=0.09). Mo phagocytosis increased (P=0.02) after treatment and correlated with increase in O3I (r=0.45, P=0.055). PMN phagocytosis also increased (P=0.003) post-supplementation. We observed decreased expression of the Mo adhesion molecule CD18 (P<0.00005), and the scavenger receptors CD163 (P=0.0006) and CD36 (P=0.0001). Within the PAD cohort, Mo expression of ICAM-1 (P=0.003) and CCR2 (P=0.006) were decreased. A decrease in MDM gene expression of iNOS and MCP-1, both associated with M1 phenotype, and an increased expression of MRC1, a M2 marker, was observed.
Conclusion: Short-term, oral supplementation with a novel marine oil fraction increased plasma SPM levels, increased the phagocytic activity of Mo and PMN, decreased the expression of Mo surface markers associated with systemic inflammation and atherosclerosis, and promoted a resolution phenotype in MDM. Collectively these data demonstrate a basis for further studies of oral SPM supplementation on inflammation and resolution pathways in patients with PAD.
M.S. Schaller: None. **M. Chen:** None. **R.A. Colas:** None. **T.A. Sorrentino:** None. **S.M. Grenon:** None. **J. Dalli:** None. **M.S. Conte:** Other Research Support; Modest; Metagenics Inc..

121
Inflammation and Resolution Phenotype is Altered in Peripheral Arterial Disease
Melinda S Schaller, UCSF, San Francisco, CA; Laura Menke, Queen Mary Univ, London, United Kingdom; Romain A Colas, William Harvey Res Inst, Queen Mary Univ, London, United Kingdom; Mian Chen, Thomas A Sorrentino, S Marlene Grenon, UCSF, San Francisco, CA; Jesmond Dalli, William Harvey Res Inst, Queen Mary Univ, London, United Kingdom; Michael S Conte, UCSF, San Francisco, CA

Introduction: Peripheral arterial disease (PAD) is best described as a disease of excess inflammation. Monocytes (Mo) and Mo-derived macrophages (MDM) play a central role in vascular inflammation and its resolution, and recent work demonstrates that specialized pro-resolving lipid mediators (SPM) derived from omega-3 fatty acids (DHA, EPA, DPA) are critical mediators.
Methods: In a cross-sectional study we profiled lipid mediators in plasma, phagocytic activity of leukocytes, Mo cell surface markers, and cytokine and gene expression of MDM. Lipid mediators were measured by liquid-chromatography-tandem mass spectrometry. Phagocytosis and surface markers were determined by flow cytometry. MDM were generated from peripheral blood Mo and ELISA and qPCR were performed.
Results: Principal component analysis demonstrated differences between plasma lipid mediators in PAD (n=10) and healthy subjects (HS) (n=10). PAD subjects trended towards lower DHA and DPA-derived resolvins. They had elevated levels of cysteinyl leukotrienes, and trended towards higher prostaglandins and thromboxane. The ratio of SPM:prostaglandins was reduced in the PAD population (p=.01). Circulating Mo and PMN from PAD patients had reduced phagocytic activity (Mo: >30%, p<.001; PMN: >25%, p<.01). Cell-surface analysis demonstrated a higher proportion of the pro-inflammatory intermediate Mo subset ($CD14^{++}16^{+}$, 1.8-fold, p=.04) in PAD subjects. MDM from PAD subjects retain their intrinsic inflammatory program and produce more IL-6 (>4 fold, p=.03) and IL-1β (>10 fold p=.04) and have increased expression of M1 genes (TNF-α, MCP-1, CXCL10) and decreased expression of M2 genes (CCL17, MRC1) versus HS.
Conclusions: PAD subjects have lower plasma levels of pro-resolving lipid mediators and higher levels of those associated with inflammation. Circulating Mo and PMN in patients with PAD have substantially lower phagocytic activity and a greater proportion of the pro-inflammatory intermediate Mo subset. MDM from PAD patients preserve their elevated inflammatory state in culture. Collectively these data demonstrate a heightened inflammatory and impaired resolution phenotype in PAD that has potential implications for disease progression and response to interventions.
M.S. Schaller: None. **L. Menke:** None. **R.A. Colas:** None. **M. Chen:** None. **T.A. Sorrentino:** None. **S.M. Grenon:** None. **J. Dalli:** None. **M.S. Conte:** Other Research Support; Modest; Metagenics Inc..

122
Increased Plasma Sulfide in Vascular Surgery Patients Correlates with Reduced Post-Operative Mortality
Kaspar Trocha, Brigham & Women's Hosp /Harvard Sch of Public Health, Boston, MA; Alban Longchamp, Dept of Vascular Surgery, Lab of Experimental Med, Ctr Hospier Univire Vaudois, Lausanne, Switzerland; Chistopher Hine, Cleveland Clinic, Cleveland, OH; Michael MacArthur, Janine Ganahl, Harvard Sch of Public Health, Boston, MA; Peter Kip, Ming Tao, Brigham & Women's Hosp, Boston, MA; Peter Nagy, Molecular Immunology and Toxicology, Natl Inst of Oncology, Budapest, Hungary, Budapest, Hungary; C. Keith Ozaki, Brigham & Women's Hosp, Boston, MA; James R. Mitchell, Harvard Sch of Public Health, Boston, MA

Objective: Hydrogen sulfide (H_2S) is an endogenously produced gaseous signaling molecule with the potential to modulate vascular functions. Free plasma sulfide can be measured by various techniques, but no consistent relationship with cardiovascular disease has yet emerged. For example, sulfide levels are decreased in CHF patients, but elevated in PAD. We therefore sought to compare plasma sulfide levels from PAD patients to matched controls, and explore links between mortality rates and sulfide levels using two assays. ***Approach & Results:*** Patients undergoing carotid endarterectomy (n=49), open lower extremity revascularization (n=44) or leg amputation (n=22) were enrolled (mean age 68.9±9.6, 67% male). Blood was collected from 20 matched control patients, without PAD or CAD (mean age 67.9± 1.3, male 65%). Plasma sulfide was measured using two methods, first detection using lead acetate, and second using mass spectrometry. Controls had increased plasma sulfide levels measured by both methods (lead acetate, Fig. A; mass spec, Fig. B) compared to PAD patients (p<0.001, p=0.013). Also, PAD patients were divided into high (n=57) and low (n=58) sulfide (lead acetate) groups by median split. Low sulfide PAD patients had increased probability of post-op mortality (p=0.0337, Fig. C). To determine the source of plasma H_2S detected by lead acetate, we tested the effects of detergent and proteolytic denaturation of plasma as well as of reducing agents on H_2S release. We found denaturation increased plasma sulfide release, and that dithiothreitol was most effective at liberating H_2S, suggesting bound sulfane sulfur as source of H_2S detected using the lead acetate assay. ***Conclusions:*** Plasma free and bound sulfide were reduced in PAD patients compared to controls, and correlated with mortality. These findings provide evidence linking circulating sulfide to clinically meaningful events, and support directed H_2S investigations toward diagnostic and therapeutic purposes.

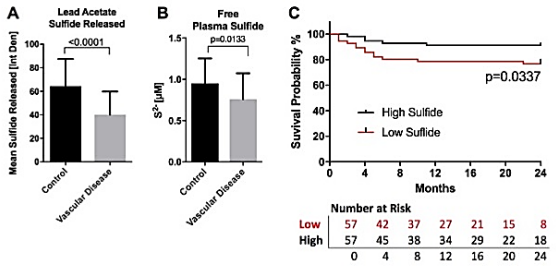

K. Trocha: None. **A. Longchamp:** None. **C. Hine:** None. **M. MacArthur:** None. **J. Ganahl:** None. **P. Kip:** None. **M. Tao:** None. **P. Nagy:** None. **C. Ozaki:** None. **J. Mitchell:** None.

This research has received full or partial funding support from the American Heart Association.

123

Establishing a Zebrafish Model of Ischemic Stroke Induced by Photochemical Thrombosis: a Novel Platform for Translational Researches

I-Ju Lee, Ya-Qi Yang, Natl Chiao Tung Univ, Hsinchu, Taiwan; **Wei-Tien Chang**, Natl Taiwan Univ Hosp, Taipei, Taiwan; Ian Liau, Natl Chiao Tung Univ, Hsinchu, Taiwan

Introduction: Ischemic stroke is a leading cause of death and disability worldwide. Animal models of stroke are important for translational researches. We herein developed a novel zebrafish model of ischemic stroke using selective photochemical thrombosis, based on which further pathophysiological studies and pharmacological screening can be done. **Method:** Using 5 day post-fertilization zebrafish larva, we injected a photosensitizer rose bengal (120 pg) into the cardinal vein and employed a green laser (λ = 532 nm) targeting at selected cerebral arteries to induce photochemical thrombosis. The fluorescent FITC-dextran was used to stain the larval blood. The dynamic cerebral blood flow was continuously monitored. The neuronal death 12 h after arterial occlusion was indicated by acridine orange (AO). A neurological scoring system measuring the movement, coordination, and response to stimuli was established to determine the neurological function at 24 h. Thrombolysis using recombinant tissue plasminogen activator (rt-PA, 300 ng) at 0.5 and 3 h post-occlusion with comparison of the above parameters was used to demonstrate the potential application of this model. **Results:** Photochemical thrombosis consistently induced occlusion of the selected cerebral arteries. Occlusion at the basilar artery led to high mortality (73.3% at 12 h). All zebrafish survived the occlusion at the 1st branch of central artery (CtA), but showed significantly increased AO stain and worsened neurological scores than control. Early treatment of rt-PA at 0.5 h post-occlusion resulted in a higher re-canalization rate than that at 3 h (40.0 vs. 26.7%). Moreover, the early treatment group exhibited significantly lower AO stain (42.2 ± 9.4 vs. 102.6 ± 17.4 a.u., $P < 0.05$) and improved neurological scores (4.2 ± 0.8 vs. 2.7 ± 1.1, $P < 0.05$). In contrast, no significant improvement was shown in the delayed treatment group even if the occluded artery had been reopened. **Conclusion:** This zebrafish model of ischemic stroke demonstrates characteristic pathophysiological responses and therapeutic effects seen in clinical stroke. With zebrafish being an increasingly employed model animal, there exist great potentials for this model to be applied in basic researches and translational studies.

I. Lee: None. **Y. Yang:** None. **W. Chang:** None. **I. Liau:** None.

124

Radiotracer Imaging of Serial Changes in Angiosome Foot Perfusion in Critical Limb Ischemia Patients Undergoing Lower Extremity Revascularization: Association With 12-month Limb Salvage Outcomes

Ting-Heng Chou, Jessica L Alvelo, Xenophon Papademetris, Bauer Sumpio, Albert J Sinusas, Carlos Mena-Hurtado, Mitchel R Stacy, Yale Univ Sch of Med, New Haven, CT

Introduction: Single photon emission computed tomography (SPECT)/CT imaging is a standard approach for assessing myocardial perfusion, but has not been traditionally applied for evaluating peripheral vascular disease (PVD). Due to the prevalence of extremity perfusion abnormalities in PVD patients, SPECT/CT imaging may allow for sensitive physiological evaluation of regional changes in perfusion within the lower extremities following revascularization. Therefore, we assessed regional changes in angiosome foot perfusion following percutaneous revascularization in diabetic patients with critical limb ischemia (CLI) to evaluate the association between treatment-induced perfusion responses and clinical outcomes. Methods: Diabetic patients with CLI and non-healing ulcers (n=24) underwent SPECT/CT perfusion imaging of the feet before and after revascularization (Fig. 1A). CT images were segmented into angiosomes (i.e. vascular territories of the foot), and radiotracer uptake was expressed as standardized uptake values (SUVs). Post-treatment changes in perfusion within ulcerated angiosomes were quantified and limb salvage outcomes were assessed for the following 12 months. Results: Post-revascularization changes in perfusion were significantly higher in patients who experienced limb salvage compared to patients who underwent amputation in the 12-months after treatment (Fig. 1B). When patients were divided into groups (high and low perfusion responders) based on median perfusion response, patients with higher percent change in perfusion demonstrated a significantly higher incidence of amputation free survival (p=0.005; Fig. 1C). Conclusion: SPECT/CT imaging detects regional changes in foot perfusion following revascularization that are associated with limb salvage outcomes. Application of SPECT/CT perfusion imaging in the evaluation of PVD could assist with characterizing treatment success and predicting clinical outcomes.

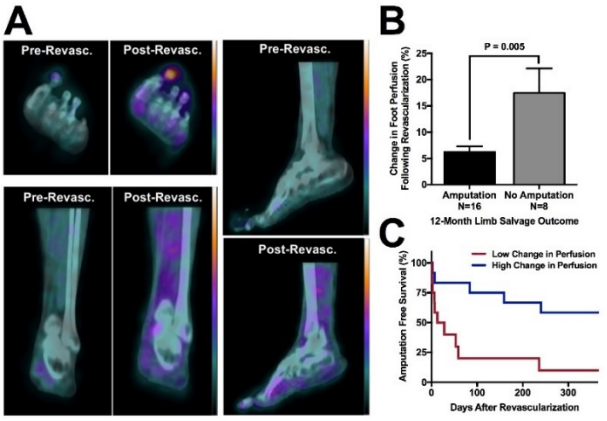

T. Chou: None. **J.L. Alvelo:** None. **X. Papademetris:** None. **B. Sumpio:** None. **A.J. Sinusas:** None. **C. Mena-Hurtado:** None. **M.R. Stacy:** None.

This research has received full or partial funding support from the American Heart Association.

125

Intensive Statin Therapy Negatively Modulates AdipoR Activity in the Monocyte-macrophage Lineage *in vivo* and *in vitro*

Karina Gasbarrino, Huaien Zheng, Stella Daskalopoulou, McGill Univ-Glen Site, Montreal, QC, Canada
Introduction. Statins are widely used for primary and secondary prevention of cardiovascular disease and its complications through cholesterol lowering and anti-inflammatory effects. Adiponectin, an anti-inflammatory adipokine, acts via 2 receptors, AdipoR1 and AdipoR2, to exert protective effects on the vasculature. Recently, we demonstrated that AdipoR are highly expressed on macrophages and that decreased AdipoR2 activity is associated with atherosclerotic plaque instability. We aimed to investigate whether statins can modulate AdipoR activity in the monocyte-macrophage lineage.
Methods. Blood monocytes were isolated from whole blood of patients (statin-naïve *vs* statin users) with severe carotid atherosclerosis by a Magnetic Cell-Sorting technique. AdipoR1 and AdipoR2 mRNA expression on circulating monocytes was determined using qRT-PCR. *In vitro*, THP-1 macrophages were treated for 24 or 72 hours with varying doses of atorvastatin or rosuvastatin (1µM, 10µM, 60µM) to determine the effect of statins on AdipoR activity (AMPK, PPAR-α) by qRT-PCR and Western Blot analyses. Macrophage cytokine secretion (IL-1β, IL-10, IL-6, TNF-α) was assessed by electrochemiluminescence.
Results. AdipoR1 and AdipoR2 mRNA expression on circulating monocytes was significantly lower by 1.36- and 1.17-fold (P<0.05), respectively, in statin users (n=157) compared to statin-naïve patients (n=37). When analyzing by statin type and dose, only patients on high doses of atorvastatin (40-80 mg) or rosuvastatin (20-40 mg) had significantly lower AdipoR expression compared to statin-naïve patients (P<0.05). Statins effects on lowering AdipoR expression was only apparent in patients with unstable but not stable plaques. *In vitro*, higher doses and longer exposure of macrophages to atorvastatin or rosuvastatin resulted in a greater decrease in AdipoR mRNA expression and signalling through AMPK and PPAR-α, and greater secretion of pro-inflammatory cytokines, IL-1β, IL-6, and TNF-α.
Conclusion. In our study, intensive statin therapy resulted in negative modulation of AdipoR expression and function. Despite their known protective properties, statins may also elicit severe adverse effects, which are often associated with long-term treatment and high doses.
K. Gasbarrino: None. **H. Zheng:** None. **S. Daskalopoulou:** None.

126
Genome Wide Association Study in the Million Veteran Program Identifies a Novel Role for Thrombosis in the Pathogenesis of Peripheral Artery Disease
Derek Klarin, Massachusetts General Hosp, Boston, MA; Julie Lynch, Dept of Veterans Affairs Salt Lake City Health Care System, Salt Lake City, UT; Krishna Aragam, Massachusetts General Hosp, Boston, MA; Tim Assimes, Stanford Univ Sch of Med, Stanford, CA; Kyung Lee, Edith Nourse Rogers VA Hosp, Bedford, MA; Qing Shao, Edith Nourse Rodgers VA Hosp, Bedford, MA; Mark Chaffin, Broad Inst, Cambridge, MA; Pradeep Natarajan, Massachusetts General Hosp, Boston, MA; Shipra Arya, Stanford Univeristy, Stanford, CA; Aeron Small, Yale Sch of Med, New Haven, CT; Yan V Sun, Emory Univ Sch of Med, Atlanta, GA; Danish Saleheen, Univ of Pennsylvania Perelman Sch of Med, Philadelphia, PA; Jennifer S Lee, Stanford Univeristy Sch of Med, Stanford, CA; Donald Miller, Boston Univ Sch of Public Health, Boston, MA; Peter Reaven, Univ of Arizona Coll of Med, Phoenix, AZ; Scott DuVall, Univ of Utah Sch of Med, Salt Lake City, UT; William Boden, Samuel S. Stratton Albany VA Medical Ctr, Albany, NY; J. Michael Gaziano, VA Boston Healthcare System, Boston, MA; John Concato, VA Connecticut Healthcare System, West Haven, CT; Sekar Kathiresan, Massachusetts General Hosp, Boston, MA; Daniel J Rader, Univ of Pennsylvania Perelman Sch of Med, Philadelphia, PA; Kelly Cho, VA Boston Healthcare System, Boston, MA; Peter W Wilson, Emory Univ Sch of Med, Atlanta, GA; Kyong-Mi Chang, Univ of Pennsylvania Perelman Sch of Med, Philadelphia, PA; Christopher J O'Donnell, VA Boston Healthcare System, Boston, MA; Phil S Tsao, Stanford Univ Sch of Med, Stanford, CA; **Scott M Damrauer**, Univ of Pennsylvania Perelman Sch of Med, Philadelphia, PA; VA Million Veteran Program

Introduction: PAD is a leading cause of cardiovascular morbidity and mortality. Previously published GWAS have been limited by small sample sizes and have only identified 3 genome-wide significant ($P<5x10^{-8}$) risk loci to date. **Hypothesis**: DNA sequence variants affecting multiple biological pathways are associated with PAD risk. **Methods**: Using electronic health record data, we identified individuals with and without clinical PAD from the 353,323 Million Veteran Program (MVP) participants genotyped on a customized Affymetrix Biobank array. We tested 32 million genotyped and imputed DNA variants for association with clinical PAD separately in participants of European (EUR), African (AFR), and Hispanic (HIS) ancestry using logistic regression models controlling for age, sex and population structure, and then performed trans-ethnic meta-analysis. The results were replicated with data from the UK Biobank. **Results**: We identified 31,307 individuals (24,009 EUR, 5,373 AFR, 1,925 HIS) with, and 211,753 individuals without, PAD. Following meta-analysis and replication, there were 19 genome-wide significant risk loci associated with PAD. We replicated a known association at *9p21* ($P=4.3 x10^{-39}$), and identified several novel loci associated with PAD that were previously known to be associated with atherosclerosis (*LPA*, *HDAC9*), diabetes (*TCF7L2*), lipid levels (*LPL*, *CELSR2*), and tobacco use (*CHRNA3*). We also identified a novel association with PAD for the Factor V Leiden (FVL) mutation (OR 1.20, $P=1.6x10^{-12}$), which remained significant after controlling for venous thromboembolism (OR 1.10, $P=8.7x10^{-4}$). Sensitivity analysis demonstrated FVL is associated with increasing risk estimates for PAD severity (claudication OR 1.19, P=0.0012; rest pain OR 1.41, P=0.004; tissue loss OR 1.57, $P=7x10^{-9}$). **Conclusions**: Using the MVP, we assembled the largest reported cohort of individuals with clinical PAD and genetic data worldwide. Our data replicate known causal risk factors and identify a novel association for FVL and its putative role for thrombosis in the development of clinical PAD.
D. Klarin: None. **J. Lynch:** None. **K. Aragam:** None. **T. Assimes:** None. **K. Lee:** None. **Q. Shao:** None. **M. Chaffin:** None. **P. Natarajan:** None. **S. Arya:** None. **A. Small:** None. **Y.V. Sun:** None. **D. Saleheen:** None. **J.S. Lee:** None. **D. Miller:** None. **P. Reaven:** None. **S. DuVall:** None. **W. Boden:** None. **J. Gaziano:** None. **J. Concato:** None. **S. Kathiresan:** None. **D.J. Rader:** None. **K. Cho:** None. **P.W.F. Wilson:** None. **K. Chang:** None. **C.J. O'Donnell:** None. **P.S. Tsao:** None. **S.M. Damrauer:** None.

127
Arterial Inflammation and Neointimal Hyperplasia Development in a Germ-free Mouse Model of Carotid Ligation
Kelly Wun, Northwestern Univ, Chicago, IL; Betty Theriault, Univ of Chicago, Chicago, IL; Joseph F. Pierre, Univ of Tennessee Health Science Ctr, Memphis, TN; Vanessa Leone, Katharine G. Harris, Univ of Chicago, Chicago, IL; Edmund B. Chen, Liqun Xiong, Qun Jiang, Owen Eskandari, Northwestern Univ, Chicago, IL; Eugene B. Chang, Univ of Chicago, Chicago, IL; **Karen J. Ho**, Northwestern Univ, Chicago, IL

BACKGOUND: The microbiome plays a functional role in a number of inflammatory processes and disease states. While neointimal hyperplasia has been linked to inflammation, there has not been direct demonstration of the role of microbiota in this process. Germ-free (GF) mice raised in complete absence of microbes are an invaluable tool for studying causative links between commensal organisms and the host. We hypothesized GF mice would exhibit altered neointimal hyperplasia following carotid

ligation compared to conventionally-raised (CONV-R) mice.
METHODS: Twenty-week-old male C57BL/6 GF mice underwent left carotid ligation under sterile conditions. Maintenance of sterility was assessed by cultivation and 16S rRNA qPCR of stool. Neointimal hyperplasia was assessed by morphometric and histologic analysis of arterial sections after 28 days. Local arterial cell proliferation and inflammation was assessed by immunofluorescence for Ki67 and inflammatory cell markers after 5 days. Systemic inflammation was assessed by multiplex immunoassays of serum. Identically treated CONV-R mice served as controls. GF and CONV-R outcomes were compared using standard statistical methods.
RESULTS: All GF mice remained sterile during the study period. Twenty-eight days after carotid ligation, CONV-R mice had significantly more neointimal hyperplasia compared to GF mice, as assessed by intima area, media area, intima+media area, and intima area/(intima+media area). Collagen content of neointimal lesions appeared qualitatively similar on Masson's trichrome staining. Ki67 immunoreactivity was significantly reduced in GF carotid arteries at 5 days with increased arterial infiltration of neutrophils and M2 macrophages compared to CONV-R. GF mice also had significantly reduced serum IL-17 concentration and nearly undetected IL-10 at 5 days but not 28 days.
CONCLUSIONS: GF mice have attenuated neointimal hyperplasia development compared to CONV-R mice, which may be related to altered kinetics of wound healing and acute inflammation. Understanding how commensal microbes regulate arterial remodeling could provide new directions in pathophysiology of restenosis and offer novel strategies to reduce restenosis risk via microbiota manipulation.
K. Wun: None. **B. Theriault:** None. **J.F. Pierre:** None. **V. Leone:** None. **K.G. Harris:** None. **E.B. Chen:** None. **L. Xiong:** None. **Q. Jiang:** None. **O. Eskandari:** None. **E.B. Chang:** None. **K.J. Ho:** None.

128
Disruption of Methylarginine Metabolism Impairs Vascular Homeostasis During Pregnancy
Aikaterini Georgopoulou, Mark Johnson, Mohd N Noor, Imperial Coll London, London, United Kingdom; **James Mitchell Leiper**, Univ of Glasgow, Glasgow, United Kingdom

Endogenously produced asymmetrically methylated forms of L-arginine (ADMA) competitively inhibit all three isoforms of nitric oxide synthase enzymes and therefore have the potential to exert significant cardiovascular effects. Elevated circulating ADMA concentrations have been reported in a number of cardiovascular disease states, including preeclampsia, suggesting that impaired ADMA metabolism may contribute to pathology. In order to test the causal relationship between ADMA concentrations and hemodynamics in pregnancy we employed radiotelemetric measurement of hemodynamic function in mice with either global or fetal-specific deletion of the predominant ADMA metabolising enzyme dimethylarginine dimethylaminohydrolase 1 (DDAH1). Global deletion of DDAH1 in non-pregnant female mice caused an elevation in circulating ADMA concentrations (2.851±0.289 vs 1.216±0.072 μM $p<0.01$) and blood pressure (118±2.28 vs 110.36±0.82 mmHg $p<0.05$). During the first and second trimesters of pregnancy DDAH1$^{-/-}$ mice showed no further elevation in ADMA and normal pregnancy related changes in blood pressure were observed. However, during the third trimester ADMA levels in DDAH1$^{-/-}$ mice increased further and this was associated with increased concentrations of sEng and sFlt1 (2288±301.58 vs 1181.35 ± 161.83 pg/ml $p<0.01$ and 153.31 ± 8.57 vs 114.42 ± 8.79 ng/ml $p<0.001$) and an exaggerated hypertensive response (115.773 ± 3.7 vs 101.93 ± 3.27 mmHg $p<0.05$). Fetal-specific deletion of DDAH1 elevated fetal ADMA concentrations (4.97 ± 0.29 μM vs 1.7 ± 0.12 μM $p<0.001$) but did not impact on maternal ADMA concentrations or blood pressure during early pregnancy. However in the third trimester a significant elevation in maternal ADMA concentrations was detected (2.49 ± 0.17 vs 1.75 ± 0.13 μM $p<0.01$) and was associated with an elevation in maternal blood pressure. No changes in sEng or sFLt1 were detectable in fetal-specific DDAH1$^{-/-}$ mice. Our data indicate that elevated ADMA is sufficient to increase levels of sFLlt1 and sEng and disrupt maternal hemodynamics. The fetus is a significant source of ADMA in late pregnancy suggesting that dysfunctional fetal ADMA metabolism is sufficient to impair maternal hemodynamic function.
A. Georgopoulou: None. **M. Johnson:** None. **M.N. Noor:** None. **J.M. Leiper:** Ownership Interest; Significant; Founder/Director of Critical Pressure Ltd.

129
Parthenolide Inhibits Inflammatory Dysfunction of Human Aortic Endothelial Cells and Proliferation of Smooth Muscle Cells in vitro and Restenosis in a Rat Model
Bowen Wang, Mengxue Zhang, The Ohio State Univ, Columbus, OH; Xudong Shi, Univ of Wisconsin-Madison, Madison, WI; Lian-Wang Guo, Craig Kent, The Ohio State Univ, Columbus, OH

Background: Cardiovascular diseases remain the leading cause of death in developed countries. Endovascular surgical interventions trigger uncontrolled proliferation of smooth muscle cells (SMCs) in the intima (intimal hyperplasia) leading to lumen re-narrowing (restenosis). Despite extensive efforts devoted to therapeutic methods with a focus on inhibiting SMC proliferation, restenosis persists at a significant rate. In recent years, a growing body of knowledge has underscored a crucial role for endothelium damage in the pathophysiology of restenosis, suggesting that preservation of the endothelium would provide an effective approach for effectively curbing restenosis.
Methods and Results: We utilized high-throughput screening methods to search for small molecules that could inhibit the proliferation of human aortic SMCs without damaging human aortic endothelial cells (ECs). We identified such a lead compound in Prestwick Library; *i.e.* Parthenolide, a sesquiterpene lactone extracted from feverfew. Treatment with a low dose (1 μM) of Parthenolide for 96h inhibited SMC but not EC proliferation. When the cells were stimulated with inflammatory cytokines (TNF-α or IL-1β), Parthenolide mitigated cytokine-induced proliferation and MCP-1 production of SMCs, but rescued cytokine-induced endothelial dysfunction, including apoptosis, proliferation, decrease of eNOS, and increase of inflammatory markers. Mechanistic studies showed that while Parthenolide treatment in both SMCs and ECs induced NRF-2 activation (nuclear translocation), NRF-2 knockdown with siRNA diminished the aforementioned beneficial effects of Parthenolide in both cell types. In contrast, NFkB activation was not significantly affected by Parthenolide. In a rat balloon angioplasty model, perivascular delivery of Parthenolide in Pluronic gel effectively inhibited intimal hyperplasia and restenosis 14 days after surgery.
Conclusion: These results indicate that the natural compound Parthenolide differentially attenuates pathological behaviors of both human vascular SMCs and ECs, whereas known agents as such are scarce. Thus Parthenolide may serve as a promising lead compound for future development of next-generation anti-restenotic therapeutics.
B. Wang: None. **M. Zhang:** None. **X. Shi:** None. **L. Guo:** None. **C. Kent:** None.

This research has received full or partial funding support from the American Heart Association.

130
Exosomal Cellular Communication in Peripheral Arterial Disease
Sarah Lewis, Univ Coll London, London, United Kingdom; Julia Konig, The Francis Crick Inst, London, United Kingdom; Charlotte Lawson, Royal Veterinary Coll, London, United Kingdom; Lucy Collinson, The Francis Crick Inst, London, United Kingdom; Xu Shiwen, George Hamilton, Daryll Baker, Janice Tsui, Univ Coll London, London, United Kingdom

Background: Exosomes are nano-meter sized vesicles that play a role in cellular communication. Their effects on target cells are influenced by their cellular source and associated niche. We hypothesize that exosomal communication is involved in the local and systemic pathology of peripheral arterial disease (PAD), where exosomes derived from ischaemic muscle contribute to impaired muscle regeneration and endothelial dysfunction. This study aims to investigate the effect of ischaemia on skeletal muscle exosomes and their potential role in PAD. **Methods:** Exosomes were isolated from C2C12 myoblasts (MB), MTs and ischaemic MTs (IMTs) through ultracentrifugation. Comparative analysis of MT and IMT exosomes was performed using Nanosight, western blotting (WB) and electron microscopy (EM). PKH26 labelled MB, MT and IMT exosomes were co-cultured with myoblasts or human umbilical vein endothelial cells (HUVECs) for 6, 12 and 24hrs. Exosome uptake was assessed by fluorescent microscopy and FACs. The effect of IMT exosomes on myoblast differentiation was assessed by WB for myogenin and myosin heavy chain. **Results:** Exosomes were secreted by MTs and IMTs at similar frequencies and were structurally similar. Both were positive for exosomal markers CD81 and Alix. Following 24hr co-culture of PKH26 labelled exosomes with myoblasts or HUVECs, over 80% (over 4000 of 5000) of cells fluoresced positively, signifying internalisation of the exosomes by myoblasts and HUVECs. IMT but not MT derived exosomes impaired myoblast differentiation. **Conclusion:** MT derived exosomes are taken up by both myoblasts and endothelial cells. Whilst ischaemia does not significantly alter MT derived exosomes quantitatively or structurally, internalisation of IMT exosomes impairs differentiation of myoblasts to myotubes. This suggests that in PAD, altered exosomal message secondary to ischaemia, contributes to muscle dysfunction. Our data also indicates that there is muscle-endothelial cell cross-talk via exosomes, which may also contribute to systemic cardiovascular morbidity. Clarification of the functional effects and delineation of the mechanisms involved may lead to new targets that can be manipulated to improve outcomes of patients with PAD.

S. Lewis: None. **J. Konig:** None. **C. Lawson:** None. **L. Collinson:** None. **X. Shiwen:** None. **G. Hamilton:** None. **D. Baker:** None. **J. Tsui:** None.

131
$P2Y_6$ Receptor Inhibition Impairs Arteriogenesis
Ryan M McEnaney, VA Pittsburgh Healthcare System, Pittsburgh, PA; Dylan McCreary, Univ of Pittsburgh, Pittsburgh, PA; Edith Tzeng, UPMC, Pittsburgh, PA

Purinergic signaling plays a role in vessel remodeling among developing collateral arteries. We have previously shown that the $P2Y_2$ receptor, an ATP/UTP receptor, mediates arteriogenesis in a murine model of hindlimb ischemia. Intra-arterial administration of UTP increases perivascular inflammation and macrophage accumulation, necessary early events of arteriogenesis, an effect which was abolished among $P2Y_2$ -/- mice. Extracellular nucleotides can be dephosphorylated by ectonuclotidases which are expressed in various tissues, converting ATP/UTP into ADP/UDP. Our objective was to identify whether receptors for these derivative nucleotides would also have a role in arteriogenesis. Muscular branches of the caudal femoral artery were explanted from rat and assessed for purinergic receptor expression by immunofluorescence. Baseline expression of $P2Y_2$ is found among endothelial cells predominantly. Conversely, the $P2Y_6$ receptor is highly expressed in the media, with no appreciable staining in the endothelium. CD39, an ectonucleotidase, is expressed among VSMCs in developing collateral arteries (Figure). We then sought to identify whether inhibition of the $P2Y_6$ receptor, the ligand for which is UDP, would alter perfusion recovery after femoral artery ligation (FAL). Selective $P2Y_6$ receptor antagonist MRS2578 was intraperitoneally delivered via osmotic minipump at a rate of 20 ng/hr. FAL was performed and perfusion recovery monitored over 14 days using laser Doppler perfusion imaging (LDPI). Perfusion recovery was reduced in animals treated with MRS2578 when compared to vehicle (DMSO) at 7 and 14 days (figure). Two (out of 12) animals receiving MRS2578 were euthanized due to gangrene of the hindlimb. We have demonstrated in this work that the $P2Y_6$ receptor is another mediator of arteriogenesis. Our results also suggest an interesting spatial localization of purinergic receptors among resident vascular cells which may facilitate their function in arteriogenesis.

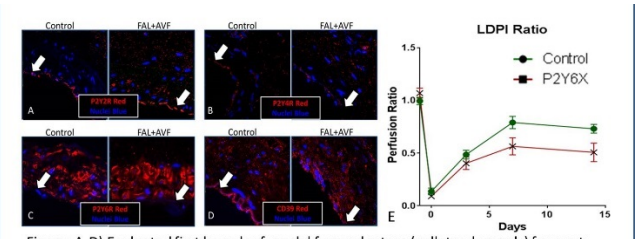

Figure: A-D) Explanted first branch of caudal femoral artery (collateral vessels) from rat hindlimb after sham operation or femoral artery ligation (FAL) with arteriovenous fistula (AVF) placement. Arrows indicate internal elastic lamina. E) Perfusion recovery is reduced in mice treated with MRS2578 after FAL. (p=0.02, n=12)

R.M. McEnaney: None. **D. McCreary:** None. **E. Tzeng:** None.

132
Application of a Cryogel-Coated Prosthetic Vascular Graft Material for Delivery of Targeted Gene Therapies in a Rabbit Model
Cindy Huynh, Beth Israel Deaconess Medical Ctr, Boston, MA; Ting Shih, Harvard Univ, Cambridge, MA; Mauricio Contreras, Beth Israel Deaconess Medical Ctr, Boston, MA; David Mooney, Harvard Univ, Cambridge, MA; Leena Pradhan-Nabzdyk, Frank LoGerfo, Beth Israel Deaconess Medical Ctr, Boston, MA

Objectives: Long-term success of prosthetic grafts (PG) in peripheral arterial disease is limited by development of anastomotic neointimal hyperplasia. We have constructed a bioactive prosthetic graft material (BPGM) capable of delivering biologic agents in vitro, and evaluate our BPGM in vivo with a rabbit carotid interposition bypass model. **Methods:** We synthesized our BPGM by cryopolymerization of RGD with methacrylated alginate and heparin, coating 1.5cm by 2mm electrospun PET (ePET) grafts, and dipcoating in fluorescent siRNA for 3 hours. Three rabbits received bare ePET and 3 received cryogel-coated ePET for a carotid interposition bypass (Figure 1). After 24 hours, bypass patency was assessed, and cell toxicity of the proximal anastomosis, mid-graft, and distal anastomosis examined with H&E staining. Confocal microscopy was used to visualize fluorescence, correlating with ability to deliver siRNA in vivo. **Results:** Graft patency was equal between groups, with no increased cell toxicity in rabbits receiving cryogel-coated ePET. Confocal microscopy demonstrated no difference in retained fluorescence between rabbits receiving cryogel-coated or bare ePET, and no increased transfection of cells at 24 hours (Figure 2). **Conclusion:** Creation of the optimal PG demands a material that is biocompatible, responsive, and nonthrombogenic. We have constructed a modified PG capable of in vitro delivery of targeted gene therapies, with comparable patency and biocompatibility in

our large animal model. Additional optimization to achieve predictable and sustained release is needed to validate this as an effective and practical method to deliver biologic agents in vivo.

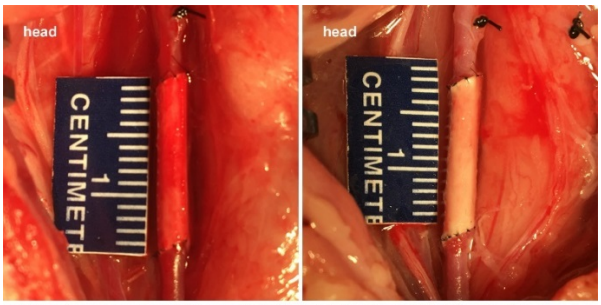

Figure 1. Cryogel-coated ePET graft with fluorescent siRNA implanted in a rabbit carotid interposition bypass model. *Intraoperative images of a rabbit undergoing carotid artery interposition bypass using our bioactive prosthetic graft material at initial surgery (left) and after 24 hours (right).*

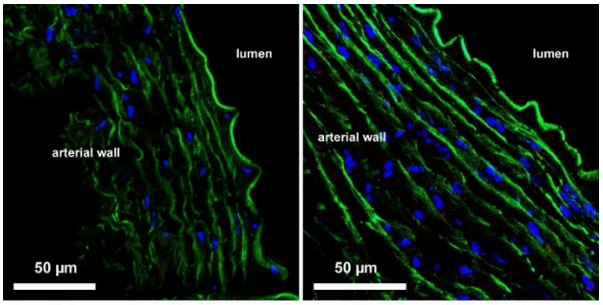

Figure 2. Cross-sections of the distal anastomosis in rabbits with bare ePET graft material compared to cryogel-coated ePET. *Confocal microscopy demonstrates no difference in retained fluorescence and no increased transfection of cells at 24 hrs in cross-sections of the distal anastomosis from rabbits receiving bare ePET graft material (left), and cryogel-coated ePET (right), with internal elastic lamina in green, fluorescent siRNA in red, and cell nuclei in blue.*

C. Huynh: None. **T. Shih:** None. **M. Contreras:** None. **D. Mooney:** None. **L. Pradhan-Nabzdyk:** None. **F. LoGerfo:** None.

133
Heterozygous Deletion of Transferrin Receptor 1 Suppresses Angiogenesis in a Mouse Model of Hind Limb Ischemia
Keisuke Okuno, Yoshiro Naito, Seiki Yasumura, Hisashi Sawada, Koichi Nishimura, Masanori Asakura, Masaharu Ishihara, Tohru Masuyama, Hyogo Coll of Med, Hyogo, Japan
Objective: Angiogenesis can be triggered under conditions of ischemia and plays a protective role in peripheral artery disease. Iron is an essential trace mineral in the living body whose intracellular metabolism is regulated by transferrin receptor 1 (TfR1). Excess iron causes tissue damage and has been reported in patients with peripheral artery disease. Therefore, we hypothesized that TfR1 contributes to the pathophysiology of hind limb ischemia through iron overload. The aim of this study is to examine whether TfR1 deletion effects angiogenesis in hind limb ischemia. **Methods and Results:** Since homozygous TfR1 deletion is embryonically lethal, mice with heterozygous TfR1 deletion and their wild type littermates were used in this study. To induce hind limb ischemia, the left femoral artery in 8 - 9 week-old male mice was ligated and stripped. The non-ligated right hind limb was used as a control. Blood flow was measured by laser Doppler blood flowmetry at both a baseline of 1 hour and 28 days after the surgery. In wild type, the ratio of ischemc/non-ischemic hind limb blood flow was significantly decreased to 12% at baseline, and recovered to 62% at day 28. On the other hand, TfR1 deleted mice also showed similar reduction of blood flow at baseline, whereas blood flow recovery at day 28 was attenuated to 42%. Subsequently, both right and left adductor muscles were harvested for Western blot and immunohistochemistry. TfR1 expression in the adductor muscle was decreased in TfR1 deleted mice compared to wild type, regardless of the ligation. Ferritin, a marker for iron storage, was 10 times higher in ischemic muscles than in wild type non-ischemic muscles. In contrast, ferritin levels in TfR1 deleted mice were not altered by the surgery. Finally, immunohistochemistry for CD31 was performed to evaluate angiogenesis. The ischemic adductor muscle of TfR1 deleted mice had few CD31 positive vascular structures. **Conclusions:** Heterozygous deletion of TfR1 attenuated iron overload and angiogenesis in a mouse model of hind limb ischemia. TfR1 may be a novel therapeutic target for the treatment of peripheral artery disease.
K. Okuno: None. **Y. Naito:** None. **S. Yasumura:** None. **H. Sawada:** None. **K. Nishimura:** None. **M. Asakura:** None. **M. Ishihara:** None. **T. Masuyama:** None.

134
The Current Patency Rate of Autologous Arteriovenous Fistula in the Snuff-Box and the Risk Factors for Its Failure
Michihiro Okuyama, Yasuhiro Fujii, Yasuyuki Kobayashi, Genya Muraoka, Dept Of Cardiovascular Surgery, Okayama Univ Graduate Sch Of Med, Dentistry, And Pharmaceutical Sciences, Okayama, Japan; Nozomu Otaka, Dept Of Chronic Kidney Disease and Cardiovascular Disease, Okayama Univ Graduate Sch Of Med, Dentistry, And Pharmaceutical Sciences, Okayama, Japan; Susumu Oozawa, Dept Of Cardiovascular Surgery, Okayama Univ Graduate Sch Of Med, Dentistry, And Pharmaceutical Sciences, Okayama, Japan; Haruhito A Uchida, Dept Of Chronic Kidney Disease and Cardiovascular Disease, Okayama Univ Graduate Sch Of Med, Dentistry, And Pharmaceutical Sciences, Okayama, Japan; Shingo Kasahara, Dept Of Cardiovascular Surgery, Okayama Univ Graduate Sch Of Med, Dentistry, And Pharmaceutical Sciences, Okayama, Japan

Introduction: Autologous snuff-box arteriovenous fistula (sAVF) is the first choice procedure as the primary AVF for chronic hemodialysis at this institution. The patency of the autologous AVF in the forearm was reported to be 43% to 85% at 1 year and 40 % to 69 % at 2 years. However, little is known about the patency of sAVF alone to date. In addition, there is a paucity of evidence for risk factors of its failure. Objectives: The purpose of this study was to describe the patency of sAVF and to verify the risk factors for its failure. Methods: Clinical records were retrospectively reviewed in 185 patients (114 male and 71 female patients) who underwent sAVF creation at our institution between March 2011 and December 2016. The average age was 64 ± 14 years (range, 23 to 90 years). The sAVF was created in the left and right arms in 155 patients and 30 patients, respectively. Nine patients had collagen vascular disease (CVD).
Results: The primary patency rates were 93.0%, 66.9%, and 59.0% at 1 month, 1 year, and 2 years after surgery, respectively. The secondary patency rates were 98.9%, 89.3%, and 85.4% at 1 month, 1 year, and at 2 years after surgery, respectively. On multivariate analysis, female gender (P = 0.002), sAVF creation in the right arm (P = 0.013), and steroid use (P = 0.019) were the significant risk factors for the decreased primary patency rate. CVD (P = 0.001) and steroid use (P = 0.005) were the significant risk factors for the decreased secondary patency rate.Conclusions: The patency rate of sAVF in our institution was comparable to previously reported patency rates for the forearm AVF. A careful observation for sAVF is needed in patients with female gender, history of smoking, sAVF creation in the right arm, CVD, and steroid use.

Factor	Primary Patency				Secondary Patency			
	Patent (N= 120)	Not patent (N= 65)	*P* (Uni)	*P* (Multi) (CI)	Patent (N= 157)	Not patent (N= 28)	*P* (Uni)	*P* (Multi) (CI)
Age(y.o.)	63.7±13.1	65.9±14.2	0.564		64.3±13.3	65.5±15.0	0.721	
Male	82 (68.3%)	29 (44.6%)	< 0.001	0.002 (0.144-0.666)	103 (65.6%)	11 (39.2%)	0.009	0.361 (0.250-1.661)
Right Arm	13 (10.8%)	17 (26.2%)	0.014	0.013 (1.256-7.567)	25 (15.9%)	4 (14.3%)	0.744	
DM	50 (41.6%)	32 (49.2%)	0.323		70 (44.6%)	12 (42.9%)	0.865	
CVD	3 (2.5%)	6 (9.2%)	0.048	0.169 (0.587-15.880)	3 (1.9%)	6 (21.4%)	< 0.001	0.001 (2.718-61.133)
IgA	11 (9.1%)	1 (1.5%)	0.025	0.009 (0.012-0.888)	10 (6.4%)	2 (7.1%)	0.880	
Nephritis	16 (13.3%)	9 (13.8%)	0.923		19 (12.1%)	6 (21.4%)	0.208	
HTN	96 (80.0%)	49 (75.4%)	0.470		124 (79.0%)	21 (75.0%)	0.642	
Statin	33 (27.5%)	21 (32.3%)	0.494		47 (30.0%)	7 (25.0%)	0.592	
Antiplatelet	31 (25.8%)	24 (36.9%)	0.118	0.079 (0.926-4.006)	48 (30.6%)	7 (25.0%)	0.547	
Anticoagulant	13(10.8%)	5 (7.7%)	0.386		15 (9.6%)	4 (14.3%)	0.466	
PCK	5 (4.1%)	2 (3.1%)	0.706		7 (4.5%)	0 (0.0%)	0.128	
Heart Failure	26 (21.7%)	10 (15.4%)	0.296		31 (19.7%)	5 (17.9%)	0.815	
Steroid	10 (8.3%)	14 (21.5%)	0.013	0.019 (1.187-8.408)	14 (8.9%)	10 (35.7%)	0.001	0.005 (1.528-11.507)
History of Smoking	50 (41.6%)	14(21.5%)	0.005	0.152 (0.240-1.257)	60 (38.2%)	4 (14.3%)	0.009	0.071 (0.098-1.176)

M. Okuyama: None. **Y. Fujii:** None. **Y. Kobayashi:** None. **G. Muraoka:** None. **N. Otaka:** None. **S. Oozawa:** None. **H.A. Uchida:** None. **S. Kasahara:** None.

135
Sterol Efflux Function and HDL Associated APOF Levels Associate with Recovery from Stroke
Deanna L. Plubell, Alexandra M Fenton, Jessica Minnier, Wayne Clark, Oregon Health & Science Univ, Portland, OR; Neil A Zakai, Univ of Vermont, Burlington, VT; Joseph F Quinn, Nabil J Alkayed, **Nathalie Pamir**, Oregon Health & Science Univ, Portland, OR

Background: Prospective cohort studies and meta-analyses examining the relationship between HDL-cholesterol (C) and stroke risk are discordant and question the value of HDL-C as a marker for stroke risk prediction. Changes in HDL-C protein composition and function after acute ischemic stroke, and their relationship to stroke recovery have not been studied. We investigated changes in HDL cholesterol efflux capacity (CEC) and proteome in response to acute ischemic stroke, and their correlation with long-term functional recovery after stroke.
Methods: Plasma samples were collected from stroke patients either at 24 (early, N = 35) or 96 hours (late, N = 20) after stroke onset, in addition to age matched healthy controls (N = 35). Samples were analyzed for HDL proteome using mass spectrometry, and CEC using three independent assays for macrophage-, ABCA1- and ABCG1-dependent efflux. Stroke recovery was assessed at 3 months after stroke using the Modified Rankin Scores (MRS) and the NIH Stroke Scale (NIHSS).
Results: Both macrophage- and ABCG1-mediated CEC were reduced by 50% (P<0.0001) and 20% (P<0.038) in early and late post stroke samples, respectively, compared to the control group. Patients who had comparable or increased CEC between the two-time points had lower NIHSS and MRS indicating better recovery. Proteomic analysis of HDL indicated a distinct time-dependent remodeling post stroke. Coagulation complement cascade proteins (FGB, FGA, A2M, C3) significantly increased (FDR>0.01) early and returned to control levels later, inflammation proteins (SAA1, SAA2, PON1, C4B) increased early and continued to increase. Interestingly, platelet adhesion proteins (DSG1, JUP, ITGB1, ITGA2, TUBB, DNAH3, PF4) were abundantly present in only later samples. Finally, apolipoprotein F (APOF) levels were 2 fold increased at 96 hour when compared to 24hour time points. APOF positively and significantly correlated with NIHSS (r=0.72, P=0.031)
Conclusion: 1) Patients with acute ischemic stroke who maintain or improve HDL CEC post stroke exhibit better recovery scores, 2) Post stroke HDL proteome remodeling is dynamic with distinct time-dependent protein signatures among which APOF correlates positively and strongly with stroke recovery.
D.L. Plubell: None. **A.M. Fenton:** None. **J. Minnier:** None. **W. Clark:** None. **N.A. Zakai:** None. **J.F. Quinn:** None. **N.J. Alkayed:** None. **N. Pamir:** None.

136
Near-Infrared Spectroscopy for Diagnosis and Characterization of Peripheral Artery Disease Severity
Matthew Fuglestad, Hernan Hernandez, Molly Schieber, Katya Brunette, Yue Gao, Univ of NE Medical Ctr, Omaha, NE; Sara Myers, Univ of NE Omaha, Omaha, NE; George Casale, Iraklis Pipinos, Univ of NE Medical Ctr, Omaha, NE

Background: Peripheral artery disease (PAD) frequently is undertreated. ABI is the standard for diagnosis of PAD but is limited in its ability to predict functional status and risk of disease progression. Previous work with Near-Infrared Spectroscopy (NIRS) has demonstrated impaired oxygen utilization in PAD muscle and may allow for improved diagnosis and stratification of disease severity. We hypothesize that exercise produces characteristic changes in lower-extremity muscle oxygenated heme percent (StO_2) which differentiates PAD from control and predicts PAD severity better than ABI. **Methods:** We recruited 31 PAD subjects with intermittent claudication (IC) (ABI < 0.9) and 9 controls (ABI ≥ 0.9 and no IC). All subjects completed a Gardner maximal treadmill test. PAD subjects walked until IC was prohibitive (peak walking time, PWT) and controls walked for 540 seconds. StO_2 measurements were taken from the lateral gastrocnemius with the wireless MOXY NIRS monitor. StO_2 was documented at baseline, 60s, claudication onset time (COT), and PWT. For each subject, StO_2 values were expressed as percent of baseline to allow for comparison across subjects. Data were analyzed by student's t-test and linear regression. **Results:** Mean baseline StO_2 values were 46±11% and 58±17%, respectively, for PAD and control subjects. Among controls, StO_2 dropped below baseline at 140±101s whereas PAD subjects dropped below baseline at 6±10s (P<0.001). PAD StO_2s at 60s, COT, and PWT were compared to control StO_2s at the corresponding time points. PAD patients' StO_2 at 60s, COT, and PWT were 65.2±37.9% (n=31), 66.4±35.5% (n=31), and 73.2±26.0% (n=25) lower than controls, respectively (P < 0.001). PAD subjects were separated into tertiles of PWT. Relative to baseline, StO_2 decreased 84.2±18.4% (n=11) in the lowest tertile compared to 29.8±30.6% (n=10) in the highest tertile (P<0.05). Percent decrease in StO_2 at 60s correlated to PWT (R^2 =0.56) in contrast to ABI (R^2=0.018). **Conclusion:** During exercise, PAD patients exhibited a characteristic change in StO_2. In contrast to ABI, StO_2 predicted PAD-related exercise limitation. These data suggest NIRS in conjunction with traditional methods could be used to guide diagnostic and treatment decisions.
M. Fuglestad: None. **H. Hernandez:** None. **M. Schieber:** None. **K. Brunette:** None. **Y. Gao:** None. **S. Myers:** None. **G. Casale:** None. **I. Pipinos:** None.

137
Right Cerebral Insufficiency Associated with Right Aortic Arch with Mirror-Image Branching: a Case Study
Joel Petit, Univ of Newcastle, Wickham, Australia; Senthil Kumar, Univ of Newcastle, Newcastle, Australia; Catherine Harrison, John Hunter Hosp, Newcastle, Australia; Aimee Scherf, Hunter New England LHD, Walcha, Australia
We report a case of right cerebral insufficiency in a 65-year-old woman with right aortic arch with mirror-image branching. The patient was found to have intermittent occlusion at the origin of the right common carotid artery between the aortic arch and the sternoclavicular joint. Duplex showed intermittent bizarre carotid artery waveforms directly related to patient positioning. The patient underwent a transposition of the right common carotid to the right subclavian artery with subsequent resolution of symptoms. Right aortic arch with mirror-image branching can rarely present with right cerebral insufficiency due to intermittent mechanical occlusion of the right common carotid artery.

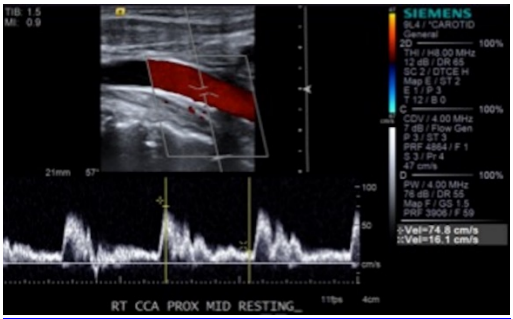

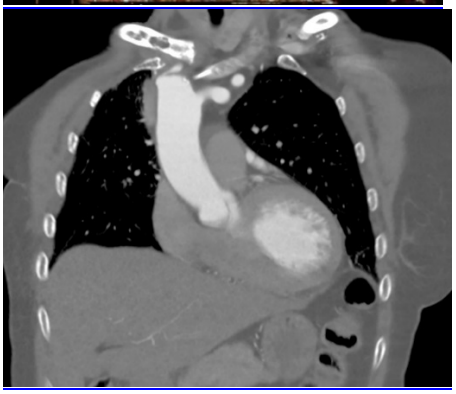

J. Petit: None. **S. Kumar:** None. **C. Harrison:** None. **A. Scherf:** None.

138
Revascularization Improves the Hemodynamics, Function, and Myopathy of the Legs of Claudicating Patients
Iraklis Pipinos, Univ of NE Medical Ctr, Omaha, NE; Sara Myers, Univ of NE Omaha, Omaha, NE; Matthew Fuglestad, Univ of NE Medical Ctr, Omaha, NE; Panagiotis Koutakis, Baylor Univ Robbins Coll of Health & Human Sciences, Waco, TX; Julian KS Kim, Zhen Zhu, Univ of NE Medical Ctr, Omaha, NE; Jonathan R Thompson, Univ of Michigan Medical Ctr, Ann Arbor, MI; Duy Ha, Jason M Johanning, George Casale, Univ of NE Medical Ctr, Omaha, NE

Introduction: Patients with claudication due to peripheral artery disease (PAD) have walking and quality of life (QOL) limitations associated with development of ischemic myopathy. Characteristics of PAD-related ischemic myopathy include myofiber degeneration, mitochondrial dysfunction, and oxidative damage. We hypothesize that revascularization operations improve lower extremity hemodynamics, function, and QOL with improvements in key indicators of PAD-related ischemic myopathy. **Methods:** Patients undergoing open or endovascular revascularization were evaluated before and 6 months after intervention. QOL was assessed by Short Form-36 (SF-36) and Walking Impairment Questionnaire (WIQ). Walking performance was measured by six-minute walking distance (6MWD) and Gardner maximal Treadmill test (Peak Walking Time - PWT). Calf muscle biomechanics were measured by plantar flexor peak force (PFPF) and power generation (PFPG). Limb hemodynamics were measured with Ankle-Brachial Index (ABI) and myopathy was assessed *via* gastrocnemius biopsy. Myofibers were evaluated for mitochondrial function *via* respirometry while slide mounted specimens of the gastrocnemius were analyzed for biomarkers of morphology (myofiber cross-sectional area) and myofiber oxidative damage (carbonyl groups) by quantitative fluorescence microscopy. **Results:** We recruited 52 patients who underwent 34 open and 18 endovascular revascularizations. Average score improved in 7 of 8 SF-36 ($p<0.03$) and 4 of 4 WIQ categories ($p<0.001$). PWT and 6MWD increased 305±75s (111.9%, $p<0.001$) and 62±17M (21.3%, $p<0.001$) respectively. PFPF and PFPG increased 9.8±3.1N (17.1%, $p=0.001$) and 1.6±0.08W/Kg (26.9%, $p<0.001$) respectively. ABI increased from 0.46±0.03 to 0.87±0.03 (90.4%, $p<0.001$). Myofiber cross-sectional area increased 458±216 μm^2 (11.1%, $p<0.05$). Complex I-mediated mitochondrial respiration (normalized to citrate synthase activity) improved 8.1±2.8 (15.4%, $p<0.01$). Oxidative damage observed as carbonyl groups was reduced 132±60 grayscale units (8.0%, $p<0.05$). **Conclusions:** Revascularization operations improved the hemodynamics, QOL and leg function of PAD patients in association with improvement in PAD-related ischemic myopathy.
I. Pipinos: None. **S. Myers:** None. **M. Fuglestad:** None. **P. Koutakis:** None. **J. Kim:** None. **Z. Zhu:** None. **J. Thompson:** None. **D. Ha:** None. **J. Johanning:** None. **G. Casale:** None.

139
PARP-1 Silencing Upregulates FOSL1 Transcription, Enhances Angiogenesis and Accelerates Ischemic-Diabetic Wound Healing
Jaideep Banerjee, Divya Cheedu, Raul Sebastian, Robyn Mascata, Anton Sidawy, Lopa Mishra, Bao Nguyen, George Washington Univ, Washington, DC

Objective: People with combined ischemic and diabetic wounds of the lower extremities have the highest risk for limb loss, especially for those without surgical revascularization options. We have demonstrated that Poly-ADP-Ribose polymerase (PARP-1) is hyperactivated in hyperglycemic/hypoxic cells and in ischemic/diabetic murine wounds. This study elucidates the molecular mechanisms of PARP-1 mediated impairment of angiogenesis in diabetic/ischemic wounds.
Methods: A model of dorsal bipedicle flap-ischemic wounds

on diabetic mice was used. The wounds were treated topically with nanoparticle-encapsulated siPARP-1 or vehicle. Wound closure rate and perfusion was analyzed using digital photography and Laser Doppler scanning, respectively. Angiogenetic markers in the tissues were measured by immunohistochemistry. In-vitro endothelial tube formation assay was performed using HUVECs cultured under hyperglycemic and hypoxic conditions.
Results: Wounds treated with topical siPARP-1 significantly accelerated wound healing compared to vehicle (from 25% ± 5% to 40%± 8% (n=7, p < .05) by day 6 and from 50% ± 15% to 75%± 3% (n=7, p < .05) by day 12, and also exhibited improved tissue perfusion (50%± 5% increase in perfusion units over control on day 6, n=47 p <0.05). Improved capillary density was also observed in the siPARP-1 treated wounds detected by immunohistochemistry for SMA (250%±35% increase in mean fluorescence intensity over control on day 12, n=4, p<0.05) and CD31 (125% ± 15% increase in mean fluorescence intensity over control on day 12, n=4, p<0.05). In-vitro angiogenesis assay showed that PARP-1-silencing significantly enhanced endothelial tube formation of hyperglycemic/hypoxic HUVECs (15± 4 complete polygons as compared to 0 in untreated, n=4, p<0.05). Human angiogenesis PCR-array analysis of pro-angiogenic factors revealed that PARP-1 silencing upregulated FOSL1 transcription by 5-fold (n=4, p<0.05). Interestingly, co-silencing of FOSL1 in PARP-1 silenced HUVECs resulted in loss of endothelial tube formation.
Conclusions: PARP-1 silencing is an effective strategy to promote ischemic-diabetic wound healing. Our data suggest that PARP-1-FOSL1 is a potential novel axis in angiogenesis and PARP-1 could be a promising therapeutic target for improving angiogenesis in these wounds.
J. Banerjee: None. **D. Cheedu:** None. **R. Sebastian:** None. **R. Mascata:** None. **A. Sidawy:** None. **L. Mishra:** None. **B. Nguyen:** None.

140
Real-time Modulation of Platelet Phenotype and Vein Wall Biology in Patients with Chronic Venous Insufficiency
Doran S Mix, Zane Young, Sandra Toth, Rachel Schmidt, Adam J Doyle, Jennifer L Ellis, Michael C Stoner, Igor Gosev, Sunil Prasad, Peter Knight, Sara Ture, Craig Morrell, Scott J Cameron, Univ of Rochester Medical Ctr, Rochester, NY

Background: The role of antiplatelet agents in the modulation of arterial disease is well described, but a paucity of data exists regarding their role in chronic venous insufficiency (CVI). We hypothesize that platelet responses to various antiplatelet agents are altered when comparing platelet function within refluxing and non-refluxing vein segments. Additionally, changes in platelet phenotype may alter vein wall biology.
Methods: Isolated platelets were obtained simultaneously from the patient antecubital vein (ACV) and a refluxing greater saphenous vein (GSV) during surgical phlebectomy and compared to platelets from healthy individuals. Non-refluxing GSV was harvested for coronary bypass. Platelet surface receptor activation was assessed through P2Y12 (clopidogrel), PAR1 (vorapaxar), and thromboxane (aspirin) pathways by flow cytometry for p-selectin. Immunoblotting assessed CD41 (platelet) and CD45 (WBC) within the wall of vein samples.
Results: Platelets from refluxing GSV showed a significant **increase** in reactivity via all platelet signaling pathways, especially P2Y12 and thromboxane when compared to platelets from the ACV in the same patient. Conversely, platelets collected from the ACV in CVI patients showed a significant **decrease** in reactivity to all agonists compared to ACV in healthy individuals without CVI. Most notably, GSV from a patient with CVI had a **reduction** in CD41 content, but a **seven-fold increase** in the CD45:CD41 ratio, compared to GSV from healthy people (Figure).
Conclusions: Platelet activation by these clinically relevant pathways is enhanced locally in the refluxing GSV, yet systemic, circulating platelets isolated from CVI patients are **2-3-fold less** active than systemic platelets from healthy people. Our data suggest that reflux may locally alter the circulating platelet phenotype and in turn also have a role in remodeling the vein wall.

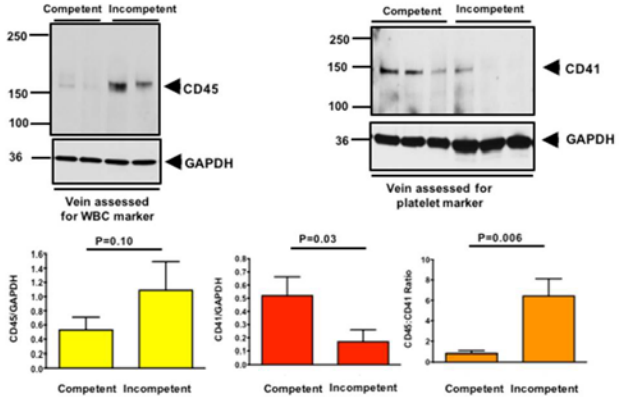

D.S. Mix: None. **Z. Young:** None. **S. Toth:** None. **R. Schmidt:** None. **A.J. Doyle:** None. **J.L. Ellis:** None. **M.C. Stoner:** None. **I. Gosev:** None. **S. Prasad:** None. **P. Knight:** None. **S. Ture:** None. **C. Morrell:** None. **S.J. Cameron:** None.

141
The Role of Epsin in Regulating Lymphangiogenesis in Diabetes
Hong Chen, Harvard Medical Sch, Boston, MA

Lymphangiogenesis occurs in adult tissues of chronic complex diseases, including diabetes. Whether lymphangiogenesis is altered owing to diabetic complication remains unknown. VEGF-C/VEGFR-3 signaling axis fuels the growth of lymphatic vessels. How VEGF-C/VEGFR3 signaling is regulated under pathological conditions, such as diabetes, however, is poorly understood. Here, we report that mice with inducible lymphatic endothelial cell-specific deficiency of epsins 1 and 2 (LEC-iDKO) display enhanced lymphangiogenesis compared to wild type (WT) in diabetic condition. A profound increase in VEGF-C-induced lymphatic vessel growth is exhibited in corneas and subcutaneous Matrigel implanted in diabetic LEC-iDKO mice compared to diabetic WT mice. Conversely, lymphatic endothelial cells isolated from diabetic WT mice show marked impairment in proliferation, migration, and tube formation in response to VEGF-C relative to those from diabetic LEC-iDKO *in vitro*. Mechanistically, reactive oxygen species (ROS) generated from hyperglycemia induces c-Src-dependent VEGFR3 phosphorylation independent of VEGF-C, which parallels c-Src-dependent epsin upregulation through the transcription factor AP-1. Heightened epsin expression induced by ROS facilitates epsin binding to VEGFR3 within Golgi compartment, promoting degradation of newly synthesized VEGFR3, and progressively reducing availability of VEGFR3 at the cell surface. Consequentially, lymphatic-specific epsin loss strengthens insufficient lymphangiogenesis and improves the resolution of tail edema in diabetic mice. Collectively, our data indicate that inhibiting epsin expression protects VEGFR3 against degradation and ameliorates diabetes-triggered downregulation of lymphangiogenesis, providing a plausible original therapeutic strategy to treat lymphatic disease in diabetic patients.
H. Chen: None.

This research has received full or partial funding support from the American Heart Association.

145
Glucocorticoid Treatment is Associated with Lower Incidence of Myocardial Infarction in Patients Hospitalized for Community-acquired Pneumonia
Roberto Cangemi, Marco Falcone, Alessio Farcomeni, Camilla Calvieri, Gabriella Scarpellini, Simona Battaglia, Giusy Tiseo, Giulio Francesco Romiti, Giuliano Bertazzoni, Gloria Taliani, **Francesco Violi**, Sapienza Univ of Rome, Rome, Italy; SIXTUS Study Group

BACKGROUND. Previous reports suggest that patients hospitalized for community-acquired pneumonia (CAP) have an enhanced risk of myocardial infarction (MI). Glucocorticoids have been proposed for the treatment of CAP. Although a recent meta-analysis showed that glucocorticoids can reduce morbidity and mortality in severe CAP, their role in the treatment of pneumonia remains unclear. Experiments in vitro and in vivo demonstrated that glucocorticoids inhibit platelet aggregation and platelet-related arterial thrombosis. Since enhanced platelet activation seems to play a role in the occurrence of MI in CAP patients, aim of the study was to assess the impact of glucocorticoids on MI occurrence in a cohort of patients hospitalized for CAP.
METHODS and RESULTS. Consecutive patients admitted to the University-Hospital Policlinico Umberto I (Rome, Italy) with CAP were recruited and prospectively followed-up until discharge. The primary outcome of the study was the occurrence of an MI during hospitalization. Seven-hundred fifty-eight patients (493 males, 265 females; age: 71.7 ± 14.4 years) were included in the study: 241 (32%) were treated with systemic glucocorticoids (methylprednisolone, betamethasone or prednisone) during in-hospital follow-up, whereas 517 patients were not treated with systemic glucocorticoids. During the follow-up, 62 patients (8.2%) had an MI. Compared to the nonglucocorticoid group, patients treated with glucocorticoids showed a lower incidence of MI (9.5% vs. 5.4%; p=0.011). A Cox regression analysis showed that age, a history of coronary heart disease, and a major degree of respiratory impairment (pO2<60mmHg and pH<7.35) was positively associated to MI incidence, whereas glucocorticoid therapy was negatively associated. Compared to patients not receiving glucocorticoids, the propensity score adjusted analysis confirmed that patients taking glucocorticoids had a lower incidence of MI (HR: 0.458; 95% CI: 0.235 - 0.893, p=0.022).
CONCLUSION. This study shows that in-hospital glucocorticoids treatment is associated with a lower incidence of MI within hospital-stay in a large cohort of patients with pneumonia.
R. Cangemi: None. **M. Falcone:** None. **A. Farcomeni:** None. **C. Calvieri:** None. **G. Scarpellini:** None. **S. Battaglia:** None. **G. Tiseo:** None. **G. Romiti:** None. **G. Bertazzoni:** None. **G. Taliani:** None. **F. Violi:** None.

146
Performance of a Chromogenic Thrombin Generation Assay in the Thrombophilia Screening in 597 Unselected Patients with a History of Venous Thromboembolism
Pierre Toulon, Pasteur Univ Hosp, Nice, France; Isabelle Martin-Toutain, Annick Ankri, La Pitie-Salpétriere Hosp, Paris, France

The HemosIL ThromboPath assay (Instrumentation Laboratory) is a chromogenic assay designed to globally evaluate the functionality of the protein C (PC) pathway. It is based on the ability of endogenous APC generated after activation of PC by a snake venom extract (Protac) to reduce the thrombin generation induced by a reagent containing tissue factor. Briefly, optical density is measured after addition of a thrombin-specific chromogenic substrate in the presence (OD A) or absence (OD B) of Protac. Test results are expressed as the Protac-Induced Coagulation Inhibition percentage (PICI%) that corresponds to the ratio [OD B-OD A]/OD B x 100. A normal test result corresponds to a PICI% above a cut-off level defined as the mean-1 SD of the values measured in 30 healthy controls. To determine the performance of that assay, we retrospectively tested frozen plasma samples from 597 consecutive patients referred for screening of biological risk factors for venous thrombosis (209 M and 388 F, mean age=45.6 years, range 15-100). None was on vitamin K-antagonist or had evidence of liver failure. PICI% was significantly lower in patients who presented with than in those without any PC pathway abnormality [median=69.0% (range: 15.3-96.8), n=101 vs. 89.8 (range: 38.5-98.0), n=496; p<0.0001]. All carriers of the Factor V Leiden mutation (32 heterozygotes, and 1 homozygote) had a PICI% below the cut-off level (88.5%). The same applied to all patients with either a PC deficiency (n=14) or a lupus anticoagulant (n=8). The test sensitivity to congenital and acquired PS deficiency was 97.7% (n=45/46). 41.5% of the patients without abnormality of the PC pathway had a decreased test result (n=206/496). The overall test sensitivity to tested thrombophilia was 99.0% (95%CI=94.6-100), its specificity 58.5% (95%CI=54.0-62.9), its negative predictive value (NPV) 99.7% (95%CI=98.1-100) and its PPV 32.7% (95%CI=27.4-38.2).
The high sensitivity of the HemosIL ThromboPath assay to PC pathway abnormalities together with a high NPV, closed to 100%, associated with a normal test result, suggest the potential interest of that assay as part of the screening strategy of PC pathway abnormalities. In that connection, the economic impact of its introduction is currently evaluated.
P. Toulon: None. **I. Martin-Toutain:** None. **A. Ankri:** None.

147
The Role of Thrombin Generation in Cardiovascular Disease and Mortality - Results from the Population-based Gutenberg Health Study
Pauline C van Paridon, Lab for Clinical Thrombosis and Hemostasis, Dept of Internal Med, Cardiovascular Res Inst Maastricht (CARIM), Maastricht, Netherlands; Marina Panova-Noeva, Ctr for Thrombosis and Hemostasis (CTH), Univ Medical Ctr of the Johannes Gutenberg-Univ Mainz, Mainz, Netherlands; Rene van Oerle, Lab for Clinical Thrombosis and Hemostasis, Dept of Internal Med, Cardiovascular Res Inst Maastricht (CARIM), Maastricht, Netherlands; Andreas Schulz, Ctr for Thrombosis and Hemostasis (CTH), Univ Medical Ctr of the Johannes Gutenberg-Univ Mainz, Mainz, Germany; Iris M. Hermanns, Preventive Cardiology and Preventive Med, Ctr for Cardiology, Univ Medical Ctr of the Johannes Gutenberg-Univ Mainz; Univ of Applied Sciences, Hochschule Fresenius Idstein, Mainz, Germany; Jürgen H Prochaska, Ctr for Thrombosis and Hemostasis (CTH), Univ Medical Ctr of the Johannes Gutenberg-Univ Mainz; Preventive Cardiology and Preventive Med, Ctr for Cardiology, Univ Medical Ctr of the Johannes Gutenberg-Univ Mainz, Mainz, Germany; Natalie Arnold, Preventive Cardiology and Preventive Med, Ctr for Cardiology, Univ Medical Ctr of the Johannes Gutenberg-Univ Mainz, Mainz, Germany; Harald Binder, Inst of Medical Biometry and Statistics, Faculty of Med and Medical Ctr - Univ of Freiburg, Freiburg; Inst of Medical Biostatistics, Epidemiology and Informatics, Univ Medical Ctr of the Johannes Gutenberg-Univ Mainz, Freiburg and Mainz, Germany; Irene Schmidtmann, Inst of Medical Biostatistics, Epidemiology and Informatics, Univ Medical Ctr of the Johannes Gutenberg-Univ Mainz, Mainz, Germany; Manfred E Beutel, Dept of Psychosomatic Med and Psychotherapy, Univ Medical Ctr of the Johannes Gutenberg-Univ Mainz, Mainz, Germany; Norbert Pfeiffer, Dept of Ophthalmology, Univ Medical Ctr of the Johannes Gutenberg-Univ Mainz, Mainz, Germany; Thomas Münzel, Cardiology I, Ctr for Cardiology, Univ Medical Ctr of the Johannes Gutenberg-Univ Mainz; DZHK (German Ctr for Cardiovascular Res), Partner Site RhineMain, Mainz, Germany; Karl J Lackner, Inst for Clinical Chemistry and Lab Med, Univ Medical Ctr of the Johannes Gutenberg-Univ Mainz; DZHK (German Ctr for Cardiovascular Res), Partner Site RhineMain, Mainz, Germany; Hugo ten Cate, Lab for Clinical Thrombosis and Hemostasis, Dept of Internal Med, Cardiovascular Res Inst Maastricht (CARIM), Maastricht,

Netherlands; Philipp S Wild, Ctr for Thrombosis and Hemostasis (CTH), Univ Medical Ctr of the Johannes Gutenberg-Univ Mainz; Preventive Cardiology and Preventive Med, Ctr for Cardiology, Univ Medical Ctr of the Johannes Gutenberg-Univ Mainz, Mainz, Germany; Henri M Spronk, Lab for Clinical Thrombosis and Hemostasis, Dept of Internal Med, Cardiovascular Res Inst Maastricht (CARIM), Maastricht, Netherlands

Background: Thrombin formation is one of the key enzymatic processes that direct the activity of the hemostatic system. Thrombin generation (TG), a method addressing the overall potential of a given plasma sample to form thrombin, may be a potential tool to improve risk stratification for cardiovascular diseases (CVD). This study aims to explore the relation between TG and cardiovascular risk factors (CVRFs), CVD, and total mortality.
Methods: For this study, N=5000 subjects from the population-based Gutenberg Health Study were analyzed in a highly standardized setting. TG was measured by the Calibrated Automated Thrombogram method at 1 and 5 pM tissue factor (TF) trigger in platelet poor plasma. Lag time, endogenous thrombin potential (ETP), and peak height were derived from the TG curve. Sex-specific multivariable linear regression analysis adjusted for age, CVRFs, CVD and therapy (vitamin K antagonists, oral contraceptives and hormonal replacement therapy), was used to analyze the determinants of TG. Cox regression models adjusted for age, sex, CVRFs and vitamin K antagonists investigated the association between TG parameters and total mortality.
Results: Lag time (at 1 and 5 pM TF) was positively associated with obesity and dyslipidemia for both sexes ($p<0.0001$). Additionally, obesity was a positive determinant of ETP (at 1pM and 5 pM TF) in both sexes ($p<0.0001$) and peak height in males (1 pM TF, $p=0.0048$) and females (1 pM TF and 5 pM TF, $p<0.0001$). Cox regression models showed an increased mortality in individuals with a lag time (1 pM TF, HR=1.46, [95% CI: 1.07; 2.00], $p=0.018$) and ETP (5 pM TF, HR = 1.50, [1.06; 2.13], $p=0.023$) above the 95th percentile of the reference group, independent of the cardiovascular risk profile. Kaplan Meier survival curves showed a decreased survival in individuals with a lag time above the 90th percentile of the reference (1 and 5 pM TF, $p<0.0001$) and ETP above the 97.5th percentile of the reference (1 pM TF, $p=0.00097$).
Conclusion: This large-scale study provides important insights in the effects of traditional CVRFs, particularly obesity, on TG in males and females. Lag time and ETP were found as potentially relevant predictors of increased mortality in the general population, which deserves further investigation.
P.C.S. van Paridon: None. **M. Panova-Noeva:** None. **R. van Oerle:** None. **A. Schulz:** None. **I.M. Hermanns:** None. **J.H. Prochaska:** None. **N. Arnold:** None. **H. Binder:** None. **I. Schmidtmann:** None. **M.E. Beutel:** None. **N. Pfeiffer:** None. **T. Münzel:** None. **K.J. Lackner:** None. **H. ten Cate:** None. **P.S. Wild:** None. **H.M.H. Spronk:** None.

148
Cardiac Myosin Promotes Thrombin Generation and Attenuates Tissue Plasminogen Activator-induced Plasma Clot Lysis
Jevgenia Zilberman-Rudenko, Oregon Health & Science Univ, Portland, OR; Hiroshi Deguchi, Jennifer Orje, Tine Wyseure, Laurent O Mosnier, The Scripps Res Inst, La Jolla, CA; Owen J McCarty, Oregon Health & Science Univ, Portland, OR; Zaverio M Ruggeri, John H Griffin, The Scripps Res Inst, La Jolla, CA

Recently we discovered that skeletal muscle myosin, which is in the same family as cardiac myosin, exerts prothrombotic effects by binding factor Xa and enhancing prothrombin activation in the presence of factor Va. Thus, we tested the influence of cardiac myosin on thrombus formation and fibrinolysis. Studies of the effects of cardiac myosin on thrombogenesis *ex vivo* using fresh human flowing blood showed that perfusion of blood over cardiac myosin-coated surfaces at 300 s^{-1} shear rate caused extensive fibrin deposition. Addition of cardiac myosin to blood also promoted the thrombotic responses of human blood flowing over collagen-coated surfaces, evidence of myosin's thrombogenicity. Further studies showed that cardiac myosin enhanced thrombin generation in whole blood, platelet rich plasma and platelet poor plasma, indicating that myosin promotes thrombin generation in plasma primarily independently of platelets or other blood cell components. In a purified system composed of factor Xa, factor Va, prothrombin and calcium ions, cardiac myosin greatly enhanced prothrombinase activity. Experiments using Gla-domainless factor Xa showed that the Gla domain of factor Xa was not required for cardiac myosin's prothrombinase enhancement in contrast to phospholipid-enhanced prothrombinase activity which requires that Gla domain. In studies of tissue plasminogen activator (tPA)-induced plasma clot lysis, increasing concentrations of cardiac myosin attenuated tPA-mediated clot lysis. The ability of cardiac myosin to inhibit tPA-induced plasma clot lysis was ablated in the presence of the carboxypeptidase inhibitor from potatoes, an inhibitor of thrombin activatable fibrinolysis inhibitor (TAFI). Clot lysis assays using TAFI-deficient plasma confirmed the requirement for TAFI for the antifibrinolytic action of cardiac myosin. We hypothesize that cardiac myosin-dependent thrombin generation increases TAFI activation and subsequent inhibition of clot lysis. In summary, here we show that cardiac myosin is both procoagulant and anti-fibrinolytic due to its ability to bind factor Xa and strongly promote thrombin generation. This raises new questions about potential procoagulant functions for cardiac myosin in coronary health and disease.
J. Zilberman-Rudenko: None. **H. Deguchi:** None. **J. Orje:** None. **T. Wyseure:** None. **L.O. Mosnier:** None. **O.J.T. McCarty:** None. **Z.M. Ruggeri:** None. **J.H. Griffin:** None.

This research has received full or partial funding support from the American Heart Association.

150
Monocyte-Platelet Aggregates Correlate With the Prevalence and Severity of Aortic Aneurysms
Tarik Hadi, Ludovic Boytard, Krista Barone, Caron Rockman, Mark Adelman, Jeffrey S Berger, Bhama Ramkhelawon, NYU Langone Medical Ctr, New York, NY

OBJECTIVE: To determine whether monocyte-platelet aggregates (MPA) correlate with aortic aneurysm (AA) prevalence and severity. **BACKGROUND**: Inflammation and intraluminal thrombus are key hallmarks of complex AA. While monocytes fuel inflammation in AA, the contribution of platelets is unknown. We hypothesized that increased platelet activity yields to MPA that drive AA development and indicate disease severity. **METHODS**: Blood was collected from 49 symptomatic patients admitted for aneurysm repair procedures (8 thoracic and 41 abdominal) and 36 matched controls. All subjects were on aspirin monotherapy. Platelet responsiveness to agonists was characterized by light transmission aggregometry. Flow cytometry analysis allowed leukocytes (CD45+)/monocytes (CD14+)-platelet (CD61+) aggregates (LPA/MPA) measurements in the blood and profiled MPA in post-surgical aneurysm tissues. **RESULTS**: Platelet aggregation in response to ADP (57% vs. 35% aggregation, $p<0.001$) and arachidonic acid (24% vs. 16% aggregation, $p=0.03$), was increased in patients with AA versus controls. LPA (17.7 vs 6.2% CD61+ leukocytes, $p=0.002$) and MPA (18.0 vs 7.2% CD61+ Monocytes, $p=0.008$) were robustly increased in AA vs controls. MPA but not LPA was strongly and positively associated with AA size ($p<0.0001$). To delve into the role of MPA *in situ* in AA sac, platelets and tissue macrophage activation was characterized. Compared to the non-diseased part of the aorta, diseased section had significantly higher platelet infiltration (7.0% vs 1.2% CD61+ cells, $p=0.006$) and

interaction with CD68+ tissue macrophages (8.3% vs. 0.7%, CD61+ macrophages p=0.03). Notably, macrophages highly expressed the adhesion protein, ICAM-1, in the diseased part (39.6 vs 3.3% in the non-diseased section, p<0.001) which further increased to 69.4% (p=0.01) when macrophages were in contact with platelets.
CONCLUSIONS: Our data highlights MPA as a novel mediator valuable to predict AA prevalence and severity.
T. Hadi: None. **L. Boytard:** None. **K. Barone:** None. **C. Rockman:** None. **M. Adelman:** None. **J.S. Berger:** None. **B. Ramkhelawon:** None.

151
Plasminogen Activator Inhibitor-1 Stimulates Smooth Muscle Senescence and Atherosclerosis Formation
Drew J Braet, Yan Ji, William P Fay, Univ of Missouri, Columbia, MO

Cell senescence, which is characterized by loss of replicative capacity and secretion of inflammatory mediators, was recently shown to play a causal role in atherosclerosis. Plasminogen activator inhibitor-1 (PAI-1), a serine protease inhibitor that regulates fibrinolysis, cell migration, and cell proliferation, promotes cell senescence. This study tested the hypotheses that 1) PAI-1 stimulates vascular smooth muscle cell (SMC) senescence and 2) pharmacologic PAI-1 inhibition attenuates senescence of SMCs and atherosclerotic plaques. Human coronary artery SMCs were grown in culture and treated with recombinant PAI-1 and PAI-039 (tiplaxtinin), a specific pharmacological inhibitor of PAI-1. SMCs were scored for the presence of senescence-associated β-galactosidase (SA-βgal), an enzyme whose expression is specifically upregulated in senescent cells. PAI-1 (10 µg/mL) significantly increased SMC senescence (28.3±1.2% senescent cells, n=6) compared to vehicle control (14.3±1.4%, n=7, p <0.05). PAI-039 (25 µM) significantly decreased PAI-1-induced SMC senescence (19.1±1.1%, n=5, p <0.05 vs PAI-1-treated cells). To examine the significance of our findings in vivo, we studied the effects of PAI-039 on cell senescence in aortas of *ldlr*$^{-/-}$ mice fed a western diet (WD) with or without PAI-039 (5 mg/g of diet). After twelve weeks of WD aortas were harvested and SA-βgal activity was measured in intact specimens with FDG substrate. SA-βgal activity was significantly less in *ldrl*$^{-/-}$ mice fed WD containing PAI-039 (366±64 FU/mg, n=7) compared to controls (591±82 FU/mg, n=7, p<0.05). The decrease in senescence was associated with a statistically significant reduction in atherosclerosis formation, assessed by quantitative Oil Red O imaging. In summary, SMC senescence is stimulated by PAI-1 and down-regulated by PAI-039, a specific PAI-1 inhibitor. PAI-039 also significantly inhibited cell senescence in aortas of *ldlr*$^{-/-}$ mice fed WD. These results suggest that PAI-1 is an important mediator of SMC senescence and that pharmacologic targeting of PAI-1 is an effective strategy to inhibit vascular senescence and atherogenesis in vivo.
D.J. Braet: None. **Y. Ji:** None. **W.P. Fay:** None.

153
Gut Microbiota-derived Lipolysaccarides Are Enhnaced in the Coronary Thrombi of Patients With Myocardial Infarction
Cristina Nocella, Roberto Carnevale, Camilla Calvieri, Roberto Cangemi, Vittoria Cammisotto, Enrico Mangeri, Sapienza Univ of Rome, Rome, Italy; Marcello Dominici, Alessio Arrivi, S. Maria Univ Hosp, Terni, Italy; Giacomo Frati, Giulia D'Amati, Gaetano Tanzilli, Francesco Violi, Sapienza Univ of Rome, Rome, Italy

Background: Gut microbiota seems to be implicated in the athero-thrombotic process. Its relationship with coronary thrombosis has never been investigated. **Methods:** Serum levels of bacterial lipopolysaccharides (LPS) against Escherichia Coli (EC) and EC DNA amplification by polymerase chain reaction, plasma sP-selectin, a marker of platelet activation, and zonulin, a marker of gut permeability, were measured in patients with ST-elevation myocardial infarction (STEMI) (n=50) or stable coronary disease (SA) (n=50) and controls (n=50). Serum LPS and sP-selectin were also measured in coronary thrombi and coronary blood of patients with STEMI and stable coronary disease, respectively. Immuno-histochemical analysis was performed in coronary thrombi of 12 STEMI patients. Finally, in vitro study was undertaken to evaluate if LPS stimulate leucocyte-platelet interaction. **Results:** Compared to controls, patients with SA and STEMI had higher systemic levels of LPS (p<0.001), sP-Selectin (p<0.001) and zonulin (p<0.001); these variables were higher in STEMI versus SA (p<0.001). LPS was significantly associated with serum zonulin (β=0.421; p<0.001), and sP-Selectin (Rs=0.501; p<0.001). Analysis of DNA Escherichia coli showed positivity in 10% of patients with coronary heart disease and no positivity in controls. Immuno-histochemical analysis of coronary thrombi showed positivity for leucocyte TLR4 and Cathepsin G (70% and 100% respectively). In vitro study showed that leucocyte incubation with LPS elicited formation of platelet aggregates, which were blunted by an inhibitor of Cathepsin G.
Conclusion: Bacterial LPS is detected in coronary thrombi of STEMI patients and may be implicated in the thrombotic process via leucocyte-mediated platelet activation.
C. Nocella: None. **R. Carnevale:** None. **C. Calvieri:** None. **R. Cangemi:** None. **V. Cammisotto:** None. **E. Mangeri:** None. **M. Dominici:** None. **A. Arrivi:** None. **G. Frati:** None. **G. D'Amati:** None. **G. Tanzilli:** None. **F. Violi:** None.

155
High sensitivity C-Reactive Protein Predicts Future Cerebrovascular Events in Patients Undergoing Carotid Endarterectomy
Megha Prasad, Valentina Nardi, Lilach Lerman, Amir Lerman, Mayo Clinic, Rochester, MN

Background High sensitivity C-reactive protein is a risk factor atherosclerosis and plaque rupture. We aimed to determine the role of high-sensitivity C reactive protein in predicting future cerebrovascular events (CVA), including stroke and transient ischemic attack, in patients undergoing routine carotid endarterectomy (CEA). Methods: A total of 251 patients underwent routine CEA without any history of stroke. At baseline prior to CEA, patients underwent routine laboratory testing, including testing for novel biomarkers including hs-CRP. Patients were followed for a median of 10.9 years (IQR 7.3, 13.4) for the development of CVA with regular nursing follow-up and/or chart review. Results: Of 251 patients enrolled in the study, 19 patients without prior CVA subsequently developed CVA during follow-up. In univariate analysis, baseline hsCRP was significantly higher in patients who developed CVA during follow-up vs. those that did not (8.1 (IQR 2.2, 46.3) mg/L vs. 3.85(0.9, 11.75) mg/L; p=0.0054)(Figure 1). After adjusting for confounders including age. diabetes mellitus, cholesterol, systolic blood pressure, history of smoking, aspirin use and duration of follow-up, log hsCRP was an independent predictor of CVA during follow-up after CEA (L-R 9.9; p=0.0016). Discussion: Hs-CRP appears to be a risk factor for CVA during follow-up after CEA. Further investigation is necessary to determine the role of risk modification in these patients and the therapeutic potential of reducing inflammation in this population.

Figure 1: Log hsCRP and Cerebrovascular Events on Follow-up

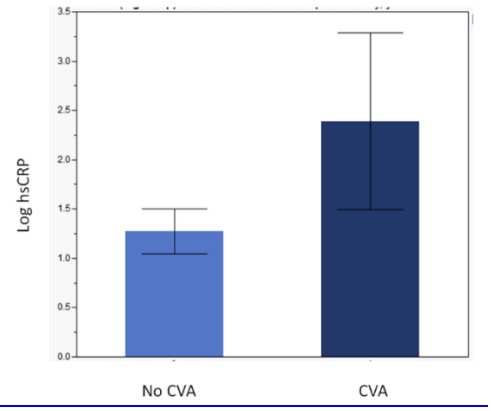

M. Prasad: None. **V. Nardi:** None. **L. Lerman:** None. **A. Lerman:** None.

156
Uric acid is an Independent Predictor of Plaque Stability and Future Cerebrovascular Events in Patients Undergoing Carotid Endarterectomy
Megha Prasad, Valentina Nardi, Lilach Lerman, amir Lerman, Mayo Clinic, Rochester, MN

Background: Uric acid is a known risk factor for atherosclerosis. We aimed to determine whether baseline uric acid levels predict plaque stability on presentation and future cerebrovascular events (CVA) in patients undergoing carotid endarterectomy (CEA). Methods: We analyzed 317 patients who underwent CEA between 2/2002 and 6/2017. Patients were stratified according to plaque stability as unstable or stable --those who presented with a history of ≥ 1 neurologic event were "unstable" and those with no history of CVA were classified as stable. All patients underwent comprehensive baseline laboratory testing at baseline prior to CEA and then were followed by a nurse coordinator and through the medical record for the development of cerebrovascular events including stroke and transient ischemic attack for a median of 10.9 years (IQR 7.3, 13.4). Results:
Baseline uric acid was significantly higher in patients presenting with unstable plaque vs. stable plaque(6.5 (IQR 5.6, 7.9) vs. 5.8(IQR 4.8,6.6); p<0.001), and was an independent predictor of plaque stability when adjusting for potential confounders including glucose, BMI, hsCRP, cholesterol, and systolic blood pressure (L-R 6.9, p=0.0096). There were a total of 58 CVA during follow-up, and baseline uric acid was higher among patients who developed CVA vs those without CVA [(6.9 ± 2.1) mg/dL vs. (6.4± 1.7) mg/dL; p=0.037]. After adjusting for diabetes, cholesterol, systolic blood pressure, smoking , age, aspirin, and creatinine, uric acid and cholesterol were both independent predictors of stroke in this population [uric acid: (LR 4.84, p=0.03); cholesterol: (L-R 11.8, p=0.0006)]. Discussion: While cholesterol has been associated with poor outcomes in patients with vascular disease, our data suggest that uric acid may be a novel risk factor for stroke in patients undergoing CEA. Further investigation is necessary to understand the therapeutic potential of reducing uric acid levels in these patients and the potential benefit of reducing overall cerebrovascular risk.
M. Prasad: None. **V. Nardi:** None. **L. Lerman:** None. **A. Lerman:** None.

157
Micromechanics of Blood Clots
Wilson Eng, Max Kim, Stephanie Pham, Amit Saha, **Anand K Ramasubramanian**, Sang-Joon Lee, SJSU, San Jose, CA

Understanding clot biomechanics is critical for the treatment of cardiovascular diseases. Based on our recent observation that that the structural configuration of the clot network correlates well with the mechanical properties such as stiffness, we hypothesized that the heterogeneity in the mechanical response of the microstructure dictates clot micromechanics and hence the macroscopic behavior. To test this hypothesis, we have custom-developed a microextensometer device coupled to a microscope to probe and image microstructural changes and micromechanical behavior of fibrin and blood clots. 20 µL clots were pulled at a prescribed strain rate of 60 µm/s using a programmable nano-positioner, and the force was measured using a 10 g load cell and acquired at 500 Hz. From the stress-strain measurements, we observed that both FFP and blood clots showed non-linear and abrupt changes in resistive tensile force in response to constant strain rate (Fig. 1A). Using fiduciary markers, we observed that cross-linked, but not uncrosslinked, fibrin clots showed a microscopically non-uniform deformation in response to macroscopically constant strain rate. Further, computational analysis of the mechanical response of clot microstructure to an applied stress revealed heterogeneity in strain energy distribution dictated by the network properties (Fig. 1B). Together, our results suggest that the heterogeneity in microscale translates to the non-linear response at the macroscale, and will ultimately dictate the pathophysiology of thrombosis.

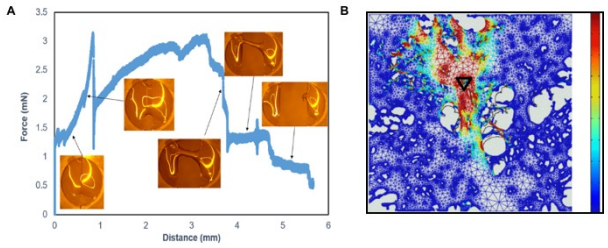

Figure 1. (A) Resistive force of FFP clots measured by microextensometry in response to a prescribed strain rate of 60 µm/s, and the inset shows instantaneous reaction of the clots (B) Fluorescence images of clots were analyzed by FEM analysis to obtain relative strain energy distribution in response to an applied contraction in the region indicated by black triangle.

W. Eng: None. **M. Kim:** None. **S. Pham:** None. **A. Saha:** None. **A.K. Ramasubramanian:** None. **S. Lee:** None.

158
Indoleamine 2,3-dioxygenase 1 is Expressed in Macrophages in Human Coronary Atherosclerotic Plaque and is Associated With Tissue Factor Expression in Activated THP-1 Macrophages
Yuki Watanabe, Shohei Koyama, Yunosuke Matsuura, Kensaku Nishihira, Atsushi Yamashita, Kazuo Kitamura, Yujiro Asada, Univ of Miyazaki, Miyazaki, Japan

Background: Recently, several clinical studies have found that changes in the kynurenine (Kyn) pathway of tryptophan (Trp) metabolism are associated with cardiovascular events. Indoleamine 2,3-dioxygenase 1 (IDO1) is a rate-limiting enzyme of the Kyn pathway and is induced by cytokines, particularly IFNγ. However, the roles of the Kyn pathway on vascular wall thrombogenicity remain unknown. *Objective:* The present study aimed to localize IDO1 in human coronary atherosclerotic plaques from patients with stable angina pectoris (SAP) and unstable angina pectoris (UAP) and define its role in plaque thrombogenicity. *Methods:* Immunohistochemical methods were applied to localize IDO1 in coronary atherosclerotic plaques from patients with SAP and UAP. We examined the role of IDO1 in tissue factor (TF) expression in THP-1 macrophages activated by interferon (IFN)γ and tissue necrosis factor (TNF)α. *Results:*

We localized IDO1 mainly in CD68-positive macrophages in atherosclerotic plaques, and in close association with TF. Areas that were immunopositive for IDO1, TF, and CD3-positive T lymphocytes were significantly larger in plaques from patients with UAP than SAP. THP-1 macrophages activated by IFNγ and TNFα upregulated IDO1 expression, increased the Kyn/Trp ratio and enhanced TF expression and activity, but not TF pathway inhibitor expression. The IDO1 inhibitor epacadostat significantly reduced the Kyn/Trp ratio, TF expression and activity, as well as NF-κB (p65) binding activity in activated THP-1 macrophages. Inhibition of the aryl hydrocarbon receptor (AHR) that binds to Kyn, also reduced Kyn-induced TF expression in activated THP-1 macrophages. Kynurenine dose-dependently increased TF expression under IDO1 inhibition whereas hydroxyanthranilic and quinolinic acids did not. *Conclusion:* The IDO1 is expressed in coronary atherosclerotic plaques and might contribute to thrombus formation through TF upregulation via NF-κB (p65) and AHR in activated macrophages.
Y. Watanabe: None. **S. Koyama:** None. **Y. Matsuura:** None. **K. Nishihira:** None. **A. Yamashita:** None. **K. Kitamura:** None. **Y. Asada:** None.

159
Neurotrophin 3 Plays a Critical Role in TLR4-mediated Fibrogenic Response in Human Aortic Valve Interstitial Cells
Qingzhou Yao, Lihua Ao, David A. Fullerton, Xianzhong Yao, 12700 E 19TH ST, Aurora, CO

Aortic stenosis is a chronic inflammatory condition, and valvular fibrosis and calcification are significant pathological changes in the progression of aortic stenosis. Aortic valve interstitial cell (AVIC) proliferation and over-expression of extracellular matrix (ECM) proteins promote valvular fibrosis. Although pro-inflammatory stimuli are the culprits of aortic valve fibrosis, the mechanism by which they induce aortic valve fibrogenic change remains incompletely understood. Our recent findings suggest that AVICs from diseased aortic valves express higher levels of neurotrophin 3 (NT3) protein and that NT3 is capable of up-regulating AVIC proliferation and ECM protein expression. In this study, we tested the **hypothesis** that pro-inflammatory stimulation up-regulates NT3 production to enhance the pro-fibrogenic activity in human AVICs. **Methods and Results:** Human AVICs isolated from normal valves were treated with Toll-like receptor 4 (TLR4) agonist lipopolysaccharide (LPS, 0.20 μg/ml) for 3 to 28 days in the presence or absence of a neutralizing antibody against NT3. LPS elevated BrdU incorporation, collagen III expression and collagen deposition. Neutralization of NT3 markedly reduced these pro-fibrogenic changes. Interestingly, LPS up-regulated NT3 levels in human AVICs in a TLR4-dependent fashion, and inhibition of either Akt or ERK1/2 attenuated the effect of LPS on NT3 expression. Recombinant NT3 induced human AVIC proliferation, collagen III expression and collagen deposition through the Trk receptors. Inhibition of the Trk receptors abrogated the pro-fibrogenic effect of LPS on AVICs. **Conclusions:** Stimulation of TLR4 in human AVICs elevates the pro-fibrogenic activity through up-regulating the production of neural growth factor NT3. The Akt and ERK1/2 pathways are involved in TLR4-mediated NT3 up-regulation, and the Trk receptors mediate the pro-fibrogenic effect of TLR4 stimulation in human AVICs. These findings reveal a molecular mechanism underlying pro-inflammatory elevation of AVIC pro-fibrogenic activity and indicate the therapeutic potential of antagonizing NT3 for suppression of aortic valve fibrosis in an inflammatory setting.
Q. Yao: None. **L. Ao:** None. **D. Fullerton:** None. **X. Yao:** None.

164
Synthetic High-Density Lipoprotein Cholesterol Scavengers for the Treatment of Niemann-Pick C Disease
Maria V. Fawaz, Mark Schultz, Ruth Azaria, Ran Ming, Andrew Lieberman, Anna Schwendeman, Univ of Michigan, Ann Arbor, MI

Background: Niemann-Pick C disease (NPC) is genetic disorder caused by an accumulation of unesterified cholesterol in late endosomes and lysosomes due to defects in *NPC* genes. The levels of ABCA1 gene expression and concentration of high-density lipoproteins (HDL) are significantly decreased in NPC patients. Infusion of synthetic HDL (sHDL) in patients with atherosclerosis has been previously found safe (up to 100 mg/kg) and effective at reducing cholesterol in atheroma. The objective of this study is to identify sHDL composition capable of rescuing cholesterol storage in NPC. **Materials and Methods:** A panel of sHDL formulations was prepared by lyophilization method using commercially available Apolipoprotein A-I mimetic peptide, 5A, complexed in various ratios with phospholipids such as sphingomyelin (SM), palmitoyl-oleoyl phosphatidylcholine (POPC), or dimyristoyl phosphatidylcholine (DMPC). The efficacy of 5A alone and sHDLs was determined in primary patient NPC and wild type fibroblast cells using fluorescent filipin staining and cholesterol efflux assay. Trafficking of sHDL in NPC fibroblasts was assessed by confocal microscopy using fluorescently-labeled sHDL. Finally, *in vivo* study was executed to examine effects of our best sHDL formulation 5A-SM in NPC1 I1061T homozygotes and littermate controls treated with vehicle or sHDL (100 mg/kg, i.p., 3x/wk) for 4 weeks, starting at 7 wks of age. Neurological correction was accessed by the balance beam tests and body weight changes were tracked. **Results:** Treatment of NPC fibroblasts with sHDL resulted in a dose- and time-dependent rescue of lipid storage (5A-POPC<5A-SM<5A-DMPC). Cellular toxicity was observed only for 5A-DMPC (~30%). HDL trafficking studies revealed that sHDLs got endocytosed into cells and co-localized with LAMP1. Additionally, administration of 100 mg/kg 5A-SM resulted in a significant rescue of body weight ($p<0.01$) in the NPC mice with no toxicity to animals. However, neuro-correction after sHDL treatment in adult mice was not detected. The absence of neuro-correction observed in adult NPC mice suggest that the alternative delivery routes, treatment durations, or sHDL compositions are still needed.
M.V. Fawaz: None. **M. Schultz:** None. **R. Azaria:** None. **R. Ming:** None. **A. Lieberman:** None. **A. Schwendeman:** None.

165
Proposed Mechanism of Inhibition of Paraoxonase 1 Activity by Isolevuglandins
Geetika Aggarwal, Sean S. Davies, Vanderbilt Univ, Nashville, TN

Paraoxonase 1 (PON1) is a High Density Lipoprotein (HDL) associated enzyme which binds to ApoAI and demonstrates lactonase, organophosphatase and arylesterase activity. Association of PON1 with ApoAI, results in a hyperactive state where PON1 activity increases 3-fold. Reduced PON1 activity has been consistently linked to increased atherosclerosis, but the mechanisms underlying this inhibition remain unclear. PON1 activity is found to be reduced in the settings of inflammation where myeloperoxidase (MPO) interacts with both ApoAI and PON1. Association of MPO with HDL generates substantial amounts of isolevuglandins (IsoLGs), lipid peroxidation products that irreversibly modify lysyl residues of proteins. We therefore hypothesized that association of MPO with HDL leads to IsoLG modifications of PON1 that reduce its activity. We found that incubating IsoLG with dextran purified HDL crosslinked PON1 and inhibited its PON1 activity (IC_{50} 7.5 μM). We then used purified recombinant PON1 to further elucidate the mechanism of inhibition. We considered four

models for inhibition of PON1 activity by IsoLG: a) IsoLG directly modifies PON1 to render it inactive; b) IsoLG modifies PON1 near the ApoAI binding site so it cannot associate with ApoAI to become hyperactivated, but PON1 retains its basal activity; c) IsoLG modifies ApoAI near the PON1 binding site, blocking PON1 association and subsequent hyperactivation; d) IsoLG crosslinks PON1 associated with ApoAI to render it inactive. We found that incubation of IsoLG with PON1 inhibited both its basal activity and its hyperactivation when modified PON1 was subsequently incubated with HDL. However incubation of HDL with IsoLG for 1 h, but not 24 h, prior to incubating with PON1 resulted in significant loss of PON1 hyperactivity. The initial reaction of IsoLG with lysines forms pyrrole adducts that can still react to crosslink other proteins, but over time these pyrrole adduct oxidize to form non-reactive lactam adducts. Therefore, modification of ApoAI by IsoLG only appears to result in reduced PON1 activity prior to oxidation of ApoAI adducts to non-reactive lactam adducts, suggesting that crosslinking of ApoAI to PON1 drives loss of PON1 activity. Future studies will examine whether small molecule IsoLG scavengers can block MPO mediated inhibition of PON1 activity.

G. Aggarwal: None. **S.S. Davies:** None.

166

Effects of Dietary Unsaturated Fat and Carbohydrate on the HDL Proteome and Metabolism of 9 HDL Proteins Across 6 HDL Size Fractions in Humans

Allison B Andraski, Harvard TH Chan Sch of Public Health, Boston, MA; Sasha A Singh, Lang Lee, Hideyuki Higashi, Ctr for Interdisciplinary Cardiovascular Sciences, Dept of Med, Brigham and Women's Hosp, Harvard Medical Sch, Boston, MA; Nathaniel Smith, Harvard TH Chan Sch of Public Health, Boston, MA; Masanori Aikawa, Ctr for Interdisciplinary Cardiovascular Sciences, Dept of Med, Brigham and Women's Hosp, Harvard Medical Sch, Boston, MA; Frank M Sacks, Harvard TH Chan Sch of Public Health, Channing Div of Network Med, Dept of Med, Brigham and Women's Hosp and Harvard Medical Sch, Boston, MA

INTRODUCTION When dietary carbohydrate replaces fat, HDL-C and apoA1 decrease. The proportion in plasma of large HDL2 decreases while small HDL3 increases. These findings suggest that diet affects metabolically important attributes of HDL that produce the size changes. We studied in humans the effect of dietary carbohydrate and unsaturated fat on the HDL proteome and metabolism of 9 HDL proteins across 6 HDL sizes.

METHODS AND RESULTS Twelve participants were placed on a controlled high unsaturated fat (HF) or high carbohydrate (HC) diet in a randomized crossover design. At the end of each 4-week diet period, subjects were infused with D3-Leu tracer, and blood was collected for 70 hrs. ApoA1-HDL was prepared by immunoaffinity purification, separated into 6 sizes α0, α1, α2, α3, preβ, and <preβ by ND-PAGE, and in-gel trypsinized for mass spectrometry. We used label free quantification to characterize the HDL proteome. The proteome composition and distribution across the 6 HDL sizes were remarkably conserved in all subjects on both diets. Diet altered the abundance of several proteins on the major HDL sizes α2 and α3. The HC diet increased proteins involved in lipid metabolism (apoC3, apoC1, apoC2-C4) and acute phase response (SAA1, 4), and decreased antioxidant (PON1, 3) and protease inhibitor (SERPINA3, G1) proteins. We also monitored the metabolism of 9 proteins that likely affect HDL metabolism – apoA1, apoA2, apoA4, apoC3, apoE, apoM, apoJ, apoL1, and LCAT. We used high resolution parallel reaction monitoring and XPI software to measure tracer enrichment in these 9 proteins across the 6 HDL sizes. We found that the HC diet increased apoA2 and decreased apoA1 and apoA4 pool sizes on large HDL. The HC diet increased apoA1 and apoE turnover on large α1 and α2 and 3, respectively.

CONCLUSIONS Dietary carbohydrate when it replaces unsaturated fat alters the HDL proteome and metabolism of several HDL proteins on specific HDL sizes. Carbohydrate increases the abundance of proteins involved in lipid metabolism and the acute phase response, decreases antioxidant and protease inhibitor proteins, and enhances turnover of apoE and apoA1. This study suggests that diet modulates HDL function by affecting HDL composition and the metabolism of major HDL proteins.

A.B. Andraski: None. **S.A. Singh:** None. **L. Lee:** None. **H. Higashi:** None. **N. Smith:** None. **M. Aikawa:** Research Grant; Significant; Kowa Company, Ltd. **F.M. Sacks:** Consultant/Advisory Board; Modest; Pfizer. Other; Modest; ApoC3 patent.

This research has received full or partial funding support from the American Heart Association.

167

Mechanism of Increased Low Density Lipoprotein Cholesterol and Decreased Triglycerides with Sodium-glucose Co-transporter 2 Inhibition

Debapriya Basu, Lesley-Ann Huggins, Diego Scerbo, Joseph Obunike, NYU Sch of Med, New York, NY; Adam E Mullick, Ionis Pharmaceuticals, Carlsbad, CA; Nicholas A Di Prospero, Janssen Res & Development, Raritan, NJ; Robert H Eckel, Univ of Colorado, Denver, CO; Ira J Goldberg, NYU Sch of Med, New York, NY

Objective: Although Sodium glucose cotransporter 2 (SGLT2) inhibition in humans sometimes leads to increased levels of low density lipoprotein (LDL) cholesterol, this therapy is associated with marked reduction in cardiovascular disease. In this study, we aimed to determine how SGLT2 inhibition alters circulating lipoproteins.Approach and Results: We used a mouse model in which plasma lipoprotein profiles were humanized by expression of human cholesteryl ester transfer protein and human apolipoprotein B100 to determine how SGLT2 inhibition alters lipoprotein profiles. The mice were fed a high fat diet and then were made partially insulin deficient using streptozotocin. SGLT2 was inhibited using a specific anti-sense oligonucleotide or canagliflozin, a clinically available oral SGLT2 inhibitor. Inhibition of SGLT2 increased circulating levels of LDL cholesterol and reduced plasma triglyceride levels. SGLT2 inhibition was associated with increased lipoprotein lipase activity in the post heparin plasma and decreased postprandial lipemia. The changes in lipoprotein metabolism were more significant in mice treated with SGLT2 ASO compared to canagliflozin.Conclusions: Our studies in mice recapitulate many of the changes in circulating lipids found with SGLT2 inhibition therapy in humans and suggest that the increased LDL cholesterol found with this therapy is due to greater lipolysis of triglyceride-rich lipoproteins. This change in lipoprotein physiology is likely, in part, to explain the reduced cardiovascular disease found with SGLT2 inhibition.

D. Basu: None. **L. Huggins:** None. **D. Scerbo:** None. **J. Obunike:** None. **A.E. Mullick:** Employment; Significant; Ionis Pharmaceuticals. Ownership Interest; Significant; Ionis Pharmaceuticals. **N.A. Di Prospero:** Employment; Significant; Janssen Research and Development. Ownership Interest; Significant; Janssen Research and Development. **R.H. Eckel:** None. **I.J. Goldberg:** Other Research Support; Significant; Janssen Research and Development.

168

Response Gene to Complement 32 Suppresses Adipose Tissue Thermogenic Genes through Inhibiting Beta3 Adrenergic Receptor mTORC1 Signaling

Sisi Chen, Xiaohan Mei, Amelia Yin, Hang Yin, **Xiao-Bing Cui**, Shi-You Chen, The Univ of Georgia, Athens, GA

Our previous study have shown that response gene to complement 32 (RGC-32) deficiency (Rgc32-/-) protects mice from diet-induced obesity and increases thermogenic

gene expression in adipose tissues. However, the underlying mechanisms by which RGC-32 regulates thermogenic gene expression remain to be determined. In the present study, we found that RGC-32 expression in white adipose tissue (WAT) was suppressed during cold exposure-induced WAT browning. Rgc32-/- significantly increased thermogenic gene expression in the differentiated stromal vascular fraction (SVF) of inguinal WAT (iWAT). Interestingly, Rgc32-/- and cold exposure regulated a common set of genes in iWAT as shown by RNA sequencing data. Pathway enrichment analyses showed that RGC-32 deficiency downregulated PI3K/Akt signaling-related genes. Consistently, Akt phosphorylation was also decreased in Rgc32-/- iWAT, which led to an increase in β3-adrenergic receptor expression and subsequent activation of mTORC1. β3-adrenergic receptor antagonist SR 59230A and mTORC1 inhibitor rapamycin blocked the Rgc32 deficiency-induced thermogenic gene expression in iWAT both in vitro and in vivo. These results indicate that RGC-32 suppressed iWAT thermogenic gene expression through down-regulation of β3-AR expression and mTORC1 activity via a PI3K/Akt-dependent mechanism.

S. Chen: None. **X. Mei:** None. **A. Yin:** None. **H. Yin:** None. **X. Cui:** None. **S. Chen:** None.

This research has received full or partial funding support from the American Heart Association.

169

Lipoproteins and their Modified Forms Regulate Smooth Muscle Cell Calcification

Emma J Akers, Jocelyne Mulangala, Peter J Psaltis, Christina Bursill, Stephen J Nicholls, **Belinda A Di Bartolo**, SAHMRI, Adelaide, Australia

Background: Vascular calcification (VC), alongside atherogenic lipoprotein profiles, have been correlated with poor cardiovascular outcome, however there is a paucity of literature exploring the relationship between the two regarding VC progression. We therefore aim to examine the roles of lipoprotein species and their oxidised forms on both medial and intimal VC. **Methods:** Human aortic smooth muscle cells (HAoSMC) were pre-treated with 200 μg/ml high (HDL), low (LDL) and very low (VLDL) density lipoproteins for 24 hours before treating cells with a calcification medium (CM; Ca 2.7mM, PO_4 2.0 mM). Cells were harvested using an alizarin red (ARS) calcification assay, or at various time points for qPCR analysis. In parallel, *in vivo* studies using apolipoprotein E knock-out mice were fed an atherogenic diet for 40 weeks and received reconstituted HDL (rHDL) infusions containing apoA-I (20mg/kg) and 1-palmitoyl-2-linoleoyl phosphatidylcholine during the final 4 weeks of the study. Tissues were harvested and stained for plaque assessment (H&E) and calcium deposits (ARS). **Results:** Pre-treatment of HAoSMC with rHDL inhibited calcification (43.9%, p<0.001), whereas ox-rHDL removed its protective effects. Likewise, ox-LDL (77.1%, p<0.05) also upregulated calcium deposition and interestingly ox-VLDL significantly decreased calcification (70.5%, p<0.05) with their native counterparts having no effects. PCR measures of calcification markers Runx2, RANKL and alkaline phosphatase show a time-dependent increase in expression as calcification occurs. In animal studies, no change in weight gain, cholesterol or triglyceride levels were observed with treatment. In addition, rHDL infusions did not alter plaque size however ARS staining of the brachiocephalic artery demonstrated a significant reduction (6.58%, p<0.05) in calcification present in the atherosclerotic plaque. **Conclusions:** This study is the first to demonstrate the effects of lipoproteins on VC *in vitro* and the effects of rHDL on *in vivo* VC. Somewhat in accordance to the roles of lipoproteins in atherosclerosis, HDL and ox-VLDL show a reduction of calcification, where-as ox-LDL enhances calcification of HAoSMC.

E.J. Akers: None. **J. Mulangala:** None. **P.J. Psaltis:** None. **C. Bursill:** None. **S.J. Nicholls:** None. **B.A. Di Bartolo:** None.

170

Deep Phenotyping of HDL Particles: Characterization of Seven HDL Species and Their Relationship to Cardiometabolic Phenotypes in a Multi-Ethnic Population (Dallas Heart Study)

Natalie Hoeting, Colby R Ayers, Anand Rohatgi, UT-Southwestern, Dallas, TX

Background: Size-based HDL particle analysis based on small, medium, and large categories has led to inconsistent associations with cardiovascular disease (CVD). A new algorithm expands characterization of HDL-P from three to seven species, but the clinical significance remains unknown. We investigated the relationships between the seven HDL species and traditional risk factors, lipids, and cardiometabolic phenotypes in the Dallas Heart Study, a multiethnic, probability-based, population cohort of Dallas county adults.

Methods: This study included 2,996 DHS participants (56% women, 50% Black), excluding those with prior CVD and statin users. HDL species were determined by nuclear magnetic resonance using the LP4 algorithm, with increasing size from H1P to H7P. Insulin resistance was determined by homeostatic model assessment index (HOMA-IR). Visceral fat was measured by MRI.

Results: The largest HDL species were most directly associated with HDL cholesterol (HDL-C) (H6P: r = 0.61, p < 0.0001; H7P: r = 0.66, p < 0.0001). H2P was inversely associated with all HDL species including H1P (r = -0.19, p < 0.0001) and HDL-C (r = -0.18, p < 0.0001), but was directly associated with total cholesterol, triglycerides, and LDL-C (p < 0.0001). Female gender and Black ethnicity were associated with lower H2P levels (p < 0.0001). H2P alone was directly associated with diabetes, hypertension, waist circumference, insulin resistance, and visceral fat (Figure, p < 0.0001 for all values)

Conclusion: Our study of a novel 7-species designation of HDL particles revealed that the smallest HDL particle species (H1P and H2P) confer differential associations with cardiometabolic phenotypes. These findings suggest further investigation specifically into the role of H2P and CVD.

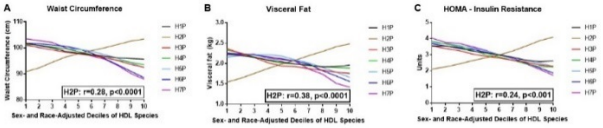

Figure 1: Mean values for waist circumference, visceral fat, and HOMA-IR were plotted across sex-and race-adjusted deciles of each HDL species. Lines depict smoothing function to display trends. All p< 0.0001.

N. Hoeting: None. **C.R. Ayers:** None. **A. Rohatgi:** Research Grant; Significant; Merck. Consultant/Advisory Board; Modest; HDL Diagnostics, Advisory Board, Merck, Consultant, CSL Limited, Consultant, Cleveland HeartLabs, Consultant.

171

Direct versus Calculated LDL Cholesterol and C Reactive Protein in Cardiovascular Disease Risk Assessment in the Framingham Offspring Study

Hiroaki Ikezaki, HNRCA at Tufts Univ, Boston, MA; Virginia A Fisher, Ching-ti Liu, L. Adrienne Cupples, Boston Univ Sch of Public Health, Boston, MA; Katsuyuki Nakajima, Gunma Univ, Maebashi, Japan; Bela F Asztalos, HNRCA at Tufts Univ, Boston, MA; Norihiro Furusyo, Kyushu Univ Hosp, Fukuoka, Japan; Jun Hayashi, Haradoi Hosp, Fukuoka, Japan; Ernst J Schaefer, HNRCA at Tufts Univ, Boston, MA

Background: Elevated serum LDL cholesterol (LDL-C) and high sensitivity C reactive protein (hsCRP) levels have been identified as major risk factors for cardiovascular disease (CVD). Our goal was to assess direct versus calculated LDL-C and hsCRP levels as compared to standard risk factors in the prospective Framingham Offspring Study. **Methods:**

Stored frozen plasma samples (-80 degrees C) obtained after an overnight fast from male and female participants free of CVD at cycle 6 of the Framingham Offspring Study were used (n=3,147, mean age 58 years) and 677 or 21.5% developed a CVD endpoint over 16 years. Total cholesterol, triglycerides, HDL cholesterol (HDL-C), direct LDL-C, and hsCRP were measured by standardized automated analysis, and LDL-C was also calculated. **Results:** For inclusive CVD risk on univariate analysis significant factors in order included the standard risk factors age, hypertension, HDL-C, hypertension treatment, gender, diabetes, smoking, and total cholesterol, as well as the non-standard risk factors non-HDL-C, direct LDL-C, calculated LDL-C, triglycerides (TG), and hsCRP. On multivariate analysis only direct LDL-C and hsCRP were still significant after inclusion of the standard model. Both parameters significantly improved the model C statistic and the net risk reclassification index. The same findings were noted for other CVD risk categories including hard CVD with procedures and hard CVD. **Conclusions:** Our data indicate that direct LDL-C is superior to calculated LDL-C in CVD risk prediction, and that both direct LDL-C and hsCRP add significant information to CVD risk prediction versus the standard model.

H. Ikezaki: None. **V.A. Fisher:** None. **C. Liu:** None. **L. Cupples:** None. **K. Nakajima:** None. **B.F. Asztalos:** None. **N. Furusyo:** None. **J. Hayashi:** None. **E.J. Schaefer:** None.

This research has received full or partial funding support from the American Heart Association.

172

Prodomain of Furin Promotes Phospholipid Transfer Protein Proteasomal Degradation in Hepatocytes

Yang Yu, Xia Lei, SUNY Downstate Medical Ctr, Brooklyn, NY; Shu-Cun Qin, Taishan Medical Univ, Taian, China; Weijun Jin, **Xian C Jiang**, SUNY Downstate Medical Ctr, Brooklyn, NY

PLTP is one of the major modulators of lipoprotein metabolism and atherosclerosis development, however, very little is known about the regulation of PLTP. The effect of hepatic profurin expression on PLTP processing and function is investigated. We utilized adenovirus overexpressing prodomain of furin (profurin) in mouse liver to evaluate PLTP activity, mass, and plasma lipid levels. We co-expressed PLTP and profurin in Huh7 cells and studied their interaction. We found profurin expression significantly reduced plasma lipids, plasma PLTP activity and mass in all tested mouse models, compared with controls. Moreover, the expression of profurin dramatically reduced liver PLTP activity and protein level. We further explore the mechanism using in vivo and ex vivo approaches. We found that profurin can interact with intracellular PLTP, and promote its ubiquitination and proteasomal degradation, resulting in less PLTP secretion from the hepatocytes. Furin does not cleave PLTP, instead it forms a complex with PLTP, likely through its prodomain. Our study reveals that hepatic PLTP protein is targeted for proteasomal degradation by profurin overexpression, which could be a novel post-translational mechanism underlying PLTP regulation.

Y. Yu: None. **X. Lei:** None. **S. Qin:** None. **W. Jin:** None. **X.C. Jiang:** None.

173

Sodium Salicylate Modulates Reverse Cholesterol Transport and HDL Proteome within Obesity

Sarina Kajani, Marcella O'Reilly, Weili Guo, Eugene Dillon, Fiona C McGillicuddy, UCD Conway Inst, Dublin, Ireland

Obesity is associated with increased risk of cardiovascular disease (CVD) due to imbalances in lipid metabolism and leads to maladaptive inflammatory responses. This study assessed the effects of an obesogenic diet supplemented with anti-inflammatory sodium salicylate (NaS) on hepatic health, HDL proteomic quality, HDL functionality and Reverse Cholesterol Transport (RCT).

RCT was assessed after 24 weeks in C57BL/6 mice fed a high fat (HFD) (60% fat) ± NaS (6g/kg) diet or low-fat diet (LFD, 10% fat) by tracing ^{3}H-cholesterol movement from labelled macrophages, injected intraperitoneally, into plasma, liver and fecal compartments. HDL particles were separated from plasma by fast protein liquid chromatography (FPLC) and associated proteins were identified by mass spectrometry. HDL particles were incubated with ^{3}H-cholesterol-labelled macrophages *ex vivo* and cholesterol efflux to HDL particles was determined by liquid scintillation counting (LSC).

Both HFDs significantly increased HDL cholesterol mass. Nonetheless, HFD alone impaired hepatic movement of ^{3}H-cholesterol to fecal compartments coincident with increased hepatic lipid infiltration and inflammation. NaS supplementation increased all steps of macrophage-to-feces RCT with partial preservation of hepatic transporters while impeding hepatic lipid load and reducing markers of inflammation (ALT & AST). HFD resulted in enrichment of HDL particles with coagulant proteins (fibrinogen, coagulation factor IX) and a dissociation of anti-thrombin and angiotensinogen compared to HFD+NaS. NaS supplementation also preserved ABCA1-mediated efflux capacity of HDL particles.

Obesogenic diets augmented with NaS resulted in profound differences within the RCT pathway and HDL proteome. HFD supplemented with NaS was associated with improved hepatic condition and HDL proteomic profile with an increase of anticoagulant and anti-atherogenic proteins on HDL despite development of obesity.

S. Kajani: None. **M. O'Reilly:** None. **W. Guo:** None. **E. Dillon:** None. **F.C. McGillicuddy:** None.

174

Lipid Levels after Acute Coronary Syndromes: a Perspective from a General Hospital

Pedro Pimentel Filho, Justo Leivas, André Galvão, Joana Carolina Junqueira de Brum, Charline Michelotti, Kauan Roessler Mohr, Hosp N S Conceição, Porto Alegre, Brazil

Background: Low-density lipoprotein cholesterol (LDL-C) is a risk factor and even cause of atherosclerosis. High dose statins early in all Acute Coronary Syndrome (ACS) patients are now recommended. . Mean serum LDL-C vary relatively little over the early days of ACS and lipid therapy generally is not considered a priority during ACS . Initiation of statin is strongly associated with their use after discharge Purpose : To evaluate our data on lipids after ACS and compare with current standards of therapy. Methods : 100 patients were analyzed during 6 months in 2016 in a step-down unit with ACS -unstable angina (UA), myocardial infarction with ST elevation (STEMI) and without ST elevation (NonSTEMI). Data regarded age, gender, type of ACS, coronary angiogram , medical therapy, lipid levels. Symmetric variables are described by mean and standard deviation(sd) and asymetric by the median and interquartile range. Categorical variables are described by frequencies and percentages . 95% confidence intervals for percentages are presented for main results.Results : 56 men, 44 women, mean ages 64 years old (sd 12.5); 36 with diabetes; 42 UA, 35 NonSTEMI and 23 STEMI. Coronary angiograms in 98 patients, 4 without lesions . Medical therapy with aspirin in 100, clopidogrel 92,beta blockers 96, ACE inhibitors 63, angiotensin receptor blockers 12, calcium channel blockers 7, diuretics 20 , nitrates 9. Previous statin use in 32 and statin use during hospital stay and discharge in 99. The range of TC was 90 to 291 mg/dL (mean: 167,1; sd 40.8), LDL-C: 39 to 194mg/dL (mean 98.0; sd: 34.1); HDL-C from 20 to 68 mg/dL (mean :34.8; sd: 99.2); Triglycerides from 55 to 615 mg/dl (median 151.5; interquartile range : 114.5 to 197.0) . Patients with LDL-C ≤ 70 mg/dL : 25% (CI 95% : 16.9- 34.7); HDL-C ≥40 : 24% (CI 95% : 16.0 - 33.6). Lipid levels were measured in only 12 patients at arrival (CI 95% : 6.4 - 20.0), in 70 during hospital stay (CI 95% : 60.0 - 78.8);

in 30 patients no measure at all (CI95% : 21.2 - 40.0) .Conclusion : Knowledge of serum lipid levels early after ACS is very relevant and should facilitate initiation of lipid lowering therapy. There is still a large gap between current recommendations and clinical practice concerning lipids in ACS, as shown with our data.
P. Pimentel Filho: None. **J. Leivas:** None. **A. Galvão:** None. **J. Junqueira de Brum:** None. **C. Michelotti:** None. **K. Roessler Mohr:** None.

175
Dynamin-Related Protein 1 Regulates Proteostasis and Proprotein Convertase Subtilisin/Kexin Type 9 Secretion
Maximillian A Rogers, Joshua D Hutcheson, Claudia Goettsch, Arda Halu, Sasha Singh, Hideyuki Higashi, Lang H Lee, Brigham and Women's Hosp, Harvard Medical Sch, Boston, MA; Lixiang Wang, Kyushu Univ, Fukuoka, Japan; Florian Schlotter, Stephanie Morgan, Takehito Okui, Yukiyoshi Yamazaki, Brigham and Women's Hosp, Harvard Medical Sch, Boston, MA; Alan Daugherty, Saha Cardiovascular Res Ctr, Univ of Kentucky, Lexington, KY; Masatoshi Nomura, Kyushu Univ, Fukuoka, Japan; Masanori Aikawa, Elena Aikawa, Brigham and Women's Hosp, Harvard Medical Sch, Boston, MA

Objective—Dysfunctional protein homeostasis (proteostasis) contributes to cardiovascular and metabolic disorders. We and others associated the mitochondrial fission protein, Dynamin-related protein 1 (DRP1) with cardiometabolic disease. Liver DRP1-deficiency reduces serum lipids and very-low density lipoprotein secretion in high-fat fed mice; whether DRP1 mediates these effects via proteostasis regulation is unknown.
Approach and Results—Using mass spectrometry integrated with network analysis to map the human liver secretome, we found DRP1 associated with cardiovascular disease modules and lipid pathways. Electron microscopy revealed human liver DRP1 at mitochondria, cytosol, vesicles, endoplasmic reticulum (ER), and clustered at membrane tethered to ER exit sites. DRP1 small molecule inhibition (Mdivi-1) or CRISPR/Cas9-mediated *DRP1* deletion in human liver cells, and *Drp1*-liver deficiency in mice reduced autophagic flux without impairing the amino acid metabolome, or activating the autophagy inhibitor, mammalian target of rapamycin complex 1. DRP1 partially co-localized and co-immunoprecipitated with the ER trafficking and autophagy regulator, Syntaxin 17, in human liver tissue and cells. DRP1 inhibition reduced Proprotein convertase subtilisin/kexin type 9 (PCSK9) secretion in human liver cells and mice (-78.5%), and altered trafficking of the PCSK9-binding and ER maintenance chaperone, Glucose-regulated protein 94. Co-treating human liver cells with Mdivi-1 and proteasome inhibitor (MG132), non-transcriptionally increased intracellular PCSK9, while maintaining Mdivi-1-mediated reduced PCSK9 secretion.
Conclusions—We propose a novel function of DRP1 in the regulation of proteostasis, wherein DRP1 may cluster, then tether and/or constrict nascent autophagy-associated membrane at the ER via its interaction with Syntaxin 17. DRP1 inhibition likely reduces lipoprotein and PCSK9 secretion in part by impairing autophagic flux leading to compensatory chaperone-mediated proteasomal degradation for ER maintenance. Proteostasis regulation and the cellular function of DRP1 is more complex than previously thought, potentially providing new avenues to therapeutically target cardiometabolic disease.
M.A. Rogers: None. **J.D. Hutcheson:** None. **C. Goettsch:** None. **A. Halu:** None. **S. Singh:** None. **H. Higashi:** Employment; Significant; Kowa Company Ltd. **L.H. Lee:** None. **L. Wang:** None. **F. Schlotter:** None. **S. Morgan:** None. **T. Okui:** Employment; Significant; Kowa Company Ltd. **Y. Yamazaki:** Employment; Significant; Kowa Company Ltd. **A. Daugherty:** None. **M. Nomura:** None. **M. Aikawa:** Research Grant; Significant; Kowa Company Ltd. **E. Aikawa:** None.

176
Preoperative Small HDL Particle Concentration is Associated with Paraoxonase-1 activity and the Risk of Acute Kidney Injury After Cardiac Surgery
Loren Smith, Derek K Smith, Vanderbilt Univ, Nashville, TN; Alan T Remaley, Natl Insts of Health, Bethesda, MD; Frederic T Billings IV, MacRae F Linton, Vanderbilt Univ, Nashville, TN

Acute kidney injury (AKI) after cardiac surgery occurs in up to 30% of patients and predicts death. We have reported that a higher preoperative HDL particle concentration is independently associated with a decreased risk of AKI after cardiac surgery. HDL has known anti-oxidant properties that may attenuate AKI. We hypothesized that HDL particle size is associated with paraoxonase-1 (PON-1) activity and with the risk of AKI after cardiac surgery.
We selected 90 patients who developed mild, moderate, severe, or no AKI from a prospective trial of perioperative atorvastatin to prevent post-cardiac surgery AKI. PON-1 paraoxonase activity was measured in apoB-depleted serum with fluorescent substrate 7-diethylphospho-6,8-dixuor-4-methylumbelliferyl. HDL particle size was assessed using the NMR Lipoprofile test. Linear regression was used to assess the association between preoperative small, medium, and large HDL particle concentrations and PON-1 activity. We assessed the association between HDL particle levels and the maximum serum creatinine change from baseline in the first 48 postoperative hours using two-component latent variable mixture models adjusted for AKI risk factors.
A higher preoperative small HDL particle concentration was associated with a higher preoperative PON-1 activity (p=0.003, Figure 1A). Medium and large HDL particle concentrations were not associated with PON-1 activity. Small HDL particle concentration was found to be independently associated with postoperative serum creatinine change (p=0.02, Figure 1B), while medium and large HDL particle concentrations were not.
Conclusions: A higher preoperative small HDL particle concentration was associated with a higher PON-1 activity and a decreased risk of AKI after cardiac surgery. Future work will characterize HDL throughout the surgical course to identify the mechanism underlying the protective association between HDL and AKI.

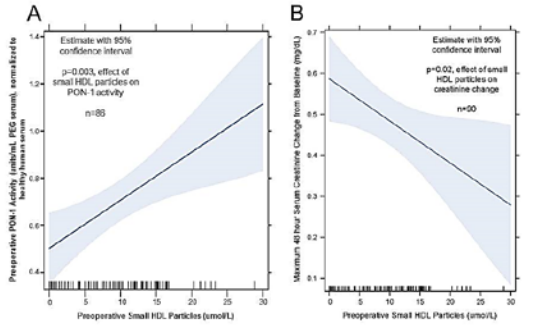

L. Smith: None. **D.K. Smith:** None. **A.T. Remaley:** None. **F.T. Billings:** None. **M.F. Linton:** None.

177
Glucagon Receptor Signaling-Mediated Regulation of PCSK9 and Cholesterol Metabolism
Stefano Spolitu, Lale Ozcan, Columbia Univ, New York City, NY

Glucagon is one of the key hormones important in hepatic glucose homeostasis, and the pathophysiological role of hyperglucagonemia and unopposed hepatic glucagon action in type 2 diabetes (T2D) is now well-established. Accordingly, there has been great interest in developing glucagon receptor antagonists (GRAs) as a treatment for T2D. Although phase 2 clinical trials have shown that GRAs effectively lower blood glucose in T2D subjects, they increase plasma low density lipoprotein cholesterol (LDL-C), which has presented a significant block to their development.

Consistent with a role of glucagon in cholesterol metabolism, recent studies suggested that proprotein convertase subtilisin/kexin type 9 (PCSK9), which increases plasma LDL-C through targeting LDL receptor (LDLR) for degradation, can be regulated by fasting, however, in-depth mechanistic information is lacking. In order to test the functional importance of hepatic glucagon action on cholesterol metabolism, we silenced hepatic glucagon receptor (GcgR) in obese mice using AAV8-mediated shRNA treatment. Consistent with previous reports, this treatment effectively lowered blood glucose in obese mice without a change in body weight. Moreover, GcgR silencing, like GRAs in humans, significantly increased plasma LDL-C. In search for the mechanism, we found that inhibition of GcgR significantly lowered hepatic LDLR protein levels and increased both hepatic and circulating PCSK9, without an effect on cholesterol synthesis. To determine causation, we silenced hepatic GcgR together with PCSK9 using AAV8 and found that this intervention restored hepatic LDLR and prevented the increase in plasma LDL-C. Further mechanistic studies showed that GcgR silencing in hepatocytes did not increase *Pcsk9* mRNA. Rather, blocking GcgR increased the half-life of PCSK9 protein by suppressing signalling through exchange protein activated by cAMP-2 (Epac2). In particular, the ability of GcgR silencing to increase PCSK9 and suppress LDLR protein levels was mimicked by hepatocytes lacking Epac2. Thus, GcgR signalling through Epac2 appears to have critical effects on processes that regulate cholesterol metabolism through PCSK9.

S. Spolitu: None. **L. Ozcan:** None.

This research has received full or partial funding support from the American Heart Association.

178

Bioactive Compounds in Fenugreek Ameliorate ER Stress and VLDL Overproduction via the Mediation of Insig Signaling

Rituraj Khound, Dipak Santra, **Qiaozhu Su**, Univ of Nebraska-Lincoln, Lincoln, NE

A number of health-enhancing bioactive compounds have been identified in the seed of fenugreek, an annual legume. These compounds have been shown to exert multiple health beneficial effects on anti-obesity and type 2 diabetes. In this study, we characterized the molecular mechanisms of fenugreek seed in regulating lipid and lipoprotein metabolism and metabolic inflammatory stress. Two groups of hyperlipidemic mice induced by depletion of cAMP responsive element binding protein H were fed either a chow containing 2% fenugreek seed or vehicle control for 7 weeks. Q-RT-PCR and immunoblotting analysis demonstrated that fenugreek seed containing diet inhibited hepatic SREBP-1c activation and the subsequent de novo lipogenesis by enhancing expression of insulin-inducible gene-1 (Insig-1) and gene-2 (Insig-2). mRNA expression of PPARα and its target genes that were involved in fatty acid β-oxidation were also upregulated in the fenugreek seed treated-mice which was accompanied by significantly reduced hepatic lipid accumulation and VLDL secretion and improved endoplasmic reticulum (ER) stress. These actions ameliorated hepatic steatosis and systemic hyperlipidemia. Fenugreek seed further improved insulin sensitivity by upregulating expression of glucose transporters Glut-2 and Glut-4 and enhancing the activity of hepatic inulin signaling molecules, insulin receptor and AKT. In vitro, treating a rat hepatoma cell line, McA-RH7777, with trigonelline, a phytochemical compound in fenugreek seed, increased expression of Insig-2 which prevented the activation of SREBP-1c and the subsequent de novo lipid synthesis, resulting in less secretion of VLDL. Trigonelline treatment also attenuated ER stress induced by a free fatty acid, palmitic acid, indicated by the downregulation of GRP94/78 and reduced phosphorylation of JNK and eIF2α. This study unveiled a novel mechanism of the bioactive compound trigonelline in ameliorating metabolic inflammatory stress, hepatic steatosis, VLDL overproduction and insulin resistance via the mediation of Insig signaling. This evidence lands support for developing fenugreek seed as a nutraceutical supplement for the prevention and treatment of nutrient-surplus associated metabolic disorders.

R. Khound: None. **D. Santra:** None. **Q. Su:** None.

179

CETP Facilitates SAA Exchange Between Lipoproteins

Patricia G Wilson, Joel C Thompson, Nancy R Webb, Frederick C de Beer, **Lisa R Tannock**, Univ of Kentucky, Lexington, KY

Serum amyloid A (SAA) is a family of acute phase reactants that are elevated in chronic inflammatory conditions such as obesity and diabetes. SAA promotes atherosclerosis in mice. Although SAA is generally thought to be exclusively an HDL apolipoprotein, we and others have detected SAA on apoB-containing lipoproteins in obese/diabetic mice and humans. The goal of this study was to investigate mechanisms underlying SAA exchange between lipoprotein fractions. Obese humans with or without metabolic syndrome or type 2 diabetes were recruited. Plasma samples were collected fasting and hourly for 8h after consumption of a high fat drink. Whereas SAA was found predominantly on HDL in fasting samples, in diabetic subjects SAA shifted from HDL to VLDL and LDL in post prandial samples. Postprandial LDL and VLDL containing SAA had increased proteoglycan binding compared to fasting LDL and VLDL from the same subject. We previously reported that HDLs remodeled by CETP release lipid-free SAA. To determine if CETP facilitates SAA exchange between particles, HDL-containing SAA was incubated with SAA-free VLDL in the presence of increasing amounts of CETP. Even in the absence of CETP, 16±3% of HDL-associated SAA shifted to VLDL; in samples with CETP, 19-28% of total SAA was found on VLDL and up to 17% was lipid-poor/lipid-free. To investigate whether CETP promotes SAA exchange in vivo, SAA-deficient mice that lack CETP were injected with HDL containing SAA and then bled at 1, 3, 6 and 24 hours. Essentially all SAA was found on HDL at each time point. In contrast, in SAA-deficient mice expressing CETP by adenoviral vector, approximately 50% and 20% of SAA was associated with the VLDL and LDL fractions, respectively, 1h after injection of HDL-containing SAA. Thus, increased CETP activity in diabetes may promote the transfer of SAA from HDL to apoB-containing lipoproteins, leading to increased retention in the vasculature.

P.G. Wilson: None. **J.C. Thompson:** None. **N.R. Webb:** None. **F.C. de Beer:** None. **L.R. Tannock:** None.

180

Missense Mutations in ABCA1 and CETP Associate with Changes in the HDL Proteome in Primate Half-Sibs Discordant for HDL Cholesterol Levels

Deanna Plubell, Irene Predazzi, Oregon Health Science Univ, Portland, OR; Jessica McKelvey, Jordyn Clarke, Oregon Health Science Univ, Beaverton, OR; John Letaw, Oregon Health Science Univ, Portland, OR; Michael J. Raboin, Oregon Health Science Univ, Beaverton, OR; Phillip A. Wilmarth, Oregon Health Science Univ, Portland, OR; Joanne Curran, South Texas Diabetes and Obesity Inst, Univ. of Texas Rio Grande Valley, Brownsville, TX; Sergio Fazio, Nathalie Pamir, Oregon Health Science Univ, Portland, OR; **Amanda Vinson**, Oregon Health Science Univ, Beaverton, OR

HDL protein composition and corresponding function may impact cardiovascular disease risk. Identifying genetic variation that influences the HDL proteome may reveal modifiable HDL functions that impact this risk. We studied genetic determinants of the HDL proteome in a cohort of rhesus macaques enriched for extreme HDL cholesterol levels (HDL-c). We selected macaques from 2 distinct

paternal half-sibships, each comprising 8 half-sib pairs matched for age-class and sex, but with large differences in HDL-c (N=22 genomes). HDL was isolated by ultracentrifugation and the protein cargo analyzed by mass spectrometry. Identified peptide sequences were compared to a Swiss-Prot canonical human protein database using BLAST to determine ortholog matches. Among the proteins identified, 64 are among the 229 reported in similar human studies, and 45 of these 64 are among the 95 highest-confidence HDL proteins tracked by the HDL Proteome Watch. We performed deep exome sequencing, and assessed predicted function for all genetic variants in macaques, among 23 genes associated with HDL disorders or variation in HDL-c in humans. We focused on the higher-impact variants most likely to have conserved effects between macaques and humans by proximity (i.e., <10 bp) to known human mutations. This produced a set of 3 missense variants in *ABCA1* associated with Tangier disease and HDL deficiency, and 4 missense variants in *CETP* associated with CETP deficiency, reduced CETP activity, and hyper- and hypoalphalipoproteinemias. Using a measured genotype approach, we tested for association of all 7 variants with adjusted spectral counts, while accounting for age and sex, and applied a false discovery rate (FDR) of 20% to all nominally significant results. After controlling for FDR, 3 missense variants in *ABCA1* were significantly associated with spectral counts for *VCAM1*, *ITGA2*, and *ITGB1* (nominal P-values 0.0005-0.0026), and 4 missense variants in *CETP* were significantly associated with spectral counts for *APOA2*, *APOC3*, *C4BPA*, and *PLTP* (nominal P-values 0.0002-0.0038). While our results require replication, these proteins suggest that changes in HDL-c in macaques are associated with changes in HDL that modulate vascular inflammation, immune response, and particle remodeling.
D. Plubell: None. **I. Predazzi:** None. **J. McKelvey:** None. **J. Clarke:** None. **J. Letaw:** None. **M.J. Raboin:** None. **P.A. Wilmarth:** None. **J. Curran:** None. **S. Fazio:** None. **N. Pamir:** None. **A. Vinson:** None.

181
The Use of Recombinant Human Lipoprotein Lipase as a Treatment for Hypertriglyceridemia
Anna Wolska, Natl Insts of Health, Bethesda, MD; Omar L. Francone, Shire Intl GmbH, Lexington, MA; Marcelo J. Amar, Milton Pryor, Alan T. Remaley, Natl Insts of Health, Bethesda, MD

Pancreatitis affects 270,000 number of people a year in the US and has a mortality rate of approximately 5%. Hypertriglyceridemia is a well established risk factor for acute pancreatitis, accounting for 10% of cases. To investigate recombinant human lipoprotein lipase (rhLPL) as a potential therapy for pancreatitis caused by hypertriglyceridemia, we examined effect of rhLPL produced in CHO cells on lipoproteins in human plasma and hypertriglyceridemic mice. IV injection of 500 µL of 20% Intralipid into mice increased plasma TG levels over 200-fold to about 6000 mg/dL at 15 min. When mice were co-injected with rhLPL (2.5 µg/g BW; IV), TG levels reached 2200 mg/dL and by 3 h were completely normal unlike control animals, which took 24 hours. Plasma TGs were decreased by 81% and 63% compared to control mice when rhLPL was administered IV at a dose 2 µg/g BW and 1 µg/g BW consecutively for mice treated IP with 1 mL of 20% Intralipid. The effect of rhLPL was sustained for 6 hours for high dose rhLPL. Enhanced lipolysis from rhLPL treatment resulted in a 2-fold increase of plasma FFA, but the albumin binding capacity for FFA did not appear to be exceeded because all FFA were bound to either lipoproteins or albumin. Moreover, no pathological changes were observed in the pancreas of treated mice, as assessed by histology. Amylase levels in rhLPL treated mice given Intralipid at 6 h were increased only 1.4-fold, whereas in control mice 2.8-fold. Addition of rhLPL in vitro (2 µg per 250 µL of human plasma) resulted in a significant decrease in lipoprotein particle numbers of all subpopulations of VLDL, small LDL, and small HDL, whereas a significant increase was observed for large LDL and large HDL particle number. The sizes of VLDL shifted towards smaller particles and the opposite was observed for LDL and HDL particles. Overall, there was a 57% reduction of TGs in plasma treated with rhLPL. In summary, rhLPL at relatively low doses accelerates the clearance of TG-rich lipoproteins in mice after a fat load. It does so without causing accumulation of toxic levels of FFA in plasma and reduces hypertriglyceridemia induced markers of pancreatitis. Furthermore, observed changes in human lipoprotein subpopulation distribution after rhLPL treatment are positive in terms of atherosclerosis risk.
A. Wolska: Research Grant; Modest; CRADA Research Grant. **O.L. Francone:** Employment; Modest; Shire International GmbH. **M.J. Amar:** Research Grant; Modest; CRADA Research Grant. **M. Pryor:** Research Grant; Modest; CRADA Research Grant. **A.T. Remaley:** Research Grant; Modest; CRADA Research Grant.

183
Association of LDL Particles With Cerebral Amyloidosis
Trusha Parekh, Univ of Southern California, Los Angeles, CA; Sarah M King, Children's Hosp of Oakland Res Inst, Oakland, CA; Bruce Reed, NIH, Bethesda, MD; Helena C, Chui, Univ of Southern California, Los Angeles, CA; Ronald M. Krauss, Children's Hosp of Oakland Res Inst and Univ of California San Francisco, Oakland, CA; **Hussein Yassine**, Univ of Southern California, Los Angeles, CA

Cerebral amyloidosis is a condition in which β-Amyloid (Aβ) proteins are deposited in the cerebral cortex and is a predictor of Alzheimer's disease (AD). In the Aging Brain Study, we reported an association between LDL cholesterol and cerebral amyloidosis assessed using PET PiB imaging. LDL comprises multiple species of varying size, density and protein composition, including very large LDL-I which is enriched in ApoE and can bind to ApoE receptors. In this study, LDL particle fractions were measured in plasma samples of 58 participants (40 women and 18 men) of the Aging Brain study. Cerebral amyloidosis was assessed using Pittsburgh Compound B index-Positron Emission Tomography (PiB-PET) imaging. LDL subfractions were analyzed by the method of ion mobility. The subjects were divided into three groups based on PiB tertiles. Compared to the first tertile, total plasma cholesterol as well as LDL cholesterol were greater in patients in the second and third PiB index tertiles (p values = 0.05 and 0.03 respectively). Amongst the LDL subfractions, levels of LDL-I as well as very small LDL-IVa particles were significantly greater in the second and third PiB index tertiles and independent of LDL cholesterol levels (p values = 0.03 and 0.04 respectively). A significant inverse association was also observed between LDL-I and hippocampal volumes (r=-0.33, p=0.02). We suggest that LDL-I level may be a mechanistic biomarker for extent of cerebral amyloidosis. Lipoprotein receptors, particularly LRP-1, participate in Aβ clearance from the brain and its hepatic degradation. One potential mechanism for our findings is competition between plasma-derived LDL-I and brain Aβ that may retard Aβ clearance and degradation.
T. Parekh: None. **S.M. King:** None. **B. Reed:** None. **H.C. Chui:** None. **R.M. Krauss:** Ownership Interest; Significant; licensed patent for ion mobility analysis. **H. Yassine:** None.

184
Hyperglycemia Enhances Pro-inflammatory Properties of Macrophage-derived Exosomes to Drive Hematopoiesis in Apolipoprotein E-deficient Mouse
Laura Bouchareychas, Allen Chung, David K Wong, Phat Duong, Robert L Raffai, Div of Vascular and Endovascular Surgery, Dept of Surgery, Univ of California San Francisco & VA Medical Ctr, San Francisco, CA

Background and Purpose: Diabetes is recognized to enhance the frequency and severity of atherosclerosis and cardiovascular disease. Recent studies have shown that hyperglycemia is associated with enhanced hematopoiesis

and macrophage accumulation in atherosclerotic lesions. We explored whether high glucose concentrations can enhance intercellular communication between mature macrophages and hematopoietic progenitors via exosomes to promote inflammation and diabetic atherosclerosis.
Methods: Bone marrow derived macrophages (BMDM) from C57BL/6 mice were cultured with normal (5mM) or high glucose concentrations (25mM). Exosomes were isolated with our cushioned-density gradient ultracentrifugation method followed by nanoparticle tracking and western blot analysis. Pro-inflammatory properties of high glucose exosomes (HGexo) were tested *in vitro* by exposing them to BMDM cultured in normal low glucose. The capacity for BMDM-derived exosomes to alter systemic and vascular inflammation were next tested by infusing 25-30 weeks-old $ApoE^{-/-}$ mice fed a chow diet with 3×10^{10} exosomes three times a week, for four weeks.
Results: Our data show that HGexo can stimulate the expression of inflammatory cytokines (IL-6, IL-1ß) as well as NADPH oxidases (Nox-1 and Nox-4) in cultured BMDM. Furthermore, our findings show that intraperitoneally injected exosomes distribute to numerous organs and tissues including the bone marrow and the spleen. Lastly, HGexo enhance the expansion of multipotent and lineage committed hematopoietic progenitors.
Conclusions: We identify that exosomes derived from cultured BMDM exposed to high glucose have the capacity to exert intercellular communication *in vitro*, and *in vivo.* Our findings suggest that exosomes produced by macrophages exposed to hyperglycemia could represent an unsuspected source of inflammation to accelerate atherosclerosis in diabetes.
L. Bouchareychas: None. **A. Chung:** None. **D.K. Wong:** None. **P. Duong:** None. **R.L. Raffai:** None.

This research has received full or partial funding support from the American Heart Association.

185
G-protein Coupled Receptor 55 Deficiency Promotes Atherosclerosis and Inflammation in Mice
Daniel Hering, Raquel Guillamat-Prats, Inst for Cardiovascular Prevention, Ludwig-Maximilians-Univ München, Munich, Germany; Petteri Rinne, Inst of Biomedicine, Univ of Turku, Turku, Finland; Martina Rami, Inst for Cardiovascular Prevention, Ludwig-Maximilians-Univ München, Munich, Germany; Sebastian Kobold, Div of Clinical Pharmacology, Dept of Med IV, Klinikum der Ludwig-Maximilians-Univ München, Munich, Germany; Yvonne Döring, Sabine Steffens, Inst for Cardiovascular Prevention, Ludwig-Maximilians-Univ München, Munich, Germany

Background: The endocannabinoid system plays a pathophysiological role in metabolic and cardiovascular disorders. G protein-coupled receptor (GPR) 55 is a novel cannabinoid receptor expressed by various lymphocyte subsets, in particular γδT cells, innate lymphoid cells and B1 cells. Its role in regulating immune functions and atherosclerosis is unknown.
Methods: We studied early and advanced atherosclerotic plaques and inflammatory parameters in apolipoprotein E deficient (ApoE-/-) and ApoE-/-GPR55-/- mice after 4 or 16 weeks Western Diet (WD), respectively (n=12-15 per group). GPR55 mRNA expression was assessed in human carotid artery plaques (n=29) and healthy control vessels (left internal thoracic arteries; n=28).
Results: ApoE-/-GPR55-/- mice had significantly 1.9 to 2.3-fold increased plaque sizes after 4 and 16 weeks WD compared to ApoE-/- controls with higher macrophage content at early stage, but less macrophage and more collagen content at advanced stage. This was accompanied by enhanced aortic pro-inflammatory cytokine mRNA expression (IL-6, TNFα, IL-1β, iNOS) as well as massively upregulated IgG1 plasma levels. Moreover, GPR55 deficiency was associated with increased circulating, splenic and aortic lymphocyte counts after 4 and 16 weeks WD. The most striking (2 to 4-fold) increase was found in γδT cells, with less pronounced increases in the total CD3+ T cell population and CD4+ and CD8+ subsets. This was paralleled by systemic increases in blood monocyte and neutrophil counts, likely due to enhanced myelopoiesis as suggested by enhanced bone marrow myeloid cell counts. At advanced atherosclerosis, ApoE-/-GPR55-/- had significantly higher NK cell numbers in blood and lymphoid organs, suggesting a possible regulation of cytotoxic lymphocyte responses. In view of a potential relevance for human pathophysiology, GPR55 mRNA levels were significantly higher in human plaque samples compared to non-atherosclerotic control vessels.
Conclusion: GPR55 deficiency promotes atherosclerosis associated with a more pro-inflammatory phenotype. We may speculate that GPR55 negatively regulates the proatherogenic activity of lymphocyte subsets such as γδT cells, which deserves further investigation.
D. Hering: None. **R. Guillamat-Prats:** None. **P. Rinne:** None. **M. Rami:** None. **S. Kobold:** None. **Y. Döring:** None. **S. Steffens:** None.

186
Deletion of Ppard in Cd11c+ Cells Attenuates Atherosclerosis in Apoe Knockout Mice
Danyang Tian, Yalan Wu, Chinese Univ Hong Kong, Sha Tin N T, Hong Kong; Ajay Chawla, Univ of California San Francisco, San Francisco, CA; Yu Huang, **Xiao Yu Tian**, Chinese Univ Hong Kong, Sha Tin N T, Hong Kong

Atherosclerosis is a chronic sterile inflammation of the vascular wall triggered by hyperlipidemia. The role of dendritic cells (DCs) in the development of atherosclerosis has not been recognised until the last decade. DCs can engulf lipids to adopt a foam cell-like appearance that may constitute the earliest stages of plaque formation. DCs may also recruit T cells to the inflamed vessel wall via secretion of chemokines and stimulate T cell responses via cytokines. PPARD is a nuclear receptor, which acts as a sensor of native and oxidized fatty acids. We examined whether PPARD regulates DC function in response to hyperlipidemia and affect atherosclerotic lesion growth. We used $Ppard^{fl/fl}$ mice and Itgax-cre (CD11c-Cre) mice crossed with $Apoe^{-/-}$ mice to generate $Ppard^{f/f}$;$CD11c^{Cre/+}$;$Apoe^{-/-}$ as DC-specific knockout of PPARD on Apoe-KO background ($Ppard^{DC\text{-}KO}$) and $Ppard^{f/f}$;$Apoe^{-/-}$ ($Ppard^{DC\text{-}WT}$) as controls. $Ppard^{DC\text{-}KO}$ and $Ppard^{DC\text{-}WT}$ were fed with high cholesterol diet for 4 months. Tissues were dissected and digested to obtain single cell suspension for flow cytometric analysis. Bone marrow derived DCs were isolated and cultured in RPMI with serum and GM-CSF and maturated with LPS.Atherosclerotic lesion size and collagen deposition decreased in $Ppard^{DC\text{-}KO}$ mice. Less CD4 and CD8 T lymphocytes were found in the atherosclerotic lesion of $Ppard^{DC\text{-}KO}$ mice comparing to $Ppard^{DC\text{-}WT}$ mice. Ppard deletion in DCs reduced DC infiltration especially $CD11b^{+}CD103^{-}$DCs in the atherosclerotic lesion. Production of IFNγ from $CD4^{+}$ T cells decreased in $Ppard^{DC\text{-}KO}$ mice. In BMDCs from $Ppard^{DC\text{-}KO}$ mice, LPS and palmitic acid induced expression of co-stimulatory molecules CD80 and CD86, as well as TNF were decreased. LDL uptake was attenuated in BMDCs from PpardDC-KO mice. Our results suggested that PPARD may be involved in DC mediated T cell activation in response to hyperlipidemia. Deletion of PPARD in DCs attenuated plaque formation in atherosclerosis. Whether lipid sensing and uptake by PPARD is required for the enhanced inflammatory response in atherosclerotic mice requires further study. (This study is supported by Hong Kong Health Bureau HMRF 05162906 and 01150057, Hong Kong RGC T402/13-N and CRF C4024-16W, and CUHK Direct grants)
D. Tian: None. **Y. Wu:** None. **A. Chawla:** None. **Y. Huang:** None. **X. Tian:** None.

187
Host Age Enhances Atherosclerotic Plaque Necrosis and Macrophage Infiltration in Mice Independently of Metabolic Alterations
Daniel J Tyrrell, Daniel R Goldstein, Univ of Michigan, Ann Arbor, MI

Traditional murine models of atherosclerosis age with mild hypercholesterolemia and metabolic derangement, which confounds determination of the intrinsic effects of aging on atherogenesis. To examine if host age enhances atherogenesis independently of metabolic alterations, we induced hypercholesterolemia in wild-type (WT) aging mice using a PCSK9 adeno-associated viral approach. Intraperitoneal PCSK9 transfection and high-fat (42% fat) feeding led to similar elevated blood cholesterol levels between young (3-months) and aged (18-months) WT mice, which were also similar to young low-density lipoprotein receptor knockout ($LDLR^{-/-}$) mice fed the same high-fat diet within 2 weeks. Elevated cholesterol levels persisted during the 10-week feeding period. Although aged mice exhibited an elevated body weight at baseline, both groups gained the same amount of weight during the high-fat feeding. Glucose and insulin resistance measured via tolerance tests were dysregulated but similar between young and aged mice. We next measured atherosclerotic plaque size and composition using H and E, Masson's trichrome, and immunohistochemical staining along with flow cytometry. There was no difference in total plaque size in the aortic sinus between the groups; however, the atherosclerotic necrotic core size and macrophage staining was significantly greater in aged mice. Flow cytometry revealed greater numbers of inflammatory monocytes in the blood along with increased macrophage infiltration in the aorta of aged hyperlipidemic mice compared to young mice. We conclude that aging induces inflammatory monocytosis and macrophage infiltration during atherosclerosis, resulting in increased plaque necrosis and progression of atherosclerosis, independently of confounding metabolic alterations. Our results indicate that aging directly impacts atherogenesis by increasing plaque instability.

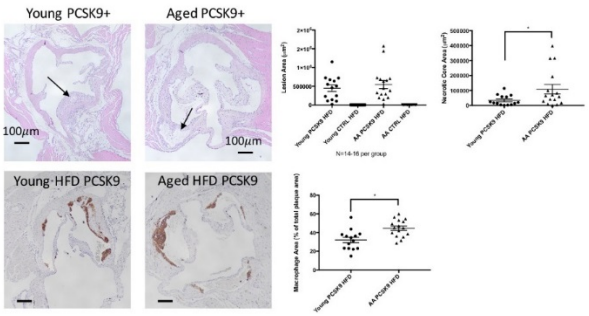

D.J. Tyrrell: None. **D.R. Goldstein:** None.

188
Macrophage-associated Lipin-1 Enzymatic Activity Primes Macrophages to Be Hyper-responsive to Additional Proinflammatory Stimulus
Aimee E Vozenilek, Cassidy M Blackburn, Ronald L Klein, A Wayne Orr, Matthew D Woolard, LSU Health Sciences Ctr, Shreveport, LA

Macrophage proinflammatory responses induced by oxidized low-density lipoproteins (oxLDL) contribute to atherosclerotic progression. Our previous data using mice lacking lipin-1 enzymatic activity in myeloid-derived cells demonstrated that stimulation of bone marrow-derived macrophages with oxLDL activates a lipin-1 dependent persistent PKCα/βII-ERK1/2-cJun signaling cascade that primes the macrophage to be hyper-responsive to subsequent proinflammatory stimulus. To further investigate the impact of lipin-1 enzymatic activity on oxLDL-induced macrophage proinflammatory responses, bone marrow-derived macrophages (BMDMs) were collected from mice lacking lipin-1 enzymatic activity in myeloid-derived cells and littermate control mice. Both the control BMDMs and BMDMs lacking lipin-1 enzymatic activity were then stimulated with oxLDL, lipopolysaccharide (LPS), or oxLDL and LPS. RNA was collected from the BMDMs and RNA sequencing was performed. The goal was to identify transcripts that are altered between the control BMDMs and BMDMs lacking lipin-1 enzymatic activity to define transcription factors and signaling pathways regulated by lipin-1 enzymatic activity on a global level. Our data demonstrates that the loss of lipin-1 enzymatic activity in BMDMs results in a reduction of proinflammatory transcripts, via loss of cJun activity, in response to the combination treatment of oxLDL and LPS when compared to the control BMDMs.

A.E. Vozenilek: Other; Significant; 17PRE33661114. **C.M.R. Blackburn:** None. **R.L. Klein:** None. **A.W. Orr:** Research Grant; Significant; HL098435, HL133497. **M.D. Woolard:** Research Grant; Significant; HL131844.

This research has received full or partial funding support from the American Heart Association.

189
Novel Drug Development Controlling Residual Inflammatory Risk in Diabetic Atherosclerotic Disease
Martin Yussman, David Wagner, Gisela Vaitaitis, Dan Waid, Univ of Colorado, Anschutz Medical Campus, Aurora, CO

Sustained inflammation is a crucial pathologic component in atherosclerosis and type 2 diabetes (T2D). A common molecular player driving auto-inflammation in both diseases is the CD40/CD154 inflammatory dyad. By normalizing the aberrant contact dependent interaction of the CD40/CD154 dyad, and resultant auto-inflammation, multiple studies have shown both prevention and therapeutic efficacy in both diseases.
We designed a series of peptides derived from the CD154 protein sequence that are capable of binding directly to the CD40 receptor to interrupt the inflammatory signal pathways. Two peptides, KGYY6 and KGYY15, were highly effective, initially demonstrating efficacy in type one diabetes mouse models. KGYY6 was chosen for additional testing in the T2D model with atherosclerosis.
ApoE-/- mice were utilized due to their ability to develop severe vascular disease and acquire the elements of T2D after 16 weeks of a high fat diet (HFD). KGYY6 was administered by IV tail injection at a dose of 1mg/kg and compared to controls given vehicle only.
Aortic en-Face analysis with Sudan IV stain demonstrated significant reduction in plaque in KGYY6 treated mice. Decreases in plaque area and changes in both smooth muscle and collagen measurement were additionally noted by sequential 5um aortic cross sections from the aortic valve leaflets into the ascending aorta. In-vitro analysis of CD3+CD4+CD40+ splenic cells demonstrated a reduction in inflammatory cytokine expression in response to KGYY6 treatment, specifically IL2, IFNγ, and IL17, which are potent cytokines in atherosclerosis.
Western blot analysis performed on adipose and muscle tissue demonstrated an increased expression of the glucose transport protein GLUT 4, with corresponding glucose tolerance testing demonstrating increased glucose tolerance and improved insulin sensitivity with lowered plasma insulin level.
KGYY6 normalizes the aberrant CD40/CD154 interaction, reducing inflammatory cytokines and regulating glucose, all together resulting in abrogating atherosclerosis.

M. Yussman: Employment; Significant; Op-T-Mune Inc.. Research Grant; Significant; R41AI131784. **D. Wagner:** Employment; Significant; Op-T-Mune Inc.. Research Grant; Significant; R41AI131784. **G. Vaitaitis:** None. **D. Waid:**

Employment; Significant; Op-T-Mune Inc.. Research Grant; Significant; R41AI131784.

190
Mir-33 Inhibition Alters Monocyte/macrophage Kinetic Processes to Promote Atherosclerotic Plaque Regression
Milessa Silva Afonso, Monika Sharma, Coen van Solingen, Graeme J Koelwyn, P. Martin Schlegel, Mireille Ouimet, Lauren Beckett, Susan Babunovic, Karishma Rahman, Edward A Fisher, Kathryn J Moore, Depts of Med (Cardiology) and Cell Biology, and the Marc and Ruti Bell Program in Vascular Biology, New York Univ Sch of Med, New York, NY

Previous studies have identified microRNA-33 (miR-33) as a key regulator of metabolic gene pathways involved in cholesterol and fatty acid homeostasis. Inhibition of miR-33 promotes the regression of atherosclerosis, in part, by enhancing plasma HDL and reverse cholesterol transport levels. However, it has become clear that miR-33 inhibition can also reduce plaque inflammation, independent of its effects on cholesterol homeostasis, yet the mechanisms of these actions are still not well understood. To investigate how miR-33 inhibition alters monocyte/macrophage dynamics during atherosclerosis regression, we fed *Ldlr*$^{-/-}$ mice a western diet for 14 weeks to establish plaques, after which mice were switched to chow diet and treated with anti-miR-33 or control anti-miR oligonucleotides for 4 weeks. As we reported previously, anti-miR-33 treatment increased plasma levels of HDL cholesterol by 30%, and concurrently reduced plaque size, macrophage content and necrotic area, compared to control anti-miR treatment. Analysis of the monocyte/macrophage kinetic processes contributing to macrophage burden in plaques revealed that anti-miR-33 treatment normalized the monocytosis associated with hypercholesterolemia. Mice treated with anti-miR33 had 40% fewer circulating monocytes than control anti-miR treated mice, and this was associated with a reduction of splenic common myeloid progenitor (CMP) cells. Surprisingly, monocyte tracking assays also revealed an increase in Ly6C^{hi} monocyte recruitment into plaques of anti-miR-33 treated mice. Although somewhat counterintuitive, these data are consistent with recent findings that Ly6C^{hi} monocytes are required for atherosclerosis regression and are a source of tissue reparative M2 macrophages. Indeed, we find that M2 macrophages, as well as atheroprotective regulatory T cells are enriched in plaques of anti-miR-33 treated mice. Collectively, our results provide insight into the mechanisms underlying anti-miR-33's atheroprotective actions, which include both anti-inflammatory and cholesterol homeostatic effects.

M.S. Afonso: None. **M. Sharma:** None. **C. van Solingen:** None. **G.J. Koelwyn:** None. **P. Schlegel:** None. **M. Ouimet:** None. **L. Beckett:** None. **S. Babunovic:** None. **K. Rahman:** None. **E.A. Fisher:** None. **K.J. Moore:** None.

191
Plan-Based Diet and Lifestyle Changes Improve Stress Test Induced ST Depression in 18 Days
Francisco E Ramirez, Neil Nedley, Nedley Clinic, Weimar, CA

Background: This study documents the effects of an intensive 18-day lifestyle program on EKG stress test readings of the ST segment. Improving EKG readings could be a positive indicator of cardiovascular improvement. Methods: The medical residential program takes place in Weimar California. The intervention could be summarized in the word NEWSTART which means Nutrition, Exercise, Water, proper Sunlight exposure, fresh Air, Rest and Trust (in relational, spiritual, and psychological aspects). Physicians, nutritionist, exercise physiologist, physical therapist, psychological and spiritual counselors are part of the team. Every patient does a treadmill test (using the Bruce protocol) before and after the 18 day program and a before and after blood tests. Board certified physicians monitored the progress of each patient. Data from 11 years of retrospective recordings were used. From n=2091 patients in the data base, n=145 were used in the study because they had a stress test induced ST depression of 2 mm on two EKG leads or more at baseline. No angiography was available at the institution. Results: Average age of patients was 64 (SD 10.5), n=81 (56%) female, and n=131 (90%) were Americans. At baseline the group with ST depression in more than two leads had a mean ST depression in mm of 3.9, SD 2.3, max 13, median 3, mode 2 in the most affected lead. At the end of the 18 days the same group had a mean ST depression in mm was 2.7, SD 2.7, max 12, median 0, mode 0 on the most affected lead. After the 18 days the stress test reported that n=70 (48.2%) had improvement as seen in an improvement of the ST depression during the stress test. While n=64 (44.1%) had the same level of ST depression during the last stress test and n=11 (7.5%) worsen the ST depression during the end stress test. The changes in the ST segment were significant according to the paired t-test t(144)=5.421 with a p<.001. The n=145 lost 4 pounds of weight on average (SD 4) at the end of the 18 days, No heart infarctions occurred during the intervention. Conclusion: The intensive lifestyle interventions seem to be effective in improving ST depression. Improvement of ST depression could improve long term prognosis. Further follow up is advised.

F.E. Ramirez: None. **N. Nedley:** Ownership Interest; Modest; Nedley Health Solutions.

192
Relation Between Poor Sleep Quality and Hypercholesteremia
Francisco E Ramirez, Neil Nedley, Nedley Clinic, Weimar, CA

Background: Problems with sleep are linked with higher risk of cardiovascular pathologies. We explore the effect that problems with sleep may have on hypercholesterolemia as well as mental health on participants of an 8-week lifestyle health program. Methods: The focus of the program is educational. Those who chose to participate met once a week for 8 weeks for a 2 hour program. It consisted of a 45 minute DVD presentation and a facilitated group discussion. The Depression and Anxiety Assessment Test (DAAT) was administered at baseline and completion. It assessed depression level based on DSM-5 [The Diagnostic and Statistical Manual of Mental Disorders Volume 5] criteria, demographics, sleep quality and inquires about cholesterol levels. The depression was classified according to DSM-5 into 4 categories as none (0-6), mild (7-10), moderate (11-19) or severe (20 or more). They were taught various healthy lifestyle habits. Sleep quality was self reported and was divided between bad quality and good quality the last two weeks. Results: Of n=5997 participants that finished the program, n=5380 knew their cholesterol levels and were used in this study. Mean age was 52.3 (SD 15.1), n=4209 (70%) females. At baseline participants that reported bad sleep were n=1124, that group baseline mean depression was 14.8 (SD 7.2), n=313 (27.8%) had hypercholesterolemia. At the end of the 8- week program their mean depression was 8.1 (SD 6.3), the change was significant with a paired t-test t(1123)=7.761 p<.001. By the end also 58.1% reported improvement in sleep quality. An improvement in cholesterol was reported in 11.8% of this group at the end of the program. At baseline those with good sleep quality were n=4256, their baseline mean depression was 11.2 (SD 7.4), n=1006 (23.6%) had hypercholesterolemia. Their end mean depression was 5.9 (SD 5.7), paired t-test reported significant change t(4255)=55.03 p<.001. An improvement in their cholesterol was reported in 26.3% of this group at the end of the program. Conclusion: The group with bad sleep quality seem to have more hypercholesterolemia and more severe depression. The 8-week program was safe and was

associated with at least some degree of improvement in the vast majority.
F.E. Ramirez: None. **N. Nedley:** Ownership Interest; Modest; Nedley Health Solutions.

195
Therapeutic Silencing of FSP27 Attenuates the Progression of Atherosclerosis in LDL-Receptor Deficient Mice
Ananthi Rajamoorthi, Saint Louis Univ, Saint Louis, MO; Richard G Lee, Ionis Pharmaceuticals, Inc., Carlsbad, CA; **Angel Baldan**, Saint Louis Univ, Saint Louis, MO

Obesity, hepatosteatosis, and hypertriglyceridemia are components of the metabolic syndrome and independent risk factors for cardiovascular disease. The lipid droplet-associated protein CIDEC (cell death-inducing DFFA-like effector C), known in mice as FSP27 (fat-specific protein 27), plays a key role in maintaining triacylglyceride (TAG) homeostasis in adipose tissue and liver, and controls circulating TAG levels in mice. Importantly, mutations and SNPs in *CIDEC* are associated to dyslipidemia and altered metabolic function in humans. Here we tested whether systemic silencing of *Fsp27* using antisense oligonucleotides (ASOs) was atheroprotective in LDL receptor knock-out (*Ldlr*$^{-/-}$) mice. Animals were fed a high-fat, high-cholesterol diet for 12 weeks while simultaneously dosed with saline, ASO-ctrl, or ASO-Fsp27. Data show that, compared to control treatments, silencing *Fsp27* significantly reduced body weight gain and visceral adiposity, prevented diet-induced hypertriglyceridemia, and reduced atherosclerotic lesion size both in *en face* aortas and in the aortic root. Our findings suggest that therapeutic silencing of *Fsp27* with ASOs may be beneficial in the prevention and management of atherogenic disease in patients with metabolic syndrome.
A. Rajamoorthi: None. **R.G. Lee:** Employment; Significant; Employee and shareholder of Ionis Pharmaceuticals.. **A. Baldan:** None.

197
Active (1,25 OH), but not Inactive (25-OH) Vitamin D levels are inversely associated with aortic Vascular Inflammation, Non-calcified Coronary Plaque Burden and Visceral Adiposity in Psoriasis
Martin Playford, Amit Dey, NIH, Bethesda, MD; Claudia Zierold, Frank Blocki, Fabrizio Bonelli, DIaSorin, Stillwater, MN; Aditya Joshi, Heather Teague, Yvonne Baumer, Nehal N Mehta, NIH, Bethesda, MD
Introduction: Psoriasis (PSO), a chronic inflammatory disease associated with increased Cardiovascular (CV) risk provides an ideal model to study the role of vitamin D, a known anti-inflammatory molecule in PSO associated CV disease. Vitamin D exists as inactive 25-hydroxyvitamin D (25(OH)D) in the bloodstream which is converted to active 1,25-dihydroxyvitaminD (1,25(OH)2D) in target tissues. Cohort studies reporting CV disease among individuals with low vitamin D are inconsistent and solely measure 25(OH)D. While serum 25(OH)D is routinely measured , we propose that measurement of 1,25(OH)2D may perform better than 25(OH)D as a surrogate for CV disease.
Methods: Consecutive PSO patients (N=122) and healthy controls (N=35) underwent FDG PET/CT and CCTA scans to measure vascular inflammation/ abdominal adiposity volume and coronary plaque burden respectively. Blood levels of both 1,25(OH)2D and 25(OH)D were measured by chemiluminescence (LIASON XL DIaSorin, Stillwater, MN).
Results: PSO patients were middle-aged, mostly male, had moderate PSO severity and were at low CV risk by 10-year Framingham risk. PSO patients had lower serum 1,25(OH)2D compared to healthy controls (mean±SEM: 52.4±1.4 pg/ml versus 57.5±2.0, p<0.037) but 25(OH)D was not significantly different (28.7±1.3 versus 27.3±2.2, p=0.30). 1,25(OH)2D, but not 25(OH)D was negatively associated with PASI score beyond adjustment for CV risk factors and systemic/ biological therapy (B=-0.20, p=0.043 vs. B=0.12, p=0.25). Furthermore, serum 1,25(OH)2D but not 25(OH)D was inversely associated with non-calcified coronary burden (B=-0.16, p<0.001 versus B=0.01, p=0.84), vascular inflammation (B=-0.24, p=0.007 versus B=-0.13, p=0.16) and visceral adiposity (B=-0.43, p=0.026 versus B=-0.26, p=0.13) independent of traditional risk factors and statin/PSO therapy.
Conclusion: Our data support that active 1,25(OH)2D may more accurately capture cardiometabolic disturbance compared to inactive 25(OH)D in humans.

M. Playford: None. **A. Dey:** None. **C. Zierold:** None. **F. Blocki:** None. **F. Bonelli:** None. **A. Joshi:** None. **H. Teague:** None. **Y. Baumer:** None. **N.N. Mehta:** Research Grant; Modest; Dr. Mehta is a full-time US Government Employee and has received research grants to the NIH from Abbvie, Janssen, Novartis and Celgene.

198
The Role of PI(4,5)P_2 in LDL Receptor Lysosomal Decay
Yuanyuan Qin, Mee J Kim, Flora Ting, Jacob Strelnikov, Joseph Harmon, Andrea Dose, Children's Hosp Oakland Res Inst (CHORI), Oakland, CA; Hua Sun, Ba-Bie Teng, Res Ctr for Human Genetics, The Brown Fndn Inst of Molecular Med, Houston, TX; Ronald Krauss, Marisa Medina, Children's Hosp Oakland Res Inst (CHORI), Oakland, CA

Upregulation of low density lipoprotein receptor (LDLR) activity reduces LDL levels and coronary disease risk. LDLR releases LDL in endosomes after internalization and then is either recycled to the cell surface or transported to lysosomes for decay. The transmembrane protein 55B (TMEM55B) is a phosphatase that hydrolyzes phosphatidylinositol-(4,5)-bisphosphate (PI(4,5)P_2) and has been found to affect lysosome function. We reported *TMEM55B* regulates cellular cholesterol metabolism by modulating LDLR protein decay.
To evaluate whether *Tmem55b* affects cholesterol metabolism *in vivo,* we treated western diet fed C57BL/6J mice with antisense oligonucleotides against either *Tmem55b* or a non-targeting control for 4 weeks. Hepatic *Tmem55b* transcript and protein levels were reduced by ~70%, resulting in increased plasma total (1.5-fold, p<0.0001) and non-HDL-cholesterol (1.8-fold, p<0.0001). FPLC and ion mobility analyses revealed increased levels of small LDL particles that were enriched in apoE as determined by immunoblot. Notably, *Tmem55b* knockdown had no effect on plasma cholesterol levels in *Ldlr*$^{-/-}$ mice. Increased LDLc (1.3-fold, p<0.05) was also observed in a murine model that lacks Ocrl, another phosphatase which hydrolyzes PI(4,5)P_2.
Given the role of the lysosome in LDLR decay, we tested whether *TMEM55B* regulates LDLR via lysosomes. Using confocal microscopy, *TMEM55B* knockdown in HepG2 cells significantly increased PI(4,5)P_2, decreased LDLR, increased lysosome staining, and reduced LDLR-lysosome colocalization. Impairment of lysosome function by incubation with NH_4Cl or knockdown of the lysosomal proteins *LAMP1* or *RAB7* abolished the effect of *TMEM55B* knockdown on LDLR. Although there was no change in RAB11 levels, a marker of recycling endosomes, LDLR-RAB11 colocalization was reduced by 50% upon *TMEM55B* knockdown. Finally, incubation of HepG2 cells with PI(4,5)P_2 increased LDL uptake and reversed the inhibitory effect of *TMEM55B* overexpression .
Together, these findings suggest that TMEM55B increases plasma cholesterol through stimulating LDLR lysosomal degradation, reducing LDLR recycling to the plasma membrane through PI(4,5)P_2, and thereby inhibiting plasma clearance of apoE-containing LDL particles.
Y. Qin: None. **M.J. Kim:** None. **F. Ting:** None. **J. Strelnikov:** None. **J. Harmon:** None. **A. Dose:** None. **H. Sun:** None. **B. Teng:** None. **R. Krauss:** None. **M. Medina:** None.

200
Behavior Modification and Hypothalamic Appetite Regulation in a Stress-less Mouse Model
Nalini Santanam, Abbagael Seidler, Debbie Amos, Lawrence Grover, Marshall Univ Sch of Med, Huntington, WV
Obesity is a major crisis in the Appalachian region. Being obese not only increases risk to heart disease and diabetes, but also promotes behavior modifications. Behavior changes such as excess food consumption, stress, depression is very commonly observed among obese individuals. We hypothesized, lower redox stress by modulating appetite regulation will decrease obesity associated behavioral stress. Behavior changes and appetite regulation were determined in C57Bl6 mice (control) and Bob-Cat mice that express high antioxidant catalase in an obese (Ob/Ob) background (stress-less mouse) (n=6-8) fed either normal chow (NC) or high-fat (HF-45% lard-TD06415) diet for eight weeks. Weekly body weights were monitored. Fat mass changes were determined using ECHO-MRI. Comprehensive lab animal monitoring system (CLAMS) was used to determine energy expenditure. Motor and anxiety-like behavior was tested using Open Field (locomotor behavior) and Rota-Rod (motor coordination and strength) testing systems at baseline and 8 weeks. Changes in appetite regulating genes in the hypothalamus were determined using real time PCR. The C57Bl6 mice on the NC stayed longer on the Rota-Rod as the weeks progressed compared to the mice on HF, where the effect was more dependent on the trials (learning) rather on endurance. The Open Field test showed that the C57Bl6 mice on HF diet were more anxious (spent more time in the edges rather than center) compared to the mice on NC. Catalase overexpression lowered levels of anxiety but had less endurance levels in the HF fed mice. CLAMS showed heat production was higher in stress-less mice vs C57Bl6. Catalase overexpression showed an induction in anorexigenic POMC, and decrease in orexigenic Npy vs C57Bl6. Redox regulation in the stress-less mice modulated both hypothalamic appetite regulation and behavior changes associated with obesity. These findings suggest that redox modulation, may be regulating metabolic pathways that lower obesity and improve the overall behavioral and nutritive state.
N. Santanam: None. **A. Seidler:** None. **D. Amos:** None. **L. Grover:** None.

201
Non-invasive, Mechanical Treatment for Atherosclerosis
Justin Urso, Chandrakala Narasimhulu, Sampath Parthasarathy, Alain Kassab, Subith Vasu, Univ of Central Florida, Orlando, FL

Background: Atherosclerosis is the foremost cause of cardiovascular diseases, and results in millions of deaths worldwide. All current treatments for atherosclerosis involve, at the least, minimally invasive surgery. The treatment procedures result in a necessary recovery time, have a risk of complication, and do not reverse plaque buildup, but rather offset the symptoms. Preventative measures depend on a reliance on pharmaceuticals to slow the growth of atherosclerotic regions. Methods: Lipoproteins were isolated from human plasma, acetylation of lipoproteins was performed. RAW 264.7 cells were incubated with Ac-LDL for 24hrs. After 24hrs of incubation, cells were treated with ultrasonic waves (Vevo 3100) followed by 2hrs incubation at 37°C. RNA was isolated, cDNA was synthesized and quantitative RT-PCR was performed to detect mRNA levels of cholesterol transport as well as pro-inflammatory gene expressions. Foam cells were stained with Oil Red O after the ultrasonic wave treatment. Results: Reduced Oil Red O staining was observed in sound waves treated foam cells as compared to untreated cells. Gene analysis showed the increased cholesterol transport genes such as ABCA1 and ABCG1, and reduced pro-inflammatory gene expressions were observed. Conclusions: This is the first study that demonstrates that ultrasonic wave treatment could be an effective non/minimally-invasive treatment for atherosclerosis. This novel treatment has the capability to reverse plaque buildup naturally, without the need for surgery, and without the use of pharmaceuticals.
J. Urso: None. **C. Narasimhulu:** None. **S. Parthasarathy:** None. **A. Kassab:** None. **S. Vasu:** None.

202
Zfp36l1 is a Post transcriptional Regulator of Hepatic Bile Acid and Lipid Metabolism
Elizabeth Tarling, Bethan Clifford, **Thomas A Vallim**, UCLA, Los Angeles, CA

Bile acids are detergents and important signaling molecules that activate the nuclear receptor FXR to control key metabolic processes, including feedback mechanisms to maintain bile acid homeostasis. FXR is the central rheostat of bile acid metabolism, and activation of FXR decreases the mRNA levels of bile acid synthetic genes, including *Cyp7a1,* the gene encoding the rate-limiting enzyme of bile acid synthesis. We show that *Cyp7a1* mRNA levels were rapidly reduced after pharmacologic FXR activation in wild-type, but not $Fxr^{-/-}$ or liver-specific *Fxr* knockout mice ($Fxr^{L\text{-}KO}$). The rapid decrease in *Cyp7a1* mRNA suggested a previously unidentified post-transcriptional mechanism. To identify the mechanism, we used synthetic and endogenous FXR agonists and found the RNA binding protein ZFP36L1 as a novel FXR target gene. ZFP36L1 mRNA and protein levels were increased as early as 30 minutes after FXR activation. ZFP36L1 is a *bona-fide* RNA binding protein that promotes degradation of mRNA targets by binding to AU-rich elements (AREs) in the 3' UTR. We generated *in vivo* and *in vitro* gain-of-function models and we used reporter assays to show that ZFP36L1 targets the *Cyp7a1* UTR. In mice, hepatic overexpression of ZFP36L1 decreased *Cyp7a1* mRNA and protein and decreased bile acid levels. To complement our gain-of-function studies, we generated liver-specific *Zfp36l1* knockout mice ($Zfp36l1^{L\text{-}KO}$) and we show that loss of *Zfp36l1* resulted in elevated *Cyp7a1* mRNA and protein, and increased bile acid levels. Given that bile acids are important metabolites that control lipid absorption and signaling, we investigated whether loss of hepatic *Zfp36l1* resulted in more broad metabolic dysfunction. Western diet fed $Zfp36l1^{L\text{-}KO}$ mice had reduced body weight gain, specifically in adipose tissue depots compared to littermate $Zfp36l1^{flox\text{-}flox}$ mice. The differences in adiposity and steatosis were attributed to reduced lipid absorption, as $Zfp36l1^{L\text{-}KO}$ mice have increased fecal caloric content and reduced triglyceride absorption as determined by an intragastric fat tolerance test. The decreased lipid absorption is consistent with an altered bile acid metabolism. Thus, we have identified a novel pathway that controls *Cyp7a1* and bile acid metabolism but may also have wider implications in diseases such as obesity and hepatosteatosis.
E. Tarling: None. **B. Clifford:** None. **T.A. Vallim:** None.

This research has received full or partial funding support from the American Heart Association.

203
Glyoxalase 1 Overexpression on Endothelial Progenitor Cell Therapy Accelerates Diabetic Wound Healing
Hainan Li, Megan O'Meara, Xiang Zhang, Yihan Wang, **Jie-Mei Wang**, Wayne State Univ, Detroit, MI

Introduction: Vascular progenitor cells (VPCs) represent the repair and regenerative potential of vasculature. VPC function has been found severely impaired in diabetes with mechanisms not fully understood. We previously demonstrated that inositol requiring-enzyme 1α (IRE1α) activity is significantly attenuated in diabetic VPCs, contributing to impaired angiogenesis *in vitro*. Methylglyoxal (MGO) is one of the highly reactive species generated in hyperglycemic environment. We hypothesize that MGO

scavenger glyoxalase 1 (GLO1) reverses VPC dysfunction through augmenting of IRE1α, resulting in improved diabetic wound healing. **Methods and Results:** VPCs were isolated and cultured from the bone marrow of adult male db/db type-2 diabetic and their healthy control db/+ mice. MGO (10μM, 24h) induced immediate and severe VPC dysfunction, including impaired tube formation (Matrigel tube formation assay) and proliferation (MTT assay), increased apoptosis (Caspase 3/7 activity), which was rescued by adenovirus-mediated GLO1 over-expression (50MOI, 48h prior to MGO exposure). IRE1α expression (by Western Blot) in VPCs was decreased upon MGO exposure, but reversed by GLO1 over-expression. IRE1α RNase activity was impaired by direct MGO modification *in vitro*. Cell therapies using db/db VPCs with GLO1 over-expression significantly improved diabetic wound healing *in vivo* (6-mm full-thickness excisional wound) through facilitating angiogenesis (detected by wound capillary density), compared with diabetic control cell therapy. **Conclusions:** Our data suggest that GLO1 can improve VPC function in diabetes and facilitate angiogenesis by rescuing compromised efficacy of diabetic cell therapies. This is at least partly through augmenting IRE1α expression and activity. We believe that our data will provide useful information for developing novel therapeutic approaches to rescue progenitor/stem cell-mediated angiogenesis and tissue repair in diabetes.

H. Li: None. **M. O'Meara:** None. **X. Zhang:** None. **Y. Wang:** None. **J. Wang:** None.

This research has received full or partial funding support from the American Heart Association.

204
Diabetes Influence Infragenicular Arterial Segment Phospholipid Profiles
Chao Yang, Fong-Fu Hsu, Yan Yan, Malik Darwesh, Mohamed Zayed, Washington Univ in St. Louis, St. Louis, MO

Diabetes patient have higher risk of PAD. Our group previously demonstrated that CEA plaque lipidomics are altered by diabetes. It remains unknown whether similar alterations also occur in infra-inguinal PAD. Between 2015 to 2017, patients undergoing major lower extremity amputation were recruited into a vascular surgery tissue biobank. At the time of amputation, infra-inguinal arterial segment with maximally (Max) and minimally (Min) disease were harvested. lipids were extracted using a modified Bligh-Dyer technique and evaluated by Electrospray-ionization tandem mass spectrometry. The relative proportions of all major phospholipid species (including phosphatidylcholine, PC; ceramide, Cer; phosphatidylethanolamine, PE; phosphatidylinositol, PI; and phsophatidylserine, PS) were derived. Paired one-sample sighed rank test was used to evaluate the differences between Max and Min diseased arterial segments, and Wilcoxon two-sample test was used between diabetic and non-diabetic group. 14 diabetic (DM) and 7 non-diabetic(NDM) patients were enrolled with well-matched demographics. Analysis of the major phospholipid families, there were no differences between DM and NDM in Max segments. However in Min segments there were differences (58% lower PI in DM patients, P<0.03). Further sub-group analysis was performed at max and min in DM and NDM separately and found differences in PCs, aPCs, PEs, pPEs, Cers. The most highly differentially expressed lipids included PC 40:3(76%, P=0.01), PC 40:5(60%,P=0.04), aPC38:3 (83%, P=0.01), aPC38:2(79%, P=0.04) ,and these have been shown previously to be important in arachidonic acid mediated inflammation. Max and Min diseased segments from infra-ingunial arterial segments from diabetic and non-diabetic patients demonstrate significantly different lipid contents. These findings highlight the profound biochemical differences in plaque phospholipid biology in the diabetes and provide a platform for future exploration in diseased oriented treatment strategies.

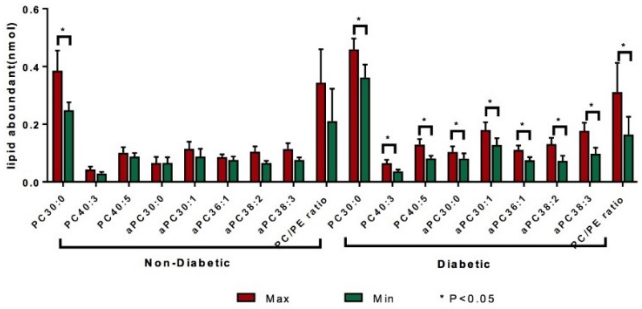

C. Yang: None. **F. Hsu:** None. **Y. Yan:** None. **M. Darwesh:** None. **M. Zayed:** None.

210
Beta-carotene Conversion to Vitamin a Delays Atherosclerosis Progression and Accelerates Atherosclerosis Regression
Jaume Amengual, Univ of Illinois, Urbana-Champaign, IL; Felix Zhou, Tessa J Barrett, Cyrus A Nikain, New York Univ, New York, NY; Johannes von Lintig, Case Western Reserve Univ, Cleveland, OH; Edward A Fisher, New York Univ, New York, NY

β-carotene (BC) from plants is strong antioxidant and is the precursor of vitamin A in animals. Human studies show that elevated BC blood levels correlate with lower incidence of heart disease, but the molecular mechanisms are unclear. While humans accumulate high amounts of BC in blood, rodents completely metabolize BC to vitamin A, precluding the possibility of studying if BC influences heart disease using mouse models. To overcome this, we used a mouse model lacking the enzyme that converts BC to vitamin A (BC oxygenase 1, BCO1) and studied if BC plays a role in atherosclerosis, the main cause of heart disease. We first crossed *Bco1*$^{-/-}$ mice with *Ldlr*$^{-/-}$ mice to generate *Bco1*$^{-/-}$/*Ldlr*$^{-/-}$ mice. These mice were fed Western diet (WD) containing BC (WD-BC) for 12 wks, accumulated levels of BC in blood comparable to those observed in humans (12±2 μM), as well as in atherosclerotic lesions, while *Ldlr*$^{-/-}$ mice fed WD-BC only accumulated trace amounts of BC in blood (0.3±0.1 μM). *Ldlr*$^{-/-}$ mice fed WD-BC showed delayed atherosclerosis progression (40% reduction in plaque size, n=10-12 mice/group) when compared to those fed WD without BC (WD-noBC). These changes were accompanied by decreased plasma cholesterol (35%) and triglyceride (~55%) levels (n=10-12 mice/group). People typically present for treatment of atherosclerotic disease after plaques have advanced. Thus, we next tested whether BC plays a role in atherosclerosis regression after lipid lowering. For this purpose, we utilized a LDLR antisense oligonucleotide (LDLR-ASO) strategy to block expression of the LDLR to induce hypercholesterolemia. Wild-type and *Bco1*$^{-/-}$ mice were fed WD-noBC and simultaneously treated with LDLR-ASO for 16 wks. After LDLR-ASO treatment was stopped, plasma cholesterol levels fell from 700mg/mL to 70mg/mL. Mice were also switched to WD-BC or continued with WD-noBC for 3 wks. Wild-type mice, but not *Bco1*$^{-/-}$ mice, fed WD-BC showed a reduced content of plaque macrophages (30%) and newly recruited monocytes (25%) (n=7 to 12 mice/group) when compared to those fed WD-noBC. We are currently in the process of elucidating the molecular mechanisms responsible of these beneficial effects of BC on atherosclerosis progression and regression.

J. Amengual: None. **F. Zhou:** None. **T.J. Barrett:** None. **C.A. Nikain:** None. **J. von Lintig:** None. **E.A. Fisher:** None.

This research has received full or partial funding support from the American Heart Association.

211
MKL1 Affects Proliferation/Survival Property of Pro-Atherogenic Macrophages
Jianbo An, Taeko K Naruse, Akinori Kimura, Tokyo Medical and Dental Univeristy, Tokyo, Japan

Coronary artery disease (CAD) is one of the leading causes of death in the most countries. Atherosclerosis of coronary arteries often results in high incidence of vascular occlusion and is recognized as the major cause of CAD. We have previously reported from a genome-wide association study that a promoter SNP in megakaryoblastic leukemia 1 gene (*MKL1*), which conferred higher transcriptional activity, was significantly associated with the susceptibility to CAD as well as coronary atherosclerosis. MKL1 is a Rho-Rock signaling-responsive co-activator of serum response factor, and regulates a variety of cellular functions. We found that MKL1 was highly expressed in activated macrophages in the neointima of atherosclerotic lesions from human and ApoE-knockout (KO) mouse. In addition, the expression level of MKL1 in lesional macrophages was increased during the development of atherosclerosis in ApoE-KO mice.
We have established a transgenic mouse line, MKL1-TgM, in which human *MKL1* was specifically overexpressed in monocyte/macrophage lineage cells. In this study, MKL1-TgM was crossbred onto ApoE-KO background. ApoE-KO/MKL1-TgM fed with normal chow developed severer atherosclerosis and showed poorer survival rate than ApoE-KO mice. Serum level of pro-inflammatory cytokines was increased in ApoE-KO/MKL1-TgM. Interestingly, ApoE-KO/MKL1-TgM also developed hypertriglyceridemia, which was associated with severe lipodystrophy.
We also investigated how MKL1 regulated macrophages function. Recently, local proliferation/accumulation of lesional macrophages was reported to be a crucial event in atherosclerosis. We treated bone marrow-derived macrophages (BMDMs) with stimuli, such as M-CSF or OxLDL, and found that proliferation property of BMDMs from MKL1-TgM was elevated. On the other hand, BMDMs from MKL1-TgM were more resistant to apoptosis. Furthermore, immunohistochemistry analyses of lesional macrophages in ApoE-KO/MKL1-TgM showed enhanced proliferation and mitigated apoptosis.
Taken together, our data indicated that MKL1 would contribute to the development of atherosclerosis by modulating pro-atherogenic functions of macrophages, providing a potential molecular target for the therapy and prevention of atherosclerosis.
J. An: None. **T.K. Naruse:** None. **A. Kimura:** None.

212
Chronic Systemic Inflammation Accelerates Endothelial Cholesterol Crystal Formation and Lysosomal Dysfunction
Yvonne Baumer, Gregory Sanda, Heather Teague, Pradeep Dagur, Qimin Ng, Charlotte Harrington, Nevin Varghese, Alexander Sorokin, NIH/NHLBI, Section of Inflammation and Cardiometabolic Diseases, Bethesda, MD; Christopher Bleck, Electron Microscopy Core NHLBI, NIH, Bethesda, MD; Justin Rodante, NIH/NHLBI, Section of Inflammation and Cardiometabolic Diseases, Bethesda, MD; Howard Kruth, Experimental Atherosclerosis NHLBI, NIH, Bethesda, MD; Aditya Joshi, Amit Dey, Martin Playford, Nehal Mehta, NIH/NHLBI, Section of Inflammation and Cardiometabolic Diseases, Bethesda, MD

Objective: Atherogenesis is an inflammatory process accelerated in psoriasis, a chronic inflammatory skin disease associated with premature cardiovascular diseases (CVD). Cholesterol crystal (CC) formation is implicated at onset and progression of atherosclerotic CVD, and we have recently shown CC formation to be upregulated in a murine model of psoriasis-related atherosclerosis. Therefore, we investigated inflammatory CC production in this psoriasis mouse model and also using psoriasis patient derived samples. **Methods:** *K14-Rac1V12* psoriasis mouse aortas were examined for CC formation and structural abnormalities, such as subendothelial spaces, via electron microscopy and histology. Human aortic endothelial cells (HAoEC) were stimulated with sera from healthy and psoriatic volunteers (n=5 each), inflammatory markers TNFα+IFNγ, LDL or combination of TNFα+IFNγ+LDL. The effect on CC formation and lysosomal function was determined by advanced microscopy and flow cytometry. HAoECs were also treated with TNFα+IFNγ+LDL combined with β-cyclodextrin (CD), a stimulant for cholesterol release from cells, and analyzed for CC formation and lysosomal function. **Results:** Psoriatic mouse aortas showed enlarged subendothelial spaces and 40% increased CC formation under normolipidemic conditions compared to littermate controls. Treatment of HAoECs with psoriasis patient-sera (severe skin disease, low CVD risk score) or TNFα+IFNγ+LDL showed a 2-fold increase in CC formation and 30% increased lysosomal frequency compared to controls. Despite an increase in lysosome frequency, TNFα+IFNγ+LDL treatment decreased overall pH-related lysosomal activity. CD treatment diminished TNFα+IFNγ+LDL-induced CC formation (compared to vehicle), and restored lysosomal function without affecting lysosome frequency. **Conclusion:** Psoriasis mice displayed accelerated CC formation in the absence of hyperlipidemic conditions suggesting chronic systemic inflammation accelerates CC formation *in vivo* and *in vitro*, accompanied by lysosomal dysfunction in ECs. These findings suggest that dyslipidemia and systemic inflammation in psoriasis are important contributors to early atherogenesis and should be treatment targets for CVD risk mitigation.
Y. Baumer: None. **G. Sanda:** None. **H. Teague:** None. **P. Dagur:** None. **Q. Ng:** None. **C. Harrington:** None. **N. Varghese:** None. **A. Sorokin:** None. **C. Bleck:** None. **J. Rodante:** None. **H. Kruth:** None. **A. Joshi:** None. **A. Dey:** None. **M. Playford:** None. **N. Mehta:** Research Grant; Significant; AbbVie, Janssen, Celgene, Novartis.

213
Human Genetic Variations in Neuroimmune Guidance Cues and their Role in Premature Atherosclerosis
Caroline S Bruikman, Academic Medical Ctr, Amsterdam, Netherlands; Dianne Vreeken, Leiden Univ Medical Ctr, Leiden, Netherlands; Julian C van Capelleveen, Academic Medical Ctr, Amsterdam, Netherlands; Huayu Zhang, Leiden Univ Medical Ctr, Leiden, Netherlands; Sara J Pinto-Sietsma, Geesje M Dallinga-Thie, Geesje M Dallinga-Thie, G. Kees Hovingh, Academic Medical Ctr, Amsterdam, Netherlands; Janine M van Gils, Leiden Univ Medical Ctr, Leiden, Netherlands

Introduction: Neuroimmune guidance cues (NGCs), a family of proteins originally known for controlling neuronal migration, have been shown to be involved in atherosclerosis in mice models by regulating adhesion of monocytes to the vascular endothelium. The NGC family consists of multiple receptors and ligands enabling an interplay between inflammatory cells and the vasculature endothelium. We set out to investigate the role of NGCs in atherosclerosis in humans.
Methods and results: We sequenced a total of 77 NGC genes in a unique cohort of 89 patients with premature atherosclerotic (PAS), in whom no clear CVD risk factor was present. A total of 178 rare variants were identified and we classified the pathogenicity of these rare (MAF<0.05) variants by high Combined Annotation Dependent Depletion (CADD) scores. Based on literature and cosegregating pedigrees of the 88 possible deleterious variants we chose two variants in Netrin1 (NTN1) and EphrinB2 (EFNB2) to explore and validate their causality in human atherosclerosis. The expression of both these genes is regulated by flow and inflammatory stimuli. Under atherosclerotic conditions endothelial cells upregulate EFNB2 while NTN1 is downregulated. In addition, using immunohistochemical staining on human aorta's, we found that NTN1, which is normally expressed on human endothelial cells, is less abundant in increasing stages of

atherosclerosis. For EFNB2, a cell surface transmembrane ligand for Eph receptors, we performed several functional assays using HUVEC cells that overexpress EFNB2 , showing that EFNB2 is affecting endothelial cell barrier function, as well as proliferation.
Conclusion: In patients with PAS rare missense variants in NGC genes were identified. Further functional- and expression assays showed an effect of NTN1 and EFNB2 on different aspects of the human atherosclerotic process. The results obtained from these studies substantiate the role of NGCs in human atherosclerotic disease and may further identify NGCs as novel potential therapeutic targets in our strive against cardiovascular disease.
C.S. Bruikman: None. **D. Vreeken:** None. **J.C. van Capelleveen:** None. **H. Zhang:** None. **S.J. Pinto-Sietsma:** None. **G.M. Dallinga-Thie:** None. **G.M. Dallinga-Thie:** None. **G.K. Hovingh:** None. **J.M. van Gils:** None.

214
Functional Analysis of the Low Density Lipoprotein Receptor Using Saturation Mutagenesis Strategies
Alexandra C Chadwick, Niklaus H Evitt, Kiran Musunuru, Univ Pennsylvania, Philadelphia, PA

Low density lipoprotein receptor (LDLR) genetic mutations are well-documented to cause familial hypercholesterolemia (FH) in patients. These mutations affect a broad range of LDLR functions, including LDL binding and receptor trafficking, and five classes exist to describe their functional consequences. Although over 1,000 LDLR mutants have been identified, an additional 15,000+ LDLR mutants are possible by only a single amino acid substitution in the ~160kDa protein. Since cataloging mutants would undoubtedly be of therapeutic benefit, we are systematically classifying the effect of every single amino acid substitution on LDLR function using saturation mutagenesis. LDLR was knocked out of HEK293 cells using standard CRISPR/Cas9 practices and decreased protein levels were assessed by flow cytometry and immunoblot staining. In order to introduce each individual mutation into the genomic DNA sequence for high-throughput, functional analyses, the PiggyBac transposon system was used to insert a serine-integrase attachment site into a single allele in the *LDLR* locus, whereby efficient knock in of LDLR mutants from a pooled cDNA library can be achieved. Mutant LDLR libraries containing ~800 single amino acid substitutions were generated using commercial oligo pools and Gibson cloning. Of particular therapeutic interest is the identification of mutations that alter LDL's ability to bind to the receptor. In our first set of experiments, fluorescently labeled LDL was incubated with cells containing pooled single amino acid substitutions in LDLR, and cells were sorted using flow cytometry. Sorted groups ranging from fluorescent negative to positive were sent for next generation sequencing in order to identify severe vs benign mutants on receptor function. As some of these mutations may decrease LDL binding activity due to inhibited receptor trafficking, we also stained pooled cells with an antibody directed against LDLR, sorted by flow cytometry and analyzed using next generation sequencing with similar strategies. Ultimately, cataloging LDLR genetic mutations should be of great therapeutic benefit, as it will allow better diagnosis and treatment of patients suffering from FH.
A.C. Chadwick: None. **N.H. Evitt:** None. **K. Musunuru:** None.

215
Glycosphingolipids Contribute to Pro-atherogenic Pathways in the Pathogenesis of Hyperglycemia-induced Atherosclerosis
Vi Dang, McMaster Univ, Hamilton, ON, Canada

Three out of every four people with diabetes will die of cardiovascular disease. However, the molecular mechanisms by which diabetes promotes atherosclerosis are not clear. In this study, comprehensive metabolomic techniques were used to investigate the molecular mechanisms by which hyperglycemia promotes accelerated atherogenesis in three distinct disease mouse models. Normoglycemic apolipoprotein E-deficient mice served as the atherosclerotic control. Hyperglycemia was induced by multiple low-dose streptozotocin injections or by introducing a point mutation in one copy of the insulin-2 gene. Glucosamine-supplemented mice, which experience accelerated atherosclerosis to a similar extent as the hyperglycemia-induced models, without alterations in the levels of glucose or insulin, were also included in the analysis. Mice with accelerated atherosclerosis showed distinct metabolomic profiles compared to the controls. We detected 6369 metabolite features in the plasma of each mouse. Second-order analysis of pair comparisons between each disease model and the control resulted in 62 commonly altered features ($p<0.05$). Identification of shared metabolites revealed alterations in glycerophospholipid and sphingolipid metabolisms, and pro-atherogenic processes including inflammation and oxidative stress. Post-multivariate and pathway analyses indicated glycosphingolipid metabolism is the most significantly altered pathway. Glycosphingolipid metabolites induced oxidative stress and inflammation in cultured human vascular cells including macrophages, endothelial and smooth muscle cells. Treatment with a known antioxidant, α-tocopherol, reduced oxidative stress and inflammation induced by glycosphingolipids. Our findings suggest that the glycosphingolipid pathway contributes to pro-atherogenic pathways in the pathogenesis of hyperglycemia-induced atherosclerosis, making it a potential therapeutic target to block or slow atherogenesis in diabetic patients.
V. Dang: None.

216
Modeling Statin Hepatotoxicity with Acute Liver Specific Deletion of HmgCoA Reductase
Marco De Giorgi, Kelsey E. Jarrett, Jason C. Burton, Alexandria M. Doerfler, Ayrea Hurley, Rachel H. Hsu, William R. Lagor, Baylor Coll of Med, Houston, TX

Hmg-CoA Reductase (Hmgcr) catalyzes the conversion of Hmg-CoA to mevalonate, which is the rate-limiting step in the cholesterol biosynthetic pathway. Hmgcr is the target of statins, which are the front line therapy for hypercholesterolemia. Statin-responsiveness varies greatly between individuals, and liver toxicity and transaminase elevations are observed in 1-3% of patients. In addition to cholesterol, *Hmgcr* activity is also required for the synthesis of heme A, dolichol, ubiquinone (Coenzyme Q), farnesylated and geranylgeranylated proteins, isopentenyl tRNA, and vitamin K2. Surprisingly, very little is known about the effects of statins on these non-sterol isoprenoids *in vivo*, which may be essential for hepatocyte viability and function. The goal of this project is to investigate the effects of *Hmgcr* inhibition in the liver, in order to better understand the physiological regulation and function of the mevalonate pathway. We have developed a new inducible genetic model of *Hmgcr* deletion, which enables us acutely inhibit the mevalonate pathway in the liver, thus avoiding well-known compensatory responses to statins in rodents. *Hmgcr* floxed mice were injected with liver-specific AAV-Cre recombinase (AAV-Cre) and followed for 1, 2, 4 and 8 weeks. We observed massive apoptosis followed by a burst of hepatocyte proliferation at 2 weeks post-injection. We also observed compensatory upregulation of genes in the mevalonate pathway, likely a response to sterol depletion. Hepatocytes from AAV-Cre mice had expanded and swollen endoplasmic reticulum (ER), and upregulation of Chop and Bax, suggesting ER stress-induced apoptosis. Genetic analysis of AAV-Cre treated livers showed progressive loss of the null allele over time, indicating a selective advantage for hepatocytes that escaped complete *Hmgcr* deletion. The injection of a five-fold higher dose of AAV-Cre was acutely lethal in less than 2 weeks, confirming that liver Hmgcr activity is essential for survival. This new model will be used to identify the essential

mevalonate-derived products in the liver, and the molecular pathways underlying statin hepatotoxicity and responsiveness.
M. De Giorgi: None. **K.E. Jarrett:** None. **J.C. Burton:** None. **A.M. Doerfler:** None. **A. Hurley:** None. **R.H. Hsu:** None. **W.R. Lagor:** None.

217
Coronary Artery Disease Locus 1p32.2 Harbors a Flow-Sensitive Endothelial Enhancer that Regulates PLPP3
Yun Fang, Matthew Krause, Univ of Chicago, Chicago, IL; Mete Civelek, Univ of Virginia, Charlottesville, VA; Casey Romanoski, Univ of Arizona, Tulsa, AZ

This research has received full or partial funding support from the American Heart Association.

Genome-wide association studies (GWAS) have identified chromosome 1p32.2 as one of the loci most strongly associated with coronary artery disease (CAD) susceptibility; however, the causal mechanism related to this CAD locus remains poorly understood. A unique feature of atherosclerotic vascular disease such as CAD is that atherosclerosis develops preferentially at arterial sites of curvature, branching, and bifurcation where endothelial cells are activated by disturbed blood flow. Recent investigations by us and others strongly implicate PhosphoLipid PhosPhatase 3 (PLPP3, also known as PhosPhatidic-Acid-Phosphatase-type-2B/ PPAP2B or Lipid Phosphate Phosphohydrolase/LPP3) as the causal gene at this locus. PLPP3 encodes an enzyme that suppresses endothelial inflammation and promotes monolayer integrity by hydrolyzing the bioactive lipid lysophosphatidic acid (LPA). Our studies demonstrated that PLPP3 is significantly reduced in vascular endothelium exposed to disturbed flow in vitro and in vivo, as the result of increased miR-92a and reduced KLF2, when compared to cells subjected to unidirectional blood flow. In addition, CAD risk allele at rs17114036 located in 1p32.2 locus is associated with reduced PLPP3 expression in an endothelium-specific manner, shown by expression quantitative trait locus (eQTL). Employing Transposase-Accessible Chromatin using Sequencing (ATAC-Seq), ChIP-Seq, CRISPR/Cas9-based genome editing, luciferase reporters, and allelic imbalance assays, we report here that CAD SNP rs17114036 is located in an endothelial enhancer that is dynamically activated by athero-protective unidirectional flow and deletion of this enhancer causatively reduces PLPP3 expression in vascular endothelium. In addition, CAD risk allele at rs17114036 is associated with reduced activity of this enhancer and its response to unidirectional flow. These results described a new molecular mechanism by which human genetic variance and mechano-transduction converge on critical vascular functions related to atherosclerosis. Moreover, we have engineered innovative polymeric nano-carriers that preferentially target inflamed endothelium and deliver therapeutic nucleotides that intervene in miR92a-PLPP3 signaling in animal models of atherosclerosis.
Y. Fang: None. **M. Krause:** None. **M. Civelek:** None. **C. Romanoski:** None.

219
Role of Transcription Co-Factor Friend of GATA 2 (FOG2) in a Hypertensive-Diabetic Mouse Model of Coronary Microvascular Disease
Marie A Guerraty, Hannah J. Szapary, Andrea Berrido, Zoltan P. Arany, Daniel J. Rader, Univ of Pennsylvania, Philadelphia, PA

Coronary microvascular disease (CMVD), or disease of the coronary pre-arterioles, arterioles, and capillaries, has become an increasingly well-recognized cardiac pathology. Characterized by microvascular remodeling, wall thickening, lumen obliteration, endothelial dysfunction, capillary rarefaction, and perivascular immune cell infiltration, CMVD can lead to inadequate myocardial perfusion, angina, heart failure, or myocardial infarction. Despite significant clinical ramifications, our understanding of the pathophysiology of CMVD remains nascent. Friend of GATA 2 (FOG2, also ZFPM2) is a crucial transcriptional co-factor in coronary development; and cardiomyocyte expression of FOG2 is required for the maintenance of the coronary microvasculature in adult mice. We hypothesize that FOG2 is activated in CMVD, and that Hypoxia-Inducible Factor 1a (HIF1a) may play a role in FOG2 activation. To test this hypothesis, we developed a hypertensive-diabetic (HTN/DM) mouse model of CMVD. Briefly, adult female C57BL/6 mice were treated with Angiotensin II (1mg/kg/day osmotic pump for 8 weeks) and low-dose streptozotocin (35 mg/kg IP for 4 days) (n=5) or saline (n=4). HTN/DM mice had increased systolic blood pressure (142±2 mmHg v 109±1 mmHg, p<1e4), mild fasting hyperglycemia (182±9 mg/dl v 149±10 mg/dl, p=0.04), and decreased glucose tolerance (p<3e4). These resulted in decreased cardiac capillary density (149±10 v 164±4 phf, p=0.008) and evidence of microvascular pathology including vessel wall thickening and immune cell infiltration. HTN/DM mice had mild LV hypertrophy, preserved EF, and diminished coronary hyperemic velocities by echocardiography. Cardiac FOG2 protein was increased in HTN/DM mice (p<0.05). To examine the relationship between HIF and FOG2 *in vitro*, AC16 cardiomyocytes were treated with HIF-hydroxylase inhibitor DMOG (0.1mM, 1mM) for 16 hours. There was a dose-dependent increase in FOG2 expression and nuclear translocation. In summary, we developed a mouse model of CMVD with mild hypertensive-diabetic insults which are relevant to human disease. We found that FOG2 protein is increased in CMVD suggesting that FOG2 may be relevant to adult CMVD pathophysiology *in vivo.* We additionally provide *in vitro* evidence that FOG2 is induced in HIF-activating conditions.
M.A. Guerraty: None. **H.J. Szapary:** None. **A. Berrido:** None. **Z.P. Arany:** None. **D.J. Rader:** None.

220
Targeting Cholesterol Efflux, Autophagy, and Inflammation to Prevent Atherosclerosis
Amanda Iacano, Harvey Lewis, Heather Andro, Jennie Hazen, Greg Brubaker, Bani Raheem, Brian Ritchey, Shuhui Lorkowski, Jonathan D Smith, **Kailash Gulshan**, Cleveland Clinic Fndn, Cleveland, OH
Introduction: The NLRP3 inflammasome and Toll-like receptor signaling is activated in advanced human atherosclerotic plaques, while autophagy and reverse cholesterol transport (RCT) become dysfunctional. Simultaneous targeting of these pathways can prevent CVD.

Objectives: To determine if Miltefosine can prevent atherosclerosis by inducing RCT/autophagy and dampening inflammation.
Methods and results: Here, we report that Miltefosine, an anti-leishmanial drug, acts to decrease atherosclerosis in vivo, and that it induced RCT/autophagy while dampening TLR signaling and NLRP3 inflammasome activity. Miltefosine treatment of macrophages disrupted lipid rafts; ~26 % decrease vs. control via alexa647-CTB binding by flow-cytometry, (p<0.005, n=4), and increased ABCA1 mediated cholesterol efflux to apoA1; ~20% increase in treated vs. control (p<0.001, n=3). Macrophages treated with Miltefosine vs. control exhibited a marked increase in autophagosomes, indicated by p62 and LC3 staining puncta. Autophagic degradative flux was not inhibited by Miltefosine. Lipid droplet degradation was induced by Miltefosine leading to ~ 50% decrease in the CE:FC (cholesterol ester:free cholesterol) ratio (p<0.005, n=3). Miltefosine treated vs. control macrophages showed ~75% reduction in pro-IL1β mRNA levels upon LPS induction (p<0.05, n=3). Miltefosine potently inhibited NLRP3 inflammasome assembly upon LPS/ATP treatment leading to ~70% reduction in ASC1 speck positive cells. Gasdermin D mediated release of mature IL1β was reduced by ~80% in Miltefosine treated vs.

controls (p<0.01, n=3), while only ~20% reduction was observed by cyclodextrin treatment, indicating that inflammasome inhibition by Miltefosine was not only due to cholesterol depletion. In vivo pilot studies showed that Miltefosine added to a chow diet increased RCT to plasma (~70% increase in 24h vs. control), and feces (~60% increase in 24h vs. control, p< 0.005, n=5) in C57BL6 mice. Atherosclerotic lesions were =50% smaller in apoE$^{-/-}$ mice fed chow diet + Miltefosine vs. controls (p<0.02, n=5). ***Conclusion:*** Miltefosine induced RCT and autophagy while dampening TLR signaling and NLRP3 inflammasome activity, and it decreased atherosclerosis lesion burden in mice.

A. Iacano: None. **H. Lewis:** None. **H. Andro:** None. **J. Hazen:** None. **G. Brubaker:** None. **B. Raheem:** None. **B. Ritchey:** None. **S. Lorkowski:** None. **J.D. Smith:** None. **K. Gulshan:** None.

This research has received full or partial funding support from the American Heart Association.

221

Crif1 deficiency-induced Mitochondrial Dysfunction Stimulates Endothelial Inflammation

Cuk Seong Kim, Su-jung Choi, Seonhee Kim, Chungnam Natl Univ, Daejeon, Korea, Republic of; Hee Jung Song, Chungnam Natl Univ Hosp, Daejeon, Korea, Republic of

CR6 interacting factor 1 (CRIF1) deficiency impairs mitochondrial oxidative phosphorylation complexes, contributing to increased mitochondrial and cellular reactive oxygen species (ROS) production. CRIF1 downregulation has also been revealed to decrease sirtuin 1 (SIRT1) expression and impair vascular function. Inhibition of SIRT1 disturbs oxidative energy metabolism and stimulates nuclear factor kappa-light-chain-enhancer of activated B cells (NF-B)-induced inflammation. Therefore, we hypothesized that both CRIF1 deficiency-induced mitochondrial ROS production and SIRT1 reduction play stimulatory roles in vascular inflammation. Plasma levels and mRNA expression of proinflammatory cytokines (tumor necrosis factor (TNF)-α, interleukin (IL)-1β, and IL-6) were markedly elevated in endothelium-specific CRIF1-knockout mice and CRIF1-silenced endothelial cells, respectively. Moreover, CRIF1 deficiency-induced vascular adhesion molecule-1 (VCAM-1) expression was consistently attenuated by the antioxidant N-acetyl-cysteine and NF-κB inhibitor (BAY11). We next showed that siRNA-mediated CRIF1 downregulation markedly activated NF-κB. SIRT1 overexpression not only rescued CRIF1 deficiency-induced NF-κB activation but also decreased inflammatory cytokines (TNF-α, IL-1β, and IL-6) and VCAM-1 expression levels in endothelial cells. These results strongly suggest that CRIF1 deficiency promotes endothelial cell inflammation by increasing VCAM-1 expression, elevating inflammatory cytokines levels, and activating the transcription factor NF-κB, all of which were inhibited by SIRT1 overexpression.

C. Kim: None. **S. Choi:** None. **S. Kim:** None. **H. Song:** None.

222

Translocator Protein as Novel Marker for Early Atherosclerosis

Chantal M Kopecky, William J Ryder, UNSW Sydney, SoMS, Sydney, Australia; Jeremy Szajer, Concord Hosp, Radiology Dept, Sydney, Australia; Arvind Parmar, ANSTO Life Sciences, Sydney, Australia; Elvis Pandzic, UNSW Sydney, Biomedical Imaging Facility, Sydney, Australia; Kerry A Rye, Blake J Cochran, UNSW Sydney, SoMS, Sydney, Australia

Atherosclerosis is characterized by lipid deposition, monocyte infiltration and foam cell formation in the artery wall. Translocator protein (TSPO) is abundantly expressed in lipid rich tissues. Recently, TSPO has been identified as a potential diagnostic tool in cardiovascular disease. Here, we aimed to determine if (i) the TSPO radioligand, ^{18}F-PBR111, can identify fatty streak formation that precedes atherosclerotic lesion development and (ii) TSPO expression can be used to identify distinct macrophage populations during different stages of lesion progression. Atherosclerosis-prone apoE$^{-/-}$ mice were maintained on a high-fat diet for 3, 9 and 12 weeks. C57BL6 mice maintained on chow diet served as controls. Mice were anesthetized, injected with ^{18}F-PBR111 (8-18 MBq, 0.1 mL, 0.2 nM) via the lateral tail vein and imaged using an Inveon PET/CT Scanner over 60 min. After euthanasia, aortas were isolated, fixed and optically cleared. Cleared aortas were immunostained with DAPI, fluorescently labelled anti-TSPO antibody and the macrophage markers F4/80 and CD11b. Tissues were visualized on a Lightsheet Z.1 microscope and analysed with 3D imaging software. A 3-fold increase in the uptake of ^{18}F-PBR111 was observed by PET/CT in the aortas of atherosclerotic mice relative to controls. Increased ^{18}F-PBR111 uptake was observed in the aortic arch and thoracic aorta, corresponding with sites of atherosclerotic lesion development. Light sheet microscopy revealed that TSPO expression increased correspondingly to atherosclerosis progression. The expression pattern of macrophage populations in early lesions differed from that in mature plaques. While F4/80-positive macrophages were evident uniformly throughout the aortas, CD11b-positive macrophages were increased in atherosclerotic areas. In conclusion, imaging TSPO expression is a new approach for studying atherosclerotic lesion progression and is associated with specific inflammatory cell infiltration. The TSPO ligand ^{18}F-PBR111 is a potential clinical diagnostic tool for the detection and quantification of atherosclerotic lesion progression in humans.

C.M. Kopecky: None. **W.J. Ryder:** None. **J. Szajer:** None. **A. Parmar:** None. **E. Pandzic:** None. **K.A. Rye:** None. **B.J. Cochran:** None.

223

Monocytes/macrophages Are Sensitized to Secondary Oxidative Insult by Cardiovascular Toxic Drugs via the P90rsk-erk5 S496 Phosphorylation Pathway, Aggrandizing Atherosclerotic Plaque Formation

Sivareddy Kotla, MD Anderson Cancer Ctr, Houston, TX; **Nhat-Tu Le**, Houston Methodist, Houston, TX; Meera V. Singh, Univ of Rochester, Rochester, NY; Kyung Ae Ko, Kyung-Sun Heo, Yuka Fujii, Hang Thi Vu, Elena McBeath, Tamlyn Thomas, Yin Wang, Young Jin Gi, MD Anderson Cancer Ctr, Houston, TX; Yunting Tao, Houston Methodist, Houston, TX; Jan Medina, MD Anderson Cancer Ctr, Houston, TX; Nicole E. Stirpe, Wang Lu, Alicia Tyrell, Kathleen J. Gates, Xing Qui, Univ of Rochester, Rochester, NY; Keigi Fujiwara, MD Anderson Cancer Ctr, Houston, TX; Sanjay B. Maggirwar, Giovanni Schifitto, Univ of Rochester, Rochester, NY; Jun-ichi Abe, MD Anderson Cancer Ctr, Houston, TX

Increased cardiovascular (CV) events in HIV patients and cancer survivors and the fact that combination antiretroviral therapy (cART) and chemotherapy induce similar unwanted CV effects are becoming evident, but the reason for this is unclear. In this study, we examined the role of p90RSK in the CV toxicity of cART and anti-cancer drugs. The level of p90RSK activation by H2O2 was higher in peripheral monocytes from cART-treated patients than in those from untreated patients. Multiple linear regression analysis involving HIV+/-, Reynolds CV risk score, and basal p90RSK activation revealed HIV+/- and basal p90RSK activation to be strong determinants for plaque formation when adjusted for other independent variables. In murine macrophages most of the cART and several chemotherapy agents activated p90RSK and reduced antioxidant molecule expression and telomere (TL) lengths. p90RSK-mediated ERK5 S496 phosphorylation inhibited transcriptional activity of ERK5 and NRF2, decreasing efferocytosis, antioxidant production and TL lengths. NRF2 activator normalized

cART-induced sensitization of p90RSK to H2O2. Lastly, we generated myeloid cells-specific wild type (WT) and dominant negative (DN) p90RSK transgenic mice, and ERK5 S496A knock-in mice, crossed with *Ldlr-/-* mice or treated with a single injection of adeno-associated virus vector (AAV) encoding a gain-of-function mutant of PCSK9 and fed a high fat diet. Our animal studies showed the crucial role of p90RSK-mediated ERK5 S496 phosphorylation in suppressing effecrocytosis and antioxidant production, and up-regulating senescence and inflammation-related molecules expression, leading to atherogenesis. Our results taken together show that p90RSK is activated by anti-HIV and anti-cancer drugs, and this activation sensitizes the monocyte/macrophages to the secondary oxidative insult by reducing NRF2 transcriptional activity and TL length. The p90RSK activation also reduces macrophage efferocytosis and antioxidant capacity, and increases inflammation and senescence via up-regulating ERK5 S496 phosphorylation, thereby accelerating atherosclerosis. Monocyte/macrophage p90RSK-ERK5 S496 phosphorylation could be a good target to prevent drugs-induced CV diseases.

S. Kotla: None. **N. Le:** None. **M. Singh:** None. **K. Ko:** None. **K. Heo:** None. **Y. Fujii:** None. **H.T. Vu:** None. **E. McBeath:** None. **T. Thomas:** None. **Y. Wang:** None. **Y. Gi:** None. **Y. Tao:** None. **J. Medina:** None. **N. Stirpe:** None. **W. Lu:** None. **A. Tyrell:** None. **K. Gates:** None. **X. Qui:** None. **K. Fujiwara:** None. **S. Maggirwar:** None. **G. Schifitto:** None. **J. Abe:** None.

This research has received full or partial funding support from the American Heart Association.

224

Notch1 Activation in Endothelial Cells Promotes Progression of Atherosclerosis

Zhao-Jun Liu, Yan Li, Leiming Zhang, Manuela M Regueiro, Yuntao Wei, Omaida C Velazquez, Univ of Miami Miller, Miami, FL

Introduction. Notch signaling plays pivotal roles in vascular development and cardiovascular disease. We previous showed that the Notch pathway is activated in luminal endothelial cells (EC) at atherosclerotic plaques, implicating a potential involvement of Notch signaling in atherosclerosis. We further demonstrated that loss of Notch1 signaling in EC suppresses progression of atherosclerosis. Here, we test the effect of activation of the Notch1 pathway in EC on atherosclerosis using mouse model with inducible EC-specific Notch1 activation on an $ApoE^{-/-}$ background.
Methods. We created a Tamoxifen-inducible EC-specific N1IC (Notch1 intracellular domain, an active Notch1 mutant) expression mouse line on atherosclerosis-prone $ApoE^{-/-}$ background: $ROSA^{LSL\text{-}N1IC}$/*VE-cadherin-CreER*^{T2}/$ApoE^{-/-}$. Mice were fed with high-fat-diet (HFD) along with or without Tamoxifen treatment (i.p. 2 mg/day for 5 consecutive days) starting from 4-wk old and terminated on 16-wk old. Aortas were harvested to study the effects of Notch1 activation in EC on the progression of aortic atherosclerosis. Expression of N1IC in EC was validated by immunostaining. Aortic plaque burden was evaluated by quantification of proportion of total aorta containing atherosclerosis detected by Oil-Red-O and hematoxylin-eosin staining using computer-aided image analysis. Blood was tested to measure lipid profile.
Results. Enforced Notch1 activation in EC is induced in Tamoxifen-treated mice. EC gain-of-function Notch1 signaling significantly increased aortic plaque burden [n=10 in both (Tamoxifen -) and (Tamoxifen +) group, $P<0.05$]. The serum levels of total cholesterol, HDL, LDL, triglycerides and glucose were comparable between Tamoxifen-treated and -untreated mice.
Conclusions. Activation of the Notch1 signaling pathway in EC facilitates atherosclerotic plaque formation. The increase in atherosclerosis was not due to changes in the serum levels of lipid, glucose, triglycerides, HDL, LDL and total cholesterol. Our findings demonstrate that activation of the Notch1 signaling pathway in EC promotes progression of atherosclerosis. It highlights Notch1 signaling as an emerging therapeutic target for the treatment of atherosclerosis.

Z. Liu: None. **Y. Li:** None. **L. Zhang:** None. **M.M. Regueiro:** None. **Y. Wei:** None. **O.C. Velazquez:** None.

225

Electronic Cigarettes Induced Exacerbation of Atherosclerosis: Contribution of MicroRNA-21

Marina V Malovichko, Nalinie S Wickramasinghe, Anuradha Kalani, Srinivas D Sithu, Univ of Louisville, Louisville, KY; Terry Gordon, Lung-Chi Chen, New York Univ, New York, NY; Aruni Bhatnagar, Tim E O'Toole, Daniel J Conklin, Sanjay Srivastava, Univ of Louisville, Louisville, KY

Smoking is the foremost cause of preventable disease and pre-mature deaths. Although the rates of smoking have declined in the recent past, advent of electronic cigarettes (e-cig) pose new challenges. E-cig are extremely popular in youth and usage of e-cig has increased by 9-fold in the youth between 2011 and 2015. E-cig are battery-operated devices used for the delivery of aerosolized nicotine. Unlike conventional cigarettes, e-cig have lower levels of carcinogens. However, aerosolization of e-liquids generates reactive chemicals such as acrolein, which has adverse effects on cardiovascular health. To examine the effect of e-cig on atherosclerosis we exposed 8-week old apoE-KO mice (maintained on Western diet) to filtered air or e-cig (36 mg/ml nicotine aerosolized in glycerol/propylene glycol, 50/50, v/v) for 12 weeks (3 h/day; 7 days a week). Our data show that exposure to e-cig increased the aortic lesion area by 24% ($P<0.05$), without affecting plasma cholesterol (e-cig 1088±61 vs air 1102±61 mg/dL) and triglyceride (e-cig 95±9 vs air 77±5 mg/dL). Exposure to e-cig also increased the expression of micro RNA-21 (miR-21) in the aorta by 26% ($P<0.05$). In situ hybridization assay showed that miR-21 co-localizes with macrophages in atherosclerotic plaques. *In vitro,* e-cig constituents acrolein and nicotine induced the expression of miR-21 by 1.8-2.0 fold, in bone marrow derived macrophages. Similarly, 4,hydroxynonenal (HNE) generated by acrolein and nicotine induced reactive oxygen species (ROS) formation by 1.3-fold, and increased the expression of miR-21 in macrophages by 2-fold. Exposure to e-cig also activated matrix metalloproteinases (MMPs) in atherosclerotic plaques. Acrolein activated MMPs *ex vivo* in atherosclerotic plaques, and increased the secretion of MMP-9 from macrophages. Acrolein-induced ROS formation and MMP-9 secretion was prevented by free radical scavengers. Moreover, we also observed that HNE-induced macrophage apoptosis was significantly increased by miR-21 deficiency. This process was mediated by the activation of both, intrinsic and extrinsic pathways of apoptosis. Collectively, these data suggest miR-21 prevents e-cig-induced atherogenesis by inhibiting inflammatory and apoptotic pathways in macrophages.

M.V. Malovichko: None. **N.S. Wickramasinghe:** None. **A. Kalani:** None. **S.D. Sithu:** None. **T. Gordon:** None. **L. Chen:** None. **A. Bhatnagar:** None. **T.E. O'Toole:** None. **D.J. Conklin:** None. **S. Srivastava:** None.

226

Proprotein Convertase Subtisilin Kexin Type 9 Knockout Mice are Protected from Valvular Calcification

Paolo Poggio, Paola Songia, Mattia Chiesa, Silvia Barbieri, Laura Cavallotti, Vincenza Valerio, Ctr Cardiologico Monzino IRCCS, Milan, Italy; Nicola Ferri, Univ degli Studi di Padova, Padua, Italy; Ilaria Zanotti, Univ degli Studi di Parma, Parma, Italy; Marina Camera, Univ degli Studi di Milano, Milan, Italy

Background: Aortic valve calcification (AVC) is one of the most common form of heart valve disease and affects 3% of the population. No pharmacological treatments have been identified yet; however, proprotein convertase subtisilin kexin type 9 (PCSK9) inhibitors have been proposed to reduce AVC progression. We aimed to evaluate the role of PCSK9

in the aortic valve calcification. **Methods:** We use PCSK9$^{-/-}$ and PCSK9$^{+/+}$ (WT) mice littermates (n=3-4 per group, 12 month-old female, normal diet). When aortic valves were excised, total calcium content was measured and valve interstitial cells (VIC) were isolated. Calcification assays were performed on aortic VICs, left untreated or treated with β-glycerophosphate and ascorbic acid (βGAA) for seven days on plastic dishes. MinION RNA-Seq was used to evaluate the differential expression patterns in the two groups. **Results:** Total calcium content of aortic valve from PCSK9$^{-/-}$ mice was significantly lower than WT (1.5±0.7 *vs* 10.1±0.5 ng of calcium/µg of total protein, respectively; p=0.0002). Calcium quantification revealed that PCSK9$^{-/-}$ VICs (untreated) were able to calcify at a less extent than WT (4.4±0.6 *vs* 8.0±0.5 ng/µg, respectively; p=0.0001). The βGAA treatment induced calcification in both cell types; however, a significant (p=0.01) lower calcification rate was noted in PCSK9$^{-/-}$ VICs (41.9±3.6 ng/µg) compared to WT (55.9±3.5 ng/µg). RNA-Seq of VICs from WT and PCSK9$^{-/-}$ mice revealed that 363 genes were differentially expressed more than two-fold (adjusted p value<0.05). Functional analysis showed that in PCSK9$^{-/-}$ VICs upregulated genes coordinate p38 cascade and cytoskeleton modifications, while downregulated ones control apoptotic signalling pathway, cell proliferation and adhesion, and oxidative stress. **Conclusion:** These preliminary results show for the first time that PCSK9 could play a direct role in AVC and thus, therapies against PCSK9 may be beneficial to patients affected by calcific aortic valve disease.

P. Poggio: None. **P. Songia:** None. **M. Chiesa:** None. **S. Barbieri:** None. **L. Cavallotti:** None. **V. Valerio:** None. **N. Ferri:** None. **I. Zanotti:** None. **M. Camera:** None.

227

Investigating the Role of Fatty Acid Binding Protein-4 in ApoE-/- Mice Aorta During Prolonged Percutaneous Retro-orbital Injections

Priyanka Prathipati, **Brian Walton**, UTHSC-Houston, Houston, TX; Cristian Rodriquez-Aguayo, Anil Sood, UT MDACC, Houston, TX; Gabriel Berestein-Lopez, UTMDACC, Houston, TX

Background: Atherosclerosis is a chronic inflammatory disease which is one of the major causes of stroke.Fatty acid binding protein-4 (FABP4) is a lipid chaperon that plays an important role in atherogenesis. It is mostly expressed in macrophages and adipocytes and acts as a mediator of inflammation. Atherosclerosis is a chronic inflammatory disease which is one of the major causes of stroke. We hypothesize that silencing FABP4 could be a novel therapeutic treatment for atherosclerosis, hence a liposomal small interfering RNA (siRNA) delivery system to silence FABP4 was developed. **Materials and methods:** Under an appproved IACUC protocol, male *ApoE*$^{-/-}$ mice (N=8) were fed high fat diet from 6 weeks of age until 12-16 weeks. At 11 weeks of age, the mice were injected with 0.1ml (500µg/ml) of FABP4/control siRNA liposomes tagged with fluorescent Qdot (QD) 625. The injections were administered through percutaneous retro-orbital route twice a week for four consecutive weeks. Starting in the 12th week, two mice from each group were sacrificed every week. Aortas and serum were collected at the time of sacrifice. Aortic arch was dissected, stored in formalin and processed for paraffin sections. The rest of aorta was flash frozen for protein analysis. Protein levels of FABP4 in aortas will be analyzed by western blot and immunohistochemistry to investigate the silencing effect of FABP4 siRNA liposomes. **Results:** ApoE-/- mice aortic tissue sections showed the successful uptake of FABP4 siRNA liposomes. **Conclusion:** Percutaneous retro-orbital injections of FABP4 siRNA liposomes for four consecutive weeks might help to silence the FABP4 to greater extent in atherosclerotic model of mice.

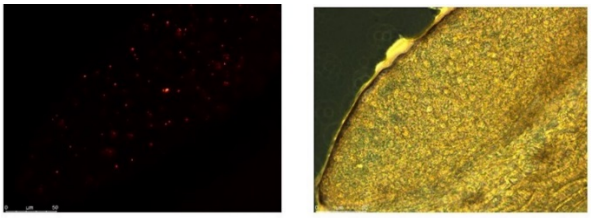

FABP4 liposomal accumulation in APOE-/- mice aorta following four weeks of siRNA treatment.
FABP4 siRNA liposomes tagged with QD reached aorta when injected through percutaneous retro-orbital route.

P. Prathipati: None. **B. Walton:** None. **C. Rodriquez-Aguayo:** None. **A. Sood:** None. **G. Berestein-Lopez:** None.

228

Multi-omics Mapping Generates a Molecular Atlas of the Aortic Valve and Reveals Networks Driving Disease

Florian Schlotter, Arda Halu, Shinji Goto, Mark C Blaser, Ctr for Interdisciplinary Cardiovascular Sciences, Div of Cardiovascular Med, Brigham and Women's Hosp, Harvard Medical Sch, Boston, MA; Simon C Body, Dept of Anesthesiology, Brigham and Women's Hosp, Boston, MA; Lang H Lee, Hideyuki Higashi, Ctr for Interdisciplinary Cardiovascular Sciences, Div of Cardiovascular Med, Brigham and Women's Hosp, Harvard Medical Sch, Boston, MA; Daniel M DeLaughter, Dept of Genetics, Harvard Medical Sch, Boston, MA; Joshua D Hutcheson, Dept of Biomedical Engineering, Florida Intl Univ, Miami, FL; Payal Vyas, Tan H Pham, Maximillian A Rogers, Ctr for Interdisciplinary Cardiovascular Sciences, Div of Cardiovascular Med, Brigham and Women's Hosp, Harvard Medical Sch, Boston, MA; Amitabh Sharma, Channing Div of Network Med, Brigham and Women's Hosp, Harvard Medical Sch, Boston, MA; Christine E Seidman, Joseph Loscalzo, Dept of Med, Brigham and Women's Hosp, Boston, MA; Jonathan G Seidman, Dept of Genetics, Harvard Medical Sch, Boston, MA; Masanori Aikawa, Sasha A Singh, Elena Aikawa, Ctr for Interdisciplinary Cardiovascular Sciences, Div of Cardiovascular Med, Brigham and Women's Hosp, Harvard Medical Sch, Boston, MA

Background: No pharmacological therapy exists for calcific aortic valve disease (CAVD), which confers a dismal prognosis without valve replacement. The search for therapeutics and early diagnostics is challenging since CAVD presents in multiple pathological stages. **Methods:** A total of 25 human stenotic aortic valves obtained from valve replacement surgery were analyzed by multiple modalities, including transcriptomics and global unlabeled and tandem-mass-tagged proteomics by liquid chromatography-mass spectrometry. **Results:** Global transcriptional and protein expression signatures differed between the non-diseased, fibrotic, and calcific stages of CAVD, with consistent trends in gene and protein expression across disease stages. Anatomical aortic valve microlayers exhibited unique proteome profiles that were maintained throughout disease progression, and revealed GFAP as a specific marker of valvular interstitial cells (VICs) from the spongiosa layer. CAVD disease progression was marked by an emergence of smooth muscle cell activation, inflammation, and calcification-related pathways. Proteins overrepresented in the disease-prone fibrosa are functionally annotated to fibrosis and calcification pathways, and we found that, *in vitro*, fibrosa-derived VICs demonstrated greater calcification potential than those from the ventricularis. These studies confirmed that the microlayer-specific proteome was preserved in cultured VICs, and that VICs exposed to TNAP-dependent and TNAP-independent calcifying stimuli had distinct proteome profiles, both of which overlapped with that of the whole tissue. Network analysis of protein-protein

interaction networks found a significant closeness to multiple inflammatory and fibrotic diseases. **Conclusions:** A spatially- and temporally-resolved multi-omics and systems biology strategy identifies the first molecular regulatory networks in CAVD, a cardiac condition without a pharmacological cure, and describes a strategy for endophenotype characterization that is broadly applicable to comprehensive omics studies of cardiovascular diseases.
F. Schlotter: None. **A. Halu:** None. **S. Goto:** None. **M.C. Blaser:** None. **S.C. Body:** Research Grant; Significant; R01 HL114823. **L.H. Lee:** None. **H. Higashi:** None. **D.M. DeLaughter:** None. **J.D. Hutcheson:** None. **P. Vyas:** None. **T.H. Pham:** None. **M.A. Rogers:** None. **A. Sharma:** None. **C.E. Seidman:** None. **J. Loscalzo:** Research Grant; Significant; R01 HL61795, GM107618. **J.G. Seidman:** None. **M. Aikawa:** None. **S.A. Singh:** None. **E. Aikawa:** Research Grant; Significant; R01 HL114805, R01 HL136431, HL119798.

229
Small GTPase Rap1 deficiency Accelerates Development of Atherosclerosis in ApoE Deficient Mice
Bandana Singh, Tara McIntyre, Sribalaji Lakshmikanthan, Blood Res Inst, Milwaukee, WI; Sushma Kaul, Mary Sorci - Thomas, Medical Coll of Wisconsin, Milwaukee, WI; Magdalena Chrzanowska-Wodnicka, Blood Res Inst, Milwaukee, WI

Rap1, a ubiquitously expressed small GTPase, integrates signals from multiple receptors and promotes activation and signaling by cell adhesion receptors. *In vivo*, endothelial (EC) Rap1 is required for normal vessel formation, angiogenesis and dynamic regulation of EC barrier. Two Rap1 isoforms, Rap1A and Rap1B, share 95% identity, and EC deletion of both isoforms leads to embryonic lethality due to cardiovascular defects. We have recently demonstrated that Rap1 is a novel regulator of shear sensing in endothelium and that it is essential for nitric oxide release, and that Rap1 deficiency leads to EC dysfunction. These findings demonstrated that Rap1 plays an essential role in vasoprotective response of endothelium in response to shear stress. The objective of this study is to determine the specific role of Rap1 response to laminar, vasoprotective flow and pro-inflammatory, disturbed flow by examining the effect of EC deletion of Rap1B, the more prominent Rap1 isoform, on progression of atherosclerosis. To investigate the role of Rap1 in progression of atherosclerosis, we crossed apolipoprotein E-deficient ($ApoE^{-/-}$) mice with tamoxifen-inducible, EC specific Rap1B-knockout ($Cadh5\text{-}CreERT^{+/0}$; $Rap1B^{f/f}$) to generate atherogenic EC-Rap1B KO (Athero-Rap1B KO) mice. We hypothesized that Rap1B deficiency will exacerbate progression of atherosclerosis. Athero-Rap1B KO and littermate controls (Cadh5-Cre-negative mice or mice injected with carrier oil only) were fed high fat, western diet (21.2% fat, 0.2% cholesterol) for 16 weeks. No difference in total cholesterol levels were observed between Athero- Rap1B KO and control mice. Atherosclerotic lesion formation was visualized with oil O red and plaque area was quantified in en-face preparations. (n=5-9). We observed increased lesion area in the descending aorta of Athero-Rap1B KO mice (0.7351 ± 0.1065 vs 0.4866 ± 0.09812; p =0.0584, one-tailed t-test, Welch corrected) and a strong trend towards larger lesion area in the total aorta (2.142 ± 0.5058 vs 1.267 ± 0.1718; p=0.0679), and the arch of the aorta (1.489 ± 0.4343 vs 0.7807 ± 0.1152; p=0.0747) compared with control mice. These findings demonstrate that Rap1B deficiency accelerates progression of atherosclerosis and show that Rap1 plays a vasoprotective role in both laminar flow and disturbed flow areas.
B. Singh: None. **T. McIntyre:** None. **S. Lakshmikanthan:** None. **S. Kaul:** None. **M. Sorci -Thomas:** None. **M. Chrzanowska-Wodnicka:** None.

This research has received full or partial funding support from the American Heart Association.

230
Matrix Regulation of Lymphangiogenesis in Atherosclerosis
Bhupesh Singla, Huiping Lin, Pushpankur Ghoshal, Augusta Univ, Augusta, GA; Catherine Martel, Univ de Montréal, Montreal, QC, Canada; Gabor Csanyi, Augusta Univ, Augusta, GA

Background: Atherosclerosis is a consequence of an imbalance of cellular uptake of lipoproteins versus removal of cholesterol from the arterial wall. The lymphatic vasculature represents the primary route of cholesterol removal from atherosclerotic vessels. Previous studies have linked matrix protein thrombospondin-1 (TSP1), a well-known inhibitor of angiogenesis, with human atherosclerotic disease; however the mechanisms by which TSP1 contributes to atherosclerosis and its effect on arterial lymphangiogenesis remain unknown. **Methods:** The effect of TSP1 on human lymphatic endothelial cell (LEC) proliferation, migration and tube formation was investigated *in vitro*. TSP1 protein expression was analyzed in human and murine ($ApoE^{-/-}$, 12 weeks Western diet) atherosclerotic aortic tissue and lesion free segments using Western blotting. The role of TSP1 and its cognate receptor CD47 in the pathogenesis of atherosclerosis was investigated using knockout animals.**Results:** TSP1 expression was significantly increased in both human and $ApoE^{-/-}$ atherosclerotic arteries compared to plaque free segments in human and wild type aortic tissue. TSP1 at physiologically relevant concentrations (11-22 nM, 24 hrs) inhibited LEC proliferation, migration, and tube formation. RT-PCR data demonstrated that CD47 is the predominant TSP1 receptor expressed in LEC (> 50-fold over CD36 mRNA levels). Finally, genome-wide deficiency in TSP1 and CD47 receptor attenuated atherosclerotic lesion formation in the aorta and brachiocephalic artery by ~50% compared to wild type controls. Importantly, there was no difference in plasma cholesterol levels, body weight, fat and lean mass, fasting plasma glucose, and blood pressure between the experimental groups.**Conclusions:** The present study suggests that matrix protein TSP1 via CD47 receptor contributes to the pathogenesis of atherosclerosis. Inhibition of arterial lymphangiogenesis by TSP1-CD47 signaling may contribute to arterial lipid accumulation and atherosclerosis.
B. Singla: None. **H. Lin:** None. **P. Ghoshal:** None. **C. Martel:** None. **G. Csanyi:** None.

This research has received full or partial funding support from the American Heart Association.

231
The Role of Epsin in Regulating SR-B1 Function and Lipid Metabolism in Atherosclerosis
Kai Song, Megan L. Brophy, Yunzhou Dong, Hao Wu, Ashiqur Rahman, Hong Chen, Boston Children's Hosp/Harvard Medical Sch, Boston, MA

Atherosclerosis is both a metabolic and inflammatory disease. Vulnerable atherosclerotic plaque forms in response to hyperlipidemia and arterial wall inflammation-associated stimuli, where macrophages represent the "Trojan horse". Owing to extreme paucity of appropriate targets that effectively block dyslipidemia and concomitantly inhibit macrophage-mediated inflammation, the battle fighting against atherosclerosis remains daunting. The discovery of new molecules and pathways that hit two birds with one stone would therefore significantly advance the development of new and more effective therapeutics to treat heart disease. In our latest study, we show that epsins 1 and 2 are upregulated in atherosclerotic plaques in apolipoprotein E deficient ApoE-/- mice fed western diet. Consequently, we show that macrophage-specific and hepatocyte-specific epsin deficiency inhibits atherosclerosis in ApoE-/- mice fed western diet. We have found that epsin

interacts with and reduces the levels of anti-atherogenic SR-B1. Furthermore, given a paramount role for epsin in promoting atherosclerosis, whether targeting epsin systemically is a viable strategy to impede atheroma progression is an extremely important and medically relevant question to be addressed. Thus, our central hypothesis is that in macrophage foam cells, epsin reduces levels of SR-B1, impeding atheroma resolution; and, in liver, epsin-mediated downregulation of SR-B1 elevates cholesterol level thus facilitating atheroma progression.
K. Song: None. **M.L. Brophy:** None. **Y. Dong:** None. **H. Wu:** None. **A. Rahman:** None. **H. Chen:** None.

232
Development and Validation of a Mathematical Model Representing Complex Cellular Interactions Within the Artery Wall: in Silico Approach to Test Targeted Interventions
Marcella Torres, Jing Wang, Virginia Commonwealth Univ, Richmond, VA; Paul Yannie, Hunter McGuire VA Medical Ctr, Richmond, VA; Rebecca Segal, Angela Reynolds, Shobha Ghosh, Virginia Commonwealth Univ, Richmond, VA

Atherosclerotic cardiovascular diseases remain the number one cause of morbidity and mortality despite significant advances in lipid management. Complex cellular interactions occur within the artery wall requiring timely infiltration/egress of immune cells and lipoproteins within a changing inflammatory milieu that determine the progression of an atherosclerotic plaque. Lack of detailed understanding of the multiple processes involved and their potential interactions has hindered development of targeted therapies. The objective of this study was to develop a computational model of the sequential influx of immune cells in response to a trigger to permit a system-level analyses of the processes involved using ordinary differential equations (ODEs). Thioglycollate induced peritonitis was used as a model to examine the infiltration of immune cells and phenotypic polarization of macrophages in response to a stimulus. Peritoneal exudates obtained at 10 different time-points over 7 days were analyzed by FACS to determine the distribution of neutrophils, macrophages and Ly6C^{Hi} (M1) or Ly6C^{Lo} (M2) polarization. Weighted least squares of the different parameters were used to calibrate the model developed in our laboratory (Panel A) to simulate inflammation/repair during sepsis using the Levenberg-Marquardt algorithm. Panels B-D show the “match” of the experimental data to the calibrated model demonstrating the validity of this model. Since the ODEs are derived from a combination of known and hypothesized kinetics of the biological system, model the changes in physiological variables over time and are based on biological interactions, our calibrated mathematical model will permit the evaluation of changes in one or more targeted parameters *in silico* on immune cell distribution/phenotype. Efficacy of various macrophage-specific interventions (e.g., reduction in cholesterol content or inflammation) can be predicted prior to preclinical experimentation.

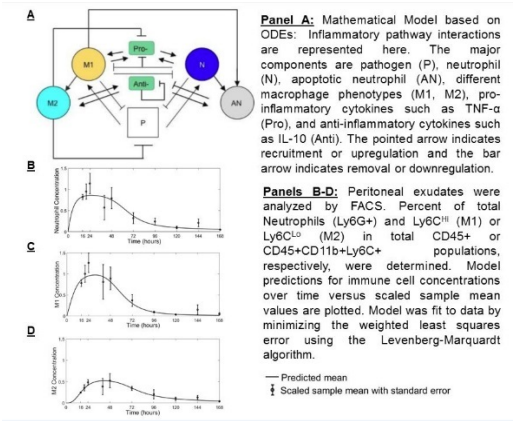

Panel A: Mathematical Model based on ODEs: Inflammatory pathway interactions are represented here. The major components are pathogen (P), neutrophil (N), apoptotic neutrophil (AN), different macrophage phenotypes (M1, M2), pro-inflammatory cytokines such as TNF-α (Pro), and anti-inflammatory cytokines such as IL-10 (Anti). The pointed arrow indicates recruitment or upregulation and the bar arrow indicates removal or downregulation.

Panels B-D: Peritoneal exudates were analyzed by FACS. Percent of total Neutrophils (Ly6G+) and Ly6C^{Hi} (M1) or Ly6C^{Lo} (M2) in total CD45+ or CD45+CD11b+Ly6C+ populations, respectively, were determined. Model predictions for immune cell concentrations over time versus scaled sample mean values are plotted. Model was fit to data by minimizing the weighted least squares error using the Levenberg-Marquardt algorithm.

M. Torres: None. **J. Wang:** None. **P. Yannie:** None. **R. Segal:** None. **A. Reynolds:** None. **S. Ghosh:** None.

233
CHI3L1 and Its Role in Vascular Smooth Muscle Cell Proliferation and Migration in Advanced Atherosclerosis
Pavlos Tsantilas, Div of Vascular Surgery, Stanford Univ Sch of Med, Stanford, CA; Shen Lao, Dept of Vascular and Endovascular Surgery, Klinikum Rechts der Isar, Technical Univ of Munich, Munich, Germany; Monika Vaerst, Div of Vascular Surgery, Stanford Univ Sch of Med, Stanford, CA; Yuhuang Li, Dept of Vascular and Endovascular Surgery, Klinikum rechts der Isar, Technical Univ of Munich, Munich, Germany; Vivek Nanda, Div of Vascular Surgery, Stanford Univ Sch of Med, Stanford, CA; Lars Maegdefessel, Dept of Vascular and Endovascular Surgery, Klinikum rechts der Isar, Technical Univ of Munich, Munich, Germany; Nicholas Leeper, Div of Vascular Surgery, Stanford Univ Sch of Med, Stanford, CA

Objectives: Stroke is one of the leading causes for death and disability worldwide. The underlying pathomechanism is most likely a thrombotic event caused by acute rupture or erosion of an unstable plaque in the carotid artery. Vascular smooth muscle cells (VSMCs) play an important role in both, development and rupture of atherosclerotic plaques. Thus, efforts have been devoted determining the characteristics of VSMCs in atherosclerotic plaques to develop novel diagnostic and therapeutic strategies to prevent unstable plaque rupture. Methods: Laser capture microdissections of the fibrous cap of ruptured plaques in symptomatic patients (n=20) and stable plaques in asymptomatic patients (n=20) were used to perform a GeneChip 2.0 Human Transcriptome Array. CHI3L1 could be detected as the most significantly upregulated transcript in ruptured plaques. Following, immunohistochemistry was performed to compare distribution of CHI3L1-positive cells, VSMCs and macrophages in ruptured and stable plaques. In-vitro MTT-assay, Boyden Chamber assay and TUNEL assay were performed to investigate the role of this gene in human VSMC proliferation, migration and apoptosis. Results: The MTT-assay revealed that silencing of CHI3L1 lead to a decreased proliferation of human VSMCs. Further, migration was reduced in absence of CHI3L1. Immunohistochemistry of human carotid plaques indicated that in stable plaques mainly macrophages were CHI3L1-postive, whereas in unstable plaques both macrophages and VSMCs were CHI3L1-positive. In-vitro knockdown of CHI3L1 in cultured human VSMCs significantly increased CD68 expression, suggesting a potential role in transformation of VSMCs to macrophages. CHI3L1/CD68-positive cells (putative macrophages) in unstable plaques appeared hyperproliferative (Ki-67 positive). Conclusion: In summary, CHI3L1 plays a role in VSMC-regulation in atherosclerotic plaques. Expression levels in unstable plaques are increased. Further, it seems to induce proliferation as well as migration in VSMCs. Results of CHI3L1-induced CD68 expression indicate a potential role in VSMC-macrophage transformation. <!--EndFragment-->
P. Tsantilas: None. **S. Lao:** None. **M. Vaerst:** None. **Y. Li:** None. **V. Nanda:** None. **L. Maegdefessel:** None. **N. Leeper:** None.

234
Nuclear Export of Telomeric Repeat Binding Factor 2 (terf2)-interacting Protein (terf2ip) Expression, One of the Sherterin Complex Molecule, is Crucial for Disturbed Flow-induced Endothelial Inflammation and Senescence via Upregulating Terf2ip S205 Phosphorylation
Hang Thi Vu, The Univ of Texas, MD Anderson Cancer Ctr, Houston, TX; Nhat-Tu Le, Houston Methodist, Houston, TX; Kyung-Sun Heo, Yuka Fujii, Sivareddy Kolta, Kyung Ae Ko, Yin Wang, Tamlyn Thomas, Elena Fujiwara, The Univ of Texas, MD Anderson Cancer Ctr, Houston, TX; Carolyn Giancursio, Houston Methodist, Houston, TX; Keigi Fujiwara,

Jun-ichi Abe, The Univ of Texas, MD Anderson Cancer Ctr, Houston, TX

Atherosclerosis is a multifactorial disease mainly caused by endothelial cell (EC) dysfunction resulting from EC senescence. Both EC inflammation and senescence are increased by disturbed flow (d-flow) but the exact mechanism is still unknown. The potential role of TERF2IP in regulating inflammation has been reported, but it has been controversial, especially in ECs. We found that d-flow-induced NF-kB activation was significantly inhibited by the depletion of TERF2IP, but TNF-induced NF-kB activation under laminar flow (l-flow) was not inhibited by TERF2IP depletion. TERF2IP S205 phosphorylation was increased by d-flow, but not by s-flow. This TERF2IP S205 phosphorylation was crucial for d-flow-induced TERF2IP nuclear export, which also caused nuclear export of its binding partner TERF2 in a piggy-back manner. Both the depletion of TERF2IP (TERF2IP siRNA) and overexpression of TERF2IP S205A mutant inhibited d-flow-induced TERF2 nuclear export as well as subsequent EC senescence. In addition, we found the key role of p90RSK activation in regulating EC inflammation and senescence via TERF2IP S205 phosphorylation. To determine the role of TERF2IP and TERF2 cellular localization in vivo, we performed in vivo en face immunostaining of mouse aortic arch in EC specific TERF2IP knock out (EC-TERF2IP-KO) and control mice using anti-TERF2IP or TEFR2 and anti-VE-cadherin antibodies. In control mice TERF2IP expression was very low in the l-flow area. In contrast we found a significant increase of TERF2IP expression, especially in the extra-nuclear region of ECs in the d-flow area. More nuclear localization of TERF2 was observed in EC-TERF2IP-KO mice than those in wild type, which supports our finding in vitro. Significant decreases of VCAM-1 expression and apoptosis were found in the d-flow area in EC-TERF2IP-KO mice compared to control mice. Lastly, we found a significant decrease in d-flow-induced atherosclerotic plaque formation after partial carotid ligation in EC-TERF2IP-KO mice crossed with Ldlr-/- mice compared to control Ldlr-/- mice. These data suggest the key role of nuclear export of TERF2IP in up-regulating EC inflammation and senescence via p90RSK-mediated TERF2IP S205 phosphorylation.

H.T. Vu: None. **N. Le:** None. **K. Heo:** None. **Y. Fujii:** None. **S. Kolta:** None. **K. Ko:** None. **Y. Wang:** None. **T. Thomas:** None. **E. Fujiwara:** None. **C. Giancursio:** None. **K. Fujiwara:** None. **J. Abe:** None.

This research has received full or partial funding support from the American Heart Association.

235

Ionizing Radiation Induces Endothelial Inflammation and Apoptosis via P90rsk-mediated Erk5 S496 Phosphorylation

Hang Thi Vu, Sivareddy Kotla, Kyung Ae Ko, Yuka Fujii, MD Anderson Cancer Ctr, Houston, TX; Yunting Tao, Houston Methodist, Houston, TX; Jan Medina, Tamlyn Thomas, MD Anderson Cancer Ctr, Houston, TX; Megumi Hada, Texas A&M Chancellor Res Initiative, Prairie View A&M Univ, Houston, TX; Anil K. Sood, The Univ of Texas MD Anderson Cancer Cente, Houston, TX; Pankaj Kumar Singh, Sarah A. Milgrom, Sunil Krishnan, Keigi Fujiwara, MD Anderson Cancer Ctr, Houston, TX; Nhat-Tu Le, Houston Methodist, Houston, TX; Jun-ichi Abe, MD Anderson Cancer Ctr, Houston, TX

Background: Adverse cardiovascular events are a leading nonmalignant cause of morbidity and mortality among cancer survivors who have been exposed to ionizing radiation (IR), but the exact mechanism of the cardiovascular complications induced by IR remains unclear. In this study we investigated the potential role of the p90RSK-ERK5 module in regulating IR-induced endothelial cell inflammation and apoptosis.

Methods and Results: Whole body radiation of mice with 2 Gy γ-ray significantly increased endothelial VCAM-1 expression; especially in the disturbed flow area *in vivo*. In vitro studies showed that IR increased p90RSK activation as well as subsequent ERK5 S496 phosphorylation in cultured human endothelial cells (ECs). A specific p90RSK inhibitor, FMK-MEA, significantly inhibited both p90RSK activation and ERK5 S496 phosphorylation, but it had no effect on IR-induced ERK5 TEY motif phosphorylation, suggesting that p90RSK regulates ERK5 transcriptional activity, but not its kinase activity. In fact, we found that IR-induced NF-kB activation and VCAM-1 expression in ECs were significantly inhibited by the over-expression of S496 phosphorylation site mutant of ERK5 (ERK5 S496A) compared to overexpression of wild type ERK5. Furthermore, when ECs were exposed to IR, the number of annexin V positive cells increased, and overexpression of ERK5 S496A, but not wild type ERK5, significantly inhibited this increase.

Conclusions: Our results demonstrate that IR augmented disturbed flow-induced VCAM-1 expression in vivo. Endothelial p90RSK was robustly activated by IR and subsequently up-regulated ERK5 S496 phosphorylation, inflammation, and apoptosis in ECs. The EC p90RSK-ERK5 signaling axis can be a good target to prevent cardiovascular events after radiation therapy in cancer patients.

H.T. Vu: None. **S. Kotla:** None. **K. Ko:** None. **Y. Fujii:** None. **Y. Tao:** None. **J. Medina:** None. **T. Thomas:** None. **M. Hada:** None. **A. Sood:** None. **P. Singh:** None. **S. Milgrom:** None. **S. Krishnan:** None. **K. Fujiwara:** None. **N. Le:** None. **J. Abe:** None.

This research has received full or partial funding support from the American Heart Association.

236

Magnetic Resonance T1 High Signal Intensity in Coronary Atherosclerotic Plaques Reflects Intraplaque Hemorrhage-derived Erythrocyte Content

Atsushi Yamashita, Miyazaki Univ, Miyazaki, Japan; Yasuyoshi Kuroiwa, Koga General Hosp, Miyazaki, Japan; Akiko Uchida, Kazunari Maekawa, Toshihiro Gi, Miyazaki Univ, Miyazaki, Japan; Takuroh Imamura, Koga General Hosp, Miyazaki, Japan; Yujiro Asada, Miyazaki Univ, Miyazaki, Japan

Objective: Acute myocardial infarction is triggered by plaque disruption and thrombus formation, therefore, it is important to detect high thrombotic risk plaque non-invasively. Coronary high signal intensity plaque (HIP) on T1 weighted magnetic resonance imaging (T1WI) was associated with future coronary events. The aim of this study is to identify pathological findings reflecting HIPs using hearts obtained from autopsy cases and blood samples.

Approach and Results: Formalin-fixed hearts (n=7) were imaged with non-contrast T1WI with a 1.5 T magnetic resonance system. We defined HIPs (n=11) or non-HIPs (n=25) as a coronary plaque to myocardial signal intensity ratio (PMR) of ≥ 1.4 or < 1.4, respectively. The corresponding histological sections were histologically and immunohistochemically analyzed. Plaque and necrotic core areas or frequency of intraplaque hemorrhage in HIPs were significantly larger or higher than those in non-HIPs. The high intensity portion in large coronary plaque was immunopositive for CD68, CD163, glycophorin A, and fibrin. Glycophorin A-, matrix metalloprotease (MMP) 9-, tissue factor-immunopositive areas were larger in HIPs than those in non-HIPs. Glycophorin A-, fibrin-, MMP9-, and tissue factor-immunopositive areas were positively correlated with PMR. We calculated T1 relaxation time of venous blood, plasma, and erythrocyte-rich blood in vitro. Blood coagulation shortened T1 relaxation time of the blood and plasma, and T1 relaxation times in coagulated whole blood and erythrocyte-rich blood were significantly shorter than those in plasma.

Conclusions: Majority of coronary HIPs may reflect intraplaque hemorrhage-derived erythrocyte content, and

may be a novel marker for plaque instability and thrombogenic potential.
A. Yamashita: None. **Y. Kuroiwa:** None. **A. Uchida:** None. **K. Maekawa:** None. **T. Gi:** None. **T. Imamura:** None. **Y. Asada:** None.

237
The Inhibitory Effect on Vascular Smooth Muscle Cell Hyperplasia in Artificial Atherosclerotic Mouse Model via miR-155 Induced NoxA1 Down Regulation
Wenwen Yan, Yian Yao, Yu Tang, Zhisong Chen, Lemin Wang, Xuebo Liu, Shanghai Tongji Hosp of Tongji Univ, Shanghai, China

Objective: To investigate the protective efficacy of miR-155 on down regulating NoxA1 gene expression, resulting in an inhibitory effect of vascular smooth muscle cell (VSMC) over proliferation and thus alleviating the progression of coronary artery atherosclerosis in mouse disease model.
Methods: Carotid artery of C57BL6 mouse was used for VSMC primary culture. The isolated VSMC was transfected with recombinant Pad2YFG adenovirus fluorescent vector with miR-155 fragment (mimic or mutant). Fluorescence microscope was applied to observe the transfection rate of miR-155 into VSMC. Artificial artery-injured mouse model fed with high-fat diet was established as host to accept VSMC transplantation via tail vein injection for 3 consecutive days. Aortic and carotid arteries were extracted at week 6. Distribution of miR-155 was quantified; protein and RNA were extracted to detect NoxA1 and NADPH expression in vehicle control, miR-155 mimic group, and the inhibitor group. Immunohistochemistry was performed in arteries section to compare the thickness of neointima and assess the severity of AS of each group.
Results: The miR-155 distribution was observed varied at week 6 in control, miR-155 mimic and inhibitor groups. The NoxA1 protein expression in VSMC was decreased in mimic group at week 6 vs control and inhibitor groups ($p<0.05$); no significant difference of NADPH expression was observed in all groups. The NoxA1 and NADPH gene expression in VSMC were both found reduced compared with those of control group at week 6 ($p<0.05$). Immunohistochemistry of artery frozen sections figured out that the thickness of neointima of carotid artery in miR-155 mimic group was significantly lower vs control and inhibitor groups ($p<0.01$) at week 6.
Conclusion: miR-155 transfection into VSMC seems to have reversed regulatory effect on NoxA1 expression resulting in amelioration of atherosclerotic lesion in artificial AS mouse model. A therapeutic strategy based on the functional role of miR-155 in VSMC over proliferation-based atherosclerosis would need to complementarily-synthesize miRNAs, which is a promising therapeutic tool due to the enhanced stability and sustained effects after intravenous injection in the arterial wall.
W. Yan: None. **Y. Yao:** None. **Y. Tang:** None. **Z. Chen:** None. **L. Wang:** None. **X. Liu:** None.

238
Biological Role and Therapeutic Potential of Nitric Oxide Signaling in Aortic Valve Stenosis: Insights From Genetic Modulation of DDAH1
Bin Zhang, Carolyn Roos, Elise Oehler, Grace Verzosa, Arman Arghami, Michael Hagler, Jordan D Miller, Mayo Clinic, Rochester, MN

The balance between local asymmetric dimethylarginine (ADMA) levels and dimethylarginine dimethylaminohydrolase 1 (DDAH1) activity is a major determinant of local nitric oxide synthase activity. Previous studies suggested that increased plasma ADMA levels are strongly associated with the aortic valve stenosis, causal or mechanistic links have yet to be elucidated. Thus, the aim of this study was to investigate whether reduction or overexpression of DDAH1 protects aortic valve dysfunction in mice. To experimentally alter DDAH1 levels, we used low density lipoprotein receptor deficient, apolipoprotein B100-only (LA) mice that were either DDAH1 wild-type ($D^{+/+}$ or $D^{0/0}$), heterozygous ($D^{+/-}$), or transgenic/overexpressing ($D^{Tg/0}$) littermates. All mice were fed a western diet for 6 months. Reducing DDAH1 increased plasma ADMA levels (LA-$D^{+/+}$=0.89 ± 0.02 µmol/L, LA-$D^{+/-}$=1.1 ± 0.02 µmol/L, $p< 0.05$) and blood pressure (LA-$D^{+/+}$ = 125 ± 4 mmHg, LA-$D^{+/-}$ = 141 ± 3 mmHg, $p< 0.05$) following 6 months of western diet feeding. Critically, aortic valve function was significantly worse in DDAH1-deficient mice (LA-$D^{+/+}$ 2.20±0.09 m/sec versus LA-$D^{+/-}$=2.41±0.11 m/sec, $p< 0.05$) and was associated with higher levels of valve cusp calcification (Alizarin Red, LA-$D^{+/+}$ = 10 ± 3% versus LA-$D^{+/-}$ = 20 ± 4%). Reciprocally, overexpression of DDAH1 in hypercholesterolemic littermates reduced ADMA levels (LA-$D^{0/0}$= 1.4 ± 0.2 µmol/L, LA-$D^{Tg/0}$= 0.7 ± 0.1µmol/L, $p< 0.05$) and systolic blood pressure (LA-$D^{0/0}$ = 136 ± 6 mmHg, LA-$D^{Tg/0}$ = 124 ± 4 mmHg, $p< 0.05$). Interestingly, aortic valve function was not improved by overexpression of DDAH1 (LA-$D^{0/0}$ = 2.36 ± 0.06 m/sec versus LA-$D^{Tg/0}$ mice (2.43 ± 0.21 m/sec), nor was valvular calcification. These results suggest that while endogenous levels of DDAH1 expression protect against increases in circulating ADMA, blood pressure, valvular calcification, and valvular dysfunction. Interestingly, overexpression of DDAH1 does not appear to confer additional protection against progression of valvular stenosis. Collectively, our data suggest effective therapeutic harnessing of the DDAH1/ADMA/NOS axis will require targeting of downstream effector molecules—such as oxidation state of soluble guanylate cyclase—known to be pathologically altered and rate limiting in a variety of cardiovascular diseases.
B. Zhang: None. **C. Roos:** None. **E. Oehler:** None. **G. Verzosa:** None. **A. Arghami:** None. **M. Hagler:** None. **J.D. Miller:** None.

241
Impact of Cigarette Smoke, Next Generation Tobacco and Nicotine Products on the Cytotoxic, Oxidative and Pro-Inflammatory Status of THP-1 Cells
Coy Brunssen, Sindy Giebe, Anja Hofmann, Melanie Brux, Univ Hosp CGC Dresden, Dresden, Germany; Katherine Hewitt, Frazer Lowe, British American Tobacco, Southampton, United Kingdom; Henning Morawietz, Univ Hosp CGC Dresden, Dresden, Germany

Monocytes exhibiting a pro-inflammatory phenotype play a key role in adhesion and development of atherosclerotic plaques. Next generation tobacco and nicotine products (NGPs) are now widely used globally as an alternative to smoking. Little is known about their pro-inflammatory effects on monocytes. We investigated cell viability, anti-oxidant and pro-inflammatory gene and protein expression in THP-1 monocytes exposed to aqueous extracts of conventional cigarettes (CSE), a tobacco heating product (THP) and an electronic cigarette (EC). Pure nicotine was used as additional control. Treatment with CSE reduced cell viability in a dose-dependent manner, whereas all other test agents showed no difference to control. At the highest non-lethal dose of CSE (20%) the following notable mRNA expression changes were observed for CSE, THP and EC respectively, relative to control; HMOX1 (6-fold, <2-fold, <2-fold), NQO1 (3.5-fold, <2-fold, <2-fold), CCL2 (4-fold, 3.5-fold, 2.5-fold), IL1B (4-fold, 3-fold, <2-fold), IL8 (5-fold, 2-fold, 2-fold), TNF (2-fold, 2-fold, <2-fold), CD31 and ICAM1 were below the 2-fold threshold for all products. With respect to protein expression; IL1B (3-fold, <2-fold, <2-fold) and IL8 (3.5-fold, 2-fold, 2-fold) were elevated over the 2-fold threshold, whereas, CD31, ICAM1, TNF and CCL2 were below 2-fold expression for all products. At higher doses, greater inductions were observed with all extracts; however NGP responses were typically lower than CSE. In conclusion, anti-oxidative and pro-inflammatory processes were activated by all products. NGPs showed similar or lower responses relative to controls than CSE exposed cells.

C. Brunssen: None. **S. Giebe:** None. **A. Hofmann:** None. **M. Brux:** None. **K. Hewitt:** None. **F. Lowe:** None. **H. Morawietz:** None.

242
Sexual Dimorphic Effects of Serum Amyloid A3 in Atherosclerosis in Mice
Laura J den Hartigh, Leela Goodspeed, Diego Gomes Kjerulf, Shari Wang, Katherine E Turk, Barbara Houston, Farah Kramer, Jenny E Kanter, Karin E Bornfeldt, Alan Chait, Univ of Washington, Seattle, WA

Introduction: The acute-phase protein serum amyloid A (SAA) exists as 4 different subtypes in mice. Levels of the SAA3 subtype increase in response to acute inflammatory stimuli, and its expression is modestly and chronically elevated in adipose tissue and macrophages in obese mice. Previously we showed that SAA3 deficiency protected C57Bl/6 female mice, but not males, from obesity, adipose tissue inflammation, and hyperlipidemia in response to a high fat high sucrose diet (HFHS: 36% calories from fat, 36% calories from sucrose with 0.15% added cholesterol). We therefore investigated whether SAA3 deficiency modulates atherosclerosis in mice deficient in the low-density lipoprotein receptor (LDLR). **Methods**: We used two models of LDLR-deficiency to promote atherosclerosis in *Saa3*$^{+/+}$ and *Saa3*$^{-/-}$ male and female mice: (1) 16 weekly injections of an LDLR antisense oligonucleotide (LDLR-ASO), or (2) genetic deletion of LDLR (*Ldlr*$^{-/-}$). All mice consumed the HFHS diet for 16 weeks. **Results**: While both models of LDLR deficiency promoted hypercholesterolemia, *Ldlr*$^{-/-}$ mice had nearly 1.5- and 2-fold higher cholesterol levels than LDLR-ASO mice (males: 753±109 vs. 560±62 mg/dL, n=8, p<0.05; females: 519±20 vs. 302±22 mg/dL, n=10, p<0.0001). There was no effect of SAA3 deficiency on plasma cholesterol in male mice from either model. However, SAA3 deficiency unexpectedly enhanced body weight gain by 15% and body fat gain by 40%, and exacerbated cholesterol levels in female *Ldlr*$^{-/-}$ mice (*Saa3*$^{-/-}$ *Ldlr*$^{-/-}$: 623±26 vs. *Saa3*$^{+/+}$*Ldlr*$^{-/-}$: 519±20 mg/dL, n=10, p<0.01). Consistent with worsened plasma cholesterol levels, *en face* aortic atherosclerotic lesion area was 2-fold greater in female *Saa3*$^{-/-}$*Ldlr*$^{-/-}$ mice than in their wild type counterparts (n=10, p<0.05). Conversely, atherosclerosis was improved by 40% in male *Saa3*$^{-/-}$ mice in both models of hypercholesterolemia (n=8). **Summary**: While both LDLR-ASO and *Ldlr*$^{-/-}$ promote hypercholesterolemia in male and female mice, SAA3 deficiency worsens hypercholesterolemia and atherosclerosis in female mice, and reduces atherosclerosis in male mice. **Conclusion**: In the setting of hypercholesterolemia, SAA3 may be pro-atherogenic in male and atheroprotective in female mice, solidifying the sexual dimorphic nature of SAA3.
L.J. den Hartigh: None. **L. Goodspeed:** None. **D. Gomes Kjerulf:** None. **S. Wang:** None. **K.E. Turk:** None. **B. Houston:** None. **F. Kramer:** None. **J.E. Kanter:** None. **K.E. Bornfeldt:** None. **A. Chait:** None.

243
Familial Hypercholesterolemia Screening at a Large Corporate Clinic in Japan
Masumi Hara, Naoyuki Iso-O, Anna Sugiura, Atsuko Takai, Hideyuki Takeuchi, Sonoka Hara, Mizonokuchi Hosp, Teikyo Univ Sch of Med, Kanagawa, Japan; Takaharu Yamada, Seigo Ito, Medical Clinic of Mitsubishi Corp, Tokyo, Japan; Kazuhisa Tsukamoto, Teikyo Univ Sch of Med, Tokyo, Japan
[Background and Aims]Familial hypercholesterolemia (FH) is a high risk of developing premature coronary artery disease even in heterozygotes. It is reported that the diagnostic rate in Japan and the United States is extremely low compared with the Netherlands and a few countries. The diagnostic criteria of FH vary from country to country. Using the JASb(Japan Atherosclerosis Society) diagnostic criteria, it has been shown that sensitivity and specificity in patients who visited lipid clinics are high, but those in the general population are not clear. In this study, we tried to screen FH in a clinic of a large Japanese corporation. [Methods] During the period from July 1, 2014 to October 31, 2017, we extracted patients suspected of FH with LDL-C≧180mg/dL or with a family history of CAD at annual and follow-up medical checkup. In the extracted patients, family history of premature CAD and Achilles tendon thickening were evaluated. For patients to which additional information was added, FH diagnosis by JAS diagnostic criteria and by Dutch criteria were performed. [Results]A total of 3,3136 medical checkups were set for about 6,300 subjects, and a total of 2,8108 visits were made (the examination rate was 84.8%). Among them, 328 patients with suspected FH were extracted due to LDL-C of 180 mg/dL or more, or family history of CAD. Among subjects additional information was obtained as of November 2017, 43 (19.6%) were diagnosed as FH on JAS criteria, and the number was higher than predicted from the estimated prevalence of FH. On the other hand, there were 24 patients who were "Definite" or "Probably" in Dutch criteria and 211 patients with LDL-C≧190 mg/dL. LDL-C of patients diagnosed as FH by JAS diagnostic criteria was 206.6 (45.3) mg/dL, while patients who did not meet the criteria also had high LDL-C values as 201.4 (18.6) mg/dL. 26.8% of patients who met the diagnostic criteria of FH had not received statin at the time of evaluation. [Conclusion]The number of patients satisfying the JAS criteria was more than predicted from the prevalence, suggesting the possibility of over-diagnosis. On the other hand, there were many patients who do not satisfy the diagnostic criteria even when LDL-C is very high.
M. Hara: None. **N. Iso-O:** None. **A. Sugiura:** None. **A. Takai:** None. **H. Takeuchi:** None. **S. Hara:** None. **T. Yamada:** None. **S. Ito:** None. **K. Tsukamoto:** None.

244
A Qualitative Evaluation of Coronary Atherosclerosis in Young and Middle-aged Dutch Tissue Donors
Jan H Lindeman, Marlieke Geerts, Leiden Univ Medical Ctr, Leiden, Netherlands; Alain van Gool, TNO Health Res, Leiden, Netherlands

Background: Ischemic coronary events relate to qualitative changes in plaque characteristics. Epidemiological data on qualitative aspects of the coronary atherosclerotic process (e.g. plaque progression and destabilization) is missing. Objective: to qualitatively map the epidemiology of atherosclerosis burden in a representative cohort of deceased individuals Methods: this is a systematic, qualitative analysis of atherosclerotic burden in the proximal left coronary artery (LCA) segment of 695 tissue donors (median age 54, range 11-65 years). Based on the cause of death, donors were dichotomized into a non-cardiovascular (non-CVD group) and a cardiovascular disease (CVD) group. Consecutive, 5 mm LCA segments were Movat stained, and the atherosclerotic burden for each segment qualitatively graded (revised AHA-classification). Results: non-CVD and CVD groups show rapid acceleration of atherosclerosis severity after the age of 40; resulting in an almost endemic presence of advanced atherosclerosis in men and women over 40 respectively 50 years. In fact, only 19% of the non-CVD and 6% of the CVD donors over 40 presented with a normal LCA or non-progressive lesion type. The consolidated fibrous calcified plaque (FCP) dominated in both non-CVD and CVD donors over 40. Estimates of atherosclerosis load (i.e. average lesion grade, proportion of FCPs, and average number of FCPs per cross-section were all higher in the CVD group ($P<1.10^{-16}$, P<0.0001 and P<0.05 respectively) Conclusions: advanced atherosclerotic disease is endemic in individuals over 40. Dominance of FCP lesions and the higher disease load in CVD donors imply that the atherosclerotic process is repetitive. Abundance of FCPs suggest that complications of plaque rupture are stochastic. This study was in part funded by the European Commission (Cartardis, FP7 HEALTH.2013.2.4.2-1).

J.H. Lindeman: None. **M. Geerts:** None. **A. van Gool:** None.

245
Phenotype Discovery in Cardiovascular Patients Using Unsupervised Learning
Elsie Ross, Stanford Health Care, Stanford, CA; Nigam Shah, Stanford Univ Sch of Med, Stanford, CA; Nicholas Leeper, Stanford Health Care, Stanford, CA

Introduction: Customer segmentation, as utilized in the retail industry, has direct applications to population health. By identifying unique patient subgroups, population health practitioners can produce health campaigns that are more effectively targeted. We describe a technique for identifying unique subgroups of patients with cardiovascular disease using unsupervised machine learning. **Methods:** Data were derived from a prospective, observational study of 1,329 patients who presented for elective, non-emergent coronary angiography at two tertiary care centers between 2004 and 2008 and were found to have CAD. Patients were measured along a total of 161 variables including demographic, clinical, physical activity, imaging, genomic and socioeconomic characteristics. We utilized a new technique called generalized low rank modeling (GLRM) coupled with K-means clustering to identify different patient subgroups. We then compared MACCE and mortality rates across clusters. **Results:** Utilizing GLRM we were able to identify 3 unique clusters of patients. While the rate of MACCE differed significantly across all 3 clusters (Figure 1), cluster 3, which represented the sickest group of patients, had significantly worse mortality rates than clusters 1 and 2. Clusters were distinguished by their prevalence of co-morbidites such as peripheral artery disease and diabetes, as well as engagement in physical activity, educational attainment, family history and genomic marker expression. **Conclusions:** Patients with cardiovascular disease are highly heterogeneous with different clinical, genomic and lifestyle traits. Unsupervised learning algorithms can be used to automate identification of important subpopulations using a wide range of data, above and beyond traditional risk factors. Identifying these unique groups of can help health practitioners better target health information and treatment strategies.

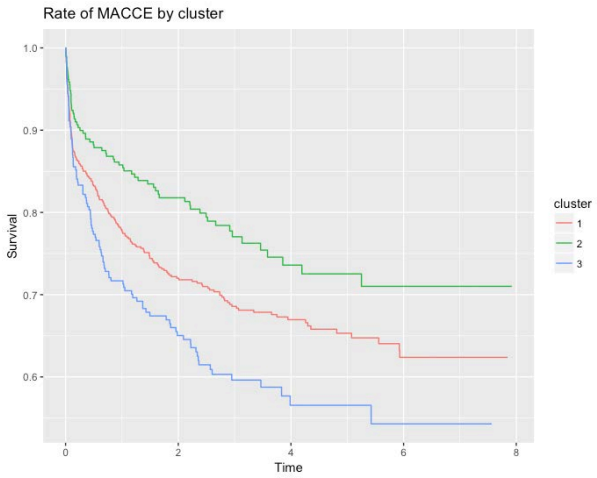

E. Ross: None. **N. Shah:** None. **N. Leeper:** None.

250
Endothelial functional Regulation by Enhancer-Associated Long Non-Coding RNAs
Zhen Chen, Yifei Miao, Feng-Mao Lin, City of Hope, Duarte, CA

Vascular endothelium constitutes the critical interface between circulating blood and vessel wall. Long non-coding RNAs (lncRNAs) are important regulators in gene expression and chromotin remodeling. We recently identified a lncRNA that enhances endothelial nitric oxide synthase (eNOS) expression (LEENE), that is encoded in a distal enhancer region and mediates long-range DNA interaction to promote the eNOS expression. We now extend from this prototype using a systematic approach to identify enhancer-associated lncRNAs and their molecular and functional regulation of endothelial gene expression. We integrate a variety of publicly available high-throughput sequencing datasets (including various chromatin immunoprecipitation-sequencing) that provide information on histone modifications and transcriptional activity and high-resolution chromatin conformation capture combined with sequencing (4C-seq) profiles generated in our own lab. From these analyses, we identified over 200 enhancer-associated lncRNA candidates with high potential to regulate endothelial gene expression. Quantitative PCR analysis verified that 7 out of the top 10 ranked candidates are differentially regulated by stimuli that alter endothelial gene expression and functions, including high-glucose, TNFα, atorvastatin, and metformin. Using CRISPR-cas9 gene editing to delete these lncRNA-associated enhancer regions and locked nucleic acid-mediated lncRNA inhibition, we demonstrated that the loss-of-function of these lncRNAs lead to significant alteration of endothelial gene expression, including those involved in angiogenesis and eNOS signaling. Collectively, these lncRNAs play an essential role in epigenetic regulation of endothelial functions; the identification of these lncRNAs can have significant impacts on understanding of endothelial homeostasis and dysfunction.

Z. Chen: None. **Y. Miao:** None. **F. Lin:** None.

251
miRNA Mapping of Cardiac Endothelial and Fibroblast Cells during Hypertrophy Progression
Seema Dangwal, Filippo Martino, Sandor Batkai, MH-Hannover, Hannover, Germany; Claus J Scholz, IKFZ, Wuerzburg, Germany; Meik Kunz, Thomas Dandekar, Univ Wuerzburg, Wuerzburg, Germany; Thomas Thum, MH-Hannover, Hannover, Germany

MicroRNAs (MiRNA/miRs) are known key players in cardiovascular disorders. Here we created and analyzed a global miRNA map in isolated cardiac endothelial and fibroblast cells during hypertrophy progression. Hypertrophy was induced in male C57BL/6 mice by trans-aortic constriction (TAC). Hypertrophic phenotyping was performed at 3 days (3d), 2 weeks (2w) or 4 weeks (4w) post- SHAM/TAC operation, using Millar system and echocardiography. Thereafter, pure single cell fractions from hearts were recovered by retrograde collagenase-II perfusion, followed by pre-plating of fibroblasts and magnetic sorting of endothelial cells. Transcriptomic analysis was performed on RNA isolated from different heart cell fractions at 3d, 2w or 4w post-SHAM/TAC. Additional 6w and 13w SHAM/TAC groups were included for validation of selected miRNAs. Cytokine secretome was performed using multiplex assay after transfection of a miR library to primary cardiac fibroblasts. Unsupervised hierarchical clustering revealed specific miRNA profile of each cardiac cell fraction. Principle component analysis projected strong effect of individual cellular compartments. Based on miRnome screening, miR-709, miR-30e-5p, miR-146a, miR-34a and miR-204, miR-1187 were validated by RTPCR to confirm spatial and temporal regulation (n=3-5, $p<0.05$) of these miRNAs in non-cardiomyocyte fractions. Corresponding time-dependent downregulation of miR-146a targets, Pten and Timp-2, was also observed. Cytokine secretome analysis upon miR-precursor library transfection in cardiac fibroblasts confirmed an increase in FGF, LIF-1, MCP-1, MIP-1 secretion (1.5-5 folds) by miR-146a and miR-34a. Gradual activation of the TGF beta pathway in endothelial cells may initiate endothelial to mesenchymal transition, whereas cytokine secretion from fibroblasts may affect the cellular hemostasis. Our study represents a global miRNome of cardiac endothelial and fibroblast compartments during progressive hypertrophy to better understand the time dependent

molecular changes in non-cardiomyocyte compartment during pressure-overload induced cardiac remodeling. The collective influence of miRNA deregulation may be linked to different pathways responsible for cell-proliferation, inflammation and fibrosis with the progression of hypertrophy.

S. Dangwal: None. **F. Martino:** None. **S. Batkai:** Employment; Significant; Cardior Pharmaceuticals. **C.J. Scholz:** None. **M. Kunz:** None. **T. Dandekar:** None. **T. Thum:** Employment; Significant; Cardior Pharmaceuticals.

252

Innovative Cell-therapy for Diabetic Kidney Disease (DKD)

Nabanita Kundu, Laureano Asico, George Washington Univ, Washington, DC; Pedro Jose, George Washington Univ, Washington, MD; **Sabyasachi Sen**, George Washington Univ Med Ctr, Washington, DC

Diabetic kidney disease (DKD) is one of the major vascular complications of diabetes, which is associated with glomerulosclerosis and poor perfusion. Therefore, improving the renal perfusion may help to halt or reverse the kidney injury. Here, we investigated whether transplanting mouse EPC (that has been modified by transiently silencing p53 gene using Adenovirus transduction ex-vivo), under renal capsule could improve angiogenesis and renal perfusion, by preventing EPC apoptosis in a hyperglycemic milieu. **Methods:** First, we confirmed hyperglycemia and progressive proteinuria in STZ-induced type 1 diabetic C57BL/6J mouse. Next, we transplanted 0.3 million p53-silenced EPCs,or Ad-Null-EPCs (control), bilaterally, under each kidney capsule. Another comparator was non-STZ normal mouse. Urine was collected weekly for volume and protein estimation. Renal blood flow was measured by laser Doppler. Kidneys were harvested post sacrifice and qRT-PCR were performed for targeted (towards angiogenic genes) gene expression assays. **Results**: Excess urine volume as noted in the hyperglycemic mouse models was reduced 4-fold post transplantation of p53sh-EPCs compared to null. There was no proteinuria after week 2 in p53sh-EPC transplanted mouse unlike control. Enhanced blood flow by laser doppler (3.2 fold) was also noted with delivery of p53sh-EPCs compared to null EPC. Absence of proteinuria (after 2wks) and renal blood flow measurements for p53sh group were similar to the non-STZ mouse. Interestingly, markers for neovascularization, such as eNOS (4.5 fold, p=0.002) and VEGF-A (1.5 fold, p=0.03) upregulated significantly post p53 silenced EPC transplantation compared to null EPC. CD31 staining is pending. **Conclusion:** Transient silencing of p53 gene in mouse EPCs help to improve proteinuria, diabetic polyuria and renal blood flow, most likely by increasing angiogenesis and perfusion and may have a prominent therapeutic role in DKD.

N. Kundu: None. **L. Asico:** None. **P. Jose:** None. **S. Sen:** None.

253

Hypercholesterolemia Reduces the Differentiation of Hematopoietic Stem Cells towards Vasculogenic Ly6C^{low} Monocytes in a Tet1 Dependent Pathway

Guodong Tie, Jinglian Yan, Lyne Khair, Amanda Tutto, Kate Hayes, Louis Messina, Univ Mass Medical Sch, Worcester, MA

Rationale: Hypercholesterolemia has been verified as an important risk factor of cardiovascular diseases. It has been shown to impair the post-ischemic arteriogenesis, the major physiological process in response to ischemic injury. As yet, the underlying mechanism is not fully illustrated. **Objective:** Our own data indicate that hematopoietic stem cells (HSCs) functions as a determinant in post-ischemic arteriogenesis by differentiating into vascular progenitors. However, the differentiation processes and the underlying mechanisms remain unknown. Ten eleven translocation (Tet) family are a group of enzymes initiating the demethylation of DNA. Tet1 is specifically downregulated in HSCs from hypercholesterolemic mice. Therefore, we hypothesized that Tet1 regulates the differentiation from HSCs towards vascular progenitors. Hypercholesterolemia reduces vascular specification of HSCs through a Tet1 dependent epigenetic pathway. **Methods and Results:** The ex vivo differentiation and in vivo transplantation experiments showed that HSC-originated Ly6C^{low} monocytes in peripheral blood possess the greatest capacity to differentiate into vascular cells and to improve the post-ischemic arteriogenesis. Ly6C^{low} monocyte population was specifically reduced in Tet1$^{-/-}$ mice after the induction of hindlimb ischemia, consequently resulting in significant impairment of post-ischemic arteriogenesis. Tet1 deficiency caused unique expression profiles of the genes involved in the differentiation of HSCs towards monocytes. RT-PCR showed that the expression of Tet1 was specifically downregulated in HSCs isolated from ApoE$^{-/-}$ mice. As expected, the Ly6C^{low} monocyte population was specifically reduced and the post-ischemic arteriogenesis was significantly impaired in ApoE$^{-/-}$ mice. **Conclusion:** Ly6C^{low} monocytes are the major vascular progenitors originated from HSCs. Tet1 dependent epigenetic regulation is critical in the differentiation process from HSCs towards Ly6C^{low} monocytes. Hypercholesterolemia inhibits the expression of Tet1 and subsequently impairs the differentiation from HSCs towards Ly6C^{low} monocytes, resulting in the impairment of post-ischemic arteriogenesis.

G. Tie: None. **J. Yan:** None. **L. Khair:** None. **A. Tutto:** None. **K. Hayes:** None. **L. Messina:** None.

254

The Bromo and Extraterminal Domain Protein (BET) Family Drives Endothelial-To-Mesenchymal Transition and Contributes to Vein Graft Stenosis

Mengxue Zhang, Bowen Wang, Go Urabe, Lian-Wang Guo, the Ohio State Univ, Columbus, OH

Background: Vein graft bypass remains the most commonly used open procedure for flow-limiting cardiovascular diseases. However, vein grafts are prone to stenosis, which ultimately leads to graft failure (4-year failure rate at ~43%). Previous studies have provided strong evidence supporting that dysfunctional endothelial cells (ECs) of the vein grafts contribute significantly to neoinitma formation (and hence stenosis) by undergoing EndoMT. Our group has recently shown that BRD4, a member of the BET epigenetic reader protein family, is up-regulated in the neointima lesion of stenotic failed vein grafts. Here we have determined whether BRD4, and possibly other BET proteins, would be involved in EndoMT in vein grafts, and ultimately vein graft stenosis/failure.

Method: For in vitro experiments, we treated rat primary vascular ECs with 100ng/ml TGFβ-1 (to induce EndoMT), and/or BET inhibitors (Pan inhibitor: JQ1; Domain-selective inhibitors: Olinone and RVX208), and/or siRNAs for BRD2, 3, and 4. For in vivo experiments, we used a cuff-based technique to establish jugular vein to carotid artery interposition graft in rats, and lentiviral shRNA delivery to achieve specific knockdown of BRD4 in the graft.

Results: BET pan-inhibition significantly reduced EndoMT of rat primary vascular ECs in vitro. Similar effects were observed via selective inhibition of bromodomain 2, but not bromodomain 1. Knockdown of BRD4 protein expression in vitro fully recapitulated the inhibitory effect of BET pan-inhibition on EndoMT, whereas knockdown of BRD2 and BRD3 could only lead to partial and marginal abrogation of EndoMT, respectively. In the rat vein graft model, local lentiviral delivery of BRD4 shRNA led to decrease of neointima formation.

Conclusion: BET proteins, especially BRD4, play an important role in EndoMT of vascular ECs and also neointima formation in vein grafts. Blockage of BRD4 protein could potentially serve as a novel strategy to achieve prolonged patency of vein graft conduits.

M. Zhang: None. **B. Wang:** None. **G. Urabe:** None. **L. Guo:** None.

This research has received full or partial funding support from the American Heart Association.

255
Fatty Acid Binding Protein 4, FABP4, Causes Impaired Wound Healing in Diabetes
Anna Boniakowski, Andrew Kimball, Frank Davis, Amrita Joshi, Matt Schaller, Aaron denDekker, Steve Kunkel, Katherine Gallagher, Univ of Michigan, Ann Arbor, MI

Wound healing in diabetes is impaired due to failed resolution of inflammation. Macrophages play a significant role in the establishment of a regulated inflammatory response during wounding. Macrophage function is dictated by metabolism, which alters gene expression. Recent studies suggest that a fatty acid binding protein, FABP4, may control macrophage function in diabetes by altering metabolism.
Thus, we examined whether FABP4 controls macrophage function and hence inflammation in diabetic wound healing. To investigate this, C57BL/6 mice were fed either a normal (12% saturated fat) diet or a high-fat (60% saturated fat) diet (HFD) for 12 weeks to induce physiologic "pre-diabetes." Wounds were created and CD3-CD19-NK1.1-CD11b+ cells (macrophages) were isolated each day following injury and FABP4 expression was quantified by qPCR and Western blot. We found that HFD wound macrophages demonstrated a significant increase in FABP4 gene expression and protein production on day 3 post-injury compared with controls.
To determine if FABP4 alters inflammatory gene expression in wound macrophages, we isolated wound macrophages with an FABP4 inhibitor, treated them, and analyzed for IL-1β and TNFα expression.
IL1β and TNFα gene expression were significantly reduced ($P<0.01$) in diabetic wound macrophages treated with the FABP4 inhibitor, suggesting that inflammatory gene expression can be controlled in diabetic wound macrophages through FABP4 modulation. As we have previously identified, epigenetic mechanisms often dictate gene expression during wound healing, thus we examined whether FABP4 expression in diabetic macrophages was regulated by histone modifications.
Chromatin immunoprecipitation (ChIP) analysis of the FABP4 promoter in wound macrophages revealed a significant increase in H3K4 trimethylation, an activating mark, on the FABP4 promoter in diabetic wound macrophages suggesting that epigenetic regulation may play an important role in the differential expression of FABP4 in diabetic wounds.
In conclusion, FABP4 appears to be upregulated in diabetic wound macrophages and contributes to increased macrophage inflammation. Modulation of FABP4 or its expression may help resolve inflammation in diabetic wounds and promote healing.
A. Boniakowski: None. **A. Kimball:** None. **F. Davis:** None. **A. Joshi:** None. **M. Schaller:** None. **A. denDekker:** None. **S. Kunkel:** None. **K. Gallagher:** None.

256
The Direct Characterization of Endothelial Inflammation in Patients with Psoriasis
Michael S Garshick, Tessa Barrett, Jose Scher, Andrea Neimann, Stuart Katz, New York Univ Medical Ctr, New York, NY; Xuan Li, Rockefeller Univ, New York, NY; Sanja Jelic, Columbia Univ Medical Ctr, New York, NY; James Krueger, Rockefeller Univ, New York, NY; Jeffrey S. Berger, New York Univ Medical Ctr, New York, NY

Objective: Psoriasis, an inflammatory autoimmune disease, increases the risk of cardiovascular disease (CVD). Active psoriatic disease is linked to systemic vascular inflammation, yet how this contributes to CVD is unknown. Using *in vivo* and *ex-vivo* measures of the vascular endothelium our study investigates the vascular health of psoriasis patients to better understand the mechanism(s) that predispose psoriatics to CVD.
Methods: Ten patients with active psoriasis (average age 46 years, 50% male (5 of 10), 6% [3.5% – 90%] body surface area involvement) were compared to age- and sex-matched controls. *In vivo* vascular endothelial function was assessed by brachial artery reactivity testing (BART, %) with high resolution ultrasonography. Venous endothelial cells were collected from the brachial vein using guidewires inserted through an angiocatheter and isolated with magnetic beads directed against CD146. Following collection, endothelial RNA was isolated, converted to cDNA and inflammatory gene profiling performed by RT-qPCR with Taqman probes and primers.
Results: Transcriptomic profiling of venous endothelial cells revealed upregulation of genes associated with inflammatory cytokines and chemokines (*lymphotoxin beta* [2.5 - fold], *CCL3* [3.5 - fold], and *IL-1β* [2.8 - fold], $P < 0.05$ for all) and genes related to intracellular adhesion and inflammation (*ICAM1* [2.3 – fold] and *COX-2* [1.4 – fold], $P < 0.05$ for both) in psoriatics vs. controls. Unexpectedly, endothelial nitric oxide synthase (eNOS) and phosphorylated eNOS (higher levels indicate healthy endothelial NO production) were upregulated (2 - 3 fold) in psoriatics vs. controls ($p = 0.24$, $p = 0.14$ respectively). BART was also higher in psoriatics when compared to controls ($7.1 \pm 1\%$ vs. $3.9 \pm 2.7\%$, $P = 0.03$).
Conclusion: This cross-sectional study is the first to directly examine the vascular endothelium of psoriatic patients. Compared to controls, active psoriatic disease was associated with upregulation of cytokines, chemokines and genes regulating intracellular adhesion as well as increased expression of eNOS, and increased BART. These findings suggest potential mechanisms to explain the increased prevalence of atherosclerosis and CVD risk seen in those with psoriasis.
M.S. Garshick: None. **T. Barrett:** None. **J. Scher:** None. **A. Neimann:** None. **S. Katz:** None. **X. Li:** None. **S. Jelic:** None. **J. Krueger:** None. **J.S. Berger:** None.

257
Apabetalone (RVX-208) Reduces Pathologic Cell-Cell Adhesion and Expression of Key Vascular Inflammation Markers in Monocytes, Endothelial Cells and Mouse Aorta
Laura Tsujikawa, Sylwia Wasiak, Emily Daze, Chris D Sarsons, Stephanie C Stotz, Ravi Jahagirdar, Resverlogix Corp., Calgary, AB, Canada; Deborah Studer, Kristina D Rinker, Univ of Calgary, Calgary, AB, Canada; Michael Sweeney, Jan O Johansson, Resverlogix Inc., San Francisco, CA; Norman C Wong, **Ewelina Kulikowski**, Resverlogix Corp., Calgary, AB, Canada

Apabetalone (RVX-208) is a bromodomain & extraterminal (BET) protein inhibitor, an epigenetic modifier of gene expression, currently in a phase 3 major adverse cardiac events outcomes trial in post-acute coronary syndrome patients with type 2 diabetes mellitus (DM) (BETonMACE). CVD patients enrolled in phase 2b trials (ASSERT, SUSTAIN and ASSURE) demonstrated a 44% relative risk reduction in cardiovascular disease (CVD) events (Nicholls et al. 2017). In CVD and DM, elevated circulating cytokines potentiate vascular inflammation (VI) through recruitment of leukocytes to the vascular endothelium, which contributes to atherosclerosis and plaque rupture. Previous studies demonstrated that apabetalone has potent anti-inflammatory effects on human aortic endothelial cells (HAEC) and macrophage-like U937 cells. Here we show that TNFα stimulation induced significant adhesion of THP-1 monocytes to inflamed endothelial cells, an outcome reversed by apabetalone treatment under both static (human umbilical vein endothelial cells - HUVEC) and flow (HAEC) conditions. Mechanistically, apabetalone suppressed the TNFα and IL-1β-induced expression of mRNAs of multiple endothelial cell adhesion molecules (CD44, E-selectin,

VCAM-1 and MCP-1) and inflammatory cytokines (IL-6, IL-8, IL-1β, and CSF2). Monocytes also respond to TNFα stimulation with an upregulation of inflammatory and adhesion marker expression. In THP-1 cells, apabetalone treatment significantly reduced mRNA expression of CCR1, CCR2, IL-1β, MCP-1, MYD88, TLR4, TNFα, and VLA-4. In the diet-induced obesity (DIO) mouse model that mimics metabolic syndrome, treatment with apabetalone, administered at 150 mg/kg BID for the last 16 weeks of a 22 week study, downregulated aortic adhesion markers (E-selectin and ICAM) and markers of infiltrating immune cells (CCR2 and CD11b). In summary, treatment with apabetalone causes transcriptional changes in monocytes and endothelial cells that translate into a reduction in adhesion under inflammatory conditions. We hypothesize that downregulation of VI by apabetalone may contribute to the reduction in CVD events observed in phase 2 studies. This hypothesis is currently being tested in the ongoing BETonMACE phase 3 trial.

L. Tsujikawa: Employment; Significant; Resverlogix Corp.. Ownership Interest; Significant; Resverlogix Corp. **S. Wasiak:** Employment; Significant; Resverlogix Corp.. Ownership Interest; Significant; Resverlogix Corp. **E. Daze:** Employment; Significant; Resverlogix Corp.. Ownership Interest; Significant; Resverlogix Corp. **C.D. Sarsons:** Employment; Significant; Resverlogix Corp.. Ownership Interest; Significant; Resverlogix Corp. **S.C. Stotz:** Employment; Significant; Resverlogix Corp.. Ownership Interest; Significant; Resverlogix Corp. **R. Jahagirdar:** Employment; Significant; Resverlogix Corp.. Ownership Interest; Significant; Resverlogix Corp.. **D. Studer:** None. **K.D. Rinker:** None. **M. Sweeney:** Employment; Significant; Resverlogix Corp.. Ownership Interest; Significant; Resverlogix Corp. **J.O. Johansson:** Employment; Significant; Resverlogix Corp.. Ownership Interest; Significant; Resverlogix Corp. **N.C. Wong:** Employment; Significant; Resverlogix Corp.. Ownership Interest; Significant; Resverlogix Corp. **E. Kulikowski:** Employment; Significant; Resverlogix Corp.. Ownership Interest; Significant; Resverlogix Corp.

258

Palmitate Regulates Diabetic Macrophage Inflammation via the Epigenetic Enzyme JMJD3

Frank M Davis, Andrew Kimball, Amrita Joshi, Anna Boniakowski, Matthew Schaller, Aaron DenDekker, Steven Kunkell, Bethany Moore, Katherine Gallagher, Univ of Michigan, Ann Arbor, MI

Macrophage (Mφ) plasticity, allowing for transition of Mφs from an inflammatory to a reparative phenotype, is critical for normal wound healing. In pathologic conditions, such as type 2 diabetes (T2D), wounds fail to heal due to impaired resolution of inflammation. The mechanism(s) responsible for the persistent inflammatory phenotype in T2D wounds are unclear. Prior studies have shown that the Toll-like receptor (TLR) 4 pathway regulates Mφ-mediated inflammation in tissues. Growing evidence indicates that TLR4 is a versatile receptor binding a spectrum of ligands including non-microbial ligands such as saturated fatty acids (SFAs). Given the excess SFAs in T2D, the purpose of this study was to examine the role of the SFA palmitate on TLR4 signaling and Mφ phenotype in diabetic wound healing. We have previously shown that Mφs isolated from wounds in a murine model of glucose intolerance (diet-induced obesity; DIO) maintained on a 60% high fat diet (HFD) for 12-18 weeks, display increased levels of inflammatory cytokines (IL-1β, IL-12, and TNFα) at both a gene expression and protein level. In the current study, we found that blood monocytes and wound Mφs from DIO mice display increased TLR4 receptors compared to control blood and wounds. To determine if altered metabolites in the diabetic environment impact Mφ phenotype, bone marrow derived macrophages (BMDMs) were incubated in serum isolated from DIO or control mice. BMDMs incubated with DIO serum displayed a hyperinflammatory response following LPS stimulation. Further, stimulation with the metabolite palmitate produced significantly increased IL-1β expression in DIO BMDMs compared to controls suggesting that DIO BMDMs are programmed toward an inflammatory response. To determine the mechanism, we examined several epigenetic enzymes known to affect Mφ polarization and found that palmitate stimulated expression of JMJD3, a histone demethylase, which increases inflammatory gene expression. In conclusion, these studies suggest that the diabetic milieu, specifically increased levels of the SFA palmitate, induces expression of the epigenetic enzyme, JMJD3, in Mφs and this regulates inflammatory gene expression and cell function.

F.M. Davis: None. **A. Kimball:** None. **A. Joshi:** None. **A. Boniakowski:** None. **M. Schaller:** None. **A. DenDekker:** None. **S. Kunkell:** None. **B. Moore:** None. **K. Gallagher:** None.

259

S100A9 is a Master Regulator of Inflammation and Repair After Myocardial Infarction

Goran Marinkovic, CRC, Lund Univ, Malmö, Sweden; Lisa DeCamp, Van Andel Inst, Grand Rapids, MI; Duco Koenis, Academic Medical Ctr, Univ of Amsterdam, Amsterdam, Netherlands; Laura Winkler, Van Andel Inst, Grand Rapids, MI; Vivian de Waard, Academic Medical Ctr, Univ of Amsterdam, Amsterdam, Netherlands; Jan Nilsson, CRC, Lund Univ, Malmö, Sweden; Stefan Jovinge, Van Andel Inst, Grand Rapids, MI; Aleaxandru Schiopu, CRC, Lund Univ, Malmö, Sweden

Background: The innate immune response plays an important role in cardiac repair following an acute myocardial infarction. The pro-inflammatory alarmin S100A8/A9 is released in high amounts locally and systemically during acute coronary events. Here, we studied the effects of S100A9 blockade on the innate immune responses involved in post-ischemic myocardial inflammation and repair.
Methods: We induced MI by permanent left coronary artery ligation in C57BL/6 mice, which were subsequently treated with the specific S100A8/A9 blocker ABR-238901 (30mg/kg) or with buffer for 21 days. Left ventricular function was assessed by echocardiography. Immune cell populations in the myocardium, blood, bone marrow and spleen were analysed by flow cytometry.
Results: The treatment induced progressive deterioration of the left ventricular systolic function and increased left ventricular volumes in ABR-238901-treated mice compared with controls, suggesting defective repair and negative myocardial remodelling. After 21 days of treatment, infarction size was significantly higher in mice receiving S100A8/A9 blockade (16.1±5.4% vs. 9.9±3.4%, P=0.03). S100A9 blockade inhibited proliferation of hematopoietic stem cells in the bone marrow, and reduced neutrophil and monocyte trafficking from bone marrow and spleen to the circulation and myocardium. Neutrophil and monocyte counts increased in the bone marrow and spleen of mice receiving S100A8/A9 blockade, possibly due to impaired egression. The presence of reparatory $CD11b^{+}F4/80^{+}Ly6C^{low}$ macrophages expressing the efferocytosis receptor MerTK was potently decreased in the myocardium by day 7 post-MI compared to controls (36 820 ± 2 538 vs. 72 371 ± 4 482 cells/heart, P=0.0001). The transcription factor Nur77 mediates phenotype switching from inflammatory $Ly6C^{hi}$ monocytes to reparatory $Ly6C^{lo}$ macrophages in MI. ABR-238901 lowered the expression of Nur77 in $Ly6C^{hi/int}$ monocytes *in-vivo*, total bone marrow derived monocytes *in-vitro*, and the activity of Nur77 in macrophages *in-vitro*. **Conclusions:** S100A8/A9 plays an important role in leukocyte trafficking after MI. Long-term S100A8/A9 blockade impairs efferocytosis and myocardial repair, leading to systolic dysfunction and detrimental remodelling.

G. Marinkovic: None. **L. DeCamp:** None. **D. Koenis:** None. **L. Winkler:** None. **V. de Waard:** None. **J. Nilsson:** None. **S. Jovinge:** None. **A. Schiopu:** None.

260
BAFF 60mer is Critical for B Cell Activation and BAFF Depletion Suppresses AAA Formation
Vlad Serbulea, Michael Spinosa, William Montgomery, Srabani Sahu, Prasad Srikakulapu, Coleen A McNamara, Gilbert R Upchurch Jr., Gorav Ailawadi, Norbert Leitinger, **Akshaya K Meher**, Univ of Virginia, Charlottesville, VA

Marginal zone and follicular B cells together constitute the B2 cell population, which is known to promote cardiovascular diseases by secretion of pathogenic antibodies. However, it is not completely understood how B2 cells are activated. Here, we tested the hypothesis that B cell activating factor (BAFF) activates B2 cells and promote abdominal aortic aneurysm (AAA) formation. Since BAFF can either exist as a 3mer or multimerize to a highly active 60mer, we further examined if the 60mer is critical for B2 cell-mediated pathogenicity. Anti-BAFF antibody (Ab) Sandy-2 was injected to C57BL/6 male mice at 1 mg/kg once in every 14 days. AAA was induced by topical elastase model after 14 days of Sandy-2 injection. Native PAGE and ELISA methods were used to determine binding of Abs to recombinant BAFF 3mer and 60mer. For *in vitro* experiments, B cells were isolated from murine spleens. Activation of B cells was examined by Western blotting and RNA sequencing and by surface expression of CD23 and MHC II by flow cytometry. Metabolic reprogramming of B cells by BAFF was determined by extracellular flux analysis using a Seahorse XF24 Flux Analyzer. Sandy-2 bound to both 3mer and 60mer, resulting in suppressed AAA formation (n=8, $p<0.05$) with (1) marked depletion of B2 cells, transitional 2, germinal center, plasma and memory B cells, but not transitional 1 and B1 cells, (2) a lower level of IgG1 and IgG2, and (3) a lack of immunoglobulin deposition in AAA sections. *In vitro*, the 60mer, but not the 3mer, significantly activated both NF-kB1 and -kB2 signaling, and induced expression of B2 cell activation markers and anti-apoptotic genes in B cells. Inhibitors of NF-kB signaling decreased B cell activation in response to 60mer. The 60mer treatment significantly increased mitochondrial respiration and glycolysis in B cells, supporting an activated status. An antibody against multimerization site of BAFF (anti-multiBAFF) significantly suppressed B cell activation relative to a control Ab, in a neutrophil:B cell co-culture model. The effect of the anti-multiBAFF Ab on AAA formation is currently being tested in our laboratory. Altogether, our results suggest a critical role for BAFF 60mer in skewing B cells to an activated B2 cell phenotype, supporting a pathogenic role of B2 cells in AAA.
V. Serbulea: None. **M. Spinosa:** None. **W. Montgomery:** None. **S. Sahu:** None. **P. Srikakulapu:** None. **C.A. McNamara:** None. **G.R. Upchurch Jr.:** None. **G. Ailawadi:** None. **N. Leitinger:** None. **A.K. Meher:** Ownership Interest; Significant; The idea and the reagents to inhibit BAFF 60mer formation.

This research has received full or partial funding support from the American Heart Association.

261
Proteomic Analysis of Infrarenal and Suprarenal Aorta in a Kawasaki Disease Vasculitis Murine Model Associated with Infrarenal Abdominal Aorta Dilatation and Aneurysms
Magali Noval Rivas, Rebecca A. Porritt, Depts of Pediatrics and Biomedical Science Cedars-Sinai Medical Ctr, Los Angeles, CA; Sarah J. Parker, Cedars-Sinai Heart Inst and Dept of Med, Los Angeles, CA; Moshe Arditi, Depts of Pediatrics and Biomedical Science Cedars-Sinai Medical Ctr, Los Angeles, CA

Background*:** Kawasaki Disease (KD) is a childhood vasculitis that leads to coronary artery aneurysms and is the leading cause of acquired heart diseases among children in the USA. We have reported that the *Lactobacillus casei*-cell wall extract (LCWE)-induced murine model of KD vasculitis and coronary arteritis also induces abdominal aorta dilatation and aneurysms (AAA) that involve exclusively the infrarenal (IR) region of the abdominal aorta (AA) without affecting the suprarenal (SR)-AA. AAA predisposes tissue to dissection and rupture, and is potentially life-threatening in humans. While differences in blood flow, tissue elasticity and different embryonic origin of vascular cells have been proposed among possible explanations for the preferential location of AAA disease in the IR aorta, the mechanism(s) for this is still not known. ***Objective: To determine and compare the proteomes of the IR vs SR aorta regions in naïve mice and during KD vasculitis induced AAA development. ***Methods and Results*:** By using data-independent mass-spectrometry, we compared the proteomes of the IR and SR aortas isolated from control naïve mice and LCWE-injected KD vasculitis mice. Proteomic analysis revealed significant differential expression of 340 proteins between the IR aorta from control vs KD mice, and 407 differentially expressed proteins between the IR and SR aorta regions of KD mice. The differentially expressed proteins include those involved in cytoskeletal reorganization, cell motility and adhesion as well as acute phase and oxidative stress responses. Ingenuity Pathway Analysis reveals the activation of key regulators of innate immune responses as well as the ER Stress response. TGF-β1, IL-6, and IL-1β are regulators of several protein that were activated in the IR aortic tissues. ***Conclusion:*** Proteomic differences exist between normal AA vs AAA and in IR vs SR aorta regions isolated from mice developing AAA. We show that a broad inflammatory response is generated in the aneurysm which maybe critical for the development and progression of the AAA and may provide possible novel therapeutic targets. (Supported by AHA 17SDG33671141 to MNR and NIH R01AI07272607 to MA).
M. Noval Rivas: None. **R.A. Porritt:** None. **S.J. Parker:** None. **M. Arditi:** None.

This research has received full or partial funding support from the American Heart Association.

262
Circulating Exosomes from PAD Patients Modulate Vascular Repair and Inflammation
Thomas A Sorrentino, Phat Duong, Laura Bouchareychas, Univ of California, San Francisco, San Francisco, CA; Brian E Sansbury, Pete Mitchell, Brigham and Women's Hosp, Boston, MA; Mian Chen, Allen Chung, Melinda S Schaller, Univ of California, San Francisco, San Francisco, CA; Matthew Spite, Brigham and Women's Hosp, Boston, MA; Robert L Raffai, Michael S Conte, Univ of California, San Francisco, San Francisco, CA

Objectives: Peripheral arterial disease (PAD) is a chronic disease characterized by inflammation. Recent work suggests that circulating exosomes may contribute to vascular injury and remodeling. We hypothesize that exosomes from PAD subjects negatively modulate vascular repair via miRNA and bioactive lipid mediators (LM).
Methods: Exosomes (particle size 30-100nm) were isolated from plasma of healthy (n=6) and PAD (n=6) subjects. Exosome miRNA was isolated and assessed by qPCR. Targeted metabolo-lipidomics was performed by liquid-chromatography-tandem mass spectrometry. VSMC and EC migration were assessed via scratch assay. Monocyte-derived macrophage gene expression after exposure to exosomes was assessed via RT-qPCR.
Results: Compared to healthy subjects, exosomes from PAD subjects contained lower levels of pro-angiogenic miR-126 and miR-210 (25.2 ± 6.4 vs 8.3 ± 1.7, $p<0.05$ and 0.29 ± 0.07 vs 0.08 ± 0.02, $p<0.05$, respectively). Exosomes contained arachidonic acid, eicosapentaenoic acid and docosapentanoic acid, as well as both pro-inflammatory and pro-resolving bioactive LMs and their pathway markers, including prostaglandins, leukotrienes, lipoxins, resolvins (D- and E-series) and maresins. By principle component analysis, exosome LM profiles differed significantly between

healthy and PAD subjects. Exosomes from PAD subjects increased VSMC migration (1.5±.09-fold vs 1.0±.09-fold wound closure, p<0.005) and decreased EC migration (1.5±.04-fold vs. 1.8±.06-fold wound closure, p<0.005) compared to healthy controls. Both PAD and healthy exosomes increased MDM expression of pro-inflammatory genes TNF-α and MCP-1.
Conclusion: Plasma-derived exosomes from PAD patients contain an altered profile of vascular-active miRNA and LMs and confer effects on VSMCs and ECs that may impair vessel remodeling. We describe the first known evidence that plasma exosomes contain pro-resolving LMs. Collectively these data suggest that circulating exosome-based signaling may modulate vascular inflammation and repair in PAD patients.
T.A. Sorrentino: None. **P. Duong:** None. **L. Bouchareychas:** None. **B.E. Sansbury:** None. **P. Mitchell:** None. **M. Chen:** None. **A. Chung:** None. **M.S. Schaller:** None. **M. Spite:** None. **R.L. Raffai:** None. **M.S. Conte:** Other Research Support; Significant; Metagenics, Inc.

263
Inhibition of Angiotensin II Signaling on LysM+ Myelomonocytic Cells and Their Depletion Improves Vascular Endothelial Dysfunction in Mice With Heart Failure After Myocardial Infarction
Wolf-Stephan Rudi, CTH, Univsmedizin Mainz, Mainz, Germany

Background: Myocardial infarction (MI) induced heart failure (HF) leads to impaired left ventricular function and endothelial dysfunction accompanied by a systemic inflammatory reaction. So far the effects of inhibition of angiotensin II-signaling in heart failure after MI regarding the endothelial function are not fully understood. **Methods and results:** 8-12 weeks old male C57BL/6 mice were subjected to permanent ligation of the left anterior descending artery (LAD) to induce ischemic heart failure. We measured a reduced vascular endothelial and smooth muscle function in isolated aortic segments 7d and 28d post MI in isometric tension studies. Vascular superoxide formation and vascular mRNA expression of monocyte chemoattractant protein-1 (*ccl2*), vascular cellular adhesion molecule-1 (*vcam-1*), inducible NO synthase (*nos2*), and angiotensin II receptor type 1 (*agtr1*) were increased in HF mice compared to sham. Flow cytometry analysis of aortic tissue of HF mice revealed an increased accumulation of CD45+ immune cells in the aortic wall, including CD11b+Gr-1lowF4/80+ macrophages and Ly6C+ monocytes. Diphteria toxin mediated depletion of lysozyme M positive cells starting 28d after MI using LysM-Cre-iDTR mice improved the endothelial function in HF mice. To test specific effects of ATII-signaling on endothelial function in heart failure we administered ramipril (10mg/kg bodyweight) or telmisartan (40mg/kg bodyweight), respectively, via drinking water, starting 1d after MI. After 28d, we assessed an improved vascular endothelial and smooth muscle function, less vascular superoxide production, less accumulation of CD45+ immune cells, reduced aortic expression of *ccl2, vcam-1, nos2* and *agtr1* mRNA of HF mice treated with ramipril as well as with telmisartan in comparison to non-treated HF controls. Importantly, left ventricular dimensions and ejection fraction was not different in treated and non-treated mice, implying a direct anti-inflammatory effect on the vasculature.
Conclusion: Our results suggest that vascular dysfunction post MI is at least in part mediated by angiotensin II, driving vascular accumulation of inflammatory monocytes and direct effects on vascular oxidative stress levels.
W. Rudi: Research Grant; Modest; 9600 €.

265
Oral Nitrite Supplementation Improves Rates of Wound Healing in Diabetic Mice
Karim M Salem, Nandan Nath, Ankur Aggarwal, Edith Tzeng, VA Medical Ctr and Univ of Pittsburgh, Pittsburgh, PA

Introduction: Nitric oxide (NO) is required for cutaneous wound healing. Impaired diabetic wound healing has been linked to a deficiency in local NO production and can be enhanced with NO delivery. NO is a short-lived, highly reactive molecule and local delivery is complicated by these properties. An alternate source of NO can be achieved through the ability of nitrite reductases to convert the stable NO end-product, nitrite, back to NO. We have previously demonstrated that skin and wound edge express high levels of xanthine oxidoreductase (XOR). XOR is a strong nitrite reductase. We hypothesize that dietary nitrite supplementation will improve wound healing in diabetic mice. **Methods:** Db/db mice (N>8/group) were pretreated for 1 week with sodium nitrite supplemented drinking water (50 mg/L), nitrite-free chow, or standard chow. Additionally, nitrite supplemented mice were gavaged with nitrite supplemented water (0.2 ml) every other day for the duration of the experiment. A 1 cm^2 excisional wound was created on the back of each mouse. Wounds were photographed every other day until closure and wound areas calculated with ImageJ and compared with ANOVA and Kaplan Meier.
Results: Time to complete healing was significantly different between nitrite supplemented (NS), nitrite depleted (ND), and control mice (18.9±0.7, 21.6±3.3, and 23±3.5 days, respectively, P = 0.035). NS mice reached 75% and 100% healed faster than ND or control mice (P = .009 and P = .042, respectively) [Figure]. Initial wound expansion on day 2 was decreased in NS mice compared to ND mice. XOR activity was increased in wounds compared to skin but similar between all treatment groups. **Conclusion:** Nitric oxide is a critical component of wound healing. Oral systemic nitrite supplementation improves diabetic wound healing in mice. Dietary nitrite may be an inexpensive and safe method of augmenting NO production through wound XOR expression to improve wound repair.

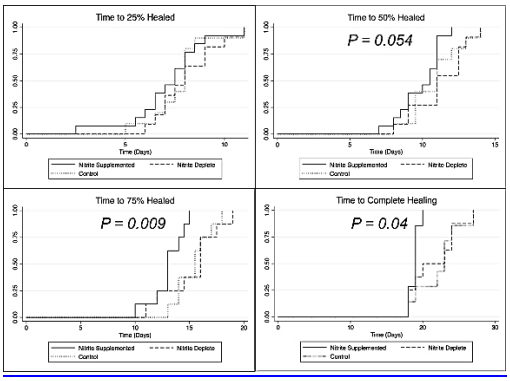

K.M. Salem: None. **N. Nath:** None. **A. Aggarwal:** None. **E. Tzeng:** Research Grant; Significant; VA Merit Award, Vascular Surgery Research T32 Training Grant.

267
Testosterone to Estradiol Ratio Reflects Systemic and Plaque Inflammation and Predicts Future Cardiovascular Events in Men with Severe Atherosclerosis
Ian David van Koeverden, Marie de Bakker, Gert J. de Borst, Gerard Pasterkamp, Hester den Ruijter, UMC Utrecht, Utrecht, Netherlands

Objective: The effects of testosterone on cardiovascular disease (CVD) as reported in literature have been ambiguous. Recently, the interplay between testosterone and estradiol as assessed by testosterone/estradiol (T/E2) ratio was suggested to be better informative on the normal

physiological balance. Considering the role in CVD, we hypothesized that a low T/E2 ratio in men with CVD is associated with increased inflammation, a more unstable plaque and a worse cardiovascular outcome.
Approach: Testosterone and estradiol concentrations were determined in blood samples of 709 male carotid endarterectomy patients included in the Athero-Express Biobank Study. T/E2 ratio was associated with baseline characteristics, atherosclerotic plaque specimens, inflammatory biomarkers and three-year follow-up information.
Results: Patients with low T/E2 ratio had more unfavorable inflammatory profiles compared to patients with high T/E2 as observed by higher levels of C-reactive protein (CRP) (3.08 µg/mL vs. 1.21 µg/mL (p<0.001)) and higher leukocyte counts (8.95*109/L vs. 7.84*109/L (p<0.001)) in blood. In atherosclerotic plaques, a negative association between T/E2 ratio and number of neutrophils (B=-0.56(p=0.010)), smooth muscle cells (B=-0.049(p=0.046)), interleukin-6 (IL-6) (B=-0.15 p=0.009) and Il-6receptor (B=-0.13 p=0.024) was found. Decreased T/E2 ratio showed an overall trend towards histological features that represent the vulnerability of atherosclerotic lesions. Furthermore, in multivariate cox regression analysis, low T/E2 ratio was independently associated with an increased risk for major cardiovascular events (MACE) during three-year follow-up (HR 1.77 (95%CI: 1.08 - 2.90 p=0.023)).
Conclusion: In male patients with manifest atherosclerotic disease, low T/E2 ratio was associated with increased systemic inflammation, increased inflammatory plaque proteins and an increased risk of future major cardiovascular events as compared to men with normal T/E2 ratio. Normalization of T/E2 ratio may be a useful tool for the secondary prevention of CVD in men.
I.D. van Koeverden: None. **M. de Bakker:** None. **G.J. de Borst:** None. **G. Pasterkamp:** None. **H. den Ruijter:** None.

268
Macrophage Depletion Attenuated Renal Injury and Fibrosis in Angiotensin II Hypertensive Mice
Lei Huang, Shenyang Medical Univ, Shenyang, China; Aimei Wang, Weihong Li, Chang Liu, Jinzhou Medical Univ, Jinzhou, China; Yueyang Liu, Zhihnag Yang, Shenyang Medical Univ, Shenyang, China; **Ming-Sheng Zhou**, Shenyang Medical Univ & Jinzhou Medical Univ, Shenyang, China

Monocyte/macrophage recruitment is closely associated with the degree of hypertensive renal injury. Here we investigated the direct role of macrophage using Liposome encapsulated clodronate (LEC) to deplete monocyte/macrophage in Ang II-induced hypertensive renal injury. C57BL/6 mice were treated with a pressor dose of angiotensin II (Ang, 1.4 mg/kg/day by mini-pump) plus LEC or the PBS-liposome for two weeks. Ang II mice developed hypertension (186 ± 5 vs. 110 ± 4 mmHg in control, p<0.05) , albuminuria (33.9 ± 4.9 vs. 83.6 ± 2.3 µg/mg creatinine in control, p<0.05), glomerulosclerosis and renal fibrosis. LEC reduced Ang II-induced albuminuria (59.6 ± 1.9 µg/mg creatinine, p<0.05) and protected against renal structural injury with a mild reduction in systolic blood pressure (153 ± 3 mmHg, p<0.05). Ang II significantly increased renal macrophage infiltration ($MOMA2^+$ cells) and the protein expression of renal tumor necrosis factor α and interleukin β1, which were significantly reduced in Ang II mice treated with LEC. Ang II increased renal oxidative stress (as demonstrated by increased oxidative fluorescence densities, NADPH oxidative activity and the protein expression of NADPH oxidase subunits gp91phox and p22phox) and the expression of profibrotic factors transform growth factor β1 and fibronectin. Ang II also inhibited the phosphorylation of endothelial nitric oxide synthesis (eNOS, ser1177). LEC revised most of the changes in the Ang II-induced molecules as mentioned above. Our results suggest that renal macrophage is a main mediator to contribute to Ang II-induced hypertensive renal injury and fibrosis, the underlying mechanisms may involve reduction in macrophage-drove renal inflammation and restoration of the balance between renal oxidative stress and eNOS. These findings may lead us to develop a novel therapy directed at targeting the infiltration of macrophages or the macrophages-derived cytokines for treatment of hypertensive renal diseases.
L. Huang: None. **A. Wang:** None. **W. Li:** None. **C. Liu:** None. **Y. Liu:** None. **Z. Yang:** None. **M. Zhou:** Research Grant; Significant; NSFC81470532, 86670384.

269
Vascular Injury-Induced ATP release leads to IL-1β Production and Endothelial Dysfunction
Joyce Cheung-Flynn, Weifeng Luo, Christy M Guth, Padmini Komalavilas, Colleen M Brophy, Vanderbilt, Nashville, TN

Introduction Injury leads to inflammation and modulates vein graft responses that result in vein graft failure. Previous work has shown that vascular injury (mechanical and chemical) leads to membrane injury, ATP release, and endothelial dysfunction. These studies were performed to determine the role of inflammation after vascular injury on endothelial dysfunction.
Methods Endothelial-dependent responses (EDR) of isolated rat aorta (RA) were determined in a muscle bath. IL-1β production in response to exogenous ATP treatment was determined in TNFα and IFNγ-primed human saphenous vein endothelial cells (HSVEC) in the presence and absence of P2X7R inhibitors A438079 (A43) and oxidized ATP (oATP), the ATP hydrolyzing enzyme apyrase, the p38MAPK inhibitor SB203580 (SB), and the MAPKAP kinase (MK2) inhibitor MMI-0100. p38MAPK and MK2 phosphorylation, and VCAM protein levels were determined by immunoblotting.
Results ATP treatment led to impaired EDR that was partially restored by oATP and apyrase (A). ATP treatment of HSVEC led to p38MAPK and MK2 activation (data not shown), delayed (2 hrs) IL-1β production (B) and increased VCAM expression (24hrs after treatment, C). P2X7R antagonism and p38MAPK/MK2 inhibition inhibited IL-1β production (D). VCAM expression was reduced by P2X7R antagonism. IL-1β treatment of RA (3hrs) led to impaired EDR (D).
Conclusions These data suggest that injury, leading to release of ATP and activation of the P2X7R/p38MAPK/MK2 signaling axis, leads to increases in the inflammatory cytokine IL-1β and expression of the endothelial inflammatory marker VCAM. Phosphorylated MK2 is known to stabilize cytokines, hence these data provide a direct link between vascular injury and endothelial inflammatory responses. Finally, IL-1β directly impaired EDR, suggesting that these data also provide a plausible mechanism for injury induced endothelial dysfunction (E).

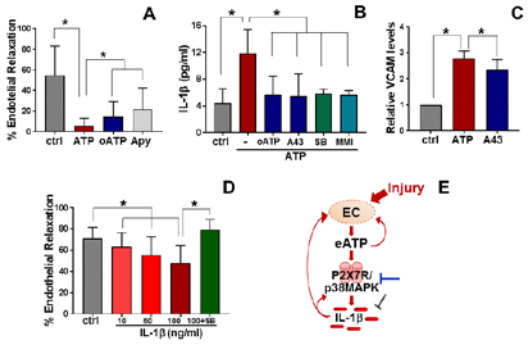

J. Cheung-Flynn: None. **W. Luo:** None. **C.M. Guth:** None. **P. Komalavilas:** None. **C.M. Brophy:** None.

270
Microsomal Prostaglandin E Synthase-1 and Endothelial EP4 Receptor Reduces Myocardial Ischemia-reperfusion Injury via Improving Microcirculatory Perfusion
Liyuan Zhu, Chuansheng Xu, Huifeng Hao, Sheng Hu, Qing Wan, Miao Wang, State Key Lab of Cardiovascular Disease,Peking Union Medical Coll, Beijing, China

Objective—Myocardial (M) ischemia/reperfusion (I/R) injury limits the efficacy of reperfusion therapy in patients with myocardial infarction (MI) and contributes to the development of heart failure. Nonsteroidal anti-inflammatory drugs (NSAIDs) that inhibit both cyclooxygenase (COX)-1 and COX-2, or those selective for COX-2 inhibition, are associated with an increased risk of heart failure. Although suppression of COX-2-derived prostaglandin (PG) I_2 predisposes cardiovascular risks, it remains unknown whether microsomal (m) PGE synthase (S)-1, a therapeutic target alternative to COX-2, might participate in MI/R injury.
Approach and Results— Mice deficient in COX-1 or -2, mPGES-1, or endothelial PGE receptor-4 (EP4), together with pharmacological interventions, were utilized in a mouse model of MI/R. Microvascular perfusion was assessed in vivo using laser Doppler flow technique. COX-1 deficiency reduced biosynthesis of PGE_2 and increased infarct size in the heart after MI/R. Deletion of mPGES-1 also depressed PGE_2 while exacerbated MI/R injury. Cardiac perfusion was impaired by mPGES-1 deletion following reperfusion, without change in baseline flow. Consistently, mPGES-1 deletion abolished arteriolar dilation in I/R, and mPGES-1-derived PGE_2 acting on EP4 receptor restrains myeloid cell adhesion to endothelial cells in vitro and limits leukocyte adhesion to vasculature in I/R in vivo. Endothelium-restricted deletion of EP4 receptor impaired microcirculatory perfusion and exacerbated cardiac injury in MI/R. By contrast, treatment with misoprostol, a clinically available PGE_2 analogue, improved cardiac microcirculation post MI and protected against I/R injury.
Conclusions—mPGES-1-derived PGE_2 and endothelial EP4 receptor protect against MI/R injury via preserving cardiac microcirculation. mPGES-1 inhibitors may harm microcirculation in patients with acute MI undergoing revascularization. Inhibition of COX-1-derived PGE_2 may contribute to the cardiovascular side effects of NSAIDs in the setting of I/R.
Key Words: myocardial infarction, ischemia reperfusion, cyclooxygenase, prostaglandin E synthase-1, PGE_2, EP4, microcirculation, endothelium
L. Zhu: None. **C. Xu:** None. **H. Hao:** None. **S. Hu:** None. **Q. Wan:** None. **M. Wang:** None.

273
Cell Mimetic Liposomal Nanocarriers Tailored for Vascular Smooth Muscle Cell Molecular Therapeutics
Samuel I Mattern-Schain, Univ of Tennessee, Knoxville, TN; Richard K Fisher, **Lauren B Grimsley**, Stacy S Kirkpatrick, Oscar H Grandas, UT Graduate Sch Med, Knoxville, TN; Michael D Best, Univ of Tennessee, Knoxville, TN; Deidra J Mountain, UT Graduate Sch Med, Knoxville, TN

Introduction: Our laboratory aims to develop biocompatible nanocarriers for molecular therapeutics aimed at vascular pathology. We have previously established a liposome platform that is an effective delivery system for RNAi in vascular smooth muscle cells (VSMC). Tailoring liposome membranes to mimic vascular cell membrane lipid constituents may be a promising strategy for increased delivery to target cells. Here we test our previously established liposome platform with the incorporation of naturally occurring signaling lipids known to influence vascular cell function as a method to increase VSMC association.
Methods: Established cell-penetrating neutral liposomes (R8-PLPs) were assembled and fluorescently tagged as previously described. The propensity of diacylglycerol (DAG) and/or phosphatidylserine (PS) to increase the association of R8-PLP to VSMCs was tested by the incorporation of gradient percentages DAG/PS alone and in combination at 5-20% membrane occupancy. Liposome stability and siRNA encapsulate retention was analyzed via dynamic light scattering and Ribo-green, respectively.
Results: DAG and PS incorporation increased VSMC association of R8-PLP, with 10% PS increased over all other groups (P10; Fig1A). Combinatorial formulations were screened for optimal DAG content with PS fixed at 10%. DAG20%+PS10% (D20P10) performed best, with increased VSMC association over all other combinatorial groups or independent P10 modification (Fig1B). Stability profiles were consistent (~50nm size and ~80% drug retention) and not significantly different among groups.
Conclusion: Signaling lipid incorporation into the nanocarrier architecture potentiates VSMC association of established R8-PLP liposomes, without sacrificing stability or drug retention. These results suggest cell mimetic tuning of liposomes to generate specificity and increase delivery efficacy is a viable strategy for advancing targeted liposomal drug delivery.

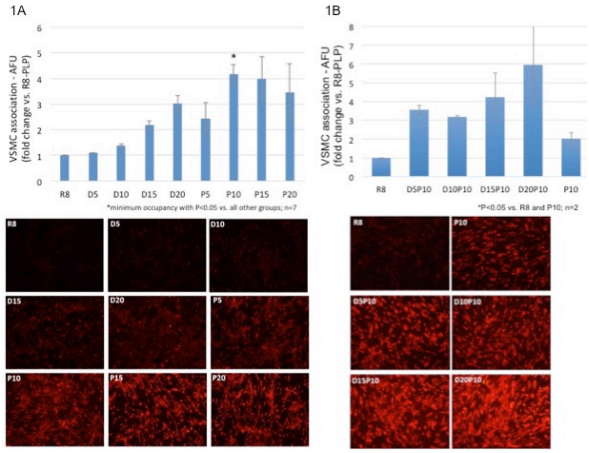

S.I. Mattern-Schain: None. **R.K. Fisher:** None. **L.B. Grimsley:** None. **S.S. Kirkpatrick:** None. **O.H. Grandas:** None. **M.D. Best:** None. **D.J.H. Mountain:** None.

274
Cd36-mediated Lipid Metabolism Promotes Endothelial Cell Angiogenic Function and Vascular Repair Ina Hindlimb Ischemia Mouse Model
Lara Bou Khzam, Ni-Huiping Son, Ira J Goldberg, New York Univ, New York, NY

Under physiological conditions, endothelial cells (ECs) play an important role in maintaining vascular integrity by acting as non-thrombogenic and non-inflammatory cells. ECs also mediate vascular repair and angiogenesis, a process by which new blood vessels are formed from pre- existing blood vessels. Hyperglycemia has been shown to alter EC angiogenic potential. However, few studies have investigated the effect of fatty acids (FAs) on EC growth and migration. CD36 is an important FA transporter expressed by ECs. We hypothesize that circulating FAs regulate angiogenic function in a CD36-dependent manner. To test this, we studied EC proliferation and migration of control and CD36 deficient mouse heart and lung ECs. siRNA- and ASO-mediated knockdown of CD36 in ECs treated with oleic acid (OA) did not affect EC proliferation. However, in wound healing experiments, OA significantly increased the migration of ECs, whereas CD36 knockdown prevented the OA-induced increase in wound healing potential. In EC transwell migration experiments, OA stimulation, which increased the recruitment and migration of ECs, was not found after CD36 knockdown. Thus, our *in vitro* results suggest that loss of CD36 hinders EC angiogenic function. In control mice, 21-day recovery post-hindlimb ischemia increased EC content in muscle, as assessed by measuring CD31 and MMP9 expression, compared to that found at

baseline in normal muscle. Mice with EC-specific CD36 deletion also showed increased CD31 and MMP9 expression. However, no further increase was found in EC-specific CD36 knockout ischemic muscle compared to normal muscle. Thus, our *in vivo* data suggest that the response to ischemia—increasing EC marker expression—is lost with EC-specific CD36 deficiency.
L. Bou Khzam: None. **N. Son:** None. **I.J. Goldberg:** None.

275
Identification of Smooth Muscle Derived Macrophages as a Novel Potential Source of Tissue Resident Macrophages
Gamze B Bulut, Anh T Nguyen, Univ of Virginia, Charlottesville, VA

Smooth muscle cells (SMC) are not terminally differentiated but display remarkable plasticity to differentiate into other cell types in response to injury or chronic disease states such as atherosclerosis. Of major significance, we previously demonstrated that nearly a third of the macrophage marker positive cells within advanced mouse and human atherosclerotic plaques are of SMC not myeloid origin. These transitions in SMC phenotype are dependent on the stem cell pluripotency gene Klf4 and play a critical role in overall lesion pathogenesis. Since atherosclerosis happens well beyond our reproductive ages, we hypothesized that transitions of SMC to a macrophage-like state also occur in normal mice and play some protective role that is likely to be evolutionarily conserved. To test this hypothesis, we performed flow cytometric evaluations of transitions of SMC to a macrophage-like state within various microvascular tissue beds of our Myh11ERT2Cre eYFP SMC-specific lineage tracing mice. Remarkably, we found that 15-20% of eYFP+ cells within the stromovascular fraction of epididymal and mesenteric fat depots were CD45+ of which >90% were also positive for the macrophage markers CD11b, F4/80, and Lgals3. Similar SMC derived macrophage-like cells were also observed in skeletal muscle and subcutaneous fat, but at much reduced levels. The percentage of SMC-derived macrophages in pathological fat depots increased about 2-fold upon four-weeks of diet-induced obesity (DIO). Interestingly, these macrophages appear to exhibit an M2-like polarization in that they were CD206+ but CD86-. We are currently ascertaining if the frequency or function of these SMC derived macrophage like cells within pathological fat depots is altered by SMC specific conditional knockout of Klf4, and/or if this is associated with alterations in insulin sensitivity or glycemia. In summary, we have discovered a novel source of tissue resident macrophages which we postulate play a protective role in regulating the inflammatory and metabolic properties of pathological adipose tissue depots.
G.B. Bulut: None. **A.T. Nguyen:** None.

276
Excessive Plasmin Activity Compromises Hepatic Sinusoidal Vascular Integrity After Acetaminophen Overdose
Siqi Gao, Robert Silasi-Mansat, Mandi Behar, Florea Lupu, **Courtney Griffin**, Oklahoma Medical Res Fndtn, Oklahoma City, OK

The serine protease plasmin degrades extracellular matrix (ECM) components both through direct cleavage and indirectly through activation of matrix metalloproteinases. We previously reported that excessive plasmin activity and subsequent ECM degradation causes hepatic sinusoidal fragility and lethal hemorrhage in developing embryos. We now report that excessive plasmin activity in a murine acetaminophen (APAP) overdose model likewise compromises postnatal hepatic sinusoidal vascular integrity. We found that hepatic plasmin activity is upregulated significantly at 6 hr after APAP overdose. This plasmin upregulation precedes both degradation of the ECM component fibronectin around liver vasculature and bleeding from centrilobular sinusoids. Importantly, administration of the pharmacological plasmin inhibitor tranexamic acid or genetic reduction of plasminogen, the circulating zymogen of plasmin, ameliorates APAP-induced hepatic fibronectin degradation and sinusoidal bleeding. In conclusion, these studies demonstrate that reduction of plasmin stabilizes hepatic sinusoidal vascular integrity after APAP overdose.
S. Gao: None. **R. Silasi-Mansat:** None. **M. Behar:** None. **F. Lupu:** None. **C. Griffin:** None.

277
Lung Gene Transfer with Sarcoplasmic Reticulum Calcium ATPase Prevent Disease Progression in Pulmonary Arterial Hypertension
Carlos Bueno-Beti, Michael G M Katz, Anthony S Fargnoli, Erik Kohlbrenner, Charles R Bridges, Yassine Sassi, Roger J Hajjar, **Lahouaria Hadri**, Mount Sinai Sch Med, New York, NY

Pulmonary arterial hypertension (PAH) is a fatal disease characterized by vascular remodeling leading to high pulmonary arterial pressure (PAP) and right ventricular (RV) heart failure. Gene therapy is a promising approach to treat PAH. The most used monocrotaline (MCT) rat model of PAH does not mimic the pathophysiology of the PAH in humans. A refined rat model, the pneumonectomy plus MCT (PNT-MCT), displays all of the features of PAH and most importantly plexiform lesions whereby therapeutics aim to reverse. In this study, we investigated whether intratracheal delivery of sarcoplasmic reticulum calcium ATPase (SERCA2a) gene reverse the severity of PAH in the PNT-MCT model. Left pneumonectomy was performed in rats. One week later, the animals received the MCT injection. At 3 weeks, the severity of PAH disease was confirmed. Thereafter, PNT-MCT rats received either intratracheal delivery of gene construct with adeno-associated virus/SERCA2a (AAV1/SERCA2a) or saline. Hemodynamic parameters were determined by magnetic resonance imaging (MRI) and RV catheterization. RV hypertrophy, heart and lung fibrosis were assessed. Molecular biology assays for gene expression and immunostaining were used to quantify SERCA2a and disease markers. Four weeks after gene delivery, RV function was improved in AAV1.SERCA2a treated-animals with an increase of stroke volume and ejection fraction compared to saline group (275 ± 22 µl vs. 192 ± 22 µl and 56 ± 3 µl vs. 44 ± 3 µl, $p<0.05$), while RV end systolic volume was decreased (199 ± 16 µl vs. 283 ± 24 µl, $p<0.05$). Hemodynamic parameters including mean pulmonary pressure were improved in AAV1.SERCA2a group (26 ± 3 mmHg vs. 61 ± 6 mmHg and 21 ± 3 mmHg vs. 41 ± 3 mmHg respectively, $p<0.01$) compared to control. RV hypertrophy was reduced in AAV1.SERCA2a treated animals (0.37g ± 0.03 vs. 0.63g ± 0.02, $p<0.0001$). All serotypes of collagen demonstrated decreased expression after AAV1/SERCA2a administration. Histologically, the animals after gene therapy showed a significant regression of plexiform lesions from grade 4 to grade 1-2. In conclusion, intratracheal administration of AAV1/SERCA2a gene can reverse the severe PAH phenotype and may be considered as a potential treatment.
C. Bueno-Beti: None. **M.M. Katz:** None. **A.S. Fargnoli:** None. **E. Kohlbrenner:** None. **C.R. Bridges:** None. **Y. Sassi:** None. **R.J. Hajjar:** None. **L. Hadri:** None.

278
Developmental Contractile Function Modulates Notch1b-Mediated Valvular Leaflet Development
Jeffrey J. Hsu, Junjie Chen, UCLA, Los Angeles, CA; Vijay Vedula, Stanford Univ, Stanford, CA; Cynthia Chen, Juhyun Lee, Yin Tintut, Linda L. Demer, UCLA, Los Angeles, CA; Alison Marsden, Stanford Univ, Stanford, CA; Tzung K. Hsiai, UCLA, Los Angeles, CA

Cardiac valve formation is a complex process affected by blood flow, but the mechanotransduction mechanisms underlying valvulogenesis remain incompletely understood. Using four-dimensional (4-D) light-sheet imaging, we evaluated the effects of pharmacological and genetic

hemodynamic modulation on ventriculobulbar (VB) valve formation in the outflow tracts (OFT) of transgenic *Tg(fli1a:GFP)* zebrafish embryos. Treatment with isoproterenol increased heart rate and cardiac contractility, increased *Notch1b* activity in the OFT, and resulted in the development of hyperplastic VB valve leaflets. While metoprolol treatment reduced heart rate without affecting contractility, there were no significant differences in *Notch1b* expression in the OFT or valve morphology. Meanwhile, BDM treatment significantly reduced heart rate and contractility, reduced *Notch1b* expression in the OFT, and prevented the formation of normal VB valve leaflets. Similarly, no VB valve leaflets were seen in the *cloche* mutant or *Tnnt2a* MO-injected embryos. Additionally, increasing blood viscosity by micro-injection of embryos with *EPO* mRNA increased *Notch1b* activity in the OFT and led to hyperplastic VB valve leaflets, but decreasing blood viscosity by *gata1a* MO micro-injection did not have any significant effect. Further, activation of the Notch signaling pathway with micro-injection of *NICD* mRNA resulted in hyperplastic VB valve leaflets. By integrating advanced optics with zebrafish genetics at the interface of developmental cardiac mechanics, we provide mechanotransduction insights into cardiac valve development within the OFT.

J.J. Hsu: None. **J. Chen:** None. **V. Vedula:** None. **C. Chen:** None. **J. Lee:** None. **Y. Tintut:** None. **L.L. Demer:** None. **A. Marsden:** None. **T.K. Hsiai:** None.

This research has received full or partial funding support from the American Heart Association.

279

Role of PDE10A in Arterial Calcification

Yujun Cai, Xue-lin Wang, Tonghui Lin, Raul J Guzman, BI Deaconess Medical Ctr, Boston, MA

Vascular calcification is highly prevalent in patients with diabetes mellitus and chronic kidney disease. When located in the media, arterial calcification is strongly associated with increased cardiovascular morbidity and mortality. The second messenger cyclic nucleotides cAMP and cGMP, controlled by distinct cyclic nucleotide phosphodiesterase (PDE) isozymes, play important regulatory roles in a variety of human diseases. Using a qPCR PDE array, we found that PDE10A was the most highly induced among all PDE genes in a rat model of medial artery calcification. PDE10A expression was markedly increased in calcified arteries from rats with chronic kidney disease and in tibial arteries from patients with peripheral artery disease. Interestingly, it co-localized with osteogenic markers in these specimens. *In vitro*, PDE10A knockdown using siRNA, and inhibition with a synthetic inhibitor markedly reduced osteogenic transformation and calcification of vascular SMC exposed to high phosphate levels. Aortic rings from PDE10A knockout mice showed significantly less Pi-induced medial calcification than those from wild-type controls. Deficiency of PDE10A also reduced medial calcification in a mouse medial calcification model *in vivo*. Mechanistic studies to elucidate the signaling alterations invoked by PDE10A are ongoing. These findings suggest that PDE10A plays a crucial role in the development of medial artery calcification, and that targeting it may provide a novel therapeutic strategy for reducing medial calcification and improving outcomes in patients with PAD.

Y. Cai: None. **X. Wang:** None. **T. Lin:** None. **R.J. Guzman:** None.

280

Are There Sex-specific Differences in Arteriovenous Fistula Maturation?

Tambudzai Kudze, Toshihiko Isaji, Shun Ono, Takuya Hashimoto, Bogdan Yatsula, Haidi Hu, Haiyang Liu, Alan Dardik, Yale Sch of Med, New Haven, CT

The arteriovenous fistula (AVF) is the preferred method of dialysis access due to its proven superior long term outcomes. However, women have lower rates of AVF maturation than men (38% vs. 60%), preventing optimal AVF use. Using a novel mouse AVF model that recapitulates human AVF maturation, we tested the hypothesis that there is a difference in male and female AVF maturation. Aortocaval fistulae were created in male and female C57BL/6 mice (9-10wk). At days 0, 3, 7, 14 and 21, aortic and IVC diameters and flow velocity were monitored by Doppler ultrasound. We then calculated shear stress. Using qPCR, we measured messenger RNA (mRNA). AVF were examined at day 21 and AVF wall thickness was measured by computer morphometry.

Female mice weighed less preoperatively and at day 21 ($p<0.05$). They also had larger suprarenal aortic diameter ($p=0.002$) but smaller infrarenal IVC diameter ($p<0.05$) at baseline. After AVF creation, there was similar dilation of the infrarenal aorta and IVC in both male and female mice ($p>0.05$). Infrarenal IVC mean velocity was decreased in female mice at baseline and at day 3, 14 and 21 ($p<0.05$). Similarly, mean laminar shear stress magnitude in the infrarenal IVC was decreased in female mice at day 7 ($p=0.03$), 14 ($p=0.04$) and 21 ($p=0.01$). There was no difference in the infrarenal aorta shear stress magnitude ($p=0.80$). mRNA of KLF2, a marker of laminar shear stress, was decreased in the venous limb of female AVF on day 21 ($p=0.048$). Preoperatively, female mice had thinner venous walls ($p=0.035$). However, at day 21, AVF wall thickness was similar ($p=0.18$).

AVF in female mice have lower magnitudes of laminar shear stress, lower expression of KLF2 mRNA and a higher percent increase in wall thickness. These findings suggest a mechanism underlying the diminished rates of AVF maturation in women.

T. Kudze: None. **T. Isaji:** None. **S. Ono:** None. **T. Hashimoto:** None. **B. Yatsula:** None. **H. Hu:** None. **H. Liu:** None. **A. Dardik:** None.

281

miR-155: a Negative Modulator of Acute Oscillatory Shear Stress (OSS)-induced Vascular Inflammation and Dysfunction

Islam Mohamed, Coll of Pharmacy, California Northstate Univ, Elk Grove, CA; Sheena Thomas, Charles Searles, Div of Cardiology, Emory Univ, Atlanta, GA

Introduction: Shear-sensitive micro-RNAs play an integral role in dictating vascular wall pro-inflammatory response and development of atherosclerosis. Previously, our group and others have identified an inverse relationship between micro-RNA-155 (miR-155) expression and inflammation in atheroprone areas of chronic low magnitude oscillatory shear stress (OSS) in vasculature and in-vitro. **Hypothesis:** we hypothesized that miR-155 negatively regulates acute OSS-induced vascular inflammation and dysfunction, via modulation of the MAPK-ETS-1 pathway. **Methods:** 12-week old C57B/6J wild type (WT) and miR-155 knockout mice (KO) were subjected to abdominal aortic coarctation (AAC), a unique model of acute induction of OSS, for 3-7 days. Downstream acute OSS segments were compared to upstream unidirectional shear stress (USS) segments of thoracic aorta using RT-PCR, western blot and two-way ANOVA followed by Tukey's multiple comparison analyses. **Results:** In WT mice, acute OSS induced vascular inflammation evidenced by upregulation of MCP-1 and VCAM-1 expression in OSS segments compared with USS. This was associated with loss of vascular barrier function as evaluated by extravasation of Evans-blue dye assay along

with increased MMP-9 and MMP-3 expression. However, vascular miR-155 levels were also higher in OSS segments compared with USS (n=6-12, P<0.05). Nevertheless, miR-155 KO mice showed enhanced expression and activation of ERK and p-38 MAPKs and downstream ETS-1, VCAM-1 and MMP-9 expression in OSS segments compared with USS versus WT controls (n=3-4, P<0.05). Tail vein injections of miR-155 overexpressing lentivirus particles in WT mice after AAC resulted in further upregulation of miR-155 and abolished OSS-induced upregulation of p-38 and downstream ETS-1, VCAM-1 and MMP-9 expression in OSS segments compared with USS versus scramble controls (n=5-6, P<0.05). **Conclusions:** Despite the early upregulation of shear-sensitive miR-155, our data suggest that miR-155 serves as a negative feedback regulator to acute OSS-induced vascular inflammation via inhibition of p-38 and ETS-1. Further studies are in progress to evaluate the effect of exogenous miR-155 on OSS-induced oxidative stress and vascular function, which can serve as basis for developing novel miRNA-based therapeutic modalities.

I. Mohamed: None. **S. Thomas:** None. **C. Searles:** None.

This research has received full or partial funding support from the American Heart Association.

282

Differential Effects of Thrombospondins on Angiogenesis Gene Expression: Contribution of Statins

Furqan Muqri, Alex Helkin, Kristopher G Maier, Vivian Gahtan, SUNY Upstate Medical Univ, Syracuse, NY

Objectives: Angiogenesis is important for vascular repair and of interest for treating peripheral arterial disease (PAD). Thrombospondins (TSP) are matricellular proteins involved in PAD. TSP-1 is the first endogenous angiogenesis inhibitor found. TSP-2, which is structurally similar, is also anti-angiogenic. TSP-5 (Cartilage Oligomeric Matrix Protein) differs structurally and may not be anti-angiogenic. Statins have pleiotropic vascular effects that impact TSPs. We studied the effects of TSPs and statin on endothelial cells (ECs). Hypothesis: TSP-1 and -2 induce anti-angiogenic genes, and inhibit EC tube formation while TSP-5 or statin induce pro-angiogenic genes and stimulate EC tube formation. **Methods**: ECs were exposed to serum free medium (SFM), TSP-1, -2, or -5 (20µg/mL) for 6 hours with or without 24 hour statin (0.5µM) pre-treatment. qrtPCR was done on 94 angiogenesis related genes. Analysis was by t-test and ANOVA, $p < 0.05$ was significant. Canonical pathways were examined with IPA software. EC tube formation and disruption were assessed with Matrigel and SFM, TSP-1, -2, or -5 (20µg/mL) treatment with or without statin. **Results**: TSP-1 and -2 downregulated pro-angiogenic genes while TSP-5 both up-regulated and downregulated pro-angiogenic genes (Fig. 1). All TSPs were affected by statin. TSP-1, and -2 decreased EC tube formation (47% and 28% respectively, p<0.05) and disrupted EC tubes (36% and 26% respectively, p<0.05). Addition of statin trends towards attentuation of TSP tube disruption. TSP-5 had no effect on EC tubes formation. **Conclusions**: TSP-1, -2, and -5 impact EC angiogenesis pathways. TSP-1 and -2 downregulated pro-angiogenic genes in similar pathways. TSP-5 upregulated pro-angiogenic genes, and statin augmented this effect. TSP-1 and -2 are anti-angiogenic while TSP-5 is not *in vitro*. The role of statin in EC tube formation is unclear but statin does impact TSP regulation of angiogenesis gene expression and thus further studies are needed.

Figure 1:

	TSP-1	TSP-2	TSP-5
Upregulated	0 genes	0 genes	1 gene HEY1 (2.923)
Downregulated	7 genes ANGPTL2 (0.567), CTGF (0.379), GRN (0.643), ITGAV (0.516), ITGB3 (0.377), NRP1 (0.479), PDGFRB (0.263),	2 genes CXCL12 (0.168), PDGFRB (0.296),	4 genes ANGPT4 (0.422), CXCL12 (0.565), ITGAV (0.638), PDGFRB (0.353),
Detectable	2 genes FLT3, ANGPTL3	4 genes FGF4, FLT3, LECT1, PRL	3 genes FLT3, LEP, PRL
Undetectable	9 gene ANGPTL1, COL15A1, FGA, FGF4, LECT1, LEP, PLG, PRL, SERPINB5	9 gene ANGPTL1, ANGPTL3, COL15A1, FGA, LEP, PLG, PROK1, TNMD, TNNI1	9 gene ANGPTL1, ANGPTL3, COL15A1, FGA, FGF4, LECT1, PLG, PROK1, TNNI1

	Control + Fluvastatin	TSP-1 + Fluvastatin	TSP-2 + Fluvastatin	TSP-5 + Fluvastatin
Upregulated	3 genes PECAM1 (1.936), TEK (1.947), TIE1 (1.258),	0 genes	1 gene ADAMTS1 (3.062),	4 genes ANG (3.267), ANGPTL4 (1.874), EDG1 (3.388), FLT1 (2.991),
Downregulated	8 genes CTGF (0.125), CXCL12 (0.230), FOXC2 (0.513), FST (0.522), HGF (0.330), ITGB3 (0.545), PDGFRB (0.501), TNF (0.028),	10 genes CD44 (0.371), CTGF (0.144), CXCL12 (0.108), ECGF1 (0.335), EDIL3 (0.175), ITGAV (0.317), ITGB3 (0.295) NRP1 (0.466), PDGFRB (0.203), PTN (0.348),	5 genes CTGF (0.367), EDIL3 (0.339), HGF (0.169), ITGAV (0.607) ITGB3 (0.336)	4 genes EDIL3 (0.433), HGF (0.387), ITGAV (0.712), ITGB3 (0.518)
Detectable	2 genes LECT1, PRL	1 gene FLT3	4 genes FGF4, FLT3, IFNG, LEP	2 genes FLT3, PLG
Undetectable	10 genes ANGPTL1, ANGPTL3, BAI1, COL15A1, FGA, FGF4, FLT3, LEP, PLG, TNNI1	11 genes ANGPTL1, ANGPTL3, COL15A1, FGA, FGF4, LECT1, LEP, PF4, PLG, PRL, SERPINB5	9 genes ANGPTL1, ANGPTL3, COL15A1, FGA, LECT1, PF4, PLG, PRL, SERPINB5	12 genes ANGPTL1, ANGPTL3, COL15A1, ENPP2, FGA, FGF4, LECT1, LEP, PRL, PROK1, TIMP3, TNNI1

F. Muqri: Research Grant; Modest; AMA Seed Grant. Research Grant; Significant; NIH RO1 HL133577. **A. Helkin:** Research Grant; Significant; NIH RO1 HL133577. **K.G. Maier:** Research Grant; Significant; NIH RO1 HL133577. **V. Gahtan:** Research Grant; Significant; NIH RO1 HL133577.

283

Fenofibrate Induces Endothelial Cell Tubule Formation Independent of Phospholipogenesis

Omar Saffaf, Larisa Belaygorod, Khalid Saffaf, Clay F. Semenkovich, Mohamed Zayed, Washington Univ Sch of Med, St Louis, MO

Fenofibrate, a proliferator-activated receptor (PPAR)α agonist, is the only oral medication demonstrated to prevent lower extremity amputations in diabetic patients. Phosphatidylcholines, generated by choline-ethanolamine phosphotransferase 1 (CEPT1) via the Kennedy Pathway, also induce PPARα activation, but their metabolism is altered in the setting of diabetes. It is unknown whether CEPT1 is essential for fenofibrate-mediated endothelial cell (EC) function. To evaluate this, we generated a murine model for conditional knockdown of *Cept1* in the endothelium (*Cept1EC*KO). Heart ECs (MHECs) were harvested from 6wk old *Cept1EC*KO and wildtype (WT) littermates, and cultured *in vitro* on growth factor-reduced Matrigel. Cultures were then supplemented with VEGF (50ng/mL), bFGF (50ng/mL), and fenofibrate (25uM), then assessed longitudinally at 0, 4, and 6 hours. We observed that compared to WT, *Cept1EC*KO MHECs had significantly less tubule formation ($p < 0.0001$). VEGF and bFGF failed to rescue *Cept1EC*KO MHECs, but demonstrated a robust agonist response in WT MHECs (bFGF: p=0.003; VEGF: p=0.0002). Interestingly, fenofibrate demonstrated complete rescue of *Cept1EC*KO MHECs at 4 and 6 hours of culture. This finding demonstrates that fenofibrate restores EC function even in the setting of impaired phospholipid biosynthesis. This observation may partially explain how fenofibrate confers added benefits in subjects with diabetic and peripheral arterial disease. Future work will further elucidate this mechanism of action in diabetic subjects.

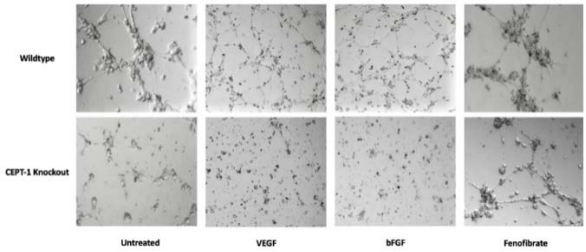

O. Saffaf: None. **L. Belaygorod:** None. **K. Saffaf:** None. **C.F. Semenkovich:** None. **M. Zayed:** None.

284
Lrp1 Regulates Smooth Muscle Contractility by Modulating Cytoskeletal Dynamics and Ca^{2+} Signaling
Selen C Muratoglu, Dianaly T Au, Zhekang Ying, Erick Hernandez-Ochoa, William E Fondrie, Brian Hampton, Mary Migliorini, Rebeca Galisteo, Martin F Schneider, Univ of Maryland, Baltimore, MD; Alan Daugherty, Debra L Rateri, Univ of Kentucky, Lexington, KY; Dudley Strickland, Univ of Maryland, Baltimore, MD

Objective - Mutations affecting proteins in the extracellular matrix (ECM), microfibrils, or vascular smooth muscle cells (VSMCs) that impact contractility can predispose individuals to thoracic aortic aneurysms. We reported previously that the low-density lipoprotein receptor-related protein 1 (LRP1) maintains vessel wall integrity, and smooth muscle LRP1-deficient (*smLRP1*$^{-/-}$) mice exhibited aortic dilatation. The current study focused on the descending thoracic aorta (DTA) and examined the role of LRP1 in VSMC contractility and its potential effect on the vascular ECM. ***Approach and Results*** - LRP1-deficient VSMCs exhibited a synthetic phenotype characterized by higher proliferation rates and an increase in synthetic organelles, mitochondria, multivesicular bodies, and macropinocytotic vesicles. LRP1-deficient VSMCs also displayed changes in their microfilament and actin structure that result in an inadequate interaction with the ECM. Quantitative proteomics identified proteins involved in actin polymerization and contraction that were downregulated significantly in the DTA of *smLRP1*$^{-/-}$ mice. Further analysis by qRT-PCR revealed attenuated mRNA levels for α-1D adrenergic receptor (*adra1d*) and calcium voltage-gated channel subunit α1 C (*cacna1c*) in *smLRP1*$^{-/-}$ aortas. Isometric contraction assays confirmed aberrant contraction of *smLRP1*$^{-/-}$ aortic rings when stimulated with vasoconstrictors. Furthermore, intracellular calcium imaging identified defects in response to a ryanodine receptor agonist in *smLRP1*$^{-/-}$ aortic rings. ***Conclusions*** - These results suggest that LRP1 is required for maintaining the VSMC contractile phenotype and identifies a novel role for LRP1 in calcium homeostasis that potentially protects against aneurysm development.
S.C. Muratoglu: None. **D.T. Au:** None. **Z. Ying:** None. **E. Hernandez-Ochoa:** None. **W.E. Fondrie:** None. **B. Hampton:** None. **M. Migliorini:** None. **R. Galisteo:** None. **M.F. Schneider:** None. **A. Daugherty:** None. **D.L. Rateri:** None. **D. Strickland:** None.

This research has received full or partial funding support from the American Heart Association.

286
Role of Glutathione in the Regulation of VEGFR2 in Human Aortic Endothelial Cells
Priya K Prasai, Christopher B Pattillo, Louisiana State Univ Health Sciences Ctr-Shreveport, Shreveport, LA

Tissue ischemia due to blood vessel occlusion favors new blood vessel formation or angiogenesis. Although hypoxia is one of the important regulators of angiogenesis, angiogenesis is a rare event in many cardiovascular diseases (CVD). This decreased angiogenesis could be attributed to many factors including altered glutathione (GSH) redox state. Previously, our laboratory has shown an intricate relationship between decreases in GSH in ischemic tissues and angiogenesis. Therefore, we hypothesized that altered GSH redox state regulates angiogenesis by affecting the vascular endothelial growth factor (VEGF)-A/VEGF receptor 2 (VEGFR2) pathway. We used human aortic endothelial cells (HAEC) and treated with diamide (DA), an oxidant that oxidizes GSH to GSSG, thereby altering GSH redox state. DA treatment decreased GSH and increased GSSG concentrations resulting in decreased GSH/GSSG. Using western blotting, we found that decreased GSH/GSSG activates VEGFR2. To identify the mechanism of VEGFR2 activation after DA treatment, we measured VEGF release into the media using ELISA. There was no difference in extracellular VEGF between the groups suggesting that DA activates VEGFR2 ligand-independently. We then investigated the role of protein tyrosine phosphatases (PTP) using a pan-PTP inhibitor, sodium orthovanadate, which did not alter VEGFR2 activation after DA treatment suggesting no role for PTPs in this pathway. We also studied the role of intracellular H_2O_2 in DA-induced activation using PEG-catalase to quench H_2O_2 and then treated with DA. PEG-catalase pretreatment did not affect VEGFR2 activation showing H_2O_2 is not involved in DA-induced VEGFR2 activation. In order to validate the DA-induced receptor activation, we inhibited glutathione reductase using 2-AAPA to increase intracellular GSSG levels. 2-AAPA treatment alone activated VEGFR2, confirming receptor activation after altering GSH/GSSG. Lastly, altering GSH/GSSG decreased the proliferation of HAECs. Our results elucidate a novel role of glutathione especially GSSG in ligand-independent VEGFR2 activation and subsequent inhibition of cell proliferation. Based on our data, GSSG could be a possible mechanism for decreased angiogenesis in CVD.
P.K. Prasai: None. **C.B. Pattillo:** None.

287
Transgenic Overexpression of Dimethylarginine Dimethylaminohydrolase 1 Protects From Angiotensin II - Induced Cardiac Hypertrophy and Vascular Remodeling
Irakli Kopaliani, Natalia Jarzebska, Silke Brilloff, Anne Kolouschek, Technische Univ Dresden, Dresden, Germany; Jens Martens-Lobenhoffer, Stefanie M. Bode-Böger, Otto-von-Guericke Univ, Magdeburg, Germany; Andreas Deussen, Norbert Weiss, **Roman N. Rodionov**, Technische Univ Dresden, Dresden, Germany

Background: Dimethylarginine dimethylaminohydrolase 1 (DDAH1) hydrolyzes the endogenous inhibitor of nitric oxide synthases asymmetric dimethylarginine (ADMA). DDAH1 is also suggested to have ADMA-independent effects. DDAH1 overexpression lowers ADMA levels and protects from renal interstitial fibrosis and vascular oxidative stress in angiotensin-II-induced hypertension. The current study was designed to test the hypothesis that DDAH1 overexpression protects from angiotensin II-induced cardiac hypertrophy and vascular remodeling.
Methods: Angiotensin II (AngII) was infused in the doses of 0.75 and 1.5 mg/kg/day, respectively, in DDAH1 transgenic mice (TG) and wild type (WT) littermates via osmotic minipumps. Echocardiography was performed in the first and fourth week after start of the infusion. Systolic blood pressure was measured by the tail-cuff method. Cardiac hypertrophy and vascular remodeling was assessed by histology after 4 weeks of AngII infusion.
Results: TG mice had decreased plasma and tissue ADMA. Infusion of Ang II resulted in an increase in systolic blood pressure, which was similar between TG and WT mice at week 1, however, TG mice were protected from a further increase in blood pressure. After 4-weeks infusion of AngII TG mice had significantly higher left ventricular lumen to wall ratio, smaller size of cardiomyocytes and reduced myocardial collagen expression compared to WT littermates. TG mice had lower left ventricular posterior wall thickness in systole and diastole as compared to WT controls. The

vasomotor function of aortic rings in response to acetylcholine was improved in the TG mice as compared to the WT mice. TG mice had less aortic hypertrophy and fibrosis and more elastin in aorta as compared to WT mice. Aortic infiltration of $CD45^+$, $CD3^+$, $CD8^+$ and $CD4^+$ T-cells was significantly lower in TG than in WT mice.
Conclusion: This study shows that upregulation of DDAH1 protects from AngII-induced cardiac hypertrophy and vascular remodeling. Upregulation of DDAH1 might be a potential therapeutic approach for protection from AngII – induced end organ damage. We are currently investigating, whether protective effects of DDAH1 are ADMA-dependent or ADMA-independent.
I. Kopaliani: None. **N. Jarzebska:** None. **S. Brilloff:** None. **A. Kolouschek:** None. **J. Martens-Lobenhoffer:** None. **S.M. Bode-Böger:** None. **A. Deussen:** None. **N. Weiss:** None. **R.N. Rodionov:** None.

288
Nitric Oxide Mediates Active Downregulation of Tissue Factor Expression in Human Pericytes
Laura Sommerville, Duke Univ Medical Ctr, Durham, NC; Dougald Monroe, Univ of North Carolina-Chapel Hill, Chapel Hill, NC; Maureane Hoffman, Durham Veterans Affairs and Duke Univ Medical Ctrs, Durham, NC

Tissue Factor (TF) is a transmembrane protein that not only expresses pro-coagulant enzymatic activity, but also mediates signal transduction by several second messenger pathways. It plays an obvious role in hemostasis and thrombosis, as well as modulating angiogenesis, inflammation, immune responses and progression of malignancy and metastasis. TF is normally expressed by a limited subset of cell types. It can also be induced on other cells by a plethora of mediators, mostly linked to inflammation and immune responses. By contrast, TF has only been shown to be actively downregulated in a single circumstance: we have reported that constitutive expression of TF by pericytes around dermal vessels disappears during angiogenesis associated with wound healing. This suggests that downregulation of pericyte TF may play a functional role in the process of angiogenesis. We previously reported that TF protein in cultured human pericytes is significantly reduced 8 hours after treatment with phorbol 12-myristate 13-acetate (PMA) (94.71% reduction $\pm$ 2.18%, $p<0.001$). This loss of TF protein is facilitated by reduction of TF mRNA. Downregulation of TF protein and mRNA depends on Protein Kinase C. The goal of the current study was to identify a physiologic mediator of pericyte TF downregulation. Treatment of human pericytes with growth factors and cytokines involved in wound healing did not change TF expression. Co-culture of human pericytes with human microvascular endothelial cells in transwells in the presence of basic fibroblast growth factor (bFGF) resulted in downregulation of pericyte TF. However, conditioned media from endothelial cells grown in the presence of bFGF did not trigger a decrease of TF in pericytes. bFGF has been shown to stimulate NO production, and both bFGF and NO have been linked to angiogenesis. This led us to consider nitric oxide (NO) as a potential labile mediator of TF downregulation. TF protein was reduced 8 hours after treatment with DETA/NO (44% reduction $\pm$ 6.1%, $p<0.01$). However, expression of TF mRNA was not reduced at this time, as it is during culture with PMA. Our working hypothesis is that TF downregulation in pericytes is partially mediated by endothelial cell-derived NO, but is also mediated by additional PKC-dependent pathways.
L. Sommerville: None. **D. Monroe:** None. **M. Hoffman:** None.

This research has received full or partial funding support from the American Heart Association.

289
Sirtuin-1 Inhibition by Peroxynitrite Contributes to Nicotine-induced Arterial Stiffness in Mice
Ye Ding, Qiulun Lu, Huaiping Zhu, Zhonglin Xie, Ming-Hui Zou, **Ping Song**, Georgia State Univ, Atlanta, GA

Cigarette smoking is a key contributor to arterial stiffness, which is a major and independent risk factor for serious cardiovascular events. Sirtuin-1 (SIRT1), a nicotinamide adenine dinucleotide-dependent protein deacetylase, plays an essential role in maintaining cardiovascular homeostasis, and *Sirt1* inhibition is linked to smoking-induced arterial damage and aortic stiffness. The mechanism behind key component of cigarette smoking, nicotine-induced SIRT1 inactivation remains unknown; therefore, we aimed to characterize the relationship between nicotine, SIRT1 inhibition, and arterial stiffness. Arterial stiffness and SIRT1 expression and activity in wild-type and *Sirt1*-overexpressing mice treated with nicotine or vehicle were monitored. Nicotine significantly increased arterial stiffness in wild type, but not *Sirt1*-overexpressing mice. Additionally, SIRT1 protein levels and activity were decreased in nicotine-treated wild-type mice, but not in *Sirt1*-overexpressing mice, and these results were reproducible in human aortic smooth muscle cells. We further determined that SIRT1 inhibition was caused by zinc release from and subsequent inhibition of deacetylation activity of SIRT1, leading to Yes-associated protein activation, and, ultimately, extracellular matrix remodeling associated with arterial stiffness. Zinc release from SIRT1 was mediated by peroxynitrite resulting from nicotine-induced increases in inducible nitric oxide synthase. Taken together, nicotine triggers arterial stiffness via extracellular matrix remodeling mediated by SIRT1 inhibition due to peroxynitrite-induced zinc release from SIRT1.
Y. Ding: None. **Q. Lu:** None. **H. Zhu:** None. **Z. Xie:** None. **M. Zou:** None. **P. Song:** None.

This research has received full or partial funding support from the American Heart Association.

290
The Transcription Factor Tead1 is Critical for Vascular Development in Mouse by Promoting Differentiation of Vascular Smooth Muscle Cells
Jiliang Zhou, Medical Coll Georgia, Augusta, GA; Tong Wen, The First Affiliated Hosp of Nanchang Univ, Nanchang, China; Kunzhe Dong, Guoqing Hu, Medical Coll Georgia, Augusta, GA; Jinhua Liu, The First Affiliated Hosp of Nanchang Univ, Nanchang University, China; Menghong Wang, Wei Zhang, The First Affiliated Hosp of Nanchang Univ, Nanchang, China

Background: Our previous study has shown that the Hippo signaling effector YAP plays a crucial role in the phenotypic modulation of vascular smooth muscle cells (VSMCs) in response to arterial injury and cardiovascular development in mice. However, the role of TEAD1, a co-factor of YAP in VSMC development is unknown.
Objective:The goal of this study to investigate the functional role of TEAD1 in cardiovascular development in mice.
Methods and Results: TEAD1 was specifically ablated in cardiomyocytes and VSMCs by crossing TEAD1 flox mice with SM22alpha-Cre transgenic mice. Cardiac/VSMC-specific deletion of TEAD1 led to embryonic lethality by E14.5 in mice due to cardiovascular defects including severe hypoplastic cardiovascular wall, resulting from impaired cardiac/VSMC proliferation. Whole transcriptomic analysis revealed deletion of TEAD1 in mouse cardiomyocytes and VSMCs significantly down-regulated expression of cardiac/VSMC differentiation genes and key transcription factors including myocardin and pitx2c that are critical for cardiovascular development. *In vitro* studies demonstrated that myocardin and pitx2c rescued TEAD1-defiency induced defects of VSMC differentiation. Furthermore, we identified pitx2c was a direct transcriptional target of TEAD1 and

pitx2c synergistically promoted VSMC differentiation with myocardin.
Conclusions: This study revealed a critical role of TEAD1 in cardiovascular development by promoting VSMC proliferation and differentiation and provided novel insights into the regulatory mechanisms for smooth muscle development.
J. Zhou: None. **T. Wen:** None. **K. Dong:** None. **G. Hu:** None. **J. Liu:** None. **M. Wang:** None. **W. Zhang:** None.

This research has received full or partial funding support from the American Heart Association.

310
Retrograde Hemorrhage and Ischemic Injury after REBOA in a Porcine Model of Uncontrolled Aortic Injury
Catherine Go, Partha Thirumala, Jenna Kuhn, Univ of Pittsburgh Med Ctr, Pittsburgh, PA; Yanfei Chen, Youngjae Chun, Univ of Pittsburgh, Pittsburgh, PA; Bryan Tillman, Univ of Pittsburgh Med Ctr, Pittsburgh, PA

Introduction Resuscitative Balloon Occlusion of the Aorta (REBOA) has gained popularity as a less invasive approach to temporize traumatic noncompressible hemorrhage, yet mortality remains over 70%. Although associated injuries may account for some deaths, contributions from ischemia and ongoing retrograde bleeding are also likely, with REBOA occlusion frequently in Zone 1 (descending thoracic aorta) and often greater than 20 minutes. This study examined retrograde blood loss and ischemic injury after REBOA in a porcine model of aortic injury. **Methods** Six anesthetized swine with invasive hemodynamic and neurophysiologic monitoring (Muscle Evoked Potentials and Somatosensory Evoked Potentials) underwent 8 Fr femoral access and Zone 1 positioning of a REBOA balloon prior to aortic injury. The thoracic aorta was injured with a 22 Fr dilator, followed by aortography and immediate REBOA inflation proximal to the injury. Profound deterioration of the first three animals with one hour of REBOA prompted the next three animals to undergo only 30 minutes of REBOA. Blood loss was recovered with a cellsaver. Animals underwent permanent stent repair of the aortic injury and resuscitation with the intent to recover. **Results:** Despite proximal hemorrhage control documented angiographically, blood loss from retrograde bleeding was substantial averaging 3.7 L and 3.5 L for the 30- and 60-minute groups, respectively. After balloon inflation, mean pressure fell an average of 62 mmHg within 20 minutes ($p < 0.001$), while cardiac output decreased 20-40%. In the lower extremities, Neuromonitoring revealed ischemic loss of motor signals at a mean of 27 minutes. Even after resuscitation with blood, bicarbonate, saline and pressors, all six animals arrested shortly after balloon deflation, amidst falling bicarbonate (p less than 0.001), and rising lactate (p less than 0.01) relative to baseline. **Conclusions:** Retrograde hemorrhage is an underappreciated event during REBOA control of aortic injuries, that may contribute to spinal cord ischemia, tissue ischemia and death. This study suggests that improved outcomes for noncompressible hemorrhage will require balance of competing goals of hemorrhage control and distal perfusion.
C. Go: None. **P. Thirumala:** None. **J. Kuhn:** None. **Y. Chen:** None. **Y. Chun:** None. **B. Tillman:** None.

311
The Role of ADAMTS-5 in Aortic Dilatation and Extracellular Matrix Remodeling
Marika Fava, Mount Sinai, New York, NY; Javier Barallobre-Barreiro, Ursula Mayr, Ruifang Lu, Athanasios Didangelos, Ferheen Baig, Marc Lynch, Norman Catibog, Abhishek Joshi, Temo Barwari, Xiaoke Yin, King's Coll London, London, United Kingdom; Marjan Jahangiri, St George's Univ of London, London, United Kingdom; Manuel Mayr, King's Coll London, London, United Kingdom

Thoracic aortic aneurysm (TAA), a degenerative disease of the aortic wall, is accompanied by changes in the structure and composition of the aortic extracellular matrix (ECM). Evidence is emerging that ECM processing by members of the ADAMTS (a disintegrin and metalloprotease with thrombospondin motifs) family could play an important role in the progression of aortic dilatation. In particular, ADAMTS-1 and -4 have been implicated in TAA. This study aimed to investigate the contribution of ADAMTS-5 to TAA development. A model of aortic dilatation by angiotensin II (AngII) infusion was adopted in mice lacking the catalytic domain of ADAMTS-5 (Adamts5$^{\Delta cat}$). Adamts5$^{\Delta cat}$ mice showed an attenuated rise in blood pressure whilst displaying increased dilatation of the ascending aorta. Interestingly, a proteomics comparison of the aortic ECM from AngII-treated wildtype and Adamts5$^{\Delta cat}$ mice revealed versican as the most up-regulated ECM protein in Adamts5$^{\Delta cat}$ mice. This was accompanied by a marked reduction of ADAMTS-specific versican cleavage products (versikine), an increase in TGFβ and a decrease of low-density lipoprotein-related protein 1 (LRP1). Silencing LRP1 expression in human aortic smooth muscle cells reduced the expression of *ADAMTS5*, attenuated the generation of versikine but increased soluble ADAMTS-1. A similar increase in ADAMTS-1 was observed in aortas of AngII-treated Adamts5$^{\Delta cat}$ mice, but was not sufficient to maintain versican processing and prevent aortic dilatation. Our results support the emerging role of ADAMTS proteases in TAA. ADAMTS-5 rather than ADAMTS-1 is the key protease for versican regulation in murine aortas. A compensatory rise in ADAMTS-1 could not prevent aortic dilatation in Adamts5$^{\Delta cat}$ mice. LRP1, which has been involved in aneurysm pathology in both human and mice, appears to be linked to ADAMTS-5 and ADAMTS-5-mediated versican cleavage. Further studies are needed to explore the ADAMTS protease family as target for therapeutic approaches aimed to reduce or halt dilatation of the aorta resulting in aneurysm.
M. Fava: None. **J. Barallobre-Barreiro:** None. **U. Mayr:** None. **R. Lu:** None. **A. Didangelos:** None. **F. Baig:** None. **M. Lynch:** None. **N. Catibog:** None. **A. Joshi:** None. **T. Barwari:** None. **X. Yin:** None. **M. Jahangiri:** None. **M. Mayr:** None.

312
Upregulation of Notch3 Contributes to Aneurysm Formation in a Murine Model of Marfan Syndrome
Matthew Fitzgerald, Trevor Meisinger, Rishi Batra, Zhibo Liu, B. Timothy Baxter, Wanfen Xiong, Univ of Nebraska, Omaha, NE

Notch3 functions as a receptor for membrane-bound ligands (Jag1, DLL1) in signaling pathways for cell-cell communication, gene regulation and control of cell differentiation during embryonic and adult vascular development. However, the role of Notch3 in Marfan Syndrome (MFS), which the main cardiovascular complication is thoracic aneurysms that results in high mortality, has yet to be fully elucidated. Previously we have shown that during aneurysm development, aortic smooth muscle cells (SMCs) in mgR mice, a murine model of MFS, display premature switch from a synthetic to a more contractile phenotype. Therefore we *hypothesized* that Notch3 could be playing a key role in this aberrant differentiation and aneurysm formation.
To test this hypothesis we examined Notch3 mRNA and protein levels in the aortic tissue and SMCs from 1, 4, and 8 weeks-old mgR mice and wild type controls by real time-PCR, Western blot, and immunohistochemistry. Aortic histological changes were examined by Verhoeff-Van Gieson (VVG) elastin staining. In addition, mice were treated with DAPT **(**N-[N-(3,5-Difluorophenacetyl)-L-alanyl]-S-phenylglycine t-butyl ester), a known γ-secretase inhibitor. The effects of notch signaling inhibition on aneurysm rupture were evaluated.
We found that aortic mRNA and protein levels of Notch3 in mgR mice was upregulated ~2 fold by 1 week, and 4-fold at

4 and 8 weeks compared to WT littermate controls. The expression levels of upstream and downstream targets of Notch3, Jagged1 and p21, respectively, were significantly increased in the aorta of mgR mice compared to wild type controls. DAPT treatment prolonged the median lifespan of mgR mice from 16 weeks (untreated) to 32 weeks (DAPT treated). The results from VVG staining of aortic tissue showed that DAPT treatment inhibited aortic elastic degradation in mgR mice.
Taken together, our findings indicate that Notch3 is upregulated in the early aortic development and continues to increase during the course of the aneurysm formation in mgR mice. The increase in Notch3 expression may contribute to aneurysm development in MFS. This study lays the groundwork to further examine Notch3 as a novel potential target for treatment.
M. Fitzgerald: None. **T. Meisinger:** None. **R. Batra:** None. **Z. Liu:** None. **B. Baxter:** None. **W. Xiong:** None.

313
Loss of Contractile Smooth Muscle Cell Phenotype in a Mouse Model of Marfan Syndrome
Nazli Gharraee, Susan M Lessner, Univ of South Carolina, Columbia, SC

Objectives: Thoracic aortic aneurysm (TAA) is a chronic vascular disease and the 15th leading cause of death in the US. TAA can result from a genetic disorder such as Marfan syndrome (MFS). MFS patients typically have fibrillin-1 deficiency, causing elastic fiber defects in the aortic media that initiate a series of cellular events. We sought to determine the association of smooth muscle cell (SMC) conversion from contractile to synthetic phenotype with changes in extracellular matrix (ECM), medial cell density, and arterial biomechanics.
Methods: A mouse model of MFS (Fbn1 C1039G/+, Het) was used to study progression of TAA and cellular events over a 3-12 month time course. Small animal ultrasound was used to image the ascending aorta and to measure diameters at several positions. Immunohistochemistry (IHC) was performed on proximal aorta sections with smooth muscle-myosin heavy chain (SM-MHC) and SM alpha actin as markers for contractile SMCs. Second harmonic generation (SHG) microscopy was used to quantitate aortic medial collagen.
Results: Ultrasound data show that aortic diameter significantly increases with time in Het mice. There is a statistically significant difference between genotypes independent of time. IHC images demonstrate that while SM-MHC expression in wild type (WT) mice remains nearly constant, in Het mice at 3 months the expression is comparable to that of WT mice but decreases at 6 months and starts to recover to the WT level by 12 months. SHG images show a time dependent increase in medial collagen expression in Het mice vs. WT. These results suggest loss of contractile SMCs in the media and remodeling of ECM.
Conclusion: Our results to date demonstrate loss of contractile SMCs and increased medial collagen deposition in the proximal aorta during TAA progression. Loss of contractile cells together with changes in ECM are expected to alter aortic biomechanics. To quantify these alterations, we are currently studying active and passive biomechanics of ascending aortas of WT and Het mice.

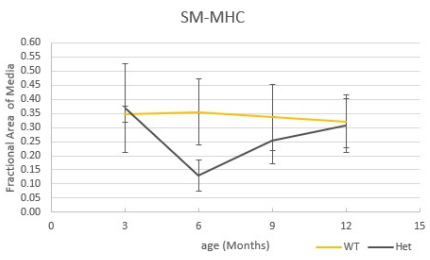

Figure1. Quantification of fractional area of media showing positive staining from the IHC images from 3-12 months mice. n=3 for each genotype.

N. Gharraee: None. **S.M. Lessner:** None.

314
H19 Induces Abdominal Aortic Aneurysm Development and Progression
Daniel Y Li, Columbia Univ Medical Ctr, New York, NY; Albert Busch, Klinikum rechts der Isar, Technical Univ Munich, Munich, Germany; Hong Jin, Ekaterina Chernogubova, Karolinska Instt, Stockholm, Sweden; Jaroslav Pelisek, Klinikum rechts der Isar, Technical Univ Munich, Munich, Germany; Per Eriksson, Joy Roy, Karolinska Instt, Stockholm, Sweden; Patrick Hofmann, Reinier Boon, Inst of Cardiovascular Regeneration, Univ Hosp Frankfurt, Frankfurt am Main, Germany; Joshua Spin, Philip Tsao, Stanford Univ, Stanford, CA; Lars Maegdefessel, Klinikum rechts der Isar, Technical Univ Munich, Munich, Germany

Background - Long noncoding RNAs (lncRNAs) have emerged as critical molecular regulators in various biological processes and diseases. Here we sought to identify and functionally characterize lncRNAs as potential mediators in abdominal aortic aneurysm (AAA) development. **Methods and results** - We profiled RNA transcript expression in two murine AAA models, Angiotensin II (ANGII) infusion in *ApoE-/-* mice (*n*=10) and porcine pancreatic elastase (PPE) instillation in C57BL/6 wildtype mice (*n*=12). The lncRNA H19 was identified as one of the most highly up-regulated transcripts in both mouse aneurysm models compared to sham-operated controls. This was confirmed by qRT-PCR and *in situ* hybridization. Experimental knock-down of H19, utilizing site-specific antisense oligonucleotides (LNA-GapmeRs) *in vivo*, significantly limited aneurysm growth in both models. Upregulated H19 correlated with smooth muscle cell (SMC) content and SMC apoptosis in progressing aneurysms. Importantly, a similar pattern could be observed in human AAA tissue samples, and in a novel preclinical *LDLR-/-* Yucatan mini-pig aneurysm model. *In vitro* knock-down of H19 markedly decreased apoptotic rates of cultured human aortic SMCs, while overexpression of H19 had the opposite effect. Notably, H19-dependent apoptosis mechanisms in SMCs appeared to be independent of miR-675, which is embedded in the first exon of the H19 gene. A customized transcription factor array identified hypoxia-inducible factor 1-alpha (HIF1α) as the main downstream effector. Increased SMC apoptosis was associated with cytoplasmic interaction between H19 and HIF1α and sequential p53 stabilization. Additionally, H19 induced transcription of HIF1α *via* recruiting specificity protein 1 (Sp1) transcription factor to the promoter region.
Conclusions - The lncRNA H19 is a novel regulator of SMC survival in AAA development and progression. Inhibition of H19 expression might serve as a novel molecular therapeutic target for aortic aneurysm disease.
D.Y. Li: None. **A. Busch:** None. **H. Jin:** None. **E. Chernogubova:** None. **J. Pelisek:** None. **P. Eriksson:** None. **J. Roy:** None. **P. Hofmann:** None. **R. Boon:** None. **J. Spin:** None. **P. Tsao:** None. **L. Maegdefessel:** None.

315
SmgGDS Prevents Thoracic Aortic Aneurysm Formation and Rupture by Phenotypic Preservation of Aortic Smooth Muscle Cells
Masamichi Nogi, Kimio Satoh, Shinichiro Sunamura, Nobuhiro Kikuchi, Taijyu Satoh, Ryo Kurosawa, Junichi Omura, MD Elias Al-Mamun, Mohammad Abdul Hai Siddique, Shun Kudo, Satoshi Miyata, Hiroaki Shimokawa, Tohoku Univ Grad Sch Med, Sendai, Japan

Background: Thoracic aortic aneurysm (TAA) and dissection (TAD) are fatal diseases, which cause aortic rupture and sudden death. The small GTP-binding protein GDP dissociation stimulator (SmgGDS) is a crucial mediator of the pleiotropic effects of statins. Previous studies revealed that reduced force generation in AoSMCs causes TAA and TAD.

Methods and Results: To examine the role of SmgGDS in TAA formation, we employed an angiotensin II (AngII, 1,000 ng/min/kg, 4weeks)-induced TAA model in *Apoe*$^{-/-}$*SmgGDS*$^{+/-}$ mice, in which 33% died suddenly due to TAA rupture, whereas there was no TAA rupture in *Apoe*$^{-/-}$ control mice. In contrast, there was no significant difference in the ratio of AAA rupture between the two genotypes. We performed ultrasound imaging every week to follow the serial changes in aortic diameters. The diameter of the ascending aorta progressively increased in *Apoe*$^{-/-}$*SmgGDS*$^{+/-}$ mice compared with *Apoe*$^{-/-}$ mice, whereas that of the abdominal aorta remained comparable between the two genotypes. Histological analysis of *Apoe*$^{-/-}$*SmgGDS*$^{+/-}$ mice showed dissections of major thoracic aorta in the early phase of AngII infusion (day 3~5) and more severe elastin degradation compared with *Apoe*$^{-/-}$ mice. Mechanistically, *Apoe*$^{-/-}$*SmgGDS*$^{+/-}$ mice showed significantly higher levels of oxidative stress, matrix metalloproteinases, and inflammatory cell migration in the ascending aorta compared with *Apoe*$^{-/-}$ mice. For mechanistic analyses, we primary cultured AoSMCs from the 2 genotypes. After AngII (100 nM) treatment for 24 hours, *Apoe*$^{-/-}$*SmgGDS*$^{+/-}$ AoSMCs showed significantly increased MMP activity and oxidative stress levels compared with Apoe$^{-/-}$ AoSMCs. In addition, SmgGDS deficiency increased cytokines/chemokines and growth factors in AoSMCs. Moreover, expressions of *FBN1*, *ACTA2*, *MYH11*, *MLK* and *PRKG1*, which are force generation genes, were significantly reduced in *Apoe*$^{-/-}$ *SmgGDS*$^{+/-}$ AoSMCs compared with Apoe$^{-/-}$ AoSMCs. Similar tendency was noted in AoSMCs from TAA patients compared with those from controls. Finally, local delivery of the SmgGDS gene construct reversed the dilation of the ascending aorta in *Apoe*$^{-/-}$*SmgGDS*$^{+/-}$ mice.
Conclusions: These results suggest that SmgGDS is a novel therapeutic target for the prevention and treatment of TAA.
M. Nogi: None. **K. Satoh:** None. **S. Sunamura:** None. **N. Kikuchi:** None. **T. Satoh:** None. **R. Kurosawa:** None. **J. Omura:** None. **M. Al-Mamun:** None. **M. Siddique:** None. **S. Kudo:** None. **S. Miyata:** None. **H. Shimokawa:** None.

316
Chronic Intermittent Hypoxia Attenuates BAPN Induced Thoracic Aortic Aneurysms in Mice
Yunyun Yang, Linyi Li, **Yan Wen Qin**, Beijing An Zhen Hosp, Capital Medical Univ, Beijing Inst of Heart, Lung and Blood Vessel Diseases, Beijing, China

Objective: Aortic aneurysm (AA) is a life-threatening cardiovascular disorder due to the predisposition for dissection and rupture. Chronic intermittent hypoxia (CIH) has protective effects on heart and brain against ischemia injury. However, whether CIH prevents against AA formation was not elucidated. The present study aimed to investigate the effect of CIH treatment on thoracic aortic aneurysms (TAA) in mice.
Approach and Results: Seventy-five C57BL/6 mice 3 weeks of age were divided into three groups, i.e. Control group (21% O_2, 24 h per day, 4 weeks, n = 15); β-aminopropionitrile (BAPN) group (oral administration BAPN 1g / kg / day, 21% O_2, 24 h per day, 4 weeks, n = 30); CIH+BAPN group (5% -21% O_2 90s / cycle, 8h per day, 4 weeks; BAPN 1g / kg / day, n = 30). We found that CIH significantly reduced the incidence of TAA (18 of 30 versus 9 of 30; p<0.05), and decreased maximal aortic diameter in BAPN group by hematoxylin and eosin staining (1.71 ± 0.35 versus 1.23± 0.15 mm; p <0.05). CIH significantly reduced elastin breaks in BAPN group by Verhoeff-van Gieson staining. The apoptosis of vascular smooth muscle cells was detected by TUNEL staining increased in BAPN group and markedly reversed by CIH. Moreover, RNA-Seq analysis and bioinformatics analysis were performed to screen the differential expression genes and possible pathway.
CIH significantly down-regulated the expression of inflammation signaling pathways, up-regulated the expression of PI3K/AKT survival pathway and extracellular matrix homeostasis related pathway in BAPN induced TAA mice. Confirmed by real-time quantitative reverse-transcription-polymerase chain reaction (qRT-PCR) assays, CIH significantly inhibited the expression of IL-1β, TNF-α, MMP-9 and Cathepsin S, and increased the expression of hypoxia inducible factor-1α (HIF-1α), Lysyl oxidase (LOX), ITGB1 and COL1A2. Our findings also showed that the expression of MMP-9, MMP-2, cathepsin S, IL-1β, MCP-1 and Mac-2 increased in BAPN group and markedly decreased in CIH+BAPN group by immunohistochemistry staining. Besides, CIH also significantly increased the protein expression of HIF-1α, LOX and p-AKT by western blot analysis.
Conclusions: The findings from our study suggest that CIH prevented the TAA development of BAPN-induced mice.
Y. Yang: None. **L. Li:** None. **Y. Qin:** None.

317
Inflammasome Inhibitor MCC950 Prevents the Development of Sporadic Thoracic and Abdominal Aortic Aneurysms and Dissections in Mice
Pingping Ren, Richard Appel, Lin Zhang, Wei Luo, Chen Zhang, Yidan Wang, Jiao Guo, Baylor Coll of Med, Houston, TX; Avril A. B. Robertson, Matthew A. Cooper, The Univ of Queensland, Brisbane St Lucia, Australia; Joseph S. Coselli, Ying H. Shen, Scott A. LeMaire, Baylor Coll of Med, Houston, TX

Background: Aortic aneurysms and dissections (AAD) are common interrelated cardiovascular diseases that cause more than 10,000 deaths in the United States each year and are a leading cause of death in people 55 years of age or older. Currently, surgery is the only effective treatment; thus, there is a critical need to develop pharmacological agents that can prevent the initiation or progression of AAD. Increasing evidence suggests that the NLRP3 inflammasome plays a critical role in aortic destruction. In this study, we aimed to test the therapeutic potential of MCC950, a potent and specific NLRP3 inhibitor, for preventing AAD.**Methods/Results :** In a sporadic AAD model induced by a high-fat diet and angiotensin II infusion,, aortic challenge induced significant aortic enlargement and the development of a range of AAD manifestations, including aneurysm without dissection, dissection, and rupture. Importantly, MCC950 treatment significantly inhibited aortic enlargement and the development of AAD, particularly in the ascending and suprarenal aorta. The overall incidence of AAD decreased from 86% in the challenged control group to 40% in the challenged MCC950 treatment group (*P*<0.001). The incidence of ascending AAD decreased from 56% in the challenged control group to 18% in the challenged MCC950 treatment group (*P*=0.0001), and the incidence of suprarenal AAD decreased from 60% in the challenged control group to 20% in the challenged MCC950 treatment group (*P*<0.001). The reduction in AAD incidence was similar in male and female mice. Furthermore, aortas from the MCC950 group showed reductions in inflammasome activation, macrophage infiltration, MMP-9 activity, and elastic fiber destruction. Likewise, in the cultured macrophages, MCC950 treatment inhibited H_2O_2-induced activation of the NLRP3 inflammasome, IL-1β secretion, and MMP-9 activation.**Conclusion:** The NLRP3 inhibitor MCC950 is effective at preventing inflammasome activation, aortic destruction, inflammation, and the development of AAD in a mouse model of sporadic disease. Further studies are needed to determine whether MCC950 has similar effects in other AAD models.
P. Ren: None. **R. Appel:** None. **L. Zhang:** None. **W. Luo:** None. **C. Zhang:** None. **Y. Wang:** None. **J. Guo:** None. **A. Robertson:** None. **M. Cooper:** None. **J. Coselli:** None. **Y. Shen:** None. **S. LeMaire:** None.

318
Perivascular Adipose Tissue-derived Pdgf-dd Contributes to Aortic Aneurysm Formation During Obesity
Cheng-Chao Ruan, Ze-Bei Zhang, Ping-Jin Gao, Shanghai Inst of Hypertension, Shanghai, China

Obesity increases the risk of vascular disease, including aortic aneurysm (AA). Perivascular adipose tissue (PVAT) surrounding arteries are altered during obesity. However, the underlying mechanism of adipose tissue especially PVAT in the pathogenesis of AA is still unclear. Here we showed that angiotensin II (AngII) infusion increases adventitial inflammation and AA formation in leptin-deficient obese mice (*ob/ob*). Transcriptomic analysis identified an increased platelet derived growth factor-DD (PDGF-DD) expression in the PVAT of AngII-infused *ob/ob* mice. PDGF-DD promotes the proliferation, migration and inflammatory factors expression in cultured adventitial fibroblasts. We further showed that inhibition of PDGF-DD signaling significantly reduces the incidence of AA in AngII-infused *ob/ob* mice. More important, adipocyte specified PDGF-DD transgenic mice (PA-Tg) is more susceptible to AA formation after AngII infusion accompanied with exaggerated adventitial fibrosis and inflammation. Collectively, our findings reveal a notable role of PDGF-DD in the AA formation during obesity, and modulation of this cytokine might be an exploitable treatment strategy for the condition.
C. Ruan: None. **Z. Zhang:** None. **P. Gao:** None.

319
Novel Method to Evaluate Nature of Vessel Wall in Abdominal Aortic Aneurysm by Fluorescent Probes Reacting Specific Protease
Akihiko Seo, Daisuke Akagi, Div of Vascular Surgery, Departmet of Surgery, Garduate of Sch of medicine, The Univ of Tokyo, Tokyo, Japan; Mako Kamiya, Lab of Chemical Biology and Molecular Imaging, Graduate Sch of Med, The Univ of Tokyo, Tokyo, Japan; Yugo Kuriki, Lab of Chemistry and Biology, Graduate Sch of Pharmaceutical Sciences, The Univ of Tokyo, Tokyo, Japan; Katsuyuki Hoshina, Div of Vascular Surgery, Departmet of Surgery, Garduate of Sch of medicine, The Univ of Tokyo, Tokyo, Japan; Yasuteru Urano, Lab of Chemistry and Biology, Graduate Sch of Pharmaceutical Sciences, The Univ of Tokyo, Tokyo, Japan

Background and Objective: Evaluation of the vessel wall condition during vascular surgery is an essential and important for technical success. However, no optimal method has been recommended for the objective assessment of the condition, and evaluation and decision of the suture/anastomotic sites are governed by the surgeon's experience during surgery. Fluorescence-based visualization is a promising method available for objective assessment; therefore, we aimed to use this technique to distinguish non-aneurysmal wall from an aneurysmal one. Various proteases are known to play a role in aneurysm formation. We synthesized over 250 kinds of aminopeptidase-activatable fluorescent probes. To optimize aneurysmal wall evaluation based on specific fluorescent activity, these probes were investigated. Methods and Results: Vessel wall specimens were clinically obtained during open surgery for the abdominal aortic aneurysm at the University of Tokyo Hospital. Initially, to screen these probes comprehensively, the vessel walls were homogenized and supernatants were obtained. After incubating each probe in the supernatant, the increment of fluorescence was measured (excitation at 485 nm and detection at 535 nm). Among the 250 probes investigated, 6 showed a difference in the fluorescent activity between aneurysmal and non-aneurysmal walls. Next, these 6 probes were applied to freshly resected vessel walls on the from luminal side in the form of a gel, and fluorescent images were obtained using the Maestro® imaging system (PerkinElmer, Waltham, MA). Two probes showed a > 2-fold stronger activity in aneurysmal walls than that observed in non-aneurysmal walls. Conclusion: These probes may be useful for the objective evaluation of the nature of vascular walls. We plan to use small fluorescent detectors for native aortic wall intraoperatively and investigate target proteases that react with these probes.
A. Seo: None. **D. Akagi:** None. **M. Kamiya:** None. **Y. Kuriki:** None. **K. Hoshina:** None. **Y. Urano:** None.

320
STAT3 deletion in Vascular Smooth Muscle Cell Disrupts Aortic Structural Integrity
Sherene Shalhub, Univ of Washington Medical Ctr, Seattle, WA; Steve Mongovin, VA Medical Ctr, Seattle, WA; Richard Kenagy, Gale Tang, Thomas Hatsukami, Michael Sobel, Univ of Washington Medical Ctr, Seattle, WA; Errol Wijelath, VA Medical Ctr, Seattle, WA

Background: The pro- and anti-inflammatory phenotypes of vascular smooth muscle cells (VSMC) are uniquely modulated by the transcription factors STAT1 and STAT3. STAT transcriptional factors are key in driving the chronic inflammation of psoriasis and rheumatoid arthritis, but their significance in degenerative aortic aneurysm pathology is unknown.
Objective: Test whether STAT3 expression within vascular smooth muscle cells (VSMC) is required for aortic wall homeostasis
Methods and Results: We created an atherosclerotic mouse model in which STAT3 or STAT1 was specifically knocked out exclusively in VSMC. $STAT3^{flox/flox}$ and SM22-CreKI were first established on an ApoE background. Female ApoE/$STAT3^{flox/flox}$ mice were then crossed with male ApoE/SM22-CreKI. F1 males from this crossing (ApoE/SM22-$Cre^{+/+}$-KI/$STAT3^{flox/wt}$ were bred with female ApoE/$STAT3^{flox/flox}$ mice to generate ApoE/SM22-$Cre^{+/o}$ KI/$STAT3^{flox/flox}$ mice. An analogous breeding strategy was employed to generate ApoE/SM22-$Cre^{+/o}$ KI/$STAT1^{flox/flox}$ mice. Both VSMC-specific STAT3 and STAT1 knockout mice were born at the expected Mendelian ratio and appeared outwardly healthy. Mice were switched from normal diet to a western diet at 6 weeks of age. All VSMC-specific STAT3 ko mice (n=8) sudden death secondary to descending thoracic and abdominal aortic rupture between 10 and 12 weeks of age. These ruptures occurred in conjunction with aortic dissection (n= 5/8). Histochemical analysis of the affected aorta revealed fragmented elastin structure and smooth muscle cell apoptosis. In-vitro studies demonstrated that STAT3-deficient VSMCs were prone to apoptosis when induced to proliferate. VSMC-specific STAT1 ko mice by comparison were viable.
Conclusion: STAT3 likely plays a nourishing role in the development and health of the VSMCs of the aortic medial layer. In the absence of STAT3 activity, there is atrophy and degeneration, leading to descending thoracic and abdominal aortic aneurysms and dissection. Derangements in the balance between STAT3 and STAT1 activity may play a role in human degenerative aortic pathology.
S. Shalhub: None. **S. Mongovin:** None. **R. Kenagy:** None. **G. Tang:** None. **T. Hatsukami:** None. **M. Sobel:** None. **E. Wijelath:** None.

321
The Aortic Luminal Area is a Potential Marker of Increased Rupture Risk in AbdominalAorticAneurysms
Antti Siika, Moritz Lindquist Liljeqvist, Rebecka Hultgren, Karolinska Inst, Stockholm, Sweden; Christian Gasser, KTH Royal Inst of Technology, Stockholm, Sweden; Joy Roy, Karolinska Inst, Stockholm, Sweden

Introduction: Diameter is currently the only factor used to estimate rupture risk of abdominal aortic aneurysms (AAAs). Many large AAAs, however, do not rupture, and a significant portion of small AAAs do. Our aim was to investigate if simple two-dimensional geometric measurements can improve rupture risk prediction in AAAs, and relate these measurements to biomechanical determinants of AAAs.
Methods: Thirty patients with ruptured AAAs (mean age was

77 ± 5 years and 23 were male) and 60 patients (mean age 60 ± 8 years, and 46 were male) with asymptomatic AAAs were included. At the location of the maximal diameter, the diameter, the luminal area and the vessel area were measured. Finite element analysis was used to compute 3D-geometric and biomechanical parameters of the asymptomatic AAAs, using A4 Clinics Software (VASCOPS, Austria). An automatic matching function was used to construct diameter-matched groups.
Results: Analysis of all stable AAAs (n=60) and ruptured AAAs (n=30) showed that ruptured AAAs had a significantly larger diameter, 77 ± 15 mm vs. 62 ± 13 mm ($p<0.01$) and significantly larger luminal area 2281 ± 1964 mm^2 vs. 1059 ± 674 mm^2 ($p<0.01$). In order to control for diameter as a confounder, two diameter-matched groups, one with ruptured AAAs (n=28) and one with stable AAAs (n=15) were formed (74 ± 12 mm vs 73 ± 11, p = .67). Diameter-matched ruptured AAAs had a larger luminal area (1954 ± 1254 mm^2 vs. 1120 ± 623 mm^2, p = .02) and a lower relative ILT area (55 ± 24 % vs 68 ± 24%, p= .03). In multivariate regression of 60 asymptomatic AAAs, including the maximal diameter, the luminal area explained the largest amount of variance in the biomechanical rupture risk parameters, followed by the ILT-area.
Conclusions: We demonstrate that the luminal area is increased in ruptured AAAs compared to stable AAAs. Further, we show that this finding may in part be explained by a correlation between luminal area and biomechanical rupture risk parameters.
A. Siika: None. **M. Lindquist Liljeqvist:** None. **R. Hultgren:** None. **C. Gasser:** Consultant/Advisory Board; Modest; Scientific Advisor for Vascops GmbH. **J. Roy:** None.

322
Exploring the Role of Triggering Receptor Expressed on Myeloid Cells-1 in Experimental Abdominal Aortic Aneurysm
Marie Vandestienne, Jérémie Joffre, Andréas Giraud, Stéphane Potteaux, Ludivine Laurans, Alain Tedgui, INSERM U970, PARIS, France; Marc Derive, INOTREM, SA, Nancy, France; Ziad Mallat, Hafid Aït-Oufella, INSERM U970, PARIS, France

Introduction: Non-syndromic Abdominal Aortic Aneurysm (AAA) is one of the leading causes of cardiovascular death in elderly men. AAA is characterized by extracellular matrix degradation, smooth muscle cell apoptosis and infiltration of inflammatory cells in the aortic wall. Monocyte recruitment particularly plays an important role in the pathophysiology of AAA. TREM (Triggering Receptor Expressed on Myeloid cells)-1, a receptor expressed by myeloid cells, is a key regulator of innate immune cell activity, and we hypothesized that it might be involved in AAA development. Objective: We aim to decipher the role of TREM-1 in the immuno-inflammatory response associated with AAA development and rupture. Method: To study the role of TREM-1 in AAA development, we used an experimental model of Angiotensin-II-induced AAA in *ApoE$^{-/-}$Trem-1$^{-/-}$ and ApoE$^{-/-}$ Trem-1$^{+/+}$* mice. At day 0, 3, 7 and 28, we analyzed monocyte trafficking (flow cytometry), inflammatory cell infiltration within the aortic wall (immunostaining, qPCR), aortic wall remodeling (histology) and finally AAA development. Results: Angiotensin II infusion induced a 2-fold increased of TREM-1 expression on classical monocytes at day 3. TREM-1 deficiency (*ApoE$^{-/-}$Trem-1$^{-/-}$*) abolished Angiotensin II-induced monocytosis at day 3 and prevented macrophage infiltration within the aorta at day 7. TREM-1 genetic deletion also limited pro-inflammatory response (*Il-1beta* and *Tnf-alpha* mRNA expression) and metalloprotease activity in the aortic wall and protected against elastin degradation at day 7. At day 28 (n=10/group), under angiotensin II infusion, *ApoE$^{-/-}$Trem-1$^{-/-}$* mice are characterized by reduced mean aorta diameter (702+/-36 µm versus 1081+/-51 µm, $p<0.01$), less severe AAA disease ($p<0.001$, Chi-squared for a trend) when compared to *ApoE$^{-/-}$Trem-1$^{+/+}$* mice. In addition, TREM-1 deficiency protected against lethal AAA rupture (28-Day survival 100% versus 82% p=0.05). Conclusion: We showed that TREM-1 deficiency reduced AAA development and rupture in an Angiotensin II-induced mouse model.
M. Vandestienne: None. **J. Joffre:** None. **A. Giraud:** None. **S. Potteaux:** None. **L. Laurans:** None. **A. Tedgui:** None. **M. Derive:** Employment; Significant; Co-founder of INOTREM. **Z. Mallat:** None. **H. Aït-Oufella:** None.

323
Hydrogen Sulfide Limits the Development of Intimal Hyperplasia in a Mouse Model of Femoral Wire Injury and in Human Veins
Alban Longchamp, Natsumi Yamagushi, Martine Lambelet, Celine Dubuis, Francois Saucy, Jean-Marc Corpataux, Florent Allagnat, Sebastien Déglise, CHUV, Lausanne, Switzerland

Objectives: Mainstays of contemporary therapies for this arterial occlusive disease include angioplasties, stents, endarterectomies and bypass surgery. However, these treatments suffer from high failure rates due to re-occlusive vascular wall adaptations, namely intimal hyperplasia (IH). IH develops in response to endothelium injury, leading to inflammation, vascular smooth muscle cells (VSMC) dedifferentiation, migration and proliferation at the site of injury. Hydrogen sulfide (H_2S) is a ubiquitous signaling gazotransmitter, which exhibits antioxidant, anti-inflammatory, and vaso-relaxant properties. Thus, we hypothesized that H_2S could reduce IH formation.
Methods: WT male C57BL6/J mice submitted to femoral wire injury surgery to induce IH were treated with an H_2S donor (NaHS) in the drinking water. IH was measured 28 days post-surgery by histology. In addition, segments of great saphenous vein obtained from patients undergoing bypass surgery were maintained in culture *ex-vivo* for 7days in presence of various H_2S donors (NaHS, GYY4137, diacyltrisulfide). Finally, primary human umbilical vein endothelial cells (HUVEC) and primary human VSMC were treated *in-vitro* with the same H_2S donors to study cellular proliferation and migration.
Results: NaHS treatment significantly reduced IH development in the mouse model of femoral wire injury (Figure 1). Similarly, the various H_2S donors prevented the development of IH in vein segments *ex-vivo. In vitro,* the same H_2S donors stimulated human endothelial cells (HUVEC) migration and proliferation, while inhibiting migration and proliferation of primary VSMC (Figure 2).
Conclusions: Exogenous H_2S prevents IH formation in mice *in-vivo* and in human veins *ex-vivo*. Importantly, H_2S reduces VSMCs but stimulates ECs proliferation and migration. These data suggest that exogenous H_2S therapy could be used in human to minimize IH, thus limiting vascular reconstruction failure.

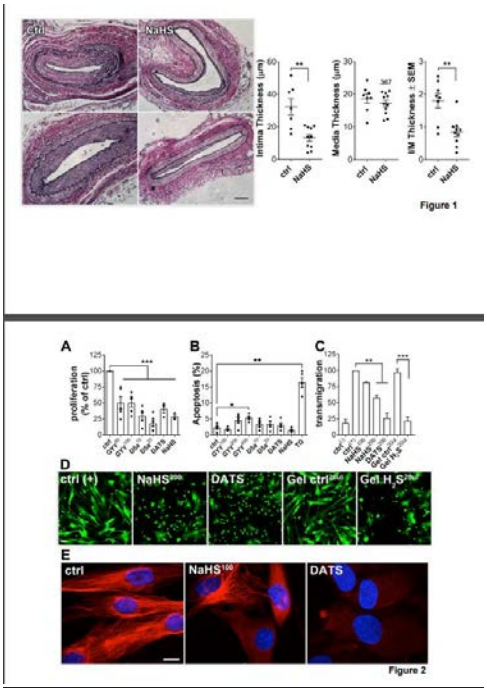

A. Longchamp: None. **N. Yamagushi:** None. **M. Lambelet:** None. **C. Dubuis:** None. **F. Saucy:** None. **J. Corpataux:** None. **F. Allagnat:** None. **S. Déglise:** None.

324

Molecular Imaging of High Risk Atherosclerotic Plaque Using Fibrin-Binding PET Probe

David Izquierdo-Garcia, Massachusetts General Hosp, Charlestown, MA; Himashinie Diyabalanage, Collagen Medical, Belmont, MA; Ian Ramsay, Nicholas J Rotile, Adam Mauskapf, Ji-Kyung Choi, Thomas Witzel, Massachusetts General Hosp, Charlestown, MA; Valerie Humblet, Collagen Medical, Belmont, MA; Anna-Liisa Brownell, Ciprian Catana, Peter Caravan, **Ilknur Ay**, Massachusetts General Hosp, Charlestown, MA

Objectives: There is a need for better stratification of atherosclerotic patients to identify individuals at high risk for a cardiovascular event. Two key hallmarks of plaque at high risk for rupture are intraplaque hemorrhage and evidence of prior rupture. The protein fibrin is strongly associated with both hemorrhage and rupture but it is not present in earlier stages of plaque development, suggesting that fibrin imaging would be sensitive for high risk plaque versus stable/early disease. Here, we describe imaging properties of a fibrin-specific PET probe for atherosclerotic plaque rupture in rabbits. Methods: Rabbits were fed with high cholesterol diet (HCD) for 8 weeks followed by 2 weeks of normal diet. Two weeks after the initiation of HCD, endothelial denudation of abdominal aorta was performed using balloon catheter. At 10 weeks, rabbits were randomly divided into plaque rupture (n=8; triggered by Russell's viper venom and histamine) and control group (n=4), injected with fibrin-binding probe [^{68}Ga]CM-246, and scanned on a PET/MRI. Then, vessels of interest were removed for ex-vivo PET, autoradiography, and histology. Results: Rabbits with plaque rupture had >2-fold increase in [^{68}Ga]CM-246 signal in the abdominal aorta compared with the control group (A). At 105-120 min post probe injection, there was a clear PET uptake on the aorta in plaque rupture rabbit (B) compared with control rabbit (C). MR images were used to differentiate abdominal aorta (green arrows) and the inferior vena cava (blue arrows). T2-dark blood images confirmed the atherosclerotic plaques in plaque rupture (D) and control rabbits (E). ToF images were used to visualize aortic lumen in plaque rupture (F) and control rabbits (G). Ex vivo PET imaging (H) and autoradiography confirmed in vivo results. Conclusions: We demonstrated that [^{68}Ga]CM-246 detects atherosclerotic plaque rupture in a rabbit model and can be a useful tool for the diagnosis of high-risk atherosclerotic plaque in patients.

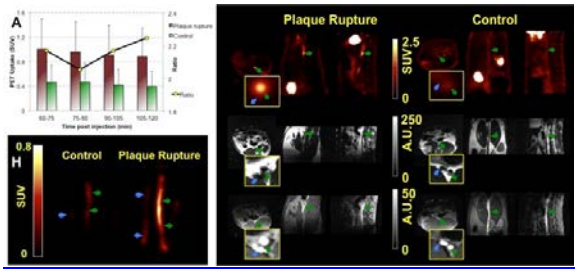

D. Izquierdo-Garcia: None. **H. Diyabalanage:** Employment; Significant; Collagen Medical. **I. Ramsay:** Employment; Significant; Collagen Medical. **N.J. Rotile:** None. **A. Mauskapf:** None. **J. Choi:** None. **T. Witzel:** None. **V. Humblet:** Employment; Significant; Collagen Medical. **A. Brownell:** None. **C. Catana:** None. **P. Caravan:** Research Grant; Significant; Pliant Therapeutics, Pfizer. Ownership Interest; Significant; Collagen Medical, Factor 1A LLC, Reveal Pharmaceuticals. Consultant/Advisory Board; Modest; Bayer, Guerbet. **I. Ay:** Research Grant; Significant; electroCore, LLC.

329

Systems-based Target Discovery Reveals PPARa as a Key Metabolic Regulator for Macrophage Activation in Vein Graft Disease

Julius Decano, Hengmin Zhang, Sasha Singh, Andrew Mlynarchik, Alexander Mojcher, Jianguo Wang, Lang Ho Lee, Arda Halu, Hideyuki Higashi, Peter Mattson, Jiao Qiao, Jung Choi, Michael Creager, Peter Libby, BWH and Harvard Medical Sch, Boston, MA; Daniel G. Anderson, Massachussetts Inst of Technology, Cambridge, MA; C. Keith Ozaki, Elena Aikawa, Masanori Aikawa, BWH and Harvard Medical Sch, Boston, MA

Objectives: Vein graft (VG) failure rates after surgical bypass for PAD remain high, which can cause limb loss. Yet, the underlying mechanisms for VG lesion development remain obscure. We took a systems approach to explore key pathways in a mouse model. **Approach and Results:** We implanted the inferior vena cava into the left carotid artery of fat-fed Ldlr-/- mice and monitored lesion development up to 4 weeks post-surgery. Unbiased proteomic profiling followed by hierarchical clustering showed distinct clusters. One protein cluster is decreased in vein grafts with overt lesions (poor outcome) relative to the group of non-diseased veins devoid of lesions and vein grafts with minimal lesion (favorable outcome). Conversely, this can be viewed as increased in the "favorable" outcome group. Using the "favorable outcome" predominant protein cluster, network analysis and pathway enrichment identified PPARα pathway as a top-ranked key hub node with high betweeness centrality measure. This implies that PPARα may play a key regulatory role in limiting lesion severity. We examined whether network-based prediction of PPARα can also serve as a therapeutic target to attenuate the development of experimental VG lesions. A blinded *in vivo* loss-of-function study using PPARα siRNA encapsulated in macrophage-targeted lipid nanoparticles (LNP) demonstrated higher plaque volume as seen by 3D ultrasound and histologic morphometry in the test group (n=7) versus the control group (n=8). In contrast, a randomized drug study on another set of VG mice using the new PPARα-selective agonist pemafibrate demonstrated less plaque lesions and macrophage accumulation in the drug group (n=11) compared to the control group (n=11). In vitro validation studies (alongside loss-of-function) including high-throughput qPCR, single cell qPCR, CyTOF, ELISA, FACS, and metabolic assays all suggested that pemafibrate-induced PPARα activation promotes a phenotype shift of activated macrophages into a less inflammatory state through

metabolic reprogramming. **Conclusion:** Systems-based target discovery on VG demonstrates that PPARα agonism reduces lesion development and inflammatory burden. Targeting this pathway might furnish a novel therapeutic option to prevent VG lesion development.
J. Decano: None. **H. Zhang:** None. **S. Singh:** None. **A. Mlynarchik:** None. **A. Mojcher:** None. **J. Wang:** None. **L. Lee:** None. **A. Halu:** None. **H. Higashi:** None. **P. Mattson:** None. **J. Qiao:** None. **J. Choi:** None. **M. Creager:** None. **P. Libby:** None. **D.G. Anderson:** None. **C. Ozaki:** None. **E. Aikawa:** None. **M. Aikawa:** None.

330
Targeted Nanotherapy for the Treatment of Atherosclerosis
Neel A Mansukhani, Miranda So, Mazen S Albaghdadi, Northwestern Univ, Chicago, IL; Erica B Peters, Univ of North Carolina at Chapel Hill, Chapel Hill, NC; Zheng Wang, Samuel I Stupp, Northwestern Univ, Chicago, IL; Melina R Kibbe, Univ of North Carolina at Chapel Hill, Chapel Hill, NC

Objective: Atherosclerosis is the leading cause of death and disability in the United States. We hypothesize that systemic administration of a novel nanofiber will target areas of atherosclerosis and regress atherosclerotic lesions.
Methods: Self assembling peptide amphiphile (PA) nanofibers were synthesized. An 18 amino acid sequence which retains the cholesterol efflux actions of apolipoprotein-A1 (apoA1) along with a Liver X Receptor (LXR) agonist, known to enhance cholesterol efflux, were incorporated into the nanofiber to both target and treat atherosclerosis. To assess the ability of the nanofiber to target and treat atherosclerosis *in vivo*, LDL receptor knockout mouse (LDLR KO) mice were fed a high fat diet (HFD) for 14 weeks after which they received bi-weekly injections of the therapeutic or control for 8 weeks. Optimum dose, concentration, binding duration, and biodistribution was determined using fluorescent microscopy and pixel quantification. Treatment groups included: PBS control, PA nanofiber with a scrambled targeting sequence, LXR agonist alone, targeted PA nanofiber (ApoA PA), and targeted PA nanofiber incorporating LXR agonist (ApoA-LXR PA). n=10/treatment group.
Results: ApoA PA and ApoA-LXR PA nanofibers effectively targeted atherosclerotic plaque in the aortic root. Optimum concentration of nanofiber was 2mg/mL, and optimum dose was 6mg/kg. There was no difference in optimum dosing or concentration between males and female mice. ApoA PA nanofiber localized to the aortic root for approximately 2-3 days, and was cleared from the aortic root by 7-10 days. Concentrations of ApoA PA in the aortic root was 5-fold higher than in the lung, liver, and kidney one day post injection. After only 8 weeks of treatment, male and female mice treated with ApoA-LXR PA had 11 and 9% plaque area reduction compared to PBS treated controls, respectively. Differences in treatment conditions vs. controls showed sex dependence, with only male mice demonstrating significantly higher plaque reduction from ApoA1-LXR PA treatment in comparison to scrambled PA treatment.
Conclusions: Our results demonstrate that a novel targeted nanofiber binds specifically to atherosclerotic lesions and reduce plaque burden after a short treatment duration.
N.A. Mansukhani: None. **M. So:** None. **M.S. Albaghdadi:** None. **E.B. Peters:** None. **Z. Wang:** None. **S.I. Stupp:** None. **M.R. Kibbe:** None.

331
Fatty Acid Synthase Expression in Peripheral Arterial Plaque
Kshitij A. Desai, Gayan DeSilva, Yang Chao, Luis Sanchez, Clay Semenkovich, Mohamed Zayed, Washington Univ in Saint Louis Sch of Med, St. Louis, MO

Introduction: Diabetic patients exhibit distinct patterns of diffuse and recalcitrant peripheral artery disease, which subsequently predisposes them to poor wound-healing, infection, and critical limb ischemia. Fatty Acid Synthase (FAS), an enzyme responsible for de novo fatty acid synthesis, exhibits elevated content in the liver tissue in diabetic mouse models and elevated serum levels in diabetic subjects with carotid artery stenosis. It is currently unknown whether tissue FAS and serum circulating FAS (cFAS) correlate with diabetic status in patients with femoral arterial-occlusive disease.
Materials and Methods: We enrolled diabetic and non-diabetic subjects undergoing femoral endarterectomy (FEA) in an IRB-approved vascular biobank. Serum and femoral endarterectomy plaque samples were collected from participants, and tissue FAS and serum cFAS, content was evaluated using ELISA. Differences in cFAS content between cohorts were summarized as mean ± SEM, and statistical significance was determined via T-test and Pearson correlation analysis.
Results: 33 patients (16 DM, 17 non-DM) who underwent femoral endarterectomy for high grade occlusive disease were evaluated. No significant difference in key demographics were observed. Tissue plaque FAS content was 69.8% (13.3 vs 7.81 ELISA: Total protein) higher in DM compared to non-DM subjects (p-value = 0.011). cFAS was also elevated by 41.7% (1.39 vs 0.98 ELISA: Total protein) in diabetic compared to non-DM subjects (p-value = 0.048). Correlation analysis of 23 patients' paired samples revealed a significant correlation between cFAS and plaque FAS content (Pearson r = 0.47, p-vale = 0.023).
Conclusion: Our study is the first to evaluate cFAS levels in patients with high grade, symptomatic, lower extremity PAD, and demonstrates evidence that cFAS and tissue FAS levels correlate in subjects with diabetes. Future studies will help determine whether cFAS is a relevant biomarker for disease severity and progression in diabetic subjects.
K.A. Desai: None. **G. DeSilva:** None. **Y. Chao:** None. **L. Sanchez:** None. **C. Semenkovich:** None. **M. Zayed:** None.

332
Fibronectin Containing Extra Domain a in the Plasma, but not Tissue, Exacerbates Stroke Outcome in the Comorbid Condition of Hyperlipidemia
Nirav Dhanesha, Mehul Chorawala, Prakash Doddapattar, Anil Chauhan, Univ of Iowa, Iowa City, IA

***Background*:** Fibronectin-splicing variant containing extra domain A (Fn-EDA) is expressed in the endothelium of atherosclerotic arteries and elevated in circulation in at risk of patients with diabetes, hypertension, and atherosclerosis. Recent studies suggest that Fn-EDA contributes to ischemic stroke. The relative contribution of plasma versus (vs.) tissue Fn-EDA in stroke outcome remains unclear. We determined the contribution of plasma vs. tissue Fn- EDA in stroke exacerbation in the comorbid condition of hyperlipidemia.
***Methods*:** We generated *Fn-EDA$^{fl/fl}$AlbCre^{+}*, which express Fn-EDA in all tissues but not in plasma, on hyperlipidemic apolipoprotein E deficient (*Apoe$^{-/-}$*) background. Controls were *Fn- EDA$^{fl/fl}$Apoe$^{-/-}$* mice, which express FN-EDA in all tissues and plasma. Susceptibility to stroke outcome was evaluated in male and female mice (8-10 weeks) by transient 1-hour ischemia followed by 1, 3, and 7 days of reperfusion. Quantitative assessment of stroke outcome was evaluated by measuring infarct volume (MRI), cerebral blood flow (laser speckle imaging), neurological outcome, and postischemic thrombo-inflammation (fibrin deposition, neutrophil, and inflammatory cytokines within the infarcted and surrounding region by Western blotting and immunohistochemistry). Susceptibility to thrombosis was evaluated in a $FeCl_3$ injury- induced carotid thrombosis model.
***Results*:** Irrespective of gender, *Fn-EDA$^{fl/fl}$AlbCre^{+}Apoe$^{-/-}$* exhibited smaller infarcts and improved neurological outcome at days 1, 3 and 7 concomitant with improved survival, and decreased post ischemic thrombo-inflammation (P<0.05 vs. *Fn-EDA$^{fl/fl}$Apoe$^{-/-}$*). Laser speckle imaging revealed improved regional cerebral blood flow in *Fn-DA$^{fl/fl}$AlbCre^{+}Apoe$^{-/-}$* mice (P<0.05 vs. *Fn-EDA$^{fl/fl}$Apoe$^{-/-}$*), suggesting that Fn-EDA present in plasma may promote intracerebral thrombosis and thereby exacerbate stroke.

Using i ntravital microscopy, we found that *Fn-EDA$^{fl/fl}$AlbCre^{+}Apoe$^{-/-}$* mice were less susceptible to experimental thrombosis (*P*<0.05 vs. *Fn-EDA$^{fl/fl}$Apoe$^{-/-}$*). **Conclusion:** Following STAIR guidelines, we provide evidence that Fn-EDA present in the plasma, but not tissue, contribute to stroke exacerbation by promoting thrombo-inflammation.
N. Dhanesha: None. **M. Chorawala:** None. **P. Doddapattar:** None. **A. Chauhan:** None.

333
Dynamic Limb-specific Metabolomics Reveals the Impact of Diabetes on Muscle and Vascular Responses to Ischemic Stress
Jane F Ferguson, Shi Huang, Vanderbilt Univ Medical Ctr, Nashville, TN; Robert E Gerszten, Beth Israel Deaconess Medical Ctr, Boston, MA; Joshua A Beckman, Vanderbilt Univ Medical Ctr, Nashville, TN

Background: Type 2 Diabetes Mellitus (T2DM) increases cardiovascular risk, but the mechanisms are incompletely understood. Blood metabolomic signatures are altered in T2DM, but the impact of ischemic stress on the local skeletal muscle signature and T2DM-related vascular dysfunction is unknown. **Methods**: We recruited 38 subjects (18 healthy, 20 T2DM), placed an antecubital intravenous catheter, and performed ipsilateral brachial artery reactivity testing. Blood samples for plasma metabolite profiling were obtained at baseline and upon cuff release after 5 minutes of ischemia. Brachial artery diameter was measured at baseline and 1 minute after cuff release. **Results**: As expected, flow-mediated vasodilation was attenuated in subjects with T2DM (p<0.01). We confirmed known T2DM-associated baseline differences in plasma metabolites, including homocysteine, dimethylguanidino valeric acid and β-alanine (all p<0.05). Metabolites were significantly altered in response to experimental ischemia. Ischemia-induced metabolite changes that differed between groups included 5-hydroxyindoleacetic acid (Healthy: -27%; T2DM +14%), orotic acid (Healthy: +5%; T2DM -7%), trimethylamine-N-oxide (Healthy: -51%; T2DM +0.2%), and glyoxylic acid (Healthy: +19%; T2DM -6%) (all p<0.05). Serine, betaine, aminoisobutyric acid and anthranilic acid associated with vessel diameter at baseline, but only in T2DM (all p<0.05). Metabolite responses to ischemia were significantly associated with vasodilation extent, but primarily observed in T2DM. Within T2DM subjects, metabolite changes predicting change in vessel diameter included enrichment in amino acid, glycerophospholipid and propanoate metabolism (all p<0.05). **Conclusion**: Our study highlights potential impairments in muscle and vascular signaling at rest and during ischemic stress in T2DM. While metabolites change in both healthy and T2DM subjects in response to ischemia, a relationship between muscle metabolism and vascular function is modified in T2DM, suggesting that dysregulated muscle metabolism in T2DM may have direct effects on vascular function.
J.F. Ferguson: None. **S. Huang:** None. **R.E. Gerszten:** None. **J.A. Beckman:** None.

This research has received full or partial funding support from the American Heart Association.

334
Collateral Development in Swine after Ligation of Native Leg Arteries
Yue Gao, Shruthi Aravind, Matthew Fuglestad, Univ of Nebraska Medical Ctr, Omaha, NE; Chris Hansen, VA Nebraska-Western Iowa Health Care System, Omaha, NE; George Casale, Mark Carlson, Iraklis Pipinos, Univ of Nebraska Medical Ctr, Omaha, NE

Introduction: The development of collateral vasculature is a key mechanism compensating for arterial occlusions in patients with Peripheral Artery Disease (PAD). We aimed to examine the development of collateral pathways after ligation of native vessels in a porcine model of PAD.
Methods: Right hindlimb Ischemia was induced in domestic swine (N=11, male, 26-57 kg) using two different versions of arterial ligation. Version 1 (N=6) consisted of ligation/division of the right external iliac, profunda femoral (RPFA) and superficial femoral arteries (RSFA). Version 2 (N=5) consisted of the ligation of Version 1 with additional ligation/division of the right internal iliac artery (RIIA). Development of collateral pathways was evaluated with standard angiography at baseline (prior to arterial ligation) and at termination (4-8 weeks later). Relative luminal diameter of the arteries supplying the ischemic right hindlimb were determined by 2D angiography, as percent of the size of the distal aortic diameter.
Results: The pathway connecting the RIIA to the RPFA and RSFA/popliteal artery of the ischemic limb was the dominant collateral pathway in version 1. Mean luminal diameter (± standard error) of the RIIA at termination increased by 39.4± 5.5% (P<0.01) compared to baseline. There were two co-dominant collateral pathways in version 2. The first pathway connected the common internal iliac trunk and left internal iliac artery to the reconstituted RIIA which then supplied the RPFA and RSFA/popliteal arteries. The second pathway connected the left profunda artery to the reconstituted RPFA. Mean diameter (± standard error) of the common internal iliac trunk and left profunda artery increased at termination by 23.7± 7.6% and 24.8± 7.4%, respectively (p < 0.05).
Conclusion: Two versions of hindlimb ischemia induction (right ilio-femoral artery ligation with and without right internal iliac artery ligation in swine produced differing collateral pathways along with changes to the diameter of the inflow vessels. Radiographic and anatomical data of the collateral formation in this porcine model has value in investigation of the pathophysiology of hindlimb ischemia, and assessment of angiogenic therapies as potential treatments for PAD.
Y. Gao: None. **S. Aravind:** None. **M. Fuglestad:** None. **C. Hansen:** None. **G. Casale:** None. **M. Carlson:** None. **I. Pipinos:** None.

335
Phase Contrast Magnetic Resonance Imaging as a Novel Complementary Tool for Investigations of Peripheral Artery Disease
Amos A Cao, Ulrich M Scheven, **Joan M Greve**, Univ of Michigan, Ann Arbor, MI

Therapeutic angiogenesis is pertinent to the acute survival of distal ischemic tissue and a relevant treatment for critical limb ischemia (CLI). Therapeutic arteriogeneis is pertinent to the restoration of function, via collateral vessel formation in proximal tissue that is not typically ischemic, and a relevant treatment for preventing intermittent claudication from advancing to CLI. In preclinical models of peripheral artery disease (PAD), laser perfusion imaging methods are applicable to the former. However, recently published results indicate they underestimate recovery and their limited penetration depth restrict their application to the latter. Our objective was to evaluate whether phase contrast magnetic resonance imaging (PC-MRI) could be used as a complementary method in murine models of PAD.
C57BL/6 male mice underwent femoral artery ligation (n=5). Mice were imaged prior to and day 3 after surgery. PC-MRI uses the phase of the MRI signal to calculate velocity of blood flow within a voxel. Integrating velocity across the vessel lumen results in flow measurements. Maximum velocity and mean volumetric flow were compared at the infrarenal aorta and ipsilateral (Ip) and contralateral (Con) iliac arteries.
Maximum velocities did not change in the aorta or Con (pre vs. day 3: aorta, 55.4±7.2 vs. 48.9±9.4 cm/sec; Con, 45.7±7.5 vs. 40.7±8.0 cm/sec). Mean volumetric flows also did not change in the aorta or Con (pre vs. day 3: aorta, 2.0±0.7 vs. 1.53±0.4 mL/min; Con, 1.1±0.4 vs. 0.92±0.3 mL/min). In the ipsilateral iliac artery, maximum velocity was

reduced by ~35% (pre vs. day 3: 43.6±5.7 vs. 28.4±5.5 cm/sec, p=0.002), leading to a reduction in mean flow of ~41% (1.1±0.4 vs. 0.63±0.3 mL/min, p=0.04). Ip/Con ratios for both metrics were: 0.98±0.2 vs. 0.74±0.2 cm/sec, p=0.03; and, 1.0±0.1 vs. 0.72±0.3 mL/min, p=0.03.
Our previous work demonstrated the ability to promote proximal-arteriogenesis by inducing distal-angiogenesis via application of a slow-release growth factor. Having developed a non-invasive method to directly quantify velocity and flow in large proximal vessels, we will have the opportunity to explore the biomechanical mechanisms coupling angio- and arterio-genesis even though they occur temporally and spatially separated.
A.A. Cao: None. **U.M. Scheven:** None. **J.M. Greve:** None.

336
MiR-126 Modified Endothelial Progenitor Cells Transplantation Contributes to Angiogenesis after Brain Focal Ischemia in SHR Rats
Jun Huang, Shanghai Inst of Hypertension, Ruijin Hosp, Shanghai, China; Meijie Qu, Yaying Song, Ruijin Hosp, Shanghai, China; Yuanyuan Lu, Pingjin Gao, Shanghai Inst of Hypertension, Ruijin Hosp, Shanghai, China

Background and Purpose—Transplantation of endothelial progenitor cells (EPCs) leads to better outcomes in experimental stroke, while improve the EPCs survival rate in ischemia area is still a challenge. MiR-126 modulates vascular development and angiogenesis. Here we overexpressed miR-126 in transplanted EPCs, to investigate the function of gene modified EPCs in angiogenesis after brain ischemia. **Methods**—Adult male SHR rats underwent permanent suture middle cerebral artery occlusion (MCAO). One week after middle cerebral artery occlusion, the animals received tail vein injection of miR-126 modified EPCs as treatment or EPCs as control and were monitored for 5 weeks. Brain water content, infarct volume, neurological score, neurogenesis and angiogenesis were examined. **Results**—Neurological score was greatly improved and brain atrophy was greatly reduced in miR-126 modified EPCs-treated SHR rats compared with the control rats 5 weeks after MCAO (P<0.05). The number of bromodeoxyuridine+/CD31+ microvessels are significantly increased. EPCs migration and proliferation were promoted after miR-126 modified in vitro. **Conclusions**—Our results showed that miR-126 modified EPCs therapyreduced ischemic brain injury, along with increased angiogenesis and neurogenesis in SHR rats, suggesting miR-126 significantly improved EPCs function in angiogenesis after MCAO. Gene modified EPCs represents a promising avenue for ischemic stroke stem cell therapy.
J. Huang: None. **M. Qu:** None. **Y. Song:** None. **Y. Lu:** None. **P. Gao:** None.

337
Short-Term Protein Restriction Attenuates Vein Graft Disease by Inhibition of Endothelial Cell Damage and Upregulates Cystathionine-g-Lyase
Peter Kip, Kaspar M Trocha, Brigham and Women's Hosp and Harvard Medical Sch, Boston, MA; Michael R MacArthur, Jose H Trevino-Villarreal, Harvard T.H. Chan Sch of Public Health, Boston, MA; Alban Longchamp, Brigham and Women's Hosp, Boston, MA; Margreet R de Vries, Leiden Univ Medical Ctr, Leiden, Netherlands; Ming Tao, Brigham and Women's Hosp and Harvard Medical Sch, Boston, MA; James R Mitchell, Harvard T.H. Chan Sch of Public Health, Boston, MA; C. Keith Ozaki, Brigham and Women's Hosp and Harvard Medical Sch, Boston, MA

Objective: Short-term protein restriction (PR) preceding surgery limits ischemia reperfusion injury and arterial intimal hyperplasia in mouse models, possibly via upregulation of endogenous enzymatic production of the gaseous messenger hydrogen sulfide (H_2S) by cystathionine-gamma-lyase (CGL). Here, we tested the hypothesis that short-term PR will limit vein graft disease (VGD) via CGL upregulation and increased H_2S production, resulting in EC cytoprotection and reduced leukocyte transmigration.
Approach and Results: $LDLR^{-/-}$ mice (male, 8-10 weeks old) were fed a high fat/high cholesterol (HF/HC) diet for two weeks. One group was then switched to a PR HF/HC diet with or without daily CGL inhibitor propargylglycine (PAG) injections. 7 days later mice underwent carotid interposition grafting with donor caval veins from mice on matched diets. Mice were euthanized at baseline (preop), post-op day 4 or 28 for analysis of the graft (histology, immunohistochemistry), aorta (western blot) and kidney EC (flow-cytometry).
PR mice showed decreased graft intimal/media+adventitia (I/M+A) area and thickness ratios (Fig. A) on post-op day 28. Staining for CD31 and neutrophil-elastase revealed a relatively intact EC layer (Fig. B-C, CD31 in brown, red arrows, p<0.001) and less neutrophil transmigration (p=0.02) on post-op day 4. PR increased baseline CGL expression in aortas (Fig. D-E) and upregulated EC H_2S (Fig. F). Our preliminary data indicates that PAG injections during PR tended to diminish its protective effects on VGD (Fig. G).
Conclusions: PR attenuated VGD via limiting of EC damage concomitant with increased CGL expression and endogenous H_2S production. Ongoing studies will further define the CGL dependence of this process. Short-term preoperative PR stands as a potentially simple, safe, cost-efficient intervention to enhance vein graft durability.

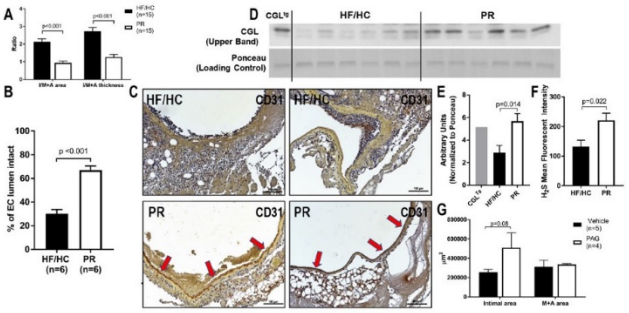

P. Kip: None. **K.M. Trocha:** None. **M.R. MacArthur:** None. **J.H. Trevino-Villarreal:** None. **A. Longchamp:** None. **M.R. de Vries:** None. **M. Tao:** None. **J.R. Mitchell:** None. **C. Ozaki:** None.

This research has received full or partial funding support from the American Heart Association.

338
Statin Therapy is Associated with Decreased Plaque Instability in Symptomatic Carotid Atherosclerotic Plaque: a Clinicopathological Analysis
Takao Konishi, Hokkaido Cardiovascular Hosp, Sapporo, Japan; Shinya Tanaka, Hokkaido Univ, Graduate Sch of Med, Sapporo, Japan

Background: Statin therapy has been shown to deplete atherosclerotic plaque instability in human carotid arteries by various imaging modalities or in animal models by pathological analysis. However, whether statin therapy attenuates plaque instability in human carotid plaque has not been fully described in a pathological analysis. The aim of this study was to analyze pathologically the possible relationships between statin therapy and plaque stability in patients undergoing carotid endarterectomy (CEA).
Methods: Among consecutive 79 patients with advanced carotid artery stenosis (>70%) between May 2015 and February 2017, 66 patients without statin therapy (group 1) and 13 patients with statin therapy (group 2) were analyzed. The specimens were stained with hematoxylin/eosin and elastica-Masson. Immunohistochemistry was performed, using an endothelial specific antibody to CD31, CD34 and PDGFRβ.

Results: Plaques from group 2 had significantly less plaque rupture (P=0.009), lumen thrombus (P=0.009), inflammatory cells (P=0.008), intraplaque hemorrhage (P=0.030) and intraplaque microvessels (P<0.001), compared with those from group 1. Among stroke patients with infarct size >1.0 cm^3 in MRI, the mean infarct volume in group 2 (4.2 ± 2.5 cm^3) was significantly smaller than that in group 1 (8.2 ± 7.1 cm^3, p = 0.031). There was no significant difference in the mean concentration of low-density lipoprotein cholesterol between group 1 and group 2 (121 ± 32 mg/dl vs. 105 ± 37 mg/dl, P=0.118).
Conclusions: This clinicopathological analysis of carotid atherosclerotic plaque suggests that statin therapy is associated with decreased plaque instability, which might result in smaller infarct volume in stroke patients undergoing CEA. This plaque stability might be derived from pleiotropic effect beyond lipid lowering of statin therapy.
T. Konishi: None. **S. Tanaka:** None.

339
Predictors of Periopertive Neurologic Outcomes Following CEA
Roland Richard Macharzina, Matthias Vogt, Carolin Mueller, Franz-Josef Neumann, Thomas Zeller, Univ Heart Ctr Freiburg Bad Krozingen, Bad Krozingen, Germany

Objective The prospective registry study intended to identify risk factors of periinterventional neurologic outcomes after carotid endarteriectomy (CEA) to improve patient selection. Neurologic outcome predicition differs from the endpoint MACCE as previously shown. **Methods** Patient characteristics and procedural factors were prospectively acquired and analysed using Cox regression to determine predictors for stroke and death within 30-days of CEA. **Results** The analysis included 748 operations, 262 (35%) asymptomatic, 208 (28%) with previous strokes, and 278 (37%) with transient ischemic attacks (TIA). The overall 30-day stroke rate was 5.5%, 3.1% in asymptomatic and 6.8% in symptomatic patients and for stroke and death 5.6%, 3.1% and 7.0% respectively. Independent predictors of stroke and death were contralateral occlusion (HR=3.826, p=0.006, CI 1.483 - 9.867), symptomatic status (HR=3.626, p=0.004, CI 1.51 - 8.706), First-degree atrioventricular block (HR=2.209, p=0.041, CI 1.034 - 4.722), resection (HR=2.448, p=0.027, CI 1.106 - 5.416) and myocardial infarction (HR=2.03, p=0.04, CI 1.032 - 3.994) compared to all patients. Similar effect estimates were found for stroke alone. Compared to lower risk patients, SHR and SEC criteria predicted stroke and death after adjustment for symptomatic status (HR=2.29, p=0.02, CI 1.142 - 4.592) and (HR=2.286, p=0.028, CI 1.094 - 4.778). Outcome in low risk patients were not related to the symptomatic status for stroke and death (HR=2.484, p=0.148, CI 0.724 - 8.524), correspondingly for stroke. **Conclusions** This is the first report identifying preprocedural myocardial infarction, first degree AV-block, SHR and SEC as predictors of stroke and stroke and death at 30 days postoperatively.
R.R. Macharzina: None. **M. Vogt:** None. **C. Mueller:** None. **F. Neumann:** None. **T. Zeller:** None.

340
Microvascular Pathology in Peripheral Artery Disease
Constance Jennifer Mietus, Timothy Lackner, Peter Karvelis, Nicholas Lambert, Hernan Hernandez, Iraklis Pipinos, George Casale, UNMC, Omaha, NE

Background: Peripheral Artery Disease (PAD) is caused by atherosclerotic narrowing of arteries supplying the legs. PAD-induced myopathy is characterized by myofiber degeneration and progressive fibrosis. Qualitative histological review suggests pathological changes in the microvasculature of PAD muscle, in association with advancing fibrosis. We tested the hypothesis that microvessel architecture, pericyte coverage, and collagen profiles systematically change with advancing disease and are consistent with advancing microvascular pathology. **Methods:** Biopsies of PAD patients at Fontaine Stage II (n=15) and IV (n=16), and controls (n=15) were labeled with antibodies specific for Col I, Col IV, αSMA, or CD31 and analyzed by quantitative wide-field, fluorescence microscopy. Thickness of the basement membrane (BM), peri-microvascular Col I density, and BM lumen diameter were measured. Pericytes were identified by abluminal location within the microvascular BM and αSMA^+ labeling. Group differences were tested by ANOVA and a *post hoc* pairwise T Test with Bonferroni correction. Correlations were determined by linear regression analysis.
Results: Thickness of the BM was greater in Stage II patients (1.58 µm) compared to controls (1.42 µm) (p<0.043) and in Stage IV (1.75 µm) compared to Stage II patients (p<0.021). Microvascular BM lumen diameter was increased (p<0.001) in Stage IV patients (3.97 µm) compared to control (3.25 µm) and Stage II patients (3.29 µm). Thickened PAD microvessels had greater pericyte coverage than control microvessels. BM thickness correlated positively with microvascular BM lumen diameter (R^2= 0.513, p<0.001). Peri-microvascular Col I deposition correlated positively with microvascular lumen diameter (R^2= 0.162, p=0.006), and was greater in Stage IV compared to Stage II patients (p=0.040).
Conclusions: Increased perivascular Col I deposition, BM thickening, and BM lumen diameter represent advancing microvascular disease in PAD patients. Pericytes, which deposit BM collagen, are more abundant in thickened microvessels. Pericyte replication and secretion of Col IV may be determining factors in the microvascular pathology of PAD muscle.
C.J. Mietus: None. **T. Lackner:** None. **P. Karvelis:** None. **N. Lambert:** None. **H. Hernandez:** None. **I. Pipinos:** None. **G. Casale:** None.

342
Helix-loop-helix Transcription Factor Id3 Promotes Ischemia-induced Angiogenesis
Victoria Osinski, Vijay C Ganta, Anh T Nguyen, Brian H Annex, Coleen A McNamara, Univ of Virginia, Charlottesville, VA

The development of new blood vessels is important during the progression of many diseases including cancer, obesity, and ischemia. While inhibiting blood vessel growth can prevent excess adiposity and tumor growth, it can also exacerbate symptoms of ischemia. Using flow cytometry to quantify total endothelial cells (ECs) in the gastrocnemius of mice who have undergone femoral artery resection (FAR), the number of ECs per gram of muscle increases approximately four-fold relative to uninjured gastrocnemius from the same mouse (442% increase, ± 208%) in a model of hindlimb ischemia. The helix-loop-helix (HLH) transcription factor Inhibitor of differentiation (ID3) promotes angiogenesis and whole tissue blood perfusion in models of cancer and obesity, but the potential role for ID3 in promoting ischemia-induced angiogenesis remains uninvestigated. Id3 mRNA levels in injured gastrocnemius are increased three days post-FAR relative to uninjured gastrocnemius ($p < 0.05$, $n = 6$). Furthermore, ID3 global knockout (KO) mice have attenuated perfusion recovery compared to wild type littermate controls at 14 days post-FAR ($p < 0.05$). Gastrocnemius muscles isolated from ID3 global KO mice 7 days post-FAR express higher levels of the cell cycle inhibitor $p21^{Cip1}$ mRNA than WT mice ($p = 0.10$, $n = 3$). Finally, flow cytometry analysis of cell subsets in a novel Id3 promoter-GFP reporter mouse line revealed that Id3 promoter activation is greater in $CD31^+$ ECs than many other cell types ($n = 10$), suggesting ECs may be an important cell type in which ID3 is promoting pro-angiogenic effects. Together, these data support the hypothesis that ID3 promotes ischemia-induced angiogenesis by promoting EC proliferation and inhibiting cell cycle inhibitor $p21^{Cip1}$. To investigate the role of ID3 in ECs during angiogenesis, an EC-specific, tamoxifen-inducible Id3 KO mouse ($Id3^{fl/fl}$ Cdh5-Cre/ERT2) has been generated.

V. Osinski: None. **V.C. Ganta:** None. **A.T. Nguyen:** None. **B.H. Annex:** None. **C.A. McNamara:** None.

343
Baseline Serum Uric Acid Predicts Future Cardiovascular Events and Death in Patients Undergoing Carotid Endarterectomy
Megha Prasad, Valentina Nardi, Fred Meyer, Lilach Lerman, Amir Lerman, Mayo Clinic, Rochester, MN

Background Serum uric acid is a marker of oxidative stress, and may serve as a marker of adverse cardiovascular events and outcomes including cardiovascular death, hospitalization and myocardial infarction. We aimed to determine whether uric acid predicts cardiovascular events and death in patients undergoing carotid endarterectomy (CEA). Methods We enrolled 327 patients undergoing CEA between February 2002 and June 2017 who had complete laboratory work up at baseline. Patients were followed through the electronic chart as well as via regular nursing follow-up for a median of 10.9 years (IQR 7.3, 13.4). There were a total of 67 adverse cardiovascular events during follow-up. Results: Baseline serum uric acid levels were significantly higher in patients who developed cardiovascular events during the follow-up period vs. those that did not [6.87$\pm$2.29 vs. 6.39 $\pm$1.61); p=0.047). Baseline serum uric was independently associated with cardiovascular events when adjusting for age, creatinine, diabetes mellitus, and hyperlipidemia (L-R 4.0, p=0.04)(Figure 1). Sex stratified analysis showed that serum uric acid was also an independent predictor of both cardiovascular events and death in men, not women undergoing after adjustment for confounders including age, cholesterol, systolic blood pressure and glucose (LR 4.97; p=0.03). Discussion: Higher uric acid levels are associated with cardiovascular events and death after CEA. Further investigation is necessary to determine the role of uric acid as a modifiable risk factor in these patients.
M. Prasad: None. **V. Nardi:** None. **F. Meyer:** None. **L. Lerman:** None. **A. Lerman:** None.

344
Reconstituted High-density Lipoprotein (rHDL) Directly Modulates Inflammatory Cells after Myocardial Infarction in Mice
Adele Richart, Medini Reddy, Baker Heart and Diabetes Inst, Melbourne, Australia; Sarah Heywood, Ctr for Physical Activity Res, Copenhagen, Denmark; Svetlana Diditchenko, Alexei Navdaev, CSL Behring AG, Berne, Switzerland; Bronwyn Kingwell, Baker Heart and Diabetes Inst, Melbourne, Australia

Aim: We have recently demonstrated that reconstituted high-density lipoprotein (rHDL) delivered immediately after myocardial infarction reduces infarct size and improves heart function in mice (*Heywood SE, Sci Transl Med, 2017*). We now examine potential immunomodulatory actions of HDL that may underlie these effects.
Methods: In male C57BL/6 mice, a single intravenous bolus of rHDL (CSL-111, 80mg/kg of human apoA-I, or saline) was delivered at the time of reperfusion following 30mins of surgically-induced ischemia. Effects on the inflammatory response were studied throughout the 5 days post ischemia-reperfusion.
Results: Twenty-four hours after ischemia-reperfusion, rHDL reduced the number of circulating leukocytes (versus saline p<0.05) and increased the number in spleen (p<0.05). rHDL inhibited the recruitment cascade of the entire spectrum of inflammatory cells into the left ventricle (LV) including neutrophils (1 day post ischemia), T and B cells (3 days after), and monocytes (5 days after) (p<0.05 for all). This was associated with lower cardiac expression of chemokines that attract neutrophils (CXCL1, CXCL2, CXCL5) and monocytes (CCL2) (ELISA, p<0.05 for all). Histochemistry at 6 and 24 hours after ischemia-reperfusion showed fluorescently labeled rHDL localized to the infarct and peri-infarct regions. There were also greater quantities of rHDL (human apoA-I) in the LV and spleen of mice subjected to ischemia versus sham-operated mice (ELISA, p<0.05); no rHDL was observed in the right ventricle. In addition, flow cytometry studies using the fluorescent rHDL indicated binding to both circulating leukocytes as well as those recruited into the ischemic LV (mostly neutrophils and monocytes). rHDL had a greater association with the circulating pro-inflammatory monocyte subtype ($Ly6C^{high}$) than the anti-inflammatory subtype ($Ly6C^{low}$; p<0.05) 24 hours post ischemia. Furthermore, there was less recruitment of $Ly6C^{High}$ monocytes 5 days post ischemia in the LV of mice treated with rHDL (p<0.05).
Conclusion: rHDL limits the myocardial post-ischemic inflammatory response by effects in both the LV and by directly modulating inflammatory cells. These finding suggest a novel treatment modality for acute coronary syndromes.
A. Richart: Research Grant; Significant; Research grant by CSL Ltd for a drug unrelated to the current submission. **M. Reddy:** None. **S. Heywood:** None. **S. Diditchenko:** None. **A. Navdaev:** None. **B. Kingwell:** Research Grant; Significant; Research grant by CSL Ltd for a drug unrelated to the current submission. Other Research Support; Modest; CSL Ltd provided the rHDL (CSL-111) to the Baker Institute for experimental studies but provided no funding and had no role in this project, Partial reimbursement of travel expenses (no honoraria). Consultant/Advisory Board; Modest; Member of International advisory board for another CSL product. No personal fees received, but modest consultation fees paid to the Baker Heart and Diabetes Institute (~$5,000)..

345
Combining Morphological and Mechanical Risk Factors May Improve Carotid Plaque Progression Prediction: an Magnetic Resonance Image-Based Follow-Up Study
Dalin Tang, Worcester Polythechnic Inst, Worcester, MA; Qingyu Wang, Southeast Univ, Nanjing, China; Gador Canton, Dept of Mechanical Engineering, Univ of Washington, Seattle, WA; Thomas S. Hatsukami, Div of Vascular Surgery, Univ of Washington, Seattle, WA; Kristen L. Billiar, Zheyang Wu, Worcester Polythechnic Inst, Worcester, MA; Chun Yuan, Dept of Radiology, Univ of Washington, Seattle, WA

It has been hypothesized that combining morphological and mechanical risk factors may improve plaque progression prediction. In this paper, plaque burden (PB), cap thickness (CT), lipid percent (LP), plaque wall stress (PWS), plaque wall strain (PWSn) and their combinations were used as predictors to identify the best predictor(s) for plaque progression measured by plaque area increase (PAI) from baseline (T1) and follow-up (T2).
In vivo magnetic resonance image (MRI) carotid plaque data were acquired from 8 patients (5 m, mean age 71) with follow-up (18 months) with informed consent obtained. We built 3D thin-layer models for the 41 matched slices to obtain plaque stress/strain data using patient-specific material properties determined from Cine MRI and patient arm blood pressure. The mean values of the 5 predictors from all lumen points of each slice were obtained for analysis. For each predictor Y, a threshold value Yc was determined so that optimal agreement rate was obtained (agreement cases are either {(Y>Yc) and (PAI >0)} or {(Y≤Yc) and (PAI ≤0)}). For PWS and PWSn, we used (either {(Y<Yc) and (PAI >0)} or {(Y≥Yc) and (PAI ≤0)}). Two combinations of predictors
COM1=a1*PB+a2*CT+a3*LP,
COM2=b1*PB+b2*CT+b3*LP+b4*PWS+b5*PWSn
were considered, where COM1 combines PB with morphological features, and COM2 combines all 5 predictors. The coefficients in these formulas were determined by using iterative linearly fitting method and initial guess of threshold values from single predictor results. The optimal threshold values for the 5 single predictors and 2 combination predictors are given in Table 1. PWSn was the best single predictor and COM2 was the best combination predictor.

The threshold value-based method is simple and easy for clinical implementation. Our preliminary results indicate that combining PB, CT, LP, PWS, and PWSn could improve the agreement rate by nearly 10%, compared to using PB alone. Large-scale patient studies are needed to confirm our findings.

Predictor	PB	CT	LP	PWS	PWSn	COM1	COM2
Threshold	51.29%	0.0196cm	14.32%	97.43kPa	0.1705	-0.0217	-0.0292
Agreement Rate	60.98%	63.41%	60.98%	65.85%	68.29%	65.85%	70.73%
COM1=0.0414*PB-0.5487*CT-0.2852*LP COM2=0.1322*PB-0.3107*CT-0.3177*LP+0.0022*PWS-1.4653*PWSn							

Table 1. Optimal threshold values and their corresponding PAI prediction agreement rates for 7 predictors considered.

D. Tang: Research Grant; Modest; NSF DMS-0540684, NIH R01 EB004759, BE2016785. **Q. Wang:** Research Grant; Modest; BE2016785. **G. Canton:** Research Grant; Modest; NSF DMS-0540684. **T.S. Hatsukami:** None. **K.L. Billiar:** Research Grant; Modest; NIH R01 EB004759. **Z. Wu:** None. **C. Yuan:** Research Grant; Modest; NSF DMS-0540684.

346

Pre-Operative Protein and Methionine Restriction Does Not Impair Wound Healing in a Murine Mcfarlane Wound Healing Model

Kaspar Trocha, Brigham and Women's Hosp, Boston, MA

Background: Numerous pre-clinical studies have demonstrated that pre-conditioning before surgery with various forms of dietary restriction enhances the surgical stress response leading to improved outcomes. However the effect of restricting proteins or amino acids for seven days prior to surgery on a healing surgical wound is currently unknown. Therefore using a using an established murine wound healing model we hypothesized that pre-operative protein restriction (PR) or methionine restriction (MR) would not impair wound healing. ***Approach & Results:*** To asses wound healing potential a Mcfarlane wound healing model was employed where a pedicle flap measuring 2.5 x 1.25cm with a silicone sheet inferior to flap to prevent angiogenesis from bellow on the dorsum of the mouse was performed. Dietary interventions included 7 days of either an iso-caloric protein restricted (90% carb., 10% fat, 0% protein) diet or 3 weeks of an methionine restricted (76% carb., 10% fat, 14% protein) diet before surgery and resumed a complete (72% carb., 10% fat, 18% protein) diet post op. Daily photographs of the wound were taken and necrotic area was calculated. PR mice revealed a trend towards accelerated wound healing, with no difference in percentage of viable skin 7 days after surgery (Fig. A). Also, daily laser Doppler imaging was performed to assess for flap perfusion and viability (Fig. B,E). MR mice displayed accelerated wound healing 3 days after surgery (Fig. C, $p<0.05$) compared to controls while after 7 days, as with PR mice, no difference in percentage viable skin was observed (Fig. D). **Conclusion:** Reducing/removing protein intake or eliminating single amino acids prior to surgery in pre-clinical models has shown to protect against surgical stress. Here we show that brief dietary-manipulations stand as simple strategies toward improving the host response to surgical injury and do not inhibit or impair wound healing in mice, thereby further enhancing clinical applicability.

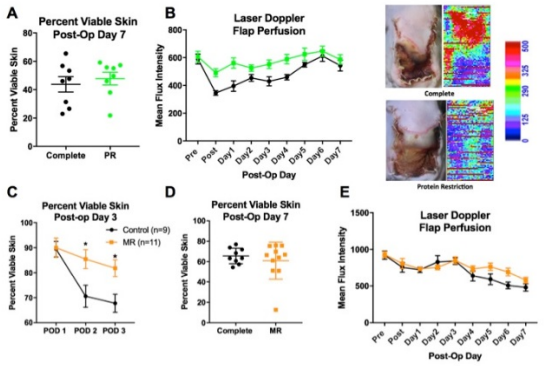

K. Trocha: None.

This research has received full or partial funding support from the American Heart Association.

347

Significant Association Between the Qualifying Neurologic Event and the In-hospital Risk of Stroke or Death Following Carotid Endarterectomy and Carotid Artery Stenting

Pavlos Tsantilas, Div of Vascular Surgery, Stanford Univ Sch of Med, Stanford, CA; Christoph Knappich, Sofie Schmid, Michael Kallmayer, Dept of Vascular and Endovascular Surgery, Klinikum rechts der Isar, Technical Univ of Munich, Munich, Germany; Thorben Breitkreuz, aQua – Inst for Applied Quality Improvement and Res in Health GmbH, Göttingen, Germany; Alexander Zimmermann, Andreas Kuehnl, Hans-Henning Eckstein, Dept of Vascular and Endovascular Surgery, Klinikum rechts der Isar, Technical Univ of Munich, Munich, Germany

Objectives: The purpose of this observational study was to analyze the association between the initial neurological status and the risk of any in-hospital stroke or death in patients treated with carotid endarterectomy (CEA) or carotid artery stenting (CAS) under routine conditions in Germany. **Methods:** Secondary data analysis based on the German statutory quality assurance database for carotid procedures between 2009-2014. The primary outcome was any periprocedural stroke or all-cause death until discharge. To analyze the association between initial neurological status and outcome, a multilevel multivariable regression analyses adjusting for confounders was performed. **Results:** From a total of 182,033 patients documented between 2009 and 2014, 144,347 patients treated with CEA and 14,794 patients treated with CAS were included in the analysis. In total, there 68% were men and the mean age of the cohort was 70.5±9.1 years. The risk of any in-hospital stroke or death in patients treated with CEA was 2.0% (n=2923/144,347). The raw risk of any in-hospital stroke or death was 1.4% in asymptomatic patients and 3.0% in symptomatic patients treated with CEA. Within the group of symptomatic patients, risk of any in-hospital stroke or death after CEA increased from 1.2% (amaurosis fugax, AFX), 2.3% (TIA), 2.8% (minor stroke), 4.4% (major stroke), 4.8% (crescendo TIA, cTIA) to 9.0% (stroke in evolution, SIE). The risk of any in-hospital stroke or death in patients treated with CAS was 3.6% (n=538/14,794). The raw risk of any in-hospital stroke or death was 1.7% in asymptomatic patients and 6.1% in symptomatic patients treated with CAS. Within the group of symptomatic patients, risk of any in-hospital stroke or death increased from 1.0% (AFX), 4.1% (TIA), 4.1% (minor stroke), 5.4% (major stroke), 5.2% (cTIA) to 11.7% (SIE). Regression analysis revealed that the severity of initial neurologic symptoms was associated with an increased risk of any in-hospital stroke or death in both patients treated for CEA and CAS. **Conclusion:** Periprocedural risk for any stroke or death did not

significantly differ between asymptomatic patients and patients with AFX but between asymptomatic patients and patients with TIA, stroke, cTIA or SIE.
P. Tsantilas: None. **C. Knappich:** None. **S. Schmid:** None. **M. Kallmayer:** None. **T. Breitkreuz:** None. **A. Zimmermann:** None. **A. Kuehnl:** None. **H. Eckstein:** None.

348
The Blood-Pressure-Lowering Effect of Moxonidine May Be Partially Through the Prostaglandin Pathway in the Kidney
Yutang Wang, Michelle Steicke, Federation Univ Australia, Ballarat, Australia; Jonathan Golledge, James Cook Univ, Townville, Australia

Objectives: Moxonidine is believed to decrease blood pressure via inhibiting sympathetic activity in the brain and consequently decreasing vascular tone. However, whether direct peripheral mechanisms are involved in this process is unknown. This study aimed to investigate possible peripheral mechanisms of moxonidine in lowering blood pressure. **Methods**: Two groups (N = 10 in each group) of apolipoprotein E-deficient mice were used. These animals were treated with or without moxonidine (18 mg/kg body weight per day) via drinking water throughout the experiment. Three days after the initiation of moxonidine treatment, hypertension was induced by subcutaneous infusion of angiotensin II (1 µg/kg body weight per min) for 28 days. Blood pressure was measured by the tail cuff method. Size and area of kidney tubules and glomeruli were analyzed by morphometric analysis. Gene expression was assessed by quantitative PCR. **Results**: Moxonidine treatment significantly decreased blood pressure ($P<0.05$). It did not change the size or area of either kidney tubules or glomeruli ($P>0.05$), nor the renal expression of inflammatory markers. Both types of moxonidine receptors (imidazoline 1 and alpha-2 adrenergic receptors) were found to be expressed in the kidney, and their gene expression was not altered by moxonidine treatment. However, moxonidine treatment significantly increased the expression of prostaglandin EP3 receptor ($P<0.05$). Increased prostaglandin EP3 receptor has been reported to be associated with promoting diuresis and natriuresis and thus decreasing blood pressure. **Summary**: The results indicate that moxonidine may lower blood pressure partially through an unrecognized non-central pathway by upregulating prostaglandin EP3 receptor in the kidney in mice.
Y. Wang: None. **M. Steicke:** None. **J. Golledge:** None.

349
The Association of Comorbid Depression with Inpatient Outcomes in Patients with Critical Limb Ischemia
Greg J Zahner, Abigail Cortez, Erin Duralde, Joel L Ramirez, Sue Wang, Jade Hiramoto, Beth E Cohen, Owen M Wolkowitz, UCSF, San Francisco, CA; Shipra Arya, Stanford, Palo Alto, CA; Nancy K Hills, Marlene Grenon, UCSF, San Francisco, CA

Background: Critical limb ischemia (CLI) is the end-stage of peripheral artery disease (PAD) and mounting evidence suggests an association between depression and PAD. The objective of this study was to determine whether outcomes, primarily major amputation, differed between CLI patients with and without comorbid depression in a large nationally-representative sample of patients in the United States. **Methods:** Patients hospitalized for CLI during 2012 and 2013 were identified from the National Inpatient Sample (NIS) using ICD-9 diagnostic and procedure codes. Depression, revascularization procedures, and relevant comorbidities were also identified. The primary outcome was major amputation and secondary outcomes were length of stay and other complications. Multivariable logistic models were run adjusting for sociodemographic factors, prior amputation, tobacco use, and several comorbidities. **Results:** The sample included 116,008 patients hospitalized for CLI of whom 10,512 (9.1%) had comorbid depression. Patients with depression were younger (64±14 yrs vs. 67±14, $p<.0001$) and more likely to be female (55% vs. 41%, $p<.001$), white (73% vs. 66%, $p<.001$), and tobacco users (46% vs. 41%, $p<.001$). They were also more likely to have prior amputations (9.8% vs. 7.9%, $p<.001$) and diabetes with chronic complications (25% vs. 20%, $p<.001$). During the hospitalization, the rate of major amputation was higher in patients with comorbid depression (11.5% vs. 9.1%, $p<.001$). In multivariable analysis, excluding patients who died prior to receiving an amputation (n=2,621), comorbid depression was associated with a 39% increased odds of major amputation (OR 1.39, 95%CI 1.30-1.49, $p<.001$). Across the entire sample, comorbid depression was also independently associated with a longer length of stay ($\beta=0.199$, 95%CI 0.155, 0.244, $p<.001$).
Conclusions: Comorbid depression was associated with 39% increased odds of major amputation among a large, nationally representative sample of CLI inpatients. These results provide further evidence that depression is a variable of interest in PAD and surgical quality databases should include mental health variables to enable further study of depression's impact on surgical patients.
G.J. Zahner: None. **A. Cortez:** None. **E. Duralde:** None. **J.L. Ramirez:** None. **S. Wang:** None. **J. Hiramoto:** None. **B.E. Cohen:** None. **O.M. Wolkowitz:** None. **S. Arya:** None. **N.K. Hills:** None. **M. Grenon:** None.

This research has received full or partial funding support from the American Heart Association.

350
Brown Adipose Tissue, a Novel Mechanism to Induce both Angiogenesis and Arteriogenesis
Jie Zhang, Marko Oydanich, Dorothy E Vatner, Stephen F Vatner, Rutgers Univ- New Jersey, Newark, NJ

Brown adipose tissue (BAT) is known to protect metabolism, but the extent to which it mediates angiogenesis and cardioprotection, the goal of this investigation, is not known. The Regulator of G Protein Signaling 14 (RGS14) knockout (KO) mouse is unique in that it not only extends longevity, but also enhances several aspects of healthful aging, i.e., protects against diabetes, obesity, exercise intolerance and increased brown adipose tissue by 47% compared with wild type littermates (WT). However, less is known about its role in cardioprotection. Accordingly we examined the effects of chronic myocardial ischemia after 1 and 3 weeks of permanent coronary artery occlusion (CAO) in 3-4 month old RGS14 KO and their WT. Scar size after 3 weeks CAO, determined by histology, was decreased by 33±5% in RGS14 KO, which was only possible in the face of permanent CAO if angiogenesis/arteriogenesis developed in the RGS14 KO mice hearts. Indeed, both angiogenesis assessed by Ki 67 endothelial cell staining and arteriogenesis, assessed by Ki 67 arteriole staining, more than doubled compared with WT. This was associated with a 206±25.5% increase in VEGF in the RGS14 KO hearts compared with WT. We then examined the role of BAT by using a simulated BAT KO, i.e., BAT was transplanted from the RGS14 KO to WT. In the WT with BAT transplants VEGF was increased by 90%. Infarct size, assessed as the fraction of area at risk, was lower, $p<0.05$, in the BAT transplants (27±2.8%), compared with infarct size in RGS14 KO donors (44±1.9%), a value similar to that observed in WT without the BAT transplant (46±1.0%). Thus, brown adipose tissue appears to be a novel mechanism to induce both angiogenesis and arteriogenesis, resulting in vascular protection from ischemia.
J. Zhang: None. **M. Oydanich:** None. **D.E. Vatner:** None. **S.F. Vatner:** None.

351
National Rates of Venous Thromboembolism in Patient with STEMI: Results from the National Inpatient Sample 2003-2013

Ali Ayoub, Ahmed Al-Ogaili, Harry E Fuentes, Jose Sleiman, Christian Torres, John H Stroger Hosp of Cook County, Chicago, IL; Luis Diaz Quintero, Alfonso Tafur, Univ of Chicago Northshore Hosp, Chicago, IL

BACKGROUND There is a growing body of evidence against the use of triple therapy (anticoagulation and dual antiplatelet) among patients with acute coronary syndrome. Venous thromboembolism (VTE) is another potential indication for triple therapy, but the magnitude of such problem is unknown. Therefore, we aimed to determine the trends of annual rate of immediate VTE occurrence in patients with ST-segment elevation myocardial infarction (STEMI) and measure its impact.
METHODS We queried the 2003-2013 Nationwide Inpatient Sample to identify adults with primary diagnosis of STEMI using ICD-9-CM codes. VTE, including limb vein thrombosis and pulmonary embolism, was allocated when present among the secondary discharge diagnosis. Demographics and inpatient outcomes were compared in the VTE and non-VTE group.
RESULTS From 2,495,757 hospitalizations for STEMI, 15,471 (0.6%) also experienced VTE. The group who experienced VTE was older (mean age: 68.44 vs 64.81, p<0.01) and had higher proportions of black patients (10.6% vs 7.7%, p<0.001) and females (42.1% vs 35%, p<0.001) compared to the non-VTE group. There was an increasing trend in the annual rate of VTE during the study period (2003: 0.3% vs 2013: 0.9%, p < 0.01). Patients with VTE had a prolonged hospitalization (12.8 vs 4.63 days, p <0.01), higher risk of gastrointestinal bleeding (OR:1.65; 95% CI 1.54-1.76, p<0.01) and intracranial hemorrhage(OR:1.52, 95% CI:1.23-1.87, P<0.01), needed more blood transfusions (OR:1.74; 95% CI:1.66-1.82, p<0.01) and had increased mortality (OR:1.53, 95%CI:1.46-1.6, p<0.01).
CONCLUSION There is an increasing annual rate in immediate VTE occurrence in patients with STEMI. VTE is associated with more bleeding complications, longer hospital stay, and higher mortality. It is plausible that individualized or more aggressive protocols of VTE prophylaxis are needed in this population.

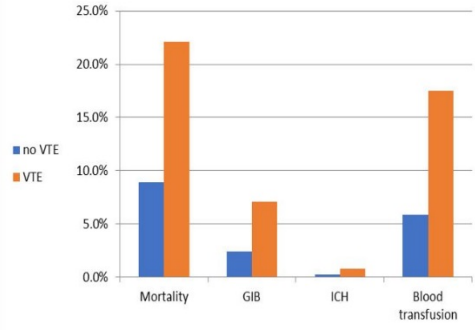

A. Ayoub: None. **A. Al-Ogaili:** None. **H.E. Fuentes:** None. **J. Sleiman:** None. **C. Torres:** None. **L. Diaz Quintero:** None. **A. Tafur:** None.

352
National Trends in Cancer-Associated Thrombosis Hospitalizations among Patients with Pancreatic, Gastric and Lung Primary: Results from Nationwide Inpatient Sample Database 2009-2014

Harry E Fuentes, **Ahmed Al-Ogaili**, Ali Ayoub, Luis H Paz, John H. Stroger Jr. Hosp of Cook County, Chicago, IL; Diana M Oramas, Univ of Illinois at Chicago, Chicago, IL; Luis Diaz Quintero, Alfonso Tafur, NorthShore Univ HealthSystem, Evanston, IL

INTRODUCTION Venous thromboembolism (**VTE**) is a leading cause of morbidity and mortality in cancer; and its occurrence leads to an increased number of hospitalizations. Therefore, we aimed to determine the trends in the annual rate of cancer-associated thrombosis (**CAT**) hospitalizations and measure its impact in patients with highly thrombogenic tumor types, such as pancreas, stomach and lung.
METHODS We queried the 2009-2014 Nationwide Inpatient Sample database to identify adults with gastric, pancreatic or lung cancer. Hospitalizations in which VTE was among the top-three discharge diagnoses, were considered as CAT admissions. In-hospital outcomes of patients with VTE were compared to those without VTE. Using SPSS, version 24, we conducted a linear regression analysis for trend and binary logistic regression analysis to obtain adjusted odds ratios (**OR**) **RESULTS** From 3 million admissions, 149.577 (4.9%) were related to VTE. The patients were mainly white (68.9%) men (53.2%) with a median age of 69 (IQR:17) years; and the predominant tumor type was lung cancer (73.4%). Although the rate of CAT admissions remained steady during the study period (2009: 5.0% vs 2014: 4.9%, p <0.01), the inpatient mortality was higher among patients admitted with CAT (10.2% vs 9.3%, OR:1.11, CI: 1.08 - 1.13, p < 0.01). The negative effect of VTE on inpatient mortality persisted after adjusting for tumor type, metastatic disease and demographics (OR:1.11, CI: 1.08 - 1.13, p < 0.01). The median length of stay was 5 days in both groups (p<0.01), but the cost was significantly higher among those admitted with CAT (USD33,468 vs USD30,452, p <0.01). Figure 1 summarizes demographics (**A**) and trends (**B**)
CONCLUSION CAT admissions in patients with stomach, pancreas and lung cancer are associated with a higher inpatient mortality and its management is costly. Conceivably, risk stratification based on early mortality may assist in therapy and resources selection to improve outcomes and cost allocation.

A	All cohort n=3041483		Non-VTE n=2422106		VTE n=125047	
Demographics						
Age (mean, SD)	68.13	6.6	68.19	11.622	66.88	11.540
Race						
White	2109759	69.4	2006007	69.4	103752	69.4
Black	368829	12.1	348413	12.0	20416	13.6
Hispanic	162514	5.3	155301	5.4	7213	4.8
Asian/Pacific Islander	76695	2.5	74582	2.6	2114	1.4
Native American	11812	0.4	11412	0.4	400	0.3
Others	66337	2.2	63155	2.2	3181	2.1
Unkown	245538	8.1	233036	8.1	12502	8.4
Male Gender	1618778	53.2	1540837	53.3	77942	52.1
Metastatic disease	983442	32.3	909526	31.5	73916	49.4
Tumor type						
Gastric Cancer	265403	8.7	255205	8.8	10198	6.8
Lung Cancer	2227243	73.2	2125652	73.5	101591	67.9
Pancreatic Cancer	543646	17.9	506130	17.5	37516	25.1
Mixed	5191	0.2	4919	0.2	272	0.2
In Hospital Outcomes						
Mortality	240260	9.4	270166	9.3	15298	10.2
Length of Stay (median, IQR)	5.0000	5.00	5.0	5.0	5.0	6.0
Cost (median, IQR)	30599	43352	30452.0	43257.0	33468	45022

B

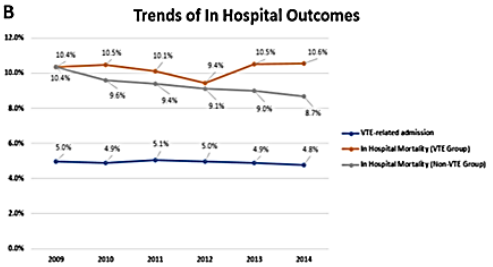

H.E. Fuentes: None. **A. Al-Ogaili:** None. **A. Ayoub:** None. **L.H. Paz:** None. **D.M. Oramas:** None. **L. Diaz Quintero:** None. **A. Tafur:** None.

353

Aldehyde Scavenging Reduces Renal Injury Role of IsoLG-modified apoAI

Valentina Kon, Vanderbilt Univ Medical Cente, Nashville, TN

Reactive aldehydes, including isolevuglandins (IsoLG) are lipoxidation products that can modify lipoproteins and promote cellular dysfunction. Previously, we showed that proteinuric injury increases urinary apoAI and causes renal lymphangiogenesis. We now investigate the role of IsoLG and effects of IsoLG scavenging on renal injury and lymphatics.

Nphs1-hCD25 mice (NEP25) expressing podocyte-specific human CD25 become proteinuric after injection of immunotoxin (LMB2). NEP25 mice were treated with the aldehyde scavenger, PPM (1g/L) or vehicle from the onset of proteinuria until sacrifice (2 weeks). We assessed proteinuria [measured as albumin:creatinine ratio (ACR)], urinary apoAI, IsoLG, KIM-1 (marker of tubular injury), and the renal expression of lymphatic markers (LYVE-1 and podoplanin). *In vitro*, we assessed the effects of apoAI or modified apoAI (IsoLG-apoAI) +/- PPM on proximal tubular cells (PTC) and lymphatic endothelial cells (LEC).

As expected, LMB2 significantly increased ACR and urinary KIM-1. Proteinuric injury also significantly increased urinary IsoLG (262%). Similar to our previous data, proteinuric kidneys increased expression of apoAI, VEGF-C, podoplanin and LYVE-1
compared to wild type mice. *In vitro,* PTC uptake of IsoLG-apoAI was significantly increased (39%), an effect that was abrogated by exposure to PPM (22%). In LECs, compared to apoAI, IsoLG-apoAI significantly increased viability (27%) and migration (13%), effects that were abrogated by exposure to PPM. *In vivo,* proteinuric NEP25 mice treated with PPM showed significantly reduced ACR (22%), urinary KIM-1 (30%) and IsoLG excretion (64%).

We conclude that aldehyde scavenger lessens proteinuric renal damage through mechanisms that include reducing proximal tubule uptake of IsoLG-modified apoAI and preserving lymphatic endothelial cell functionality.

V. Kon: None.

354

Early Intentional Restoration of Blood Flow Reduces Thrombus Burden and Vein Wall Scarring Following Dvt: Implications for Preventing the Post-thrombotic Syndrome

Wenzhu Li, Chase Kessinger, Makoto Orii, Stephan Kellnberger, Jie Cui, Adam Mauskapf, Lang Wang, Xiaoxin Zheng, Cardiovascular Res Ctr, Massachusetts General Hosp, Boston, MA; Peter Henke, Section of Vascular Surgery, Univ of Michigan, Ann Arbor, MI; Farouc Jaffer, Cardiovascular Res Ctr, Massachusetts General Hosp, Boston, MA

Background: Despite anticoagulation therapy, up to 50% of deep vein thrombosis (DVT) patients still develop the post-thrombotic syndrome (PTS), a condition that arises from thrombus obstruction and vein wall damage, leading to venous hypertension. While catheter-based intervention may reduce PTS, the CaVenT and ATTRACT trials demonstrated little clinical benefit of intentional restoration of blood flow (RBF) for reducing PTS. However, these trials have not explored the time-dependence of RBF, a key factor as aging VT are associated with greater vein wall injury.

Methods: To investigate the temporal effects of intentional RBF following VT, we modified a classic complete ligation inferior vena cava (IVC) stasis VT protocol in C57BL/6 mice by de-ligating the day 0 ligature at day 2 to allow RBF. Compared to intravital microscopy, the sensitivity and specificity of noninvasive ultrasound (US) to detect RBF was 82.1% and 94.4%, respectively. Serial US was then performed on mice. Mice were classified as early RBF (RBF by day 4), late RBF (RBF after day 4), no RBF, or sham de-ligation groups. Follow day 8 sacrifice, thrombus burden (mg/cm) and vein wall scarring (VWS) were measured. Kruskal-Wallis followed by Dunn's test was used to compare statistical significance between groups.

Results: After de-ligation, RBF through VT increased gradually over time (Fig. A). The early RBF group exhibited significant reductions in VT burden (N=9) and VWS (N=5) at day 8 (p<0.05 vs. comparator groups, Fig B-C). In contrast, the late RBF group did not experience significant reductions in thrombus burden (N=6) nor VWS (N=4), with measures similar to mice with no RBF (N=3-4), or sham de-ligation (N=8-9).

Conclusions: Intentional early RBF reduces venous thrombus burden and VWS, factors that drive PTS. Mechanistic studies to address these findings are going. The overall results suggest that anti-PTS benefits of catheter-based intervention may be enhanced in subjects receiving early RBF.

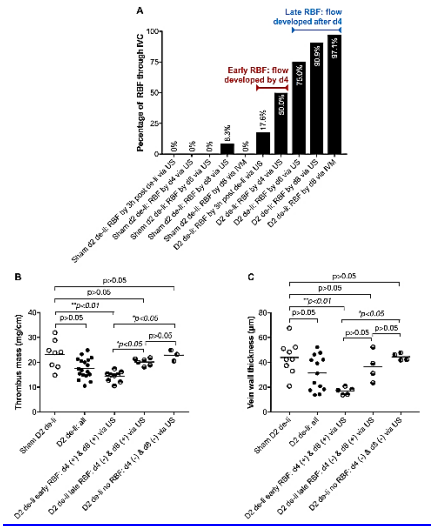

W. Li: None. **C. Kessinger:** None. **M. Orii:** None. **S. Kellnberger:** None. **J. Cui:** None. **A. Mauskapf:** None. **L. Wang:** None. **X. Zheng:** None. **P. Henke:** None. **F. Jaffer:** None.

360
Rivaroxaban Enhances the Antiplatelet Activity of Aspirin via Inhibition of Nox2-mediated Thromboxane A_2 and Isoprostane Biosynthesis
Vittoria Cammisotto, Roberto Carnevale, Cristina Nocella, Lucia Stefanini, Daniele Pastori, Simona Bartimoccia, Pasquale Pignatelli, Francesco Violi, Sapienza Univ of Rome, Rome, Italy

Background: A recent study demonstrated that a combination of rivaroxaban, an inhibitor of factor Xa, plus aspirin (100mg/day) reduces cardiovascular events in patients with stable vascular disease, compared to aspirin alone but the underlying mechanism is still unknown.
Methods: In vitro study was performed consisting in measuring agonist-induced platelet aggregation, thromboxane (Tx)B_2 and isoprostane biosynthesis, soluble Nox_2-dp, a marker of Nox2 activation, and PLA_2 activation in platelets from healthy subjects (n=5) added with or without scalar doses of aspirin (25-100 uM) and/or rivaroxaban (15-120 ng/ml). Furthermore, we measured urinary excretion of isoprostanes, and soluble Nox2 before and after 3 months of 20 mg rivaroxaban (n=25) or warfarin (n=25) treatment in atrial fibrillation(AF) patients. **Results:** In vitro study showed that rivaroxaban significantly reduced platelet aggregation, TxB_2 and isoprostane biosynthesis and Nox2 and PLA_2 activation in a dose-dependent fashion. Also, rivaroxaban dose-dependently inhibited aggregation of platelets treated with low-(25uM) as well as high-(100uM) aspirin doses. In low-dose aspirin-treated samples an incremental inhibition of platelet TxB_2 biosynthesis was achieved; conversely, in platelets treated with high doses of aspirin a significant inhibition of isoprostanes and Nox2 was observed. Inhibition of platelet aggregation by rivaroxaban was detected also in platelets stimulated with convulxin suggesting that its antiplatelet effect was GPVI-dependent. In addition, convulxin elicited PLA_2 activation, that was inhibited by rivaroxaban as well as by a Nox2 inhibitor. Finally, in AF patients treated with rivaroxaban a significant reduction of urinary isoprostanes and soluble Nox2 and GPVI as compared to warfarin-treated ones was detected.
Conclusion: Here we show that rivaroxaban inhibits platelet aggregation via GPVI interaction and eventually Nox2-mediated thromboxane and isoprostane biosynthesis in aspirin-treated platelets so providing a novel mechanistic insight into the beneficial effects of combining rivaroxaban with aspirin.

V. Cammisotto: None. **R. Carnevale:** None. **C. Nocella:** None. **L. Stefanini:** None. **D. Pastori:** None. **S. Bartimoccia:** None. **P. Pignatelli:** None. **F. Violi:** None.

361
Multifocal Vascular Disorders Due to the Uncommon Anti-phosholipid Antibody Syndrome
Yasutaka Kawanura, Harue Hosp, Fukui, Japan; Masato Ai, Masafumi Nakaki, Awa Regional Medical Ctr, Chiba, Japan

Purpose: We report three cases with uncommon anti-phosholipid antibody syndrome. The difficulty in diagnosing as well as treatment procedures for multifocal vascular disorders is discussed.
Patients and Methods: All patients were examined and were initially treated for digestive disorders.
Patient 1, 84-year-old woman, with gastrointestinal bleeding
Patient 2, 76-year-old man, with sudden onset of upper abdominal pain
Patient 3, 54-year-old man, with nausea and vomiting, liver dysfunctionClinical manifestation was superior mesenteric artery (SMA) thrombosis in the patient 1 and 2, and portal vein thrombosis in the patient 3.
Serial CT scans were examined on 64 multidetector-row CT; Hitachi and GE, with bolus injection of contrast media for CT angiography.
Abdominal angiography and coronary angiography with endovascular intervention performed on were performed on Allura; Philips.
Results: CTA of for patient 1 and 2 showed decreased contrast enhancement of SMA and SMV enhancement. The intestinal enhancement was poor in patient 1 and well preserved in patient 2. A week later, patient 1 died suddenly due to multiple organ failure. Although the symptom improved in patient 2, the follow-up CT revealed the enlargement ofSMA thrombosis. The aspiration and the dissolution of SMA thrombosis were performed and resulted in complete recanalization. Then he felt chest oppression and 75% stenosis of RCA #4, followed by complete spastic occlusion on Acetylcholine loading on the coronary angiography, which recovered perfectly with intracoronary nitroglycerin administration. He discharged our hospital with health, while he developed cerebellar infarction. On patient 3, to resolve portal hypertension, balloon-occluded retrograde transvenous obliteration and splenic arterial embolization were successfully performed.
Discussion and Conclusions: Acute deterioration encountered in patient 1, the progressive SMA thrombosis with coronary disease and subsequent cerebellar occlusion seen in patient 2, and portal vein thrombosis and portal hypertension without chronic hepatitis, cirrhosis or alcoholic liver damage in the patient 3 were seemed to be unusual. To discover underlining disorders such as uncommon anti-phosholipid antibody syndrome is important to prevent serious vascular diseases in sequence.
Y. Kawanura: None. **M. Ai:** None. **M. Nakaki:** None.

362
Plasminogen Activator Inhibitor 1 Forms a Complex With FXIa on the Surface of Endothelial Cells, Blocking Its Activity and Inducing the Clearance, Internalization and Degradation of FXIa
Cristina Puy, Anh Ngo, Oregon Health Science Univ, Portland, OR; David Gailani, Vanderbilt Univ, Nashville, TN; Andras Gruber, **Owen J McCarty**, Oregon Health Science Univ, Portland, OR

Background: The activation of coagulation factor (F) XI by activated coagulation FXII (FXIIa) is a prothrombotic process. The endothelium is known to play an antithrombotic role by preventing thrombin generation and platelet activation. It is unknown whether the antithrombotic role of the endothelium includes regulation of activated FXI (FXIa) activity. Hypothesis: Endothelial cells (ECs) express anticoagulant properties that block the procoagulant activity of FXIa. Methods: We used a chromogenic assay to

measure FXIa, kallikrein or FXIIa activity on cultured human umbilical vein ECs (HUVECs). To detect FXIa-inhibitor complexes in either the supernatant (SN) or cell lysate (CL), HUVECs were exposed to FXIa for 2 hrs at 4°C, then washed and lysed, followed by immunoprecipitation and western blot (WB) using an anti-FXIa mAb to the catalytic domain. To assess FXIa binding and internalization, HUVECs were exposed to FXIa for 2 hrs a 4C, washed and incubated at 37C for 5 min to 2 hrs, followed by fixation, and immunostaining with an anti-FXI antibody. Results: HUVECs block the activity of FXIa but not kallikrein or FXIIa activity. The catalytic domain of FXIa (30 kDa) formed a covalent bond with one inhibitor generating one band at 80 kDa. The formation of FXIa-inhibitor complexes appeared in the SN when ECs were transferred to 37C. Mass spectrometry analysis of the 80kDa band revealed that FXIa forms a complex with plasminogen activator inhibitor 1 (PAI-1). WB for PAI-1 from the SN and CL detected a band at 80 kDa, while the expression of PAI-1 on the HUVEC surface decreased after incubation with FXIa. FXIa bound to the EC surface at 4C. After 5 mins at 37C, FXIa was internalized and localized beneath the plasma membrane, and after 30 mins to 2 hr at 37C, FXIa accumulated in the early and late endosomes and lysosomes. The serine protease inhibitor PPACK blocked FXIa-PAI-1 complex formation and internalization of FXIa. A blocking anti-PAI-1 antibody increased the cleavage of the chromogenic substrate by FXIa and the capacity of FXIa to promote fibrin formation on ECs in recalcified plasma. Summary: FXIa forms a complex with PAI-1 on the surface of ECs blocking its activity. Inhibition of FXIa on the endothelium may support internalization and clearance of FXIa from the circulation.
C. Puy: None. **A. Ngo:** None. **D. Gailani:** None. **A. Gruber:** Employment; Significant; Aronora, Inc.. Ownership Interest; Significant; Aronora, Inc. **O.J. McCarty:** None.

This research has received full or partial funding support from the American Heart Association.

363
Platelet Mass Retraction is a Negative Feedback Regulator of Thrombin Generation and Activity
Timothy J Stalker, Leonard Nettey, Chelsea Matzko, Izmarie Poventud-Fuentes, Talid Sinno, Lawrence F Brass, **Maurizio Tomaiuolo**, Univ of Pennsylvania, Philadelphia, PA

Endogenous anticoagulants, including antithrombin III, tissue factor pathway inhibitor, and activated protein C (aPC) provide a biochemical means to inhibit thrombin generation and/or activity. In addition, we have previously shown that platelet mass retraction prevents the escape and exchange of solutes, thereby providing a biophysical mechanism to limit thrombin generation and activity. The relative contribution of each of these biochemical and biophysical mechanisms to the termination of thrombin activity during the hemostatic response *in vivo* remains poorly understood. Here, using computational simulations coupled with *in vivo* experimental models, we tested the hypotheses that 1) platelet mass retraction itself is physiologically relevant to inhibit thrombin generation; and 2) that given the spatial localization of protein C activation on the endothelial cell surface, aPC mediated thrombin inhibition has negligible effects on the hemostatic response. Our computational model has several innovative aspects, including 3D representations of the vessel, extravascular space, and injury, blood flow, and a simplified but anatomically correct model of coagulation. Our simulations show that tissue factor localization combined with flow exiting the injury limit thrombin generation/activity to the extravascular space. Our experiments using a mouse jugular puncture injury model show rich deposition of fibrin in the extravascular space and little to no fibrin in the luminal side. Additionally, our simulations illustrate how platelet mass retraction inhibits thrombin generation by decreasing the delivery of substrates, such as prothrombin and factor X, and at the same time it limits thrombin activity by constraining its movement. These effects are mediated by physical forces only and are independent of the biochemical inhibitory pathways. Our *in vivo* experiments using aPC inhibitory antibodies show that lack of aPC mediated thrombin inhibition has negligible effects on the hemostatic response. In conclusion, this study suggests that platelet mass retraction is an underappreciated mechanism that negatively regulates thrombin generation, while aPC mediated inhibition of thrombin generation plays a minor role in hemostasis.
T.J. Stalker: None. **L. Nettey:** None. **C. Matzko:** None. **I. Poventud-Fuentes:** None. **T. Sinno:** None. **L.F. Brass:** None. **M. Tomaiuolo:** None.

367
Quantitative Phosphoproteomic Profiling and Causal Pathway Analysis Reveal Novel Mediators and Mechanisms Supporting Glycoprotein VI (GPVI) Signaling and Platelet Function
Özgün Babur, Anh T Ngo, Jevgenia Zilberman-Rudenko, Owen J McCarty, Emek Demir, Larry L David, **Joseph E Aslan**, Oregon Health & Science Univ, Portland, OR

Intracellular signaling systems associated with the platelet glycoprotein VI receptor (GPVI) are essential to hemostasis and also initiate atherothrombotic events in cardiovascular disease contexts. While many separable molecular entities linked to GPVI-mediated platelet activation have been characterized, a systemic understanding of GPVI signaling over the context of the entire platelet proteome remains far from complete. To test the hypothesis that specific, intact signaling systems downstream of GPVI regulate platelet function, we used a combination of tandem mass tag (TMT) labeling and high-resolution, multidimensional mass spectrometry and informatics tools to quantify and model protein phosphorylation events reproducibly measurable in platelets from healthy human subjects (n=5) in response to the GPVI specific agonist collagen-related peptide (CRP). Following CRP treatment, platelets rapidly regulated the phosphorylation state of 1004 serine, threonine and tyrosine residues on 542 proteins (fold change > 1.5; false discovery rate < 0.05). In addition to regulatory sites on kinases, phospholipases and other well-known targets, the majority of phosphorylation events following CRP stimulation occurred on proteins with uncharacterized roles in platelet function. CausalPath analysis of this data mapped 46 high confidence pathway relations, suggesting that Syk, PKCs and MAPKs ultimately drive the phosphorylation of several novel effectors specifically downstream of GPVI in platelet regulation, including CRMP-2, RAD23B and caldesmon. In addition to comprehensively mapping out known signaling relations while illuminating previously unrecognized regulatory mechanisms of platelet function around GPVI, our work provides a platform to generate novel, mechanistic and testable hypotheses from omics data sets for subsequent discovery-driven efforts to identify platelet-based therapeutic and biomarker targets relevant to cardiovascular disease risk, progression and mortality.
Ö. Babur: None. **A.T.P. Ngo:** None. **J. Zilberman-Rudenko:** None. **O.J.T. McCarty:** None. **E. Demir:** None. **L.L. David:** None. **J.E. Aslan:** None.

This research has received full or partial funding support from the American Heart Association.

368
Severe Obesity and Bariatric Surgery Alter the Platelet mRNA Profile
Sean P Heffron, Christian Marier, Manish Parikh, Edward A Fisher, Jeffrey S Berger, NYU Sch Med, New York, NY

Mechanisms explaining the relationship between obesity and CVD are needed. Platelets are increasingly recognized as immune cells; the platelet transcriptome and sheddome can modulate the function of disparate cells and tissues. Despite

growing recognition of the importance of the platelet transcriptome, low levels of RNA in platelets makes assessment difficult. Unbiased platelet RNA profiling specifically in obesity has not previously been performed. We performed a prospective study investigating the association between severe obesity and weight loss via bariatric surgery and platelet function and RNA profile in 25 pre-menopausal, non-diabetic women (31.9 ± 7.6 years; 43.0 ± 6.5 kg/m^2) who underwent sleeve gastrectomy. Ten women of similar age and racial background with normal BMI (22.8 ± 2.3kg/m^2) served as control subjects.
Platelet function via light transmission aggregometry and surface expression via flow cytometry was assessed before and after surgery. RNAseq was performed on platelet RNA isolates of 8 obese women before and 5 after surgery and 5 control subjects.
Platelet count, size, age (reticulated platelets) and aggregation measures did not differ between control and obese women. However, surface markers (eg P-selectin and CD40) of platelet activation were significantly higher in obesity. mRNA sequencing demonstrated >600 RNA transcripts differentially abundant (P<0.05 and base mean counts ≥5) in obesity. Notably, platelet *S100A9* and *AGER*, established markers of CV risk, were 2 of the most highly upregulated transcripts in obesity. Pathway analyses identified eIF2 and mTOR signaling and protein translation broadly to be upregulated. At 6 months after surgery, subjects lost 26.1 ± 5.8% body weight, but only a small fraction of transcripts (46/630; which included *AGER)* exhibited significantly altered expression.
Platelet activation (not aggregation) was increased and the platelet transcriptome was altered in obesity. Given platelets' ability to act as immune cells and transfer their RNA cargo to other cells important in atherothrombosis, the altered platelet RNA profile in obesity may contribute to increased risk of CVD. More substantial degrees or duration of weight loss may be necessary to rectify the altered platelet RNA profile.
S.P. Heffron: None. **C. Marier:** None. **M. Parikh:** None. **E.A. Fisher:** None. **J.S. Berger:** None.

369
Muscle Ischemia Induces Nlrp3 Inflammasome Activation in Platelets via Tlr4, Promoting Platelet Aggregation and Interfering With Perfusion Recovery
Sebastian Vogel, Pranav Murthy, Xiangdong Cui, Bowen Xie, Ulka Sachdev, UPMC, Pittsburgh, PA

Introduction: Angiogenesis is an adaptive response to chronic ischemia, but is deficient in peripheral arterial disease (PAD). We have recently shown that the pattern recognition receptors toll-like receptor 4 (TLR4) and nucleotide-binding domain leucine rich repeat containing protein 3 (NLRP3) expressed by platelets control aggregation and thrombosis. The role of platelet TLR4 and NLRP3 in PAD is unexplored.
Methods: Unilateral femoral artery ligation (FAL) was performed in transgenic mice with platelet-specific ablation of TLR4 (TLR4 PF4) and in global NLRP3 knockout (NLRP3 KO) mice. Platelet NLRP3 inflammasome activation was monitored by caspase-1 activation (fluorescent labeled inhibitor of caspase-1, FLICA) and cleavage of IL1β (Western blot). Platelet aggregation was evaluated with impedance aggregometry. Laser Doppler perfusion imaging (LDPI) verified perfusion in the ischemic (right) and non-ischemic (left) limb over time. Angiogenesis and myoblast regeneration were measured histologically.
Results: Platelet NLRP3 inflammasome activity was significantly upregulated following FAL (p<0.001), and reversed with TAK242, a TLR4 inhibitor. FAL significantly increased aggregation of circulating platelets, which was significantly suppressed in TLR4 PF4 (p<0.01) and NLRP3 KO mice (p<0.001). Down-regulation of platelet aggregation and caspase-1 activity in TLR4 PF4 mice was nearly completely reversed by nigericin, a NLRP3 activator. Ischemic limb perfusion (Fig 1A) was significantly higher in TLR4 PF4 (Fig1B, p<0.05) and NLRP3 KO mice (Fig1C, p<0.001) than in controls 14d after FAL. Angiogenesis and regeneration were significantly improved in TLR4 PF4 mice (p<0.05).
Conclusion: We show that the platelet NLRP3 inflammasome is activated in muscle ischemia via platelet TLR4, which upregulates platelet aggregation and deters recovery from FAL. Thus, platelet TRL4/NLRP3 activation may be a therapeutic target to improve limb salvage in PAD.

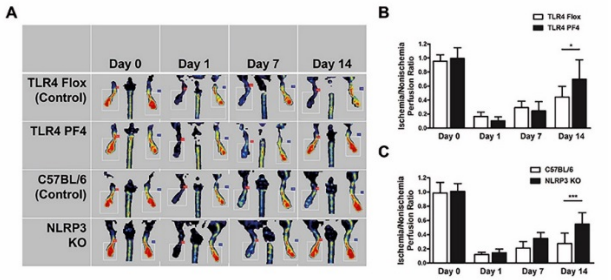

S. Vogel: None. **P. Murthy:** None. **X. Cui:** None. **B. Xie:** None. **U. Sachdev:** None.

373
An Animal Model of Left Atrial Thrombus
Jiqiu Chen, Delaine Ceholski, Lifan Liang, Roger Hajjar, Mount Sinai Sch Med, New York, NY

Left atrial thrombus (LAT) is a common funding of some cardiovascular diseases such as congestive heart failure (CHF), atrial fibrillation and myocardial injury. There is no proper animal model of LAT to date. The present study reports a model of congestive heart failure in rats that is characterized by LAT. **Methods**: LAT were induced by aortic banding 2 months plus 30 minutes ischemia and reperfusion 1 m followed with aortic de-banding 1 m in rats. Cardiac function and blood flow velocity were assessed by echocardiography. Masson's stainings were conducted for histology. **Results**: congestive heart failure (CHF) in rats with LAT showed significant dilatation in left atrium (CHF = 56 ± 18 mm, N = 7, Control = 25 ± 6 mm, N = 10), significant decrease in left appendage blood flow velocity (CHF = 4.20 ± 0.09, Control = 0.21 ± 0.05 m/s) and mitral valve blood velocity (CHF = 0.76 ± 0.09 m/s, Control = 1.01 ± 0.04 m/s). Histology data showed that mature LAT had a complete membrane; the thrombus was characterized by significant fibrosis in middle and out layers. The outer layer of thrombus had microvessels and the cells were nucleated. The central part of the thrombus had very little fibrosis and showed necrosis. Small thrombus (0.05 - 0.1 mm) had a base from which the blood clot grew. Atrial neo-intimal fibrosis plays an important role in the formation of the base of microembolization. However, in some cases, micro-thrombi (<0.01 mm) showed no fibrotic base. Conclusion: left atrial thrombus results from blood flow congestion. However, it is still not clear whether the thrombus is due to vascular proliferation from the atrial wall or through adhesion of coagulation fibers to the atrial wall.
Figure. A. echocardiographic imaging. B. left atrial area . C. mitral valve blood velocity. D. echocardiography of left atrial blood velocity. E. left atrial blood flow velocity. F. regular imaging of LAT. G. cross sectional imaging. H. small LAT. I. endometrial fibrosis. J. micro thrombus. K. coagulation fiber.

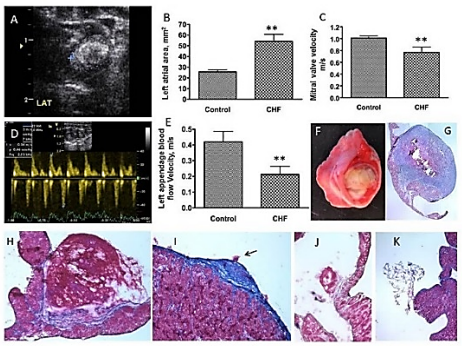

J. Chen: None. **D. Ceholski:** None. **L. Liang:** None. **R. Hajjar:** None.

374
Lack of Fibronectin Containing Extra Domain a Attenuates Acute Myocardial Ischemia/Reperfusion Injury in Hyperlipidemic Mice by Limiting Postischemic Thrombo-inflammation
Mehul Chorawala, Univ of Iowa, iowa city, IA; Prem Prakash, Univ of Iowa, Iowa City, IA; Prakash Doddapattar, Nirav Dhanesha, Anil Chauhan, Univ of Iowa, Iowa city, IA

Background: Reperfusion therapy is standard care for patients following acute myocardial infarction. Fibronectin-splicing variant containing extra domain A (Fn-EDA), which is an endogenous ligand for toll-like-receptor 4 (TLR4), is upregulated during vascular hypertension, myocardial injury, and atherosclerosis. An earlier study done in rabbit showed that Fn-EDA accumulates more rapidly (within 24 hrs) in the reperfused hearts. Very little is known about the mechanistic role of Fn-EDA in the pathophysiology of myocardial infarction (MI) in the comorbid condition of hyperlipidemia.
Methods: Susceptibility to MI outcome was evaluated in hyperlipidemic Apoe$^{-/-}$, Fn-EDA$^{-/-}$Apoe$^{-/-}$, TLR4$^{-/-}$Apoe$^{-/-}$ and Fn-EDA$^{-/-}$TLR4$^{-/-}$Apoe$^{-/-}$ mice (male and female; 8-10 weeks old) by transient 1-hour ischemia/23 hours of reperfusion (I/R). Myocardial I/R injury outcome was evaluated by measuring infarct area, cardiac Troponin I (cTnI) levels in plasma, postischemic thrombo-inflammation (thrombi and neutrophil influx) and myocyte apoptosis.
*Results***:** Irrespective of gender, Fn-EDA$^{-/-}$Apoe$^{-/-}$ mice (Apoe$^{-/-}$ mice expressing Fn deficient in EDA) exhibited smaller infarcts and decreased cTnI levels concomitant with reduced postischemic thrombosis, inflammation and myocyte apoptosis (P<0.05 vs. Apoe$^{-/-}$ mice). Genetic ablation of TLR4 attenuated myocardial I/R injury outcome in Apoe$^{-/-}$ mice (P<0.05 vs. Apoe$^{-/-}$ mice), but did not further reduce in Fn-EDA$^{-/-}$ Apoe$^{-/-}$ mice, suggesting Fn-EDA modulates TLR4-dependent MI exacerbation. Bone marrow transplantation experiments revealed that nonhematopoietic cells-derived Fn-EDA exacerbates myocardial I/R injury through TLR4 expressed on the hematopoietic cell. Infusion of a specific inhibitor of Fn-EDA into Apoe$^{-/-}$ mice significantly reduced myocardial I/R injury.
Conclusions: Hyperlipidemic mice deficient in Fn-EDA exhibit TLR4-dependent reduced myocardial I/R injury that was associated with decreased thrombo-inflammatory response. These findings suggest that targeting Fn-EDA combined with thrombolytic agents could be an effective therapeutic strategy to inhibit myocardial I/R injury in patients with hyperlipidemia.
M. Chorawala: None. **P. Prakash:** None. **P. Doddapattar:** None. **N. Dhanesha:** None. **A. Chauhan:** None.

This research has received full or partial funding support from the American Heart Association.

375
Interaction of Plasma Autotaxin and Extracellular Vesicles in Rheumatoid Disease Patients Induces Circulating Cell Activation
Anne-Claire Duchez, Stephan Hasse, Paul R Fortin, Eric Boilard, Sylvain G Bourgoin, Ctr de recherche du CHU de Quebec-Univ Laval, Quebec, QC, Canada

Background: the frequency and severity of cardiovascular disease (CVD) is higher in patients suffering from Rhumatoid Arthritis (RA) and Systemic Lupus Erythematosus (SLE) than healthy individuals, likely due to the direct impact of systemic inflammation on the atherosclerotic plaque. Several factors can contribute to cardiovascular damage, including pro-inflammatory lipid mediators such as lysophosphatidic acid (LPA) produced by a lysophospholipase enzyme named autotaxin (ATX). Extracellular vesicles (EVs) are also abundant in blood from patient developing atherosclerotic plaque, and recently EVs from arthritic synovial fluid were found to interact with phospholipase and release inflammatory lipids. **Objective:** we therefore sought to understand how EVs and ATX may cooperate in the context of rheumatoid disease to promote inflammation. **Results:** we observed that plasma from RA and SLE patients, analysed by ELISA, contained high concentrations of ATX compared to the plasma from healthy people (pvalue =0.0001). The plasma of these patients, analysed by nanoparticle flow cytometry, also contained high concentration of EVs and these EVs are decorated by ATX, on their surface. As the presence of EVs indicated cell activation due to different endogenous stimuli such as LPA, we found in vitro that different species of LPA activate circulating blood cell to produce EVs (observed by flow cytometry and electronic microscopy), suggesting that LPA serves as an activating signal for EV production. In summary, our results show that ATX bind EVs and produces LPA that activates circulating cells in RA and SLE patients. ATX and LPA could serve as biomarkers and therapeutic target in accelerated CVD in patients with rheumatoid diseases.
A. Duchez: None. **S. Hasse:** None. **P.R. Fortin:** None. **E. Boilard:** None. **S.G. Bourgoin:** None.

378
Predilection of Low Protein C-induced Spontaneous Atherothrombosis for the Right Coronary Sinus in Apolipoprotein E-deficient mice
Marco Heestermans, Leiden Univ Medical Ctr, Leiden, Netherlands; Amber B Ouweneel, Leiden Academic Ctr for Drug Res, Leiden, Netherlands; **Chrissta X Maracle**, Leiden Univ Medical Ctr, Leiden, Netherlands; Jasmin Hassan, Leiden Academic Ctr for Drug Res, Leiden, Netherlands; Meander Kloosterman, Pieter H Reitsma, Leiden Univ Medical Ctr, Leiden, Netherlands; Marion J Gijbels, Cardiovascular Res Inst Maastricht, Maastricht, Netherlands; Bart J van Vlijmen, Leiden Univ Medical Ctr, Leiden, Netherlands; Miranda Van Eck, Miranda Van Eck, Leiden Academic Ctr for Drug Res, Leiden, Netherlands

Atherothrombosis is the cause of death of over 14 million people per year worldwide and murine models to replicate this process *in vivo* are mostly lacking. Previously we demonstrated that silencing of anticoagulant protein C using RNA interference (*siProc*) induces spontaneous atherothrombosis in the aortic root of apolipoprotein E-deficient (*Apoe*$^{-/-}$) mice, albeit at a low incidence rate. Here we aim to determine if plaque susceptibility for rupture can be linked to plaque characteristics and/or blood composition, and moreover, we attempt to boost incidence through a transient increase in blood pressure as well as to localize atherothrombosis to an additional predefined vascular site by means of a semi-constrictive collar around the carotid artery. In the current study, si*Proc*-driven spontaneous atherothrombosis in the aortic root of Apoe-/- mice was reproduced and occurred at an incidence of 23% (9 out of 39 mice), while the incidence of collar-induced atherothrombosis in the carotid artery was 2.6% (1 out of 39

mice). Treatment with phenylephrine, to transiently increase blood pressure, did not increase atherothrombosis in the aortic root of the *Apoe*$^{-/-}$ mice nor in the carotid arteries with collars. Plaques in the aortic root with an associated thrombus were lower in collagen and macrophage content, and mice with atherothrombosis had significantly more circulating platelets. Plasma protein C, white blood cell counts, total cholesterol, fibrinogen, and serum amyloid A were not different amongst si*Proc*-treated mice with or without thrombosis. Remarkably, our data revealed that thrombus formation preferably occurred on plaques in the right coronary sinus of the aortic root. In conclusion, there is a predilection of low protein C-induced spontaneous atherothrombosis in *Apoe*$^{-/-}$ mice for the right coronary sinus, a process that is associated with an increase in platelets and plaques lower in collagen and macrophage content.
M. Heestermans: None. **A.B. Ouweneel:** None. **C.X. Maracle:** None. **J. Hassan:** None. **M. Kloosterman:** None. **P.H. Reitsma:** None. **M.J.J. Gijbels:** None. **B.J.M. van Vlijmen:** None. **M. Van Eck:** None. **M. Van Eck:** None.

379
Platelet-driven Contraction of Venous Thrombi Modulates Their Obstructiveness and Embologenicity
Valerie Tutwiler, Univ of Pennsylvania, Philadelphia, PA; Alina D Peshkova, Giang Le Minh, Izabella A Andrianova, Kazan Federal Univ, Kazan, Russian Federation; John W Weisel, Rustem I Litvinov, Univ of Pennsylvania, Philadelphia, PA

Contraction (retraction) of the blood clot is a part of the clotting process driven by activated platelets attached to fibrin. The aim of this work was to reveal the pathogenic importance of contraction of clots and thrombi in venous thromboembolism (VTE). We investigated the kinetics of clot contraction in clots made from the blood of 55 patients with VTE not receiving antiplatelet and anticoagulant medications. In addition, we studied the ultrastructure of *ex vivo* venous thrombi, as well as the morphology and functionality of isolated platelets. Thrombi from VTE patients contained compressed polyhedral erythrocytes, a marker for clot contraction *in vivo*. The extent and rate of contraction of in vitro clots were reduced by 2-fold in clots from the blood of VTE patients compared to healthy controls. The contraction of clots from the blood of patients with pulmonary embolism was significantly impaired compared to that of those with isolated venous thrombosis, suggesting that less compacted thrombi may be prone to embolization. The reduced ability of clots to contract correlated with continuous platelet activation followed by their partial refractoriness to stimulation. Morphologically, 75% of platelets from VTE patients were spontaneously partially activated (with filopodia) compared to only 21% of those from healthy controls. At the same time, platelets from VTE patients showed a 1.4-fold reduction in activation markers expressed in response to chemical activation when compared to platelets from healthy individuals. The results obtained suggest that the impaired contraction of thrombi resulting from platelet dysfunction is an underappreciated pathogenic mechanism in VTE that may regulate the obstructiveness and embologenicity of venous thrombi. Furthermore, an assay for clot contraction may have diagnostic and prognostic value for venous thromboembolism.
The work was supported by the Program for Competitive Growth at Kazan Federal University.
V. Tutwiler: None. **A.D. Peshkova:** None. **G. Le Minh:** None. **I.A. Andrianova:** None. **J.W. Weisel:** None. **R.I. Litvinov:** None.

383
HDL Particles, Cell-Cholesterol Efflux, and CHD Risk: the Preβ-1 Paradox
Bela F Asztalos, Katalin V Horvath, Ernst J Schaefer, Tufts Univ, Boston, MA

Objective: The cell-cholesterol efflux capacity (CEC) of high-density lipoprotein (HDL) is inversely associated with coronary heart disease (CHD) risk. ATP-binding cassette transporter-A1 (ABCA1) plays a crucial role in cholesterol efflux from macrophages to preβ-1-HDL. We tested the hypothesis that CHD patients have functionally abnormal preβ-1-HDL. **Approach and Results**: We measured HDL CEC via the ABCA1 and the scavenger receptor class B type-I (SR-BI) pathways, HDL anti-oxidative capacity, apolipoprotein A-I-containing HDL particles, and inflammatory- and oxidative-stress markers in 64 CHD cases and 64 gender-matched controls. There were significant positive correlations between ABCA1-dependent cholesterol efflux and the levels of small lipid-poor preβ-1-particles in both cases (R^2=0.541) and controls (R^2=0.350). Cases had almost twice the levels of preβ-1-HDL than controls, but the functionality of their preβ-1 particles (preβ-1-concentration-normalized ABCA1-dependent efflux capacity) was significantly lower (-39%). There were significant positive correlations between SR-BI-dependent cholesterol efflux and the levels of large lipid-rich (α-1 + α-2) HDL particles in both cases (R2=0.828) and controls (R2=0.671). Cases had significantly lower (-11%) levels of large HDL particles, but the functionality of their particles (large-HDL-concentration-normalized SR-BI-dependent efflux capacity) was significantly higher (+27%) compared to controls. High plasma levels of inflammatory and oxidative stress markers were not associated with the functionality of HDL particles. High plasma levels of triglycerides were associated with increased HDL particle functionality. HDL anti-oxidative capacity was significantly lower (-15%) in cases than in controls. There were no significant correlations between HDL anti-oxidative capacity and the concentrations of inflammatory- and oxidative-stress markers or HDL CEC. **Conclusions**: HDL CEC is significantly influenced by both the concentration and the functionality of specific HDL particles. CHD patients have higher than normal preβ-1 concentration with decreased functionality and lower than normal large-HDL particle concentration with enhanced functionality.
B.F. Asztalos: Consultant/Advisory Board; Significant; Boston Heart Diagnostics. **K.V. Horvath:** Employment; Significant; Boston Heart Diagnostics. **E.J. Schaefer:** Employment; Significant; Boston Heart Diagnostics.

384
Differential Effects of Niacin and Omega-3 Fatty Acids on HDL-apolipoprotein A-I Exhange and Cholesterol Efflux Capacity in Subjects with Metabolic Syndrome
Mark S Borja, Bradley Hammerson, Children's Hosp Oakland Res Inst, Oakland, CA; Chongren Tang, Univ of Washington, Seattle, WA; Olga V. Savinova, Sanford Res, Univ of South Dakota, Sioux Falls, CA; William S. Harris, Gregory C. Shearer, Sanford Res, Univ of South Dakota, Sioux Falls, SD; Michael N. Oda, Children's Hosp Oakland Res Inst, Oakland, CA

Objective: Niacin and omega-3 fatty acids are two therapeutic agents that have been extensively studied for their ability to reduce cardiovascular disease risk, but their effectiveness has more recently been called into question. In this study, we investigate whether these agents alone and in combination alter HDL function, in particular, HDL-apolipoprotein A-I exchange (HAE), a measure of HDL dynamics, and serum cholesterol efflux capacity (CEC).
Approach: Fifty-six subjects with metabolic syndrome (MetSyn) were recruited to a double-blind trial and randomized to 16 weeks of treatment with dual placebo, extended release niacin (ERN, 2g/day), prescription omega-3 ethyl esters (P-OM3, 4g/day), or combination. HDL function was assessed at baseline and following 16 weeks of treatment by measuring HAE, macrophage CEC, and ABCA1-specific CEC.
Results: Compared to placebo, ERN and P-OM3 alone significantly increased HAE by 15.1 [8.2, 22.0] ($p<0.0001$) and 12.4% [5.9, 18.9] ($P<0.0001$) respectively while the

combination therapy increased HAE by 10.0% [3.2, 16.8] (*P*=0.002). When evaluated by HAE:apoA-I ratio (a measure of apoA-I specific activity), ERN increased apoA-I specific activity by 20.1% [4.8, 36.9] (*P*=0.008), P-OM3 by 30.1% [14.4, 45.9] (*P*<0.0001), however with combination there was no increase, 9% [-6.6, 26.6] (*P*=0.34). Triglyceride-adjusted macrophage CEC showed marginally significant increases with P-OM3 therapy (*P*=0.05). No therapy significantly improved ABCA1-specific CEC.
Conclusions: Much of the effect of ERN on HDL function can be attributed to this therapy raising apoA-I levels, but P-OM3 raises HDL function by independent means, increasing apoA-I specific activity. Future investigation is needed to determine whether interaction between ERN and P-OM3 therapies in combination reduces their overall effectiveness.
M.S. Borja: None. **B. Hammerson:** None. **C. Tang:** None. **O.V. Savinova:** None. **W.S. Harris:** None. **G.C. Shearer:** None. **M.N. Oda:** None.

This research has received full or partial funding support from the American Heart Association.

385
Ultracentrifugation and Depletion Methods of High-density Lipoprotein Isolation Yield Particles That Are Functionally Distinct in Some of Their Vasoprotective Functions
Emily Button, Jerome Robert, Megan Gilmour, Harleen Cheema, Cheryl Wellington, Univ of British Columbia, Vancouver, BC, Canada
The evaluation of the functional capabilities of high-density lipoproteins (HDL) has been shown to be a better predictor of several cardiometabolic diseases than the traditional marker of plasma HDL cholesterol. An important, yet often unconsidered, factor in clinically evaluating HDL function is the method used to purify HDL from plasma. It has been shown that the method of HDL isolation can impact the composition of the HDL produced yet the effect of these compositional changes on HDL function has been explored very little. The evaluation of isolation method is especially important when studying novel HDL functions, such as the vasoprotective functions relevant to Alzheimer's disease (AD) recently discovered on brain vascular cells and in 3-dimensional brain vessel models. We compared the high-throughput HDL isolation method of polyethylene glycol (PEG) precipitation to the more time-consuming but purer method of sequential density gradient ultracentrifugation (UC) in several of these novel, brain-relevant vasoprotective functions. HDL isolated from young, healthy human plasma by PEG precipitation and UC were equal in their capacity for effluxing cholesterol from macrophages, suppressing TNFα-induced inflammation in brain endothelial cells, and preventing the pathological accumulation of the AD protein amyloid beta (Aβ) in 3D vessel models. However, only HDL isolated by UC, and not PEG precipitation, could induce nitric oxide production and inhibit Aβ-induced inflammation in brain endothelial cells. These findings highlight the importance of HDL isolation method in the composition and function of the HDL produced. Furthermore, that HDL isolation method affected some but not all HDL functions shows that HDL may act on brain vascular cells to protect against AD through more than one pathway.
E. Button: None. **J. Robert:** None. **M. Gilmour:** None. **H. Cheema:** None. **C. Wellington:** None.

386
Dietary Oxidized Linoleic Acid Modulates PCSK9 and Associated Genes
Chinedu Ochin, **Mahdi O Garelnabi**, Univ of Massachusetts, Lowell, MA

Introduction: We have previously shown that oxidized linoleic acid (OxLA) modulate plasma lipids. In this study we investigated the role of dietary OxLA on PCSK-9 and its associated genes. **Method:** Liver tissue from four groups of normal C57BL6 mice were feed; plain chow, chow supplemented with linoleic acid (9mg), chow supplemented with a low concentration of OxLA (9mg) and chow supplemented with a high concentration of OxLA (18mg) were analyzed for PCSK-9 and related genes. RNA from these livers samples was extracted with Trizol, assessed for purity by agarose gel electrophoresis and quantified using fluorometry. cDNA was synthesized from total extracted RNA and subsequently used for qRT-PCR analysis. Gene expressions of **PCSK-9, SREBP-1, HNF-1α** and **PPARα** were measured and normalized to **GAPDH**. **Total, free** and **cholesterol ester** levels in the liver were analyzed spectrophotometrically. Experiments were performed in triplicates and the difference between means was determined using a student's T-test with a p value of <0.05 accepted as statistically significant. **Results:** PCSK-9 gene expression was markedly elevated in the mice fed high concentration OxLA, SREBP-1 gene levels in these of mice was also significantly elevated in comparison to the other 3 groups which had relatively the same levels of SREBP-1 gene expression. Conversely HNF-1α gene expression levels were elevated in all groups except the mice on low concentration OxLA. PPARα gene levels were significantly down regulated in the mouse on high concentration OxLA. Plasma total cholesterol levels were significantly elevated in both groups on OxLA. **Conclusion:** Elevated cholesterol levels in the livers of mice fed high concentration OxLA was accompanied with increased PCSK-9 expression. These results show that OxLA modulate PCSK-9 and its associated genes expression and promote accumulation of liver cholesterol.
C. Ochin: None. **M.O. Garelnabi:** None.

387
Apolipoprotein E Receptor-2 Restricts Cardiomyocyte Proliferation and Controls Heart Size
Anja Jaeschke, Eddy S. Konaniah, Dept of Pathology, Metabolic Diseases Inst, Univ of Cincinnati Coll of Med, Cincinnati, OH; Nathan J. Robbins, Sheryl E. Koch, Jack Rubinstein, Dept of Internal Med, Div of Cardiovascular Diseases, Univ of Cincinnati Coll of Med, Cincinnati, OH; David Y. Hui, Dept of Pathology, Metabolic Diseases Inst, Univ of Cincinnati Coll of Med, Cincinnati, OH

Introduction: Apolipoprotein E receptor 2 (ApoER2) is highly expressed in brain and testes, but also in macrophages, endothelial and vascular smooth muscle cells, as well as heart. Importantly, genome-wide association studies have linked polymorphisms in the LRP8 gene to familial and premature coronary artery disease (CAD) and myocardial infarction (MI). However, the mechanisms by which ApoER2, the protein encoded by the LRP8 gene, affect CAD and MI are incompletely understood.
Hypothesis: The goal of the current study was to examine the function of ApoER2 in the heart.
Methods and Results: Morphological analysis revealed an increase in heart size and cross-sectional area with elevated cardiomyocyte proliferation in mice deficient for ApoER2 compared to wild-type control mice. Echocardiography showed a significant increase in left ventricular diameter in ApoER2 KO mice, while no significant differences in fractional shortening and ejection fraction were observed. Loss of ApoER2 attenuated expression of Disabled-2 (Dab2) and Axin2, thereby preventing formation of the destruction complex, resulting in increased levels of β-catenin. Consistent with previous studies that demonstrated that stabilized β-catenin alters expression of the T-box protein Tbx20, ApoER2 deficiency was associated with increased Tbx20 expression, a transcription factor necessary and sufficient to promote cardiomyocyte proliferation.
Conclusions: Together, these data indicate that ApoER2 promotes β-catenin degradation and modulates Tbx20 expression to restrain cardiomyocyte proliferation and heart size, providing a mechanism by which ApoER2 dysfunction may contribute to premature CAD and MI.

A. Jaeschke: None. **E.S. Konaniah:** None. **N.J. Robbins:** None. **S.E. Koch:** None. **J. Rubinstein:** None. **D.Y. Hui:** None.

388
High-density Lipoprotein Cholesterol Efflux Capacity is not associated with Atherosclerosis and Cardiovascular Events: the CODAM Study

Tatjana Josefs, Div of Cardiology, Dept of Med, New York Univ Sch of Med, New York, NY; Kristiaan Wouters, Dept of Internal Med and CARIM Sch for Cardiovascular Diseases, Maastricht Univ Medical Ctr, Maastricht, Netherlands; Uwe J Tietge, Dept of Pediatrics, Univ of Groningen, Groningen, Netherlands; Robin P Dullaart, Dept of Endocrinology, Univ of Groningen, Univ Medical Ctr Groningen, Groningen, Netherlands; Carla J van der Kallen, Dept of Internal Med and CARIM Sch for Cardiovascular Diseases, Maastricht Univ Medical Ctr, Maastricht, Netherlands; Coen D Stehouwer, Dept of Internal Med and CARIM Sch for Cardiovascular Diseases, Maastricht Univ Medical Ctr, Maastricht University, Netherlands; Casper G Schalkwijk, Dept of Internal Med and CARIM Sch for Cardiovascular Diseases, Maastricht Univ Medical Ctr, Maastricht, Netherlands; Ira J Goldberg, Div of Endocrinology, Diabetes and Metabolism, Dept of Med, New York Univ Sch of Med, New York, NY; Edward A Fisher, Div of Cardiology, Dept of Med, New York Univ Sch of Med, New York, NY; Marleen M van Greevenbroek, Dept of Internal Med and CARIM Sch for Cardiovascular Diseases, Maastricht Univ Medical Ctr, Maastricht, Netherlands

Cholesterol Efflux Capacity (CEC) is considered to be a key atheroprotective property of high-density lipoproteins (HDL). However, its role in atherosclerosis risk is still controversial. In this study, we have analyzed the relationship between HDL CEC and atherosclerosis surrogates (carotid intima media thickness (cIMT), endothelial dysfunction (EnD); Z-Scores) in a well-characterized clinical population in the Cohort of Diabetes and Atherosclerosis Maastricht (CODAM) study, which consists of 574 individuals (age 59.6±0.3yrs, 61.3% men, 24.4% T2DM). Multiple linear regression analyses were performed to identify the associations in baseline data between HDL CEC (%), plasma HDL cholesterol (HDL-C, mmol/L), HDL size (nm), apoprotein A1 (ApoA1, g/L), and HDL Particle Concentration (HDL-P, nmol/L (LN), by NMR) with cIMT and EnD. Logistic regression analyses were done to identify the association of the above-mentioned HDL characteristics and CV events (CVE; N=499, 80 CVE cases). Analyses were adjusted for lifestyle, medication and metabolic confounders.
The results show that HDL-C (ß=-0.65, 95%CI -0.91; -0.42), HDL size (ß=-0.57, 95%CI -0.98; -0.15), apoA1 (ß=-0.65, 96%CI -1.01; -0.29), and HDL-P (ß=-0.77, 95%CI -1.47; -0.11) were inversely associated with EnD (N=532), whereas HDL CEC was not (ß=-0.03, 95%CI=-0.24;0.24). Interestingly, preliminary analyses show that these associations are lost in diabetic subjects (N=131), but not in non-diabetics (N=401). An inverse association also exists between HDL-C, HDL size, apoA1, and HDL-P with cIMT (N=494), which was not statistically significant likely due to variability and relative insensitivity of cIMT measurements. Further, a 1 unit increase of HDL-C was associated with ~4fold lower prevalence of CVE (OR=0.25, 95%CI 0.08;0.83), and for HDL-P, with ~20fold less CVE (OR=0.05, 95%CI 0.00;0.70), but no association was found between HDL CEC and CVE (OR=1.26, 95%CI 0.41;3.84).
Our results show that certain HDL-related parameters have atheroprotective associations, but HDL-CEC is not one of them. This result agrees with, but differs from, some other studies, and might reflect population differences in the relationships between measurements of HDL lipids/particle number, and HDL CEC.
T. Josefs: None. **K. Wouters:** None. **U.J.F. Tietge:** None. **R.P.F. Dullaart:** None. **C.J.H. van der Kallen:** None. **C.D.A. Stehouwer:** None. **C.G. Schalkwijk:** None. **I.J. Goldberg:** None. **E.A. Fisher:** None. **M.M.J. van Greevenbroek:** None.

389
The Impact of Phospholipid Composition of Synthetic High-Density Lipoprotein on Its Pharmacological Activity

Sang Yeop Kim, Dan Li, Maria V Fawaz, Emily E Morin, Karl Olsen, Univ of Michigan, Ann Arbor, Ann Abor, MI; Xiang-An Li, Univ of Kentucky, Lexington, KY; Anna Schwendeman, Univ of Michigan, Ann Arbor, Ann Abor, MI

Objective: Synthetic high-density lipoprotein (sHDL) is a nanoparticle that can mimic biological activities of endogenous HDL such as reverse cholesterol transport (RCT) and anti-inflammatory properties. We hypothesize that differences in the fluidity of sHDL phospholipids at body temperature effect plasma stability of sHDL, particle ability to efflux cholesterol and inhibit inflammation.
Methods: sHDL particles with different membrane fluidities were prepared complexing phospholipids with different fatty acid chain length and saturation (POPC, DMPC, DPPC, and DSPC) with the apoA-I mimetic peptide, PVLDLFRELLNELLEALKQKLK (22A). The ability of various sHDL compositions to efflux cholesterol, inhibit NF-kB activation and cytokine release, and cause lipid raft disruption was examined in RAW264.7 macrophages. Various sHDL were administered to mice challenged by injection of 0.05 mg/kg LPS at 10 mg/kg dose and the levels of cytokine release were measured at 2 hours post-dose. Various sHDL were dosed to normal rats at 50 mg/kg and cholesterol mobilization and pharmacokinetics were examined.
Results: 22A-POPC and 22A-DMPC sHDL have relatively fluid phospholipid layer at body temperature compared to 22A-DPPC and 22A-DSPC sHDL due to lower phospholipid transition temperature. 22A-POPC and 22A-DMPC sHDL inhibited NF-κB activation and cytokine release in a concentration-dependent manner. From murine endotoxin infusion studies, 22A-DMPC displayed the significant inhibition of cytokine release. Cholesterol efflux studies demonstrated that 22A-POPC and 22A-DMPC displayed highest cholesterol efflux. Interestingly, *in vivo* RCT study showed that 22A-DSPC had longest plasma residence time and resulted in greatest cholesterol mobilization.
Conclusions: Phospholipid composition of sHDL particles has a significant effect on its cholesterol efflux and anti-inflammatory properties, yet the effect appears to be different *in vitro* and *in vivo*. *in vitro* effect is driven by the ability of fluid phospholipid bilayer to bind LPS, cholesterol, and LCAT, while *in vivo* effect is defined by particle stability in plasma and residence time in the body.
S. Kim: None. **D. Li:** None. **M.V. Fawaz:** None. **E.E. Morin:** None. **K. Olsen:** None. **X. Li:** None. **A. Schwendeman:** None.

This research has received full or partial funding support from the American Heart Association.

390
A New Humanized Mouse Model to Study Lipid Abnormalities and HDL Function in Poorly Controlled Type 1 Diabetes Mellitus

Vishal Kothari, Yi He, Farah Kramer, Shelley Barnhart, Jenny E Kanter, Alan Chait, Univ of Washington, Seattle, WA; Ira J Goldberg, New York Univ, New York, NY; Tomas Vaisar, Jay W Heinecke, Karin E Bornfeldt, Univ of Washington, Seattle, WA

Elevated plasma triglycerides (TG) and VLDL are often present in poorly controlled type 1 diabetes mellitus (T1DM). Furthermore, T1DM patients exhibit an increased risk of cardiovascular disease (CVD) despite normal or high HDL-cholesterol. There is a need for new mouse models to study T1DM lipid abnormalities because mice do not express cholesteryl ester transfer protein (CETP), which transfers

cholesteryl ester (CE) from HDL to VLDL and other lipoproteins in exchange for TG, and because mice do not exhibit human-like HDL populations. To develop a physiologically relevant model, we crossed a virally-induced mouse model of T1DM (*Ldlr*$^{-/-}$*;Gp*^{Tg}) deficient in the LDL receptor with human apolipoprotein A-I (*APOA1*) transgenic mice. These mice (n=8-10) were injected with a liver-specific adeno-associated virus driving expression of human CETP, mimicking the human CETP activity/apoA-I ratio, and the 3 major human HDL subpopulations. Using this model (*APOA1*^{Tg}*;Ldlr*$^{-/-}$*;Gp*^{Tg}), we examined the impact of diabetes on dyslipidemia, HDL particle concentration (HDL-P), and serum HDL function. Induction of diabetes increased plasma TG and cholesterol, primarily due to an increase in VLDL, as compared with non-diabetic (ND) littermates. The dyslipidemia was associated with increases in hepatic TG content and hepatic TG production rate (2-fold over ND). Moreover, resident peritoneal macrophages from diabetic mice exhibited a 5-fold increase in CE loading, increased lipid raft content (20%), and increased *Tnfa* (3-fold) and *Il1b* mRNA (4-fold), as compared with ND littermates. In addition, T1DM mice had increased small, medium and large HDL-P (2-fold) concentrations compared with ND controls. Serum HDL from T1DM mice showed a significant increase in its cholesterol efflux capacity through both ABCA1 and ABCG1. Thus, in this humanized mouse model, poorly controlled T1DM leads to elevated plasma TG and VLDL due in part to increased hepatic TG production. This dyslipidemia is associated with higher HDL-P and an increase in serum HDL's cholesterol efflux capacity, likely due to the increased plasma HDL-P. We have found similar changes in HDL concentration and function in humans with T1DM, suggesting that our mouse model might provide insights into CVD risk in T1DM patients.

V. Kothari: None. **Y. He:** None. **F. Kramer:** None. **S. Barnhart:** None. **J.E. Kanter:** None. **A. Chait:** None. **I.J. Goldberg:** None. **T. Vaisar:** None. **J.W. Heinecke:** None. **K.E. Bornfeldt:** None.

391

Flow Field-flow Fractionation: a Powerful Underused Size Fractionation Technique for Composition Analysis of Lipoprotein Particles

Zsuzsanna Kuklenyik, Kevin Bierboum, Jeffrey Jones, Yulanda Williamson, John R Barr, Ctrs for Disease Control, Atlanta, GA

Multiplexed mass spectrometry (MS) techniques have substantially improved the ability to characterize the composition of lipoproteins. However, these advanced MS techniques for composition analysis of lipoproteins are limited by traditional preparative fractionation techniques that compromise the structural integrity of lipoprotein particles during separation from serum or plasma. In this work a highly effective but underused size fractionation technique, asymmetric flow field-flow fractionation (AFFFF) was applied. We compared AFFFF with traditional techniques, including gel electrophoresis (GE), size exclusion chromatography (SEC), and gradient ultracentrifugation (GUC). Direct comparison of the techniques was performed by analysis of the same set of samples using sudan black staining. The AFFFF size separation allowed size resolution most similar to GE techniques, either tube gel or gradient gel. In addition, AFFFF and SEC was compared by collection of fractions where the average size in each fraction was measured by dynamic light scattering, and all major lipids and apolipoproteins were quantified by liquid chromatography tandem mass spectrometry methods (LC-MS/MS) in each fraction. The size resolution by AFFFF vs. SEC was compared based on the elution profiles of endogenous plasma proteins. On the hydrodynamic size scale, the half peak width of individual size species were 0.8-1 nm by AFFFF vs. 3-8 nm by SEC, showing the superior size resolution capability of the AFFFF technique. The gentle nature of the AFFFF separation relative to GUC was demonstrated by AFFFF separation of HDL sub-fractions with and without pre-fractionation by GUC, showing the significant loss of apoA-IV and apoCs, as well as a general shift of all lipid and protein profiles to smaller hydrodynamic size as a result of intense shearing forces and high salt conditions during GUC. Our results demonstrate that AFFFF coupled with LC-MS/MS deserves to be among the gold standard techniques for size and composition analysis of HDL, LDL and VLDL sub-classes.

Z. Kuklenyik: None. **K. Bierboum:** None. **J. Jones:** None. **Y. Williamson:** None. **J.R. Barr:** None.

392

Nanoparticle-based Biosensors for Measuring Apolipoprotein A-I and HDL Function

Rohun U Palekar, Jonathan S. Rink, Kaylin M McMahon, C Shad Thaxton, Northwestern Univ, Chicago, IL

Background: High-density lipoproteins (HDL) are dynamic circulating nanoparticles that carry cholesterol and have numerous functions. Rapid measurement of HDL, the HDL-associated protein apolipoprotein A-I (apoAI), or HDL function(s) is not currently possible. Such technology may provide new opportunities for HDL monitoring. We utilized nanoparticles to develop a method of sequestering apoAI from solution, including human serum, and for measuring the activity of the HDL-maturing and apoAI-dependent enzyme, lecithin:cholesterol acyl transferase (LCAT).
Methods: Gold nanoparticles were surface-functionalized with phospholipids. The synthesized particles were incubated with various amounts of apoAI or with purchased, LDL-depleted, human serum samples where the apoAI amount was measured using an ELISA. After incubation, the particles were easily isolated and apoAI sequestration by the nanoparticles was measured using ELISA. As apoAI is a cofactor that activates LCAT, nanoparticles were incubated with various amounts of apoA1, LCAT, and free cholesterol or with the LDL-depleted human serum samples (diluted) for 1 hour at 37ºC to enable binding of apoAI, cholesterol, and LCAT activity. The nanoparticles were easily isolated and the particle-associated cholesteryl ester was measured using an Amplex Red Cholesterol Assay kit.
Results: The nanoparticles sequester apoAI according to the concentration of apoAI in solution ($R = 0.668$, $p = 0.035$, $N = 10$). Also, data reveal that the LCAT binds the nanoparticle-apoAI structures and catalyzes the conversion of cholesterol to cholesteryl ester. The amount of cholesteryl ester bound to the nanoparticles is directly dependent on the amount of apoAI ($R = 0.729$, $p = 0.016$, $N=10$).
Conclusion: These results demonstrate that specific, functionalized nanoparticles can be added to serum to sequester apoAI in dose-response. Also, the formed conjugate structures activate LCAT whereby the amount of cholesteryl ester formed on the nanoparticle directly correlates with apoAI. Overall, this technology provides a framework and new approach for developing next generation HDL- and HDL-function specific biosensors.

R.U. Palekar: None. **J.S. Rink:** None. **K.M. McMahon:** None. **C.S. Thaxton:** None.

This research has received full or partial funding support from the American Heart Association.

393

Differential Regulation of Lipoprotein Assembly and Secretion and Mtp Expression in Intestinal and Hepatic Cells by Oleoylethanolamide

Xiaoyue Pan, Mahmood M. Hussain, NYU Winthrop Hosp, Mineola, NY

Dietary fat triggers synthesis of OEA in enterocytes of the upper small intestine. OEA initiates a cascade of events to optimize fatty acid uptake and reduce feeding frequency. Effects of OEA have been studied after oral gavage and intraperitoneal injections. Here, we studied dose dependent effects of OEA on the assembly and secretion of lipoproteins

in differentiated human colon carcinoma Caco-2, human hepatoma Huh-7 and HepG2 cells as well as in mouse primary enterocytes and hepatocytes. Differentiated Caco-2 cells were treated with OEA or oleic acid for 16 h. OEA increased synthesis of triglycerides in dose dependent manner compared with oleic acid:taurocholate micelles. Further, OEA increased secretion of triglycerides and apolipoprotein B (apoB) in chylomicrons. Expression and activity of microsomal triglyceride transfer protein (MTP) was increased by OEA in a dose dependent manner in these cells. Next, mouse primary enterocytes were incubated with OEA or oleic acid for 4 h. OEA increased MTP activity and secretion of triglycerides in these cells as well. These studies suggest that OEA enhances MTP expression, lipid synthesis and lipoprotein assembly in intestinal cells more than oleic acid.
To study the effect of OEA on liver derived cells, these cells were exposed to OEA or no lipids for 16 h. OEA reduced secretion of triglycerides and apoB in Huh-7 and HepG2 cells without affecting the secretion of apoAI. Further, MTP expression and activity was reduced in these cells after OEA treatment compared to no OEA controls. Similarly, OEA reduced MTP expression and activity as well as secretion of triglycerides in mouse primary hepatocytes. These studies indicate that OEA reduces MTP expression, lipid synthesis and lipoproteins secretion in liver derived cells. Thus, OEA has differential effects on MTP expression and lipoprotein assembly and secretion in intestine and liver derived cells. It is likely that OEA regulates postprandial response to optimize exogenous lipid absorption and reduce endogenous lipid mobilization.
X. Pan: Research Grant; Modest; AHA GIA. **M.M. Hussain:** None.

394
Bacterial Serum Opacity Factor Rescues HDL Functionality in SR-B1$^{-/-}$ Mice
Corina Rosales, Dedipya Yelamanchili, Baiba K. Gillard, Methodist Hosp Res Inst, Houston, TX; Antonio M. Gotto, Weill Cornell Med, New York, NY; Henry J. Pownall, Methodist Hosp Res Inst, Houston, TX

Although plasma HDL-C levels negatively correlate with atherosclerotic cardiovascular disease (ACVD), attempts to reduce ACVD risk by raising plasma HDL have disappointed. Thus, hypotheses about salutary HDL effects have shifted from higher-is-better to function-is-more-important. The SR-B1$^{-/-}$ mouse is an extreme model of HDL dsyfunctionality; compared to WT mice, SR-B1$^{-/-}$ mice have higher plasma HDL levels and an HDL surface that is free cholesterol (FC)-rich (60 vs. 15 mol%). This would be expected to increase HDL-FC bioavailability to cytotoxic levels. HDL dysfunctionality among SR-B1$^{-/-}$ mice is associated with multiple metabolic abnormalities—impaired cell membrane structure and function and atherosusceptibility, despite having high plasma HDL-C levels; moreover, female SR-B1$^{-/-}$ mice are infertile. Liver-specific SR-B1 expression in SR-B1$^{-/-}$ mice normalizes HDL size and FC content. Thus, the SR-B1$^{-/-}$ mouse phenotype is due to lack of hepatic clearance of lipids from dysfunctional HDL. Serum opacity factor (SOF) is a bacterial protein that catalyzes the quantitative disproportionation of HDL into a cholesteryl ester-rich micro emulsion (CERM), neo HDL, and lipid-free apo AI. The CERM contains apo E and all HDL-CE. Injection of SOF (4 µg) into WT mice lowers plasma cholesterol by diverting the CERM to hepatic LDLR. Thus, we began testing whether adeno-viral delivery of SOF (AAV_{SOF}) to SR-B1$^{-/-}$ mice rescues HDL functionality. A plasmid encoding the SOF gene was synthesized; SOF DNA was isolated by restriction enzyme digestion and cloned into a pAAV-TBG-mcs plasmid that was submitted to the PENN Vector Lab for virus production and isolation. AAV_{GFP} plasmid (UPENN) was used as control. Good SOF production and secretion was confirmed by transfection of Huh7 hepatocytes. AAV_{SOF} injection into SR-B1$^{-/-}$ mice induced constitutive plasma SOF activity and reduced HDL-C levels to nil. Superposition of high plasma HDL levels and a high mol% FC in SR-B1$^{-/-}$ is expected to increase HDL-FC bioavailablity that contributes to whole-body FC-toxicity and the observed metabolic abnormalities. Future tests will determine whether ablation of dysfunctional HDL in SR-B1$^{-/-}$ mice rescues their pathological phenotype, especially atherosclerosis.
C. Rosales: None. **D. Yelamanchili:** None. **B.K. Gillard:** None. **A.M. Gotto:** None. **H.J. Pownall:** None.

395
Changes in the HDL Lipidome With Regular Exercise: a Pilot Study
Mark A Sarzynski, Univ of South Carolina, Columbia, SC; Dinesh K Barupal, Megan R Showalter, UC Davis, Davis, CA; Jacob L Barber, Jonathan J Ruiz-Ramie, Univ of South Carolina, Columbia, SC; Claude Bouchard, Pennington Biomedical Res Ctr, Baton Rouge, LA; Oliver Fiehn, UC Davis, Davis, CA

Background: Over 200 individual molecular lipid species have been found to reside on high-density lipoproteins (HDL). The effects of exercise on the HDL lipidome profile is unknown.
Methods: We examined changes in the HDL lipidome after regular exercise in 20 individuals who completed a 20-week endurance exercise program as part of the HERITAGE Family Study. The 20 subjects were selected based on discordance for exercise-induced increases in mean HDL particle (HDL-P) size (10 high-responders, 10 non-responders). The abundance of 184 known individual lipid species was quantified in baseline and post-training HDL plasma samples by UPLC-QTOF-MS. HDL was isolated through gel filtration chromatography.
Results: Seven lipid species, particularly classes of triacylglycerols, cholesteryl esters, phosphatidylcholines, and sphingomyelins, showed nominal ($p<0.05$) increases in abundance with exercise training, with fold changes ranging from 1.13 to 1.65 (**Figure 1**). Three lipids showed differential responses to exercise between high- and non-responders of HDL-P size, including one lipid and metabolite each that showed an overall effect of training (**Figure 1**). For example, the abundance of sphingomyelin d39:2 decreased by an average of 23% in the high-responders of HDL size to exercise, whereas abundance increased by 71% in the non-responders ($p=0.004$ for difference between groups). None of the exercise-induced changes in lipid levels were statistically significant after accounting for multiple testing.
Discussion: This pilot study showed limited evidence of systematic remodeling of the HDL lipidome in response to regular endurance exercise. Future studies are needed with larger sample sizes, diverse populations, and differing exercise protocols to further examine how the molecular composition of HDL particles changes in response to exercise and potentially contributes to its atheroprotective functions.

Figure 1: Changes in the HDL lipidome with regular exercise

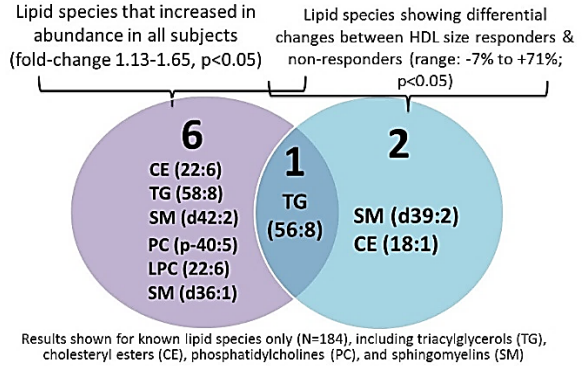

M.A. Sarzynski: Consultant/Advisory Board; Significant; Genetic Direction, LLC. **D.K. Barupal:** None. **M.R.**

Showalter: None. **J.L. Barber:** None. **J.J. Ruiz-Ramie:** None. **C. Bouchard:** None. **O. Fiehn:** None.

396
A Unique Case of Artefactual and Real HDL Disappearance Due to Isolevuglandins Adducts
Hagai Tavori, Oregon Health & Science Univ, Portland, OR; Jonathan Stringer, CHI St. Vincent Diabetes and Endocrinology Clinic,, Hot Springs, AR; Monica Agarwal, Univ of Alabama at Birmingham, Birmingham, AL; Jessica S Lilley, Mississippi Ctr for Advanced Med,, Madison, MS; Linda Zhang, Sean S Davies, Vanderbilt Univ Medical Ctr, Nashville, TN; MacRae F Linton, Vanderbilt Univ Medical Ctr, Nashvile, TN; Michael D Shapiro, Serg Fazio, Oregon Health & Science Univ, Portland, OR; Michelle J Ormseth, Vanderbilt Universtiy Medical Ctr, Nashville, TN

We report a case of acquired, progressive, and severe HDL cholesterol (HDL-C) deficiency that emerged in an individual with multiple myeloma. An 81 year-old white male presented with extremely low HDL-c (≤5 mg/dL). Between the ages of 69 - 73 years old, his annual lipid panels demonstrated HDL-c >70 mg/dL. At that point, his HDL-C levels progressively decreased until their virtual disappearance over a period of 12 years. During this time, he developed anemia, an IgG-kappa M-spike, and increased plasma cells on bone marrow biopsy, compatible with a diagnosis of multiple myeloma. Review of his medications, medical history, and metabolic status failed to identify a cause for his progressive decine of HDL-C. Parallel analyses of plasma samples using detergent to solubilize and release HDL-associated cholesterol (SYNCHRO LX, Beckman) and separation of non-HDL precipitated by dextran sulfate yielded HDL-C values of 5 mg/dL and 47 mg/dL, respectively. Furthermore, HDL-C levels of 52 mg/dL and 54 mg/dL were confirmed using ultracentrifugation and NMR-based methods, respectively. Serum apoAI concentration was 153 mg/dL, suggesting normal levels of HDL, in contrast with the ultra-low HDL-C reported in one method. The patient's alpha migrating band on lipoprotein gel electrophoresis also appeared normal, suggesting the presence of roughly normal amounts of HDL. Methodological artifact alone, however, did not explain the significant "real" decrease in HDL-C (from the upper 70's mg/dL to the 40's mg/dL) recorded during 12 years of monitoring. Isolevuglandins (IsoLG) are highly reactive ketoaldehydes that interact with lysine residues of proteins and head groups of phosphatidylethanolamine. It was recently proposed that IsoLG adducts on HDL can result in deleterious structural and functional changes in the particle. Interestingly, the patient's serum showed high titers of autoantibodies to IsoLG-apoAI, but low titers against native apoAI. We further studied the turnover of IsoLG-apoAI and native apoAI in mice. This case of artefactual and real HDL-C disappearance in a patient with multiple myeloma is likely due to paraprotein-related interference of HDL-C assays and increased plasma clearance of modified apoA1.
H. Tavori: None. **J. Stringer:** None. **M. Agarwal:** None. **J.S. Lilley:** None. **L. Zhang:** None. **S.S. Davies:** None. **M.F. Linton:** None. **M.D. Shapiro:** None. **S. Fazio:** None. **M.J. Ormseth:** None.

397
Cotinine, but Not Nicotine, Increased ApoA-I Mediated HDL Synthesis in THP-1 Cells
Maki Tsujita, Nagoya City Univ Graduate Sch Med Sci, Nagoya, Japan; Vasanthy Narayanaswami, California State Univ Long Beach, Long Beach, CA

Aim: Cotinine is known as a stable metabolite of nicotine, the plasma half-life is over 20-30 hrs. Here, we evaluated its characteristic properties on the apoA-I mediated HDL generation. Method: Cotinine (5.6 to 11.2μM), or nicotine (5 to 150μM) were supplemented to medium and co-incubated with apoA-I (10μg/mL) for 18 hrs with THP-1 cells to determine their effect on efflux activity. Cellular ACAT accessible cholesterol pool size was determined by [^{14}C]oleic acid labeling of cells for 60 min immediately after removal of the culture medium. The culture medium and the cellular lipids were extracted by organic solvents and cholesterol and phospholipids content were determined. Nicotine was administered orally as an aqueous solution (10 μM) to C57BL/6 mice for 10 days and the plasma lipoprotein profiles were measured by gel-HPLC (tandem TSK-lipopropak$_{XL}$) with online enzymatic lipid assay system (Skylight biotech, Inc.). Results: Supplementation of nicotine into the medium showed no effect on the apoA-I mediated cellular cholesterol release from THP-1 cells. On the other hand, cotinine increased apoA-I mediated cellular cholesterol efflux 2.8 fold. ACAT accessible cholesterol pool size was dramatically decreased to 80% and 58% of control with 5 and 10 μM cotinine treatment, respectively, indicating that cotinine effectively increased apoA-I/ABCA1 mediated cellular cholesterol efflux. Mice with oral nicotine administration showed increased plasma HDL by 11.4% (50.1±4.4 and 55.8±3.9 mg/dL for control and nicotine treatment, respectively). Conclusions: Cotinine increased apoA-I mediated cellular cholesterol efflux in THP-1 cells. The cellular ACAT accessible cholesterol pool size reduction is one of the early reactions of apoA-I/ABCA1 mediated cellular cholesterol efflux. Cotinine seemingly modifies cellular factor/factors to induce a change in cholesterol distribution. Mice administrated oral nicotine may convert the compound to cotinine by CYP2A6 and aldehyde oxidase activities in their liver, and which likely increased HDL generation. Further experiments are necessary to examine the direct effect of cotinine on the ABCA1 transporter for increasing HDL assembly system.
M. Tsujita: None. **V. Narayanaswami:** None.

398
Gut Microbiota Facilitates Apolipoprotein A1 and HDL Production Through Hepatic TLR5
Jensen Hc Yiu, Wai-Lun W Fung, Jin Li, Jamie Cheung, The Univ of Hong Kong, Pokfulam, Hong Kong; Patrick Tso, Univ of Cincinnati, Cincinnati, OH; Aimin Xu, **Connie W Woo**, The Univ of Hong Kong, Pokfulam, Hong Kong

Gut microbiota is considered as an external organ as these trillions of commensal microbes in our gut interact with our body to regulate various physiological responses. The pattern and composition of gut bacteria is subject to alteration by our diet. High fat diet not only decreases the β-diversity of gut microbiota but also increases gut permeability, leading to the leak of bacterial products into circulation, which aggravates various diseases including atherosclerosis by escalating inflammation. Paradoxically high fat intake can augment HDL level (J Clin Invest 91:1665-71, 1993). Moreover, gut microbiota was shown to contribute the variation of HDL but not LDL or total cholesterol level in a human study. (Circ Res 117: 817-24, 2015) We speculate that gut microbiota may provide an adaptive protection by upregulating HDL level. In this study, we investigated the possible underlying mechanism of how gut microbiota affects HDL level. C57BL/6J mice were fed a normal chow diet and a high fat diet (HFD, 45% fat kcal) for 10 weeks. Other than decreasing the β-diversity of gut microbiota, HFD increased the portion of flagellated bacteria, resulting in the increase of hepatic but not circulating level of flagellin, the ligand of toll-like receptor (TLR5). Deletion of TLR5 in mice suppressed HFD-stimulated HDL level. Treatment with flagellin in hepatocytes was able to stimulate apolipoprotein A1 (apoA), the primary apolipoprotein on HDL in TLR5-dependent manner. Blocking the downstream signaling of TLR5 by silencing MYD88 blocked the flagellin-induced apoA1 production in wild type hepatocytes. Lipopolysaccharides, another important bacterial product which can activate MYD88 signaling, failed to elicit the same effect. It might be due to the different degree of sensitivity of these TLRs in hepatocytes. In addition, supplementation of flagellin to atherogenic mice (apoE knockout mice) by oral gavage was able to elevate apoA1 and HDL levels in circulation, partially protecting against atherosclerosis. Our

data provides a molecular explanation of how commensal bacteria in gut stimulate HDL production upon HFD, and such finding will provide an insight in developing alternative strategy to stimulate HDL production and prevent atherosclerosis.
J.H. Yiu: None. **W.W. Fung:** None. **J. Li:** None. **J. Cheung:** None. **P. Tso:** None. **A. Xu:** None. **C.W. Woo:** None.

399
Cell, Mice and Human CSF Studies Indicate Impaired Interactions Between ABCA-1 and ApoE4 in ApoE4 Driven Alzheimer's Disease
Varun Rawat, Univ of Southern California, Los Angeles, CA; Anat Boehm-Cagan, Tel Aviv Univ, Tel Aviv, Israel; Jan Johansson, Artery Therapeutics, San Ramon, CA; John Bielicki, Univ of California, Berkely, Berkely, CA; Helena Chui, Univ of Southern California, Los Angeles, CA; Michael Harrington, Huntington Medical Res Inst, Pasadena, CA; Daniel Michaelson, Tel Aviv Univ, Tel Aviv, Israel; **Hussein Yassine**, Univ of Southern California, Los Angeles, Los Angeles, CA

Background: Loss-of-function mutations in the ATP Binding Cassette A-1 (ABCA-1) transporter and the ApoE4 allele are associated with increased Alzheimer's disease (AD) risk. We recently reported decreased ABCA-1 activity of cerebrospinal fluid (CSF) from participants with AD. Our aim is to study the interaction of ApoE4 with ABCA-1 activity in astrocytes, in human apoE4 (hApoE4) targeted replacement (TR) mice, and in CSF from humans grouped by APOE genotype. **Methods:** ABCA-1 expression and activity were assessed in astrocytes that express human ApoE isoforms and in hApoE mice. The ability of CSF to activate ABCA-1 was examined in cells. CSF from 59 older individuals with or without cognitive impairment was analyzed for ApoE particle size using native gel electrophoresis, and ABCA-1 cholesterol efflux activity. The effect of the ABCA-1 agonist CS-6253 on ABCA-1 activity and AD pathology was examined. **Results:** ApoE4 vs. apoE3 expressing astrocytes had decreased ABCA-1 expression that was associated with hypolipidated ApoE4. A similar discrepancy for ABCA-1 and apoE lipidation was found between hApoE4 and hApoE3 TR mice. CSF ApoE was resolved in four distinct bands by electrophoresis α_0 (>669 KDa), α_1 (600 KDa), α_2 (440 KDa) and α_3 (232-140 KDa). The amount of total ApoE present in α_0 size was reduced in ε4/ε4 vs ε3/ε3 individuals (3.208 % (SD 0.6156; N=3) vs 8.904 % (SD 0.6156; N=29), $p<0.05$), whereas total ApoE in α_2 size was increased in ε4/ε4 vs ε3/ε3 individuals (60.68 % (SD 8.207; N=3) vs 37.34 % (SD 16.80; N=31), $p<0.05$). CSF from ε4/ε4 individuals (N=3) has reduced capacity to induce ABCA-1 mediated cholesterol efflux compared to CSF from non ε4 individuals (N=9) (adjusted efflux 1.288 vs 1.594, $p<0.05$). CS6253 incubation with CSF increased ABCA1 mediated efflux in hApoE3 and hApoE4 TR mice, respectively. Treatment with the ABCA-1 agonist CS-6253 enhanced CSF cholesterol efflux capacity and reversed cognitive deficits in hApoE4 TR mice. **Conclusions:** ApoE4 was associated with reduced ABCA-1 activity and hypolipidated ApoE4 *in vivo, in vitro and in CSF*. The ABCA-1 agonist CS6253 improved apoE lipidation in astrocytes, CSF and in hApoE4 TR mice. The findings stress the importance of ABCA-1 in apoE4 driven AD and ABCA-1 activity of CSF as a biomarker in AD.
V. Rawat: None. **A. Boehm-Cagan:** None. **J. Johansson:** Ownership Interest; Significant; Artery Therapeutics. **J. Bielicki:** Ownership Interest; Modest; Peptide inventor. **H. Chui:** None. **M. Harrington:** None. **D. Michaelson:** None. **H. Yassine:** None.

408
ApoE Regulation of Hematopoiesis Suppresses Atherosclerosis by Reducing Adaptive Immunity in Hyperlipidemic Mice
Laura Bouchareychas, Div of Vascular and Endovascular Surgery, Dept of Surgery, Univ of California San Francisco & VA Medical Ctr, San Francisco, CA; Ryo Yamamoto, Inst for Stem Cell Biology and Regenerative Med, Stanford Univ Sch of Med, Stanford, CA; Fu Sang Luk, Roy Y Kim, David Wong, Div of Vascular and Endovascular Surgery, Dept of Surgery, Univ of California San Francisco & VA Medical Ctr, San Francisco, CA; Jonathan Villeneuva, Inst for Stem Cell Biology and Regenerative Med, Stanford Univ Sch of Med, Stanford, CA; Phat Duong, Allen Chung, Div of Vascular and Endovascular Surgery, Dept of Surgery, Univ of California San Francisco & VA Medical Ctr, San Francisco, CA; Hiromitsu Nakauchi, Inst for Stem Cell Biology and Regenerative Med, Stanford Univ Sch of Med, Stanford, CA; Robert Raffai, Div of Vascular and Endovascular Surgery, Dept of Surgery, Univ of California San Francisco & VA Medical Ctr, San Francisco, CA

Background and Purpose: Apolipoprotein (apo) E suppresses atherosclerosis by exerting a profound control over cells of the innate immune system including monocytes and macrophages. In mice with hyperlipidemia, apoE also prevents an exaggerated proliferation of hematopoietic stem and progenitor cells (HSPC) to further limit the expansion of innate immune cells. However, apoE's control over hematopoiesis and its subsequent shaping of adaptive immunity remains unexplored. **Methods:** We explored this question by studying HypoE mice deficient in the LDL receptor (*Apoe*$^{h/h}$*Ldlr*$^{-/-}$ mice) that display plasma lipid levels similar to those of *Apoe*$^{-/-}$*Ldlr*$^{-/-}$ mice when fed a chow diet, but accumulate apoE in plasma and display reduced atherosclerosis. Populations of HSPC were examined in the bone marrow (BM) and spleen, while populations of mature immune cells and their levels of cellular activation were examined in the blood, spleen, lymph nodes and aorta of twenty-week-old mice.**Results:** Our findings show that apoE suppressed the expansion of HSPC in both the spleen and BM of *Apoe*$^{h/h}$*Ldlr*$^{-/-}$ mice, which remained similar to levels seen in normal wildtype mice. Specifically, in the spleens of *Apoe*$^{h/h}$*Ldlr*$^{-/-}$ mice, apoE reduced the expansion of a population of multi-potent progenitors termed MPP4 responsible for lineages of lymphoid cells. Accordingly, *Apoe*$^{h/h}$*Ldlr*$^{-/-}$ mice displayed smaller spleens and lymph nodes that contained fewer myeloid- and lymphoid-derived leukocytes compared to *Apoe*$^{-/-}$*Ldlr*$^{-/-}$ mice. The spleens and lymph nodes of *Apoe*$^{h/h}$*Ldlr*$^{-/-}$ mice had a higher percentage of T cells that displayed a naïve phenotype, while the percentage of effector T cells was decreased and produced 50% less IFN-γ. Dendritic cells isolated from spleens of *Apoe*$^{h/h}$*Ldlr*$^{-/-}$ mice showed reduced levels of CD86 that plays a key role in T cell activation. Digested aortas of *Apoe*$^{h/h}$*Ldlr*$^{-/-}$ mice revealed a decrease in both T cell and myeloid cell number that also displayed a lower percentage of the pro-inflammatory CD11b^{+} subtype but a higher percentage of the anti-inflammatory CD103^{+} subtype. **Conclusion:** Collectively, our findings show that the control of hematopoiesis exerted by apoE results in reduced adaptive immunity to suppress atherosclerosis in hyperlipidemic mice.
L. Bouchareychas: None. **R. Yamamoto:** None. **F. Luk:** None. **R.Y. Kim:** None. **D. Wong:** None. **J. Villeneuva:** None. **P. Duong:** None. **A. Chung:** None. **H. Nakauchi:** None. **R. Raffai:** None.

409
Ambient Fine Particulate Matter Impairs Endothelial Progenitor Cells Through Card9-mediated Innate Immune Response
Yuqi Cui, Xuanyou Liu, Zhiheng Chen, Huifang Xu, Hong Hao, Hong Hao, Qingyi Zhu, Meng Jiang, Univ of Missouri, Columbia, MO; Xin Lin, Univ of Texas, Houston, TX; Qinghua Sun, The Ohio State Univ, Columbus, OH; Lianqun Cui, Shandong Univ, Jinan, China; Zhenguo Liu, Univ of Missouri, Columbia, MO

Background/Aims: Endothelial progenitor cells (EPCs) play a critical role in angiogenesis and vascular repair. Some environmental insults, like fine particulate matter (PM) exposure, significantly impair EPCs through inflammation and ROS production. Cytosolic adaptor caspase recruitment

domain 9 (CARD9) is important to the function of macrophages and involved in the innate immune response. The present study was to determine the role of macrophage-mediated immune response in PM-induced adverse effects on EPCs. **Methods:** PM was intranasal-distilled into male C57BL/6 mice for 1, 2, 7, 14 and 28 days. The level of EPCs ($CD34^+/Flk\text{-}1^+$, $Sca\text{-}1^+/Flk\text{-}1^+$, $c\text{-}Kit^+/CD31^+$ and $CD34^+/CD133^+$) in the bone marrow (BM) and circulation was determined using flow cytometry along with the proliferation and apoptotic level of EPCs as well as intracellular reactive oxygen species (ROS) formation. Serum TNF-α, IL-1β, IL-6 and IL-10 were measured using ELISA. To determine the role of CARD9-mediated signaling in PM-induced detrimental effects on EPCs, CARD9 knock out ($CARD9^{-/-}$) mice were used to repeat the experiment. The population of total macrophages as well as M1 and M2 subpopulations in both BM and blood were analyzed in the mice with and without PM exposure. To study the function of macrophages after PM exposure, the peritoneal macrophages were isolated and cultured for 48 hours to measure the production of TNF- α, IL-1β, IL-6 and IL-10 in the media. **Results:** PM exposure significantly decreased BM and circulating $CD34^+/FLk\text{-}1^+$ as well as BM $Scal\text{-}1^+/Flk\text{-}1^+$ population, promoted apoptosis and inhibited proliferation of EPCs in association with increased ROS production, serum TNF-α, IL-1β, IL-6 and decreased serum IL-10 level. These PM-induced effects on EPC population and cytokine production were largely prevented in $CARD9^{-/-}$ mice along with increased M2 population in both BM and blood. The production of TNF-α, IL-1β and IL-6 was significantly decreased, while the IL-10 level increased, from cultured macrophage of $CARD9^{-/-}$ mice compared with WT control. **Conclusion:** PM exposure significantly decreased BM and circulating EPCs population due to CARD9-mediated innate immune response.

Y. Cui: None. **X. Liu:** None. **Z. Chen:** None. **H. Xu:** None. **H. Hao:** None. **H. Hao:** None. **Q. Zhu:** None. **M. Jiang:** None. **X. Lin:** None. **Q. Sun:** None. **L. Cui:** None. **Z. Liu:** None.

410

Statin Use May Alleviate Coagulation- and Inflammation-associated Gene Expression in Circulating Classical Monocytes in Women with Chronic HIV-1 Infection

Erik Ehinger, Pramod Akula Bala, La Jolla Inst, La Jolla, CA; Juan Lin, David B Hanna, Albert Einstein Coll of Med, Bronx, NY; Karin Mueller, Livia Baas, La Jolla Inst, La Jolla, CA; Qibin Qi, Tao Wang, Albert Einstein Coll of Med, Bronx, NY; Konrad Buscher, La Jolla Inst, La Jolla, CA; Yongmei Liu, Wake Forest Univ Sch of Med, Winston-Salem, NC; Kathryn Anastos, Albert Einstein Coll of Med, Bronx, NY; Jason M Lazar, State Univ of New York, Downstate Medical Ctr, Brooklyn, NY; Wendy J Mack, Keck Sch of Med, Univ of Southern California, Los Angeles, CA; Phyllis C Tien, San Francisco VA Medical Ctr, San Francisco, CA; Mardge H Cohen, John Stroger Hosp and Rush Univ, Chicago, IL; Igho Ofotokun, Emory Univ Sch of Med, Atlanta, GA; Stephen Gange, Johns Hopkins Univ, Baltimore, MD; Sonya L Heath, Univ of Alabama at Birmingham, Birmingham, AL; Howard N Hodis, Keck Sch of Med, Los Angeles, CA; Russell P Tracy, Univ of Vermont Larner Coll of Med, Colchester, VT; Alan L Landay, Rush Univ Medical Ctr, Chicago, IL; Robert C Kaplan, Albert Einstein Coll of Med, Bronx, NY; Klaus Ley, La Jolla Inst, La Jolla, CA

During virally-suppressed chronic human immunodeficiency virus (HIV) infection, persistent inflammation contributes to the development of cardiovascular disease, a major comorbidity in people living with HIV. Monocytes play a key role in atherosclerotic plaque development, inflammation, and stability, but their contribution to the CVD under viral suppression in people living with HIV remains unknown. Here, we investigated the transcriptomes of classical ($CD14^{++}CD16^-$) blood monocytes from 92 women with and without chronic HIV infection and subclinical cardiovascular disease (sCVD), defined as the presence of focal carotid artery plaque, from the Women's Interagency HIV Study (WIHS). Differential gene expression, based on four two-way comparisons among participant groups (HIV-sCVD-, HIV+sCVD-, HIV-sCVD+, and HIV+sCVD+, 23 subjects each), identified large pro-inflammatory gene signatures for both sCVD and virally-suppressed HIV. These findings were further corroborated by Ingenuity Pathway Analysis. We found that classical monocytes persistently express common CVD-related markers of inflammation, including IL6, IL1β, and IL12B; overlapping with many transcripts identified in sCVD+ participants. In comorbid disease (HIV+sCVD+), those reporting statin use showed dramatically reduced pro-coagulant tissue factor (F3) and tissue factor pathway inhibitor (TFPI and TFPI2) gene expression to a level comparable with healthy participants. Cytokine expression profiles associated with the tissue factor pathway were also modified in participants on statins, suggesting that statins may benefit women with chronic HIV infection by limiting pro-coagulation and inflammation pathways in classical monocytes.

E. Ehinger: None. **P. Akula Bala:** None. **J. Lin:** None. **D.B. Hanna:** None. **K. Mueller:** None. **L. Baas:** None. **Q. Qi:** None. **T. Wang:** None. **K. Buscher:** None. **Y. Liu:** None. **K. Anastos:** None. **J.M. Lazar:** None. **W.J. Mack:** None. **P.C. Tien:** None. **M.H. Cohen:** None. **I. Ofotokun:** None. **S. Gange:** None. **S.L. Heath:** None. **H.N. Hodis:** None. **R.P. Tracy:** None. **A.L. Landay:** None. **R.C. Kaplan:** None. **K. Ley:** None.

411

Human Species-specific Loss of the CMP-N-acetylneuraminic Acid Hydroxylase Fuels Atherosclerosis Development via Intrinsic and Extrinsic Mechanisms

Kunio Kawanishi, Bastian Ramms, Sandra Diaz, Raymond Do, Nissi Varki, Ajit Varki, **Philip Gordts**, UCSD, La Jolla, CA

Cardiovascular disease (CVD) events due to atherosclerosis are very common in humans, but rarely occur spontaneously in other mammals, absent experimental manipulation. All humans exhibit a species-specific deficiency of the common mammalian sialic acid N-glycolylneuraminic acid (Neu5Gc), due to pseudogenization of the CMP-N-acetylneuraminic acid (Neu5Ac) hydroxylase (CMAH) gene, which occurred in hominin ancestors about 2-3 million years ago. Human-like $Cmah^{-/-}$ mice that express only the precursor sialic acid Neu5Ac are more prone to insulin resistance and have more reactive macrophages and T cells. Human dietary consumption of Neu5Gc (primarily from red meat), can acts as a foreign “xenoantigen” in humans that gets metabolically incorporated into endogenous glycoproteins. Humans with circulating anti-Neu5Gc “xeno-autoantibodies” can thus potentially develop local chronic inflammation or “xenosialitis” at sites of Neu5Gc accumulation such as endothelial cells and in atherosclerotic plaques. In this study we set out to test if human CMAH deficiency contributes to CVD via multiple intrinsic and extrinsic mechanisms. $Cmah^{-/-}Ldlr^{-/-}$ mice had increased atherogenesis on a Neu5Gc-free high fat diet (HFD), compared to $Cmah^{+/+}Ldlr^{-/-}$ mice. This was not associated with cytokine levels in plasma, but increased cytokine expression was seen in $Cmah^{-/-}Ldlr^{-/-}$ macrophages in comparison to $Cmah^{+/+}Ldlr^{-/-}$. The baseline relative hyperglycemia of the $Cmah^{-/-}Ldlr^{-/-}$mice was also enhanced on a Neu5Gc-free HFD. When such mice were immunized to develop human-like levels of anti-Neu5Gc antibodies, they had a 2.5-fold increase in atherosclerosis on a Neu5Gc-rich HFD compared to control Neu5Ac-rich or sialic acid-free HFD feeding. Drastically advanced lesions with increased necrotic core areas and infiltration of macrophages and T-cells accompanied increases in atherosclerotic area and lesion volume. None of these differences were explained by changes in lipoprotein profiles or insulin sensing. Human evolutionary loss of CMAH likely contributes to atherosclerosis propensity, via both intrinsic mechanisms such as amplified chronic inflammatory

response and hyperglycemia; and extrinsic mechanisms such as red meat-derived Neu5Gc-induced xenosialitis.
K. Kawanishi: None. **B. Ramms:** None. **S. Diaz:** None. **R. Do:** None. **N. Varki:** None. **A. Varki:** None. **P. Gordts:** None.

412
Dietary Lectins Cause Coronary Artery Disease via an Autoimmune Endothelial Attack Mediated by Interleukin 16
Steven R Gundry, The Intl Heart and Lung Inst, Palm Springs, CA

Interleukin 16 (IL-16) is a chemoattractant released by endothelial and other cells to attract activated T cells. It has previously been shown to have expression in many autoimmune diseases (AI). Based on our previous reports using elevated adiponectin levels of 16 ug/mL to predict lectin sensitivity, and showing an association between lectins and AI causation, we have treated a large pt population with known autoimmune disease (as confirmed by markers). We recently began using the PULS Cardiac Test (GD Biosciences Lab, Irvine, CA) a validated blood test for predicting 5 year risk of acute coronary syndrome (ACS) to examine which measured biomarkers predominate in these patients.
325 consecutive pts aged 25-89 had PULS tested as part of a comprehensive blood panel, which also screens for 14 autoimmune disease markers. The PULS tests ranks 9 biomarkers, including IL-16, MCP-3, Eotaxin, CTACK, sFas, Fas Ligand, HGF for ACS risk, ranking each biomarker from lowest to highest level contributing to risk.
241 pts (74%) were positive for elevated adiponectin, hx of AI, and/or markers for AI. Of these pts, 223 (93%) were positive for IL-16 as the highest PULS risk factor. In contrast, of the other 84 pts without AI or adiponectin elevation, only 5 (6%) had IL-16 recorded as a risk.
We conclude that based on IL-16 testing via PULS, that this provides further evidence to support an autoimmune cause of coronary artery disease at the endothelial level via T cell activation and attraction in patients with gluten and lectin sensitivity or known autoimmune disease. It also explains the known high association of autoimmune disease and ACS.
S.R. Gundry: None.

413
CD11c/CD18 Affinity Modulates Monocyte Inflammatory in Primary and Recurrent Myocardial Infarction
Alfredo A Hernandez, Greg Foster, Andrea Fernandez, Scott Simon, Gagan Singh, UC Davis, Davis, CA

Several studies address the role of $CD11c^{+}$ monocytes in the exacerbation of atherosclerosis through the maintenance of macrophages, notably foam cells, however this cell type remains elusive in the context of human atherosclerosis. Intermediate monocytes (CD14+CD16+, Mon2) have a high degree of potential participation in atherosclerosis through the upregulation of membrane β2-integrin CD11c/CD18 expression that functionally orchestrates their recruitment to VCAM-1 activating VLA-4 leading to focal clustering and shear resistant arrest. Both Mon2 frequency and CD11c expression remain critical factors associated with the extent of coronary artery disease (CAD) related to persistent inflammation, plaque growth and destabilization, myocardial infarction and morbidity. Understanding dynamic alteration of Mon2 CD11c and its function in promoting macrophage accumulation in plaques that exacerbate and progress atherosclerotic disease progression toward myocardial infarction remains undetermined. In this study, we investigated the activation status of circulating Mon2 in patients experiencing non-ST myocardial infarction (NSTEMI) compared to those undergoing angiography in the cardiac clinic. Mon2 activation status and CD11c function was gauged using flow cytometry and real-time microfluidics using an *Artery-on-a-Chip* (A-Chip) device. Circulating Mon2 upregulated CD11c receptors to the greatest extent in patients experiencing myocardial infarct that increase with recurrence and lead to enhanced CD11c dependent capture on VCAM-1 relative to patients being treated in the cardiac clinic. Arrest on VCAM-1 under shear flow resulted in time-dependent phenotypic alteration including the loss of CD16 over 45 min and was dependent on atherosclerotic disease but independent of NSTEMI and involved CD11c outside-in signaling. A shift from a high to low affinity state of CD11c triggered the translocation of several activation and differentiation markers such as NfKB, and upregulation of MMP-9 associated with an M1 phenotype. CD11c receptor number and subsequent signaling provides a potential target for intervention of atherogenesis by altering Mon2 differentiation potential and inflammatory capacity.
A.A. Hernandez: None. **G. Foster:** None. **A. Fernandez:** None. **S. Simon:** None. **G. Singh:** None.

414
Local Artery Wall Inflammation Overrides Systemic Inflammation in Diabetes-Accelerated Atherosclerosis
Jenny E Kanter, Farah Kramer, Shelley Barnhart, Univ of Washington, Seattle, WA; Karishma Rahman, Jaume Amengual, NYU, New York, NY; Xiaochao Wei, Washington Univ, St Louis, MO; Tessa Bergsbaken, Alan Chait, Pamela J Fink, Univ of Washington, Seattle, WA; Daniel A Winer, Univ of Toronto, Toronto, ON, Canada; Edward A Fisher, Ira J Goldberg, NYU, New York, NY; Clay F Semenkovich, Washington Univ, St Louis, MO; Karin E Bornfeldt, Univ of Washington, Seattle, WA

Human genomic studies have highlighted the importance of arterial wall-specific inflammatory processes in cardiovascular disease (CVD) risk. Diabetes increases systemic inflammation, local arterial inflammation, and CVD risk. To clarify the relative contributions of systemic inflammation versus artery wall inflammatory processes in atherosclerosis, we studied LDL receptor-deficient mice with streptozotocin-induced diabetes. The damage-associated molecular pattern protein S100A9 and toll-like receptor 4 (TLR4) have both been implicated in diabetes-induced inflammation. S100A9-deficient bone marrow chimeras were used to inhibit systemic inflammation, 5-aminosalicylic acid (5-ASA) was used to inhibit intestinal inflammation, and TLR4-deficient bone marrow chimeras were used to inhibit artery wall inflammation. No model affected the severity of diabetes, plasma cholesterol or blood leukocyte numbers. Hematopoietic S100A9-deficiency, but not TLR4-deficiency, reduced diabetes-associated systemic inflammation to levels observed in non-diabetic mice. 5-ASA differentially altered measures of systemic inflammation. Thus, diabetes induced a 2-fold increase in circulating leukocyte *Il1b* mRNA, which was normalized by S100A9-deficiency ($p<0.01$, n=7-10) and 5-ASA, but was not reduced by hematopoietic TLR4-deficiency (n=11-14). Similarly, diabetes increased plasma levels of the acute-phase protein serum amyloid-A (SAA), which were normalized by S100A9-deficiency ($p<0.01$, n=5-12), but not by TLR4-deficiency (n=5-10) or 5-ASA. Conversely, hematopoietic TLR4-deficiency ($p<0.05$), but not hematopoietic S100A9-deficiency or 5-ASA, reduced diabetes-accelerated myeloid cell accumulation in the artery wall determined by aortic *en face* Sudan IV staining (n=16-21). Finally, laser capture microdissection of CD68-positive lesional macrophages revealed that hematopoietic TLR4-deficiency prevents diabetes-induced inflammatory processes in the artery wall including expression of *Il1b, Ccr2*, and *S100a9* mRNA. Together, our data strongly suggest that although systemic inflammation is increased in diabetes, inhibition of inflammatory processes in the artery wall is required to prevent lesional macrophage accumulation.
J.E. Kanter: None. **F. Kramer:** None. **S. Barnhart:** None. **K. Rahman:** None. **J. Amengual:** None. **X. Wei:** None. **T. Bergsbaken:** None. **A. Chait:** None. **P.J. Fink:** None. **D.A. Winer:** None. **E.A. Fisher:** None. **I.J. Goldberg:** None. **C.F. Semenkovich:** None. **K.E. Bornfeldt:** None.

415
HDL-small RNA Gene Regulatory Networks Alter T Cell Signalling
Danielle L Michell, Shilin Zhao, Quanhu Sheng, Michelle J Ormseth, C. Michael Stein, Amy S Major, Kasey C Vickers, Vanderbilt Univ, Nashville, TN

Small non-coding RNAs (sRNA) are critical regulators of adaptive immunity and the flow of information between immune cells likely extends beyond cytokines and danger signals to sRNAs. microRNAs (miRNA) are sRNAs that post-transcriptionally regulate gene expression and are transferred between cells within intercellular communication networks. In addition to miRNAs, another class of sRNAs has emerged as critical regulators of gene expression - tRNA-derived small RNAs (tDRs). During cell stress, parent tRNAs are cleaved by RNaseIII enzymes, e.g. Angiogenin (ANG), and tDRs suppresses protein synthesis and gene expression; however, the functional relevance of ANG and tDRs in T cell activation is unknown. To determine if ANG is altered during T cell activation, ANG expression was quantified in anti-CD3 and anti-CD28 activated human CD4+ T cells, and we found that both mRNA and protein levels were significantly (p<0.05) increased compared to non-activated T cells by real-time PCR and ELISA, respectively. Strikingly, 12 T cell tDRs were significantly upregulated (p<0.05) during activation, as quantified by high-throughput sRNA sequencing (sRNA-seq). In addition, tDR-GlyGCC was found to be readily exported from CD4+ T cells to HDL after 24 hr post-activation. Moreover, sRNA-seq analysis showed that tDRs (e.g. tDR-GlyGCC) are highly abundant on human HDL. Based on these results, we hypothesized that HDL mediates T cell-originating tDR intercellular communication networks. In support, we found that HDL transferred tDR-GlyGCC from T cells to monocytes, as evidenced by an 18-fold increase (p<0.05) in tDR-GlyGCC in recipient cells. In conclusion, we demonstrate that HDL facilitates a novel intercellular communication network of tDRs between immune cells which is likely enhanced during T cell activation.
D.L. Michell: None. **S. Zhao:** None. **Q. Sheng:** None. **M.J. Ormseth:** None. **C. Stein:** None. **A.S. Major:** None. **K.C. Vickers:** None.

This research has received full or partial funding support from the American Heart Association.

416
Are Good and Evil Polarized? - How Murine Rgs5 knock-out Influences Macrophage Polarization and Aortic Atherosclerosis and Dissection
Isabel N Schellinger, Houra Loghmani, Niandan Hu, Greta Ginski, Franziska Wendt, Nicolina Wibbe, Dept. of Med, Univ of Oldenburg, Oldenburg, Germany; Uwe Raaz, Univ Heart Ctr Goettingen, Goettingen, Germany; Gregor Theilmeier, Dept. of Med, Univ of Oldenburg, Oldenburg, Germany

Background: Aortic atherosclerosis and dissection cause significant morbidity and mortality. Although atherosclerosis is associated with aortic dissection, points of interaction are unclear. Regulator-of-G-protein signaling 5 (RGS5) is still insufficiently characterized regarding its role in aortic atherosclerosis and dissection. **Objectives:** We investigated Rgs5-deficiencie's effects on aortic atherosclerosis and dissection. **Methods:** $ApoE^{-/-}$ $Rgs5^{GFP/GFP}$ double knockout mice (rraa, n=15) and WT littermates (RRaa, n=17) were fed a cholesterol-rich diet for 14weeks. Plaque size, plaque morphology (composition and a validated vulnerability score based on Stary criteria), macrophage phenotype and aortic dissection were evaluated. **Results:** rraa mice displayed more aortic dissections (5/15) compared to WT (0/17; p<0.05 in Chi^2-test). Surprisingly, rraa showed significantly smaller (rraa plaque size 190 657 μm^2 ± 93184 vs. control 398 279 μm^2 ± 153339) and less complicated plaques (5 of 15 mice with >2 vulnerability features) compared to RRaa (14 of 15 with >2 vulnerability features, p<0.01). While relative areas of aSMA and lipids did not differ between genotypes, relative plaque areas positive for collagen and CD45 were increased in rraa (n=15/17, p<0.01) compared to RRaa. Due to smaller plaque sizes were anti-inflammatory macrophages reduced and pro-inflammatory macrophages increased in absolute numbers (p<0.05). Phenotyping of $CD45^+$-myeloid cells revealed increased proportions of macrophages staining positive for pro-inflammatory markers (Cd86/Cd45: 24.71 area% ± 3.75 for RRaa; 60.95 area% ± 5.909, for rraa and iNOS/Cd45: 37.22 area% ± 6.37, for RRaa; 73.99 area% ± 3.997 for rraa, p<0.01), while anti-inflammatory markers (Cd163/Cd45 and Dectin/Cd45 double stainings) remained unchanged. **Conclusions:** rraa mice are more prone to aortic dissection despite smaller and less complex plaques with reduced anti-inflammatory but increased numbers of pro-inflammatory macrophages. We hypothesize that pro-inflammatory macrophage polarization along with evasion of anti-inflammatory macrophages in rraa mice could be causative for higher dissection numbers. Our data warrant further studies into the diverging pathomechanistic roles of Rgs5 in aortic dissection and atherosclerosis.
I.N. Schellinger: None. **H. Loghmani:** None. **N. Hu:** None. **G. Ginski:** None. **F. Wendt:** None. **N. Wibbe:** None. **U. Raaz:** None. **G. Theilmeier:** None.

417
CXCR4 Distinguishes and Maintains Atheroprotective IgM-producing B-1 cells
Aditi Upadhye, Prasad Srikakulapu, Heather Perry, Claire Rosean, Anh Nguyen, Chantel McSkimming, Univ of Virginia, Charlottesville, VA; Ayelet Gonen, Sabrina Hendrikx, Univ of California, San Diego, La Jolla, CA; Angela Taylor, Univ of Virginia, Charlottesville, VA; Sotirios Tsimikas, Joseph Witztum, Univ of California, San Diego, La Jolla, CA; Coleen McNamara, Univ of Virginia, Charlottesville, VA

B1 cells exert protective effects in atherosclerosis through production of anti-inflammatory IgM antibodies recognizing oxidation-specific epitopes, such as MDA-LDL, present in diseased arteries. However, factors mediating B1 IgM production are currently unclear. We evaluated MDA-LDL binding and chemokine receptor expression on human B1 cells in a cohort of subjects undergoing intravascular ultrasound (IVUS) for coronary artery assessment. Results demonstrate that a subset of human B1 cells (~35%) is able to bind MDA-LDL. Moreover, expression of the chemokine receptor CXCR4 on circulating B1 cells associates with increased plasma levels of anti-MDA-LDL IgM antibodies (p=0.0009), and decreased plaque burden in coronary arteries (p=0.0002). Mice with B cell-specific loss of CXCR4 on the atherogenic $ApoE^{-/-}$ background ($CXCR4^{BKO}$) demonstrate fewer B1a cells (n=6-8,p<0.0001) and IgM antibody-secreting cells (n=6,p<0.01) in the bone marrow, and reduced plasma IgM levels (n=6-8,p<0.05), relative to littermate controls ($CXCR4^{WT}$). Furthermore, retroviral-mediated overexpression of CXCR4 on B1a cells *in vivo* is associated with increased B1a localization to the bone marrow (p<0.01) and increased circulating levels of anti-MDA-LDL IgM antibodies (p<0.05). To determine the atheroprotective role of CXCR4 on the B1a cell subset, we adoptively transferred $CXCR4^{WT}$ or $CXCR4^{BKO}$ B1a cells into lymphocyte-deficient $Rag1^{-/-}ApoE^{-/-}$ mice. After 16 weeks of Western diet feeding, recipients given $CXCR4^{BKO}$ B1a cells demonstrate reduced plasma IgM levels (n=7,p<0.001), and fewer donor B1a cells in the bone marrow and spleen (n=7,p<0.05) compared to recipients given $CXCR4^{WT}$ B1a cells. Intriguingly, B1a transfer reduces plasma cholesterol levels in mice regardless of CXCR4 expression (n=7,p<0.05). However, CXCR4 further strengthens the atheroprotective ability of B1a cells, as recipients given $CXCR4^{WT}$ B1a cells have reduced aortic lesion area compared to PBS controls (n=7,p<0.01) while recipients given $CXCR4^{BKO}$ B1a cells did not attain the same level of protection. Overall, these data suggest that CXCR4 is an

important regulator of IgM production and B1a-mediated atheroprotection.
A. Upadhye: None. **P. Srikakulapu:** None. **H. Perry:** None. **C. Rosean:** None. **A. Nguyen:** None. **C. McSkimming:** None. **A. Gonen:** None. **S. Hendrikx:** None. **A. Taylor:** None. **S. Tsimikas:** None. **J. Witztum:** None. **C. McNamara:** None.

This research has received full or partial funding support from the American Heart Association.

422
Association of Remnant Lipoprotein Cholesterol and Levels of Glucose and Insulin: the Very Large Database of Lipids
Renato Quispe, Johns Hopkins Univ, Jacobi Medical Ctr/Albert Einstein Coll of Med, New York, NY; **Behnoud Baradaran Noveiry**, Johns Hopkins Univ, Baltimore, MD; Kamil F Faridi, Beth Israel Deaconess Medical Ctr, Boston, MA; Seth S Martin, Johns Hopkins Univ, Baltimore, MD; Peter P Toth, CGH Medical Ctr, Peoria, IL; Steven R Jones, Johns Hopkins Univ, Baltimore, MD

Background: A defining feature of diabetic dyslipidemia is elevation of triglyceride-rich lipoproteins, particularly remnant lipoprotein cholesterol (RLP-C). Lowering these lipoproteins may reduce risk of atherosclerotic cardiovascular disease in diabetic patients, though the relationship between RLP-C and hyperglycemia as well as hyperinsulinemia remains inadequately characterized. The purpose of this study was to determine the association of RLP-C with serum glucose and insulin across a broad range of insulin resistance. **Methods:** We used a sample of individuals from the Very Large Database of Lipids with measured fasting serum glucose and insulin levels, as well as lipoprotein cholesterol levels measured by the Vertical Auto Profile test (Atherotech, Birmingham, AL). RLP-C was defined as the sum of $VLDL_3$-C + IDL-C. The study population was divided into deciles of HOMA-IR, calculated as [Insulin × Glucose/405]. We performed multivariable linear regression models to determine associations of RLP-C with insulin and glucose after adjusting for age, sex, real LDL-C, triglycerides, AST, BUN and creatinine. Covariates not normally distributed were log-transformed. Analysis was performed in overall population and across HOMA-IR deciles. **Results:** We included a total of 146,826 individuals (43.6% male, mean age 54.9 ± 15.9 years). Median values were: insulin, 9 uU/mL; glucose, 95 mg/dL; RLP-C, 26 mg/dL. The models in our Table explained 60% of variance in RLP-C. Overall, insulin (β=-1.85, p<0.001) and glucose (β=-0.84, p<0.001) had significant negative associations with RLP-C. However, levels of RLP-C were significantly associated with insulin but not glucose across most HOMA-IR deciles (Table). **Conclusion:** RLP-C is significantly associated with levels of serum insulin but not with glucose across a spectrum of insulin resistance. Further characterization of the relationship between RLP-C and serum insulin is needed to help guide future therapies for patients with diabetes.

Table. The association of RLP-C with insulin, glucose, and other covariates in overall population and across HOMA-IR deciles.

Variables	HOMA-IR deciles										
	1st	2nd	3rd	4th	5th	6th	7th	8th	9th	10th	Overall
Insulin*	-0.2509	-3.0588	-1.8054	-3.3602	-4.0177	-3.6843	-3.9494	-3.6152	-0.6915	-0.5811	-1.8499
Glucose*	1.2311	-0.9192	0.0936	-1.2845	-1.0317	-1.0876	-3.2271	-1.7388	-0.6346	-0.2636	-0.8388
Triglycerides*	16.9127	17.2530	17.3825	17.5576	18.4343	17.4154	17.8127	18.3927	17.8364	16.9218	17.4660
Age	-0.0120	-0.0079	-0.0048	-0.0034	-0.0025	0.0040	0.0123	0.0098	0.0142	0.0175	0.0021
Sex	-0.7331	-0.9432	-1.2942	-1.7610	-1.9786	-2.1670	-2.3295	-2.4429	-2.7460	-3.0077	-1.9875
AST*	0.1140	0.2936	0.5412	0.8814	0.7775	1.0472	1.0838	0.5901	0.9512	0.7742	0.6679
BUN	0.0809	0.0949	0.1316	0.1301	0.1394	0.0943	0.0916	0.1239	0.0900	0.0910	0.1095
Creatinine*	1.6394	2.2430	2.1571	2.9217	2.6843	3.2266	3.6333	3.6622	3.7332	4.1950	3.1716
LDLr-C	0.0669	0.0737	0.0784	0.0838	0.0838	0.0861	0.0896	0.0886	0.0915	0.0926	0.0841
R-squared	0.6057	0.6100	0.5976	0.5934	0.5884	0.5735	0.5866	0.5774	0.5645	0.5690	0.6000

P-value >= 0.05
P-value < 0.05
P-value < 0.001

**Log-transformed values were used as the variable was not normally distributed.*
Values in cells represent β-coefficients from multivariate linear regressions.
AST, Aspartate aminotransferase; BUN, Blood urea nitrogen; LDLr-C, real low density lipoprotein cholesterol, Calculated as LDL-C – (IDL-C + Lp(a)-c); HOMA-IR, Homeostatic Model Assessment of Insulin Resistance.

R. Quispe: None. **B. Baradaran Noveiry:** None. **K.F. Faridi:** None. **S.S. Martin:** Consultant/Advisory Board; Modest; Quest Diagnostics, Amgen, Pew Research Center, Regeneron, Sanofi. **P.P. Toth:** Speakers Bureau; Modest; Amarin, Amgen, Kowa, Merck, Novo-Nordisk, Regeneron, Sanofi. Consultant/Advisory Board; Modest; Amarin, Amgen, Kowa, Merck, Novo-Nordisk, Regeneron, Sanofi, Gemphire. **S.R. Jones:** Consultant/Advisory Board; Modest; Sanofi, Regeneron.

423
Role of Autophagy in Macrophages During Acute Myocardial Infraction
Shuang Chen, Kenichi Shimada, Timothy R Crother, Michifumi Yamashita, Moshe Arditi, Cedars-Sinai Medical Ctr, Los Angeles, CA

Acute myocardial infarction (AMI) is associated with inflammation and proinflammatory cytokine release, including IL-1β, but the role of NLRP3 inflammasome in cardiac injury remains controversial and requires further investigation. Autophagy, important for stress responses in injury and diseases, is a self-digestion process for the recycling of cytosolic macromolecules and damaged organelles. While autophagy has been previously investigated in cardiac muscle cells in AMI, its role in inflammatory cells is unknown. We generated macrophage (Mϕ)-specific Atg16L1 KO mice (*Atg16l1*$^{fl/fl}$ LysM-Cre) and performed permanent ligation of the left anterior descending artery (LAD) using closed-chest model. 24 hours post ligation, Mϕ-specific Atg16L1 KO mice had significantly larger infarction area as measured by myoglobin staining, and more TUNEL staining compared with control groups. This suggested that autophagy in macrophages plays a cardioprotective role during AMI. Since autophagy negatively regulates NLRP3 inflammasome activation and IL-1β secretion, we investigated the role of NLRP3 inflammasome in AMI. NLRP3 KO mice were subjected to LAD ligation and KO mice had less infarction compared with control mice. We also observed reduced infarction in IL-1R1 deficient mice, suggesting that NLRP3 inflammasome and subsequent IL-1β secretion and signaling play a role in AMI pathology. Multiple reports indicate that autophagy associated proteins induction have reduced expression in aged tissues and that autophagy diminishes with aging. We therefore investigated IL-1 signaling blockade with Anakinra (IL-1 receptor antagonist) in aged C57BL/6 mice. Mice were injected with Anakinra daily 10 mg/kg starting 1 h after LAD ligation. While we observed 14% larger infarct size in aged mice (18 months) compared to young mice (12 weeks), Anakinra treatment displayed significantly reduced infarction compared with age matched controls and the reduction of infarction by anakinra treatment was significantly greater in aged mice (75% reduction) compared with young mice (50% reduction). Taken together, these data demonstrate that autophagy plays a protective role in macrophages and NLRP3 and IL-1β mediate pathology, with an increased effect on aged mice during AMI.
S. Chen: None. **K. Shimada:** None. **T.R. Crother:** None. **M. Yamashita:** None. **M. Arditi:** None.

424
Waist Circumference for the Diagnosis of Metabolic Syndrome on Risks of Arterial Stiffness and Diabetes
Sung-Sheng Tsai, **Pao Hsien Chu**, Chang Gung Memorial Hosp, Taipei, Taiwan

Background. Published studies seldom tested the weight of different waist circumference (WC) cut-off values for the diagnosis of metabolic syndrome (MetS) in predicting clinical outcomes, including cardiovascular disease and diabetes. *Methods.* This is a Chinese population-based cross-sectional study screening subjects from a Health Examination Program since 1999 to 2015. The MetS identification and scores were determined either according to the Adult Treatment Panel III/ American Heart Association/National Heart, Lung, and Blood Institute (ATP III/AHA/NHLBI)- or Asian-WC cut-off points. The developments of a higher brachial-ankle pulse wave velocity (baPWV) and diabetic-

level hyperglycemia were surveyed by comparing the areas under receiver operating characteristic curves (AUC-ROC) for both MetS scores. *Results.* According to the ATP III/AHA/NHLBI- or Asian-MetS criteria, 6633 (24.8%) or 9133 (34.2%) subjects were diagnosed as the MetS among 26735 study subjects with a mean age of 55 ± 12 years. The stepwise increases in baPWV and prevalence of diabetic-level hyperglycemia were associated with both MetS scores after adjusting for age and sex. The AUC-ROC for the ATP III/AHA/NHLBI- vs Asian-MetS scores to predict a higher baPWV (0.685 vs 0.680, *p*=0.271) and diabetic-level hyperglycemia (0.791 vs 0.784, *p*=0.546) were similar. Conclusions. In a stepwise manner, both ATP III/AHA/NHLBI- or Asian-MetS scores were strong risk factors for arterial stiffness and diabetes. Through a novel and holistic approach, the predictive performance of the ATP III/AHA/NHLBI-MetS score for the risks of arterial stiffness and diabetes was comparable to the Asian-MetS score among a Chinese population. <!--EndFragment-->
S. Tsai: None. **P. Chu:** None.

425
Resistin induced Differential Global Protein Expression in Human Macrophage
Nezam Haider, Univ of Arizona, Tucson, AZ

BACKGROUND: Human resistin synthesized by macrophages is shown to be associated with insulin resistance, type 2 diabetes, atherosclerosis, and chronic inflammation. However, there are several missing links related to downstream targets and intracellular signaling pathways involving hyper-resistinemia-associated metabolic disorders. In this study, we used a comparative global protein expression profiling of human macrophage treated with resistin to identify some of these missing links.
METHODS: Human macrophage (Mφ) derived from THP1 cells were treated with 10ng/ml of human resistin for 48 hrs. Samples of total protein tryptic digest of untreated control and resistin-treated Mφ were analyzed by HPLC-ESI-MS/MS. Differentially expressed proteins were analyzed by using the Gene Ontology (GO), DAVID, and KEGG databases to characterize their potential functional roles and related pathways.
RESULTS: Proteins with significant ($\rho < 0.05$) differences in expression between control and resistin treated groups are shown in Table I. The differentially expressed proteins were mainly involved in metabolic process, cell-cell adhesion, MAPK cascade, protein polyubiquitination, autophagy, and NIK/NF-κB signaling. Majority of the differentially expressed proteins were located in the extracellular exosome, mitochondrion, nucleoplasm, and proteasome complex Table II & III.
CONCLUSION: Resistin significantly changed the expression of ~162 proteins in human macrophage. The differentially expressed proteins are involved in metabolic process, signal transduction pathways, immunological and inflammatory response, exosome and mitochondrial function. This work provides the foundation for future in-depth understanding of resistin-associated metabolic derangement.

Table-I
Summary of Mass Spectrometry Data

Categories	No. Proteins
Identified Proteins	6547
Quantified Proteins	5230
Significantly altered proteins (p-value<0.05)	162
up-regulated	78
down-regulated	84

Table-II
Resistin induced Up-regulated Proteins

Categories	No. Proteins
Biological process	
MAPK cascade	5
cell-cell adhesion	5
I-kappaB /NF-kappaB signaling	4
Inflammatory response	2
Cellular component	
extracellular exosome	32
nucleoplasm	23
proteasome complex	5
Functional	
Acetylation	33
Phosphoprotein	52
Autophagy	3

Table-III
Resistin induced Down-regulated Proteins

Categories	No. Proteins
Biological process	
succinyl-CoA metabolism	2
protein import into nucleus	2
metabolic process	4
cell proliferation	5
Cellular component	
mitochondrion	36
extracellular exosome	23
nucleoplasm	22
endoplasmic reticulum	10
KEGG Pathway	
Citrate cycle (TCA cycle)	3
Metabolic pathways	12

N. Haider: None.

426
Atherosclerotic Risk Factors Correlate with Carotid Intimal Media Thickness in Participants of the Childhood Obesity Study in South Texas: Preliminary Results
Genesio Karere, Andrew Bishop, Texas Biomedical Res Inst, San Antonio, TX; Laura Cox, Wake Forest Baptist Univ, Winston-Salem, NC; Maria-Gisera Mercado-Deane, Suzanne Cuda, The Children's Hosp of San Antonio, San Antonio, TX

Rationale: The prevalence of childhood and adolescent obesity is increasing in the United States, where one-third of children and adolescents are affected. This is especially true in the Hispanic population. It is well known that obesity is positively associated with increased atherosclerosis, the primary cause of cardiovascular disease (CVD).
Our study objective was to determine whether carotid intima-media thickness (CIMT) is associated with the severity of obesity and cardiovascular risk factors in obese Hispanic adolescents in San Antonio, Texas. We present for the first time, preliminary results for an on-going, Childhood Obesity Study at The Children's Hospital of San Antonio, where obese children in South Texas are referred for weight management.
Methods: We present data for 36 obese subjects (males= 21) with an average % of the CDC 95th BMI percentile of 139 at baseline (first clinic visit). The mean age was 15±1 years. We assessed cardiovascular risk factors and measured CIMT using B-mode ultrasonography on the left and right carotid arteries. For each patient, we calculated mean CIMT for carotid internal artery, common carotid artery, and carotid bulb, and the mean for all the CIMT measurements.
Results: There were no age-sex differences in BMI, plasma LDL-C, high sensitivity C-reactive protein (hs-CRP) and CIMT. The mean CIMT for the common carotid artery (CIMT-CCA), carotid internal artery (CIMT-CIA), and carotid bulb (CIMT-CB) were 0.50±0.12, 0.43±0.22, and 0.60±0.29 mm respectively. BMI correlated with CIMT-CIA (p= 0.012) and CIMT-CB (p= 0.002). The correlation remained significant with the means of all the CIMT measurements (p= 0.002). Plasma hs-CRP and LDL-C concentrations correlated with CIMT-CIA (p= 0.045) and the means for all CIMT measurements (p= 0.027). We did not observe significant correlations with CIMT for the common carotid artery.
Conclusion: Cardiovascular risk factors assessed in adolescents who are obese correlate with CIMT, a surrogate for atherosclerotic burden, suggesting that these obese adolescents have early onset atherosclerosis. Our results are preliminary and should be interpreted cautiously.

G. Karere: None. **A. Bishop:** None. **L. Cox:** None. **M. Mercado-Deane:** None. **S. Cuda:** None.

427
Chronic Intermittent Hypoxia Induces Endothelial Insulin Resistance *in vivo* and *in vitro*
Linyi Li, Yunyun Yang, Xinliang Ma, Yongxiang Wei, Yanwen Qin, Beijing Inst of Heart, Lung and Blood Vessel Diseases, Beijing, China

Introduction: Obstructive sleep apnea, a condition leading to chronic intermittent hypoxia (CIH), is an independent risk factor for cardiovascular disease and type 2 diabetes and is correlated with insulin resistance. Insulin stimulates production of nitric oxide (NO) in vascular endothelial cells through the IRS-1/PI3K/Akt/eNOS pathway (IRS-1, insulin receptor substrate 1; PI3K, phosphatidylinositol 3-kinase; eNOS, endothelial NO synthase). Endothelial cells directly expose to blood flow and respond to oxygen concentration change in flow. We wondered if and how CIH would affect insulin signalling/action in endothelial cells. Methods and Results: C57BL/6J mice were exposed to CIH (21%-5%, 90 s/cycle, 10 h/day) or intermittent air for 7 weeks. HUVECs were exposed to CIH (21%-5%, 1 h/cycle) for 24 h or 48 h with or without insulin. We observed that CIH increased systolic blood pressure and impaired endothelium-dependent relaxation of aortas in C57BL/6J mice. CIH increased IRS-1 phosphorylation at Ser307 and Ser612 and impaired insulin-stimulated phosphorylation of IRS-1 at Tyr896 and Akt/eNOS pathway in aortas. Furthermore, CIH activated hypoxia-inducible factor 1α (HIF-1α) and nuclear factor kappa B (NF-κB) in aortas. In vitro, CIH activated endothelial HIF-1α signaling, impaired endothelial insulin signaling and reduced insulin-mediated NO production. In addition, CIH resulted in mitochondria proton leak and elevated oxygen consumption in HUVECs. Increased oxygen consumption further leaded to endothelial hypoxia and HIF-1α induction. Pharmacological inhibition of proton leak ameliorated CIH-induced endothelial insulin resistance in HUVECs. Conclusion: Our data suggest that CIH induces insulin resistant endothelial dysfunction, which may be associated with HIF-1α induction and proton leak.
L. Li: None. **Y. Yang:** None. **X. Ma:** None. **Y. Wei:** None. **Y. Qin:** None.

428
An Unexpected Role for ACC in Lipid Droplet Formation in Macrophages in Response to Acellular Adipocyte Fat
Akshaya Kumar Meher, Vlad Serbulea, Clint M Upchurch, Victoria Osinski, Srabani Sahu, Stefan Hargett, Kyle L Hoehn, Thurl E Harris, Alexander L Klibanov, Coleen A McNamara, Norbert Leitinger, Univ of Virginia, Charlottesville, VA

In adipose tissues of obese mice, macrophages accumulate in crown-like structures (CLS) formed around dying adipocytes. The CLS macrophages are thought to clear the dead adipocytes by exophagy, which involves exocytosis of lysosomes and digestion of apoptotic adipocytes. After digesting the plasma membrane and other cytosolic contents of the adipocyte, CLS macrophages come in contact with the large lipid droplet, however, it is unknown how macrophages response to such acellular adipocytes. We hypothesized that the acelular adipocytes in CLSs promote inflammation and metabolically activate the macrophages to promote clearance of the lipid. To mimic the *in vivo* scenario, we exposed cultured murine bone marrow-derived macrophages to lipid droplets isolated from the adipocytes of high-fat diet-induced obese C57BL/6 mice. In response to adipocyte lipid, macrophages accumulated lipid droplets, which were similar in size and number to lipid droplets of CLS macrophages *in vivo*. Acellular lipid exposure significantly increased TNF-α gene expression, which was suppressed by the CD36 inhibitor sulfo-N-succinimidyl oleate, supporting CD36-mediated inflammatory response. Moreover, lipid exposure significantly lowered metabolic activity of macrophages and impaired clearance of apoptotic bodies from 3T3-L1 adipocytes. Using specific inhibitors, unexpectedly we found that lipid droplet accumulation in macrophages was independent of CD36 activity or processes involved in exophagy such as exocytosis of lysosomes, extracellular lipase activity, lipolysis and phagocytosis. Interestingly, lipid droplet accumulation was dependent on acetyl-CoA carboxylase (ACC) as determined by use of ACC inhibitors soraphen A and TOFA, and siRNA knock-down of ACC in macrophages. Furthermore, confocal microscopy of whole mount adipose tissue revealed expression of ACC in CLS macrophages. Altogether, using a novel *in vitro* model we demonstrate that acelular adipocytes suppress metabolic activity, but induce inflammation and *de novo* lipogenesis-mediated lipid droplet formation in macrophages.
A.K. Meher: None. **V. Serbulea:** None. **C.M. Upchurch:** None. **V. Osinski:** None. **S. Sahu:** None. **S. Hargett:** None. **K.L. Hoehn:** None. **T.E. Harris:** None. **A.L. Klibanov:** None. **C.A. McNamara:** None. **N. Leitinger:** None.

This research has received full or partial funding support from the American Heart Association.

429
Exercise and Heart Healthy Lifestyle Program Also Improve Mental Health
Francisco E Ramirez, Neil Nedley, Nedley Clinic, Weimar, CA

Background: Exercise conveys benefits to cardiovascular and mental health. A program that uses exercise is analyzed. Methods: Retrospective data from 5221 participants (n=3680, 70% women) that finished the educational program was used, which taught heart healthy lifestyle changes such exercise, plant-based nutrition, stress management among many interventions. The program meet once a week for 8-week, emphasis is given to reach the goal of exercising at least 4 times a week for at least 30 minutes (ideally 60 minutes). Participants completed at baseline, and at the end, the Depression and Anxiety Assessment Test (DAAT), a 75-item questionnaire assessing depression, anxiety, emotional intelligence (EQ), demographic data, and exercise habits. Results: At baseline depression was 12 (moderate level) SD 7.59, anxiety of 7 (mild) SD 4.6, EQ 100 SD 15.1 not all the participants were depressed. At baseline 64.8% (n=3385) acknowledged that they didn't do exercise more than 4 times a week on a regular basis. By the end of the 8-weeks, participants mean depression was 6 (moderate) SD 6, anxiety of 3 (none) SD 3.6, EQ 109 SD 14.3 and 46% (n=2402) of them did not exercise more than 4 times a week. There was a significant difference in the depression scores $t(5220)=66.44$, $p<.001$ and anxiety scores $t(5220)=62.07$, $p<.001$. Table 1 highlights more results. The depression was classified according to DSM-5 into 4 categories as none (0-6), mild (7-10), moderate (11-19) or severe (20 or more). Conclusion: Four or more sessions of physical exercise a week was related to improvement in overall health including depression, anxiety and EQ level, even before the program started.

Table 1: Results

Table 1	*n*	Depression	Depression level	Depression SD	Anxiety	Anxiety Level	Anxiety SD
Before program, did not meet exercise goal	3385	14	Moderate	7.4	8	Mild	4.5
Before program, meet exercise goal	1836	10	Mild	7.3	6	Mild	4.4
After 8-week, did not meet exercise goal	2402	7.9	Mild	6.3	4.4	None	3.9
After 8-week, meet exercise goal	2819	5.5	None	5.4	3.2	None	3.4

F.E. Ramirez: None. **N. Nedley:** Ownership Interest; Modest; Owner of Nedley Health Solutions.

430
Development of a Gut-microbe Targeted Non-Lethal Therapeutic to Inhibit Thrombosis Potential Without Enhanced Bleeding
Adam Roberts, Xiaodong Gu, Jennifer A Buffa, Weifei Zhu, Stanley L Hazen, Cleveland Clinic Fndn, Cleveland, OH

Recent clinical and animal studies show trimethylamine-N-oxide (TMAO), a microbiota-dependent metabolite derived from trimethylamine (TMA)-containing nutrients abundant in a Western diet, both promotes platelet hyperresponsiveness and thrombosis potential and is predictive of incident atherothrombotic event risks in large-scale clinical investigations. Utilizing a mechanism-based inhibitor approach targeting a major gut microbial enzyme (CutC/D) in the TMAO meta-organismal pathway, we developed choline analogues with cryptic reactive moieties that upon interaction with the microbial TMA generating enzyme, display potent, time-dependent and irreversible inhibition without affecting commensal microbial viability. In animal models, a single oral dose of mechanism-based microbial choline TMA lyase inhibitor significantly reduced (> 95% inhibition, $p < 0.0001$) plasma TMAO levels over a sustained period of time (up to 3 days), while limiting systemic exposure in the host. This was achieved by the selective accumulation of inhibitor at the site of action, within intestinal microbes, to millimolar levels, a concentration over a million-fold higher than needed for therapeutic effect. In animal models, inhibition of microbial TMA generation was shown to rescue diet-induced platelet hyperresponsiveness and enhanced thrombosis potential, both without increasing enhanced bleeding risk and observable toxicity. The present studies reveal mechanism-based inhibition of microbial TMA lyase activity as a therapeutic target for reducing thrombosis potential, a critical adverse complication in heart disease. They also suggest mechanism-based inhibitors designed to concomitantly accumulate within the gut microbe may serve as a generalizable approach for the selective targeting of microbial catabolic enzymes linked to host diseases, while limiting systemic exposure in the host.
A. Roberts: None. **X. Gu:** None. **J.A. Buffa:** None. **W. Zhu:** None. **S.L. Hazen:** None.

This research has received full or partial funding support from the American Heart Association.

431
Sex Differences in Manifestation of Subclinical Coronary Atherosclerosis: Analysis of Lipoprotein Sub-Fractions in Healthy but High Risk Individuals
Emir Veledar, Anshul Saxena, Lara Arias, Baptist Health South Florida, Coral Gables, FL; Ehimen Aneni, Mount Sinai Medical Ctr, Miami Beach, FL; Mahdi Garelnabi, Univ of Massachusetts Lowell, Lowell, MA; Khurram Nasir, Baptist Health South Florida, Coral Gables, FL

Background: Lipoproteins-rich triglycerides are associated with markers of coronary atherosclerosis such as coronary artery calcification (CAC) in young high-risk population. This study examines differences between sexes associated with lipoprotein sub-fractions and atherosclerosis. **Methods:** The study presents analysis from baseline data of a randomized trial of employees of Baptist Health South Florida with metabolic syndrome or diabetes. Participants completed lipoprotein sub-fraction analysis at baseline using ion mobility technique. Subjects above 35 years had a CAC test completed. We tested for differences between correlational matrices of the original variables. The same analysis was repeated for sets of 3 principal components (PC) that were computed for the combination of all lipoprotein subclasses. **Results:** The study population (N=170) was largely female (128) with a mean age of 58 years. Three PCs accounted for 83% variation in the sample. Distribution of atherosclerostic PC2 by sex was entirely different between sexes (Wishart test p=.004). In addition, a significant Jennrich's test ($p < .0045$) implied that the inter-correlations among all dependent variables for different groups were dissimilar; with the finding of significant angles between PC components by sex. PC2, with main contributions from VLDL particles, was in the positive direction; however PC3 with large LDL particles was in the negative direction. Atherogenic lipoprotein profiles were significant only for males, with PC keeping their independent predictability. **Conclusion:** In a relatively young high-risk population, there were sex-specific differences in lipoprotein sub-fractions profiles that are associated with increased risk of atherosclerosis. The relationship was much weaker for males compared to females (see graph). These findings points towards a possible sex-linked lipoprotein sub-fraction association with the atherosclerosis pathogenesis.

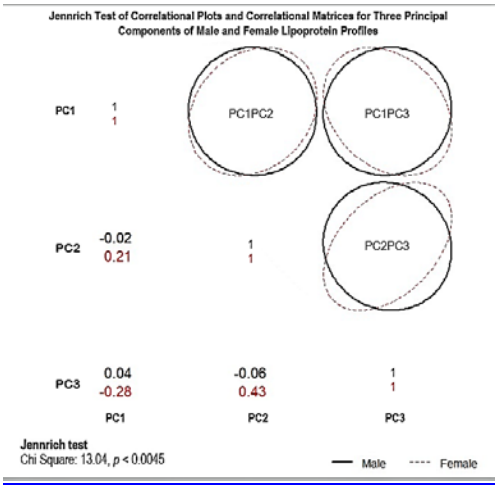

E. Veledar: None. **A. Saxena:** None. **L. Arias:** None. **E. Aneni:** None. **M. Garelnabi:** None. **K. Nasir:** None.

432
Differential MicroRNA Expression in Subcutaneous Abdominal and Lower-body Fat Depots
Jared Evans, Zhifu Sun, Naima Covassin, Fatima H Sert-Kuniyoshi, Virend K Somers, **Prachi Singh**, Mayo Clinic, Rochester, MN

Background: Abdominal fat elevates while lower-body (LB) fat diminishes cardiovascular risk. However, molecular mechanisms differentiating the two fat depots are not completely understood. MicroRNA (miRNA) are important regulators of gene expression with widespread effects on several proteins.
Objective: To explore miRNA differences between the two fat depots using unbiased next-generation sequencing (NGS) approach.
Methods: Total RNA isolated from paired subcutaneous (sc) fat tissue obtained from abdomen (ABD) and LB (femoral) region of 12 healthy subjects (7 male; age: 27 ± 5 years;

BMI: 23.5 ± 3.2 kg/m^2) was used to quantify miRNA expression. Body fat distribution was determined using dual-energy X-ray absorptiometry and abdominal computed tomography scans. RNA was prepped using the NEBNext small RNA library prep kit and sequenced using Illumina HiSeq 2000. Raw sequence data were processed using CAP-miRSeq pipeline. miRNA expression between the two depots was evaluated using EdgeR. Relationship between miRNA and regional fat depots were examined using Spearman's correlation. Adjusted or unadjusted P value <0.05 was considered significant.
Results: Using NGS, 383 ± 55 known miRNA with ≥5 raw reads were detected in the study samples. Principal component analysis including all miRNAs showed no any clear separation between ABD or LB fat tissue. However, 37 miRNAs were found to have altered expression in the two depots. miR-196a-5p (log2FC=1.138, p<0.001), miR-146b-5p (log2FC=1.388, p<0.001), miR-1287 (log2FC=1.059, p<0.001), miR-1247-5p (1.002, p<0.001), and miR-346 (log2FC =-1.240, p=0.002) were among the top five differentially expressed miRNA in ABD Vs. LB fat. Interestingly, ABD fat tissue expression of miR196a-5p (rho=-0.58, p=0.047) and miR146b-5p (rho=0.76, p=0.004) correlated with visceral fat while miR146b-5p (rho=0.66, p=0.02) and miR1287 (rho=0.79, p=0.002) correlated with ABD sc fat.
Conclusions: Several miRNAs are differentially expressed between ABD and LB fat tissue which may partly contribute to depot specific alterations in adipose tissue function and consequent cardiometabolic risk. Furthermore, the associations between miRNA and regional fat depots suggest a functional role of these miRNA in fat distribution.
J. Evans: None. **Z. Sun:** None. **N. Covassin:** None. **F.H. Sert-Kuniyoshi:** None. **V.K. Somers:** None. **P. Singh:** None.

This research has received full or partial funding support from the American Heart Association.

433
Difference in pAAV/D377Y-mPCSK9-induced Expression of mPCSK9 Between Male and Female Mice
Aimee E Vozenilek, Sunitha Chandran, Cassidy M Blackburn, Louisiana State Univ Health Sciences Ctr, Shreveport, LA; Reneau Castore, Feist-Weiller Cancer Ctr, Shreveport, LA; Ronald L Klein, Matthew D Woolard, Louisiana State Univ Health Sciences Ctr, Shreveport, LA

Objective: The recombinant adeno-associated viral vector serotype 8 (AAV8) expressing the gain-of-function mutation of mouse proprotein convertase subtilisin/kexin type 9 (PCSK9) is a new model for the induction of hypercholesterolemia and atherosclerosis development. AAV8 tends to preferentially infect hepatocytes and the liver-specific promoter should ensure expression of PCSK9 results in reduced hepatic low-density lipoprotein receptor levels. However, the tissue distribution of adeno-associated viral vectors can differ between male and female mice. Therefore, we set out to investigate differences in PCSK9 expression and hypercholesterolemia development in male and female mice using the AAV8-PCSK9 model.
Approach and Results: Male and female C57BL/6 mice were retro-orbitally injected with a low-dose (3x10^{10} vector genomes) of AAV8-PCSK9 and fed a high-fat diet for 8 weeks. Inoculation of male mice with low dose AAV8-PCSK9 dramatically elevated both serum PCSK9 and cholesterol levels, which was not observed in female mice. Increasing the inoculation dose of AAV8-PCSK9 threefold (9x10^{10} vector genomes) in female mice induced serum cholesterol and PCSK9 concentration to levels equivalent with low-dose inoculated male mice. Although increasing the dose of AAV8-PCSK9 induces a hypercholesterolemia phenotype in female mice, it did not result in an increased amount of AAV8 virus nor increased mRNA expression of mPCSK9 in female livers but did increase mRNA expression of mPCSK9 in the brains of these mice.
Conclusions: Our data demonstrate that AAV8-PCSK9 inoculation results in differences between male and female mice in the localization and production of mPCSK9. These differences do not hinder the use of female mice in hypercholesterolemia and atherosclerosis studies when AAV8-PCSK9 doses are taken into consideration. However, localization to and production of AAV8-PCSK9 in organs besides the liver in female mice may introduce confounding factors into studies and should be considered during experimental design.
A.E. Vozenilek: Other; Significant; 17PRE33661114. **S. Chandran:** None. **C.M.R. Blackburn:** None. **R. Castore:** None. **R.L. Klein:** None. **M.D. Woolard:** Research Grant; Significant; HL131844, GM104940.

This research has received full or partial funding support from the American Heart Association.

434
Nogo-B Regulates Hyperglycemia Induced Endothelial Dysfunction by Modulating Mitochondria Function
Cheng Zhang, Jun Yu, Temple Univ, Philadelphia, PA
Objective--As an important part of the vasculature, the endothelium plays multiple functions in maintenance of vascular homeostasis. Endothelial dysfunction is associated with several pathologies, including but not limited to diabetes, hypertension and atherosclerosis. Emerging evidence suggest that mitochondrial have a profound impact on endothelial cell function. Hyperglycemia induced mitochondrial defects are associated with endothelial dysfunction and pathogenesis of diabetes related microvascular and macrovascular diseases. However, the mechanism by which hyperglycemia causes mitochondrial dysfunction are not fully elaborate. ***Approach and Results***--Here we examined the role of Nogo-B, a regulator of mitochondria-endoplasmic reticulum unit, in mitochondrial dysfunction that triggered by hyperglycemia. Our data show that compared to control, depletion of Nogo-B enhanced high glucose induced mitochondrial fission; suppressed mitochondrial membrane potential and respiration rate in endothelial cells. Furthermore, Nogo-B deficiency resulted in elevated JNK phosphorylation, which then led to MFN2 degradation and cell apoptosis. ***Conclusion***--Taken together, our findings provide novel insights into an unexpected role of Nogo-B. Nogo-B is a regulator of mitochondrial morphology and function under high glucose treatment in endothelial cells. The results from this study deepen our understanding on the mechanism of diabetic related endothelium dysfunction.
C. Zhang: None. **J. Yu:** None.

This research has received full or partial funding support from the American Heart Association.

435
Inhibition of the Key Glycolytic Enzyme PFKFB3 with Novel Compounds Suppresses Angiogenesis
Anahita Abdali, Alberto Corsini, Univ of Milan, Milan, Italy; Denisa Baci, IRCCS MultiMedica, Milan, Italy; Carlo De Dominicis, Matteo Zanda, Univ of Aberdeen, Aberdeen, United Kingdom; Maria Luisa Gelmi, Stefano Bellosta, Univ of Milan, Milan, Italy

Aim Intraplaque angiogenesis is an important contributor to atherosclerotic plaque growth and instability. Angiogenic signals induce endothelial cells (ECs) to switch their metabolism to being highly glycolytic, enabling their growth and division. Glycolytic modulation by inhibition of the glycolytic activator 6-phosphofructo-2-kinase/fructose-2,6-bisphosphatase (PFKFB3) has been shown to reduce angiogenesis. The objective of this study was to identify novel anti-angiogenic compounds with a potential to efficiently modulate (inhibit) angiogenesis. **Methods** Using

the human EC line EA.hy926, we studied the effects of PFKFB3 inhibition with 3PO, a weak competitive inhibitor of PFKFB3, and of two potent self-synthesized phenoxindazole analogues (PA-1 and PA-2) on glycolysis, proliferation, migration, matrix metalloproteinase (MMP) activity, and capillary tube formation. Moreover, gene expression of important markers related to angiogenesis were measured at mRNA level by real-time PCR. **Results** PFKFB3 inhibition with all three tested compounds significantly reduced glycolytic activity. While PA-1 and PA-2 suppressed capillary tube formation, 3PO did not have any effect. Accordingly, PA-1 and PA-2 markedly inhibited EC migration, proliferation and wound closing capacity which are essential for neovessel formation. Moreover, these inhibitors downregulated gelatinase gene expression up to 6-fold, as well reduced the activity of proMMP-9 and MMP-2 up to 50% and 30% compared to control, respectively. Gene expression analysis revealed that the PA compounds downregulated PFKFB3 expression whilst 3PO did not. Similarly, markers of migration and angiogenesis, such as CCL5, VCAM-1, VEGFA and VEGFR2, were also markedly reduced (up to 10-fold) by the PA compounds. **Conclusions** These findings suggest that PFKFB3 inhibition with PA compounds may interfere with key pro-angiogenic functions, such as endothelial migration, proliferation and capillary-like structure formation and this exerts a multitarget anti-angiogenic activity. Hence, PFKFB3 inhibition with PA compounds is a promising therapeutic approach to promote plaque stability.

A. Abdali: None. **A. Corsini:** None. **D. Baci:** None. **C. De Dominicis:** None. **M. Zanda:** None. **M. Gelmi:** None. **S. Bellosta:** None.

436

Talin1-Dependent Integrin Activation Drives Endothelial Inflammation and Fibronectin Deposition

Zaki Al-Yafeai 71103, Lsu health sciences center-shreveport, SHREVEPORT, LA; Arif Yurdagul, Columbia Univ, New York, NY; Brian Petrich, Emory Univ Sch of Med, Atlanta, GA; A. Wayne Orr, A. Wayne Orr, Lsu health sciences center-shreveport, SHREVEPORT, LA

Integrin activation plays a critical role in regulating leukocyte and platelet adhesion, but less is known concerning integrin activation in adherent cells. In endothelial cells (ECs), both shear stress and oxidized LDL (oxLDL) promote integrin activation, and blocking the interactions between integrins and provisional matrix proteins, such as fibronectin, limits proinflammatory responses. However, current studies fail to demonstrate a causal role for integrin activation in this response due to the inability to specifically uncouple integrin activation while maintaining integrin function in cell adhesion. Therefore, we isolated ECs from mice containing an L325R mutation in talin1, the classic mediator of integrin activation, that selectively inhibits talin1-induced integrin activation while preserving its ability to link integrins to the actin cytoskeleton. We now show that talin1 L325R ECs show slowed adhesion and spreading, but cells eventually adhere, spread, and form focal adhesions. In addition, talin1 L325R ECs lack shear stress and oxLDL-induced α5β1 integrin activation, but basal levels of integrin activation remain similar between wildtype and Talin1 L325R ECs. Additionally, shear stress does not induce NF-κB activation or proinflammatory gene expression in talin1 L325R ECs. Consistent with abrogating inflammation, talin1 L325R completely blunts shear stress-induced fibronectin fibrillogenesis, a main initiating event in atherosclerosis development, through mechanisms involve blunting translocation of tensin1- α5β1 to fibrillar adhesions, the primary machinery of fibronectin assembly. Similarly, talin1 L325R ECs blocks endothelial inflammation and fibronectin deposition in response to oxLDL. However, preventing talin1-dependent integrin activation does not block all shear stress-mediated signaling, and proinflammatory responses to cytokines and LPS remain unchanged. These data suggest a model whereby flow and oxLDL mediate talin1-induced α5β1 integrin activation, which is required for flow and oxLDL-induced inflammation and fibronectin assembly.

Z. Al-Yafeai: None. **A. Yurdagul:** None. **B. Petrich:** None. **A. Orr:** None. **A. Orr:** None.

437

Large-scale Validation of Zebrafish Larvae as a Model System for Systematic Genetic Screens in Dyslipidemia, Atherosclerosis and Coronary Artery Disease

Manoj Bandaru, Uppsala Univ, Uppsala, Sweden

Background: Genome-wide association studies have identified hundreds of loci that are robustly associated with circulating lipids, atherosclerosis and coronary artery disease (CAD). In all but a few of these loci the causal genes and mechanisms remain unknown. Small-scale studies suggest that zebrafish larvae represent a promising model system for genetic screens in dyslipidemia, early-stage atherosclerosis and CAD. We expanded the phenotypic pipeline, increased the throughput, and performed a large-scale validation study. **Methods:** We used a three-tiered approach to validate the zebrafish model system: 1) a dietary intervention to examine the effect of overfeeding and cholesterol supplementation (N=1956); 2) treatment with atorvastatin and ezetimibe (N=835); and 3) a genetic screen for zebrafish orthologues of *APOE, APOB* and *LDLR* using a multiplex CRISPR-Cas9 approach (N=330). After imaging of vascular atherogenic traits and body size, whole-body lipid and glucose levels were assessed using enzymatic assays, and CRISPR-Cas9 target sites were sequenced on a MiSeq. **Results:** Overfeeding and cholesterol supplementation have independent pro-atherogenic effects, including higher LDLc and triglyceride levels, more vascular infiltration by lipids and oxidized LDLc, and more vascular co-localization of lipids with macrophages and neutrophils. Treatment with atorvastatin and ezetimibe can largely prevent this diet-induced pro-atherogenic state, but results in higher glucose levels. Finally, mutations in *apoea* and *apoeb* result in higher whole-body LDLc levels; mutations in *apobb.1* result in more vascular co-localization of lipids and neutrophils; and mutations in *ldlra* result in more vascular infiltration by lipids, and in more vascular co-localization of lipids and macrophages. Data from all larvae combined show that atherosclerosis in 10-day-old zebrafish larvae is mainly driven by higher triglyceride levels. **Conclusion:** Systematic genetic screens in zebrafish larvae will likely help increase our understanding of disease aetiology and identify new targets that can be translated into efficient medication for prevention and treatment.

M. Bandaru: Research Grant; Significant; Anastasia Emmanouilidou, Petter Ranefall, Benedikt von der Heyde, Tiffany Klingström, Johan Ledin, Anders Larsson, Hannah Brooke, Carolina Wählb, Erik Ingelsson and Marcel den Hoed.

438

Promyelocytic Leukemia Protein (pml), an Antagonist of Arteriosclerotic Plaque Rupture

Janine Berkholz, Andreas Zakrzewicz, Eugeny Ermilov, Guenter Siegel, Charite - Univ Clinic Berlin, Berlin, Germany

Aims: A growing body of evidence exists that PML, a constitutive component of PML nuclear bodies, is a key regulator of inflammatory responses. In this study, we aimed at demonstrating its presence and distribution in arteriosclerotic plaques of human coronary arteries (from heart transplantations), a prerequisite for a role of PML in atherogenesis. *Methods:* Nanotechnologic biosensor ellipsometry, photometric methods, ELISAs and EIAs, confocal laser scanning microscopy. *Results and Discussion:* Western blot, ELISA and IHC studies were performed on samples of human coronary arteries without and with macroscopic signs of arteriosclerosis. We compared protein expression and spatial distribution of PML between plaque and non-plaque regions of the same artery as well as between coronaries without and with

arteriosclerosis. PML was significantly higher in arteriosclerotic vessels with the highest amount occurring in the vulnerable shoulder region of the plaque, a critical domain for plaque rupture. In this inflamed tissue, PML seems to counteract this degradation. Moreover, PML had been shown to positively regulate cytokine signaling, reversely, a regulatory influence of PML in atherogenesis can be suggested. In a molecular biological approach, we show that in human coronary artery plaque ruptures, PML is dramatically upregulated to combat reactive oxygen species (ROS)-induced plaque fibrous cap disintegration at this blood-tissue interface. The biochemical correlations, with co-operation of the transcription factors NFκB and CIITA, can simplistically be portrayed by a two-armed control loop both with negative and positive feedbacks (Figure). Since we measured all controlled variables and actuators quantitatively, the entire control cycle can be specified utilizing a set of differential equations. *Perspective:* This quantitative molecular-biological approach aims at determining the constellation for a possible plaque rupture.

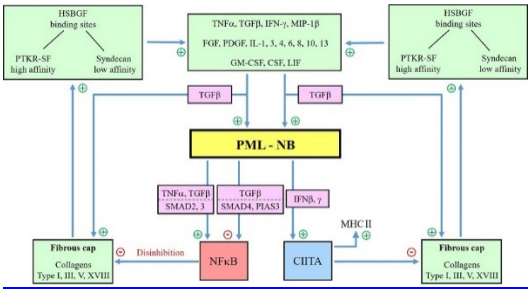

J. Berkholz: None. **A. Zakrzewicz:** None. **E. Ermilov:** None. **G. Siegel:** None.

439
Statins Disrupt Rac Regulation Leading to Increased Atherosclerotic Calcification
Abigail Healy, Chris Mantsounga, **Joshua Michael Berus**, Jared Christensen, Jerome Watt, Nicole Ceneri, Rachael Nilson, Jade Neverson, Gaurav Choudhary, Alan Morrison, Brown Univ, Providence, RI

Coronary artery disease caused by atherosclerosis is the leading cause of morbidity and mortality in the world. Calcification of atherosclerotic plaque is predictive of increased cardiovascular events; however, recent studies demonstrate that increased calcium density may be associated with more stable disease. Therapeutic modulation of calcified atherosclerotic plaque composition may have potential to reduce event risk. HMG-CoA reductase inhibitors (statins) reduce the risk of cardiovascular events. Moreover, recent data demonstrate that statin use is associated with increased plaque calcification, yet the underlying mechanisms for this process are not well understood. Our laboratory identified a Rac-dependent pathway that promotes IL1B-driven atherosclerotic calcification. Here, we hypothesize that statins disrupt isoprenylation of Rac1, resulting in increased activation of Rac1 and consequent IL1B expression. Results demonstrated statin-induced loss of Rac1 isoprenylation disrupted a complex between Rac1 and its inhibitor, Rho-GDI, in primary macrophages. This led to increased GTP-bound (activated) Rac1 in a statin dose-dependent manner. This phenomena was rescued by a precursor isoprenyl group for Rac1. Statin-treated primary macrophages expressed higher IL1B mRNA and secreted more IL1B protein in response to inflammasome activation. Small molecule inhibition of Rac1 and *Rac1* gene-deletion mitigated this statin-induced effect. *ApoE*$^{-/-}$ mice placed on high fat diet with statin therapy revealed increased plaque calcification in association with elevated serum IL1B protein. In summary, we have defined a potential mechanism of statin-induced calcification, whereby statins disrupt Rho-GDI-mediated inhibition of Rac1.

A. Healy: None. **C. Mantsounga:** None. **J.M. Berus:** None. **J. Christensen:** None. **J. Watt:** None. **N. Ceneri:** None. **R. Nilson:** None. **J. Neverson:** None. **G. Choudhary:** None. **A. Morrison:** None.

440
Targeting LOX-1 Scavenger Receptor and oxLDL Uptake with Affimers
Gary A Cuthbert, Jonathan DeSiqueira, Leeds Vascular Inst, Leeds, United Kingdom; Izma Abdul-Zani, Darren C Tomlinson, Sreenivasan Ponnambalam, Univ of Leeds, Leeds, United Kingdom; Shervanthi Homer-Vanniasinkam, Leeds Vascular Inst, Leeds, United Kingdom

Introduction: Lectin-like oxidized low density lipoprotein receptor 1 (LOX-1, SREC-1, OLR1) is a class E scavenger receptor which binds oxidized low density lipoprotein (oxLDL) particles implicated in promoting atherosclerosis. Affimers are non-antibody synthetic protein-based scaffolds that enable recognition of a wide range of molecular targets.
Aims: To investigate the ability of Affimers to bind LOX-1 and modulate oxLDL accumulation and effects on cellular responses.
Methods: Recombinant soluble human LOX-1 was screened with an Affimer library and LOX-1-specific Affimers were isolated and characterized. Human embryonic kidney (HEK293T) cells inducibly expressing human LOX-1 were incubated with labeled oxLDL and Affimers to modulate LOX-1 and oxLDL uptake and trafficking. Furthermore, Affimer-mediated effects on oxLDL-regulated metabolism and apoptosis was evaluated.
Results: Five Affimers specific for human LOX-1 were identified. Fluorescent labelled Affimers demonstrate specific binding to LOX-1 expressing HEK293T cells and modulate LOX-1 and oxLDL trafficking and accumulation in endosomes and lysosomes. LOX-1-specific Affimers also show effects in modulating oxLDL-mediated effects in specific cellular responses.
Conclusion: LOX-1-specific Affimers are a new class of synthetic molecules that have therapeutic potential in targeting LOX-1, a key mediator of inflammation and arterial dysfunction in cardiovascular disease.

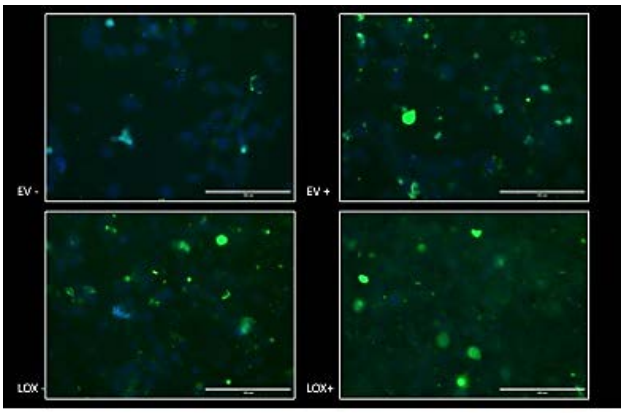

Membrane specific binding is demonstrated only in induced LOX-1 expressing cells (LOX+).

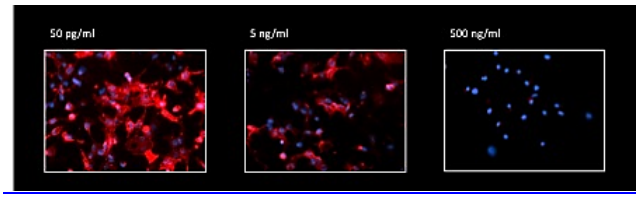

Increasing concentration of affimer prior to incubation with DiI labelled oxLDL.

G.A. Cuthbert: None. **J. DeSiqueira:** None. **I. Abdul-Zani:** None. **D.C. Tomlinson:** None. **S. Ponnambalam:** None. **S. Homer-Vanniasinkam:** None.

441
Zebrafish Larvae as a Model System for High-throughput, Image-based Genetic Screens in Dyslipidemia and Atherosclerosis
Manoj Bandaru, Benedikt von der Heyde, Anastasia Emmanouilidou, Dept of Immunology, Genetics and Pathology, Uppsala Univ, Uppsala, Sweden; Petter Ranefall, Amin Allalou, Dept of Information Technology, Div of Visual Information and Interaction, Uppsala Univ, Uppsala, Sweden; Hannah Brooke, Inst of Environmental Med, Karolinska Inst, Stockholm, Sweden; Anders Larsson, Dept of Medical Sciences, Clinical Chemistry, Uppsala Univ, Uppsala, Sweden; Carolina Wählby, Dept of Information Technology, Div of Visual Information and Interaction, Uppsala Univ, Uppsala, Sweden; Erik Ingelsson, Dept of Med, Div of Cardiovascular Med, Stanford Univ Sch of Med, Stanford, CA; **Marcel den Hoed**, Dept of Immunology, Genetics and Pathology, Uppsala Univ, Uppsala, Sweden

Background: Genome-wide association (GWAS) have identified hundreds of loci that are robustly associated with the risk of cardiometabolic risk factors and diseases. With few exceptions, the causal genes through which these loci influence disease risk remain uncharacterized. Since murine model systems are not suitable for systematic characterization of candidate genes in hundreds of loci, novel *in vivo* model systems are desirable.
Methods: My group has developed and validated zebrafish model systems that make optimal use of: 1) the zebrafish' well-annotated genome, with orthologues of at least 71.4% of human genes; 2) recent developments in multiplex CRISPR-Cas9-based mutagenesis; 3) advances in automated positioning of non-embedded zebrafish larvae; 4) fluorescent transgenes and dyes; and 5) custom-written image-quantification pipelines.
Results: Five days of overfeeding, dietary cholesterol supplementation and/or exposure to glucose induce atherogenic and insulin resistant phenotypes (higher/more whole-body LDL cholesterol (LDLc) and triglyceride levels; vascular foam cell formation and inflammation; beta-cell number and volume; subcutaneous and hepatic accumulation of fat) that can largely be prevented by concomitant treatment with lipid-lowering or diabetes medication (N>4000). In line with recent results in humans, treatment with atorvastatin and ezetimibe results in higher whole-body glucose levels (N~835). Each additional mutated allele in zebrafish orthologues of *APOE* results in higher LDLc levels, while mutations in *LDLR* affect vascular infiltration by lipids and macrophages (N~330). Ongoing characterization of 37 prioritized genes in GWAS-identified loci for triglyceride levels identified genes that influence triglycerides, LDLc, and/or vascular inflammatory and atherogenic traits, while characterizing prioritized genes in loci associated with heart rate variability yielded genes that influence cardiac rate and rhythm.
Conclusions: Systematic characterization of candidate genes for cardiometabolic traits in zebrafish model systems will help increase our understanding of human disease and identify novel targets that can be translated into efficient therapeutics.
M. Bandaru: None. **B. von der Heyde:** None. **A. Emmanouilidou:** None. **P. Ranefall:** None. **A. Allalou:** None. **H. Brooke:** None. **A. Larsson:** None. **C. Wählby:** None. **E. Ingelsson:** None. **M. den Hoed:** None.

442
Loss of *Kiaa1462*, a Coronary Artery Disease Associated Gene, Decreases Atherosclerosis
Gillian Douglas, Theodosios Kyriakou, Victoria S Rashbrook, Ayman Al Haj Zen, Lucy Trelfa, Vedanta Mehta, Ellie Tzima, Hugh Watkins, Keith Channon, Div Cardiovascular Med, Oxford, United Kingdom

Introduction: *KIAA1462* is the only coding gene in a chromosome 10 genomic locus consistently associated with Coronary Artery Disease (CAD) in Genome Wide Association Studies. KIAA1462 has no recognizable functional domains and little homology to other protein families, but has been previously implicated in endothelial cell proliferation and angiogenesis. We used a murine knock out (KO) model to investigate the role of *Kiaa1462* in the development of atherosclerosis. **Methods and Results**: *Kiaa1462* global KO mice were generated by replacing exon 3 with a reporter/selection cassette harbouring LacZ. *Kiaa1462* KO mice bred normally with offspring born in the expected Mendelian ratio. X-gal staining of aortas showed *Kiaa1462* expression in vascular smooth muscle cells (VSMC) and endothelial cells. This was confirmed by qRT-PCR with expression of *Kiaa1462* observed in both isolated endothelial cells and VSMC from WT but not KO mice. Loss of *Kiaa1462* did not alter blood pressure or heart rate. Furthermore, no difference in vascular contractile function, or either endothelial cell dependent or independent dilation in the aorta was observed between WT and KO mice. To assess the role of *Kiaa1462* in the development of atherosclerosis we crossed *Kiaa1462* KO mice with hyperlipidaemic ApoE$^{-/-}$ mice. Heterozygous breeding pairs were used to generate matched WT, heterozygous and homozygous KO mice. On an ApoE$^{-/-}$ background *Kiaa1462* KO mice were no longer born at the expected Mendelian ratio with a significant (~50%) decrease in KO mice alive 21 days after birth. Surviving KO mice were indistinguishable from their littermates with no difference in body or organ weight observed. Atherosclerosis was assessed after high fat feeding for 10 weeks (6 to 16wk of age). Loss of *Kiaa1462* caused a significant decrease in plaque burden in the aortic root of both male and female KO mice vs. WT mice, with no difference observed between WT and heterozygous KO mice. Despite the decrease in plaque size there was no significant difference in macrophage or collagen content between genotypes. **Conclusions**: Our findings support that *Kiaa1462* a GWAS gene candidate plays a critical role in the development of atherosclerosis.
G. Douglas: None. **T. Kyriakou:** None. **V.S. Rashbrook:** None. **A. Al Haj Zen:** None. **L. Trelfa:** None. **V. Mehta:** None. **E. Tzima:** None. **H. Watkins:** None. **K. Channon:** None.

443
Cushioned-Density Gradient Ultracentrifugation (C-DGUC) Improves the Isolation Efficiency of Exosomes for their use in Atherosclerosis Research
Phat Duong, Allen Chung, David K Wong, Kang Li, King Yeung Hong, Laura Bouchareychas, Robert L Raffai, Div of Vascular and Endovascular Surgery, Dept of Surgery, Univ of California San Francisco & VA Medical Ctr, San Francisco, CA

Background and Purpose: Ultracentrifugation (UC) is recognized as a robust approach for the isolation of exosomes especially when combined with a second step that involves density gradient ultracentrifugation (DGUC). However, recent studies have highlighted limitations associated with the use of UC including low recovery efficiencies and possible aggregation of exosomes. Such effects could subsequently impact on downstream assessments of exosome function in biological systems.
Methods: We tested the benefit of using a liquid cushion of iodixanol during the first UC step to improve the yield of exosomes that are concentrated from the conditioned media (CM) of J774.1 murine macrophages in a method we recently termed Cushioned(C)-DGUC. We also compared the yield and purity of exosomes isolated by C-DGUC with those isolated by first subjecting CM to two other forms of concentration that included: ultrafiltration (UF) and polyethylene glycol (PEG) sedimentation prior to DGUC.
Results: Our data show that the concentration step largely determines the yield and purity of exosomes isolated following the second DGUC step. The use of a high-density iodixanol cushion in cushioned-UC (C-UC) led to a threefold improvement in exosome yield over conventional UC. Although subjecting the CM to UF resulted in a similar

exosome recovery efficiency, it retained eight-fold more soluble proteins than C-UC method. Strikingly, PEG precipitation of the CM generated a substantial number of non-exosomal nanoparticles, which could not be efficiently eliminated by the DGUC step. Western blot analysis reproducibly detected exosome markers CD-81, TSG101 and Alix in fractions 6 and 7. Finally, an *in vitro* assay of exosome-mediated microRNA delivery confirmed that C-DGUC provided the highest yield of functional exosomes. **Conclusions:** Collectively, our data demonstrate that the use of a high-density liquid cushion of iodixanol during the concentration step of C-DGUC substantially improves the yield and purity of exosomes derived from cell culture media. This approach can therefore facilitate functional studies of cell-derived exosomes in atherosclerosis.
P. Duong: None. **A. Chung:** None. **D.K. Wong:** None. **K. Li:** None. **K.Y. Hong:** None. **L. Bouchareychas:** None. **R.L. Raffai:** None.

This research has received full or partial funding support from the American Heart Association.

444
Role of CaMKII in Atherosclerotic Plaque Progression in ApoE-Deficient Mice
Obialunanma V Ebenebe, Alison K Heather, Jeffrey R Erickson, Univ of Otago, Dunedin, New Zealand

Non-obstructive mixed atherosclerotic plaques are an independent risk factor in predicting mortality in coronary artery disease patients. The multifactorial process of plaque progression and complication is a result of proliferation and migration of VSMCs and macrophages, apoptosis and calcification. A number of osteogenic regulators and inflammatory stimuli driving these processes in plaque advancement have been identified. Yet rupture, a result of complex mixed plaques, remains the leading cause of fatal cardiovascular events. Further understanding of the mechanisms underlying plaque progression is required to identify potential targets for therapies. Key signalling factors that modulate cell proliferation and migration, which potentially underlie plaque complication include the nodal multifunctional calcium/calmodulin dependent protein kinase II (CaMKII). Thus we hypothesized that, as plaques progress in a mouse model of atherosclerosis ($ApoE^{-/-}$), CaMKII activity would increase. We also hypothesized that systemic inhibition of CaMKII would impede plaque progression. Our data show a trend towards increased CaMKII phosphorylation, an indirect measure of kinase activity, in plaques as mice advance from 26 to 30 weeks. Pharmacological inhibition of CaMKII with KN-93, on alternate days for 4 weeks, in 30 week old mice reduced the incidence of calcification from 50% (KN-92 control: 4 out of 8) to 25% (KN-93: 2 out of 8). This was associated with a trend towards reduced calcification area (KN-92 control: $0.43mm^2$ vs. KN-93: $0.06mm^2$). These results suggest that CaMKII is activated during atherosclerosis and may be involved with plaque progression through calcification.
O.V. Ebenebe: None. **A.K. Heather:** None. **J.R. Erickson:** None.

446
Ampk Regulates Endothelial Mirna Biogenesis Through Nucleolin
Brendan Gongol, Univ of California, San Diego, San Diego, CA; Traci Marin, Loma Linda Univ, Loma Linda, CA; John Shyy, Univ of California, San Diego, San Diego, CA

Background A characteristic of atherosclerosis is the focal distribution of lesions in the arterial tree despite the systemic nature of cardiovascular impairments such as hyperlipidemia. While pulsatile shear stress (PS, atheroprotective) maintains endothelial homeostasis, oscillatory shear stress (OS, atherogenic) causes endothelial dysfunction. Previously, we and others have identified AMP activated protein kinase (AMPK) is a master regulator in vascular endothelial cells (ECs) in response to PS. To further decipher the atheroprotective effect of AMPK, bioinformatic approaches identified a broad array of AMPK-regulated pathways that regulate cellular functions beyond its canonical catabolic regulation. Among other newly identified substrates, nucleolin (NCL) is a multifunctional protein and the newly identified AMPK phosphorylation of NCL S328 may be a major mechanotransduction event hindering miRNA biogenesis in ECs. **Methods and Results** Using AMPK kinase assays and phospho-S328 NCL antibody, we identify that the PS-activated AMPK increased phospho-S328 NCL. Cellular fractionation and immunofluorescence indicated NCL localization throughout the nucleus and cytoplasm which was sequestered to the nucleus following AMPK activation. This indicated bipartite NCL functions, acting as a chaperone under dephospho-S328 conditions and maintaining a transcriptional function upon phosphorylation. Bioinformatics analysis validated by RNA immunoprecipitation showed that the OS-induced miR-93 and miR-484 were novel NCL-regulated miRNAs. Putative miR-93 and miR-484 targets, including eNOS and BMPR2 were cross referenced to RNA-seq data from ECs exposed to PS and OS. ECs transfected with anti-miR-93 and anti-miR-484 exhibited ratified NO bioavailability and attenuated inflammation. In response to PS stimulation, however, AMPK activation increased NCL phosphorylation resulting in its binding to the KLF2 promoter to induce KLF2 that increased NO bioavailability and inhibited miR-93 and miR-484 induction. **Conclusions** These results demonstrate that AMPK can inhibit the expression of atherogenic miR-93 and miR-484 in ECs through AMPK phosphorylation of NCL S328.
B. Gongol: None. **T. Marin:** None. **J. Shyy:** None.

447
Lipid Droplet Associated Hydrolase (LDAH) Impacts Oxysterol Metabolism and Prevents Atherosclerosis
Young-Hwa Goo, Inhwa Lee, Albany Medical Coll, Albany, NY; Todd A Lydic, Michigan state university, East Lansing, MI; Sushant Bangru, Univ of Illinois, Urbana, IL; Pradip Saha, Baylor Coll of Med, Houston, TX; Auinash Kalsotra, Univ of Illinois, Uraban, IL; Lawrence C Chan, Baylor Coll of Med, Houston, TX; Antoni Paul, Albany Medical Coll, Albany, NY

Macrophage/foam cells in the arterial wall engulf apolipoprotein B-containing lipoproteins and store the surplus of lipids derived from these particles in lipid droplets (LDs). Even though cholesterol is abundant in the LDs of atheroma, the lipidome of LDs displays a variety of lipid species, including other sterols that have a deep impact on foam cell and plaque biology. While the LD is increasingly seen as a reservoir of signaling precursors, how the bioactive lipids are mobilized from the LDs remains elusive. Previously, we identified LDAH as a novel LD protein that contains a lipase/esterase sequence and reported it as a CE hydrolase. Our in vivo atherosclerosis studies on LDAH knock-out (KO) and transgenic (Tg) mice in apoE KO background revealed an athero-protective role of LDAH driven by its ability to reduce lipid accumulation in the lesional foam cells. LDAH increases expression of ATP-binding cassettes (ABC) A1 and G1, two cholesterol transporters that are regulated by liver X receptor (LXR). Interestingly, we also found that LDAH promotes favorable tissue remodeling, evidenced by a remarkable increase in lesional collagen content, which is known to contribute to plaque stability. To determine molecular mechanism behind these phenotypes we performed combinatory “omics” studies of LDAH WT, KO, and Tg foam cells: lipidomics (targeted and untargeted) and transcriptomics. Lipidomics analyses confirmed that LDAH inversely regulates total cholesterol levels, and revealed that several other lipid species were also altered by LDAH. Interestingly, among sterol lipids, LDAH preferentially targets esterified oxysterols whose free forms are LXR ligands. RNA-seq analysis

identified several collagen synthesis genes regulated by LDAH, supporting the phenotype seen in the atheroma. Overall, our studies suggest that LDAH might play a central role in the production of messengers from ester precursors stored in LDs of foam cells. Therefore, unraveling the mechanisms of trafficking through LDs may be key to exploit the atheroprotective potential of endogenous lipid mediators.
Y. Goo: None. **I. Lee:** None. **T.A. Lydic:** None. **S. Bangru:** None. **P. Saha:** None. **A. Kalsotra:** None. **L.C.B. Chan:** None. **A. Paul:** None.

This research has received full or partial funding support from the American Heart Association.

448
Stress Granule Formation as a Molecular Indicator of Atherosclerotic and Vascular Disease Progression
Allison B Herman, Christine N. Vrakas, Mitali Ray, Sheri E. Kelemen, Michael V Autieri, Temple Univ Lewis Katz Sch of Med, Philadelphia, PA

The molecular mechanisms by which atherogenic stress contributes to the pathophysiology of disease remain to be fully characterized. RNA-binding proteins (RBPs) regulate vascular cell (VSMCs and ECs) response to inflammatory stimuli by fine-tuning mRNA stability, and protein abundance. RBPs such as HuR and FXR1 regulate mRNA transcript abundance by binding AU-rich elements (AREs) in the 3'UTR permitting the transcript stabilization or destabilization, respectively. Most inflammatory transcripts including TNFα contain conserved AREs in their 3'UTR, and inflammatory stimuli activate RBPs to alter the landscape of inflammatory mediators. This post-transcriptional regulation of inflammatory transcripts by RBPs islocalized to structures called stress granules (SGs), which are mRNA-protein assemblies formed from non-translating mRNAs, ribosomal subunits, among other components. The manner by which these complexes form between mRNA and RBPs (mRNPs) under inflammatory or pathological conditions remains unknown, particularly with respect to vascular inflammatory disease. We hypothesize that the presence and quantity of stress granules are a critical cellular response to atherogenic stimuli. We identified SGs in cultured VSMCs and ECs treated with clotrimazole, a known inducer of SGs by co-staining for PABP, a SG marker, along with RBPs HuR and FXR1, both known to co-localize to SGs. VSMC treated with clotrimazole had increased eIF2α phosphorylation. LDLR-/- mice fed high fat diet for 14 weeks also demonstrated significantly increased PABP expression in the smooth muscle and endothelial cells of the aortic arch as compared to WT control. Atherogenic and hypoxic stimuli induced the formation of SGs in cultured primary human VSMCs and ECs. Interestingly, we found VSMCs pre-treated with anti-inflammatory cytokine IL-19 followed by clotrimazole significantly reduced the formation of SGs per cell in a time dependent manner ($n=50$, $p<0.05$) as well as reduction in PABP expression, suggesting anti-inflammatory treatment effects SG formation. Taken together, these results have led to the hypothesis that SG formation in atherosclerosis is driven by inflammatory stimuli, and that anti-inflammatory treatment may lessen atherosclerosis progression and plaque formation by reduction of SGs.
A.B. Herman: None. **C.N. Vrakas:** None. **M. Ray:** None. **S.E. Kelemen:** None. **M.V. Autieri:** None.

This research has received full or partial funding support from the American Heart Association.

449
Dimerization of Sortilin Regulates its Trafficking to Extracellular Vesicles and Leads to Secretion of Soluble Sortilin Homodimers, a Potential Novel Biomarker
Shinsuke Itoh, Ken Mizuno, Masanori Aikawa, Elena Aikawa, Ctr for Interdisciplinary Cardiovascular Sciences, Brigham and Women's Hosp, Harvard Medical Sch, Boston, MA

Objective Extracellular vesicles (EVs) play a critical role in intercellular communication by transferring microRNAs, lipids and proteins to neighboring cells. Sortilin, a sorting receptor that directs target proteins to the secretary or endocytic compartments of cells, is found in both EVs and cells. In many diseases, including cardiovascular calcification and cancer, sortilin expression levels are atypically high. We previously demonstrated that sortilin promotes vascular calcification via its trafficking of tissue-nonspecific alkaline phosphatase to EVs. Therefore, suppressing trafficking of sortilin to EVs may act as a novel therapy against EV-associated diseases. However, the precise mechanisms of sortilin trafficking remain to be determined. In this study, we hypothesized that dimerization of sortilin regulates its trafficking to EVs. **Approach and Results** We found that sortilin forms a homodimer with an intermolecular disulfide bond (IDB) at Cysteine783 (Cys783) residue. Palmitoylation and the IDB formation compete for Cys783. Formation of the IDB led to trafficking of sortilin to EVs by preventing palmitoylation, which further promoted sortilin trafficking to the Golgi apparatus. Moreover, addition of sortilin-derived propeptide decreased sortilin homodimers within EVs, suggesting that the propeptide binding suppresses sortilin trafficking to EVs through prevention of its dimerization. We also found that soluble sortilin secreted by cells overexpressing full-length sortilin forms homodimers with IDBs using various commercially available antibodies against sortilin, thus providing an opportunity for diagnosis of EV-associated diseases by detection of sortilin homodimers in patients. **Conclusions** Sortilin is transported to EVs via the formation of homodimers with an IDB, which is endogenously regulated by its own propeptide. Therefore, inhibiting sortilin dimerization may provide a novel therapy against EV-associated diseases, including cardiovascular calcification and cancer. In addition, soluble sortilin homodimer with IDBs could be detected and used as a novel diagnostic biomarker for EV-associated diseases.
S. Itoh: Employment; Significant; Kowa Company, Ltd. **K. Mizuno:** Employment; Significant; Kowa Company, Ltd. **M. Aikawa:** Research Grant; Significant; Research Grant from Kowa Company, Ltd. **E. Aikawa:** Research Grant; Significant; R01HL 114805 and R01HL 136431.

450
Vascular Smooth Muscle Cell-expressed Tie2 Controls Atherosclerosis Progression
Stephanie S Kapel, Jingjing Shi, Zulfiyya Hasanov, German Cancer Res Ctr, Heidelberg, Germany; Sila Appak-Baskoy, Ryerson Univ and Li Ka Shing Knowledge Inst, Keenan Res Ctr, Toronto, ON, Canada; Mahak Singhal, Jessica Wojtarowicz, Stella Hertel, Damir Krunic, German Cancer Res Ctr, Heidelberg, Germany; Claudia Korn, Univ of Cambridge, and Natl Health Service Blood and Transplant, Cambridge, United Kingdom; Junhao Hu, Interdisciplinary Res Ctr on Biology and Chemistry, Shanghai, China; Caroline Arnold, Inst of Physiology and Pathophysiology, Heidelberg, Germany; Marius Robciuc, Wihuri Res Inst, Helsinki, Finland; Thomas Korff, Inst of Physiology and Pathophysiology, Heidelberg, Germany; Hellmut G Augustin, German Cancer Res Ctr, Heidelberg, Germany

Angiopoietin (Angpt)/Tie signaling in microvascular endothelial cells (EC) controls vascular development, remodeling and maturation. Biomarker studies also imply a role of macrovascular Angpt/Tie signaling. The model of Angpt1/stimulation versus Angpt2/destabilization would imply an anti-atherosclerotic function of Angpt1 and a pro-atherosclerotic function of Angpt2. Yet, experimental studies on the role of the Angpt ligands and the Tie receptors in atherosclerosis have yielded conflicting results suggesting spatiotemporally context-dependent pro- and anti-atherosclerotic functions in different experimental settings. The endotheliocentric view of Angpt/Tie signaling is not

sufficient to mechanistically explain the divergent roles of Angpt/Tie signaling during atherosclerosis. We hypothesized that vascular smooth muscle cell (VSMC)-expressed Tie2 may contribute to the pathogenesis of atherosclerosis. Employing genetic models, the present study was aimed at elucidating the role of VSMC-expressed Tie2 during atherosclerosis. Compared to EC, VSMC express lower, but consistently detectable levels of functional Tie2. We therefore generated VSMC-specific Tie2-deficient mice (*Tie2*$^{SMC-KO}$), using a mural cell-specific *Sm22α-Cre* driver line. These were crossed with atherosclerosis-prone *ApoE*-deficient mice (*ApoE*^{KO}*Tie2*$^{SMC-KO}$). *ApoE*^{KO}*Tie2*$^{SMC-KO}$ mice, fed a Western-type diet for 14 weeks, showed significantly reduced atherosclerotic lesion progression with less VSMC content. Transcriptionally, Tie2 controlled the phenotypic switch of VSMC with increased contractile and reduced synthetic phenotype-specific gene expression in isolated Tie2-deficient VSMC. Correspondingly, migration and proliferation was significantly reduced in Tie2-deficient cultured VSMC. Serum Angpt2 as well as the Angpt2/Angpt1 ratio were significantly increased in *ApoE*^{KO}*Tie2*$^{SMC-KO}$ mice. Collectively, the data expand and revise the endotheliocentric Tie2 signaling concept to show that mural cell-expressed Tie2 is involved in regulating macrovascular functions related to atherosclerosis. VSMC-expressed Tie2 acts pro-atherosclerotic to control the phenotypic switch towards a proliferative and migratory synthetic VSMC phenotype.

S.S. Kapel: None. **J. Shi:** None. **Z. Hasanov:** None. **S. Appak-Baskoy:** None. **M. Singhal:** None. **J. Wojtarowicz:** None. **S. Hertel:** None. **D. Krunic:** None. **C. Korn:** None. **J. Hu:** None. **C. Arnold:** None. **M. Robciuc:** None. **T. Korff:** None. **H.G. Augustin:** None.

451

Radiation Induced Atherosclerosis on Mice

Kyung-Ae Ko, Sivareddy Kotla, Yin Wang, Yuka Fujii, Hang T Vu, Bhanu P Vankatesulu, Tamlyn N Thoman, Jan Medina, Young Jin Gi, MD Anderson Cancer Ctr, Houston, TX; Megumi Hada, Prairie View A&M Univ, Houston, TX; Jane Grande-Allen, Rice Univ, Houston, TX; Zarana S Patel, KBRwyle, Houston, TX; Sarah A Milgrom, Sunil Kirshnan, Keigi Fujiwara, Jun-ichi Abe, MD Anderson Cancer Ctr, Houston, TX

Rationale: The high prevalence of cardiovascular disease (CVD) in cancer survivors after ionizing radiation (IR) therapy has long been recognized, but the mechanism for this is unknown. Previous studies reported that the plaques in IR therapy survivors exhibit characteristics of increased instability without changes in the plaque size. **Objective**: To study the mechanism of IR induced CVD in humans, we decided to develop an IR mouse model that mimics human CV events. **Methods and Results:** We fed *LDLR-/-* mice or C57 mice with a single injection of adeno -associated virus vector(AAV) encoding a gain-of function of PCSK9 with a high fat diet, then irradiated the mice with different doses of IR (2 Gy, 5 Gy, 10 Gy). Whole body radiation was given 2 Gy, while localized IR to the neck and thoracic area was given at 5 Gy (1 time) or 10Gy (weekly 5 Gy, twice).About 2~3 weeks after the IR treatment, we performed left partial carotid artery ligation (PCL), and 3 weeks later examined the extent of plaque formation and cardiac abnormality by comparing those detected in non-irradiated control mice. The lesion area ratio between the partially ligated left carotid artery (LCA) and the right carotid artery (RCA) was significantly increased in the IR-treated group compared to the non-IR-treated group (3.1 ± 0.3 vs.1.8 ± 0.4, $n = 7$-8, $p = 0.03$). In addition, the lesion in the IR-treated of mice had significantly larger necrotic cores with a thinner fibrous cap when compared to those in non-irradiate mice. Furthermore, IR-treated mice showed cardiac hypertrophy, in which we found a significant increase of the wall thickness of mid-to small sized arteries as well as perivascular fibrosis, which were not noticed in the non-IR-treated mice. **Conclusions:** Our results demonstrate that IR not only increases atherosclerotic and vulnerable plaque formation but also cardiac hypertrophy with mid- and micro-vascular wall swelling. The increase of mid- and micro-vascular wall thickness may explain the heart failure preserved heart failure, which is observed in the majority of heart failure patients after IR treatment.

K. Ko: None. **S. Kotla:** None. **Y. Wang:** None. **Y. Fujii:** None. **H.T. Vu:** None. **B.P. Vankatesulu:** None. **T.N. Thoman:** None. **J. Medina:** None. **Y. Gi:** None. **M. Hada:** None. **J. Grande-Allen:** None. **Z.S. Patel:** None. **S.A. Milgrom:** None. **S. Kirshnan:** None. **K. Fujiwara:** None. **J. Abe:** None.

452

Estrogen Inhibits LDL Transcytosis by Coronary Artery Endothelial Cells via GPER and SR-BI

Siavash Ghaffari, Michael G. Sugiyama, Farnoosh Naderi Nabi, Keenan Res Ctr, St. Michael's Hosp, Toronto, ON, Canada; **Warren L. Lee**, Keenan Res Ctr, St. Michael's Hosp and the Univ of Toronto, Toronto, ON, Canada

Objectives Premenopausal women have a significantly lower rate of atherosclerosis than men, an effect attributed to estrogen. The atheroprotective effects of estrogen are independent of circulating lipid levels and may be due to an effect on the vessel wall. Early on in atherosclerosis, circulating LDL is able to cross an intact endothelial monolayer by transcytosis and accumulate in the intima. Little is known about the mechanisms of transcytosis but using novel assays we recently discovered a role for the SR-BI and ALK1 receptors. We hypothesized that estrogen can attenuate LDL transcytosis by coronary artery endothelial cells.

Approach and Results Using a recently described assay based on total internal reflection fluorescence microscopy, we quantified transcytosis of LDL across human coronary artery endothelial cells treated with physiological concentrations of estrogen. Estrogen significantly attenuated LDL transcytosis by endothelial cells from male donors; the effect was ligand-specific as transcytosis of albumin was not affected. Estrogen caused down-regulation of endothelial SR-BI but not ALK1 and over-expression of SR-BI was sufficient to restore LDL transcytosis. Similarly, depletion of SR-BI by siRNA attenuated endothelial LDL transcytosis and prevented any further effect of estrogen. In contrast, treatment with estrogen had no effect on SR-BI expression by liver cells from a male donor. Inhibition of estrogen receptors α and β had no effect on estrogen-mediated attenuation of LDL transcytosis. However, estrogen's effect was blocked by depletion of the G-protein coupled estrogen receptor (GPER) by siRNA. GPER was found to be enriched in endothelial cells compared to hepatocytes and is known to signal via transactivation of the epidermal growth factor receptor (EGFR); we observed that inhibition of EGFR also prevented the effect of estrogen on LDL transcytosis. Lastly, male mice demonstrated more vascular deposition of LDL than age-matched female mice after acute injection.

Conclusions Physiological concentrations of estrogen significantly inhibit LDL transcytosis by down-regulating endothelial SR-BI; this effect requires GPER. This may contribute to the lower rates of atherosclerosis in premenopausal women.

S. Ghaffari: None. **M.G. Sugiyama:** None. **F. Naderi Nabi:** None. **W.L. Lee:** None.

453

Sestrin1 is Required to Maintain Plasma Cholesterol Homeostasis During Cholesterol Feeding

Zhonggang Li, Sophia M. Ly, Sabrina L. Belisle, Fernanda B. Leyva Jaimes, Brian W Parks, Univ of Wisconsin-Madison, Madison, WI

Elevated plasma cholesterol is an established risk factor in the development of heart disease; however, the detailed mechanisms controlling plasma cholesterol levels are complex and under active investigation. Integrating mouse

liver global co-expression networks along with human lipid genome-wide association study (GWAS) data, we identified *Sestrin1* as a candidate gene associated with cholesterol in mice and humans. To test the role of *Sestrin1* in cholesterol metabolism, we performed *in vitro* and *in vivo* studies to determine its sensitivity to cholesterol and influence on cellular and plasma cholesterol levels. *In vitro*, *Sestrin1* mRNA is upregulated following cellular cholesterol depletion with methyl-β-cyclodextrin for 4 hours in AML12 hepatocyte cells. This upregulation is blocked when cholesterol complexes or Low-Density Lipoprotein (LDL)-cholesterol is supplemented back into the media. *In vivo*, hepatic *Sestrin1* mRNA is downregulated when mice after feeding a 0.2% cholesterol diet for 8 weeks. In contrast, treatment of mice with 0.02% Lovastatin for 1 week results in upregulation of hepatic *Sestrin1* mRNA. Consistent with transcriptional regulation by cholesterol *in vitro* and *in vivo*, siRNA knockdown of Sterol regulatory element-binding protein 2 (Srebp2) represses *Sestrin1* transcription and prevents the transcriptional regulation of *Sestrin1* by cholesterol. Knockdown of *Sestrin1* with siRNA in AML12 cells results in cellular cholesterol accumulation along with altered cholesterol related gene expression, indicating *Sestrin1* can regulate cholesterol metabolism *in vitro*. *In vivo*, homozygote or heterozygote *Sestrin1* knockout mice fed a 0.2% cholesterol diet for 4 weeks show elevated plasma cholesterol levels compared to littermate control mice. Our results establish *Sestrin1* as a *Srebp2* target gene that is capable of modulating cellular cholesterol levels *in vitro* and regulating plasma cholesterol homeostasis *in vivo*.

Z. Li: None. **S.M. Ly:** None. **S.L. Belisle:** None. **F.B. Leyva Jaimes:** None. **B.W. Parks:** None.

454

Repression of Map1lc3a During Atherosclerosis Progression Plays an Important Role in the Regulation of Vascular Smooth Muscle Cell Phenotype

Joelle Magné, St Jude Children's Hosp, Memphis, TN; Valentina Paloschi, Technical Univ Munich, Dept of Vascular and Endovascular Surgery, Munich, Germany; Isabel Gonçalves, Experimental Cardiovascular Res Group and Cardiology Dept, Clinical Res Ctr, Clinical Sciences Malmö, Lund Univ, Malmö, Sweden; Peter Saliba-Gustafsson, Cardiovascular Med Unit, Dept of Med, Ctr for Molecular Med, Karolinska Univ Hosp, Karolinska Instt, Stockholm, Sweden; Josefin Skogsberg, Vascular Biology Unit, Dept of Medical Biochemistry and Biophysics, Karolinska Instt, Stockholm, Sweden; Anton Razuvaev, Dept of Molecular Med and Surgery, Ctr for Molecular Med, Karolinska Univ Hosp, Karolinska Instt, Stockholm, Sweden; Hong Jin, Cardiovascular Med Unit, Dept of Med, Ctr for Molecular Med, Karolinska Univ Hosp, Karolinska Instt, Stockholm, Sweden; Yuhuang Li, Technical Univ Munich, Dept of Vascular and Endovascular Surgery, Munich, Germany; Daniel F.J. Ketelhuth, Cardiovascular Med Unit, Dept of Med, Ctr for Molecular Med, Karolinska Univ Hosp, Karolinska Instt, Stockholm, Sweden; Lars Maegdefessel, Technical Univ Munich, Dept of Vascular and Endovascular Surgery, Munich, Germany; Ulf Hedin, Dept of Molecular Med and Surgery, Ctr for Molecular Med, Karolinska Univ Hosp, Karolinska Instt, Stockholm, Sweden; Per Eriksson, Ewa Ehrenborg, Cardiovascular Med Unit, Dept of Med, Ctr for Molecular Med, Karolinska Univ Hosp, Karolinska Instt, Stockholm, Sweden

Background: Autophagy is a cell survival mechanism, which has been implicated in atherogenesis in mouse models by studying core autophagy machinery proteins using knock-out models. MAP1LC3A and MAP1LC3B play a key role in autophagy activity and have been implicated as prognostic factors in several human cancers. However, data on the involvement of autophagy in human atherosclerotic disease and plaque vulnerability are still sparse and completely lacking with regards to the involvement of MAP1LC3. Approach and Results: Using two independent biobanks of human carotid atherosclerotic plaques, we observe that MAP1LC3A mRNA and protein levels are decreased in plaques from patients with symptomatic disease compared to asymptomatic. Notably, MAP1LC3A mRNA levels strongly correlate with vascular smooth muscle cell markers, while MAP1LC3B does not. In in vivo models, we show that MAP1LC3A mRNA is downregulated during the progression of atherosclerosis in hypercholesterolemic mice as well as upon hyperplasia induced by balloon-injury in rats. In vitro, we show that ablation of MAP1LC3A in human carotid VSMC induces a transient compensatory increase in myocardin, a master regulator of vascular smooth muscle cell phenotypic switch.
Conclusions: Taken together, these results demonstrate that reduced MAP1LC3A expression is a relevant marker of vulnerable plaque phenotype, suggesting an impact on vascular smooth muscle cell biology in the context of atherogenesis.

J. Magné: None. **V. Paloschi:** None. **I. Gonçalves:** None. **P. Saliba-Gustafsson:** None. **J. Skogsberg:** None. **A. Razuvaev:** None. **H. Jin:** None. **Y. Li:** None. **D. Ketelhuth:** None. **L. Maegdefessel:** None. **U. Hedin:** None. **P. Eriksson:** None. **E. Ehrenborg:** None.

455

Inhibition of Histone Deacetylase 6 Activity Provides Protection Against Atherogenesis: a Role for HDAC6 NEDDylation

Yohei Nomura, Max C Rossberg, Anil Bhatta, Lew Romer, Dan Berkowitz, **Deepesh Pandey**, John Hopkins Univ, Baltimore, MD

Rationale: Histone Deacetylase 6 (HDAC6) regulates Cystathionine Gamma Lyase (CSEγ)- hydrogen sulfide producing enzyme known to play a critical role in endothelial function. However, a role for HDAC6 in atherogenesis is unknown. **Objective:** To determine whether pharmacological inhibition of HDAC6 inhibition by tubacin would attenuate atherogenesis and to elucidate specific molecular mechanism(s) that regulate endothelial HDAC6 activity. **Methods and Results:** We evaluated whether administration of tubacin attenuated or reversed the endothelial dysfunction and atherosclerosis induced in mice by a single i.p injection of PCSK9 AAV followed by a high fat diet (HFD) for 12 weeks. Tubacin significantly blunted PCSK9-induced increases in pulse wave velocity (index of vascular stiffness and overall vascular health) that are also seen in atherogenic mice. Furthermore, tubacin protected vessels from defective vasorelaxation, as evaluated by acetycholine-mediated relaxation using wire myograph. Plaque burden defined by Oil Red O staining was also found to be significantly less in mice that received tubacin than in those that received PCSK9 alone. Inhibition of the NEDD8 - activating enzyme 1 (NAE1) by MLN4924 significantly increased HDAC6 activity in Human Aortic Endothelial Cells (HAEC). Interestingly, levels of HDAC6 remain unchanged. This finding is consistent with the etiology of the change in function being the post-translational modification of HDAC6 by NEDD8, and not due to its overall abundance. HAEC exposed to the atherogenic stimulus OxLDL exhibited enhanced HDAC6 activity which was attenuated in a dose-response manner by pre-treatment with MLN4924. Conclusion: HDAC6 inhibition by tubacin and/or MLN4924 represents a novel pharmacological intervention for atherogenesis.

Y. Nomura: None. **M.C. Rossberg:** None. **A. Bhatta:** None. **L. Romer:** None. **D. Berkowitz:** None. **D. Pandey:** None.

This research has received full or partial funding support from the American Heart Association.

456
LncRNA *CHROME* is Increased in Cardiovascular Disease and Regulates Inflammatory Gene Expression
Kaitlyn R. Scacalossi, Coen van Solingen, Elizabeth J. Hennessy, Barbara Rizzacasa, Jeffrey S Berger, New York Univ, New York, NY; Hilal Kazan, Antalya Intl Univ, Antalya, Turkey; Kathryn J. Moore, New York Univ, New York, NY

Long non-coding RNAs (lncRNAs) are a class of regulatory RNAs capable of binding DNA, RNA, and/or protein to regulate transcriptional and epigenetic networks. Although thousands of lncRNAs have been identified, relatively few have been functionally characterized. Here we identify a primate-specific lncRNA, *CHROME*, encoded in a locus associated with cardiovascular disease. We found that *CHROME* expression is increased in the plasma of patients with inflammatory conditions, including coronary artery disease and lupus, compared to control subjects. Using FANTOM, a database of transcriptome analyses, we found the *CHROME* locus is transcriptionally activated in human monocytes and macrophages stimulated with microbial ligands and inflammatory cytokines. To investigate CHROME's molecular mechanisms, we used RNA immunoprecipitation (RIP) and chromatin isolation by RNA purification (ChIRP) to map *CHROME* lncRNA -protein and -DNA interactions, respectively. We found that *CHROME* has a strong histone binding affinity and its DNA binding pattern was consistent with interaction of *CHROME* with numerous inflammatory transcription factor motifs, including sites for CEBPβ, SPI1, NFKB, and RELA. To investigate the impact of CHROME's interaction with DNA in macrophages, we used gain and loss of function studies combined with RNA-sequencing. Ingenuity Pathway Analysis of genes most significantly altered with both CHROME knockdown and overexpression identified the inflammatory response as the pathway most significantly altered by *CHROME*. In particular, repression of *CHROME* led to a decrease in the expression of interferon stimulated genes and receptors involved in macrophage motility. Together, these data suggest that *CHROME* contributes to the transcriptional regulation of inflammatory gene expression and its dysregulation in the setting of atherosclerotic cardiovascular disease may contribute to the maintenance of chronic inflammation.
K.R. Scacalossi: None. **C. van Solingen:** None. **E.J. Hennessy:** None. **B. Rizzacasa:** None. **J.S. Berger:** None. **H. Kazan:** None. **K.J. Moore:** None.

This research has received full or partial funding support from the American Heart Association.

457
Feedback Regulation of 3-Hydroxy-3-methylglutaryl-coenzyme a Reductase in Livers of Mice
Shan Su, Kristina Garland, Youngah Jo, Seonghwan Hwang, Gennipher Young, Iris Fuentes, Marc Schumacher, Rania Elsabrouty, Brittany Johnson, Russell A. Debose-Boyd, UT Southwestern Medical Ctr, Dallas, TX

Introduction: HMG-CoA reductase is a membrane protein of the endoplasmic reticulum that catalyzes reduction of HMG-CoA to mevalonate, a rate-limiting step in the synthesis of cholesterol and nonsterol isoprenoids, which exert feedback control on HMGCR through multiple mechanisms. These mechanisms ensure constant synthesis of essential nonsterol isoprenoids, while avoiding toxic cholesterol accumulation. One mechanism involves sterol-induced ubiquitination of HMGCR, marking the enzyme for degradation from ER membranes, a process augmented by nonsterol isoprenoids. We examine the contribution of sterol-accelerated ubiquitination/degradation to overall regulation of HMGCR in livers of mice. **Methods:** Forty mice, including 20 wild-type (WT) and 20 knock-in (Ki) mice expressing ubiquitination-resistant HMGCR, were fed diets containing only chow, or chow supplemented with 0.1, 0.3, or 1% cholesterol. After five days of feeding, livers were harvested for measurements of cholesterol and triglycerides, immunoblot analysis, and qRT-PCR of genes related to cholesterol, nonsterol isoprenoid, and fatty acid synthesis. **Results:** Normalization of mRNA to protein levels indicates that HMGCR Ki livers contain a more HMGCR protein despite mRNA downregulation. Protein and gene expression of SREBP2 and its target genes, which contribute to cholesterol synthesis, decreased as expected with increased dietary cholesterol. Conversely, protein and gene expression of SREBP1 and its target genes increased, likely due to SREBP1c predominance toward fatty acid synthesis, which prevents cholesterol accumulation. **Conclusion:** The increase in HMGCR protein relative to mRNA suggests that significant post-transcriptional regulation exists in the form of impaired degradation. Furthermore, these normalized values indicate that accumulation of protein is primarily due to impaired degradation at lower cholesterol levels (chow, 0.1%); however, at high cholesterol levels (0.3, 1%), a greater degree of transcriptional control from sterol-mediated inhibition of SREBP2 regulates HMGCR due to negative feedback. This study demonstrates the role of degradative control on inhibition of HMGCR and may assist in reducing HMGCR accumulation during statin therapy.
S. Su: None. **K. Garland:** None. **Y. Jo:** None. **S. Hwang:** None. **G. Young:** None. **I. Fuentes:** None. **M. Schumacher:** None. **R. Elsabrouty:** None. **B. Johnson:** None. **R.A. Debose-Boyd:** Research Grant; Modest; NIH grants HL020948 and GM112409.

459
Protein Glutathionylation Promotes Calcification via Oxidative DNA Damage in Human Valve Endothelial Cells
Vincenza Valerio, Ctr Cardiologico Monzino, Milano, Italy; Silvia Montanari, Paola Songia, Benedetta Porro, Donato Moschetta, Laura Cavallotti, Veronika Myasoedova, Paolo Poggio, Ctr Cardiologico Monzino IRCCS, Milan, Italy

Background: Calcific aortic valve disease (CAVD) is one of the most common form of heart valve disease and affects 3% of the population. The initial phase, called aortic valve sclerosis (AVSc), is linked to inflammation and oxidative stress with direct consequences on endothelial cells. Thus, we aimed to evaluate the effects of protein glutathionylation caused by oxidative damage in endothelial cells. **Methods:** We analysed blood samples from 58 subjects, 29 with AVSc and 29 without (no-AVSc). The levels of oxidized (GSSG) and reduced (GSH) forms of glutathione were measured by a liquid chromatography-tandem mass spectrometry method and their ratio (GSH/GSSG) represent a recognized an oxidative stress status index. 2-AAPA, a glutathione reductase inhibitor, was used to increase GSSG levels. Human umbilical vein endothelial cells (HUVEC) were employed to create a model of protein glutathionylation. Valve endothelial cells (VEC) were isolated from pig and human aortic valves and were used to test and to validate this model. **Results:** Subjects with AVSc had a circulating GSH/GSSG ratio lower than no-AVSc (17.0±1.7 vs 24.4±2.6, respectively; p=0.02), indicating an increased systemic oxidative stress status in AVSc. Protein glutathionylation was increased more than 9-fold in human specimens from AVSc compared to no-AVSc subjects (p=0.03). In HUVECs, 2-AAPA significantly reduced the GSH/GSSG ratio (p=0.003) and induced an increment in protein glutathionylation of 1.91±0.17 fold compared to untreated cells (p=0.006). In pig VECs, 2-AAPA caused a 2-fold increment in reactive oxygen species production and an activation of the histone H2AX. In human VECs, protein glutathionylation caused an upregulation of smooth muscle actin (+0.7±0.16; p=0.004) and a downregulation of vascular endothelial cadherin (-0.4±0.02; p<0.0001) and, after 7 days, treated VECs were able to calcify at a greater extent (+2.83±0.4) than untreated cells (p<0.0001). **Conclusion:** These preliminary results show for the first time that protein glutathionylation could play a direct role in CAVD development via oxidative DNA damage. Restoring the proper balance of GSH and GSSG

may be beneficial to reduce the endothelial damage occurring in patients affected by CAVD.
V. Valerio: None. **S. Montanari:** None. **P. Songia:** None. **B. Porro:** None. **D. Moschetta:** None. **L. Cavallotti:** None. **V. Myasoedova:** None. **P. Poggio:** None.

460
Modulation of the SUMOylation of Fish Oil Receptor G-protein Coupled Receptor (GPR) 120 by AMP-activated Protein Kinase α2 Controls the Anti-Atherosclerotic Effects of Fish Oils in vivo
Chenghui Yan, Qulun Lu, Ping Song, Ctr for Molecular and Translational Med, Georgia State Univ, Atlanta, GA; Yaling Han, Cardiovascular Res Inst and Dept of Cardiology, General Hosp of Shenyang Military Region, Shenyang, China; Ming-hui Zou, Ctr for Molecular and Translational Med, Georgia State Univ, Atlanta, GA

BACKGROUND: Fish oils including eicosapentaenoic acid (EPA) and docosahexaenoic acid (DHA) have cardiovascular benefits in general population but fail to show therapeutic effects in patients with cardiovascular diseases (CVD). The aim of this study was to determine how fish oils are ineffective in CVD patients. **METHODS:** The effects of fish oils on atherosclerosis, the expression of AMP-activated protein kinase (AMPK), fish oil receptor G-protein coupled receptor (GPR) 120, and inflammation were assessed in CVD patients, atherosclerosis prone $LDLR^{-/-}$ mice with or without AMPKα2, lipid reversal atherosclerotic mouse model ($LDLR^{-/-}ApoB100^{+/+}$) and cultured cells. **RESULTS:** Healthy individuals had significant higher levels of EPA and DHA in blood than CVD patients. The levels of EPA or DHA were negatively correlated with SYTNAX scores in CVD patients with high AMPKα2 expression but had no correlation in those patients with low AMPKα2 expression. Administration of fish oils (5%, 12 weeks) significantly reduced aortic lesions and inflammation in both $LDLR^{-/-}$ mice and $LDLR^{-/-}ApoB100^{+/+}$ but not in $LDLR^{-/-}/AMPK\alpha2^{-/-}$ mice. In both human and mouse arteries, AMPKα2 was inversely correlated with GPR120. Further, AMPKα2 suppresses GPR120 SUMOylation resulting in an increase of GPR120 internalization. Consistently, GPR120 inhibition abolished the anti-atherosclerotic effects of fish oils in cultured cells. Moreover, selective inhibition of AMPKα2 but not AMPKα1 increased both SUMOylated protein UBC9 and its transcriptional factor c-myc expression. Furthermore, inhibition of c-myc ablated UBC9 transcription and GPR120 SUMOylation. Mechanistically, we found that AMPKα2 controls c-myc stability by phosphorylating c-myc at serine 67, a key site for its degradation. **CONCLUSION:** We conclude that AMPK α2 mediates the anti-atherosclerotic effects of fish oils by modulating GPR120 SUMOylation and internalization.
C. Yan: None. **Q. Lu:** None. **P. Song:** None. **Y. Han:** None. **M. Zou:** None.

461
Enhanced Glycolysis in Endothelial Cells Protects Against Atherosclerosis
Qiuhua Yang, Jiean Xu, Peking Univ, Shenzhen, China; Zhiping Liu, Varadarajan Sudhahar, Augusta Univ, augusta, GA; Qian Ma, Yapeng Cao, Lina Wang, Xianqiu Zeng, Yaqi Zhou, Min Zhang, Peking Univ, Shenzhen, China; Yiming Xu, Guangzhou Medical Univ, Guangzhou, China; Yong Wang, Chengdu Univ of TCM, Chengdu, China; Neal Weintraub, Augusta Univ, Augusta, GA; Chunxiang Zhang, Univ of Alabama at Birmingham, Birmingham, AL; Tohru Fukai, Augusta Univ, Augusta, GA; Chaodong Wu, Texas A&M Univ, College Station, TX; Mei Hong, Peking Univ, Shenzhen, China; Fulton David, Yuqing Huo, Augusta Univ, Augusta, GA

Background: Increased aerobic glycolysis in endothelial cells (ECs) of atheroprone areas of blood vessels is hypothesized to drive increased inflammation and lesion burden but the direct links are not yet established. The goal of this study was to determine how metabolic adaptation in ECs impacts atherosclerosis. **Methods**: The immunostaining, Real-time PCR, Western blots, Seahorse assayes are used to analyze the expression and activity of PRKA/AMPKs and metabolic glycolysis in the arterial endothelium of mice and cultured endothelial cells under disturbed flows. Staining of Edu, TUNNEL and Evans blue were utilized to evaluate endothelial turnover and endothelium integrity. Oil Red O staining and histological cellular characterization were performed to evaluate atherosclerosis. **Results**: ECs exposed to disturbed flow in vivo and in vitro exhibit increased levels of PRKA/AMPKs (protein kinase AMP-activated; AMP-activated protein kinases) and glycolysis. Selective deletion of endothelial Prkaa1 (protein kinase AMP-activated catalytic subunit alpha1) reduced glycolysis, compromised EC proliferation and EC monolayer integrity, and accelerated the formation of atherosclerotic lesions in hyperlipidemic mice. Rescue of impaired glycolysis in Prkaa1-deficient ECs through Slc2a1 transfection enhanced EC viability and integrity of the EC barrier and reversed susceptibility to atherosclerosis. These results suggest that increased glycolysis in the endothelium of atheroprone arteries is a protective mechanism. **Conclusions**: Endothelial glycolysis plays a vital role in EC proliferation, repair of the EC monolayer, and protects mice from atherosclerosis. Thus, approaches such as activating AMPK activity or increasing endothelial glycolysis are preventive and therapeutic for arterial diseases.

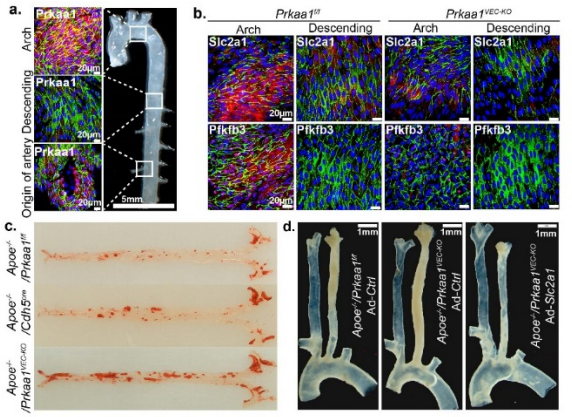

Figure. Enhanced glycolysis in endothelial cells protects against atherosclerosis. a. Increased expression of Prkaa1/AMPK in the endothelium of lesion-prone artery. **b.** The endothelial glycolysis is decreased on the endothelium of lesion-prone artrey in *Prkaa1* EC deficient mice. **c.** Loss of endothelial *Prkaa1* increases atherosclerosis in *Apoe*$^{-/-}$ mice. **d.** Overexpression of endothelial *Slc2a1* suppresses aggravated atherosclerosis in *Apoe*$^{-/-}$/*Prkaa1*$^{VEC-KO}$ mice.

Q. Yang: None. **J. Xu:** None. **Z. Liu:** None. **V. Sudhahar:** None. **Q. Ma:** None. **Y. Cao:** None. **L. Wang:** None. **X. Zeng:** None. **Y. Zhou:** None. **M. Zhang:** None. **Y. Xu:** None. **Y. Wang:** None. **N. Weintraub:** None. **C. Zhang:** None. **T. Fukai:** None. **C. Wu:** None. **M. Hong:** None. **F. David:** None. **Y. Huo:** None.

462
Low Carbohydrate High Protein (LCHP) Diets Are Atherogenic by Modulating Macrophage Mtorc1-mitophagy Signaling to Accelerate Apoptosis and Plaque Complexity
Xiangyu Zhang, Washington Univ, Saint Louis, MO

Low carbohydrate high protein (LCHP) diets which are commonly utilized for weight loss have been reported to raise cardiovascular risk. However, the mechanisms underlying this risk are unknown. We first confirm that LCHP diets increase atherosclerotic lesion area with a particular rise in plaque complexity. Mass spectrometry analysis reveals protein ingestion acutely elevates amino acid levels in blood and atherosclerotic plaques with concomitant stimulation of macrophage mTORC1 signaling. This activation is causal as LCHP diet-induced plaque progression is abrogated in macrophage-specific Raptor-null mice. A prominent effect of certain amino acids, such as leucine, on macrophages is the synergistic exacerbation of

macrophage apoptosis induced by atherogenic lipids. More specifically, leucine stimulates mTORC1-dependent inhibition of autophagy which hinders the mitophagic removal of dysfunctional and pro-apoptotic mitochondria. This amino acid-mTORC1-autophagy signaling axis is supported in vivo by 1) the absence of reduced atherosclerosis in mice dually deficient in macrophage mTORC1 and autophagy (Raptor/ATG5-/-) and 2) the absence of increased atherosclerosis in macrophage autophagy-deficient (ATG5-/-) mice fed a LCHP diet. Our data provide the first mechanistic details of the deleterious effects of high protein diets on macrophages and atherosclerotic progression. Incorporation of these concepts in clinical studies will be important to define the vascular effects of dietary protein.
X. Zhang: None.

466
Carotid Atherosclerosis on the Association Between Hypothyroidism and Renal Dysfunction in a Healthy Japanese Population
Norihiro Furusyo, Yuuki Tanaka, Hiroaki Ikezaki, Masayuki Murata, Jun Hayashi, Kyushu Univ Hosp, Fukuoka, Japan

Aim: This large-scale Japanese population study was done to evaluate the relation between the serum thyroid stimulating hormone (TSH) level and renal function. Methods: Among 1,374 residents who attended a free public physical examination between 2010 and 2011, we evaluated the data of 888 for whom the serum TSH level and estimated glomerular filtration rate (eGFR) were successfully measured. The participants were divided into three groups by TSH level (normal TSH, ≤2.4; high-normal TSH, 2.5-4.4; subclinical hypothyroid, ≥4.5 μIU/L). Multiple linear regression analysis adjusted for cardiovascular risk factors was done to determine the relation between serum TSH level and renal function. Results: The mean ± SD TSH level was 2.0±1.4 μIU/mL. Of the participants, 75.9% (n=674) had a normal TSH level, 17.9% (n=159) were high-normal TSH, and 6.2% (n=55) were subclinical hypothyroid. The mean eGFR significantly decreased with increased TSH level (normal TSH group, 79.3±14.1; high-normal TSH group, 77.4±13.0; subclinical hypothyroid group; 72.3±12.2 mL/min/1.73m2: P for trend <0.01). Multiple linear regression analysis extracted log-transformed TSH level as an independent factor correlated with eGFR in the high-normal TSH group (beta=-0.18, P=0.02). Conclusions: The eGFR level significantly decreased with increased TSH level. Significant correlation between TSH and eGFR levels was found only in high-normal TSH individuals. Even in healthy individuals, increase risk of chronic kidney disease could be started from high-normal TSH level.
N. Furusyo: None. **Y. Tanaka:** None. **H. Ikezaki:** None. **M. Murata:** None. **J. Hayashi:** None.

467
Lipoproteins and Cardiovacular Disease Risk
Hiroaki Ikezaki, Tufts Univ, Boston, MA; Virginia A. Fisher, Ching-ti Liu, L. Adrienne Cupples, Boston Univ, Boston, MA; Ernst J Schaefer, Tufts Univ, Boston, MA

Objectives: Elevated serum levels of low density lipoprotein cholesterol (LDL-C), small dense LDL-C (sdLDL-C), remnant lipoprotein cholesterol (RLP-C), and lipoprotein (a) or Lp(a) and low high density lipoprotein cholesterol (HDL-C) have all been associated with increased cardiovascular disease (CVD) risk. Our goal was to assess direct measurements of these lipoproteins as compared to standard risk factors (age, gender, hypertension, hypertension treatment, diabetes, smoking, total cholesterol, and HDL-C) in the Framingham Offspring Study (FOS). **Methods:** Stored frozen plasma samples (-80 degrees C) obtained after an overnight fast from male and female participants free of CVD at cycle 6 of FOS were used (n=3,147, mean age 58 years, with 677 (21.5%) developing CVD over 16 years. Total cholesterol, HDL-C, direct LDL-C, sdLDL-C, remnant lipoprotein cholesterol (RLP-C), Lp(a), and high sensitivity C reactive protein (hsCRP) were measured by standardized automated analysis. Large buoyant LDL-C (lbLDL-C) (direct LDL-C - sdLDL-C) and calculated LDL-C (total cholesterol-HDL-C - TG/5) were also calculated. **Results**: For all CVD risk on univariate analysis significant factors with p values in parentheses in order of significance were: age ($8.1x10^{-41}$), hypertension ($3.2x10^{-23}$), HDL-C ($4.2x10^{-16}$), sdLDL-C ($4.2x10^{-14}$), hypertension treatment ($1.5x10^{-14}$), gender ($1.7x10^{-10}$), diabetes ($5.1x10^{-9}$), direct LDL-C ($8.2x10^{-9}$), body mass index ($9.2x10^{-7}$), calculated LDL-C ($6.2X10^{-6}$), RLP-C ($8.0 X 10^{-4}$) cholesterol medication ($1.8 X 10^{-4}$), total cholesterol (0.00081) smoking (0.0024), hsCRP (0.005), and Lp(a) (0.024). On multivariate analysis sdLDL-C, direct LDL-C, hsCRP, and Lp(a) were still significant using the model including all standard risk factors. All four parameters significantly improved the model C statistic and net risk reclassification. **Conclusions:** Our data indicate that for CVD risk prediction in FOS direct LDL-C is significantly better than calculated LDL-C, that HDL-C, sdLDL-C, direct LDL-C, RLP-C, and Lp(a) are all atherogenic, and that after standard risk factors, sdLDL-C, direct LDL-C, Lp(a), and hsCRP all add significant information.
H. Ikezaki: None. **V.A. Fisher:** None. **C. Liu:** None. **L. Cupples:** None. **E.J. Schaefer:** None.

468
Cross-species Comparison of Genetic Networks of Coronary Artery Disease
Zeyneb Kurt, Rio Elizabeth Barrere-Cain, Christine Sun, Yuqi Zhao, Calvin Pan, UCLA, Los Angeles, CA; Arno Ruusalepp, Dept of Cardiac Surgery, Tartu Univ Hosp, Tartu, Estonia; Oscar Franzén, Simon Koplev, Johan L Bjorkegren, Icahn Sch of Med at Mount Sinai, New York, NY; Aldons J Lusis, Xia Yang, UCLA, Los Angeles, CA

The genetic architecture of coronary artery disease (CAD), which represents the leading cause of death worldwide, has been investigated in both human populations and mouse models. However, whether the two species share similar genetic underpinnings has not been thoroughly evaluated. We hypothesize that a comprehensive data-driven integrative study leveraging multi-omics data resources will allow a tissue-specific, systems level assessment of the key similarities and differences in disease networks between mouse and man. To derive CAD genetic networks in mouse, we used genetic data from genome-wide association studies (GWAS) of atherosclerosis and functional genomics data of aorta and liver tissues from >100 strains profiled in an Atherosclerosis Hybrid Mouse Diversity Panel. To model human CAD genetic networks, we used human CAD GWAS from CARDIoGRAM+C4D, and functional genomics data from aorta and coronary arteries, and liver tissues from the Stockholm-Tartu Atherosclerosis Reverse Networks Engineering Task and Genotype-Tissue Expression biobanks. We identified coexpression network modules and biological pathways that were significantly associated with genetic signals in each species. This tissue-specific analysis revealed that ~75 and ~80% of the pathways and networks were shared between species for vascular and liver tissues, respectively. The shared processes between species for both tissues included lipid and lipoprotein metabolism, MAPK, TCA, and notch signaling pathways; for vascular tissues the shared terms included biological oxidations, interferon, and cytokine signaling; for liver tissue, fatty acid metabolism, TGF-beta signaling, leukocyte transendothelial migration were shared between species. Viral myocarditis, platelet-derived growth factor signaling, fibrinolysis, and IL6/7 pathways were identified as human-specific, while insulin and nerve growth factor signaling were found to be mouse-specific. This cross-species tissue-specific integrative analysis provides insights into the convergent and divergent causal mechanisms underlying CAD between species and highlights the conditions in which mouse may or may not serve as a surrogate model for human CAD in disease mechanistic and preclinical studies.

Z. Kurt: None. **R.E. Barrere-Cain:** None. **C. Sun:** None. **Y. Zhao:** None. **C. Pan:** None. **A. Ruusalepp:** None. **O. Franzén:** None. **S. Koplev:** None. **J.L.M. Bjorkegren:** None. **A.J. Lusis:** None. **X. Yang:** None.

This research has received full or partial funding support from the American Heart Association.

469

APOL1 Genotypes and Risk of Heart Failure: an Additive Genetic Effect in the Elderly, but Not in the Young Adults in Patients with Chronic Kidney Disease

Longjian Liu, Drexel Univ, Philadelphia, PA; Ming Chen, Chongqing Medical Univ, Chongqing, China; Yuna Kim, Drexel Univ, Philadelphia, PA; Hong Jia, Southwest Medical Univ, Luzhou, China; Yong Long, The Fourth Military Medical Univ, Xi'an, China; Yichen Zhong, Drexel Univ, Philadelphia, PA; Ellie Kelepouris, Howard J Eisen, Drexel Univ Coll of Med, Philadelphia, PA

Objective; Apolipoprotein L1 (APOL1), the major protein component of HDL, is identified having an association with renal disease in African Americans (AA). We assessed the hypothesis that the genetic variations in APOL1 (G1 and G2 alleles) are associated with risk of heart failure (HF), and this effect is modified by age.
Methods: Subjects aged 21-75, with an estimated GFR (eGFR) of 20 to 70 ml/min/1.73 m^2 at baseline recruitments (April 2003-Sept 2008), who were free of HF participating in the Chronic Renal Insufficiency Cohort (CRIC) Study and followed-up through March 2013 are analyzed (White: 1335, AA:1323). The associations of APOL1 risk genotype (assessed by either 1 of the G1 and G2, or 2 of their combinations, i.e., G1/G1, G1/G2 or G2/G2) with incident HF and mortality are examined using Cox's regression models.
Results: Within a mean 7-year (SD: 2.1) follow-up, AA had a significantly higher incidence of HF than White (2.62 vs. 1.67 per 100 person-year (PY), p=0.006) in those aged<65, and 3.94 vs. 2.71 per 100 PY (p=0.026) in those aged≥65. Cox's models, with adjusted age, sex, eGFR and HDL, indicate that compared to White, AA aged<65 without or with 1 of either G1 or G2 had a significantly higher risk of HF [Hazard Ratio, HR: 2.15 (95%CI: 1.59-2.92, p<.0001), followed by those with either 2 of G1/G1, G1/G2 or G2/G2 alleles (1.47, 0.88-2.48, p=0.15)]. However, a significant additive genetic effect of the number of risk alleles (i.e., 0,1,2) is observed in AA aged ≥65. The corresponding HRs (95%CI) are 1.73 (1.17-2.57, p=0.007) in those without or with either 1 of the G1 or G2, and 2.17 (1.20-3.94, p=0.011) in those with either 2 of the G1 and G2 combination. A significant interaction effect of age (≥65 vs. <65) and the risk alleles (2 vs. 0/1) is observed (HR: 2.45, 95%CI: 1.14-5.28, p=0.02). Similar associations between APOL1 alleles and mortality from HF and all-cause are seen by the two age groups.
Conclusion: African Americans with APOL1 risk alleles have significantly higher risk of HF and mortality than White. An additive genetic effect of the number of APOL1 risk alleles is shown among AA aged ≥65, but not in the younger adults. The modifying effect of age suggests that a possible 'different genetic-risk window' by ages warrants consideration in HF control and prevention.
L. Liu: None. **M. Chen:** None. **Y. Kim:** None. **H. Jia:** None. **Y. Long:** None. **Y. Zhong:** None. **E. Kelepouris:** None. **H.J. Eisen:** None.

470

Ultrasound Carotid Plaque Features, Cardiovascular Disease Risk Factors and Events: the Multi-Ethnic Study of Atherosclerosis

Carol Mitchell, Claudia E Korcarz, Univ of Wisconsin Madison, Madison, WI; Adam D Gepner, Univ of Wisconsin Madison, Willliam S. Middleton VA Memorial Hosp, Madison, WI; Joel D Kaufman, Univ of Washington, Seattle, WA; Wendy S Post, Johns Hopkins Hosp, Baltimore, MD; Russell Tracy, Univ of Vermont, Colchester, VT; Amanda J Gassett, Nanxun Ma, Robyn L McClelland, Univ of Washington, Seattle, WA; James H Stein, Univ of Wisconsin Madison, Madison, WI

Background: Grayscale ultrasound atherosclerotic plaque characteristics may predict cardiovascular disease (CVD) events, though they have not been investigated in a large primary prevention cohort. This study determined if CVD risk factors were associated with carotid plaque ultrasound characteristics and if these characteristics could predict future coronary heart disease (CHD) and stroke/transient ischemic attack (TIA) events in a multi-ethnic cohort free of known CVD at baseline.
Methods: We measured carotid artery total plaque area (TPA) and grayscale carotid plaque features (grayscale median, black areas, and discrete white areas) at baseline in participants of the Multi-Ethnic Study of Atherosclerosis that had B-mode carotid ultrasound examinations. There were 2205 participants with images available for TPA analyses and 1703 with images available for grayscale analyses. Multivariable linear regression analysis was used to examine relationships between baseline ultrasound carotid plaque features and CVD risk factors. Cox proportional hazards models were used to assess their ability to predict incident CHD and stroke/TIA events over an average follow-up of 13.3 years. The predictive characteristics of TPA and carotid plaque features were compared to carotid plaque score and coronary artery calcification (CAC) score.
Results: Participants were mean (standard deviation) 65.4 (9.6) years old, 49% male, 39% White, 28% Black, 22% Hispanic, and 11% Chinese. Mean TPA (27.7 [24.7] $mm^{2)}$, but not grayscale plaque features, were associated with several CVD risk factors. In risk factor-adjusted models, TPA was the only plaque feature that predicted incident CHD events (HR 1.23; 95% CI 1.11-1.36; p<0.001) with C-statistics for CHD that were similar to carotid plaque score, but lower than CAC score. TPA did not independently predict stroke/TIA events. No gray scale plaque feature predicted future CHD or stroke/TIA events.
Conclusions*:* In middle-aged individuals free of known CVD, carotid TPA was associated with CVD risk factors and predicted incident CHD events while grayscale plaque features did not. For CHD, predictive characteristics of TPA were similar to carotid plaque score but lower than CAC score.
C. Mitchell: Other; Modest; Davies Publishing Inc., authorship for two echocardiography textbooks, currently under review, may have future royalties. Elsevier, Wolters Kluwer, author textbook chapters, may have future royalties.. **C.E. Korcarz:** None. **A.D. Gepner:** None. **J.D. Kaufman:** None. **W.S. Post:** None. **R. Tracy:** None. **A.J. Gassett:** None. **N. Ma:** None. **R.L. McClelland:** None. **J.H. Stein:** Other; Significant; Wisconsin Alumni Research Foundation - patent related to carotid wall thickness and vascular age.

471

Influence of Platelet-specific Soluble Guanylyl Cyclase Deficiency on Atherosclerotic Plaque Formation

Marlène Stroth, Noomen Bettaga, Jana Wobst, Julia Werner, Anna-Sophia Zimmermann, German Heart Ctr Munich, Munich, Germany; Andreas Friebe, Univ of Wuerzburg, Wuerzburg, Germany; Hendrik B. Sager, Heribert Schunkert, Thorsten Kessler, German Heart Ctr Munich, Munich, Germany

Introduction: The genomic locus harboring the *GUCY1A3* gene has been associated with coronary artery disease (CAD) with the risk variant reducing *GUCY1A3* expression via allele-specific transcription factor binding. The gene encodes the $alpha_1$-subunit of the soluble guanylyl cyclase (sGC) which produces the second messenger cyclic guanosine monophosphate (cGMP) upon activation by nitric oxide, thereby influencing the function of vascular smooth muscle cells and platelets. **Aim**: To investigate whether a reduction in sGC expression specifically in platelets

influences atherosclerotic plaque formation. **Methods**: By crossbreeding Pf4-Cre and sGC $\beta_1^{fl/fl}$ mice, platelet-specific sGC knockout (PS-sGC$^{-/-}$) mice were generated. These were crossbred with *Ldlr*$^{-/-}$ mice to generate PS-sGC$^{-/-}$*Ldlr*$^{-/-}$ mice. PS-sGC$^{-/-}$*Ldlr*$^{-/-}$ and *Ldlr*$^{-/-}$ mice were fed a high-cholesterol diet (HCD) for 10 weeks. Serial sections of the aortic root were analyzed by Masson-Trichrome staining. Inflammatory cells in aortae were assessed using flow cytometry. *In vitro* adhesion assays using wildtype endothelial cells (EC) and monocytes were performed in presence of plasma of activated platelets. **Results**: PS-sGC$^{-/-}$*Ldlr*$^{-/-}$ (n=13) mice displayed enhanced total plaque size compared to *Ldlr*$^{-/-}$ (n=15) mice ($247 \cdot 10^3$ vs. $190 \cdot 10^3$ µm^2, p<0.05). After HCD, more neutrophils (747 vs. 448, p<0.05) and Ly6C^{high} monocytes (366 vs. 207, p<0.05) were detected in PS-sGC$^{-/-}$ *Ldlr*$^{-/-}$ compared to *Ldlr*$^{-/-}$ mice indicating enhanced recruitment of these cells in PS-sGC$^{-/-}$*Ldlr*$^{-/-}$ mice. In *in vitro* adhesion assays, incubation of mouse aortic EC and monocytes with plasma from PS-sGC$^{-/-}$ platelets resulted in enhanced adhesion of monocytes to EC compared to plasma from wildtype platelets (13%, p<0.01). **Conclusion and Outlook**: Platelet-specific knockout of sGC led to increased atherosclerotic plaque formation and inflammation. *In vitro* adhesion assay results point to an enhanced stimulation of leukocyte adhesion to endothelial cells in PS-sGC$^{-/-}$ mice. Hence, factors released by platelets secondary to reduced sGC expression could mediate increased risk of CAD. Inhibiting platelet activation in carriers of the human risk variant might therefore be a promising therapeutic strategy to reduce risk of CAD.
M. Stroth: None. **N. Bettaga:** None. **J. Wobst:** None. **J. Werner:** None. **A. Zimmermann:** None. **A. Friebe:** None. **H.B. Sager:** None. **H. Schunkert:** None. **T. Kessler:** None.

472
Identifying and Characterizing Causal Genes in GWAS-identified Loci for Triglyceride Levels Using High-throughput, Image-based Screens in Zebrafish Larvae
Benedikt von der Heyde, Uppsala Univ, IGP, Uppsala, Sweden; Mauro Masiero, ETH Zuerich, Zuerich, Switzerland; Anastasia Emmanouilidou, Tiffany Klingström, Marcel den Hoed, Uppsala Univ, IGP, Uppsala, Sweden

Background: High triglyceride levels are an established risk factor for coronary artery disease (CAD). Unpublished results from our proof-of-principle studies show that triglyceride-levels are also associated with atherosclerosis in zebrafish larvae. Identifying and characterizing causal genes for triglyceride levels may yield novel drug targets. In 2013, a meta-analysis of genome-wide association studies identified 37 previously unanticipated loci that are associated with triglyceride levels. We aim to characterize positional candidate genes in these loci using a zebrafish model system. **Methods**: We prioritized 37 candidate genes for functional-follow up. These genes together have 41 zebrafish orthologues, which were targeted in five lines of ~8 genes each using a multiplex CRISPR-Cas9 approach. Founder mutants have been raised and 384 offspring for two of the five lines have so far been screened for body size as well as fluorescently labeled lipids, macrophages and neutrophils in the vessel wall, using a high-throughput imaging set-up. Image quantification was performed using automated, custom-written pipelines in CellProfiler and ImageJ. Additionally, whole body lipid fractions and glucose levels were measured in each larva using enzymatic assays. CRISPR-induced mutations were quantified using paired-end sequencing and data were analyzed using hierarchical mixed models and (zero-inflated) negative binomial regression.
Results: Each additional disrupted allele in *pepd* resulted in higher triglyceride levels (beta±SE 0.21±0.09 SD). Mutants for *met* have less vascular infiltration by macrophages (-0.31±0.13), and less co-localization of macrophages with lipids (-0.56±0.21) and neutrophils (-0.49±0.18). Mutants for *lpar2* have lower LDLc (-0.54±0.27) and HDLc levels (-0.57±0.27), while *gmip* mutants have less vascular lipid deposition (-1.05±0.43), and less co-localizing lipids and neutrophils (-1.26±0.56). **Conclusion**: By characterizing candidate genes for triglyceride levels using a high-throughput, largely image-based approach in zebrafish larvae, we identified previously unanticipated genes that influence a range of cardiometabolic risk factors. This approach is anticipated to identify novel drug targets.
B. von der Heyde: None. **M. Masiero:** None. **A. Emmanouilidou:** None. **T. Klingström:** None. **M. den Hoed:** None.

476
The Role of N-glycosylation in the Myogenic Differentiation of Stem Cells to Vascular Smooth Muscle Cells
Eoin Corcoran, Abidemi Olayinka, Brendan O'Connor, Paul A Cahill, Dublin City Univ, Dublin, Ireland

Cell fate decisions within the vasculature are crucial to the pathogenesis of vascular diseases, including, arteriosclerosis, atherosclerosis and restenosis after angioplasty. Notch signalling is involved in regulating cell fate in vasculature development during embryogenesis resulting in altered cell fate decisions leading to vascular disease. The Notch signalling pathway is highly regulated by a number of mechanisms including glycosylation, a post-translational modification.
Our main objective was to define a putative role for N-glycosylation of the Notch1 receptor in controlling resident vascular stem cell fate *in vitro*. Utilising ligand Jagged-induced Notch signalling assay, qRT-PCR, immunocytochemistry, ectopic expression of Notch1 receptor, siRNA knockdown, pharmacological inhibition and enzyme linked lectin assay (ELLA), alterations in N-glycan decoration of the Notch1 receptor were assessed before evaluation of their effects on Notch signalling and Notch ligand promotion of myogenic differentiation.
N-glycosylation of the Notch1 receptor was assessed using a combination of the HPLC and ELLA assays and confirmed the presence of N-glycans on the receptor, an effect that was abrogated following inhibition of glycosyltransferase activity with tunicamycin and lunatic fringe (Lfng) knockdown. Jagged1-induced Notch activation increased Notch target gene expression and promoted myogenic differentiation of bone-marrow derived mesenchymal stem cells and resident vascular stem cells. Selective knockdown of the Notch1 receptor in stem cells resulted in a significant decrease in Jagged1 stimulated Hey1 expression, a Notch1 target gene, concomitant with a reduction in myogenic differentiation due to decreased smooth muscle differentiation marker expression (CNN1 and MYH11 mRNA and protein levels). Inhibition of N-glycosylation with tunicamycin lead to a down regulation of smooth muscle differentiation markers, CNN1 and MYH11 independent of a reduction in Notch target gene expression. Lfng knockdown lead to a similar significant reduction in Jagged1 induced myogenic differentiation (reduced CNN1 expression). Collectively, these results suggest that N-glycosylation of Notch1 receptor is involved in Notch signalling leading to altered resident vascular stem cell fate.
E. Corcoran: None. **A. Olayinka:** None. **B. O'Connor:** None. **P.A. Cahill:** None.

477
Platelet microRNAs Crosstalk with Vascular Endothelial Cells in Diabetes
Seema Dangwal, Inst for Molecular and Translational Therapeutic Strategies, Hanover Medical Sch, Hanover, Germany; Bernd Stratmann, Heart and Diabetes Ctr NRW, Ruhr Univ Bochum, Bad Oeynhausen, Germany; Xiao Ke, Inst for Molecular and Translational Therapeutic Strategies, MH-Hannover, Hannover, Germany; Petra Kleinbongard, Gerd Heusch, Inst for Pathophysiology, West German Heart and Vascular Ctr, Univ of Essen Medical Sch, Essen, Germany; Raimund Erbel, West German Heart and Vascular Ctr, Univ of Essen Medical Sch, Essen, Germany; Diethelm

Tschoepe, Heart and Diabetes Ctr NRW, Bad Oeynhausen, Germany; Thomas Thum, Inst for Molecular and Translational Therapeutic Strategies, Hanover Medical Sch, Hannover, Germany

Platelets are major source of extracellular miRNAs (miRs) constituting the plasma miR-pool. Here we generated miR-profile of leukocyte depleted platelets (LDP) isolated from type-2 diabetic (T2DM) or healthy subjects and investigated mechanism of miRNA mediated vascular crosstalk.
LDPs were obtained by leukocyte filtration of platelet rich plasma isolated from blood withdrawn from T2DM (6 males, age: 54.8±7.6 yr; HbA1c: 8.9±0.6%; BMI: 30.9±2.8kg/m2) and healthy subjects (10 males, age: 49.2±6.8yr; HbA1c: 5.3±0.2%; BMI: 26.6±3.8kg/m2). MiR-profile was generated using total RNA isolated from T2DM or healthy LDPs. Students t-test applied to compare groups and $p \leq 0.05$ considered significant.
Among all detected 735 miRs (cutoff<29 Ct), 19.5% miRs were depleted, whereas 7.5% showed >2 fold increase in T2DM-LDPs. Compared to healthy LDPs (n=10), depletion of 14 platelet-enriched miR candidates, including miR-21 and -22, were validated by RTPCR in individual T2DM-LDPs (n=11) irrespective of aspirin intake or presence of coronary heart disease.Ex-vivo thrombin stimulation of washed healthy platelets increased the release of miRNA into cellular-supernatants and confocal microscopy confirmed the cellular uptake of platelet released miRNA-carrying microparticles into human coronary artery endothelial cells (ECs) within 2-24h. In addition, EC overexpression of miR-21 or -22 decreased cell proliferation, whereas miR-22 also attenuated their tube forming capacity. MiR-21 or -22 modulations inversely regulated gene expression of their common predicted target, the cell-cycle regulator gene-CDK-6. MiR concentrations were also measured in particulate debris and plasma derived from coronary aspirates retrieved during stent implantation from 3 T2DM or 4 non-diabetic patients. In line, higher miR-21 or -22 ratios in plasma to particulate debris in T2DM vs non-diabetic aspirates indicated miR release from particulate debris into coronary plasma. This in turn provides relatively richer miR-21 or -22 microenvironment to the vicinal vascular ECs.
T2DM platelets show distinct miR-profile compared to healthy platelets and depletion of miRNAs may represent their active secretion from diabetic platelets. Altered coronary microenvironment may lead to altered cellular responses to injury in diabetic vessels.
S. Dangwal: None. **B. Stratmann:** None. **X. Ke:** None. **P. Kleinbongard:** None. **G. Heusch:** None. **R. Erbel:** None. **D. Tschoepe:** None. **T. Thum:** Employment; Significant; Cardior Pharmaceuticals.

478
Resident Multipotent Vascular Stem Cells Isolated From Susceptible and Non-susceptible Arteriosclerotic Regions of the Mouse Aorta Are Sca1/s100β/nestin$^+$ and Respond Similarly to the Same Myogenic Inductive Stimulus
Mariana Di Luca, Emma Fitzpatrick, Dublin City Univ, Dublin, Ireland; Weimin Liu, David Morrow, Eileen M Redmond, Univ of Rochester, Rochester, NY; Paul A Cahill, Dublin City Univ, Dublin, Ireland

Vascular remodeling leading to arterial obstruction is a hallmark of arteriosclerosis and in-stent restenosis and is due in part to the accumulation of vascular smooth muscle (SMC)-like cells within the vessel wall. The source of these vascular cells has been controversial with many studies providing compelling evidence for a putative role for stem cell-derived myogenic progeny. It is known that neuroectoderm-derived vascular regions (ascending aorta, aortic arch, carotid artery) are more susceptible to arteriosclerotic lesion formation in comparison with mesoderm derived regions (descending and abdominal aorta, femoral artery). Our aim was to isolate and characterize stem cells from arteriosclerotic-susceptible and non-susceptible regions and determine their differential responsiveness to discrete myogenic inductive stimuli. A population of myosin heavy chain (Myh11$^-$) negative, Sca1/S100β/Nestin$^+$ multipotent vascular stem cells (MVSCs) was first shown to accumulate within the intima of murine carotid arteries following injury using Sca1 and S100β e-GFP transgenic mice. Resident MVSCs were isolated from mouse aorta arch (susceptible) and descending aorta (non-susceptible) by enzymatic dissociation and initial seeding on non-adherent plates for 48 h before suspended cells were re-seeded on adherent plates and grown in B27 supplemented maintenance media. Cells were characterized by fluorescent immunocytochemistry using stem (Sca1/S100β/Nestin) and vascular SMC cell markers (CNN1 and Myh11). MVSCs from both aortic arch and descending aorta were positive for stem cell markers but negative for Myh11 and Cnn1. Treatment of both cell populations with TGF-β1 or the Notch ligand, Jagged-1 for 7 days promoted myogenic differentiation by increasing the number of cells expressing SMC markers concomitant with increased Myh11 and CNN1 mRNA levels, respectively. There was no difference in the responsiveness of stem cells from either arteriosclerotic-prone and non-prone regions. We conclude that the aortic arch and descending aortic region both house a neuroectoderm-derived Sca1/S100β/Nestin$^+$ stem cell population that responds similarly to myogenic inductive stimulation.
M. Di Luca: None. **E. Fitzpatrick:** None. **W. Liu:** None. **D. Morrow:** None. **E.M. Redmond:** None. **P.A. Cahill:** None.

479
Dickkopf-3 Binds to CXCR7 of Vascular Progenitor Cells to Enhance Degradable Graft Regeneration
Shirin Issa Bhaloo, Yifan Wu, Alexandra Le Bras, **Yanhua Hu**, Qingbo Xu, King's Coll London, London, United Kingdom; Qiang Zhao, Nankai Univ, Tianjin, China

Background: Dickkopf-3 (Dkk3) is a secreted protein that may have a role in vascular diseases by promoting smooth muscle cell (SMC) differentiation and endothelial repair, two processes in which vascular stem/progenitor cells could be involved. However, the effect of Dkk3 on stem/progenitor cell migration and its specific receptor on these cells remain unknown. **Methods:** Vascular stem/progenitor cells (VPCs) were isolated from murine aortic adventitia and selected for the Sca-1 marker. The chemotactic ability of Dkk3 for Sca-1+ cells was tested *in vitro* using transwell and wound healing assays and *ex vivo* by the aortic ring assay. Chemokine receptors identification was carried out using Western blot (WB), siRNA-mediated knockdown, co-Immunoprecipitation (Co-IP) and saturation binding assays. To assess *in vivo* the role of Dkk3 in recruiting Sca-1+ cells, tissue-engineered vessel grafts, with or without Dkk3, were fabricated and implanted to replace the rat abdominal aorta. **Results:** We demonstrated that Dkk3 induced the chemotaxis of Sca-1+ cells *in vitro,* and *ex vivo* in culture of aortic rings derived from Sca-1-GFP transgenic mice. Flow cytometry and WB analysis revealed that Sca-1+ cells expressed CXCR7, while overexpression or knockdown of CXCR7 resulted in alterations in cell migration. Interestingly, Co-IP experiments showed the physical interaction between DKK3 and CXCR7, and specific saturation binding assays identified a high affinity Dkk3-receptor binding with a dissociation constant of 14.14 nM. Activation of CXCR7 by Dkk3 triggered the ERK1/2, PI3K/AKT, Rac1 and RhoA signalling pathways. Furthermore, when Dkk3-loaded tissue-engineered vessels were grafted to the abdominal artery of rats, the grafts showed efficient endothelization and recruitment of VPCs, which had acquired characteristics of mature SMCs. CXCR7 blocking using specific antibodies in our vessel graft model hampered stem/progenitor cell recruitment into the vessel wall, thus compromising vascular remodelling.
Conclusions: We provide novel and solid evidence that CXCR7 serves as Dkk3 receptor, which mediates Dkk3-induced VPCs migration *in vitro* and in tissue-engineered vessels, hence harnessing patent grafts resembling native blood vessels.

S. Issa Bhaloo: None. **Y. Wu:** None. **A. Le Bras:** None. **Y. Hu:** None. **Q. Xu:** None. **Q. Zhao:** None.

480
Injury-Activated Vascular Cells Share a Common Photonic Fingerprint with Stem Cell-Derived Myogenic Progeny Following Interrogation Using a Lab-on-a-Disc (Load) Platform
Claire Molony, Damien King, Lourdes A Julius, Emma Fitzpatrick, Mariana Di Luca, Gillian Casey, Roya Hakimjavadi, Denise Burtenshaw, Killian Healy, Daniel Canning, David Kernan, Dublin City Univ, Dublin, Ireland; Andreu Llobera, Ctr Nacional de Microelectronica, Campus UAB,, Barcelona, Spain; Weimin Liu, David Morrow, Eileen M Redmond, Univ of Rochester, Rochester, NY; Jens Ducree, Paul A Cahill, Dublin City Univ, Dublin, Ireland

The accumulation of vascular smooth muscle (SMC)-like cells within the intima contributes significantly to intimal medial thickening (IMT) and vascular remodeling typical of arteriosclerotic disease. Light has emerged as a powerful tool to interrogate cells label-free and facilitates discriminant observations both *in vitro* and *in vivo*. The auto-fluorescence (AF) profile of individual cells isolated from arteriosclerotic vessels, captured on V-cup array and interrogated across five wavelengths using a novel Lab-on-a-Disc platform, was significantly increased at the 565 ± 20nm wavelength concomitant with a reduction in Myh11 expression, when compared to differentiated vascular smooth muscle (SMC) cells from control vessels. In vitro, TGF-β1 promoted myogenic differentiation of murine bone-marrow derived $Sca1^+/CD44^+$ mesenchymal stem cells (MSC) and murine $Sca1^+$ C3H 10T1/2 cells concomitant with enrichment of the specific SMC epigenetic histone mark, H3K4me2 at the Myh11 promoter, Myh11 promoter transactivation and increased SMC differentiation marker mRNA and protein expression. Myogenic differentiation resulted in a significant increase in the AF intensity across 565 ± 20nm wavelength, an effect not observed for TGF-β1 treated RAMOS human B lymphocytes but mimicked by Notch activation of resident $Sca1^+$ multipotent vascular stem cells (MVSCs) with Jagged1 and inhibited following elastin and collagen III depletion, respectively. Moreover, the temporal increase in the AF intensity at 565 ± 20nm wavelength during myogenic differentiation was similar to the AF profile of dissociated cells from arteriosclerotic vessels at this same wavelength. These data suggest that an AF photonic fingerprint of stem cell-derived myogenic progeny *in vitro* mimics that of vascular cells *ex vivo* following injury.
C. Molony: None. **D. King:** None. **L.A.N. Julius:** None. **E. Fitzpatrick:** None. **M. Di Luca:** None. **G. Casey:** None. **R. Hakimjavadi:** None. **D. Burtenshaw:** None. **K. Healy:** None. **D. Canning:** None. **D. Kernan:** None. **A. Llobera:** None. **W. Liu:** None. **D. Morrow:** None. **E.M. Redmond:** None. **J. Ducree:** None. **P.A. Cahill:** None.

485
Novel Mechanisms at Immune-vascular Interfaces Regulates Myogenic Tone of Resistance Arteries and Induce Hypertension in Mice
Daniela Carnevale, Sapienza Univ/IRCCS Neuromed, Pozzilli, Italy; Iolanda Vinciguerra, Manuel Casaburo, IRCCS Neuromed, Pozzilli, Italy; Marialuisa Perrotta, Sapienza Univ, Pozzilli, Italy; Roberta Iacobucci, Daniele Iodice, IRCCS Neuromed, Pozzilli, Italy; Giuseppe Lembo, Sapienza Univ/IRCCS Neuromed, Pozzilli, Italy

In the search for mechanisms regulating the pathophysiological relationship existing between hypertension and immune system, CD8 effector T cells emerge as possible mediators of target organ colonization. However, how the crosstalk at vascular interfaces is established still remains unidentified. Phosphatidylinositol-3-kinase gamma (PI3Kγ) is an intracellular signaling involved in the acquisition of CD8 effectors functions and was previously showed by our group as involved in hypertension. The hypothesis here tested rely on the possibility that PI3Kγ could regulate trafficking of immune cells at vascular interfaces relevant for hypertension. By taking advantage of a knock-in mouse model, expressing a constitutively active PI3Kγ isoform ($PI3K\gamma^{CX/CX}$), we conceived an experimental setting allowing to assess the direct crosstalk between immune cells and vasculature, obtained by co-culturing CD8 T cells with isolated resistance arteries mounted in pressurized systems. Thus, CD8 isolated from $PI3K\gamma^{CX/CX}$ mice were co-cultured for 3 days with WT resistance arteries and, after the incubation period, vascular function was tested by challenging arteries to increasing intraluminal pressure to detect myogenic tone (MT). CD8 T cells with constitutively active PI3Kγ spontaneously increased MT of mesenteric arteries, a behavior typically associated with hypertension. Conversely, the same T cell population from WT mice, had no effect when cultured with vessels. In addition, $PI3K\gamma^{CX/CX}$ CD8 infiltrated naïve vessels upon co-culture suggesting an intrinsic ability to colonize resistance districts relevant for hypertension. To test the in vivo relevance of the observed phenotype, we performed an adoptive transfer of $PI3K\gamma^{CX/CX}$ CD8 in WT mice, finding that they developed spontaneous hypertension, accompanied by infiltration of effector CD8 in perivascular spaces of resistance districts as kidneys. Taken together these data show that PI3Kγ signaling in CD8 T cells is crucial for their effector functions in target vasculature of hypertension, likely contributing to BP increase by increasing peripheral resistance. These results also suggest translational potential as PI3Kγ inhibitors could modulate the immune response involved in hypertension.
D. Carnevale: None. **I. Vinciguerra:** None. **M. Casaburo:** None. **M. Perrotta:** None. **R. Iacobucci:** None. **D. Iodice:** None. **G. Lembo:** None.

This research has received full or partial funding support from the American Heart Association.

486
Type 2 Cytokines Are Required for the Resolution of Injury in Neonatal Hearts Following Ischemic Injury
Francis M Chen, Fung Ping Leung, Gary Tse, Jack Wing Tak Wong, Chinese Univ of Hong Kong, Shatin, Hong Kong
Background: Type 2 signals such as interleukin-4 (IL-4) and interleukin-13 (IL-13) have been canonically defined as skewing naïve T-cells to Th2 cells and upregulating anti-inflammatory immune programs following injury. As opposed to adults, the immature immune system of the neonate basally prefers a Th2 versus a Th1 profile to maintain fetomaternal tolerance during development. **Hypothesis:** Due to the required activation of type 2 immunity for proper resolution of injury coupled with the inherent Th2 immune profile of the neonate, we hypothesized that IL-4 and IL-13 play an indispensable role in the proper resolution of injury in the neonatal heart niche by fostering an anti-inflammatory response conducive for niche remodeling and growth factor release. **Methods and Results:** Neonatal Balb/C and $IL\text{-}4^{-/-}$ /$IL\text{-}13^{-/-}$ (DKO) immune populations and overall heart regenerative capacity after left anterior descending (LAD) coronary artery ligation were profiled using flow cytometry and transthoracic echocardiography. DKO mice had significantly reduced CD4/CD8 ratios and suppression of $CD206^+$ alternatively activated macrophages whilst increasing the population of pro-inflammatory $Ly6c^{Hi}$ monocytes. WT Balb/C mice had high CD4/CD8 ratios and actively reduced $Ly6c^{Hi}$ populations, preferring $Ly6c^{Mid}$ populations and anti-inflammatory $CD206^+$ alternatively-activated macrophages. Furthermore, echocardiography demonstrated a reduction in both EF and FS in DKO mice following LAD ligation compared to control mice, which had complete restoration of EF and FS. **Summary:** Our results confirmed that both IL-4 and IL-13 are required for mediating a Th2/M2 immune response following LAD ligation in the neonate, thereby permitting a niche that is conducive for regeneration. Future studies are needed to determine whether application of IL-4 and IL-13 in adult mice with

myocardial infarction can similarly promote cardiac regeneration.
F.M. Chen: None. **F. Leung:** None. **G. Tse:** None. **J. Wong:** None.

487
Myocardial Infarction is Associated with Changes in Innate Immunity that Drive Breast Cancer Progression
Graeme J Koelwyn, New York Univ Langone Health, New York, NY

Cardiovascular (CV) disease and cancer-specific mortality compete as the leading causes of mortality in women with early-stage breast cancer. Following treatment for early-stage disease, breast cancer patients are 5 times more likely to develop CV complications such as myocardial infarction (MI) compared to age-matched controls, due to the 'cardiotoxic' effects of anti-cancer therapies on CV tissues (e.g. chemotherapy, radiation). As CV disease and cancer progression share many common risk factors and etiologies, we hypothesized that CV disease may also influence cancer progression. To investigate this potential cross-disease communication, we developed a mouse model using the left anterior descending (LAD) coronary artery permanent ligation technique of MI in the E0771 orthotopic breast cancer model. LAD ligation significantly increased tumor growth over 20 days compared to sham surgery controls (SHAM) ($p<0.001$). This was associated with an altered tumor microenvironment and tumor immune cell landscape, most notably increased proportions of CD11b+Ly6C+Ly6G- myeloid cells in LAD vs SHAM ($p<0.01$). RNA and ATAC sequencing of these cells from the bone marrow, circulation, and tumor showed distinct functional and chromatin-based changes following LAD ligation, including increased expression of genes associated with cell proliferation, mitochondria and lipid transport, and enrichment of transcription factor binding motifs within differentially accessible regions, including PU.1, Ets1, Runx1 and Cebp. Using monocyte adoptive transfer experiments, we also show that recruitment of bone marrow monocytes to the tumor microenvironment was increased in LAD vs SHAM mice. Collectively, these findings suggest that MI can accelerate breast cancer progression and provide insight into molecular mechanisms driving innate immune adaptations that promote cross-disease communication.
G.J. Koelwyn: None.

488
Plasma Lipoproteins in Alzheimer's Disease
Danni Li, Univ of Minnesota, Minneapolis, MN

Introduction: Scientific evidence continues to identify vascular contributions to Alzheimer disease (AD); as such, the vasculature may even be the site of the earliest AD-associated pathological dysregulation. In particular, plasma lipoproteins have long been implicated in cerebrovascular health and disease because of their roles in maintaining the integrity of vascular systems. Delineating the relationships between the four major classes of plasma lipoproteins and AD sequelae (amyloid plaques, thinning of cortical thickness, cognitive decline, and development of incident mild cognitive impairment [MCI]/dementia) will identify novel biomarkers and advance our understanding of vascular mechanisms that contribute to AD pathophysiology. The objective of this study was to provide initial proof-of-concept that plasma lipoproteome likely differ between AD cases and controls when measured in plasma lipoprotein fractions than unfractionated plasma. **Methods:** In this case-control study of 5 AD cases and 5 sex- and age-matched controls, we applied a targeted proteomic method to measure 79 proteins in plasma lipoprotein fractions (fractionated by sequential gradient ultracentrifugation) and in unfractionated plasma (removed of albumin and IgG by immunoaffinity depletion). **Results:** We demonstrated that protein differences between the AD cases and controls were much more remarkably when measured in plasma lipoprotein fractions than when measured in unfractionated plasma. **Discussion:** The findings provided the initial proof of concept evidence that proteome in plasma lipoprotein fractions might increase the accuracy in diagnosing AD, which should be further tested.
D. Li: None.

489
Disruption of HuR-mediated VEGF-A mRNA Stabilization as a Mechanism of Age-related Defects in Arteriogenesis
Chris Sorel Mantsounga, Brown Univ/Rhode Hosp/ Providence VA Medical Ctr, Providence, RI; Abigail Healy, Nicole Ceneri, Joshua Berus, Brown Univ, Providence, RI; Jerome Watts, Brown Univ/Providence VA Medical Ctr, Providence, RI; Hyung Chun, Yale Univ, New Haven, RI; Gaurav Choudhary, Brown Univ/ Providence VA Medical Ctr, Providence, RI; Alan R. Morrison, Brown Univ/Providence VA Medical Ctr, Providence, RI

Aging and age-related diseases like peripheral arterial disease are associated with impaired inflammatory arteriogenesis in response to injury. Macrophage expression of pro-inflammatory and pro-angiogenenic factors can be altered during aging. We seek to define the molecular mechanism that determine the impact of aging on macrophage-dependent arteriogenesis. Recently, we defined a critical signaling pathway that involves CCL2 stimulation coupled to ICAM-1 adhesion, resulting in rapid nuclear-to-cytosolic translocation of the RNA-binding protein, HuR, with its consequent stabilization of VEGF-A mRNA. Preliminary data from bone marrow-derived macrophages (BMDMs) demonstrated decreased VEGF-A level by both mRNA and protein in aged mice (52-week old) when compared to young (10-week old). BMDMs from aged mice also revealed increased markers of senescence. The hypothesis is that age-related changes in arteriogenesis are a conseqeuence of altered HuR-mediated VEGF-A stabilization. In a hindlimb ischemia model of arteriogenesis, we found reduced flow recovery in aged mice. Moreover, small arterial angiography by microCT confirmed decreased arteriogenesis. Loss of functional arteriogenesis was associated with decreased muscle tissue VEGF-A levels despite adequate macrophage recruitment to the muscle tissue. BMDM HuR expression was unaffected in aged mice, and CCL2-coupled ICAM-1 adhesion demonstrated comparable nuclear-to-cytosolic translocation in aged BMDMs, indicating the signaling of HuR activation remained intact. However, BMDMs demonstrated a loss of HuR binding to VEGF-A mRNA with consequent decreased VEGF-A mRNA half-life. In summary, HuR-mediated VEGF-A mRNA stabilization and consequent inflammatory-mediated arteriogenesis is disrupted in aged animals.
C.S. Mantsounga: None. **A. Healy:** None. **N. Ceneri:** None. **J. Berus:** None. **J. Watts:** None. **H. Chun:** None. **G. Choudhary:** None. **A.R. Morrison:** None.

491
Production of Fatty Acid Binding Protein-4 by Macrophages in Atherosclerotic Human Coronary Arteries
Priyanka Prathipati, **Brian Walton**, Univ of Texas Health Science Ctr Houston, Houston, TX

Background: Fatty acid binding protein-4 (FABP4) is a lipid chaperon that carries fatty acids and other lipophilic substances to specific compartments in the cell. It is mostly expressed in macrophages and adipocytes and is associated with insulin resistance, obesity and atherosclerosis. Previous studies have shown the role of FABP4 in high risk phenotypes of atherosclerotic plaques featuring inflammation and vulnerability of the plaques in cardiovascular diseases. Hence we hypothesis that FABP4 is produced by macrophages in the human coronary atherosclerosis and might be involved in aggravation of the disease.**Materials and methods:** Human coronary arteries which were formalin fixed and paraffin embedded were used with IRB review. Immunohistochemistry was performed on these samples to analyze the expression of FABP4 and co-

localization of CD68 (macrophage marker) in the atherosclerotic plaques of these human coronary arteries.**Results:** Atherosclerotic plaques in the human coronary arteries expressed both FABP4 and CD68.**Conclusion:** Macrophages in the plaques of human plaques secrete FABP4 which is evident from the co-existence of both molecules in the atherosclerotic coronary arteries.

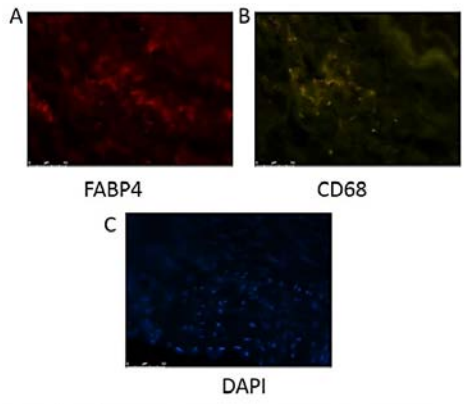

Expression of FABP4 and CD68 in human coronary artery: A)Immunofluorescence staining of FABP4 (red), B) CD68 (green) and C) DAPI nuclear staining (blue) in the human coronary artery samples.

P. Prathipati: None. **B. Walton:** None.

493
Neutrophil and Macrophage Cell Surface Colony-Stimulating Factor-1 is Shed by a Disintegrin and Metalloprotease 17 and Contributes to Stimulating Macrophage Proliferation in Inflammation
Jingjing Tang, Jeremy M Frey, Univ of Washington, Seattle, WA; Carole L Wilson, Medical Univ of South Carolina, Charleston, SC; Angela Moncada-Pazos, Clemence Levet, Matthew Freeman, Univ of Oxford, Oxford, United Kingdom; E. Richard Stanley, Albert Einstein Coll of Med, New York, NY; Michael E Rosenfeld, Karin E Bornfeldt, Elaine W Raines, Univ of Washington, Seattle, WA

Recent studies highlight a role for macrophage proliferation post monocyte recruitment in inflammatory conditions, such as atherosclerosis. However, the mechanisms regulating macrophage proliferation are not well understood. Using an acute peritonitis model, we identified a 40 ± 8% reduction (mean ± SEM; n=5; p<0.01) in macrophages in the S phase of the cell cycle 40 hrs post thioglycollate injection in mice lacking the transmembrane protease ADAM17 in hematopoietic cells. ADAM17 is a member of a disintegrin and metalloprotease family that cleaves many cell surface proteins involved in inflammation. The macrophage proliferation defect in ADAM17 null chimeras was associated with a 60 ± 10% (n=5; p<0.001) decrease in soluble macrophage colony-stimulating factor (CSF)-1 in the peritoneum, and was rescued by intraperitoneal injection of CSF-1. We demonstrate that neutrophils, the first innate immune cell that migrates into inflammatory sites, and macrophages are both major sources of cell surface (cs)CSF-1 in this acute inflammation model, adding to the current knowledge that stromal, epithelial and endothelial cells are sources of CSF-1. We show that ADAM17 is critical in mediating csCSF-1 release in the inflamed peritoneum, and that this release following neutrophil extravasation is associated with elevated expression of iRhom2, a member of the rhomboid-like superfamily, which promotes ADAM17 maturation and trafficking to the cell surface. Accordingly, deletion of hematopoietic iRhom2 is sufficient to prevent csCSF-1 release from neutrophils and macrophages, thus recapitulating the defect in macrophage proliferation seen in ADAM17 null cells. Our data indicate that csCSF-1 release and macrophage proliferation is self-limiting in states of acute inflammation due to the transient nature of leukocyte recruitment and temporally restricted csCSF-1 expression and release. In chronic inflammation such as atherosclerosis, we show that macrophage proliferation is decreased by 30 ± 7% (n=6; p<0.01) in atherosclerotic lesions of ADAM17 hematopoietic null LDL receptor-deficient mice fed a high fat diet for 16 weeks. Together, these results demonstrate a novel mechanism governing macrophage proliferation in both acute and chronic inflammation.

J. Tang: None. **J.M. Frey:** None. **C.L. Wilson:** None. **A. Moncada-Pazos:** None. **C. Levet:** None. **M. Freeman:** None. **E.R. Stanley:** None. **M.E. Rosenfeld:** None. **K.E. Bornfeldt:** None. **E.W. Raines:** None.

494
Endothelial Cell Heterogeneity Governs Basal and Inducible Inflammatory Responses Relevant to Allograft Injury
Gianna Zufall, UCLA, Los Angeles, CA; **Nicole Valenzuela**, UCLA Immunogenetics Ctr, Los Angeles, CA

Introduction: Transplanted organs are not equally susceptible to rejection, suggesting a role for site specialization of vascular endothelial cells (EC). Most studies of leukocyte recruitment employ umbilical vein or aorta EC, and fail to capture physiological differences among EC. ***Methods:*** EC were left unstimulated or treated with TNFα or IL-1β (0.01-10ng/mL, 4-24hr). Confluent primary human EC from aorta (AEC), coronary artery (CAEC), cardiac microvessel (CMVEC), pulmonary artery (PAEC), lung microvessel (LMVEC), skin blood microvessel (DMVEC), liver sinusoids (LSEC), kidney glomerulus (RGEC) and brain microvessel (HMBVEC) were compared for expression of adhesion molecules and chemokines by Nanostring Human Immunology 594 gene panel, flow cytometry and 38-plex Luminex assay (n=3 donors). A novel adhesion assay enabled immunophenotyping of allogeneic leukocyte subsets (T, B, NK and monocytes) adherent to EC (n=4 PBMC donors).
Results >200 immunology-related genes were differentially expressed (fold >1.5, p<0.05) across untreated EC. Microvascular EC expressed higher baseline levels of ICAM-1, E-selectin and VCAM-1. TNFα and IL-1β increased these adhesion molecules, but there were clear differences in the magnitude and kinetics across cells. Most notably, LSEC failed to significantly upregulate E-selectin, and exhibited the lowest adherence of leukocytes. Only LSEC constitutively expressed suppressors of cytokine signaling (SOCS1 and SOCS3).
After stimulation with TNFα and IL-1β, cardiac EC produced more fractalkine than other EC irrespective of vessel size; but large vessel (AEC, PAEC) produced the most IL-6 and G-CSF. AEC were a poor source of RANTES and IP-10, while LSEC did not increase fractalkine or GM-CSF. IL-1β increased GM-CSF, G-CSF, and GROα and IL-6. TNFα increased RANTES. More NK and B cells were recruited to TNFα than IL-1β activated EC. IL-1β selectively increased the nuclear cofactor NFKBIZ (IκBζ), but TNFα promoted Bcl-3 expression, suggesting different transcriptional programs.
Conclusion: These findings demonstrate heterogeneity among EC from different vascular beds and organs. SOCS proteins may be potential therapeutic targets to reduce the inflammatory responses of ECs in multiple vascular disease models.

G. Zufall: None. **N. Valenzuela:** None.

495
Nicotine Promotes Endothelial Dysfunction and Vascular Inflammation in Diet-induced Obese Rats: Role of Macrophage TNFa
Chang Liu, Aimei Wang, Yun Hao, Jinzhou Medical Univ, Jinzhou, China; Lei Huang, Yang Zhihang, Shenyan Medical Univ, Shenyang, China; Runxia Tian, Leopoldo Raij, Univ of Miami, VAMC, Miami, FL; **Ming Sheng Zhou**, Jinzhou Medical Univ & Shenyan Medical Univ, Jinzhou, China

Obesity and cigarette smoke are major cardiovascular (CV) risk factors and, when coexisting in the same individuals, have additive/synergistic effects upon CVD. We studied the mechanisms involved in nicotine enhancement of CVD in Sprague Dawley rats with diet-induced obesity**.** The rats were fed either a high fat (HFD) or normal rat chow (NFD) diet with or without nicotine (100 mg/L in drinking water) for 20 weeks. HFD rats developed central obesity, increased systolic blood pressure (SBP 146 ± 3 vs. 130 ± 5 mmHg in NFD , p<0.05), aortic superoxide (O_2^- 1357 ± 142 vs. 847 ± 102 counts/min/mg in NFD, p<0.05) production, and impaired endothelial nitric oxide synthase (eNOS) and endothelium-dependent relaxation to acetylcholine (EDR, Emax: 85 ± 5 vs. 99 ± 1% in NFD, p<0.05). Nicotine further increased SBP (159 ± 5 mmHg, p<0.05), O_2^- (1689 ± 87 counts/min/mg, p<0.05) and impaired eNOS and EDR (Emax: 72 ± 4%, p<0.05) in obese rats. In the peritoneal macrophages from obese rats, tumor necrosis factor (TNF) α, interleukin 1β and CD36 were increased, and were further increased in nicotine-treated obese rats. Using PCR array we found that 3 of 84 target proinflammatory genes were increased by 2-4 fold in the aorta of obese rats, 11 of the target genes were further increased in nicotine-treated obese rats. HUVECs, incubated with conditioned medium from the peritoneal macrophages of nicotine treated-obese rats, exhibited reduced eNOS and increased NADPH oxidase subunits gp91phox and p22phox expression. Those effects were partially prevented by adding anti-TNFα antibody to the conditioned medium. Our results suggest that nicotine aggravates the CV effects of diet–induced obesity including the oxidative stress, vascular inflammation and endothelial dysfunction. The underlying mechanisms may involve in targeting endothelium by enhancement of macrophage-derived TNFα.

C. Liu: None. **A. Wang:** None. **Y. Hao:** None. **L. Huang:** None. **Y. Zhihang:** None. **R. Tian:** None. **L. Raij:** None. **M. Zhou:** Other Research Support; Significant; National Science Foundation of China 81470532, 86670384.

500
Endothelial Specific *Meis1* Knockout Protects Cells from Doxorubicin-Induced Apoptosis
Miao Chen, Benjamin Ledford, Catherine Mary Barron, Jia-Qiang He, Virginia Tech, Blacksburg, VA

Introduction: *Meis1* belongs to the TALE (three amino-acid loop extension) subclass of the homeobox gene families. It is a highly conserved transcription factor in all eukaryotes and plays a crucial role in anatomical development during embryogenesis and maintaining homeostasis after birth. However, little is known about the role of *Meis1* gene on regulating functions of endothelial cells (ECs). Our preliminary study found that EC-specific knockout (KO) of *Meis1* showed protective benefits in response to hindlimb ischemia, such as increased blood flow and decreased toe apoptosis. We hypothesize that deletion of *Meis1* may enhance EC viability or resistance to harsh environment. The present study aims to explore the potential underlying mechanisms using an *in vitro* apoptotic condition induced by doxorubicin (Dox).
Methods: EC-specific deletion of *Meis1* gene was generated by crossbreeding *Meis1*$^{flox/flox}$ mice with *Tie2-Cre* mice. Following confirmation of genotyping, ECs were isolated from the lungs of 3-5 WT and KO newborn pups using CD31 microbeads. Cells were then plated and treated with 0, 0.5, and 1 μM Dox for 24 hours prior to various assays.
Results: Our qPCR data indicated that *KDR* expression was ~100-times more in $CD31^+$ fraction than in $CD31^-$ fraction both in WT and KO groups (n=4); while in KO group, *Meis1* expression was significantly decreased to 20% of WT control, suggesting the successful isolation of *Meis1-KO* ECs. Further analysis with immunocytochemistry indicated that 83.1±2.3% $CD31^+$ cells were also KDR^+, compared to 8.3±1.2% KDR^+ cells in $CD31^-$ fraction (n=7-8). Using EC-specific dye uptake assay, we found that 84.6±2.4% $CD31^+$ cells were positive for Dil-Ac-LDL, compared to 7.9±3.2% in $CD31^-$ cells (n=6), which appears to correspond to more tube formation observed in KO than WT groups. As we expected, *Meis1-KO* ECs demonstrated greater cell viability (81.2±6.1%) than WT cells (58.0±1.6%) under 0.5 μM Dox treatment (n=5-6). The increased viability in KO ECs may be due to the decreased expression of *Bax*, a pro-apoptotic factor.
Conclusions: We conclude that activation of *Meis1* gene may facilitate EC death under ischemic condition while deletion of *Mei1* gene promote protective effects on ECs.

M. Chen: None. **B. Ledford:** None. **C.M. Barron:** None. **J. He:** None.

501
Angiotensin II Increases Angiogenesis by Nf-κB-mediated Transcriptional Activation of Angiogenic Factor Aggf1
Wenxia Si, Wen Xie, Wenbing Deng, Huazhong Univ of Science and Technology, Wuhan, China; Sadashiva S Karnik, Cleveland Clinic, Cleveland, OH; Chengqi Xu, Huazhong Univ of Science and Technology, Wuhan, China; **Qiuyun Chen**, Qing K Wang, Cleveland Clinic, Cleveland, OH

Angiogenic factor AGGF1 is involved in the specification of hemangioblasts, vascular development, differentiation of veins, angiogenesis, neointimal formation after vascular injury, and cardiac hypertrophy and heart failure. However, the regulation of the expression of AGGF1 remains incompletely characterized. In this study, we show that vasoconstrictor angiotensin II (AngII), the major effector of the renin-angiotensin system (RAS) and one of the most important regulators of the cardiovascular system, induces the expression of AGGF1 through NF-κB, and up-regulation of AGGF1 plays a key role in AngII-induced angiogenesis. AngII significantly up-regulated the levels of AGGF1 mRNA and protein at low doses (10-40 μM), but not at high doses in HUVECs (>60 μM). AngII receptor AT1R inhibitor losartan inhibited AngII-induced up-regulation of AGGF1, whereas AT2R inhibitor PD123319 further increased AngII-induced up-regulation of AGGF1, suggesting that up-regulation of AGGF1 by AngII was through AT1R. Up-regulation of AGGF1 by AngII was blocked by NF-κB inhibitors PDTC and quinacrine. A binding site for p65 was identified at the 5'-UTR of *AGGF1* and shown to bind p65 directly using chromatin immunoprecipitation analysis (CHIP) and electrophoretic mobility shift assays (EMSA). Western blot, real-time RT-PCR and luciferase assays revealed that p65 transcriptionally activated *AGGF1* expression. Capillary tube formation assays showed that knockdown of *AGGF1* expression inhibited angiogenesis induced by AngII. These data suggest that AngII acts as a critical regulator of AGGF1 expression through NF-κB, and AGGF1 plays a key role in AngII-induced angiogenesis.

W. Si: Research Grant; Modest; National Natural Science Foundation of China. **W. Xie:** Research Grant; Modest; National Natural Science Foundation of China. **W. Deng:** Research Grant; Modest; National Natural Science Foundation of China. **S.S. Karnik:** None. **C. Xu:** Research Grant; Modest; National Natural Science Foundation of China. **Q. Chen:** Research Grant; Significant; NIH. **Q.K. Wang:** Research Grant; Significant; NIH.

502
Glucose-6-Phosphate Dehydrogenase Regulates MYH11 and MYOCD Expression in HDAC and miR-1 Dependent Manner
Vidhi Dhagia, SachindraRaj Joshi, Vasiliki Soldatos, John G Edwards, Sachin A Gupte, New York Medical Coll, Valhalla, NY

Vascular smooth muscle cell (VSMC) phenotype and function is altered in diabetic and obese patients and animals. Increased activity of glucose-6-phosphate dehydrogenase (G6PD), the rate-limiting enzyme in Pentose Phosphate Pathway, in diabetic and obese animals is associated with decreased expression of MYOCD and MYOCD-dependent genes in the arteries of these animals. Therefore, we hypothesize that reprogrammed metabolism and increased G6PD activity is critical in switching the VSMC from a differentiated to a dedifferentiated phenotype. Our results demonstrated metabolic reprogramming and decrease in MYOCD and MYOCD-driven MYH11 in the aorta of normal chow- and high fat diet (HFD)-fed diabetic Goto-Kakizaki (GK) as compared to control rats. Up regulated G6PD activity in the aorta of these animals positively correlated with increased arterial elastance (R^2 = 0.8322) and total peripheral resistance (R^2 = 0.8364). *In vitro*, VSMCs (A7r5) treated with Ad-shRNA for G6PD, epiandrosterone (Epi), G6PD inhibitor, and PD2958, a selective inhibitor of G6PD activity, increased ($P<0.05$) *Myocd* and *Myh11* levels and MYOCD-regulated MYH11 and CNN1 expressions as compared to untreated cells. Furthermore, we found that G6PD-mediated expression of MYOCD and MYH11 expressions was regulated at transcriptional and post transcriptional level. Inhibition of G6PD by PD2958 or Epi decreased histone deacetylase (HDAC) activity by 70-80% ($P<0.05$), and concomitantly, PD2958 and Ad-shRNA-G6PD up regulated H3K9Ac expression in A7r5 cells as compared to their respective controls. Next, we compared the expression of VSMC-restricted MYH11 in A7r5 cells treated with HDAC inhibitor, Trichostatin (TSA), and PD2958+TSA. Our results demonstrated that MYH11 expression increased by TSA and PD2958 was not further potentiated by PD2958+TSA, suggesting that G6PD inhibition up regulated MYH11 via HDAC inhibition. We also found that G6PD inhibition increased miR-1 levels, which post-transcriptionally regulates MYOCD and MYOCD-dependent gene expression. Therefore, our results collectively suggest that increased G6PD activity is associated with switching of VSMCs from a differentiated to a dedifferentiated phenotype in HDAC and miR-1 dependent manner.
V. Dhagia: None. **S. Joshi:** None. **V. Soldatos:** None. **J.G. Edwards:** None. **S.A. Gupte:** None.

503
Smooth Muscle Cell Cytochrome B5 reductase < CYB5R3 > expression modulates vascular tone
Brittany G Durgin, Scott A. Hahn, Megan P. Miller, Megan P. Miller, Adam C Straub, Univ of Pittsburgh, Pittsburgh, PA

Hypertension is a major risk factor for cardiovascular-related morbidity and mortality. Nitric oxide (NO) resistance results in an inability of arterial blood vessels to relax contributing to hypertension. NO relaxes vascular smooth muscle cells (SMCs) by stimulating soluble guanylyl cyclase (sGC) to generate cyclic guanosine monophosphate (cGMP) which leads to downstream activation of protein kinase G (PKG) and vasodilation. Importantly, the sGC heme iron is required to be in the reduced (Fe^{2+}) state in order for NO to bind and activate sGC. When the sGC heme iron is oxidized (Fe^{3+}), sGC is insensitive to NO signaling for cGMP production, resulting in hypertension. We recently published evidence that NADH cytochrome b5 reductase 3 (CYB5R3) is a sGC heme reductase that maintains sGC in the reduced (Fe^{2+}), NO-sensitive state. Transient knockdown and pharmacological inhibition of CYB5R3 in SMCs blocks NO-mediated cGMP production and aortic relaxation. Combined, these data implicated CYB5R3 as a potential regulator of systemic blood pressure. To test this, we created tamoxifen-inducible SMC-specific CYB5R3 knockout mice (SMC CYB5R3 KO) and measured systemic blood pressure. We found SMC CYB5R3 KO mice have ~ 5 mmHg increase in mean arterial blood pressure at baseline relative to SMC CYB5R3 WT mice. Subsequently, Angiotensin II (Ang II) infusion resulted in a further ~ 15 mmHg increase in blood pressure respective to SMC CYB5R3 WT mice. Future studies will test whether SMC CYB5R3 may confer vascular protection against Ang II-induced HTN, vessel fibrosis, and SMC dysfunction by maintaining sGC in the reduced, NO sensitive state**.**
B.G. Durgin: None. **S.A. Hahn:** None. **M.P. Miller:** None. **M.P. Miller:** None. **A.C. Straub:** None.

504
MicroRNA Signatures in Murine Aorta and Carotid Arteries
Debora Faffe, Ernesto Curty-Costa, Luisa Hoffmann, Rosane Silva, Turan P. Urmenyi, Federal Univ of Rio de Janeir, Rio de Janeiro, Brazil

Atherosclerosis, a major cause of mortality, affects arteries diffusely. However, some vascular beds are preferably involved. In the last decade microRNAs (miRs) have emerged as key regulators of gene expression in physiological or pathophysiological processes. Here, we investigated whether different arteries, commonly affected by atherosclerosis, present specific miR expression signatures. For this purpose, aorta (Ao) and carotid (Ca) arteries of four healthy male Wistar rats were dissected, total RNA was extracted with Trizol, and enriched for small RNA fraction. MicroRNAs were then sequenced using massive parallel sequencing (RNA-Seq) on Ion Torrent PGM platform. Data were analyzed using CLC Genomics Workbench software. We identified 266 mature miRs in Ao and 421 in Ca, 260 were common between arteries. Differential expression analysis (EDGE) showed increased expression (IE) of 16 miRs in Ao and reduced expression (RE) of 54 miRs in Ao, relative to Ca. The lists of differently expressed miRs were subjected to *in silico* functional analyzes: (1) computational target prediction, using miRWalk tool, identified 1,094 target genes for IE list and 3,574 for RE list; (2) gene-set enrichment analysis in the lists of putative target genes, using EnrichR tool, showed differences in enriched biological processes, such as response to shear stress, regulation of endothelial proliferation, smooth muscle metabolism, and response to FGF signaling (which were enriched in RE list); (3) construction of regulatory networks for differently expressed miRs, using miRnet, identified metabolic pathway components differently regulated between arteries, such as inhibition of SIRT1 and increased expression of HIF1-alpha in Ao. Taken together, our results show differences in miR signature between arteries, suggesting that specific expression profiles of miR may play a role in the vascular behavior as well as in atherosclerosis pathophysiology.
D. Faffe: None. **E. Curty-Costa:** None. **L. Hoffmann:** None. **R. Silva:** None. **T.P. Urmenyi:** None.

505
Targeting FOXM1 in Vascular Smooth Muscle Cells Induces Apoptotic Cell Death
Sarah R Franco, Amelia Stranz, Fiona Ljumani, Univ of Wisconsin-Madison, Madison, WI; Go Urabe, The Ohio State Univ, Columbus, OH; Danielle Stewart, Univ of Wisconsin-Madison, Madison, WI; Mirnal Chaudhary, Wright State Univ, Dayton, WI; Bo Liu, Univ of Wisconsin-Madison, Madison, WI

Objectives: Vascular smooth muscle cell (VSMC) proliferation and dedifferentiation are key contributors to the initiation and progression of vascular diseases including restenosis. Forkhead Box M1 (FOXM1) is a proliferation-associated transcription factor shown to play a role in a variety of biological processes including cell cycle progression, cell survival, and apoptosis in many cell types.

However, the role of FOXM1 in VSMC phenotypic transformation as a result of vascular injury following balloon angioplasty has not been studied. We hypothesize that FOXM1 modulates VSMC response by enhancing pro-proliferative and pro-survival signaling following vascular injury. **Methods & Results:** The rat carotid artery balloon injury was used to model vascular injury. Immunofluorescence staining was carried out on sections from injured carotid arteries or uninjured controls collected at 3, 7, or 14 days post injury (dpi). We observed that FOXM1 expression was upregulated in injured arteries at 7 and 14 dpi**.** Expression of FOXM1 in injured arteries co-localized with PCNA, a marker of proliferation. The upregulation of FOXM1 protein was replicated in cultured rat VSMCs by serum stimulation. Using thymidine synchronization, we observed that FOXM1 expression followed a cell cycle specific pattern *in vitro*. Chemical inhibition of FOXM1 using thiostrepton or FDI-6, or via siRNA resulted in decreased VSMC viability as measured by CCK-8, induction of apoptosis as measured by flow cytometry, and cleaved caspase 3 induction. More detailed immunocytochemistry analysis revealed that FDI-6 treated VSMCs exhibit disorganized microtubule networks. Furthermore, FDI-6 treatment decreased expression of Eg5, a motor protein essential for microtubule orientation and critical for mitosis execution. Additionally, FOXM1 inhibition decreased levels of β-catenin, a known activator of cell cycle-related genes and proliferation. **Conclusions:** In conclusion, our data suggest FOXM1 is critical to VSMC viability and may modulate VSMC proliferation and survival via regulation of important cell cycle and pro-proliferative proteins, and therefore may serve as a novel therapeutic target to prevent VSMC pathophysiology in the context of restenosis.
S.R. Franco: None. **A. Stranz:** None. **F. Ljumani:** None. **G. Urabe:** None. **D. Stewart:** None. **M. Chaudhary:** None. **B. Liu:** None.

506
Pharmacological Inhibition of Forkhead-box Class O Transcription Factors Reduces Nitric Oxide Signaling Through Downregulation of Soluble Guanylate Cyclase
Joseph C. Galley, Univ of Pittsburgh, Pittsburgh, PA

Dysregulated vascular tone contributes to hypertension. Nitric oxide (NO) activated soluble guanylate cyclase (sGC) is an integral player in the regulation of vasodilation capacity through production of the secondary messenger cyclic guanosine monophosphate (cGMP) to induce vasorelaxation. Impaired NO-stimulated cGMP production through sGC has previously been shown to significantly contribute to the development and acceleration of hypertension. To date, little is understood concerning the transcriptional regulation of sGC expression in vascular smooth muscle cells (VSMCs). It has been established that the class O forkhead-box (FoxO) family of transcription factors play important roles in the regulation of cell growth, proliferation, metabolism, survival, lifespan, and tissue differentiation. Therefore, we hypothesize that FoxO transcription factors play an important role in sGC regulation and hypertension. Here we show that pan-pharmacological inhibition of FoxO transcription factors using AS1842856 significantly reduced sGC mRNA expression rapidly and in a dose dependent manner. Similarly, sGC protein expression significantly decreased quickly and dose-dependently upon FoxO protein inhibition. Furthermore, VSMC FoxO inhibitor pre-treatment significantly decreased cGMP production under basal and after stimulation with DEA-NONOate, a NO-donor molecule. Functionally, *Ex vivo* two-pin myography experiments show that FoxO inhibitor-treated C57BL/6 mouse aortas have significantly blunted sodium nitroprusside (SNP)-induced (NO-dependent) vasorelaxation. Taken together, our data suggest FoxO transcription factor activity is necessary for the maintenance of sGC expression and NO-dependent vascular tone modulation.
J.C. Galley: None.

507
Dedicator of Cytokinesis 2 Regulates Smooth Muscle Cell Proliferation via p38 Mitogen-Activated Protein Kinase Signaling Pathway
Xia Guo, FeiFei Li, Yung-Chun Wang, Kun Dong, Shi-You Chen, Univ of Georgia, Athens, GA

Smooth muscle cell (SMC) proliferation is an important process during vascular development and involved in vascular remodeling of a number of cardiovascular diseases including atherosclerosis, hypertension, and restenosis after angioplasty. However, the underlying mechanisms are not completely understood. In the present study, we identified dedicator of cytokinesis 2 (DOCK2) as one of the factors mediating the SMC proliferation. Knockout of DOCK2 (DOCK2-/-) caused abnormal blood vessel development in yolk sac and hemorrhage in mouse embryos. In addition, dorsal aorta wall structure was disrupted in DOCK2-/- embryos, and the SMC numbers in the dorsal aorta were decreased by 49% compared with wild type (WT). Consistently, proliferating cell nuclear antigen (PCNA)-positive cells in DOCK2-/- dorsal aorta media were much less the WT. These data suggest that the abnormal vascular development in DOCK2-/- embryos was due to the defective SMC proliferation. In vitro, platelet-derived growth factor (PDGF)-BB and serum upregulated DOCK2 along with PCNA expression in SMCs. Knockout or knockdown of DOCK2 by its shRNA inhibited the PDGF-BB-induced PCNA expression while forced expression of DOCK2 induced PCNA expression in SMCs. 5-ethynyl-2'-deoxyuridine (EdU) assay showed that knockdown of DOCK2 blocked PDGF-BB-induced SMC proliferation. Mechanistically, DOCK2 induced SMC proliferation by activating p38 mitogen-activated protein kinase (MAPK). Overexpression of DOCK2 induced while knockdown of DOCK2 inhibited p38 phosphorylation. Blockade of p38 MAPK signaling by its pathway-specific inhibitor diminished DOCK2-induced SMC proliferation. In a rat carotid artery balloon-injury model, knockdown of DOCK2 by adenoviral delivery of its shRNA blocked the injury-induced neointima formation and attenuated the PCNA expression. Furthermore, deletion of DOCK2 blocked ligation-induced neointima formation and PCNA expression in mouse arteries. Taken together, our studies demonstrated that DOCK2 is an important factor regulating SMC proliferation during embryo development as well as vascular remodeling in pathological conditions.
X. Guo: None. **F. Li:** None. **Y. Wang:** None. **K. Dong:** None. **S. Chen:** None.

This research has received full or partial funding support from the American Heart Association.

508
Endothelial Cell Telomerase Promotes Aberrant Cell Proliferation in Pulmonary Hypertension
Eric Hyzny, Univ of Pittsburgh, Pittsburgh, PA; Genevieve Doyon, Elena Goncharova, Dennis Bruemmer, Univ of Pittsburgh Medical Ctr, Pittsburgh, PA

Background: Pulmonary arterial hypertension (PAH) is a progressive, severe disease with high morbidity and mortality. Mechanistically, early pulmonary vasoconstriction promotes cell proliferation and extensive vascular remodeling. Mammalian cell proliferation is dependent on telomerase expression; however, a mechanistic link between endothelial cell telomerase reverse transcriptase (TERT) and the control of mitogenic responses during the development of PAH has never been established.
Hypothesis: Elevated telomerase levels in the diseased pulmonary endothelium induce proliferation of endothelial and smooth muscle cells in the pulmonary vasculature.
Methods: We first received isolated pulmonary arterial endothelial cells from control subjects and patients with PAH. Autopsy sections obtained from patients were stained

for endothelial cells, mitogenic markers, and TERT. Pooled primary pulmonary endothelial cells were used for in vitro experiments.
Results: TERT expression was increased in the endothelium of pulmonary artery specimens of patients with PAH. Co-staining for the mitogenic marker PCNA confirmed high TERT expression specifically in proliferating cells. Key mechanistic stimuli causally involved in PAH, including hypoxia, inflammation, and vascular injury, increased mRNA and protein expression of TERT in pulmonary artery endothelial cells. TERT expression is necessary and sufficient for endothelial cell proliferation, as demonstrated through genetic TERT depletion and overexpression. Mechanistically, TERT supports the transcription of key endothelial growth factors, including vascular endothelial growth factor and epidermal growth factor, an effect that is mediated through TERT-dependent regulation of the transcription factor HIF1α.
Conclusions: These data support the hypothesis that TERT promotes a proliferative phenotype of endothelial cells in PAH. Future experiments will investigate the cell-specific role of TERT in endothelial cell function and proliferation during the development of PAH using Cre/loxP recombination in mice harboring floxed TERT alleles.
E. Hyzny: None. **G. Doyon:** None. **E. Goncharova:** None. **D. Bruemmer:** None.

509
Fibronectin Containing Extra Domain a Modulates TLR4-Dependent Smooth Muscle Cell Proliferation and Neointimal Hyperplasia in Apolipoprotein E-Deficient Mice
Manish Jain, Prakash Doddapattar, Mehul Chorawala, Nirav Dhanesha, Anil Chauhan, university of Iowa, Iowa City, IA

Background: Fibronectin-splice variant containing extra domain A (Fn-EDA), an endogenous ligand of toll-like-receptor 4 (TLR4), is a characteristic feature of proliferating vascular smooth muscle cells (VSMCs) that contributes to intimal thickening and atherosclerosis. Very little is known about the role of Fn-EDA in VSMC proliferation or its clinical implication in neointima formation after vascular injury in the comorbid condition of hyperlipidemia.
*Methods***:** To explore the mechanism and therapeutic potential of targeting Fn-EDA in vascular diseases, we used carotid wire-injury model to induce neointimal hyperplasia (28 days) in hyperlipidemic Apoe$^{-/-}$, Fn-EDA$^{-/-}$Apoe$^{-/-}$, TLR4$^{-/-}$Apoe$^{-/-}$, Fn-EDA$^{-/-}$ TLR4$^{-/-}$Apoe$^{-/-}$ and SMC- specific Fn-EDA$^{-/-}$ mice (Fn-EDA$^{fl/fl}$αSMACre^{+}Apoe$^{-/-}$) (male and female; 10 weeks old). Furthermore, VSMCs were isolated from different genotypes and stimulated with PDGF to dissect the mechanisms.
Results: Using immunostaining, we found increased expression of Fn-EDA in human atheroma, injured carotid artery and proliferating VSMCs of Apoe$^{-/-}$ mice (P<0.05 vs. control). Irrespective of gender, genetic deletion of Fn-EDA in Apoe$^{-/-}$ mice reduced neointimal area after vascular injury (P<0.05 vs. Apoe$^{-/-}$). Aortic VSMCs isolated from Fn-EDA$^{-/-}$ Apoe$^{-/-}$ mice exhibited reduced cell proliferation (BrdU assay, G1/S phase transition) and migration (wound healing assay) that was concomitant with elevated pAKT2 and pFOXO4 expression and reduction in pAKT1, pmTOR, pNFκB, TNF-α and IL-1β secretion levels (P<0.05 vs. Apoe$^{-/-}$). Genetic ablation of TLR4 in Apoe$^{-/-}$ mice reduced neointimal hyperplasia concomitant with decreased VSMCs proliferation and migration (P<0.05 vs. Apoe$^{-/-}$), but had no additive effect in Fn-EDA$^{-/-}$Apoe$^{-/-}$ mice. Purified cellular Fn, which contains EDA, attenuated pAKT2 and pFOXO4 and potentiated pAKT1, pmTOR, pNFκB, TNF-α and IL-1β secretion in SMCs from Fn-EDA$^{-/-}$Apoe$^{-/-}$ mice (P<0.05 vs. plasma Fn that lacks Fn-EDA) but not from Fn-EDA$^{-/-}$TLR4$^{-/-}$Apoe$^{-/-}$ mice. Finally, SMC-specific Fn-EDA$^{-/-}$ mice (Fn-EDA$^{fl/fl}$αSMACre^{+}Apoe$^{-/-}$) exhibited reduced neointimal hyperplasia.
*Conclusion***:** Fn-EDA modulates TLR4-dependent VSMCs proliferation and intimal hyperplasia after vascular injury in the comorbid condition of hyperlipidemia.
M. Jain: None. **P. Doddapattar:** None. **M. Chorawala:** None. **N. Dhanesha:** None. **A. Chauhan:** None.

510
Extracellular cAMP as a Novel Therapeutic Strategy in Pulmonary Arterial Hypertension
Yassine Sassi, Carlos Bueno-Beti, Carly Jones, Guillaume Bonnet, Susana Neves, Lahouaria Hadri, Roger J Hajjar, Ichan Sch of Med Mt Sinai, New York, NY
Cyclic adenosine monophosphate (cAMP) is a cellular second messenger that mediates physiological effects of G protein-coupled receptors. Yet, the last two decades of research have shown that there is more to the role of cAMP than ever expected from this small molecule. Stimulated cells transport cAMP outside the cells, a process that is mediated by the multidrug resistance-associated proteins (MRPs). The present study investigated the role of extracellular cAMP in the lung and asked whether it may act on pulmonary vasculature remodeling. By employing a fluorescence resonance energy transfer (FRET)-based sensor, we found that extracellular cAMP activates intracellular cAMP formation in human pulmonary artery smooth muscle cells (hPASMC) and endothelial cells (hPAEC). Extracellular cAMP, via binding of its metabolite adenosine to the type A2 receptor, reduced hPASMC and hPAEC growth by controlling the PKA/CREB pathway. To test for a role of extracellular cAMP in the pulmonary vasculature, we chose rat-monocrotaline and mouse-hypoxia as *in vivo* models for pulmonary arterial hypertension (PAH). Rats treated with monocrotaline developed PAH with increased pulmonary artery pressures (PAP) and right ventricular (RV) hypertrophy. Extracellular cAMP infusion significantly prevented and reversed these structural changes. Extracellular cAMP-treated rats displayed lower RV systolic pressure and Fulton index, as well as decreased PAP. In line with these observations, we found infused cAMP to potently repress RV hypertrophy, RV systolic pressure, perivascular lung fibrosis and pulmonary arteries remodeling in mice exposed to Sugen5416 and chronic hypoxia. Together, our results assign extracellular cAMP a potent regulatory role in pulmonary vascular cells, and suggest targeting the extracellular cAMP signaling pathway to limit pulmonary vascular remodeling and PAH.
Y. Sassi: None. **C. Bueno-Beti:** None. **C. Jones:** None. **G. Bonnet:** None. **S. Neves:** None. **L. Hadri:** None. **R.J. Hajjar:** None.

This research has received full or partial funding support from the American Heart Association.

511
Mef2 Transcription Factors are Essential Regulators of Endothelial Morphology and Functions
John Schwarz, Yao Wei Lu, Albany Medical Coll, Albany, NY

Background: Laminar shear stress on the endothelium promotes atheroprotecive gene expression. In vitro experiments support a model of laminar shear stress activating the Mef2 transcription factors that in turn induce transcription of Klf2 and Klf4, which regulate many anti-inflammatory and anti-thrombotic genes. However, this model has not been tested in vivo. Three Mef2 transcription factors (Mef2a, -c, and -d) are expressed in the endothelium. To understand their functions and test this model, we generated mice with inducible, endothelial-specific deletions of Mef2c, Mef2a/c, and Mef2a/c/d.
Methods & Results: We previously reported that endothelial Mef2c inhibits the formation of endothelial actin stress fibers and migration of smooth muscle cells across the internal elastic lamina into the intima. Combined deletion of endothelial Mef2a/c produced a similar phenotype. Neither of these deletions affected survival or altered the levels of Klf2

or Klf4. However, combined deletions of Mef2a/c/d led to death 10-14 days after induction. Pulmonary hemorrhage was consistently observed as was variable amounts in other organs. En face imaging of the aorta and vena cava revealed a substantial increase in endothelial cell density and proliferation. The aortic endothelium displayed extensive actin stress fibers but the overall organization was not substantially changed. However, the vena cava was disorganized with endothelial cell aggregation. Transcriptome analysis showed ≥ 2-fold alterations in expression of 894 genes, with many important for endothelial function. Notably, Klf2 and Klf4 were both decreased in Mef2a/c/d deficient aortic endothelium to a similar extent as the Mef2s. This is consistent with the phenotypic similarity of Klf2/4 and Mef2a/c/d deletions. Comparison of genes altered by Klf2/4 and Mef2a/c/d deletions revealed that 37% of Mef2-dependent genes are also Klf2/4-dependent. **Conclusions:** Together, these data support a model in which Mef2 transcription factors redundantly regulate endothelial expression of Klf2 and Klf4 in response to shear stress to promote atheroprotective gene expression. They further regulate expression of many genes important for endothelial function independently of Klf2/4.
J. Schwarz: None. **Y. Lu:** None.

512
Bcl11b is a Newly Identified Regulator of Vascular Smooth Muscle Function and Stiffness
Jeff Arni Valisno, Pavania Elavalakanar, Christopher Nicholson, Kuldeep Singh, Boston Univ, Boston, MA; Dorina Avram, Univ of Florida, Gainesville, FL; Richard A. Cohen, Boston Univ, Boston, MA; Gary F. Mitchell, Cardiovascular Engineering, Norwood, MA; Kathleen G. Morgan, **Francesca Seta**, Boston Univ, Boston, MA

Background. B-cell leukemia 11b (Bcl11b) is a zinc-finger transcription factor known as master regulator of T lymphocytes and neuronal development during embryogenesis. However, a role for Bcl11b in the cardiovascular system has never been described. Based on human findings from a genome-wide association study (GWAS) that a gene desert region downstream of *BCL11B,* known to function as *BCL11B* enhancer, harbors single nucleotide polymorphisms (SNPs) associated with increased arterial stiffness, we sought to examine relations between Bcl11b and arterial function. ***Methods and Results.*** We found for the first time that Bcl11b is expressed in the vascular smooth muscle (VSM) of human and murine vasculature and transcriptionally regulates the expression of VSM contractile proteins smooth muscle myosin and smooth muscle α-actin. Lack of Bcl11b in VSM-specific Bcl11b null mice (BSMKO) resulted in an increased expression of Ca^{++}-calmodulin-dependent serine/threonine phosphatase calcineurin in BSMKO VSM cells and aortas, which were inversely correlated with levels of phosphorylated $VASP^{S239}$, a calcineurin de-phosphorylation target. Decreased $pVASP^{S239}$ in BSMKO aortas was associated with increased actin polymerization (F/G actin ratio), consistent with $pVASP^{S239}$'s function as regulator of cytoskeletal actin rearrangements, and was normalized by treatment with calcineurin inhibitor cyclosporine A. Functionally, Bcl11b deletion in VSM cells translated in increased aortic force, stress and wall tension, measured ex vivo in BSMKO aortas in organ baths, and increased pulse wave velocity, the *in vivo* index of arterial stiffness, in BSMKO mice compared to WT littermates. Moreover, Bcl11b and $pVASP^{S239}$ expression were decreased in aortas of obese and aged mice, two models of arterial stiffness. Bcl11b deletion in VSM had no effect on baseline blood pressure or angiotensin II-induced hypertension, measured in conscious WT and BSMKO mice by radiotelemetry, but dramatically increased the incidence of angII-induced aortic aneurysms in BSMKO mice. ***Conclusions.*** Taken together, our results identify VSM Bcl11b as a novel and crucial regulator of VSM cell phenotype and vascular structural and functional integrity
J. Valisno: None. **P. Elavalakanar:** None. **C. Nicholson:** None. **K. Singh:** None. **D. Avram:** None. **R.A. Cohen:** None. **G.F. Mitchell:** None. **K.G. Morgan:** None. **F. Seta:** None.

513
ACE2-EPCs Protect Ecs Majorly Through Their Exosomal Effects on Mitochondria
Jinju Wang, Wright State Univ, Dayton, OH; Xiaotang Ma, Guangdong Key Lab of Age-Related Cardiac and Cerebral Diseases, Inst of Neurology, Affiliated Hosp of Guangdong Medical Univ, Zhanjiang, China; Chuanfang Cheng, Dept of Cardiology, Guangzhou Inst of Cardiovascular Disease, the Second Hosp of Guangzhou Medical Univ, Guangzhou, China; Shuzhen Chen, Wright State Univ, Dayton, OH; Shiming Liu, Dept of Cardiology, Guangzhou Inst of Cardiovascular Disease, the Second Hosp of Guangzhou Medical Univ, Guangzhou, China; Bin Zhao, Guangdong Key Lab of Age-Related Cardiac and Cerebral Diseases, Inst of Neurology, Affiliated Hosp of Guangdong Medical Univ, Zhanjiang, China; Ji Bihl, Wright State Univ, Dayton, OH

Angiotensin-converting enzyme 2 (ACE2) is an emerging cardiovascular protective target which mediates the metabolism of angiotensin (Ang) II into Ang (1-7). Our group has demonstrated that ACE2 overexpression enhances the therapeutic efficacy of endothelial progenitor cells (EPCs) for ischemic stroke. Here, we investigated whether ACE2-primed EPCs (ACE2-EPCs) can protect cerebral microvascular endothelial cells (ECs) against injury and dysfunction in an *in vitro* model, with focusing on their exosomal and cytokine paracrine effects on endothelial mitochondria. Human EPCs were transfected with lentivirus containing null or human ACE2 cDNA (denoted as Null-EPCs, ACE2-EPCs, respectively). Their conditioned culture media, w/wo ultra-centrifugation for depletion of exosomes ($ACE2\text{-}EPC\text{-}CM^{EX-}$, $Null\text{-}EPC\text{-}CM^{EX-}$, ACE2-EPC-CM and Null-EPC-CM), were used for co-culture experiments. ECs injury and dysfunction model was induced by Ang II (10^{-7} M) for 8 hrs before 16 hr co-culture. After that, ECs were collected for analyses of apoptosis, angiogenic ability, mitochondrion functions (ROS production, membrane potential, fragmentation), and gene expressions (ACE2, Nox2 and Nox4). The co-culture medium was collected for measuring the levels of ACE2, Ang II / Ang-(1-7) and growth factors (VEGF and IGF). Our results showed that: 1) ACE2-EPC-CM had higher levels of ACE2, Ang (1-7), VEGF and IGF than that of Null-EPC-CM. 2) Ang II-injured ECs displayed increase of apoptotic rate and reduction in tube formation and migration abilities, which were associated with ACE2 downregulation, Ang II / Ang (1-7) imbalance, Nox2/Nox4 upregulation, ROS overproduction, increase of mitochondrion fragmentation and decrease of membrane potential. 3) ACE2-EPC-CM had better protective effects than Null-EPC-CM on Ang II-injured ECs, which were associated with the improvements on ACE2 expression, Ang II / Ang (1-7) balance and mitochondrial functions. 4) $ACE2\text{-}EPC\text{-}CM^{EX-}$ and $Null\text{-}EPC\text{-}CM^{EX-}$ had remarkably reduced effects by over 70% as respectively compared to ACE2-EPCs-CM and Null-EPCs-CM. In conclusion, our data demonstrate that ACE2 overexpression can enhance the protective effects of EPCs on ECs injury, majorly through the exosomal effects on mitochondrial function.
J. Wang: None. **X. Ma:** None. **C. Cheng:** None. **S. Chen:** None. **S. Liu:** None. **B. Zhao:** None. **J. Bihl:** None.

This research has received full or partial funding support from the American Heart Association.

514
Netrin 4 Deficiency Leads to Endothelial Cell Senescence
HUAYU ZHANG, Dianne Vreeken, Ruben G de Bruin, Danielle G Leuning, Mehdi Maanaoui, Wendy M Sol, Eric P van der Veer, Ton J Rabelink, Anton Jan van Zonneveld, Janine M van Gils, Leiden Univ Medical Ctr, Leiden, Netherlands

Senescence phenotype of endothelial cells (ECs) has pathophysiological consequences, such as decreased regeneration capacity, pro-atherogenic tendency and dysregulated vessel tune. We find that netrin 4 (NTN4), recognized in neural and vascular development, is highly expressed by mature ECs. Remarkably, little is known about its role in vascular biology after development. NTN4 is deposited in the extracellular matrix. Using human decellularized kidney extracelluar matrix scaffolds, we found that pre-treatment of the scaffolds with NTN4 increased numbers of EC adhesion to the matrix, showing a pro-survival effect of NTN4.
Subsequently we explored the regulation of NTN4 expression in ECs. We found a 1.8-fold (±0.3; $p<0.05$) upregulation in NTN4 expression in ECs cultured under laminar flow conditions compared to static culture conditions. In contrast, ECs stimulated with TNFα resulted in decreased NTN4 expression (0.17 ± 0.06 fold; $p<0.05$), indicating a role for NTN4 in quiescent healthy endothelium. Silencing of NTN4 in ECs, to investigate the necessity of NTN4 in ECs, markedly resulted in more senescent associated β-galactosidase activity (20-50%; $p<0.05$) that could be rescued by NTN4 protein coating. Consistent with increased senescence, NTN4 reduction is accompanied with increased expression of senescence-associated transcription factors, CDKN1A and CDKN2A, as well as decreased ability to proliferate. Importantly, ECs with reduced levels of NTN4 have also increased expression of ICAM-1 and VCAM-1, are more prone to adhesion of human monocyte and have impaired barrier function, measured in an electric cell-substrate impedance sensing system as well as 'organ-on-a-chip' microfluidic system.
In conclusion, our results identified the anti-senescence function of NTN4 and thereby provides novel insights in the role of NTN4 in EC function. In situations like acute inflammation and unfavourable hemodynamic conditions, NTN4 expression decreases, so that there is a possible window for us to improve EC function by normalizing NTN4 expression.
H. Zhang: None. **D. Vreeken:** None. **R.G. de Bruin:** None. **D.G. Leuning:** None. **M. Maanaoui:** None. **W.M.P. Sol:** None. **E.P. van der Veer:** None. **T.J. Rabelink:** None. **A. van Zonneveld:** None. **J.M. van Gils:** None.

515
Shear Stress Regulation of Angiotensin Converting Enzyme 2 Contributing to the Endothelial Homeostasis
Jiao Zhang, UCSD, La Jolla, CA

Background The angiotensin-converting enzyme 2 (ACE2)-angiotensin 1-7 (Ang 1-7)-Mas pathway is the vasoprotective axis in the renin-angiotensin system and hence plays an essential role in maintaining vascular health. Although shear stresses are principal physiological and pathophysiological stimuli regulating endothelial function or dysfunction, information is scant whether the athero-protective and athero-prone flow patterns distinctly regulate ACE2 in the endothelium and the underlying mechanism.
Methods and Results Bioinformatics prediction, kinase assay, and antibody against phosphorylated ACE2 Ser-680 (p-ACE2 Ser-680) were used to investigate AMP-activated protein kinase (AMPK) phosphorylation of ACE2 in vascular endothelial cells (ECs). Pulsatile shear stress (PS) mimicking athero-protective flow with its activation of AMPK caused increased phosphorylation of ACE2 at Ser-680. This AMPK-dependent ACE2 phosphorylation enhanced the stability and activity of ACE2 with ensuing increase in Ang 1-7 level, eNOS-derived NO bioavailability, and mitochondrial function in ECs. The PS-activated AMPK also regulated ACE2 at the transcriptional level via krüppel-like factor 2 (KLF2). Evidence supporting KLF2 transactivation of ACE2 included the decreased methylation of the promoter region of the *ACE2* gene in ECs overexpressing KLF2. *In vivo*, the thoracic aorta (TA, athero-protective) of C57BL6 mice exhibited higher levels of p-ACE2 and ACE2 compared to aortic arch (AA, athero-prone). Using CRISPR-Cas9 genomic editing, we created gain-of-function ACE2 S680D (a phspho-mimetic mutant) knock-in and loss-of-function ACE2 S680L (a dephspho-mimetic mutant) knock-in mice. Lung ECs isolated from these mice showing that ECs with ectopic expression of ACE2 S680D had higher ACE2 expression than those of ACE2 S680L. Consistently, the flow-mediated vasodilation was attenuated in ACE2 S680L mice compared to ACE2 S680D mice.
Conclusions The athero-protective PS regulates ACE2 in ECs through AMPK phosphorylation of ACE2 Ser-680 as well as KLF2 mediation of ACE2 transcription. Thus, the AMPK-ACE2 pathway plays a beneficial role in endothelial homeostasis.
J. Zhang: None.

516
Endothelial Foxp1 Regulates Cardiac Remodeling via Tgfbeta and Et-1 Signal Pathway
Jie Liu, Tao Zhuang, Xiaoli Chen, Jinjiang Pi, Yashu Kuang, Sheng Peng, Lin Zhang, **Yuzhen Zhang**, Shanghai East Hosp-Tongji U Sch of Med, Pudong New Area Shanghai, China

Rationale: Cardiac fibrosis and hypertrophy is common features in left ventricular remodeling that leads to heart failure. Forkhead box protein P-1 (Foxp1), a large modular transcriptional repressor that binds to DNA via the highly conserved forkhead DNA-binding domain, is crucial in coordinating the balance of cardiomyocyte proliferation and differentiation through cell lineage-specific regulation during cardiac development. However, its role in adult pathological cardiac remodel remains to be clarified. **Objective:** We seek to determine the role and the underlying mechanisms of Foxp1 in cardiac fibrosis and hypertrophy. **Methods and Results:** Foxp1 was highly expressed in endocardium and cardiac microvascular endothelial cells, significantly reduced following AngII stimulation. Loss of endothelial Foxp1 increased AngII-mediated cardiac fibrosis, which was accompanied by myofibroblast proliferation and endothelial-mesenchymal transition (endMT) with elevated expression of fibrotic matrix genes. TGF-β signal pathway was identified as Foxp1 direct downstream target gene in endothelial cells to regulate the fibrosis. Increased AngII-mediated cardiac hypertrophy was observed when loss of endothelial Foxp1, with elevated cardiac hypertrophic genes and fetal myosin gene (myh7) expression but reduced adult mature myosin gene (myh6) expression via endothelial ET-1 signal. The pathological remodel in endothelial Foxp1 deficient mutant mice finally led to worsen cardiac diastolic dysfunction as shown by elevated E/e' ratio in echocardiogram. Moreover, the similar pathological remodel and worsen cardiac diastolic and systolic dysfunction as shown by reduction of LV fractional shortening (FS) and ejection fraction (EF) were observed in pressure overload transverse aortic constriction (TAC) model when loss of endothelial Foxp1. **Conclusions:** This study uncovered a previously unrecognized anti-fibrotic and anti-hypertrophic role of Foxp1 in pathological cardiac remodel, which is achieved through the regulation of endothelial TGF-β/ET-1 signals, implying the promising therapeutic targets in pathological cardiac remodeling diseases and heart failure.
J. Liu: None. **T. Zhuang:** None. **X. Chen:** None. **J. Pi:** None. **Y. Kuang:** None. **S. Peng:** None. **L. Zhang:** None. **Y. Zhang:** None.

520
Skeletal Muscle Myosin Supports the Anticoagulant Functions of Activated Protein C and Protein S but not Protein C Activation by Thrombin:Thrombomodulin
Mary Jo Heeb, Olivia McDowell, Atsuki Yamashita, Jose' A. Fernandez, Laurent O. Mosnier, Hiroshi Deguchi, John H. Griffin, The Scripps Res Inst, La Jolla, CA

Skeletal muscle myosin was reported by Deguchi et al to promote thrombus formation ex vivo for flowing human whole blood, to support prothrombinase activity in plasma and to promote prothrombin activation by factors (F) Xa and Va in purified systems. Skeletal muscle myosin binds FXa and FVa and effectively replaces the procoagulant activity of phospholipid vesicles. We therefore assessed whether myosin might replace phospholipids in support of the anticoagulant function of activated protein C (APC) and its cofactor protein S (ProS) for inactivation of purified FVa. When purified component prothrombinase assays were used to monitor FVa inactivation by APC, FVa activity was significantly reduced by APC in the presence of myosin compared to controls, and FVa inactivation in the presence of 40 nM myosin over 25 min was much greater than that in the presence of 40 nM phospholipids and similar to the rate of FVa inactivation in the presence of 25 μM phospholipids (see Figure). Inhibition of the APC-enhancing effects of myosin were confirmed to be specific for myosin because the anti-myosin inhibitor, myoVin-1, inhibited myosin's effects. ProS at ≥ 25 nM enhanced the myosin-stimulated inactivation of FVa by APC. The ProS anticoagulant enhancement effect was most obvious at lower APC concentrations, as expected. Immunoblots showed that myosin enhanced Arg506 cleavage in FVa by APC alone; but notably in the presence of ProS, myosin enhanced both Arg506 and Arg306 cleavages in FVa. Myosin did not enhance activation of protein C by thrombin in the presence or absence of thrombomodulin. Thus, in purified reaction mixtures, skeletal muscle myosin remarkably can support both procoagulant thrombin generation, as previously reported, and compensatory anticoagulant mechanisms in the presence of APC and ProS, as shown here. Further studies are needed to determine the molecular basis for these reactions and to assess the physiologic and pathologic relevance of these reaction mechanisms.

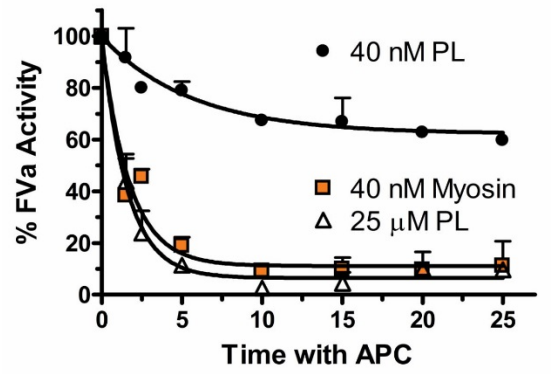

M.J. Heeb: None. **O. McDowell:** None. **A. Yamashita:** None. **J.A. Fernandez:** None. **L.O. Mosnier:** None. **H. Deguchi:** None. **J.H. Griffin:** None.

521
Pharmacological Profile of JNJ-64179375: A Novel, Long Acting Exosite-1 Thrombin Inhibitor
Zheng Huang Devine, Qiu Li, Madhu Chintala, Johnson & Johnson, Spring House, PA

Background: Thrombin is a key serine protease involved in hemostasis and thrombosis by mediating the conversion of soluble fibrinogen to insoluble fibrin that forms the meshwork of a clot. In addition, it is the most potent activator of platelets. Hence thrombin inhibition has been a target for the development of anticoagulant drugs. Recently, an IgA that binds to the exosite 1 region of thrombin was identified in a patient that was profoundly anticoagulated but without any abnormal bleeding episodes over a prolonged follow-up. JNJ-64179375 (JNJ-9375) is a monoclonal antibody derivative of the IgA which by selectively inhibiting exosite 1 may allow for some of thrombin functions mediated by exosite 2 and the active site which might be important for hemostasis. JNJ-9375 is being developed as a new long-acting anti-coagulant with a potential for better efficacy with a reduced bleeding liability.
Objectives: To assess the in vitro effects of spiked JNJ-9375 on various clotting assays in human and animal plasma and to evaluate the antithrombotic activity in a rat A-V shunt model of thrombosis.
Methods and results: JNJ-9375 produced a concentration-dependent prolongation of thrombin time (TT), ecarin clotting time (ECT), prothrombin time (PT), and activated partial thromboplastin time (aPTT) when added to normal human plasma. The concentrations required to prolong clotting time by twofold (EC2Xs) were 4.4, 12.4, 202.7, and 172.6 μg/ml for TT, ECT, aPTT, and PT respectively. Therefore, TT was the most sensitive assay to show pharmacodynamic activity of JNJ-9375. Similar effects were observed in other species studied including monkey, rat, and mouse. In the rat A-V shunt model of thrombosis, JNJ-9375 dose dependently inhibited thrombus weight with an efficacious dose of 0.3 mg/kg, which was accompanied by prolongation of TT, ECT, PT, and aPTT from ex vivo plasma samples.
Conclusion: Results from these studies demonstrate that selective inhibition of exosite 1 on thrombin leads to robust anticoagulation and antithrombotic efficacy. JNJ-9375 is currently in early clinical development.

Z. Huang Devine: Employment; Significant; Janssen Research & Development, LLC. **Q. Li:** Employment; Significant; Janssen Research & Development, LLC. **M. Chintala:** Employment; Significant; Janssen Research & Development, LLC.

522
VWF Inhibition by an RNA Aptamer Improves Functional Outcome Compared to rTPA in Ferric Chloride-induced Carotid Artery Thrombosis in Mice
Jenna Wilson, Debra Wheeler, Allyson Huttinger, Cole Anderson, Spencer Talentino, Maria Balch, Cameron Rink, **Shahid Nimjee**, The Ohio State Univ Med Ctr, Columbus, OH

Objective: To compare the functional effects of von Willebrand Factor (VWF) inhibition by RNA aptamer (T79) vs rTPA utilizing *in vivo* arterial thrombosis in mice. ***Approach and Results:*** We previously demonstrated that inhibition of VWF by a targeted RNA aptamer (T79) both prevents thrombosis and thrombolyses stabilized clots in a murine model of ferric chloride ($FeCl_3$)-induced vascular injury suggesting a pivotal role for VWF in the pro-thrombotic and anti-thrombotic milieu. We hypothesized that T79 treatment, which demonstrated no hemorrhagic complications and greater re-perfusion compared to rTPA, would result in improved behavioral outcome with 7 day survival after vascular injury. Baseline locomotor testing in an open field was performed on both male and female, 8-16 week old, wild-type C57BL/6J mice. Occlusive arterial thrombus formation was induced by a 3 minute exposure to 10% $FeCl_3$ on the right common carotid monitored by Doppler flow and time to occlusion (blood flow of 0 ml/min) was measured. Twenty minutes after thrombus stabilization either T79 (0.1 mg/kg or 0.5 mg/kg bolus), rTPA (10 mg/kg 45 min infusion) or saline vehicle (45 min infusion) was introduced via a saphenous catheter. Animals were recovered and locomotor testing was repeated 48 hours and 7 days after injury with baseline set as 100%. All groups including vehicle control resulted in a statistically significant decrease in distance traveled (meters) and speed (meters/sec) at 48 hours after injury. At 7 days, 0.1 mg/kg T79 increased 29.89% from 48 hours, 0.5 mg/kg T79 increased 22.50% from 48 hours but

rTPA treatment showed no significant improvement (2.79% increase) (n=4, p<0.001). In addition, 0.1 mg/kg and 0.5 mg/kg T79 resulted in a 28.46% and 22.44% increase in speed, respectively, at 7 days compared to 48 hours whereas rTPA did not (2.94% increase) (n=4, p<0.001). Interestingly, males scored lower on most behavioral parameters at 48 hours, but recovered to the same level as females by 7 days. No significant differences in time to occlusion or baseline locomotor testing were observed in any group. ***Conclusion***: Inhibition of VWF by T79 aptamer markedly improves behavioral outcomes compared to rTPA after survival carotid artery occlusion following ferric chloride-induced injury in mice.

J. Wilson: None. **D. Wheeler:** None. **A. Huttinger:** None. **C. Anderson:** None. **S. Talentino:** None. **M. Balch:** None. **C. Rink:** None. **S. Nimjee:** None.

523

The Effects of Spontaneous Exercise on Murine Model of Deep Vein Thrombosis

Olivia R Palmer, Jose A Diaz, Joan M Greve, Univ of Michigan, Ann Arbor, MI

Introduction: Recent studies suggest physical activity may have beneficial effects on deep vein thrombosis (VT). Long-term moderate exercise has been shown to reduce inflammatory cytokines and attenuate plasma fibrinogen compared to uninterrupted sitting. However, the effect exercise may have in VT is unknown. Our objective is to quantify the effects of prophylactic exercise on the thrombotic process in a murine model of VT. Methods: C57BL6 male mice were either provided in-cage running wheels (E: n=6) starting 2 weeks prior to and continuously following VT induction, or no wheel exposure (C: n=4). VT was induced with the electrolytic inferior vena cava model (EIM), which induces thrombosis in the continuous presence of blood flow. MR images were acquired days 2 (acute) or 6 (chronic) post VT using a T2-weighted sequence sensitive to edema-related fluid, then the thrombi were harvested for histology. Results: Four of six mice engaged in exercise. Three of four mice continued running after thrombus induction, with reduced activity (88 ± 11% reduction). While thrombus volume was not significantly different between groups, the volume of thrombus exhibiting high T2 signal was reduced by ~57% at day 6 in exercising mice, suggesting a decreased inflammatory response with exercise (C 0.81 ± 0.13 mm^3 vs. E 0.35 ± 0.07 mm^3, p=0.08). Fibrin content, assessed by Picro-Mallory staining, was reduced by 60% at day 2 in exercising mice (C 2.08 ± 0.29 um^2 vs. E 0.83 ± 0.45 um^2, p=0.09). Conclusion: Our results suggest that exercise may reduce inflammation in VT and lead to less fibrin-rich clots. Future studies will increase the number of animals, investigate inflammatory components, and extend to more chronic time points. Understanding the impact of exercise on specific thrombotic components could lead to better recommendations for patients with DVT.

O.R. Palmer: None. **J.A. Diaz:** Consultant/Advisory Board; Modest; American Venous Forum, Board of Directors. **J.M. Greve:** None.

524

Fibrinogen Depletion Attenuates Angiotensin II-induced Abdominal Aortic Aneurysm

Hannah M Russell, Keith Saum, Alexandra C Sundermann, Shannon M Jones, Anders Wanhainen, Todd L Edwards, Lori A Holle, Alisa S Wolberg, A. Phillip Owens III, Univ of Cincinnati, Cincinnati, OH

Background: Fibrinogen and fibrin provide physical and biochemical support to a developing clot and is defined as one of the most crucial independent risk factors for cardiovascular diseases (CVDs). In addition to clot formation, fibrinogen promotes wound healing and powerful inflammatory and immune responses by engagement of leukocytes. Increased circulating fibrinogen and fibrin degradation products are correlated with increased diameter and progression of abdominal aortic aneurysm (AAA). However, a causal link between fibrinogen and AAA has not yet been established. The objective of this study was to determine the role of fibrinogen depletion in a mouse model of AAA. ***Methods and results:*** To determine whether aneurysm resulted in a procoagulant environment, we examined plasma levels of thrombin generation by calibrated automated thrombography (CAT), thrombin anti-thrombin (TAT), and fibrinogen in control and AAA plasma from mice and humans. Patients and mice with AAA had significant elevations in thrombin generation, TAT, and fibrinogen versus saline controls (mice) and control patients (human). To determine the effect of fibrinogen, in vivo, low density lipoprotein receptor deficient ($Ldlr^{-/-}$) mice were injected with scrambled anti-sense oligonucleotide (ASO) or β-fibrinogen ASO (30 mg/kg) 3 weeks prior to experimentation and throughout the study. Fibrinogen ASO treatment achieved > 90% depletion of fibrinogen. After 3 weeks, mice were fed a fat and cholesterol enriched diet (42% milk fat; 0.2% cholesterol) 1 week prior to and throughout infusion with angiotensin II (AngII; 1,000 ng/kg/day) for 28 days. Fibrinogen ASO attenuated abdominal diameter (33% decrease; P = 0.001), and inflammatory cytokines (>75% decreased IL-1 and IL-6; P = 0.001) versus scrambled ASO control. Further, fibrinogen depletion significantly attenuated aneurysm incidence and rupture-induced death (P < 0.05). ***Conclusions:*** Our results demonstrate that AAAs augment procoagulant markers in both humans and mice. Importantly, fibrinogen depletion attenuates AAA incidence, diameter, rupture-induced death, and inflammation. Therefore, reduction of plasma fibrinogen may be a novel treatment strategy in patients with AAA.

H.M. Russell: None. **K. Saum:** None. **A.C. Sundermann:** None. **S.M. Jones:** None. **A. Wanhainen:** None. **T.L. Edwards:** None. **L.A. Holle:** None. **A.S. Wolberg:** None. **A. Owens III:** None.

525

Contraction of Blood Clots Influences Their Susceptibility to Fibrinolysis

Valerie Tutwiler, Univ of Pennsylvania, Philadelphia, PA; Alina D Peshkova, Giang Le Minh, Kazan Federal Univ, Kazan, Russian Federation; Sergei Zaitsev, Rustem I Litvinov, John W Weisel, Univ of Pennsylvania, Philadelphia, PA

The success of endogenous and therapeutic fibrinolysis is governed in part by the structure of the fibrin clot. An understudied feature that potentially affects fibrinolysis is the degree of platelet-driven shrinkage, i.e. contraction, of blood clots and thrombi. The aim of this work was to examine the effect of clot contraction on the rate of naturally occurring fibrinolysis from within and external fibrinolysis to simulate therapeutic thrombolysis. Clot contraction, which was initatied with 2mM $CaCl_2$ and 1U/ml thrombin, was impaired by ~75% by inhibiting platelet non-muscle myosin IIa activity (blebbistatin), actin polymerization (latrunculin A), and platelet-fibin(ogen) binding (abciximab). Internal fibrinolysis measured using dynamic optical tracking of clot size as a function of time occurred 2X faster in contracted clots compared to uncontracted clots in the presence of 75ng/ml tPA. In direct contrast, the dynamic release of radioactive fibrin degradation products as a measure of external fibrinolysis was 4X faster in uncontracted clots when 75 ng/ml tPA was added to the surface of preformed clots. This difference in the susceptibility of contracted and uncontracted clots to internal versus external lysis suggests that the lysis rate is dominated by the interplay of clot permeability to fibrinolytic enzymes as well as the spatial proximity of the fibrin fibers themselves. These results have implications for understanding clot stability in patients with thrombotic disorders and improving clot lysis by impairing platelet-mediated clot contraction.

V. Tutwiler: None. **A.D. Peshkova:** None. **G. Le Minh:** None. **S. Zaitsev:** None. **R.I. Litvinov:** None. **J.W. Weisel:** None.

This research has received full or partial funding support from the American Heart Association.

529
Digoxin and Platelet Activation in Atrial Fibrillation Patients
Daniele Pastori, Roberto carnevale, Simona Bartimoccia, Cristina Nocella, Marta Novo, Francesco Violi, **Pasquale Pignatelli**, Sapienza Univ, Rome, Italy

Background: digoxin use was shown to be associated with an increased risk of cardiovascular events In atrial fibrillation (AF). We hypothesized that digoxin may affect cardiovascular risk by increasing platelet activation. **Methods:** This is a post-hoc analysis from an observational prospective study of AF patients treated with vitamin K antagonists. Patients were divided into two groups balanced for age, sex and cardiovascular risk factors: digoxin users (n=132) and non-users (n=388). Urinary excretion of 11-dehydro-thromboxane B_2 (TxB_2), a marker of platelet activation and serum digoxin concentration (SDC) were measured. In vitro experiments were performed on platelets from healthy subjects treated with scalar doses of digoxin (0.6 - 2.4 ng/ml). **Results:** Mean age of digoxin users was 75.2±7.2 years and 47.7% were women. Median overall 11-dehydro-TxB_2 was 105.0 (IQR 60.0-190.0) ng/mg creatinine, and median SDC was 0.65 (IQR 0.40-1.00) ng/ml. Urinary 11-dehydro-TxB_2 and SDC were significantly correlated (rS=0.350, p<0.001). Patients in the upper tertile of SDC showed significantly higher urinary11-dehydro-TxB_2 compared to non-digoxin users (p=0.019). In vitro study showed that digoxin at concentration ≥1.2 ng/ml induced calcium mobilization, arachidonic acid (AA) release, TxB_2 biosynthesis and platelet aggregation, that were inhibited by the calcium chelator Ethylenediaminetetraacetic acid (EDTA) or by the specific phospholipase A_2 (PLA_2) inhibitor Arachidonyl trifluoromethyl ketone (ACOOCF3). **Conclusion:** We found a significant in vivo correlation between SDC and platelet activation. In vitro study showed that supra-therapeutic digoxin concentrations increased platelet aggregation via calcium-related PLA_2 phosphorylation. This finding provides new insights into the association between digoxin use and cardiovascular complications in AF patients.
D. Pastori: None. **R. carnevale:** None. **S. Bartimoccia:** None. **C. Nocella:** None. **M. Novo:** None. **F. Violi:** None. **P. Pignatelli:** None.

530
Hemostasis Revisited: a Combined Light and Electron Microscopy Analysis of Hemostatic Plug Formation *in vivo*
Maurizio Tomaiuolo, Chelsea N. Matzko, Izmarie Poventud-Fuentes, John W. Weisel, Lawrence F. Brass, **Timothy J Stalker**, Univ Pennsylvania, Philadelphia, PA

We have previously shown in the microcirculation that gradients of platelet agonists develop during the hemostatic response as a consequence of the solute transport properties within the evolving platelet mass. These agonist gradients result in the formation of a gradient of platelet activation extending from the site of vascular injury. Here we utilized a combined light and electron microscopy approach to examine the organization of hemostatic plugs formed in response to larger injuries that result in significant bleeding in the mouse jugular vein. The results show that the hemostatic response to vessel wall puncture in a large vein is similarly characterized by a gradient of platelet activation. Specifically, we found that 1) platelets are the primary cellular component of hemostatic plugs in large veins; 2) platelet activation is heterogeneous, with fully activated and degranulated platelets present at the interface of the damaged vessel wall and extending to the extravascular side of hemostatic plugs, while platelets aggregated on the luminal side of plugs were minimally activated; 3) fibrin, and by extension thrombin activity, is localized primarily in the extravascular space; 4) $P2Y_{12}$ antagonism impairs platelet aggregation, resulting in a prolonged bleeding time when the hole created by the puncture injury does not completely fill with platelets; and 5) the importance of $P2Y_{12}$ signaling in establishing a hemostatically competent plug is related to the size of the hole through which blood escapes the vasculature. Taken together, these results provide novel insights into the mechanisms of hemostatic plug formation in vivo, demonstrate in detail the mechanism by which $P2Y_{12}$ antagonists result in bleeding, and highlight differences in the composition and morphology of hemostatic plugs versus pathologic thrombi.
M. Tomaiuolo: None. **C.N. Matzko:** None. **I. Poventud-Fuentes:** None. **J.W. Weisel:** None. **L.F. Brass:** None. **T.J. Stalker:** None.

532
Shear-induced Release of Platelet Receptors Contributes to Bleeding Outcomes in Patients With Lvads or Exposed to Ecmo
Elizabeth E Gardiner, The Australian Natl Univ, Canberra, Australia; Joshua Casan, The Alfred Hosp, Melbourne, Australia; Samantha J Montague, The Australian Natl Univ, Canberra, Australia; Pohan Lukito, The Alfred Hosp, Melbourne, Australia; Robert K Andrews, Monash Univ, Melbourne, Australia; Amanda K Davis, The Alfred Hosp, Melbourne, Australia

Despite advances in design and materials, as well as pharmacological prophylaxis, hemostatic complications continue to plague device recipients. Ventricular assist devices (VADs) and extracorporeal membrane oxygenation (ECMO) are associated with bleeding that is not fully explained by anticoagulant or antiplatelet use. Exposure of platelets to elevated shear in vitro leads to increased shedding. We examined blood samples from patients with heart failure or in receipt of high fluid shear mechanocirculatory support to assess whether loss of platelet receptors occurs *in vivo*, and the relationship with acquired von Willebrand syndrome (AVWS) and changes in inflammatory cytokines. Platelet counts, levels of inflammatory cytokines IL-1β, IL-6, TNFα, MCP-1, IL-17A and IFNγ, coagulation tests and von Willebrand factor (VWF) analyses were performed on samples from 13 continuous flow VAD (CF-VAD), 14 ECMO, and 24 heart failure patients. Levels of platelet receptors were measured by flow cytometry or ELISA. The loss of high molecular weight VWF multimers was observed in 12 of 13 CF-VAD and 7 of 14 ECMO patients, consistent with AVWS. Platelet receptor shedding was demonstrated by elevated soluble glycoprotein (GP) VI levels in plasma and significantly reduced surface GPIbα and GPVI levels in CF-VAD and ECMO patients as compared with healthy donors. Platelet receptor levels were also significantly reduced in heart failure patients. Significant differences in levels of inflammatory cytokines monocyte-chemoattractant protein and tissue necrosis factor-a in a subset of patients with decompensated HF. These data link AVWS and increased platelet receptor shedding in patients with CFVADs or ECMO. Loss of the platelet surface receptors GPIbα and GPVI in heart failure, CFVAD and ECMO patients may be linked with extent of inflammation and may contribute to ablated platelet adhesion/activation, and limit thrombus formation under high/pathologic shear conditions.
E.E. Gardiner: None. **J. Casan:** None. **S.J. Montague:** None. **P. Lukito:** None. **R.K. Andrews:** None. **A.K. Davis:** None.

533
Gold Nanoparticles Allow CT Imaging of Experimental Atherosclerosis
Hisanori Kosuge, Tsukuba Advanced Imaging Ctr, Ibaraki, Japan; Maki Nakamura, Ayako Oyane, Nanomaterials Res Inst, Natl Inst of Advanced Industrial Science and Technology, Ibaraki, Japan; Kazuko Tajiri, Nobuyuki Murakoshi, Satoshi Sakai, Akira Sato, Kazutaka Aonuma,

Dept of Cardiology, Faculty of Med, Univ of Tsukuba, Ibaraki, Japan

Background: Macrophages play a key role in the development of atherosclerosis, and are important targets for the detection of vascular inflammation. Gold nanoparticles (GNPs) are widely used as contrast agents for computed tomography (CT) due to high X-ray attenuation. We evaluated GNPs for imaging of macrophages, both *in vitro* and in murine carotid arteries.
Methods: Mouse macrophage cells (RAW 264.7) were incubated with GNPs (AuroVist™ 15 nm, Nanoprobes, Yaphank, NY) at doses of 0, 50, 100 µg Au/ml for 24 hours. Cells were scanned with micro-CT imaging system (LaTheta LCT-100A, Hitachi-Aloka, Tokyo) for cellular uptake. Cell viability was assessed by MTT assay. FVB mice (N=3) induced diabetes and hyperlipidemia were developed macrophage-rich atherosclerotic lesions by left carotid ligation (operation group). After 2 weeks, mice were injected with GNPs (2 mice: 10 mg Au/mouse, one mouse: 20 mg Au/mouse) via tail vein and scanned with micro-CT imaging system at 24 hours after injection. One mouse without induction of hyperlipidemia and diabetes and carotid ligation (control group) was also scanned after injection of GNPs (10 mg Au/mouse).
Results: The CT values of macrophage cells incubated with GNPs were significantly higher compared to those of Au-free cells ($p<0.02$) (Figure 1). Macrophages incubated with GNPs showed a similar viability as control cells (Figure 2). The CT values of a ligated left carotid artery injected with 20 mg Au was higher compared to those of a ligated left carotid with 10 mg Au, a non-ligated left carotid of a control, and non-ligated right carotids (operation group and control) at 24 hours after injection (Figure 3).
Conclusion: CT imaging can detect macrophages with GNPs *in vitro* and accumulation of higher dose of GNPs in vascular lesion. GNPs have the potential as a contrast agent for imaging of atherosclerosis.

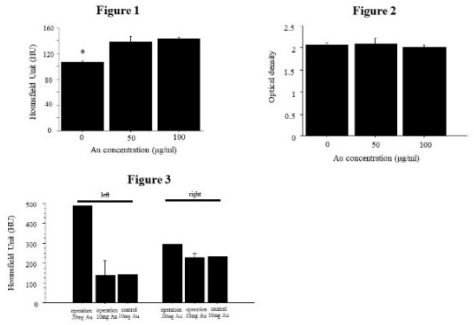

H. Kosuge: Research Grant; Significant; JSPS KAKENHI Grant Number JP16K09511. **M. Nakamura:** Research Grant; Significant; JSPS KAKENHI Grant Number JP16H03831. **A. Oyane:** None. **K. Tajiri:** None. **N. Murakoshi:** None. **S. Sakai:** None. **A. Sato:** None. **K. Aonuma:** None.

534
Aging is Associated with Peroxide Mediated Increased Thrombin Generation
Rahul Kumar, Vijay Sonkar, Lauren Wegman-Points, Anjali Sharathkumar, Gary L Pierce, Sanjana Dayal, Univ of Iowa Health Care, Iowa City, IA

Human aging is associated with increased incidence of deep vein thrombosis (DVT), but the mechanisms are not fully elucidated. Using experimental models of DVT, we and others have demonstrated that mice also display increased susceptibility to thrombosis during aging. Further, we established that aged mice overexpressing antioxidant glutathione peroxidase (Gpx1; that converts peroxides to water) are protected from age associated increased susceptibility to DVT. However, the mechanistic pathway for peroxide-dependent thrombosis remains elusive. Recent studies have suggested that hydrogen peroxide mediated activation of neutrophils causes release of neutrophil extracellular traps (NETs). NETs are known to activate coagulation and contribute to the development of DVT. We hypothesized that aging cause peroxide-dependent increased release of NETs and increased thrombin generation. We studied Gpx1 Tg mice and their wild type (WT) littermates at 4 (young) and 20 months (old) of age. Cell-free DNA (cfDNA), a circulating marker of NETs was measured in the plasma using Qubit assay. We observed a significant increase in cfDNA in old WT mice compared to young WT mice (28.2±2.2 vs. 11.4±0.8 ng/µl, $P<0.001$), but there was no difference in cfDNA between old WT and old Gpx1 Tg mice. Next, we assessed thrombin generation using a Calibrated Automated Thrombogram (Daignostic Stago). The aged WT mice showed significant increase in endogenous thrombin potential (ETP, 430.2±26.7 vs. 277.9±42.1 nM.min, $P<0.05$) as well as peak amplitude, compared to young WT mice (65.4±4.3 vs. 40.8±7.1 nM, $P<0.05$). Interestingly, ETP was significantly decreased in aged Gpx1 Tg mice ($P<0.05$ vs. aged WT), suggesting a peroxide mediated effect on thrombin generation with aging. To examine how the findings in aged mice translate to human aging, we examined plasma samples from healthy young (18-39 years, n=11) and older (50-79 years, n=17) human subjects. We observed a significant increase in cfDNA and ETP in older compared to younger humans (13.4±.9 vs. 12.3±.4 ng/µl, $p<0.05$ for cfDNA and 1917.6±141.2 vs 1475.9±66.3 nM.min, $p<0.05$ for ETP). These data suggest that both mouse and human aging is associated with increased release of cfDNA and higher ETP, and that in mice peroxide mediates effects of aging on thrombin generation.

R. Kumar: None. **V. Sonkar:** None. **L. Wegman-Points:** None. **A. Sharathkumar:** None. **G.L. Pierce:** None. **S. Dayal:** None.

535
Proteomics Identifies Endothelium-derived Clusterin as a Novel Regulator of Von Willebrand Factor Multimerization
Jincai Luo, Peking Univ, Beijing, China

*Background***:** Secretion of vascular endothelial cells (ECs) is considered to be the first line of defense against vascular injury. Vascular endothelial growth factor (VEGF) is one of the most important endothelial growth factors, involved in various endothelial functions including the regulatory secretion of ECs. However, the systematic analysis of the VEGF-induced secretory proteins has not yet been carried out. *Objectives*: To investigate the secretory proteins rapidly released from ECs under VEGF stimulation and their functions on the ECs. *Methods:* A non-serum culture system was established for analyzing the proteins secreted form human primary ECs in response to VEGF with mass spectrometry. *Results*: In the proteomic result, 362 proteins were identified and assigned to the VEGF-induced secretome, including the known von Willebrand factor (VWF), a multimeric protein mediating adhesion of platelets at vascular injury sites. Clusterin, a multifunctional protein involved in various diseases including Alzheimer disease and cancers, was selected for further study as a new VEGF-induced secretory protein. Clusterin was co-localized with VWF both in Weibel-Palade bodies (WPBs) and extracellular VWF strings of ECs. We showed that the localization of clusterin in pseudo-WPBs in 293T cells depends on the carboxy-terminal domains of VWF. Functional study showed that deficiency of clusterin in ECs increased the size of VWF multimers. *Conclusions*: We not only obtained a VEGF-induced secretome using primary ECs, but also determined clusterin as a novel component of WPBs, which is capable of maintaining the normal pattern of VWF multimers, and suggest its function on vascular thrombosis and haemostasis.

J. Luo: None.

537
Nature's Surfaces: a Potential Role for Arterial Wrinkles in Vascular Homeostasis
Nandan Nath, Luka Pocacivsek, UPMC Vascular Surgery, Pittsburgh, PA; Ya Gao, Univ of Pittsburgh Dept of Chemical Engineering, Pittsburgh, PA; Karim Salem, UPMC Vascular Surgery, Pittsburgh, PA; Sachin Velankar, Dept of Chemical Engineering, Pittsburgh, PA; Edith Tzeng, UPMC Vascular Surgery, Pittsburgh, PA

Biologic interfaces play important roles in tissue function. The tissue-blood interface in blood vessels represents a dynamic interaction between the endothelium and circulating RBCs, platelets and inflammatory cells. This interface is critical in regulating vascular thrombosis. While the study of vascular homeostasis has focused on the endothelium, the arterial lumen has been shown to possess a regular wrinkled pattern that has been previously attributed to fixation artifact. We hypothesize that the arterial luminal surface undergoes phasic wrinkling and flattening driven by the cardiac cycle and this dynamic topography may represent a novel mechanism of resisting platelet adhesion. Using an *ex vivo* pulsatile pump system to actuate arteries and grafts, we examined the effect of physiologic pressures on luminal topography and the effect of dynamic topography on platelet adhesion in vascular graft function. Pig carotid arteries were distended to 40-140 mmHg, fixed, and examined histologically for luminal surface wrinkle amplitudes. Arteries at 40 mmHg had an average wrinkle amplitude of 20.52 ± 4.13 µm which decreased to 5.86 ± 1.69 µm at 140 mmHg (p<0.05; Figure 1A-D). We synthesized silicone grafts with a wrinkled luminal surface similar to the arteries or with a smooth surface. The grafts were placed on a pulsatile pump circuit set to a systolic pressure of 100-120 mmHg and activated platelets were circulated through the graft. Wrinkled grafts undergoing pulsatile flow exhibited an 87% reduction in platelet deposition by Giemsa stain in comparison to grafts with smooth luminal surfaces (p<0.05, Figure1E,F). These findings confirm that arteries do possess luminal topography that varies with physiologic ranges in blood pressure. Grafts that mimic this behavior show reduced platelet accumulation, suggesting that dynamic topography contributes to vascular homeostasis. Incorporation of this topography into vascular grafts may improve graft patency.

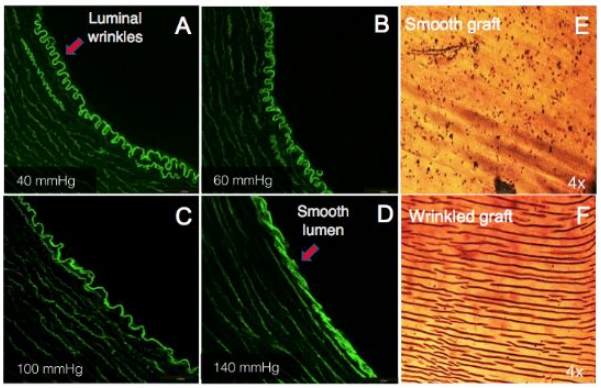

N. Nath: None. **L. Pocacivsek:** None. **Y. Gao:** None. **K. Salem:** None. **S. Velankar:** None. **E. Tzeng:** None.

538
Procedural Characteristics and Outcomes in Women with Hyperuricemia after Percutaneous Coronary Intervention
Megha Prasad, Charanjit Rihal, Lilach Lerman, Ryan Lennon, Amir Lerman, Mayo Clinic, Rochester, MN

Background: Serum uric acid may serve as a marker of cardiovascular events and outcomes in men, but further studies are required to determine its role in women. We aimed to determine differences in procedural characteristics and outcomes in women undergoing percutaneous coronary intervention(PCI). Methods: We retrospectively analyzed the Mayo Clinic Cardiovascular Catheterization Laboratory database, and included patients undergoing PCI from 1/1/2000 to 12/31/2007. There were 495 women who underwent PCI in this time period. Patients were divided into normal uric acid (n=240) and high uric acid (n=255) groups, and high uric acid was defined as >6.0 mg/dL. Patients were followed for adverse outcomes for a median of 47.1 (IQR 23.8, 62.8) months. Results: Mean age was 66.6±12.7 years in the normal group vs. 70.5 ± 11.2 years in the elevated uric acid group(p=0.01). Hypertension and diabetes were more prevalent in the elevated uric acid group (p<0.01). BMI was significantly higher in the elevated uric acid group (p=0.001). There was a higher prevalence of calcified lesions among women with elevated uric acid when compared to those with normal uric acid levels (47% vs. 30% p<0.001). There was significantly lower TIMI=3 flow postprocedurally in those with elevated uric acid levels when compared to those with normal uric acid levels (91 % vs. 97%, p=0.003). After adjusting for potential confounders including age, hyperlipidemia, hypertension, BMI, diabetes, and chronic kidney disease, elevated uric acid was associated with increased likelihood of death (HR 1.8, p=0.01) and the composite endpoint of death or subsequent myocardial infarction (HR 1.5, p=0.03). Discussion: Uric acid may be an independent determinant of procedural characteristics and a predictor of outcomes after percutaneous intervention. Further studies are required to better understand the effect of uric acid on cardiovascular events in women.

M. Prasad: None. **C. Rihal:** None. **L. Lerman:** None. **R. Lennon:** None. **A. Lerman:** None.

545
Evolocumab Alters LDL-cholesterol Levels but Not Glycemic Profile and Liver Lipids in Chow Fed and High fat/Cholesterol/Fructose Fed Golden Syrian Hamsters
Francois Briand, Noémie Burr, Emmanuel Brousseau, Thierry Sulpice, Physiogenex SAS, Labege, France

Background - Beside its effect on LDL-cholesterol levels, proprotein convertase subtilisin/kexin9 (PCSK9) could also be linked to glucose metabolism and non-alcoholic fatty liver diseases. Here we evaluated whether Evolocumab (EVO), a monoclonal antibody targeting PCSK9, may alter glycemic profile and liver lipids in hamsters. Methods - Hamsters were maintained on either a control chow (CC) or high fat/cholesterol/fructose (HFCF) diet for 5 weeks. After 2 weeks of diet, hamsters were randomized into 2 groups, control or EVO at 30mg/kg s.c. once weekly for 3 weeks, to evaluate the effects on lipoprotein/glycemic profiles, and liver lipids. Results - When compared with CC diet, HFCF diet significantly increased total cholesterol and LDL-cholesterol levels by 87% and 102%. Hamsters fed the HFCF diet also showed higher HOMA-IR index of insulin resistance, higher blood glucose area under the curve (AUC) during an oral glucose tolerance test (OGTT), and higher liver lipids (triglycerides: +197%, total cholesterol: +421%, both p<0.001 vs. CC). However, plasma PCSK9 levels were markedly reduced by 47% in HFCF fed hamsters (p<0.001 vs. CC). As expected, treatment with EVO significantly increased hepatic LDL-receptor protein levels by 1.74-fold and reduced plasma LDL-cholesterol by up to 28% in CC fed hamsters (p<0.01 vs. CC control). The LDL-cholesterol reduction was also observed in HFCF fed hamsters treated with EVO, but to a lesser extent (up to 16%). In both CC and HFCF fed hamsters, EVO did not alter fasting glycemia and plasma insulin levels. IN CC fed hamsters, EVO transiently reduced blood glucose levels by 15% at time 15 minutes (p<0.01 vs. CC control) after an oral glucose load. However, EVO did not change blood glucose levels AUC or plasma insulin levels during the OGTT, in neither CC nor HFCF fed hamsters. As well, no change in liver lipids levels was observed in CC or HFCF fed hamsters treated with EVO. Conclusion - Our data indicate that diet-induced insulin resistance and liver steatosis in hamsters are not associated with elevated plasma PCSK9 levels, and are not altered by

Evolocumab. Whether these results are specific to our hamster model and can translate to humans remains to be further investigated.
F. Briand: Employment; Significant; PHYSIOGENEX SAS. Ownership Interest; Modest; PHYSIOGENEX SAS. **N. Burr:** Employment; Significant; PHYSIOGENEX SAS. **E. Brousseau:** Employment; Significant; PHYSIOGENEX SAS. **T. Sulpice:** Employment; Significant; PHYSIOGENEX SAS. Ownership Interest; Significant; PHYSIOGENEX SAS.

547
High-density Lipoprotein Particle Diversity from Selective Combinatorial Assembly of Particle Constituents Result in a Dynamic Particle Population
Steven G Fried, **Scott W Altmann**, HDL Apomics, Allenhurst, NJ

Introduction: Mass spectrometry is starting to elucidate the extent of lipoprotein diversity. It is believed that HDL is comprised of proteins encoded by >100 genes and ~200 distinct lipid species in an undetermined number of combinations. Multiple proteoforms derived from a single gene contribute to particle complexity, confound proteome identification and makes differentiation of distinct subpopulations a challenge. Subtle proteoform variants can account for alterations in particle physicochemical properties and critical functions. Refining high-definition constituent identification within a structured atlas may reveal mechanism-based pathophysiology of a variety of diseases.
Hypothesis: The ongoing identification of HDL constituents necessitates an effort to catalogue, categorize, map and relate entities in a framework that organizes this knowledge in a form of testable observations, explanations and predictions. Defining constituent interactions will advance knowledge and guide inquiry that enables HDL research, clinical diagnostics and subsequent therapeutic strategies.
Methods: Informatic analysis of the literature produced an HDL proteome reference set. Proteome specific analysis of gene isoforms, proteolytic products, amino acid modifications and cSNPs were used to prepare a proteoform index. Theoretical tryptic peptide maps were generated and referenced to the PeptideAtlas and available published mass spec peptide lists.
Results: Over 380 non-immunoglobulin proteins were identified in high-density lipoprotein fractions from human samples. A consensus-based scoring produced an “unofficial” list of 122 genes. UniProtKB was used to expand an index of potential proteoforms and derive a theoretical peptide mass library used to map empirically defined peptide spectral lists.
Conclusions: Utilizing a reductionism model to HDL measurement has proven insufficient and undermines the application of Precision Medicine for CAD. Understanding the health benefits of HDL requires clinical diagnostics that captures particle diversity and population heterogeneity. Constructing a conceptual framework that unifies a constituent map is the initial step to resolving their relational context and functional consequences.
S.G. Fried: Employment; Significant; HDL Apomics. **S.W. Altmann:** Ownership Interest; Significant; Founder/Owner HDL Apomics.

548
Separation of Lipoprotein Particles Utilizing Asymmetric Flow Field-flow Fractionation and Quantitation of Apolipoprotein L1 in Human Plasma with IMER-UPLC-MS/MS
Michael Andrews, Zsuzsanna Kuklenyik, Yulanda Williamson, Kevin Bierbaum, David Schieltz, Bryan Parks, Christopher Toth, Michael Gardner, Lisa McWilliams, Anthony Lehtikoski, Jon Rees, John Barr, Ctr for Disease Control & Prevention, Atlanta, GA

Apolipoprotein L1 (ApoL1) is an intriguing protein and was shown to be involved in numerous diseases states such as chronic kidney disease (CKD), cardiovascular diseases(CVD), Human Immunodeficiency Virus associated Nephropathy (HIVAN), systemic lupus erythematosus (SLE) (associated collapsing glomerulopathy), and type 2 diabetes (especially for people of African descent). People of African ancestry were shown to have either one or two alleles which contribute to their susceptibility of diseases related to CKD. ApoL1 is characterized as a HDL binding protein. In this work we studied ApoL1 binding to HDL by using a gentle size fractionation technique, asymmetric flow field-flow fractionation (AF4), and liquid chromatography (LC) with quantitative tandem mass spectrometry (MS/MS) detection. We injected 50 uL of whole plasma onto the AF4 system, where smaller HDL particles eluted first followed by the larger HDL, and then by LDL, IDL and VLDL particles. The lipoproteins were separated into 40 fractions and quantitatively analyzed using on-line trypsin digestion coupled with LC-MS/MS analysis. We analyzed plasma samples both with and without purification by UC. When HDL particles were separated by UC, apoL1 was found in the higher density HDL fractions, as was also found by previous studies. When HDL separated using AF4 with or without UC, apoL1 eluted in the larger HDL size region (12-13 nm). With UC vs. without UC, the apoL1 peptide signal intensities were reduced by more than 50%, indicating significant loss of apoL1 from the surface of HDL particles during UC. Our data on apoL1 provides further evidence for the fact that size and density are not directly interconvertible physical characteristics of lipoproteins. Furthermore, our data shows that apoL1 is also an example of exchangeable apolipoproteins whose binding can be significantly diminished due to the effect of intense shear forces during UC separation. This work also demonstrates the advantages of utilizing AF4-IMER-UPLC-MS/MS methodology to separate lipoprotein particles and study of their apolipoprotein composition.
M. Andrews: None. **Z. Kuklenyik:** None. **Y. Williamson:** None. **K. Bierbaum:** None. **D. Schieltz:** None. **B. Parks:** None. **C. Toth:** None. **M. Gardner:** None. **L. McWilliams:** None. **A. Lehtikoski:** None. **J. Rees:** None. **J. Barr:** None.

549
Improvement in Large Density HDL Particle Number by NMR is Associated with Reduction in Coronary Soft Plaque Burden by Coronary Computed Tomography Angiography in Psoriasis
Yousssef A Elnabawi, Amit K Dey, Aditya Goyal, Jacob W Groenendyk, Leonard D Genovese, Agastya D Belur, Justin A Rodante, Marcus Y Chen, David A Bluemke, Alan T Remaley, Martin P Playford, Nehal N Mehta, NIH, Bethesda, MD

Background: Patients with psoriasis (PSO), a chronic inflammatory disease associated with dysfunctional lipoprotein profile and accelerated risk of MI, have increased burden of subclinical atherogenesis by coronary computed tomography angiography (CCTA). Large HDL particle (l-HDLp) number by NMR has been shown to associate negatively with cardiovascular (CV) events independent of traditional lipoprotein levels. We hypothesize that increase in l-HDLp would inversely associate with soft plaque volume (PV) as well as non-calcified coronary burden (NCB).
Methods: Consecutive treatment naïve PSO patients (n= 92 arteries) underwent CCTA (320 detector row, Toshiba) at baseline and one-year. Soft plaque volume and non-calcified burden were assessed using a semi-automated software (QAngio, Medis). Lipoprotein profiling and cholesterol efflux capacity was done by NMR. **Results**: Patients were middle aged and at low CV risk by traditional risk scores (Table 1). With improvement of PSO severity at one year and no change in traditional CV risks, l-HDLp increased (5.8 ± 0.4 vs. 6.3 ± 0.5, p=0.007) concurrently with cholesterol efflux capacity (0.95 ± 0.02 vs 1.01 ± 0.02, p=0.003). PV reduced at one-year (3.7 ± 1.2 vs. 2.9 ± 1.1 mm^3, p=0.01), as well as NCB (1.20 ± 0.06 vs. 1.07 ± 0.06 mm^2, p<0.001). Coronary burden was inversely associated with l-HDLp beyond traditional CV risk factors (β = -0.47, p<0.001).
Conclusions: Increase in l-HDLp was inversely associated

with coronary plaque burden possibly through improvement in HDL function via cholesterol efflux capacity, suggesting a role for NMR lipoprotein profiling in assessment of CVD in chronic inflammatory states.

Table 1: Characteristics of Psoriasis Patients at Baseline and One year

Parameter	Baseline (n=92)	One-year (n=92)	P-value
Demographics and medical history			
Age, years	50.3 ± 11.8	51.6 ± 1.6	**<0.001**
Males	51 (55)	51 (55)	1.00
Body mass index	29.0 ± 0.65	29.0 ± 0.68	0.44
Hypertension	30 (33)	30 (33)	1.00
Hyperlipidemia	32 (35)	32 (35)	1.00
Statin treatment	22 (24)	21 (23)	0.65
Type-2 diabetes mellitus	8 (9)	5 (5)	0.83
Current smoker	11 (12)	10 (11)	0.16
Clinical and laboratory values			
Total cholesterol (mg/dL)	181.5 ± 5.2	177.9 ± 5.2	0.20
HDL cholesterol (mg/dL)	56.7 ± 2.4	58.9 ± 2.7	0.06
LDL cholesterol (mg/dL)	97.5 ± 3.4	97.2 ± 3.7	0.43
Framingham risk score	2 (1-4)	2 (1-5)	0.28
C-reactive protein (mg/L)	4.1 ± 1.6	2.7 ± 0.64	**0.03**
Cholesterol efflux capacity	0.95 ± 0.02	1.01 ± 0.02	**0.003**
Large HDL particle number	5.8 ± 0.4	6.3 ± 0.5	**0.007**
Psoriasis characterization			
Psoriasis area severity index score	7.6 (3.2-16.3)	3.3 (1.3-5.5)	**<0.001**
Disease duration, years	20 (10-24)	21 (11-27)	**<0.001**
Systemic/Biologic Treatment	52 (57)	64 (69)	**<0.001**
Coronary characterization, proximal			
Total burden, mm^2 (x100)	1.27 ± 0.06	1.17 ± 0.05	**0.009**
Dense calcified burden, mm^2 (x100)	0.068 ± 0.01	0.072 ± 0.01	0.36
Non-calcified burden, mm^2 (x100)	1.20 ± 0.06	1.07 ± 0.06	**<0.001**
Focal plaque analysis			
Plaque volume (mm^3)	3.7 ± 1.2	2.9 ± 1.1	**0.01**
%Stenosis	48.4 ± 1.2	47.6 ± 1.2	0.17

Values are reported as mean ± SD/median (IQR) for continuous variables and n (%) for categorical variables. P-values were calculated by Student t-test for normally distributed continuous variables and by Mann-Whitney U-test for non-normally distributed continuous variables. Pearson's chi-square test was performed for categorical variables. P-value<0.05 deemed significant.

Y.A. Elnabawi: None. **A.K. Dey:** None. **A. Goyal:** None. **J.W. Groenendyk:** None. **L.D. Genovese:** None. **A.D. Belur:** None. **J.A. Rodante:** None. **M.Y. Chen:** None. **D.A. Bluemke:** None. **A.T. Remaley:** None. **M.P. Playford:** None. **N.N. Mehta:** Research Grant; Modest; Abbvie, Janssen, Novartis, Celgene.

551
Is Free Cholesterol Bioavailability a Determinant of Dysfunctional, Atherogenic High Density Lipoproteins? Refining the Model of Reverse Cholesterol Transport
Baiba K Gillard, Dedipya Yelamanchili, Antonio M Gotto Jr, Corina Rosales, Henry J Pownall, Houston Methodist Res Inst, Houston, TX

Although cardiovascular disease (CVD) negatively correlates with high-density lipoprotein-cholesterol (HDL-C) levels, to date HDL-raising therapies have not reduced CVD; thus, in the context of reverse cholesterol transport (RCT), HDL quality, i.e., functionality, may be more important to atheroprotection than HDL quantity. The current RCT model comprises free cholesterol (FC) efflux from macrophages to apo AI to give nHDL, LCAT-mediated nHDL-FC esterification forming mature HDL, SR-B1-mediated hepatic uptake of HDL lipids, followed by sterol metabolism and excretion. Our recent studies challenge this model: We observed that nHDL apo AI, FC and phospholipid (PL) metabolically segregate. In mice, plasma nHDL FC and PL are hepatically cleared with $t_{1/2}$ ~3 min; nHDL-apo AI is cleared more slowly with $t_{1/2}$ = 460 min. FC esterification is 100X slower, and thus a minor RCT step. These results and the observation that nHDL is FC-rich (~64 mol%) led to a revised model of RCT, with a focus on FC bioavailabilty rather than CE uptake. HDL from SR-B1$^{-/-}$ mice is also FC-rich and associated with atherosclerosis. Moreover, the magnitude of HDL-C content/particle is associated with carotid artery atheroprogression (Qi et al JACC 2015 65:355-363), and HDL from hyperlipidemic HIV patients, which are at increased CVD risk, also have a high mol% FC compared to controls (29 vs 16 mol%, p<0.05). Thus, we hypothesize that high HDL-FC bioavailability, measured as the product of mol% HDL-FC and HDL particle number, is a metric for dysfunctional, atherogenic HDL. We studied SRB1$^{-/-}$ mice, which are atherosusceptible and a model of dysfunctional HDL. Compared to WT mice, SR-B1$^{-/-}$ mice have a higher HDL particle number and mol% FC (~58 vs. 15). Compared to WT HDL, SRB1$^{-/-}$ HDL is more resistant to disruption by GdmHCl and serum opacity factor, indicating a resistance to remodeling. We plan to compare FC bioavailability of WT and SRB1$^{-/-}$ HDL according to the kinetics of HDL-FC transfer to LDL. Our studies will determine if increased HDL-FC bioavailability in dysfunctional FC-rich HDL supports whole-body hypercholesterolemia that could increase CVD risk.

B.K. Gillard: None. **D. Yelamanchili:** None. **A.M. Gotto:** None. **C. Rosales:** None. **H.J. Pownall:** None.

552
Enhancement of Rat Lymphatic Lipid Transport by Glucose or Amino Acids Ingestion
Hiroshi Hayashi, Tokyo Ariake Univ of Med and Hlth Sci, Tokyo, Japan

Objectives: Dietary lipid absorption usually occurs with absorption of other nutrients because lipid is contained in foods fed as a meal. The effect of simultaneously fed carbohydrate and protein on lipid absorption is not clear. In this study, lymphatic lipid transports in the rat intestine were observed during intraduodenal lipid feeding with or without simultaneous feeding of glucose or amino acids.
Methods: Mesenteric lymph duct was cannulated in male SD rats and a feeding tube was inserted into the duodenum through the fundus of the stomach. Postoperatively, the rats were intraduodenally infused with saline. On the day after surgery, the saline infusion was replaced by a lipid infusion containing 40 µmol/h (35.4 mg/h) of triolein, 2.74 µmol/h (1.06 mg/h) of cholesterol, 7.8 µmol/h (6.08 mg/h) of egg lecithin with 300 mg/h of glucose (the Glucose group), with 150 mg/h of amino acids derived from medical amino acid injections (the Amino Acids group), or without any additive (the Control group). The lipid emulsion was infused at 3mL/h for 8 hours.
Results: The amounts of triglyceride transported in lymph for 8 hours were 185 ± 12 (mean ± SE) mg in the Amino Acids group (n=4), 175 ± 3 mg in the Glucose group (n=5), and 147 ± 7 mg in the Control group (n=4), respectively, with a statistically significant difference ($p < 0.05$) among the groups. The amount of cholesterol transported in lymph for 8 hours were 7.30 ± 0.63 mg in the Amino Acids group, 6.82 ± 0.46 mg in the Glucose group, and 5.96 ± 0.17 mg in the Control group, respectively. The amount of phosphatidylcholine transported in lymph for 8 hours were 16.4 ± 1.0 mg in the Amino Acids group, 15.7 ± 0.4 mg in the Glucose group, and 12.4 ± 0.3 mg in the Control group, respectively, with a statistically significant difference ($p < 0.01$) among the groups.
Conclusions: Simultaneous glucose or amino acids feeding enhanced lymphatic lipid transport in the rat intestine during lipid feeding.

H. Hayashi: None.

553
Scavenging Reactive Aldehydes With 5'-o-pentyl-pyridoxamine (PPM) Improves HDL Function and Reduces Atherosclerosis in Ldlr Deficient Mice
Jiansheng Huang, Vanderbilt Univ Medical Ctr, Nashville, TN; Linda Zhang, Vanderbilt Univ, Nashville, TN; Patricia Yancey, Huan Tao, Lei Ding, Youmin Zhang, John Oates, Venkataraman Amarnath, Jackson Roberts II, Sean Davies, MacRae F. Linton, Vanderbilt Univ Medical Ctr, Nashville, TN

Background: Lipid peroxidation products impair the cholesterol efflux capacity of high-density lipoprotein (HDL) and contribute to the development of atherosclerosis. The effect of inhibition of HDL dysfunction by scavengers on HDL function and whether scavenging reactive aldehydes with PPM protects against the development of atherosclerosis was examined. **Methods and Results:** HDL of familial hypercholesterolemia (FH) subjects have impaired ability to promote cholesterol efflux and FH-HDL contain 5-fold more malondialdehyde adducts (MDA) than control HDL. In vitro studies revealed that reactive aldehyde MDA crosslinks apolipoprotein AI (apoAI) and impairs the ability of HDL to

promote cholesterol efflux from *Apoe*$^{-/-}$ macrophages. 5'-O-pentyl-pyridoxamine (PPM), a potent scavenger of reactive aldehydes, abolished MDA-mediated crosslinking of apoA-I in HDL by 80 % (P<0.05). PPM prevents the reduction in cholesterol efflux capacity of MDA treated HDL in Apoe-/- macrophages. Furthermore, PPM significantly improved the cholesterol efflux capacity of HDL from *Ldlr*$^{-/-}$ mice fed a Western diet (WD) for 16 weeks (P<0.05), indicating that PPM protects HDL from modifications by reactive aldehydes and maintains HDL function in vivo. Importantly, administration of 1 mg/mL of the reactive aldehyde scavenger PPM, versus 1 mg/mL of the nonreactive analogue PPO, to *Ldlr*$^{-/-}$ mice consuming a WD for 16 weeks reduced the extent of proximal aortic atherosclerosis by 45% (P<0.05). Immunohistochemistry studies revealed that PPM reduced the macrophage content and the number of TUNEL positive cells by 55% (P<0.05) and by 60% (P<0.01) in advanced atherosclerotic lesions of *Ldlr*$^{-/-}$ mice, respectively. In addition, the necrotic core area was reduced by 52% (P<0.05) in advanced atherosclerotic lesions in *Ldlr*$^{-/-}$ mice treated with PPM compared to the control group.
Conclusions: Treatment with PPM, a reactive aldehyde scavenger: 1) inhibits MDA-ApoA1 adduct formation thereby preserving HDL cholesterol efflux capacity in *Ldlr*$^{-/-}$ mice; 2) reduces the number of apoptotic cells in atherosclerotic lesions and the necrotic core area in lesions of *Ldlr*$^{-/-}$ mice. These results support the therapeutic potential of PPM in the treatment of atherosclerotic cardiovascular disease.
J. Huang: None. **L. Zhang:** None. **P. Yancey:** None. **H. Tao:** None. **L. Ding:** None. **Y. Zhang:** None. **J. Oates:** None. **V. Amarnath:** None. **J. Roberts II:** None. **S. Davies:** None. **M.F. Linton:** None.

554
FoxO Transcription Factors are Required for Hepatic HDL-Cholesterol Clearance
Samuel X Lee, Columbia Univ Medical Ctr, New York, NY

Insulin resistance and type 2 diabetes are associated with low levels of high-density lipoprotein-cholesterol (HDL-C). The insulin-repressible FoxO transcription factors are potential mediators of insulin's effect on HDL-C. FoxOs mediate a substantial portion of insulin-regulated transcription, and poor FoxO repression is thought to contribute to the excessive glucose production in diabetes. In this work, we show that mice with liver-specific triple FoxO knockout (L-FoxO1,3,4), which are known to have reduced hepatic glucose production, also have increased HDL-C. This was associated with decreased expression of HDL-C clearance factors, scavenger receptor class B type I (SR-BI) and hepatic lipase, and defective selective uptake of HDL-cholesteryl ester by the liver. The phenotype could be rescued by re-expression of SR-BI. These findings demonstrate that hepatic FoxOs are required for cholesterol homeostasis and HDL-mediated reverse cholesterol transport to the liver.
S.X. Lee: None.

555
Investigation of 4-oxo-2-nonenal Mediated HDL Dysfunction and the Use of Lipid Dicarbonyl Scavengers in Preserving HDL Function
Linda S May-Zhang, Vanderbilt Univ, Nashville, TN; Mark S. Borja, California State Univ East Bay, Hayward, CA; Tiffany Pleasent, Meharry Medical Coll, Nashville, TN; Amarnath Venkataraman, Vanderbilt Univ, Nashville, TN; Patricia G. Yancey, MacRae F. Linton, Vanderbilt Medical Ctr, Nashville, TN; Sean S. Davies, Vanderbilt Univ, Nashville, TN

Background: Lipid peroxidation products such as hydroxy-2-nonenal (HNE) are elevated in atherosclerosis and cause HDL dysfunction. Generated in parallel to HNE is 4-oxo-2-nonenal (ONE), a less studied lipid dicarbonyl possibly due to its far greater reactivity. The consequences of ONE modification of HDL have not been studied. We have recently found that scavengers of lipid dicarbonyls such as salicylamine (SAM) and pentylpyridoxamine (PPM) prevent HDL dysfunction induced by malondialdehyde and isolevuglandin (IsoLG). In this study, we examine the impact of ONE adduct formation on HDL structure-function, and the scavenging abilities of various small molecules in preventing ONE modification. **Methods and Results:** By Western blot analysis, ONE crosslinked apoA-I on HDL at a concentration of 3 ONE molecules for every 10 apoA-I proteins (0.3 molar equivalence, eq.), which is 100 fold lower than HNE but comparable to IsoLG. ONE-mediated crosslinking of HDL proteins preferentially produced a 39 kDa band on SDS-PAGE, likely an apoA-I/apoA-II heterodimer. ONE-modified HDL partially inhibited the ability of HDL to protect against the inflammatory response of macrophages (as shown in TNFα and IL-1β mRNA expression), but did not render HDL pro-inflammatory. At 3 eq., ONE dramatically decreased the ability of apoA-I to exchange among HDLs, from ~46.5% to only ~18.4% (P<0.001). HDL-mediated macrophage cholesterol efflux was decreased by ~70.6% (P<0.005) and 56.1% (P<0.001) by HDL modified by 0.3 and 3 eq. ONE, respectively. Investigation of various scavenger analogues in protecting HDL from ONE modification showed that while SAM and its fluoro- and chloro- analogues partially prevented ONE-mediated HDL protein crosslinking, PPM nearly completely blocked crosslinking. PPM pretreatment of HDL prior to 3 eq. ONE modification was also able to restore HDL-mediated macrophage cholesterol efflux, from 56.1~ to ~83.0% (P<0.01) while the inactive analogue pentylpyridoxine had no effect. **Conclusions:** Our study is the first to show that ONE causes HDL dysfunction, and demonstrates that not all modified HDLs result in the same "dysfunction". We also demonstrate the use of PPM in preferentially scavenging ONE in biological systems.
L.S. May-Zhang: None. **M.S. Borja:** None. **T. Pleasent:** None. **A. Venkataraman:** None. **P.G. Yancey:** None. **M.F. Linton:** None. **S.S. Davies:** None.

This research has received full or partial funding support from the American Heart Association.

556
Structural Characterization of Distinct Subparticles of Human High-density Lipoproteins Isolated from Plasma
John T Melchior, Scott E Street, Univ of Cincinnati, Cincinnati, OH; Amy S Shah, Cincinnati Children's Hosp, Cincinnati, OH; W. Jay Jerome, Rachel Hart, Vanderbilt Univ Sch of Med, Nashville, TN; Jay W Heinecke, Yi He, Univ of Washington, Seattle, WA; Allison B Andraski, Jeremy D Furtado, Frank M Sacks, Harvard Sch of Public Health, Boston, MA; W. Sean Davidson, Univ of Cincinnati, Cincinnati, OH

High-density lipoproteins (HDL) play a critical role in lipid transport and the maintenance of vascular homeostasis. HDL consists of a heterogeneous population of particles that vary in size, composition, and functionality. HDL is proteomically diverse; it can host at least 95 different proteins and structure-function studies suggest that specific protein complements on the surface of the particles are responsible for the broad spectrum of HDL function.
The goal of this study was to isolate and fully characterize specific subspecies of HDL based on their protein complement and particle size. We built upon our previous studies where we segregated lipoproteins using immunoaffinity chromatography using antibodies specific to the two major scaffold proteins of HDL; apolipoprotein (apo)A-I and apoA-II. Two populations were obtained directly from plasma that either had both apoA-I and apoA-II (LpA-I/A-II) or just apoA-I with no apoA-II (LpA-I). These subpopulations were further fractionated using size exclusion chromatography using four superdex columns in series.
We observed at least three distinctly sized particles within the LpA-I/A-II subfraction and two distinctly sized particles in

the LpA-I subfraction which all elute in the size range of HDL. We successfully isolated the “large” and “small” subpopulations observed in the LpA-I subfraction and compositional analysis revealed profound proteomic differences between the two populations. Particles in the larger fraction were enriched in more common apolipoprotiens important for lipid metabolic processes such as apoL-I, apoD, apoM and apoE. Conversely, the smaller LpA-I particles were enriched in proteins important for immune response and complement activation. Using multiple cross-linking reagents, we have mapped the protein-protein interactions on each of these subpopulations to begin generating detailed structural models of these particles *in silico*.

J.T. Melchior: None. **S.E. Street:** None. **A.S. Shah:** None. **W. Jerome:** None. **R. Hart:** None. **J.W. Heinecke:** None. **Y. He:** None. **A.B. Andraski:** None. **J.D. Furtado:** None. **F.M. Sacks:** None. **W. Davidson:** None.

This research has received full or partial funding support from the American Heart Association.

557

The Effect of Dietary Fat and Carbohydrate on the Metabolism of HDL Subspecies Containing ApoE in Humans

Allyson Morton, Carlos Mendivil, Jeremy Furtado, Frank M Sacks, Harvard T.H. Chan Sch of Public Health, Boston, MA

Background The effect of diet on the metabolism of HDL subspecies defined by protein content remains undetermined. ApoE forms subspecies on HDL with unique metabolic properties. HDL containing apoE have dramatically increased clearance from plasma compared to HDL not containing apoE, and also participate in size expansion from small to large HDL (a marker of cholesterol uptake).
Methods We enrolled ten adults who were overweight or obese and had low HDL-C (≤45 mg/dl for men, ≤55 mg/dl for women). Each participant received two diets in a random-crossover design: a high-unsaturated fat diet (40% fat [10% sat, 23% MUFA, 7% PUFA], 45% carbohydrate) and a low fat diet (65% carbohydrate, 20% fat [10% sat, 8% MUFA, 7% PUFA]), each for 28 days. At the end of each diet period, participants received a bolus infusion of tri-deuterated (D3-) leucine, a stable isotope tracer, to label apoA1, and plasma was collected at 18 time points up to 94 hours post-tracer infusion. We isolated from plasma HDL subspecies containing or not containing apoE, and used compartmental modeling of apoA1 tracer enrichment and pool size to study the kinetic behavior of each HDL subspecies during each diet.
Results HDL containing apoE comprises about 5% of apoA1 HDL mass in plasma. On both diets, apoA1 in HDL containing apoE turns over about ten times more quickly than in HDL not containing apoE. The high-unsaturated fat diet increased the synthesis and clearance of apoA-I on HDL containing apoE by about 250% compared to the low fat diet. There was also greater evidence of HDL size interconversion in this subspecies on the high fat diet. In contrast, the high-unsaturated fat diet did not significantly affect the metabolism of apoA1 of HDL not containing apoE.
Conclusions Dietary unsaturated fat compared to carbohydrate increases the secretion of HDL subspecies containing apoE, and renders them more biologically active in metabolic pathways that involve reverse cholesterol transport.

A. Morton: None. **C. Mendivil:** None. **J. Furtado:** Other; Modest; inventor on patents awarded to Harvard University pertaining to HDL: US 8,846,321 B2; US 9,494,606 B2. **F.M. Sacks:** Other; Modest; Inventor on patents awarded to Harvard University pertaining to HDL: US 8,846,321 B2; US 9,494,606 B2.

560

Protein and Lipid Composition of HDL Particles

Katrin Niisuke, Tufts Univ, Boston, MA; Zsuzsanna Kuklenyik, CDC/ONDIEH/NCEH, Atlanta, GA; Tomas Vaisar, Univ of Washington, Seattle, WA; Bela F Asztalos, Tufts Univ, Boston, MA

Objective: HDL cell-cholesterol efflux capacity is influenced by both the concentration and the functionality (efflux capacity per particle) of HDL particles. It is assumed that the lipid and protein composition of HDL particles significantly influence their functionality; however there is little data to support that. Our aim was to determine the protein and lipid composition of individual HDL particles to better understand the large variability observed in HDL functionality studies. **Approach**: ApoA-I-containing HDL particles (preβ-1, α-4, α-3, α-2, and α-1) were separated by non-denaturing 2d-PAGE, electro-eluted from the gel, and purified by immuno-affinity chromatography using anti-human apoA-I IgG. The protein and lipid composition of the particles were assessed by mass-spectrometry. The number of apoA-I molecules in each particle was determined by cross-linking experiments. **Results**: The number of protein species, associated with HDL particles, increased with particle size: the largest (α-1) particles carried more than 50, while the smallest (preβ-1) particles carried only a few different proteins. ApoE was present in trace amount, if any, in these HDL particles. The apoA-II/apoA-I ratio was very low in the α-1, α-4, and preβ-1 particles but substantially higher in the α-2 and α-3 particles. The maximum number of apoA-I molecules was 4 in α-1 and 3 in α-2, α-3, and α-4 particles. The largest (α-1) particles contained significantly more lipid molecules, especially triglycerides, for each apoA-I molecule compared to smaller particles. The lipid composition of the intermediate-size α-2 and α-3 particles was similar. In contrast to larger HDL particles, the small α-4 particles were enriched in sphingomyelin. Interestingly, the very-small preβ-1 particles contained about equal amounts of polar (phospholipids and free cholesterol) and non-polar (cholesteryl ester and triglycerides) lipids. Phospholipids were represented only by sphingomyelin. These findings contradict previous models that indicated that each preβ-1 particle contained one or two apoA-I and a few polar lipid molecules. **Conclusions**: Both the protein and the lipid composition of HDL particles are size dependent. Further studies are needed to determine how the protein and lipid composition of HDL particles influence HDL functions.

K. Niisuke: None. **Z. Kuklenyik:** None. **T. Vaisar:** None. **B.F. Asztalos:** None.

561

Reduced Serum Efflux Capacity Associates With Elevated Plasma Lp(a) Levels

Alexandra M Fenton, Jessica Minnier, Deanna L Plubell, Paige Bergstrom, Hagai Tavori, Sergio Fazio, **Nathalie Pamir**, Oregon Health & Science Univ, Portland, OR

Background: Plasminogen, is a potent acceptor of cholesterol by the ABCA1 transporter in peripheral cells, and this function is inhibited by lipoprotein (a) [Lp(a)]. Patients with high Lp(a) have increased cardiovascular disease risk, but the mechanism for this effect is not known. The interplay of plasminogen and Lp(a) in contributing to the total sterol efflux capacity of whole serum (TSEC) could explain the influence of Lp(a) on vascular health. We investigated TSEC in patients with low and high plasma Lp(a) levels.
Methods: TSEC (measured in cAMP-stimulated J774 murine macrophages), lipid profile, Lp(a), and plasminogen levels were measured in a cohort of patients (N=58) followed for standard-of-care in our lipid clinic. We used a linear regression model with sex, age, Lp(a), plasminogen, LDL and HDL cholesterol levels, and use of lipid-lowering drugs to understand the predictors of TSEC. The interaction between plasminogen, ABCA1, and Lp(a) was further characterized by biochemical studies of Lp(a) isoforms, cell based assays, and label free protein-protein interaction

assays.
Results: TSEC was 30% lower (p=0.002) in patients with plasma Lp(a) levels >50mg/dl compared with those below 50mg/dl. Plasminogen, Lp(a), Lp(a)/plasminogen interaction, and LDL-C were significant predictors of TSEC (adjusted R^2=0.48, p<0.01). The regression model revealed varying associations of Lp(a) with TSEC for different values of plasminogen: At low plasminogen, Lp(a) showed a negative association, whereas for higher values of plasminogen, Lp(a) showed no association. Additionally, sterol efflux to increasing plasminogen concentrations was reduced when samples were co-treated with plasma from patients with Lp(a) levels >20mg/dl when compared to samples co-treated with plasma from patients with lower Lp(a) levels. Furthermore, two distinct Lp(a) isoforms isolated from different patients inhibited plasminogen mediated sterol efflux. Finally, label free protein-protein interaction assays showed that plasminogen binds to ABCA1 in a process inhibited by the presence of Lp(a).
Conclusion: Our results support an interaction between plasminogen and Lp(a) that contribute to the total sterol efflux capacity of the serum, an atheroprotective process.
A.M. Fenton: None. **J. Minnier:** None. **D.L. Plubell:** None. **P. Bergstrom:** None. **H. Tavori:** None. **S. Fazio:** None. **N. Pamir:** None.

562
Foamy Monocytes in Hypertriglyceridemia
Xueying Peng, Zeqin Lian, Xiaoyuan Dai Perrard, Baylor Coll of Med, Houston, TX; Henry Dong, Univ of Pittsburgh Sch of medicine, Pittsburgh, PA; Aparna Mukherjee, Baylor Coll of Med, Houston, TX; Haibo Zhu, Inst of Materia Medica, Chinese Acad of Medical Sciences & Peking Union Medical Coll, Beijing, China; Christie M. Ballantyne, Huaizhu Wu, Baylor Coll of Med, Houston, TX

Objective Hypertriglyceridemia (HTG) increases risk for atherosclerotic cardiovascular disease, but the mechanisms remain poorly defined. Foamy monocytes are lipid-loaded monocytes in circulation that contribute to atherosclerosis under hypercholesterolemia. Human study has proved that HTG is associated with formation of foamy monocytes. Our study is to examine formation of foamy monocytes in HTG and their potential contribution to atherosclerosis in mouse models.
Approach and results In vivo mouse models of HTG included wild-type C57BL/6 mice on high fat diet (HFD) injected intraperitoneally with LPL inhibitor, Poloxamer 407 (P407, 0.25mg/g, every two days), as a chemically-induced model and mice with transgenic overexpression of human ApoCIII (ApoCIIItg) as a genetic model. Based on CD11c and CD36, monocytes were identified as $CD36^-CD11c^-$, $CD36^+CD11c^-$ and $CD36^+CD11c^+$ subsets. In the first model, at 24h of the first injection, triglyceride levels increased to 367 ±84 mg/dL, higher than that of control group with saline injection (60 ±22 mg/dL, n=4, P<0.001). Meanwhile, the side scatter (SSC, representing cell granularity) values and Nile red staining for lipids of $CD36^+CD11c^+$ monocytes increased significantly, indicating formation of foamy monocytes, in mice with HTG. Furthermore, CD11c mean fluorescence intensity of $CD36^+CD11c^+$ foamy monocytes increased significantly at 2 weeks of P407 injection. In ApoCIIItg mice fed HFD (5 weeks), the percentage and SSC value of $CD36^+CD11c^+$ monocytes increased significantly (37%±5%, 247±8), also indicating elevated granularity and lipid accumulation of these monocytes, compared to wild-type mice (26%±3%, p<0.05; 226±8, p<0.05, n=4-6). In vitro treatment with human triglyceride-rich lipoprotein (hTGRL) for 24h increased the granularity and Nile red staining intensity of THP-1 monocytes, indicating foamy monocyte formation. hTGRL treatment also increased THP-1 monocyte expression of CD36, with greater uptake of cholesteryl ester-rich lipoprotein.
Conclusion High triglyceride promotes foamy monocyte formation and induces monocyte phenotypic changes in mice and tissue culture, with increased expression of CD11c and CD36, which may contribute to development of atherosclerosis under HTG.
X. Peng: None. **Z. Lian:** None. **X.D. Perrard:** None. **H. Dong:** None. **A. Mukherjee:** None. **H. Zhu:** None. **C.M. Ballantyne:** None. **H. Wu:** None.

This research has received full or partial funding support from the American Heart Association.

563
Working Out the Kinks of SR-BI-mediated Cholesterol Transport
Sarah C Proudfoot, Alexandra C Chadwick, Daisy Sahoo, Medical Coll of Wisconsin, Milwaukee, WI

High density lipoproteins (HDL) facilitate reverse cholesterol transport (RCT), the process by which cholesterol effluxed from peripheral tissues is delivered via selective uptake to the liver for excretion. These processes are mediated by HDL's high-affinity receptor, scavenger receptor BI (SR-BI). SR-BI is an 82 kDa glycoprotein with two transmembrane domains (TMD), two short cytoplasmic N/C-terminal domains, and a large extracellular domain. Our laboratory solved the NMR structure of the C-terminal TMD and nearby extracellular domain. This peptide contains four conserved proline residues, an amino acid that confers structural flexibility. In our structure, P408 and P412 are in an extracellular alpha-helix, P438 lies at a helix-loop junction, and P459 introduces a kink into the TMD helix. We hypothesized that these proline residues support SR-BI-mediated cholesterol transport. To test this hypothesis, we mutated each proline to alanine and transiently expressed wild-type (WT), P408A-, P412A-, P438A-, or P459A-SR-BI in COS-7 cells. Total lysate and cell surface expression of SR-BI was examined by immunoblot analysis and flow cytometry, respectively. All mutants expressed on the cell surface, except P408A-SR-BI, which was absent from whole cell lysates. P412A- and P438A-SR-BI were significantly impaired in their ability to efflux cell-associated [^{3}H]cholesterol to HDL, as compared to WT-SR-BI. Likewise, cellular binding of [^{125}I]HDL and selective uptake of [^{3}H]cholesteryl oleyl ether were reduced with P412A- and P438A-SR-BI. We assessed SR-BI's ability to modulate membrane cholesterol pools by cholesterol oxidase treatment. SR-BI enhances the accessibility of cholesterol to the exogenous enzyme, and a proportional increase in cholestenone is detected by thin layer chromatography. Cholestenone was increased with WT-SR-BI but not P412A- or P438A-SR-BI, suggesting defective membrane cholesterol distribution. Taken together, key proline residues in the near-C-TMD extracellular domain support efficient HDL binding, selective uptake, cholesterol efflux, and membrane cholesterol organization. These critical residues appear to support SR-BI in a conformation that allows for efficient RCT.
S.C. Proudfoot: None. **A.C. Chadwick:** None. **D. Sahoo:** None.

This research has received full or partial funding support from the American Heart Association.

565
Effects of PCSK9 Inhibition on Plasma PCSK9 Concentration and Hepatic *PCSK9* Expression
Michael D Shapiro, Hagai Tavori, Carlota Oleaga, Joshua Miles, Sergio Fazio, Oregon Health Science Univ, Portland, OR

Background: We previously reported a marked (~7-fold) increase in plasma PCSK9 concentrations in patients treated with monoclonal antibodies blocking PCSK9 action. It is unclear whether this pronounced increase in plasma PCSK9 is due to increased hepatic production of PCSK9, slow plasma clearance of the antibody/PCSK9 complex, or both.

Objectives: To determine whether hepatic *PCSK9* gene expression increases after exposure to a therapeutic monoclonal antibody targeted to PCSK9. **Methods:** C57Bl/6 wild-type (WT) mice and human PCSK9 transgenic (PCSK9tg) mice were treated with a single injection (10 mg/kg) of a monoclonal antibody targeted to PCSK9. Plasma samples were collected at baseline and then at 1, 2, 4, 8, 24, 48, 72, 192 and 336 hours after injection. Livers were sampled from age-matched mice (n=4) at baseline and 24 hours post injection for gene expression analyses. **Results:** In WT mice (n=8), mean baseline plasma PCSK9 level was 69±28 ng/mL and mean peak plasma PCSK9 level was 719±239 ng/mL (a 10.4-fold increase). Peak PCSK9 levels were reached at 24 hours after injection of the monoclonal antibody. At 24 hours after injection a statistically significant 3-fold increase in hepatic *PCSK9* gene expression was observed, compared with baseline, in WT mice. On the other hand, treatment with the antibody increased human PCSK9 levels only by 2-fold in our transgenic mice, whose human PCSK9 is expressed by extrahepatic tissues and in a stable and unregulated fashion. **Conclusion:** We observed a much larger increase in plasma PCSK9 levels in WT vs. PCSK9tg mice 24 hours after injection of a monoclonal antibody that blocks plasma PCSK9. This finding suggests that the striking increase in plasma PCSK9 in WT mice, which mirrors the effects seen in patients under treatment with PCSK9 blocking antibodies, is mostly due to increased hepatic production and only modestly due to reduced plasma clearance of the antibody/PCSK9 complex.

M.D. Shapiro: Consultant/Advisory Board; Modest; Akcea, Amgen, Kastle, Novartis, Regeneron. **H. Tavori:** None. **C. Oleaga:** None. **J. Miles:** None. **S. Fazio:** Consultant/Advisory Board; Modest; Amarin, Amgen, Akcea, Kowa.

566

High-density Lipoprotein Inhibits Serum Amyloid a -Mediated Inflammasome Activation

Preetha Shridas, Maria C de Beer, Nancy R Webb, Univ of Kentucky, Lexington, KY

Objectives: Interleukin-1beta (IL-1β) has been implicated in inflammatory diseases, including atherosclerosis and abdominal aortic aneurysm (AAA). Production of bioactive IL-1β is controlled by the inflammasome, a multi-protein complex that regulates caspase-1 activity. Serum Amyloid A (SAA) is an acute-phase protein whose levels in circulation is elevated in individuals with chronic inflammation. We previously reported that deficiency of SAA protects mice from angiotensin II (AngII)-induced AAA. Here we report that reduced AngII-induced AAA in SAA-deficient mice is accompanied by significant reductions in plasma IL-1β, indicating that SAA is required for inflammasome activation in AngII-infused mice. The objective of this study is to investigate mechanisms involved in SAA-mediated inflammasome activation. **Methods/Results:** SAA dose-dependently induced both caspase-1 activation and IL-1β secretion in J774 macrophage-like cells incubated with 0-25 µg/ml purified mouse SAA. The ability of SAA to induce IL-1β secretion was significantly reduced in bone marrow-derived macrophages deficient in NLRP3. A caspase-1inhibitor, Z-YVAD-FMK, significantly suppressed IL-1β secretion induced by SAA, whereas the P2X7-receptor antagonist, AA38079, had no effect. Inhibition of reactive oxygen species (ROS), cathepsin-B activation, and cellular potassium efflux by N-acetyl-L-cysteine, CA-074, and glyburide, respectively, blocked NLRP3 inflammasome activation by SAA. Pre-incubating SAA with HDL prior to cell treatments completely abrogated SAA-mediated inflammasome activation. In contrast, HDL did not alter inflammasome activation triggered by ATP. **Conclusions:** SAA-mediated NLRP3 inflammasome activation in macrophages is dependent on ROS generation, release of cathepsin-B, and potassium efflux, and is independent of the P2X7 receptor. Moreover, our data identify a novel mechanism by which HDL may exert cardioprotective effects.

P. Shridas: None. **M.C. de Beer:** None. **N.R. Webb:** None.

567

Insulin Reverses Mcp-1 Suppressed Cholesterol Efflux to Hdl3/apoa1 Through Up-regulation of Abca1, Abcg1 and Sr-bi in Differentiated 3t3-l1 Adipocytes

Runlu Sun, Canxia Huang, Sun Yat-sen Memorial Hosp, Sun Yat-sen Univ, Guangzhou, China; Jieyu Jiang, Graceland Medical Ctr, the Sixth Affiliated Hosp, Sun Yat-sen Univ, Guangzhou, China; Jinlan Bao, Yuling Zhang, Sun Yat-sen Memorial Hosp, Sun Yat-sen Univ, Guangzhou, China

Aims- Insulin has been reported to influence cholesterol removal from different cells, but the results have been controversial. Based on our previous study, which we found that insulin promote cholesterol efflux from HepG2 cells and can reverse the decreased cholesterol efflux to HDL though PI3K-Akt pathway, we further investigate the effects of insulin on damaged cholesterol efflux by MCP-1 in this report.

Methods- 3T3-L1 preadipocytes were differentiated into adipocytes as described previously. Fully differentiated adipocytes (day 13) were labeled with ^{3}H-cholesterol (1 Ci/ml) for 24 h. Cellular cholesterol efflux was initiated by 20µg/ml human apoA1 or 50 µg/ml HDL_3 with the indicated dose of MCP-1 for the indicated period of time in the presence or absence of insulin. After incubation, the radioactivity of the medium and cells was measured using a liquid scintillation counter. Cholesterol efflux was calculated as the percentage of total [^{3}H]-cholesterol released into the medium after subtraction of the values obtained in the absence of a cholesterol acceptor. 3T3-L1 adipocytes were harvested for PCR , western blotting, cell-surface protein assays and Confocal microscopy.

Results-1. MCP-1 reduced cholesterol efflux to HDL3 and apoA1 in differentiated 3T3-L1 adipocytes. 2. In differentiated 3T3-L1 adipocytes, MCP-1 reduced cholesterol efflux to HDL_3 mainly by inhibiting SR-BI and ABCG1 and to apoA1 mainly by inhibiting ABCA1. 3. MCP-1 decreased ABCA1 and SR-BI mRNA expression but not ABCG1. 4. MCP-1 decreased total and cell surface ABCA1, ABCG1, and SR-BI protein expression as shown by Western blotting and confocal microscopy in differentiated 3T3-L1 adipocytes. 5. Insulin increased MCP-1 suppressed cholesterol efflux to HDL_3 and apoA1 depending on Akt phosphorylation. 6. Insulin reversed MCP-1 suppressed ABCA1 and SR-BI mRNA expression, and ABCA1, ABCG1 and SR-BI protein expression via PI3K/Akt pathway.

Conclusions- Insulin reverses the suppressed cholesterol efflux to HDL3 and apoA1 by MCP-1 through up-regulation of ABCA1, ABCG1 and SR-BI through PI3K/Akt pathway in 3T3-L1 adipocytes, which provides evidences that insulin may improve the MCP-1-induced adipocyte cholesterol imbalance to exert the anti-inflammatory effect.

R. Sun: None. **C. Huang:** None. **J. Jiang:** None. **J. Bao:** None. **Y. Zhang:** None.

569

Pnpla2 Influences Secretion of Triglyceride-rich Lipoproteins but Does Not Affect Lipid-droplet Metabolism of Human Hepatoma Cells

Apostolos Taxiarchis, Hovsep Mahdessian, Angela Silveira, Per Eriksson, Rachel Fisher, Ferdinand M. van ´t Hooft, Karolinska Instt, Stockholm, Sweden

Background. Increased hepatic secretion of triglyceride (TG)-rich lipoproteins and cellular TG-accumulation are associated with enhanced risk for cardiovascular disease and diabetes mellitus but the factors regulating these processes are largely unknown. KO studies demonstrated that patatin-domain containing protein 2 (PNPLA2), also known as ATGL, is largely responsible for hepatic TG-hydrolysis in mice but the physiological role of PNPLA2 in

human liver metabolism has thus far not been evaluated. *Aim*. To investigate the role of PNPLA2 in the secretion of TG-rich lipoproteins and TG-accumulation in human hepatoma Huh7 and HepG2 cell-lines. *Results.* Gene-specific siRNA silencing of PNPLA2 generated mRNA reductions of 88±9% and 82±5% in Huh7 and HepG2 cells, respectively. PNPLA2-silencing was associated with 48±5% and 45±12% decreases in cellular TG-hydrolysis in both hepatoma cell-lines as measured by an *in vivo* assay. Secretion of TG-rich lipoproteins was analyzed using an ELISA for apolipoprotein B (APOB) and quantification of ^{14}C -TG following incubation with ^{14}C-TG labelled glycerol. It was found that PNPLA2-silencing reduced the secretion of APOB and TG by 35±3% and 37±10% in Huh7 cells and by 23±13% and 29±6% in HepG2 cells, respectively. Surprisingly, no changes in cellular TG-accumulation were observed following PNPLA2-inhibition in Huh7 and HepG2 cells. Confocal microscopy studies confirmed that PNPLA2 inhibition did not change the lipid-droplet content of the hepatoma cells. Subcellular localization studies with a monoclonal PNPLA2 antibody found no evidence for the colocalization of PNPLA2 with lipid droplets. In contrast, considerable overlap was observed between PNPLA2 and the endoplasmic reticulum (ER) marker protein disulphide isomerase (PDI). The colocalization was quantified using Pearson correlation analysis (Rcoloc). The Rcoloc value for PNPLA2 and PDI was 0.78 ±0.06, compatible with predominant localization of PNPLA2 in the ER in human hepatoma cells.*Conclusion.* These studies demonstrate that PNPLA2 acts as a TG-hydrolase in human hepatoma cells and it is involved in the secretion of TG-rich lipoproteins. However, PNPLA2 does not influence hepatic lipid-droplet homeostasis and is not co-localized with large lipid-droplets.
A. Taxiarchis: None. **H. Mahdessian:** None. **A. Silveira:** None. **P. Eriksson:** None. **R. Fisher:** None. **F. van ´t Hooft:** None.

576
LDL-Trafficked Small RNAs Promote Atherosclerosis through TLR Signaling in Macrophages
Ryan M Allen, Shilin Zhao, Marisol A Ramirez-Solano, Wanying Zhu, Bradley W. Richmond, Timothy Blackwell, Quanhu Sheng, Kasey C Vickers, Vanderbilt Univ Medical Ctr, Nashville, TN

Atherosclerosis is a chronic inflammatory disease, and despite resounding success in lipid management to reduce cardiovascular events, most heart attacks in the US occur in patients with clinically normal LDL-C levels. The next generation of therapies for cardiovascular disease (CVD) will include inflammation-based targets; however, systemic immune suppression has limitations. Thus, the critical barrier for successful targeting of inflammation in CVD is the identification of vascular ligands that drive immune cell activation. Previously, we demonstrated that low-density lipoproteins (LDL) transport microRNAs. Here, we report that LDL traffic a wide-diversity of small non-coding RNAs (sRNA) in circulation, many of which are derived from exogenous species, e.g. bacteria and fungi. Moreover, using high-throughput sRNA sequencing, we found that LDL-sRNA signatures are influenced primarily by environmental microbiota, as opposed to commensal bacteria in the gut microbiome. Using a mouse model of compromised mucosal immunity, we identified a process by which LDL accumulates bacterial sRNAs. Next, we demonstrated that native LDL potently stimulated cytokine release from macrophages through activation of single-stranded RNA (ssRNA)-sensing toll-like receptor (TLR) signaling, which was blunted by partial silencing of ssRNA-sensing TLRs in macrophages. Most importantly, preliminary results in mice suggest that targeting ssRNA-sensing TLRs is a potential strategy to suppress atherosclerosis. Taken together, we put forth a novel paradigm in which, LDL scavenge microbial sRNAs to promote clearance during health, yet serve as TLR-ligands that propagate macrophage inflammation in hypercholesterolemia, which likely contributes to the underlying inflammation in the pathogenesis of CVD.
R.M. Allen: None. **S. Zhao:** None. **M.A. Ramirez-Solano:** None. **W. Zhu:** None. **B.W. Richmond:** None. **T. Blackwell:** None. **Q. Sheng:** None. **K.C. Vickers:** None.

This research has received full or partial funding support from the American Heart Association.

577
NF-kB Inhibition via Celastrol-Loaded Nanocarriers Induces Distinct Changes in Atheroma-Resident Immune Cell Composition in Male vs. Female ldlr -/- Mice
Sean D Allen, Yugang Liu, **Evan A Scott**, Northwestern Univ, Evanston, IL

The immune component of atherosclerosis is strongly influenced by inflammatory signaling. Although NF-kB signaling is a key regulator of cytokine expression and activation of atheroma-resident macrophages and dendritic cells, previous attempts at its therapeutic inhibition have generated inconsistent results. These difficulties may arise from nonspecific systemic administration of inhibitors that have pleiotropic effects in both immune and non-immune cells in multiple organs.
To address these concerns, we have developed a nanocarrier delivery system (NCs) capable of transporting both hydrophobic and hydrophilic therapeutics to the cytosol of specific immune cell subsets. Following I.V. administration, our NCs are readily endocytosed by macrophages and dendritic cells within atheromas for modulation of signaling pathways. We hypothesized that delivery of the NF-kB pathway inhibitor celastrol to these cells *via* celastrol-loaded NCs (Cel-NCs) may alleviate atherosclerotic inflammation while minimizing off-target effects. Celastrol has potent anti-inflammatory effects, but also modulates unrelated signaling pathways in a range of cells and is cytotoxic near its effective inhibitory concentration (EIC). The low water solubility of celastrol is not amenable to I.V. injection, and oral administration achieves poor bioavailability and specificity for atheroma-resident cells.
We have found that loading celastrol into Cel-NCs expands its EIC, reduces cytotoxicity, and allows it to be administered *via* I.V. injection for improved targeting of atheroma. When injected into ldlr -/- mice, Cel-NCs modulated the immune composition within the aorta and spleen. Notably, these changes differed between male and female mice, possibly due to immuno-endocrine related mechanisms. Our work introduces a nanotherapeutic to reduce atherosclerotic inflammation and highlights the need to identify the effects of anti-inflammatory strategies in both sexes.

Percent Change in Immune Cell Populations Following I.V. Administration of Cel-NC in ldlr-/- Mice

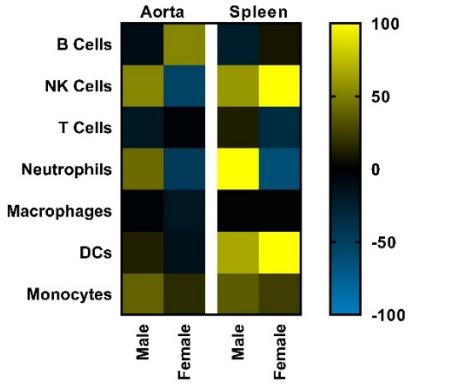

S.D. Allen: None. **Y. Liu:** None. **E.A. Scott:** None.

This research has received full or partial funding support from the American Heart Association.

578
Macrophage Cholesterol Levels Modulate Ion Channel Activity: Effect(s) on Ion Flux Dependent Inflammatory Events
Hongliang He, Jing Wang, Virginia Commonwealth Univ, Richmond, VA; Paul Yannie, Hunter McGuire VA Medical Ctr, Richmond, VA; Sung Park, Clive Baumgarten, Shobha Ghosh, Virginia Commonwealth Univ, Richmond, VA

Accumulation of cholesterol loaded macrophage foam cells is the hallmark of atherosclerotic lesions where high cellular cholesterol content not only contributes to the plaque volume but is also responsible for the inflammatory milieu. Causal relationship exist between macrophage cholesterol content and inflammatory status involving TLR4, NFκB or cholesterol crystal mediated activation of inflammasome and IL1β secretion. Since K+ efflux is central to inflammasome activation, in this study we examined the hypothesis that cellular cholesterol content directly affects K+ channel activity as well as K+ efflux. K+ currents were monitored in mouse peritoneal macrophages (MPMs) from chow or western diet (WD) fed LDLR-/- or LDLR-/-CEHTg mice. WD feeding led to a significant increase in the K+ currents in MPMs from LDLR-/- mice (A, red). In contrast, WD feeding did not affect K+ currents in MPMs from LDLR-/-CEHTg mice; these MPMs have reduced cellular cholesterol accumulation due to increased efflux. Consistently, cholesterol loading with AcLDL led to an increase in K+ currents in THP1 macrophages (B, red) and this increase was attenuated following cholesterol efflux. The physiological effect of changes in K+ channel activity or K+ efflux on inflammasome activation in MPMs by different activators (K+ ionophore Nigericin, N or ALUM crystals) was examined. Increase in extracellular K+ (+KCl) or inhibition of K+ efflux by glyburide significantly reduced IL1β secretion (C&D). Consistently, cellular K+ levels after LPS+N or LPS+ALUM treatment were significantly reduced (E). While in MPMs only K_{ATP} channel inhibitors reduced IL1β secretion (F), in human THP1 macrophages inhibition of K_{ATP} as well as Na/K pump inhibitors significantly reduced IL1β secretion (G). These data demonstrate a novel mechanism for cholesterol mediated regulation of inflammatory pathways by regulation of K+ channel activity and also illustrate species specific differences in K+ channels involved

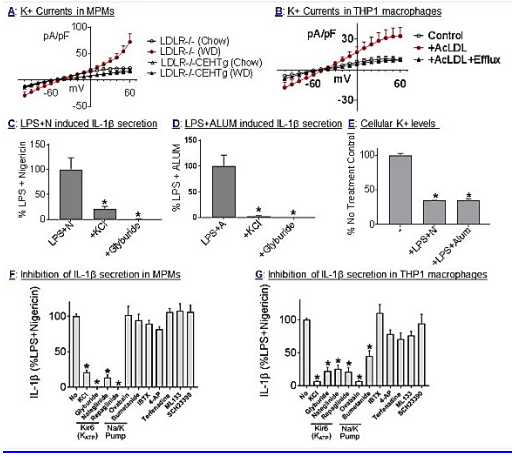

H. He: None. **J. Wang:** None. **P. Yannie:** None. **S. Park:** None. **C. Baumgarten:** None. **S. Ghosh:** None.

579
Anti-apolipoprotein A-I Antibody Profile Correlates With Cardiovascular Disease Outcomes
David Henson, Univ of Kentucky, Lexington, KY; Ayman Samman Tahhan, Emory Univ, Atlanta, GA; Sierra Schlicht, Ryan Temel, Univ of Kentucky, Lexington, KY; Arshed Quyyumi, Emory Univ, Atlanta, GA; Vincent Venditto, Univ of Kentucky, Lexington, KY

Apolipoprotein A-I (ApoA-I) is a target of IgG autoantibody induction in patients, but the role of these antibodies has not been fully elucidated. Previous research has characterized anti-ApoA-I IgG antibodies targeting delipidated ApoA-I as a biomarker of cardiovascular progression, but only a moderate association was observed. We hypothesize that free anti-ApoA-I IgG is a single component of the anti-ApoA-I response and characterization of anti-ApoA-I antibody profiles will be more predictive of adverse cardiovascular outcomes. Given the relative concentrations of ApoA-I and anti-ApoA-I antibodies, we examined sera samples from 375 patients with coronary artery disease (CAD) to quantify soluble ApoA-I/IgG immune complexes (ICs). We found a range of ApoA-I/IgG IC concentrations in patients, irrespective of free anti-ApoA-I antibodies. While free antibodies failed to predict outcomes in this CAD cohort, a median Cox regression analysis over 6 years of follow-up determined a hazard ratio of 1.5 (95% CI: 1.03-2.18, p = 0.03) for patients with below median ApoA-I/IgG ICs levels after adjusting for 11 traditional cardiovascular risk factors. In comparison, a cohort of healthy subjects exhibited significantly higher ApoA-I/IgG ICs. Pearson correlation analysis between ApoA-I/IgG ICs in the 375 patients with CAD and 25 patient characteristics found that only hypertension showed a significant association with ApoA-I/IgG ICs (r = -0.154, p = 0.003). In addition, no significant relationship between ApoA-I/IgG ICs and total ApoA-I concentration (r = -0.0601, p = 0.51) or total IgG concentration (r = 0.134, p = 0.137) was observed. Continued characterization of the molecular characteristics and immunologic sequelae associated with the immune complexes will help determine the functional implications of ApoA-I/IgG ICs *in vivo*. Current data using affinity column purification shows co-elution of ApoA-I and IgG in patients with elevated levels of ApoA-I/IgG ICs. Furthermore, ApoA-I/IgG ICs elute through size exclusion chromatography in the HDL fraction. The identification and characterization of ApoA-I/IgG ICs has the potential to guide clinical diagnosis and intervention strategies in patients with atherosclerotic cardiovascular disease.

D. Henson: None. **A. Samman Tahhan:** None. **S. Schlicht:** None. **R. Temel:** None. **A. Quyyumi:** None. **V. Venditto:** None.

This research has received full or partial funding support from the American Heart Association.

581
Identification on Anti-Atherosclerotic Mechanism of SGLT-2 Inhibitor in Diabetic Rabbit Model
Seulgee Lee, Jung-Sun Kim, Jaewon Oh, Sung-Kyung Bong, jung-jae lee, Yonsei Univ, seoul, Korea, Republic of

Aim: The sodium-glucose cotransporter 2 inhibitor (SGLT-2i) suggested a possible anti-atherosclerotic and cardioprotective effects beyond glucose lowering effect. However, further study is needed to prove underlying mechanisms of improve on cardiovascular outcomes by SGLT-2i. Therefore, we investigated possible underlying anti-atherosclerotic effect of SGLT-2i 'Dapagliflozin' with diabetic rabbit model by inducing atherosclerosis. Methods: Rabbit divided into two groups (each group/n=10); DA: Diabetic atherosclerosis, DAD: Diabetic atherosclerosis + Dapagliflozin. Dapagliflozin was given for a total of 8 weeks. Atherosclerotic plaques were induced with a high cholesterol (HC) diet and balloon inflation. In vivo intravascular imaging and histological assessment was performed. Results: From the histologic evaluation, atheromatous plaque and lipid accumulation were significantly less developed in the Diabetic atherosclerosis + Dapagliflozin group compared to the Diabetic atherosclerosis group. Significantly less macrophage infiltration and inflammatory proteins expression level was observed in the Diabetic atherosclerosis + Dapagliflozin group. The mRNA and

protein level of pro-inflammatory markers such as HMGB1, TNF-α, iNOS, and RAGE were significantly lower in the Diabetic atherosclerosis + Dapagliflozin group. The polarization of M1 macrophages was also significantly lower in the Dapagliflozin treated group. The fibronectin and type IV collagen were less observed in the glomerulus of kidney in the Dapagliflozin treated group. The lipid droplet area and size in the liver of Dapagliflozin treated group was smaller and fewer than those in the non-treated group. Conclusion: These results suggest that dapagliflozin may prevent an acceleration atherosclerosis by reducing a vascular inflammation and modifying the macrophage polarization in diabetic animal model. This preliminary clinical observation demonstrates the therapeutic potential of dapagliflozin in diabetic patients with cardiovascular disease.

S. Lee: Research Grant; Modest; HI08C2149, Graduate School of YONSEI University Research Scholarship Grants in 2017. Research Grant; Significant; No.2017R1A2B2003191. **J. Kim:** Research Grant; Significant; No.2017R1A2B2003191. **J. Oh:** None. **S. Bong:** None. **J. lee:** None.

582

Vascular Smooth Muscle-derived Macrophage are a Major Source of MCP1 in Atherosclerosis

Katherine Owsiany, Anh Nguyen, Gary K Owens, Univ of Virginia, Charlottesville, VA

Smooth muscle cells (SMC) are conventionally thought to promote atherosclerotic plaque stability by investing within the fibrous cap and protecting the blood flow from the harmful inflammatory plaque core. However, lineage tracing studies have shown that SMC in plaque can undergo a Klf4-dependent transition *in vivo* to a macrophage-like state, characterized by loss of SMC markers and expression of multiple macrophage markers, lipid accumulation, and phagocytic activity. Of major interest, SMC induced to the macrophage state in vitro by cholesterol loading also show increased production of the atheropromoting cytokine MCP1 (Monocyte chemoattractant protein 1). These results are surprising since it has been largely assumed that monocyte derived macrophages are the major source of MCP1 and that this acts to exacerbate lesion pathogenesis by inducing recruitment of additional circulating monocytes. Using MCP1-mCherry reporter mice on an $ApoE^{-/-}$ background, we show that MCP1 is highly expressed by medial and fibrous cap SMC. Further, we show that SMC-specific KLF4 knockout mice, which show marked reductions in the frequency of SMC-derived macrophages, show a 50% decrease in MCP1 immunostaining in late stage atherosclerotic lesions, suggesting that these cells are a major source of MCP-1 and produce it via a Klf4-dependent mechanism. Consistent with this possibility, we demonstrated that SMC-specific tamoxifen conditional MCP1 knockout mice on an $ApoE^{-/-}$ background (Myh11-CreERT2 eYFP $ApoE^{-/-}$ MCP1-mCherry), showed greatly decreased total MCP1 protein level within the aorta. We are currently completing examination of the effects of SMC specific MCP1 KO on late stage lesion pathogenesis in our Myh11-CreERT2 eYFP $ApoE^{-/-}$ MCP1-mCherry mice following 18 weeks of Western diet feeding. Taken together results provide evidence that SMC derived cells are an unexpected major source of MCP1 within lesions.

K. Owsiany: None. **A. Nguyen:** None. **G.K. Owens:** None.

This research has received full or partial funding support from the American Heart Association.

583

Targeting of Macrophage Netrin-1 Expression Promotes Plaque Regression and Resolution of Chronic Inflammation in Atherosclerosis

Martin Schlegel, Monika Sharma, Milessa Afonso, Lauren Beckett, Susan Babunovic, Kathryn J Moore, Marc and Ruti Bell Vascular Biology and Disease Program, Leon H. Charney Div of Cardiology, Dept of Med, New York Univ Medical Ctr, New York, NY

Chronic inflammation in atherosclerosis is driven by the accumulation of cholesterol-laden macrophages in the arterial wall. These pro-inflammatory macrophages persist in this site, and sustain local and systemic inflammation. Recently, we reported that the neuronal guidance protein netrin-1 plays a pivotal role in the retention of macrophages in plaques and the progression of atherosclerosis. To test whether targeting netrin-1 in established atherosclerotic plaques could promote the resolution of chronic inflammation in atherosclerosis and/or induce plaque regression, we developed mice in which macrophage netrin-1 expression could be inducibly deleted by tamoxifen administration ($Ntn1^{fl/fl}CX3CR1^{CreER2+}$ mice). We first induced atherosclerosis in $Ntn1^{fl/fl}CX3CR1^{CreER2+}$ and control $Ntn1^{fl/fl}CX3CR1^{CreER2-}$ using a recombinant AAV-vector overexpressing PSCK9 and Western diet feeding. After 20 weeks, 10 mice from each group were sacrificed for baseline plaque measurements, while the remaining mice were switched to chow diet to stop further progression of atherosclerosis and treated with tamoxifen (n=14/group). After 4 weeks, mice were sacrificed to assess the effects of macrophage-specific netrin-1 deletion on plaque size and composition. Analysis of peritoneal macrophages confirmed robust deletion of netrin-1 in tamoxifen treated $Ntn1^{fl/fl}CX3CR1^{CreER2+}$ but not control $Ntn1^{fl/fl}CX3CR1^{CreER2-}$ mice. Macrophage-specific deletion of netrin-1 caused a 30% reduction in plaque burden in the aortic arch as measured by en face analysis, compared to control mice. While we observed no change in aortic macrophage content, macrophage-specific netrin-1 deletion was associated with a shift in effector T cell populations in the aorta: we observed a decrease in Th1 cells and an enrichment of Th2 and Treg cells in aortic plaques of $Ntn1^{fl/fl}CX3CR1^{CreER2+}$ compared to control $Ntn1^{fl/fl}CX3CR1^{CreER2-}$. Furthermore, deletion of macrophage netrin-1 expression was associated with a reduction of systemic IL-1β levels. Collectively, these data suggest that targeting macrophage expression of netrin-1 in established atherosclerosis fosters a local pro-resolving and atheroprotective T cell phenotype in plaques and reduces systemic inflammation.

M. Schlegel: None. **M. Sharma:** None. **M. Afonso:** None. **L. Beckett:** None. **S. Babunovic:** None. **K.J. Moore:** None.

584

Neuroimmune Guidance Cues Important for Monocyte-Endothelial Cell Interaction and Monocyte to Macrophage Differentiation

Dianne Vreeken, Leiden Univ Medical Ctr, Leiden, Netherlands; Caroline S. Bruikman, Academic Medical Ctr, Amsterdam, Netherlands; Huayu Zhang, Wendy M.P.J. Sol, Anton Jan van Zonneveld, Leiden Univ Medical Ctr, Leiden, Netherlands; G. Kees Hovingh, Academic Medical Ctr, Amsterdam, Netherlands; Janine M. van Gils, Leiden Univ Medical Ctr, Leiden, Netherlands

Introduction: Atherosclerosis is a systemic inflammatory disease, characterized by the accumulation of macrophages in the vascular wall. Studies in mice showed that neuroimmune guidance cues (NGCs) are involved in atherosclerosis-related processes. In this study we aimed to determine the NGCs involved in monocyte-endothelium adhesion and transmigration, and subsequent macrophage differentiation.

Methods and Results: Combining publically available gene expression data of >600 endothelial, monocytes or macrophage samples we determined the specific NGCs expressed by these cells involved in the onset and progression of atherosclerosis. Next, the mRNA levels of the expressed NGCs were analyzed in primary human endothelial cells and monocytes upon TNFα, IL1β or oxidized LDL stimulation (5 or 24 hours), as wells as in human monocytes differentiated into macrophages.

In endothelial cells a significant (P<0.05, abs(logFC)>1) downregulation was observed for *NTN4, SEMA6C* and *PLXNA4* while a significant upregulation was observed for *EFNA1, EFNB1, UNC5B, ROBO1, SEMA6D* and *SEMA7A* upon stimulation. In monocytes a significant downregulation was detected for *SEMA6B, PLXNC1, NRP1, NRP2* and *EPHB6,* while *SEMA7A* and *EPHB2* were significantly upregulated upon stimulation. These findings combined resulted in potentially interesting concurrent changes in the NGC ligand-receptor combinations; (1) endothelial *PLXNA4* receptor with monocyte *SEMA3A* and (2) endothelial *EFNB1* ligand with monocyte *EPHB2* receptor. These changes seen at mRNA were validated at protein level. Remarkably, monocyte to macrophage differentiation induced a major increase and change in NGC expression levels, mainly in the SEMA family of ligands and receptors (including *SEMA3G*, *SEMA7A, NRP1, and NRP2*), as well as in *EPHB2* as seen in monocyte stimulation.
Conclusion: In conclusion, in our current study we observed a differential expression of NGC ligands and receptors in endothelial cells, monocytes and macrophages, culprit cell types in atherosclerosis, once subjected to pro-atherogenic stimuli. Our findings confirm a potential role for NGCs in human atherosclerosis. The next step is to further investigate the underlying mechanism of these NGCs and their role in atherosclerosis.
D. Vreeken: None. **C. Bruikman:** None. **H. Zhang:** None. **W. Sol:** None. **A. van Zonneveld:** None. **G. Hovingh:** None. **J. van Gils:** None.

585
Card9 Deficiency Accelerates Experimental Atherosclerosis
Yujiao Zhang, Lynda Zeboudj, Jeremie Joffre, Marie Vandestienne, Soraya Taleb, Ludivine Laurans, Alain Tedgui, Inserm U970, Paris Cardiovascular Res Ctr, Paris, France, Univ René Descartes Paris 5, Paris, France; Ziad Mallat, Inserm U970, Paris Cardiovascular Res Ctr, Paris, France, Univ René Descartes Paris 5; Dept of Med, Div of Cardiovascular Med, Univ of Cambridge, Cambridge, UK, Paris, France; Harry Sokol, Avenir Team Gut Microbiota and Immunity, UMR 7203, Saint-Antoine Hosp, Paris, France; Sorbonne Univ-UPMC Univ Paris 06, Paris, France; Hafid Ait-Oufella, Inserm U970, Paris Cardiovascular Res Ctr, Paris, France, Univ René Descartes Paris 5; Service de Réanimation Médicale, Saint-Antoine Hosp, Paris, France; Sorbonne Univ-UPMC Univ Paris 06, Paris, France

Introduction: There are accumulating evidences that innate and adaptive immunity play a major role in the development of atherosclerosis. Pattern-recognition receptors (PRRs) engagement including Toll-like receptors and Dectins are involved in the modulation of immune responses and atherosclerosis development but little is known about downstream signaling pathways. Card9 for Caspase recruitment domain-containing protein-9, is an adaptor protein expressed by antigen presenting cells required for PRRs-induced activation of myeloid cells. We hypothesized that Card9 pathway regulates systemic immune response and impacts on the development of atherosclerosis. **Method and results:** To evaluate the effect of Card9 deficiency on experimental atherosclerosis, $Ldlr^{-/-}$ mice were lethally irradiated and reconstituted with $Card9^{-/-}$ or $Card9^{+/+}$ bone marrow cells and put under a high fat diet during 8 weeks. Animal weight and cholesterolemia were not different between groups. We observed an increase of atherosclerosis plaque size in the aortic sinus in chimeric $Ldlr^{-/-}Card9^{-/-}$ mice compared to chimeric $Ldlr^{-/-}Card9^{+/+}$ mice (+32%, P=0.04). A more inflammatory plaque phenotype was found in chimeric $Ldlr^{-/-}Card9^{-/-}$ mice compared to control mice with an increase in both macrophage accumulation (+86%, P=0.0005) and necrotic core size (+102%, P=0.006). Card9 deficiency induced a deviation of the systemic immune response toward a pro-inflammatory profile. Lps/Ifn-γ-stimulated $Card9^{-/-}$ bone marrow-derived macrophages (BMDM) produced less IL-10 (-22%, P<0.05) than $Card9^{+/+}$ BMDM. Lps/Ifn-γ-stimulated splenocytes from chimeric $LDLr^{-/-}Card9^{-/-}$ mice produced more IL-12p70 (+151%, P<0.01) than splenocytes from control mice. Anti-CD3 stimulated $CD4^+$ T cells from chimeric $Ldlr^{-/-}Card9^{-/-}$ mice produced less Ifn-γ (-92%, P<0.05) and IL-17A (-100%, P<0.05) than control $CD4^+$ T cells. A second atherosclerosis mouse model $ApoE^{-/-}Card9^{-/-}$ confirmed the protective role of Card9 with an increase in both atherosclerosis plaque size and macrophage accumulation in $ApoE^{-/-}Card9^{-/-}$ mice compared to $ApoE^{-/-}Card9^{+/+}$ mice. **Conclusion:** Card9 deficiency accelerated atherosclerosis development in mice and induced a more inflammatory plaque phenotype.
Y. Zhang: None. **L. Zeboudj:** None. **J. Joffre:** None. **M. Vandestienne:** None. **S. Taleb:** None. **L. Laurans:** None. **A. Tedgui:** None. **Z. Mallat:** None. **H. Sokol:** None. **H. Ait-Oufella:** None.

586
Oxidized LDL Induce a Metabolic Switch Through CD36 in Macrophages
Yiliang Chen, Wenxin Huang, Moua Yang, Roy Silverstein, Blood Ctr of Wisconsin, Brookfield, WI

Under atherogenic conditions, low-density lipoproteins are converted to oxidized forms (oxLDL) by reactive oxygen species. They are then recognized by scavenger receptors such as CD36 in macrophages and stimulate pro-inflammatory functions of those innate immune cells. Although oxLDL are believed to contribute to chronic inflammation during atherosclerosis development, how the inflammatory status is sustained is not well understood. In this study, we explored how oxLDL affects the metabolic status of macrophages, which is increasingly being recognized as a key regulator of macrophage phenotypes. Exposure of wild type macrophages to oxLDL, but not native LDL, suppressed mitochondria oxidative phosphorylation (OXPHOS) as measured by oxygen consumption rate (OCAR), and increased glycolysis as measured by extracellular acidification rate (ECAR), in a dose-dependent manner. At 50μg/ml oxLDL for 24h there was a 79% reduction in OXPHOS and 60% elevation in glycolysis. Exposure to 50μg/ml oxLDL increased glucose uptake by 1.4 fold. Inhibition of glycolysis with 2-deoxy-glucose blocked oxLDL-induced HIF-1α expression as well as cytokine production, linking glycolytic metabolism to the pro-inflammatory response to oxLDL. These metabolic changes were not seen in *cd36* null macrophages.
In conclusion, oxLDL induce a metabolic switch in macrophages from mitochondrial OXPHOS to glycolysis through CD36-mediated signaling. This metabolic switch is important for inflammatory activation of macrophages and may be an underlying mechanism for sustained inflammatory status of those cells in the context of atherosclerosis.
Y. Chen: None. **W. Huang:** None. **M. Yang:** None. **R. Silverstein:** None.

This research has received full or partial funding support from the American Heart Association.

587
Inflammatory Status and Macrophage Infiltration in Relation to Insulin Resistance and Dyslipidemia among Morbid Obese Subjects
Nain-Feng Chu, Kaohsiung VGH, Nat. Def. Med. Ctr, Taipei, Taiwan; Tian-Jong Chang, Natl Defense Medical Ctr, Taipei, Taiwan
Inflammatory response and macrophage infiltration in adipocyte is associated with the development of insulin resistance status and obesity-related co-morbidities. This study is to examine the inflammatory status and macrophage infiltration in adipose tissues and their relationship with insulin resistance (IR) and dyslipidemia among morbidly obese patients.We collected blood and omental visceral fat samples from 35 morbidly obese subjects (BMI ≧ 35 kg/m^2) and used HOMA-IR (≧2.4) and prescription history to divide the subjects into normal and insulin resistant sub-groups.

We used enzyme-linked immunosorbent assay (ELISA) to determine the advanced glycation end products (AGEs) and plasma growth arrest-specific protein 6 (GAS-6) expression levels. We used turbidimetric method to determine the concentration of high sensitivity C-reactive protein (hs-CRP) level. For adipocyte, the cluster of differentiation 68 (CD68) antibody, as macrophages infiltration of adipocyte, was determined using immunohistochemistry (IHC) methods.The mean BMI among these 35 morbidly obese subjects (20 male, 15 female) is 41.2 kg/m^2. There are 15 subjects with normal HOMA and 20 subjects with insulin resistant HOMA. Among the IR group, the fasting glucose, insulin, triglyceride, GAS-6, CD68, levels are significantly higher than those of the normal HOMA group. CD68 level are positively correlated with fasting glucose, insulin, cholesterol and HOMA-IR level and negatively correlated with HDL-C level. After adjusting for age, gender and BMI, every increase of 1ng/mL AGEs, 1ng/mL GAS-6, 1mg/L hs-CRP, and 1μm^2 CD68 is associated with increasing of HOMA-IR by 1.323 units (p=0.030), 0.118 unit (p=0.681), 2.787 units (p=0.059), and 0.0002 unit (p=0.019), respectively.Inflammation response, especially CD68 level, is associated with the insulin resistance and dyslipidemia among the morbidly obese subjects. Additionally, it is imperative to examine the interactions between inflammation response, macrophage infiltration and inflammatory status on insulin resistance and obesity-related co-morbidities.

N. Chu: None. **T. Chang:** None.

588

Corticotropin-releasing Hormone via Its Type2 Receptor Inhibits Insulin-stimulated NO Formation in HUVECs

Ick-Mo Chung, Hai Dan Jin, Hyang Kim, Ewha Womens Sch of Med, Seoul, Korea, Republic of

Background: Stress may provoke endothelial dysfunction thereby inducing atherosclerotic cardiovascular diseases (ASCVD). Corticotropin-releasing hormone (CRH) is recognized as a key regulator of hypothalamo-pituitary-adrenal axis under stress, however, its role in endothelial function and ASCVD is not known well. Insulin can produce NO formation in endothelial cells through eNOS activation. We studied effect of CRH and urocortin 2 (UCN2) on insulin-stimulated NO formation in HUVECs. *Methods and Results:* HUVECs were incubated in serum-free media for 8 h prior to the experiment. Treatment of HUVECs with insulin (100 nM) enhanced NO production detected by 5 μM 4,5-diaminofluorescein-diacetate. Fluorescent and phase contrast images were obtained using an fluorescence microscope (Em max : 515 nm), using an exposure time based on control conditions, and mean fluorescence intensity was calculated with ImageJ. Insulin-stimulated NO production was markedly inhibited by either CRH or UCN2 (100 nM each), which was reversed mostly by 100 nM astressin 2B (CRH receptor type 2 (CRHR2) inhibitor) and partly by 100 nM NBI35965 (CRHR1 inhibitor). CRH induced Rho-associated kinase (ROCK) and p-IRS-1(Ser). Insulin (2nM) stimulated p-eNOS (Ser1177), which was inhibited by CRH. *Conclusions:* Taken together, CRH/UCN2 via mainly its type 2 receptor signaling can inhibit insulin-stimulated eNOS/NO pathway. This CRH's inhibitory effect on insulin signaling is mediated at least partly by activation of ROCK/ p-IRS-1 (Ser).

Fig. 1. Effects of CRH and UCN2 on insulin-stimulated NO production in HUVECs
*p<0.05 and **p<0.01

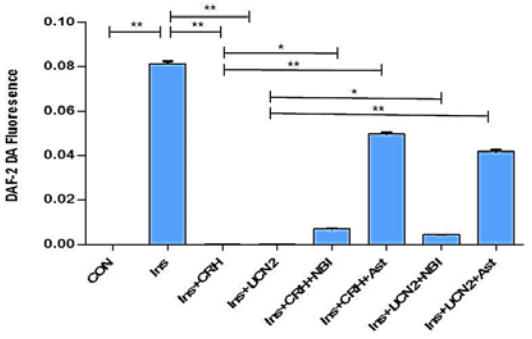

I. Chung: None. **H. Jin:** None. **H. Kim:** None.

589

Amygdala Activity Assessed by 18-FDG PET/CT Associates with Coronary Plaque Burden Quantified by Coronary Computed Tomography Angiography in Psoriasis

Aditya Goyal, Abhishek Chaturvedi, **Youssef Elnabawi**, Jonathan Chung, Amit Dey, Tsion Aberra, Agastya Belur, Joshua Rivers, Leonard Genovese, Jacob Groenendyk, Joseph Lerman, Aditya Joshi, Justin Rodante, Martin Playford, David Bluemke, Marcus Chen, NHLBI, NIH, Bethesda, MD; Joel Gelfand, Univ of Pennsylvania, Philadelphia, PA; Nehal Mehta, NHLBI, NIH, Bethesda, MD

Introduction: Psoriasis (PSO), a chronic inflammatory disease associated with increased prevalence of both stress and coronary artery disease, provides a model to study the role of perceived stress in cardiovascular (CV) disease. While stress perception quantified as resting amygdala activity (RAA) is associated with CV events, its association psoriasis severity as well subclinical CV indices is not well known. We thus, sought to look into the relationship between RAA, psoriasis area severity index (PASI) score and Non-calcified burden (NCB) in PSO. **Methods:** 150 consecutive PSO patients and 58 healthy volunteers (HV) underwent 18-FDG PET/CT and CCTA scans (Toshiba, 320-detector row) to quantify RAA and NCB respectively. Skin disease severity was assessed as PASI score, RAA as target-to-background ratio (Osirix) and NCB using prior published methods (QAngio). The relationship between them was analyzed using multivariable regressions (STATA 12).**Results:** Despite older age, both PSO & HV were at low CV risk by traditional risk score. RAA was higher in PSO compared to HV (Table 1). Moreover, PASI score correlated positively with RAA in treatment naïve psoriasis patients (β=0.22, p=0.03). Furthermore, RAA associated with NCB (β=0.27, p<0.001), which persisted independent of traditional risk factors (β=0.19, p<0.001). Similar relationship was not observed in HV. **Conclusion:** In conclusion, PSO skin disease severity relates to amygdalar activity by 18-FDG PET/CT suggesting the role of chronic inflammatory disease like PSO in triggering perceived psychological stress. Moreover, there is a direct association between amygdalar activity and coronary plaque burden suggesting a role for perceived stress in subclinical CV disease in these patients. Larger studies are needed to confirm these findings.

Table 1: Baseline characteristics of study cohorts.

Parameter	PSO (N = 150)	Controls (N = 58)	p-value
Demographics and medical history			
Age, years	50.6 ± 12.7	36.4 ± 12.5	**<0.001**
Males	85 (57)	41 (71)	0.06
Ethnicity, Caucasians	123 (82)	38 (66)	**0.003**
Hypertension	40 (27)	7 (12)	**0.02**
Hyperlipidemia	70 (47)	16 (28)	**0.01**
Type 2 diabetes mellitus	14 (9)	4 (7)	0.58
Current tobacco use	12 (8)	3 (5)	0.50
Lipid treatment	49 (33)	8 (14)	**0.01**
Body mass index	29.3 ± 5.8	26.3 ± 4.9	**<0.001**
Waist-to-hip ratio	0.95 (0.88 - 1.0)	0.94 (0.87 - 0.99)	0.27
Clinical and laboratory values			
Total cholesterol	180.6 ± 37.3	178.5 ± 37.3	0.36
HDL cholesterol	55.8 ± 17.9	57.1 ± 18.0	0.32
LDL cholesterol	100.5 ± 30.3	97.4 ± 32.7	0.26
Triglycerides	120.5 ± 74.1	120.0 ± 91.1	0.49
Framingham risk score	3.0 (1.0 – 6.0)	1.0 (1.0 – 2.1)	**<0.001**
C-reactive protein	1.8 (0.7 - 4.0)	1.0 (0.6 - 2.6)	**0.02**
HOMA-IR‡	2.8 (1.6 – 4.7)	2.1 (1.1 – 2.8)	**0.002**
Cholesterol efflux capacity	0.95 ± 0.16	1.00 ± 0.17	**0.02**
Psoriasis Characterization			
Psoriasis area severity index score	5.7 (3.0 – 10.0)	-	-
Systemic or biologic treatment	54 (36)	-	-
Coronary Plaque Burden (x100)			
Total Burden, mm^2	1.14 ± 0.42	1.02 ± 0.32	**<0.001**
Non-Calcified Burden, mm^2	1.10 ± 0.44	1.00 ± 0.32	**0.005**
Amygdalar Activity (FDG PET/CT)			
Target-to-background ratio	1.10 ± 0.11	1.04 ± 0.12	**<0.001**

Values reported in the table as Mean ± SD or Median (IQR) for continuous data and N (%) for categorical data. P value less than or equal to 0.05 deemed significant. P values were calculated by using student's t-test or Mann-Whitney U test for continuous variables and Pearson's chi-squared test for categorical variables. ‡ HOMA-IR: Homeostasis model assessment of insulin resistance.

A. Goyal: None. **A. Chaturvedi:** None. **Y. Elnabawi:** None. **J. Chung:** None. **A. Dey:** None. **T. Aberra:** None. **A. Belur:** None. **J. Rivers:** None. **L. Genovese:** None. **J. Groenendyk:** None. **J. Lerman:** None. **A. Joshi:** None. **J. Rodante:** None. **M. Playford:** None. **D. Bluemke:** None. **M. Chen:** None. **J. Gelfand:** Research Grant; Significant; Abbvie, Janssen, Novartis Corp, Sanofi, Celgene, Pfizer. Consultant/Advisory Board; Modest; Sanofi-Aventis, Janssen Scientific Affairs, LLC, AstraZeneca Pharmaceuticals, Coherus, GSK, Menlo Therapeutics, Novartis Pharmaceuticals, Eli Lilly and Company, BMS, Dermira, Regeneron. Consultant/Advisory Board; Significant; Pfizer Inc. **N. Mehta:** Research Grant; Significant; Abbvie, Janssen, Novartis, Celgene.

595

Transcriptional Control of Intestinal Cholesterol Absorption, Adipose Energy Expenditure and Lipid Handling by Sortilin

Sumihiko Hagita, Maximillian Rogers, Tan Pham, Jennifer Wen, Andrew Mlynarchik, Masanori Aikawa, Elena Aikawa, Ctr for Interdisciplinary Cardiovascular Sciences, Boston, MA

Objective—The sorting receptor Sortilin functions in the regulation of glucose and lipid metabolism. Dysfunctional lipid uptake, storage, and metabolism contribute to several major human diseases including atherosclerosis and obesity. Sortilin associates with cardiovascular disease; however, the role of Sortilin in adipose tissue and lipid metabolism remains unclear. **Approach and Results—**Here we show that in the low-density lipoprotein receptor-deficient ($Ldlr^{-/-}$) atherosclerosis model, Sortilin deficiency ($Sort1^{-/-}$) in female mice inhibits intestinal Niemann-Pick type C1-Like 1 (Npc1l1) expression (-60.6 %, p<0.01), reduces body (-17.2 %, p<0.01) and white adipose tissue weight (-35.2 %, p<0.05), and improves brown adipose tissue function partially via transcriptional downregulation of Krüppel-like factor 4 and Liver X receptor (Figure). Female $Ldlr^{-/-}Sort1^{-/-}$ mice on a high fat/cholesterol diet had elevated plasma Fibroblast growth factor 21 (+89.1 %, p<0.05) and Adiponectin (+37.7 %, p<0.01), an adipokine that when reduced is associated with obesity and cardiovascular disease related factors. Additionally, Sortilin deficiency suppressed cholesterol absorption in both human colon Caco-2 cells (-16.5 %, p<0.05) and mouse ex vivo intestinal tissue (-16.9 %, p<0.05) in a similar manner to treatment with the Npc1l1 inhibitor - ezetimibe. **Conclusions—** Together our findings support a novel role of Sortilin in energy regulation and lipid homeostasis in female mice, which may be a potential therapeutic target for obesity and cardiovascular disease.

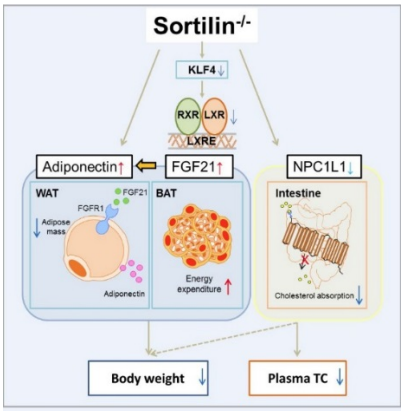

Figure. Working model for the role of Sortilin in female *Ldlr-/-* mouse body weight and Plasma total cholesterol (TC) regulation.

S. Hagita: None. **M. Rogers:** None. **T. Pham:** None. **J. Wen:** None. **A. Mlynarchik:** None. **M. Aikawa:** Research Grant; Significant; Kowa Company, Ltd. **E. Aikawa:** Research Grant; Significant; National Institutes of Health grants R01HL114805 and R01HL136431.

596

Disruption of Cholesterol Metabolism and Substrate Stiffness Coordinate to Regulate Cellular Biomechanics and Induce Cytoskeletal Remodeling in Vascular Smooth Muscle Cells

Hanna Sanyour, Na Li, Alex RIckel, **Zhongkui Hong**, Univ of South Dakota, Sioux Falls, SD

Cholesterol is the main culprit contributing to the development of atherosclerosis by inducing the endothelial dysfunction, triggering the inflammatory response in the blood vessel wall, and deposition in the foam cell at the atherosclerotic plaque. However, growing evidence suggests that the role cholesterol plays during the process of atherogenesis is not only triggering the inflammation, but also plays an important role as a regulator of cellular mechanics, cell spreading, and cell migration, which is the critical step in atherogenesis. In addition, the mechanical environment of the VSMCs in blood vessel undergoes progressive stiffening along with aging, which may potentially affect the development of atherosclerosis. In this study, our main hypothesis is that membrane cholesterol affects the VSMCs migration during the progression of atherosclerosis by regulating the integrin- and cadherin-mediated cell adhesion and this effect highly depends on the mechanical properties of extracellular matrix (ECM). VSMCs used were enzymatically isolated from the descending thoracic aorta of male Sprague-Dawley rats. Cell mechanics was measured using an atomic force microscope (AFM). F-actin cytoskeleton was visualized with confocal microscopy and AFM imaging. 1 μM fluvastatin was used to reduce the endogenous cellular cholesterol. Our results showed that fluvastatin treatment dramatically decreased cell E-modulus, but, significantly increased the average rupture force of collagen I-, fibronectin-, and N-cadherin-mediated cell adhesion. In addition, the confocal microscopy and AFM imaging studies showed that the fluvastatin treatment significantly disrupted the actin stress fiber organization. Interestingly, the effect of fluvastatin on the biomechanics and the architecture of cytoskeleton of VSMCs decreased on the soft substrate. These results indicate that cholesterol and ECM stiffness play the roles synergistically in biomechanics, cytoskeleton architecture, and thus in migration of VSMCs. The knowledge that we obtained in this project will lead to a novel therapeutic strategy to prevent the VSMCs migration and then formation of atherosclerotic plaque by regulating VSMCs biomechanics.

H. Sanyour: None. **N. Li:** None. **A. RIckel:** None. **Z. Hong:** None.

This research has received full or partial funding support from the American Heart Association.

597
Disruptions in Hepatic Insulin Signaling Reveal an Enterohepatic Signaling Pathway that Regulates the ABCG5 ABCG8 Sterol Transporter and Biliary Cholesterol Secretion
Ailing Ji, Xuebing Wang, Sonja Pijut, Lisa Bennett, Deneys R van der Westhuyzen, Gregory A Graf, Univ Kentucky, Lexington, KY

Insulin resistance is associated with increased risk for cholesterol gallstones as well as the development of diabetic dyslipidemia. HDL is the primary cholesterol carrier in the reverse cholesterol transport (RCT) pathway, the process by which cholesterol is delivered from peripheral organs to the liver for elimination in bile. Therefore, we hypothesized that insulin signaling regulates hepatobiliary cholesterol transport in the RCT pathway. To test the role of insulin signaling, we utilized mice harboring insulin receptor flanked by loxP sites ($IR^{fl/fl}$) in combination with adenoassociated viral vectors containing no transgene (empty) or Cre recombinase to generate control and liver insulin receptor knock out (LIRKO) mice, respectively. As with previous LIRKO models, our mice showed markedly reduced insulin receptor mRNA and protein in liver, but not skeletal muscle or adipose tissue, and impaired glucose tolerance. LIRKO mice had increased biliary cholesterol secretion as well as increased expression of the ABCG5 ABCG8 sterol transporter, the primary mediator of biliary cholesterol secretion. Levels of SR-BI, the primary HDL receptor, were unchanged as were rates of HDL clearance from plasma and selective delivery of HDL cholesterol to the liver. We also observed increased ileal fibroblast growth factor (FGF)15 mRNA. Wild-type mice treated with FGF19 exhibited increased ABCG5 ABCG8 protein expression in the liver. Immunofluorescence microscopy was used to examine the subcellular localization of ABCG5 in the liver following FGF19 administration. Under control conditions, G5 appeared in puncta, diffusely distributed within hepatocytes. Following treatment with FGF19, G5 signal intensity was substantially increased and juxtaposed to zonula occcludin-1 (ZO-1), a tight junction protein the delineates the canalicular channels within the liver. In conclusion, depletion of hepatic insulin receptors increases G5G8 abundance and promotes its localization to the canalicular surface. This effect is associated with an increase in ileal FGF15 expression which promotes its localization to the apical surface and drives biliary cholesterol secretion.
A. Ji: None. **X. Wang:** None. **S. Pijut:** None. **L. Bennett:** None. **D.R. van der Westhuyzen:** None. **G.A. Graf:** None.

598
Monounsaturated Fat Reduces Foamy Monocyte Formation and Atherosclerosis Development in $Ldlr^{-/-}$ Mice Compared to Western High Saturated Fat Diet
Zeqin Lian, Baylor Coll of Med, Houston, TX; Xiao-yuan Dai Perrard, Baylor Coll of Med, Houston, TX; Xueying Peng, Raya Joe L., Baylor Coll of Med, Houston, TX; Alfredo A. Hernandez, Univ of California, Davis, Davis, CA; Collin G. Johnson, William Lagor, Ron Hoogeveen, Baylor Coll of Med, Houston, TX; Scott I. Simon, Univ of California, Davis, Davis, CA; Frank Sacks, Harvard Medical Sch, Boston, MA; Christie Ballantyne, Huaizhu Wu, Baylor Coll of Med, Houston, TX

Monounsaturated fat (MUF)-rich Mediterranean-type diet (MedD) has been reported to improve atherosclerotic outcome in clinical studies, but the underlying mechanism is ill defined. Circulating foamy monocytes (FMs, monocytes with intracellular lipid droplets), which are $CD11c^+$ and highly adherent to inflamed endothelium, contribute to atherosclerosis development. In the present study, we investigated the influence of MedD on FM formation and its contribution to atherosclerosis in mice. $LDLR^{-/-}$ mice were fed MedD with high cholesterol (MedD [w/w, 21% total fat from olive oil and nut] containing 2.6% saturated fat and 13.4% MUF; 0.2% cholesterol) or western diet (WD, 21% milkfat-containing 13.3% saturated fat and 5.9% MUF; 0.2% cholesterol), with normal diet (ND) as control. Lesion area of the whole aorta examined by oil red staining at 3 months was significantly reduced in mice on MedD, compared to WD. Although plasma triglyceride levels were lower in mice on MedD than on WD, the free fatty acid profile indicated that MUFs concentration in plasma significantly increased in mice on MedD. Further, FMs from mice on MedD circulated at lower proportions and exhibited lower side scatter (SSC) than WD, indicating less lipid accumulation. Lipid accumulation in FMs from mice on WD accelerated their conversion from $CD11c^-/CD36^+$ to $CD11c^+/CD36^+$ compared to mice on ND. In contrast, this accelerated conversion did not occur in mice on MedD. Compared to WD, MedD reduced the number of firmly arrested $CD11c^+$ monocytes on vascular cell adhesion molecule-1 and E-selectin coated coverslips detected in an ex-vivo shear flow assay. Similarly, fewer $CD11c^+$ macrophages were observed in the lesion of aortic sinus in mice on MedD than on WD. In summary, compared to WD high in saturated fat and cholesterol, MedD high in MUF and cholesterol lowered triglyceride levels, inhibited foamy monocyte formation and adhesion, and reduced atherosclerosis in $LDLR^{-/-}$ mice.
Z. Lian: None. **X.D. Perrard:** None. **X. Peng:** None. **R. Joe L.:** None. **A.A. Hernandez:** None. **C.G. Johnson:** None. **W. Lagor:** None. **R. Hoogeveen:** None. **S.I. Simon:** None. **F. Sacks:** None. **C. Ballantyne:** None. **H. Wu:** None.

This research has received full or partial funding support from the American Heart Association.

599
Exposure to Biodiesel Exhaust Triggers Atherosclerotic Plaque Destabilisation through Increased Apoptosis of Vascular Smooth Muscle Cells in the Arterial Vessel Wall
Jens J Posma, Evrin Kilinç, Julian I Borissoff, Astrid Haegens, Maastricht Univ, Maastricht, Netherlands; Aleksandra D Jedynska, TNO Built, Utrecht, Netherlands; Hugo Ten Cate, Maastricht Univ, Maastricht, Netherlands; Ingeborg M Kooter, TNO Built, Utrecht, Netherlands; Henri M Spronk, Maastricht Univ, Maastricht, Netherlands

Introduction Long-term exposure to air pollutants increases cardiovascular morbidity and mortality. Particulate matter (PM) derived from diesel exhaust has been documented to be pro-atherogenic in animal studies. Biodiesels are widely introduced as new fuels with improved emission characteristics. However, biodiesel contains relatively more polycyclic aromatic carbohydrates (PAH) compared to diesel. Therefore, we hypothesise that exposure to biodiesel as compared to diesel exhaust results in increased atherosclerosis. **Methods and Results:** In a carotid cuff atherosclerosis model, the effects of exposure to exhaust PM of biodiesel vs. diesel PM vs. saline (control) on atherosclerosis were evaluated. Both common carotid arteries in $LDLR^{-/-}$ mice were cuffed at week 2 in the course of an 8-week high-fat diet regimen. All mice were intratracheally instilled with saline, PM biodiesel or biodiesel once-weekly for 5 times. Immunohistochemistry and primary human vascular smooth muscle cells (hVSMC) were used for evaluation. Results: Exposure to both biodiesel and diesel didn't exacerbate atherosclerosis development, however, biodiesel affected plaque composition towards a more vulnerable phenotype as compared to diesel with decreased total collagen content and hVSMC (respectively -100%, p=0.09 and -339%, p<0.01 and tend to increase necrotic core volumes (37.5% vs 28.9 % p=0.2). Exposure to biodiesel PM triggered loss of hVSMC in tunica-media, strongly correlating with apoptosis in the vessel wall (Pearson r=0.7, p<0.01). These findings were supported by dose-dependent apoptosis of hVSMCs upon 2-hour PAH treatment. **Conclusions:** This study demonstrates that exposure to biodiesel exhaust PM dramatically modulates atherosclerotic plaque composition, resulting in an unstable

plaque phenotype through enhanced pro-apoptotic mechanisms.
J.J.N. Posma: None. **E. Kilinç:** None. **J.I. Borissoff:** None. **A. Haegens:** None. **A.D. Jedynska:** None. **H. Ten Cate:** None. **I.M. Kooter:** None. **H.M.H. Spronk:** None.

600
Hepatic (Pro)renin Receptor Inhibition Decreases Plasma Cholesterol and Triglyceride Levels but Does Not Ameliorate Atherosclerosis in LDLR$^{-/-}$ Mice
Liwei Ren, Yuan Sun, Shenzhen Univ, Shenzhen, China; A.H. Jan Danser, Div of Pharmacology and Vascular Med at the Erasmus Medical Ctr, Rotterdam, Netherlands; Xifeng Lu, Shenzhen Univ, Shenzhen, China

Rationale: Cardiovascular diseases (CVD) are the leading cause of death worldwide. Atherosclerosis, dyslipidemia, hypertension, obesity and diabetes are major risk factors for CVD. Elevated plasma cholesterol, especially low-density lipoprotein cholesterol (LDL-c), accelerates atherosclerosis development by inducing lipid accumulation in the vascular wall, foam cell formation and chronic inflammation. Hypertriglyceridemia has also been identified as a risk factor for CVD. Recently, we have identified the (pro)renin receptor [(P)RR], a signaling receptor for renin/prorenin, as a key regulator of lipid metabolism. Inhibiting the (P)RR receptor prevented diet-induced obesity and dyslipidemia in C57BL/6J mice, suggesting that (P)RR inhibition might be used to treat atherosclerosis. Therefore, in the current study, we aimed to explore whether inhibiting the hepatic (P)RR in LDLR$^{-/-}$ mice could reduce plasma lipid levels and attenuate atherosclerosis.
Methods and Results: Eight week-old male LDLR$^{-/-}$ mice were injected with GalNAc-modified (liver-specific) antisense oligos against the (P)RR weekly, and fed a high-fat diet (HFD) for 16 weeks. Inhibiting the hepatic (P)RR prevented HFD-induced obesity in LDLR$^{-/-}$ mice, similar to our previous observation in C57BL/6J mice. Moreover, (P)RR inhibition decreased the HFD-induced increase in plasma cholesterol levels by almost 50%. FPLC analysis revealed that the VLDL fraction but not the IDL/LDL fraction was reduced by (P)RR inhibition. Plasma triglyceride levels decreased from 1249 ± 136 to 207 ± 32 mg/dL. Remarkably, despite these changes, (P)RR inhibition did not reduce atherosclerotic lesion areas in the aortic root, and even increased plaque size in the entire aorta.
Conclusion: Hepatic (P)RR inhibition reduces obesity and plasma cholesterol in HFD-fed LDLR$^{-/-}$ mice, yet failed to ameliorate atherosclerosis. The latter most likely relates to the lack of effect of (P)RR inhibition on LDL-c, and implies that only LDL-c, and not triglycerides contribute to atherosclerosis progression.
L. Ren: None. **Y. Sun:** None. **A. Danser:** None. **X. Lu:** None.

601
MicroRNAs and Hedgehog Signaling in the Pathogenesis of Progressive Liver Injury from NAFLD to Fibrosis
Xiao Cheng, Edward Harris, Juan Cui, **Neetu Su**, Univ of Nebraska-Lincoln, Lincoln, NE

Non-alcoholic fatty liver disease (NAFLD) is very common (~70%) in subjects with diabetes and is associated, independently of several confounding factors, with an increased risk of cardiovascular disease (CVD). Diabetes is an independent risk factor for progression of liver fibrosis. Recent studies in human subjects with NAFLD and animal models have demonstrated that microRNAs, a group of noncoding small RNAs, are intimately involved in the development and progression of liver injury, and act to alter expression of genes involved in lipid metabolism and apoptosis. MiR-34a and miR-29 family were among the most frequently dysregulated miRNAs in NAFLD. Thus, the objective of this study was to determine the role of miR-34a and miR-29 in the onset and progression of hepatic steatosis to liver fibrosis in a diabetic mouse model. We showed that streptozotocin (STZ)-induced diabetes predisposed mice to a high-fat-diet (HFD) induced severe liver injury in a much short time course compared to non-diabetic mice. The livers exhibited the development of a spectrum pathological change, with hepatic steatosis at week 6, NASH at week 8 and liver fibrosis at week 12 upon high fat feeding. More importantly, the progressive live injury was closely associated with significantly increased or reduced expression of miR-34a and miR-29 family, respectively, resulting in the activation of hedgehog signaling and the markers of fibrogenesis, Col1A1 and alpha-SMA. Treatment with nanoparticles carrying miR-29b1 mimics improved insulin sensitivity and prevented HFD induced liver fibrosis. In vitro, treatment of McA-RH7777 cells, a rat hepatoma cell line, with a hedgehog signaling inhibitor MDB5 prevented overexpression of miR-34a induced by a free fatty acid, palmitic acid but significantly enhanced expression of miR-29 family in both hepatocytes and hepatic stellate cells. This action hindered the activation of fibrogenesis by lipotoxicity and inflammatory cytokine TNFα. Our study, for the first time, delineates the interaction between miR-34a and miR-29 family and hedgehog signaling in the development of NAFLD and liver fibrosis. This novel finding may provide rationale for developing miRNAs as pharmaceutical targets for the prevention and treatment of liver injury.
X. Cheng: None. **E. Harris:** None. **J. Cui:** None. **N. Su:** None.

602
The Role of Interleukin-19 in Adipose Tissue Homeostasis
Christine N Vrakas, Allison B Herman, Mitali Ray, Gavin Landesberg, Sheri E Kelemen, Michael V Autieri, Rosario Scalia, Lewis Katz SOM at Temple Univ, Philadelphia, PA

Expanding adipose depots experience hypoxia and inflammation, a phenomenon considered pathogenic of metabolic and cardiovascular complications. Currently very little is known about the potential for endogenously expressed anti-inflammatory cytokines to attenuate inflammation and also provide pro-angiogenic effects. Interleukin-19 is a uniquely anti-inflammatory, pro-angiogenic cytokine expressed in adipose tissue. We hypothesized that in the inflamed adipose depots of the overweight-obese organism IL-19 promotes a compensatory, anti-inflammatory and pro-angiogenic action to restore adipocyte homeostasis in the face of excess energy intake. We report that IL-19 is constitutively expressed in visceral and subcutaneous adipose depots of lean wild-type mice. We also found evidence of significantly increased IL-19 expression in the visceral adipose depots of diet-induced obese mice ($p<0.001$ vs lean mice). Using *Il19*$^{-/-}$ mice, we first demonstrate that the loss of IL-19 leads to a reduction in the metabolically protective and anti-inflammatory genes PPARγ and adiponectin. Simultaneously, pro-inflammatory factors including TNFα and IL-6 are increased, and pro-angiogenic factors such as VEGF are down regulated. *Il19*$^{-/-}$ mice display elevated fasted blood glucose levels relative to WT controls ($p<0.05$). Insulin tolerance tests revealed that *Il19*$^{-/-}$ mice exhibit insulin resistance compared to WT controls. The metabolic profile of *Il19*$^{-/-}$ mice appears to be related to IL-19 actions on adipose tissue as suggested by the fact that *Il19*$^{-/-}$ mice fed high fat diet experience significant down-regulation of IL-19 receptor (IL-20Rα/IL-20Rβ) expression in the visceral adipose tissue, but not in the liver and skeletal muscle. Mechanistic studies in differentiated 3T3-L1 adipocytes demonstrated that addition of rIL-19 increases PPARγ and adiponectin at both the transcript and protein level. These data suggest that potentiation of endogenous IL-19 activity may represent a novel therapeutic strategy to avert the inflammatory and metabolic complications associated with the adipose tissue dysfunction of diet-induced obesity.
C.N. Vrakas: None. **A.B. Herman:** None. **M. Ray:** None. **G. Landesberg:** None. **S.E. Kelemen:** None. **M.V. Autieri:** None. **R. Scalia:** None.

603
Sequences Proximate to the Renin Cleavage Site in Angiotensinogen Do Not Affect Angiotensin II-mediated Functions
Chia-Hua Wu, Congqing Wu, Feiming Ye, Deborah Howatt, Anju Balakrishnan, Jessica Moorleghen, Craig Vander Kooi, Alan Daugherty, Hong Lu, Univ of Kentucky, Lexington, KY

Objective: Angiotensinogen (AGT) cleavage by renin is the rate limiting step to produce angiotensin (Ang)II, a critical contributor to hypertension and atherosclerosis. Human AGT can not be cleaved by mouse renin as demonstrated by a transgenic mouse model expressing human AGT. Amino acids at positions 11 and 12, adjacent to the renin cleavage site in AGT, have been proposed to regulate renin cleavage between human and mouse. This study determined whether these two residues affect renin cleavage and the consequent AngII-mediated functions.
Methods and Results: Hepatocyte-specific AGT deficient (hepAGT-/-) mice have low plasma AGT but high renin concentrations. This mouse model injected with adeno-associated viral vectors (AAV) encoding AGT was used to repopulate AGT. We first determined whether repopulation of human AGT using AAV recapitulate phenotypes of human AGT transgenic mice. HepAGT-/- mice were injected with AAV having a null insert or encoding human AGT, while wild type littermates (hepAGT+/+) were injected with the null AAV. Administration of AAV encoding human AGT led to high plasma human AGT concentrations without affecting plasma mouse renin concentrations, and had no effect on blood pressure and atherosclerosis. In a subsequent study, AAV encoding mutated mouse AGT with Leu11Val and Tyr12Ile that were same as the two residues in human were injected into hepAGT-/- mice. Repopulation of the mutated mouse AGT resulted in increased plasma mouse AGT concentrations and reduced renin concentrations that were comparable to their concentrations in hepAGT+/+ mice injected with the null AAV. Consequently, AAV-driven expression of mutated mouse AGT increased blood pressure and atherosclerosis in hepAGT-/- mice that were comparable to their magnitudes in hepAGT+/+ mice injected with the null AAV. Conclusion: The two amino acids proximate to renin cleavage site do not affect AngII-mediated effects.
C. Wu: None. **C. Wu:** None. **F. Ye:** None. **D. Howatt:** None. **A. Balakrishnan:** None. **J. Moorleghen:** None. **C. Vander Kooi:** None. **A. Daugherty:** None. **H. Lu:** None.

604
Anti-apoptotic Role of Leptin in Adipose Tissue
Yuebo Zhang, Virend K Somers, Yu Dong, Prachi Singh, Mayo Clinic, Rochester, MN

Background: Leptin contributes to obesity-related cardiometabolic pathology. While the role of adipose tissue dysfunction in altering metabolic profile in obesity is recognized, the direct effects of leptin signaling in adipose tissue are not completely understood. Among factors impacting adipose tissue function in obesity, adipocyte death is associated with increased inflammation with consequent adipose tissue insulin-resistance. Furthermore, apoptosis of adipocyte progenitor cells (preadipocytes) is important as it lowers adipose tissue capacity to maintain and expand fat storage. **Objective:** To determine the effects of leptin on regulation of proteins important to apoptotic pathways in cultured human white preadipocytes (HWP) and differentiated HWP (dHWP). **Methods:** Cells were exposed to increasing concentrations of leptin to evaluate the role of leptin on regulation of anti-apoptotic Bcl2, and pro-apoptotic Bax and CD95 expression. Next, we examined if pre-exposure to leptin attenuated TNF-α and FasL induced apoptosis. **Results:** Leptin upregulated transcription of Bcl2 (p=0.02) and down-regulated transcription of Bax (p=0.02) and CD95 (p=0.04) in a leptin-concentration dependent manner in dHWP. Leptin dependent increases in Bcl2 (p=0.004) and decreases in Bax (p=0.003) and CD95 (P=0.03) protein expression were also observed. Furthermore, 24 hour pre-exposure to leptin protected cells from TNF-α (p=0.01; p=0.006) and FasL (p=0.03; p=0.007) induced apoptosis in dHWP and HWP respectively. Additionally, leptin attenuated TNF-mediated activation of the p53 pathway, suggesting another mechanism by which leptin mediates its inhibitory effects on TNF-induced apoptosis. **Conclusion:** Leptin regulates the expression of proteins involved in the apoptotic pathway such that it decreases the apoptotic potential of adipose tissue by increasing anti-apoptotic Bcl2 and decreasing pro-apoptotic Bax and CD95 protein expression. In contrast to our in-vitro findings, prior studies in adipose tissue from obese humans report decreased Bcl2 and increased Bax protein expression, along with high leptin expression. This suggests that increased adipose tissue apoptosis in obesity may at least in part be secondary to altered leptin signaling.
Y. Zhang: None. **V. Somers:** None. **Y. Dong:** None. **P. Singh:** None.

This research has received full or partial funding support from the American Heart Association.

605
Inhibition of the Key Glycolytic Enzyme PFKFB3 with Novel Compounds Suppresses Angiogenesis
Anahita Abdali, Alberto Corsini, Univ of Milan, Milan, Italy; Denisa Baci, IRCCS MultiMedica, Milan, Italy; Carlo De Dominicis, Matteo Zanda, Univ of Aberdeen, Aberdeen, United Kingdom; Maria Luisa Gelmi, Stefano Bellosta, Univ of Milan, Milan, Italy

Aim Intraplaque angiogenesis is an important contributor to atherosclerotic plaque growth and instability. Angiogenic signals induce endothelial cells (ECs) to switch their metabolism to being highly glycolytic, enabling their growth and division. Glycolytic modulation by inhibition of theglycolytic activator 6-phosphofructo-2-kinase/fructose-2,6-bisphosphatase (PFKFB3) has been shown to reduce angiogenesis. The objective of this study was to identify novel anti-angiogenic compoundswith a potential to efficiently modulate (inhibit) angiogenesis. **Methods** Using the human EC line EA.hy926, we studied the effects of PFKFB3 inhibition with 3PO, a weak competitive inhibitor of PFKFB3, and of two potent self-synthesized phenoxindazole analogues (PA-1 and PA-2) on glycolysis, proliferation, migration, matrix metalloproteinase (MMP) activity, and capillary tube formation. Moreover, gene expression of important markers related to angiogenesis were measured at mRNA levelby real-time PCR. **Results** PFKFB3 inhibition with all three tested compounds significantly reduced glycolytic activity. While PA-1 and PA-2suppressedcapillary tube formation, 3PO did not have any effect. Accordingly, PA-1 and PA-2 markedly inhibited EC migration, proliferation and wound closing capacity which are essential for neovessel formation. Moreover, these inhibitors downregulated gelatinase gene expression up to 6-fold, as well reduced the activity of proMMP-9 and MMP-2 up to 50% and 30% compared to control, respectively. Gene expression analysis revealed that the PA compounds downregulated PFKFB3 expression whilst 3PO did not. Similarly, markers of migration and angiogenesis, such as CCL5, VCAM-1, VEGFA and VEGFR2, were also markedly reduced (up to 10-fold) by the PA compounds. **Conclusions** These findings suggest that PFKFB3 inhibition with PA compounds may interfere with key pro-angiogenic functions, such as endothelial migration, proliferation and capillary-like structure formation and this exerts a multitarget anti-angiogenic activity. Hence, PFKFB3 inhibition with PA compounds is a promising therapeuticapproach to promote plaque stability.
A. Abdali: None. **A. Corsini:** None. **D. Baci:** None. **C. De Dominicis:** None. **M. Zanda:** None. **M. Gelmi:** None. **S. Bellosta:** None.

606
The Differential Roles of the Adaptor Proteins Nck1 and Nck2 in Shear Stress-Induced Endothelial Activation *in vitro* and *in vivo*
Mabruka Alfaidi, Jonette M. Green, A. Wayne Orr, LSU Health Sciences Ctr-Shrevepo, Shreveport, LA

Hemodynamic shear stress critically regulates endothelial activation and atherogenesis by affecting cytoskeletal dynamics and endothelial gene expression. The Nck adaptor proteins (Nck1 and Nck2) couple tyrosine kinase signaling to induction of cytoskeletal remodeling pathways, and we previously demonstrated that a peptide corresponding to a Nck-binding sequence in p21 activate kinase (PAK) blunts shear stress-induced proinflammatory signaling (PAK, NF-κB) and permeability *in vitro* and *in vivo*. However, the specific roles of Nck1 and Nck2 in flow-induced endothelial activation remain to be elucidated. Here, we demonstrate that Nck1, but not Nck2, critically regulates shear stress-induced endothelial activation. We show that Nck1 deficiency (siRNA knockdown, genetic knockout) decreases basal and shear stress-induced proinflammatory signaling (PAK2, NF-κB) and proinflammatory gene expression (ICAM-1, VCAM-1). In addition, only Nck1, but not Nck2, knockdown/knockout limited shear-induced endothelial permeability. However, other shear stress-dependent pathways, such as Akt activation, proved Nck1-independent. By contrast, selective Nck2 depletion paradoxically increased basal PAK2 activation without significant effects on NF-κB signaling or permeability. Using the partial carotid ligation model of disturbed flow, we found that Nck1 knockout mice showed significantly reduced proinflammatory gene expression that was not further diminished upon Nck2 deletion. However, Nck2 was not inconsequential to the flow response, as Nck2 knockdown or knockout reduced actin cytoskeletal alignment with laminar flow. Taken together, our data suggests that Nck1 plays a dominant role in flow-induced endothelial activation in response to shear stress, whereas Nck2 may critically regulate flow-induced cytoskeletal remodeling and endothelial alignment.
M. Alfaidi: None. **J. Green:** None. **A. Orr:** None.

607
Increased Vitamin D_3-induced Kidney Dysfunction Associates With Intrarenal VascularCalcification in Type 2 Diabetes Mellitus Murine Model
Youri E Almeida, Melissa R Fessel, Luciana S Carmo, Elisangela Farias-Silva, Luciana P Alves, Hosp Albert Einstein, São Paulo, Brazil; Vanda Jorgetti, Univ São Paulo - Faculdade de Medicina, São Paulo, Brazil; Lionel L Contreras, Erika B Rangel, Marcel Liberman, Hosp Albert Einstein, São Paulo, Brazil

Vascular calcification associates with increased cardiovascular morbidity and mortality in patients with diabetes mellitus and end-stage renal disease. We evaluated intrarenal vascular calcification and renal dysfunction after either vitamin D_3 ($VitD_3$ 4.4-6.4x104 IU/day i.p. for 21 days) or saline in ob/ob mice (n=12), a murine model of type 2 diabetes mellitus (T2DM), in comparison to paired C57BL/6 mice (n=12). The animal protocol #2242-14 was approved by Institutional ethics committee. VitD3 increased serum calcium levels in both animal strains. Serum creatinine increased in VitD3-treated mice (92% and 43% in ob/ob and C57BL/6 respectively), while serum urea levels decreased in ob/ob and increased in C57BL/6 after calcifying protocol. Both $VitD_3$-treated ob/ob and C57BL/6 decreased 24-hour urine volume, which was more pronounced in diabetic animals (~5 times and ~1.5 reduction in ob/ob and in C57BL/6 respectively). Moreover, creatinine clearance decreased in $VitD_3$-treated mice, especially in ob/ob animals (~7 and ~3 fold reduction in ob/ob and C57BL/6, respectively). Additionally, urinary albumin/creatinine ratio increased after $VitD_3$ administration in ob/ob mice only (~13 times in comparison to control ob/ob). Alizarin Red S, Von Kossa and Osteosense™ revealed that only ob/ob mice developed extensive intrarenal vascular calcification after $VitD_3$. Interestingly, histomorphometric analysis of the femur showed that $VitD_3$ induced similar osteomalacia in both ob/ob and C57BL/6 mice. Coincidently with increased intrarenal vascular mineralization in ob/ob, confocal immunofluorescence analysis demonstrated that Bone Morphogenetic Protein-2 (BMP-2) was highly expressed in these arteries exclusively in ob/ob. These data suggest a greater susceptibility of T2DM murine model to $VitD_3$, in comparison to paired C57BL/6 littermates to induce kidney dysfunction associated with increased intrarenal vascular calcification, together with BMP-2 signaling pathway activation. These findings were independent of bone remodeling and serum calcium levels. In conclusion, this study unfolded novel mechanisms of progressive renal dysfunction in T2DM after $VitD_3$ in vivo associated with increased intrarenal vascular calcification.
Y.E. Almeida: None. **M.R. Fessel:** None. **L.S. Carmo:** None. **E. Farias-Silva:** None. **L.P. Alves:** None. **V. Jorgetti:** None. **L.L.F. Contreras:** None. **E.B. Rangel:** None. **M. Liberman:** None.

608
Integrated Omics and Network Analysis Identify Drivers of Calcific Bicuspid Aortic Valve Disease
Mark C Blaser, Florian Schlotter, Lang H Lee, Ctr for Interdisciplinary Cardiovascular Sciences, Div of Cardiovascular Med, Dept of Med, Brigham and Women's Hosp, Harvard Medical Sch, Boston, MA; Arda Halu, Ctr for Interdisciplinary Cardiovascular Sciences, Div of Cardiovascular Med, Channing Div of Network Med, Dept of Med, Brigham and Women's Hosp, Harvard Medical Sch, Boston, MA; Wunan Zhou, Dept of Radiology, Brigham and Women's Hosp, Harvard Medical Sch, Boston, MA; Livia S Passos, Ctr for Excellence in Vascular Biology, Div of Cardiovascular Med, Dept of Med, Brigham and Women's Hosp, Harvard Medical Sch, Boston, MA; Hideyuki Higashi, Tan H Pham, Ctr for Interdisciplinary Cardiovascular Sciences, Div of Cardiovascular Med, Dept of Med, Brigham and Women's Hosp, Harvard Medical Sch, Boston, MA; Amitabh Sharma, Ctr for Interdisciplinary Cardiovascular Sciences, Div of Cardiovascular Med, Channing Div of Network Med, Dept of Med, Brigham and Women's Hosp, Harvard Medical Sch, Boston, MA; Maria C Nunes, Dept of Clinical Med, Federal Univ of Minas Gerais, Belo Horizonte, Brazil; Ron Blankstein, Marcelo F DiCarli, Div of Cardiovascular Med, Dept of Med, Dept of Radiology, Brigham and Women's Hosp, Harvard Medical Sch, Boston, MA; Masanori Aikawa, Ctr for Interdisciplinary Cardiovascular Sciences, Ctr for Excellence in Vascular Biology, Div of Cardiovascular Med, Channing Div of Network Med, Dept of Med, Brigham and Women's Hosp, Harvard Medical Sch, Boston, MA; Sasha A Singh, Ctr for Interdisciplinary Cardiovascular Sciences, Div of Cardiovascular Med, Dept of Med, Brigham and Women's Hosp, Harvard Medical Sch, Boston, MA; Simon C Body, Ctr for Perioperative Genomics, Dept of Anesthesiology, Perioperative and Pain Med, Brigham and Women's Hosp, Harvard Medical Sch, Boston, MA; Elena Aikawa, Ctr for Interdisciplinary Cardiovascular Sciences, Ctr for Excellence in Vascular Biology, Div of Cardiovascular Med, Dept of Med, Brigham and Women's Hosp, Harvard Medical Sch, Boston, MA

Objectives Calcific aortic valve disease (CAVD) shares risk factors with atherosclerosis but has no pharmacotherapy. Bicuspid aortic valve (BAV) is the most common congenital cardiac defect (2% of humans), and individuals with BAVs acquire CAVD at a rate >15-25x of those with tricuspid aortic valves (TAVs). The causes and mechanisms of accelerated BAV-CAVD remain unclear. This study demonstrates the integrated transcriptome and proteome of BAV-CAVD.
Methods Quantification of gated chest CTs assessed aortic valve calcification. We performed transcriptomics using Illumina sequencing and global unlabeled proteomics by LC-

MS/MS in a total of 55 human aortic valves (24 stenotic TAVs and 25 stenotic BAVs from valve replacement surgeries segmented into fibrotic and calcific portions, and 6 non-diseased aortic valves from heart transplants).
Results
Calcific burden did not differ between BAVs and TAVs (Agatston score: p = 0.88), but BAV mineralization was significantly accelerated as BAVs underwent surgery 11.5±1.74 years earlier than TAVs (p < 0.01). Transcriptomics sequenced 11,223 genes and proteomics identified 1,798 proteins. Of these, 174 genes (fibrotic = 121, calcified = 53) and 98 proteins (fibrotic = 24, calcified = 74) were differentially expressed between BAV- and TAV-CAVD. Pathway analysis of proteins enriched in BAVs vs. TAVs found significant enhancement of iron metabolism and proteoglycan function in BAV-CAVD, while complement activation and collagen biosynthesis distinguished TAVs. When overrepresented proteins were mapped to the protein-protein interactome, network analysis identified disease stage- and valve type-specific subnetworks. While numerous protein-protein interactions existed between the fibrosis and calcification subnetworks of TAVs, a disconnection between these two pathological processes was identified in BAV subnetworks.
Conclusions Integrated multi-omics of CAVD stratified by disease stage and valve type identify unique contributors to BAV pathogenesis and shed light on molecular drivers of disease. Network analysis finds that while fibrocalcific responses are linked in TAVs, fibrosis and calcification may develop independently in BAVs, with vital implications for targeting of therapeutics.
M.C. Blaser: None. **F. Schlotter:** None. **L.H. Lee:** None. **A. Halu:** None. **W. Zhou:** None. **L.S.A. Passos:** None. **H. Higashi:** None. **T.H. Pham:** None. **A. Sharma:** None. **M.C.P. Nunes:** None. **R. Blankstein:** None. **M.F. DiCarli:** None. **M. Aikawa:** None. **S.A. Singh:** None. **S.C. Body:** None. **E. Aikawa:** None.

609
Pro-atherosclerotic Low-density Neutrophils Are Present in Hypercholesterolemia
Blake J Cochran, UNSW Sydney, UNSW Sydney, Australia; Damilola Pinheiro, Maria Prendecki, Ben Jones, Jaimini Cegla, Imperial Coll London, London, United Kingdom; Victoria Lee, Philip J Barter, UNSW Sydney, Sydney, Australia; Andrew J Murphy, Baker Heart and Diabetes Inst, Melbourne, Australia; Kerry-Anne Rye, UNSW Sydney, Sydney, Australia; Kevin J Woollard, Imperial Coll London, London, United Kingdom

Introduction: Elevated cholesterol levels and increased accumulation of myeloid cells are key risk factors in the development of atherosclerosis. Whilst there is significant understanding of the impact of hypercholesterolemia on monocyte function, less is known about the impact of cholesterol on neutrophils. Neutrophils contain the necessary machinery to take up, synthesize, efflux and esterify cholesterol and unique neutrophil phenotypes have been shown in various pathologies, including low density neutrophils (LDNs) described in inflammatory diseases.
Aim: Determine if cholesterol loading of neutrophils occurs in hypercholesterolemia and characterize the associated phenotypic and functional consequences.
Methods: Patients (n=13) were a mix of familial hypercholesterolemia and mixed dyslipidemia all with total cholesterol > 7.0 mmol/L. Age and sex matched healthy donors were used as controls. Normal and low density neutrophils were isolated using a percoll density protocol and further purified by FACS selecting for $CD66b^{+}CD15^{+}$ cells.
Results: LDNs were only present in hypercholesterolemic patients, accounting for 12.29.6% of the cells in the lower density percoll fraction (p<0.01 vs control). LDNs were morphologically similar to mature high density neutrophils and stained positive for neutral lipid. Functionally, LDNs secreted significantly more extracellular traps (NETs) in response to PMA treatment relative to normal density neutrophils isolated from the same patients or healthy controls (p<0.005). Cholesterol loaded neutrophils were more adhesive to endothelial cells compared to controls (p<0.005). Increased NETosis and neutrophil adhesion have been demonstrated to be atherogenic. Phagocytosis was increased in LDNs vs controls (p<0.05). These functional changes could all be replicated in vitro via treatment of neutrophils from healthy subjects with cholesterol or oxLDL.
Conclusion: Hypercholesterolemia results in cholesterol loading and a pro-atherosclerotic phenotype in neutrophils. Our data provides evidence that this cholesterol loading occurs in the circulation. More work is now being carried out to further characterize the phenotype of LDNs and mechanisms of maturation during hypercholesterolemia.
B.J. Cochran: None. **D. Pinheiro:** None. **M. Prendecki:** None. **B. Jones:** None. **J. Cegla:** None. **V. Lee:** None. **P.J. Barter:** None. **A.J. Murphy:** None. **K. Rye:** None. **K.J. Woollard:** None.

610
Functional Relationship of The *CARS2* Locus to Coronary Artery Disease
AnhThu Dang, Adam Turner, Paulina Lau, Sébastien Soubeyrand, Ruth McPherson, Univ of Ottawa Heart Inst, Ottawa, ON, Canada

In a recent meta-analysis of GWAS for cardiovascular disease (CAD) with imputation from 1000 Genomes (Nat Genet 2015), we identified 202 significant CAD associated variants (FDR q< 0.05) in 129 loci. Seven independent association signals were identified in a gene cluster at chromosome 13q34 including rs61969072. This SNP is located in an intergenic region proximal to the *ING1*, *CARKD* and *CARS2* genes. Expression data (eQTL) obtained from the GTEx Project demonstrate a strong association of rs61969072 with *CARS2* mRNA abundance in artery with decreased *CARS2* expression in carriers of the risk G allele, hinting that *CARS2* may be a causal CAD gene. *CARS2* encodes a putative mitochondrial cysteinyl t-RNA synthetase. Bioinformatics data (BioGPS) indicate high gene expression of *CARS2* in monocytes, a precursor of macrophages. Having then demonstrated that *CARS2* mRNA expression is decreased in M1 macrophages compared to M0 and M2 macrophages, we examined the role of *CARS2* in the anti-inflammatory pathway in macrophages using THP-1 cells, a macrophage model system. Gene expression profiling of 84 key players of the inflammatory response was performed on siRNA mediated knockdown of *CARS2* samples. Comparisons between knockdown and control samples (n=4) identified 12 upregulated and 4 down regulated genes with ≥ 1.25 or ≤0.75 fold difference in expression (p<0.05). Gene Set Enrichment Analysis (GSEA), using inflammatory response PCR array data, identified the interleukin-10 signaling pathway as an enriched category (FDR q<0.05). IL-10 has an atheroprotective effect against plaque rupture and thrombus formation by influencing the local inflammatory process in the lesion. IL-10 activates the STAT3 cascade, where phosphorylated STAT3 homodimers translocate to the nucleus to activate specific target effector genes which repress the proinflammatory genes at the transcriptional level. IL-10 induced STAT3 phosphorylation was measured by Western blotting in THP-1 cells. In response to IL-10, *CARS2* knockdown samples showed dampened STAT3 phosphorylation compared to control suggesting that *CARS2* serves an anti-inflammatory function within the IL-10 signaling pathway.
A. Dang: None. **A. Turner:** None. **P. Lau:** None. **S. Soubeyrand:** None. **R. McPherson:** None.

611
Association Between Thoracic Irradiation and Increased Progression of Coronary Artery Calcium
Mark A Davison, Anel Yakupovich, Michael Z Kharouta, Julius Turian, Christopher W Seder, Marta Batus, Dinesh Kalra, Mark Kosinski, Tuncay Taskesen, Tochukwu M Okwuosa, Rush Univ, Chicago, IL

INTRODUCTION Thoracic irradiation (TIR) is associated with increased risk of coronary artery disease (CAD) and coronary death. Coronary artery calcium (CAC) is the result of coronary plaque accumulation and has been shown to predict CAD and overall cardiovascular mortality. We hypothesized that TIR in lung cancer patients receiving radiotherapy would be associated with CAC progression.
METHODS We evaluated CAC progression (pre- and post-TIR) from chest CT scans of lung cancer patients identified from a cancer registry at an urban academic medical center. A 2:1 matched control population was established controlling for age, gender, race, and CT scan interval. Vessel-specific CAC progression and extension in pre- and post-interval CT studies was evaluated by 2 independent reviewers using existing standard methodologies. Whole heart and the left anterior descending (LAD) coronary artery were retrospectively segmented on the CT study used for treatment planning. The volume of each structure and associated dose metrics were obtained using the standard tools available in the Pinnacle Treatment Planning software. Chi squared tests were used to compare vessel-specific CAC progression (increase in CAC volume) and extension (CAC lengthening within a vessel) between groups. Pearson correlation analysis explored associations between radiation volume and CAC progression.
RESULTS We included 35 patients and 65 controls (50% female). Mean and max whole heart TIR doses: 13.5 Gy (95% CI 10.3-16.7 Gy) and 52.1 Gy (95% CI 46.2 – 58.0 Gy); LAD: 21.4 Gy (95% CI 16.0 – 26.8 Gy) and 34.9 Gy (95% CI 28.7 – 41.1 Gy), respectively. CAC progression and extension in LAD and left circumflex coronary artery (LCx) were significantly greater in patients vs. controls (p<0.03 for all). There was statistically significant correlation between LAD radiation volume and CAC progression in the left main coronary artery (LM) (r =0.33, p=0.05).
CONCLUSIONS TIR is associated with CAC progression in the LAD and LCx. For LAD and LM, the CAC progression correlated with the irradiated volume of these structures although neither a dose nor a volume threshold could be established. Future studies examining the utility of CAC screening for radiation-induced CAD and cardiovascular mortality are required.
M.A. Davison: None. **A. Yakupovich:** None. **M.Z. Kharouta:** None. **J. Turian:** None. **C.W. Seder:** None. **M. Batus:** None. **D. Kalra:** None. **M. Kosinski:** None. **T. Taskesen:** None. **T.M. Okwuosa:** None.

612
Low Expression of Lysosomal Acid Lipase in Smooth Muscle Cells Relative to Macrophages Provides New Insights into Foam Cell Lipid Accumulation
Joshua A. Dubland, Kamel Boukais, St. Pauls Hosp, Vancouver, BC, Canada; Ying Wang, Stanford Univ, Stanford, CA; Sima Allahverdian, Collin S. Pryma, Teddy Chan, Gordon A. Francis, St. Pauls Hosp, Vancouver, BC, Canada

Background and Hypothesis: Smooth muscle cells (SMCs) are the predominant cell type within the intima of human atherosclerosis-prone arteries and promote initial retention of atherogenic lipoproteins in the deep intima. We previously found that ≥50% of foam cells in intermediate coronary atheromas are of SMC origin and that intimal SMCs have reduced expression of the ATP-binding cassette transporter A1 (ABCA1). Previously we also found that ABCA1 expression is acutely dependent on the flux of cholesterol out of lysosomes and subsequent generation of oxysterols for promotion of gene transcription by the nuclear liver X receptor (LXR). **Hypothesis:** In the present studies we tested the hypothesis that SMCs have lysosomal dysfunction that contributes to foam cell formation. **Methods and Results:** Human monocyte-derived macrophages (HMMs) and arterial SMCs were treated with aggregated LDL (agLDL) to increase intracellular cholesterol. Unlike HMMs, agLDL treatment failed to upregulate ABCA1 expression in SMCs and did not significantly increase 27-hydroxycholesterol levels. Also in contrast to HMMs, SMCs did not downregulate new cholesterol synthesis and displayed minimal increases in cholesteryl ester formation with agLDL loading. This data suggested retention of lipids within lysosomal compartments. Indeed, confocal microscopy revealed retention of lipids identified by the neutral lipid dye BODIPY within lysosomal compartments stained with LAMP1 in SMCs, while HMMs showed mostly cytosolic lipid droplets [Pearson correlation of colocalization of +0.3197±0.0123 in SMCs and -0.0897±0.0143 in HMMs (p<0.0001, avg±SEM, n>100 cells)]. *LIPA* mRNA levels and LAL protein were markedly reduced in SMCs relative to HMMs, with LAL activity being 23.4-times higher in HMMs compared to SMCs (p<0.0001, n=4). Similarly, we found reduced LAL levels in mouse SMCs relative to macrophages. Incubation of SMCs with medium containing LAL reduced lysosomal lipid accumulation, resulting in decreased new cholesterol synthesis and increased cholesterol efflux. **Conclusions:** We find that arterial SMCs have a relative deficiency in LAL expression resulting in defects in downstream sterol regulatory events compared to macrophages. Our results provide a novel reason for SMC foam cell formation and a potential therapeutic target.
J.A. Dubland: None. **K. Boukais:** None. **Y. Wang:** None. **S. Allahverdian:** None. **C.S. Pryma:** None. **T. Chan:** None. **G.A. Francis:** None.

613
Disturbed Flow-induced Telomeric Repeat Binding Factor 2 (terf2)-interacting Protein (terf2ip) K240 Sumoylation is Critical for Endothelial Senescence but Not Inflammation
Yuka Fujii, MD Anderson Cancer Ctr, Houston, TX; Nhat-Tu Le, Houston Methodist, Houston, TX; Kyung-Sun Heo, Hang T Vu, Sivareddy Kolta, Kyung-Ae Ko, Yin Wang, Tamlyn N Thomas, Elena McBeath, MD Anderson Cancer Ctr, Houston, TX; Carolyn Giancursio, Houston Methodist, Houston, TX; Keigi Fujiwara, Jun-ichi Abe, MD Anderson Cancer Ctr, Houston, TX

Upregulation of both inflammation and senescence (Sen) of endothelial cells (ECs) in the disturbed flow area within the aortic arch is well established, but the exact mechanisms and the relationship between inflammation and senescence remain unclear. TERF2IP is involved in regulation of DNA double strand break (DSB) repair of telomeres (TLs) as a component of the shelterin complex and in IκB kinase (IKK)-NF-kB signaling in the cytosol. TERF2IP and TERF2 form a stable heterodimer to protect the duplex region of TLs. Recent studies showed that TERF2IP or TERF2 deficiency caused TL shortening in mice. We studied how TERF2IP SUMOylation is regulated in ECs and what role it may play in EC inflammation and Sen. We found that disturbed flow (d-flow) activated p90RSK and increased TERF2IP S205 phosphorylation and subsequently K240 SUMOylation. Overexpression of dominant negative p90RSK inhibited d-flow-induced TERF2IP S205 phosphorylation and K240 SUMOylation, and also inhibited EC inflammation and Sen provoked by d-flow. TERF2IP S205 phosphorylation induced TERF2IP nuclear export, which then caused EC inflammation and Sen. In contrast, TERF2IP K240 SUMOylation had no effect on TERF2IP nuclear export, and the TERF2IP K240R SUMOylation site mutant failed to inhibit d-flow-induced NF-kB activation. Interestingly, this point mutation inhibited d-flow-induced Sen with reduced d-flow-induced TL shortening, 8-OHdG level, and apoptosis. Overexpression of a de-SUMOylation enzyme SENP2 and SENP2 T368 mutant significantly inhibited d-flow-induced TERF2IP SUMOylation, suggesting that SENP2 regulates

nuclear TERF2IP SUMOylation. Lastly, EC Sen increased when SENP2 was specifically knocked out in ECs in mice, suggesting that TERF2IP K240 SUMOylation may play a role in d-flow-induced EC Sen. These data suggest that TERF2IP post-translational modifications play roles in regulating EC inflammation and Sen, which are differentially regulated by S205 phosphorylation and K240 SUMOylation. TERF2IP K240R knock-in mice will be used to determine the role of TERF2IP K240 SUMOylation in d-flow-induced atherogenesis. We suggest that TERF2IP SUMOylation promotes TL dysfunction, but it does not interfere with TERF2IP-mediated IKK-NF-kB activation in the cytosol.
Y. Fujii: None. **N. Le:** None. **K. Heo:** None. **H.T. Vu:** None. **S. Kolta:** None. **K. Ko:** None. **Y. Wang:** None. **T.N. Thomas:** None. **E. McBeath:** None. **C. Giancursio:** None. **K. Fujiwara:** None. **J. Abe:** None.

614
From Genotype to Phenotype: Molecular and Functional Characterization of the CVD-associated SNP rs11574 in *ID3*
Christopher A Henderson, Dept of Biochemistry and Molecular Genetics, Robert M. Berne Cardiovascular Res Ctr, Univ of Virginia, Charlottesville, VA; Michael Lipinski, Andrea Zhou, James Garmey, Robert M. Berne Cardiovascular Res Ctr, Univ of Virginia, Charlottesville, VA; Coleen A McNamara, Dept of Med/Cardiovascular Div, Robert M. Berne Cardiovascular Res Ctr, Univ of Virginia, Charlottesville, VA

Atherosclerosis is the primary pathological process of CVD and is strongly controlled by heritable factors; however, the mechanisms and pathways through which many of these genetic components regulate plaque development are poorly understood. Recently, a SNP in the coding region of the gene inhibitor of differentiation 3 (*ID3*) at rs11574 was identified in multiple studies to be associated with CVD. Mutation of rs11574 from the major allele (G) to the minor allele (A) changes the 105th amino acid of ID3 from an alanine to a threonine and is associated with an attenuated ability of ID3 to antagonize bHLH transcription factors and to prevent them from binding to DNA and activating transcription.
The current study utilized co-immunoprecipitation to demonstrate that the minor allele of rs11574 specifically impairs the ability of ID3 to bind to and sequester E12 and no other member of the bHLH family. ChIP studies further demonstrated that the impaired regulatory ability of the ID3 minor allele variant increases E12 occupancy at promoter regions and enhances transcription of E12 target genes including smooth muscle alpha actin (*Acta2*) and p21 in murine vascular smooth muscle cells (VSMCs). To study the role of this SNP in human cells in intact chromatin under endogenous regulation, we genome edited human 293T cells using CRISPR/Cas9 to produce the allelic variants of rs11574 in the *ID3* gene (GG, AG, and AA). Edited cells showed significant changes in cellular proliferation, gene expression, and promoter occupancy depending upon genotype at rs11574. Cells containing the minor allele of rs11574 displayed significantly increased p21 expression and proliferated more slowly than cells containing the major allele of rs11574; whereas, cells heterozygote at rs11574 displayed an intermediate phenotype. These data implicate rs11574 in the regulation of cellular proliferation and mature VSMC marker expression, key phenotypes regulated in the processes of lesion development and formation.
C.A. Henderson: None. **M. Lipinski:** None. **A. Zhou:** None. **J. Garmey:** None. **C.A. McNamara:** None.

615
Absence of RIP3 Reduces Atherosclerotic Progression in Type 1 Diabetes
Denuja Karunakaran, Michele Geoffrion, Leah Susser, Katey Rayner, Univ of Ottawa Heart Inst, Ottawa, ON, Canada

Introduction: Patients suffering from Type 1 diabetes (T1D) have increased risk of developing atherosclerosis. T1D is a chronic autoimmune metabolic disease characterized by a deficiency in insulin secretion and hyperglycemia, promoting oxidative stress and low-grade inflammation in part via advanced glycation end products (AGE). Recently, we and others showed that necroptosis, a newly defined pro-inflammatory programmed cell death, drives advanced atherosclerosis. Given that diabetes accelerates inflammation and atherosclerosis, we ***hypothesized*** that hyperglycemia may exacerbate macrophage necroptosis to drive atherosclerotic lesion formation. **Methods/Results:** Male *Ldlr-/-* mice were lethally irradiated, transplanted with bone-marrow from WT or *Rip3*$^{-/-}$ mice and then administered streptozotocin (STZ) or vehicle daily for 5 days to induce T1D, prior to being fed a western diet for 6 wks. As expected, STZ-treated WT BMT *Ldlr*$^{-/-}$ mice had a marked increased in atherosclerotic aortic lesion area compared to non-diabetic mice (1.08%±0.30 vs 2.13%±0.45). which was blunted in *Rip3*$^{-/-}$ BMT *Ldr*$^{-/-}$ mice (arch: 49% reduction, sinus: 54% reduction, $p<0.05$). Bone marrow derived macrophages (BMDMs) cultured in high glucose (HG) increased cell death in response to necroptotic stimuli (oxidized LDL ± caspase inhibitor zVAD) relative to those cultured in low glucose (LG). Further, the addition of recombinant s100A8/9, a soluble AGE, markedly amplified oxLDL-induced death in HG cultured BMDMs with minimal effects on LG cultured BMDMs, suggesting that pro-inflammatory AGEs released in diabetes can augment macrophage cell death. Further, the increased cell death induced by oxLDL+S100A8/9 was inhibited by a necroptotic inhibitor, Nec-1, or in *Rip3*$^{-/-}$ BMDMs cultured in HG. Mechanistically, treatment of BMDMs cultured in HG with oxLDL+s100A8/9 increased the expression of Rip3 and Mlkl (~5-fold and ~2-fold respectively), which may drive necroptotic cell death during hyperglycemia. **Conclusion:** Deletion of Rip3 markedly halts atherosclerotic progression in a STZ-induced T1D mouse model by inhibiting macrophage necroptosis induced by both atherogenic ligands (oxLDL) and soluble AGE products (s100A8/9).
D. Karunakaran: None. **M. Geoffrion:** None. **L. Susser:** None. **K. Rayner:** None.

617
Apolipoprotein E Receptor-2 Deficiency Accelerates Smooth Muscle Cell Senescence via Impairment of Protein Phosphatase-2-mediated Cytokinesis
Ravi K Komaravolu, Meaghan D Waltmann, Anja Jaeschke, David Y Hui, Dept of Pathology, Metabolic Diseases Inst, Univ of Cincinnati Coll of Med, Cincinnati, OH

Objective*:** Genome-wide association studies revealed apoE receptor-2 (apoER2) variants increase atherosclerosis risk in humans. ApoER2 deficiency in hypercholesterolemic *Ldlr*$^{-/-}$ mice also displayed accelerated atherosclerosis with more complex lesions and extensive lesion necrosis. While loss of apoER2 in macrophages contributes to the advanced lesion phenotype, apoER2 is also expressed in vascular smooth muscle cells (SMC). This study explores the role of apoER2 in SMC functions. ***Methods and Results: Freshly isolated aortic SMC from apoER2 knockout mice showed ~40% less proliferative capacity and displayed a significant reduction in their population doubling when compared to SMC from wild-type (WT) mice. Despite the reduced proliferative rate, apoER2-deficient SMC responded more robustly to TGF-β induced fibronectin synthesis, suggesting a senescence-associated secretory phenotype with increased fibrosis. Accelerated senescence of apoER2-deficient SMC was confirmed by cytochemical staining of β-galactosidase activity and by the increased number of multinucleated polyploidy cells compared to control. Western blot analysis of cell cycle proteins revealed the accumulation of cyclin B1, D1 and securin in apoER2-deficient SMC, indicating that loss of apoER2 does not affect cell cycle entry but promotes cell cycle arrest at the metaphase/anaphase. Increased levels of phosphorylated aurora kinases A/B/C were also

observed in apoER2-deficient SMC, suggesting the impairment of protein phosphatases during cell cycle exit. Interestingly, co-immunoprecipitation experiments showed that apoER2 interacts with the catalytic subunit of protein phosphatase 2A (PP2A-C). In the absence of apoER2, PP2A-C failed to interact with cell-division cycle protein 20 (CDC20) thus resulting in inactive anaphase promoting complex (APC/C^{CDC20}) and the impairment of cell cycle exit. ***Conclusion***s: This study identifies a novel function of the lipoprotein receptor apoER2 in SMC mitosis. The data indicate that apoER2 promotes the recruitment of PP2A-C to the anaphase complex, and the impairment of this process accelerates premature smooth muscle cell senescence similar to that observed in the aging vessel wall.
R.K. Komaravolu: None. **M.D. Waltmann:** None. **A. Jaeschke:** None. **D.Y. Hui:** None.

618
Identification of Novel Disease Genes for Metabolic Syndrome
Arya Mani, Neha Bhat, Sahar Esteghamat, Yale Univ, New Haven, CT

Factors that underlie the association of diverse traits of the metabolic syndrome have remained largely unknown. The strong heritable nature of this condition provides an exceptional avenue for discovery of the disease mechanisms by using modern techniques of human molecular genetics. Strikingly, efforts by genome-wide association studies to identify common variants that show association with two or more traits have largely failed. Growing evidence indicates excess of rare genetic variants through recent exponential population growth, raising the possibility for their causal role in common diseases. With the advent of high throughput sequencing the power for identification of functional rare variants has dramatically increased. By biasing for extreme phenotypes and utilizing traditional method of segregation analysis we have discovered a number of disease genes for metabolic syndrome and coronary artery disease. A major benefit of this strategy is that true causal relationships has been established between rare variations in a gene, its cognate pathways and the disease of interest. These, in turn, have provided fundamental new insight into pathogenesis of poorly understood diseases such as plaque erosion, and logical starting points for identifying new targets and pathways for therapeutic intervention. By dissecting cognate pathways, we have identified novel targets, including Dyrk1B kinase, a novel incretin and components of Wnt signaling pathway to treat CAD, diabetes and hyperlipidemia and have implemented those succesfuly in animal models.
A. Mani: None. **N. Bhat:** None. **S. Esteghamat:** None.

This research has received full or partial funding support from the American Heart Association.

619
Regulatory Mechanism of Lmod1 Mediated Predisposition to Coronary Artery Disease
Vivek Nanda, Ting Wang, Milos Pjanic, Boxiang Liu, Thomas Quertermous, Stanford Univ, Stanford, CA; Joseph Miano, Univ of Rochester, Rochester, NY; Nicholas Leeper, Clint L Miller, Stanford Univ, Stanford, CA

Atherosclerotic coronary artery disease (CAD) continues to be the leading cause of mortality and morbidity worldwide, with an estimated 40% of one's lifetime risk attributed to genetic factors. Meta-analysis of genome-wide association studies implemented to identify this risk in human populations, has now identified rs2820315 (P=7.7E-10; OR=1.05), in the smooth muscle cell-restricted gene, Leiomodin 1 (LMOD1), as the leading genetic polymorphism associated with CAD. However, the causal mechanism by which this polymorphism is responsible for predisposition to CAD remains to be identified. Expression quantitative trait loci (eQTL) mapping in GTEx and STARNET databases revealed that carriers of the risk allele, rs34091558, which is in tight linkage disequilibrium with rs2820315, display significantly attenuated LMOD1 expression in vascular tissues than carriers of the ancestral allele. Allelic expression imbalance analyses in heterozygous HCASMC donors further demonstrated cis-acting effects of the polymorphism on LMOD1 gene expression. To determine the mechanism responsible for this reduction in LMOD1 expression, we performed position weight matrix (PWM) motif analyses and found that rs34091558 disrupts the binding site of a transcription factor called forkhead box O3 (FOXO3). Subsequent chromatin immunoprecipitation and reporter assays demonstrated reduced FOXO3 binding and transcriptional activity by the risk allele in cultured HCASMCs. Platelet-derived growth factor BB (PDGF-BB) stimulation also significantly reduced LMOD1 expression coincident with FOXO3 knockdown. Finally, both gain and loss-of-function for FOXO3 and LMOD1 in HCASMC delineated a regulatory circuit by which LMOD1 regulates SMC proliferation, migration and contraction, characteristic features of atherosclerotic lesion progression. Taken together, these results provide compelling functional evidence that: 1) rs3091558 is associated with reduced LMOD1 expression, 2) this reduction appears to be mediated through the inhibition of FOXO3 binding and 3) changes in vessel wall processes through LMOD1 dysregulation may partially explain the heritable risk for CAD.
V. Nanda: None. **T. Wang:** None. **M. Pjanic:** None. **B. Liu:** None. **T. Quertermous:** None. **J. Miano:** None. **N. Leeper:** None. **C.L. Miller:** None.

This research has received full or partial funding support from the American Heart Association.

620
miRNA Nanoparticles Targeting Cholesterol Efflux: a Promising Tool for the Treatment of Atherosclerosis
My-Anh Nguyen, Leah Susser, UOttawa Heart Inst, Ottawa, ON, Canada; Suresh Gadde, UOttawa, Ottawa, ON, Canada; Katey Rayner, UOttawa Heart Inst, Ottawa, ON, Canada

The prevention and treatment of cardiovascular diseases (CVD) has largely focused on lowering circulating LDL cholesterol, yet a significant burden of atherosclerotic disease remains even with low LDL. Recently, microRNAs (miRNAs) have emerged as exciting therapeutic targets for CVD. miRNAs are small noncoding RNAs that post-transcriptionally regulate gene expression by degradation or translational inhibition of target mRNAs. A number of miRNAs have been found to modulate all stages of atherosclerosis, particularly those that promote cholesterol efflux from lipid laden macrophages in the vessel wall. However, one of the major challenges of miRNA-based therapy is to achieve tissue-specific, efficient and safe delivery of miRNAs *in vivo*. **Objective**: We therefore sought to develop chitosan/miRNA nanoparticles, deliver them to the plaque, and determine if these miRNAs can promote cholesterol efflux to decrease atherosclerosis. **Results**: We conjugated negatively charged miRNAs with tripolyphosphate (TPP) to support crosslinks between polymeric and nucleic acid units, which were then mixed with varying ratios of chitosan polymer to form nanoparticles that ranged from 150-180nm in size. We next optimized the efficiency of intracellular delivery of different chitosan/miRNA ratios to mouse macrophages (MΦ). We find chitosan nanoparticles can protect as well as transfer exogenous miR-33 to naïve MΦ and reduce mRNA and protein expression of its target gene, ABCA1, confirming that miRNAs delivered via nanoparticle can escape the endosomal system and function in the RISC complex. Because ABCA1 plays a key role in stimulating the efflux of cholesterol from MΦ, we also confirmed that MΦ treated with

chitosan/miR-33 nanoparticles exhibited reduced cholesterol efflux to Apolipoprotein A1, further confirming functional delivery of the miRNA. Using this formulation, we have developed a panel of miRNA nanoparticles delivering miRNAs that enhance ABCA1 expression and promote cholesterol efflux. **Conclusions**: miRNAs can be efficiently delivered to macrophages via nanoparticles where they can function to regulate ABCA1 expression and cholesterol efflux, suggesting that these miRNA-nanoparticles can be used *in vivo* to target atherosclerotic lesions.
M. Nguyen: None. **L. Susser:** None. **S. Gadde:** None. **K. Rayner:** None.

621
Vascular Smooth Muscle EphA2 Signaling Regulates Fibrillar Adhesion Formation to Drive Fibronectin Deposition
Alexandra C. Finney, Jonette M. Green, J. Steven Alexander, James G. Traylor, Anthony Wayne Orr, LSU Health Sciences Ctr, Shreveport, LA

During atherosclerosis, synthetic vascular smooth muscle cells drive development of the fibrous cap through extracellular matrix deposition. Deposition of the provisional matrix protein fibronectin appears to critically regulate fibrous cap development by promoting smooth muscle recruitment and by providing a critical scaffold for assembly of fibrillar collagens. We previously showed that deletion of the receptor tyrosine kinase EphA2 in ApoE knockout mice attenuated plaque size and progression, characterized by a reduction of both smooth muscle content and fibrosis, and we further demonstrated that EphA2 depletion attenuates smooth muscle fibronectin deposition *in vitro.* Despite this, the mechanisms by which EphA2 regulates smooth muscle matrix deposition remains unknown. Fibronectin fibrillogenesis involves both the formation of α5β1 integrin-rich fibrillar adhesions and contractility-dependent fibronectin unfolding. We now show EphA2 localizes to integrin adhesions and appears to regulate matrix deposition through multiple mechanisms. Knockdown of EphA2 reduces the formation of fibrillar adhesions characterized by a loss of α5β1 integrins and tensin, whereas EphA2 overexpression is sufficient to induce fibrillar adhesion formation in contractile smooth muscle cells. In addition, vascular smooth muscle cells show diminished collagen gel contraction following EphA2 knockdown, and EphA2 depletion significantly reduces smooth muscle myosin light chain phosphorylation, suggesting that EphA2 expression is required to generate the contractive forces required for matrix remodeling in synthetic smooth muscle cells. Together these data identify a novel role for EphA2 in the regulation of smooth muscle matrix deposition through effects on both integrin adhesion structure and cytoskeletal contractility.
A.C. Finney: None. **J.M. Green:** None. **J.S. Alexander:** None. **J.G. Traylor:** None. **A.W. Orr:** None.

This research has received full or partial funding support from the American Heart Association.

622
Expression of Fatty Acid Binding Protein-4 in Atherosclerotic Watanabe Heritable Hyperlipidemic (WHHL) Rabbit Aortas
Priyanka Prathipati, **Brian Walton**, UTHSC-Houston, Houston, TX

Background: Atherosclerotic diseases are among the prime cause of mortality globally. Proper animal model that can resemble the lipid metabolism and atherosclerotic lesions in humans is key to study the pathophysiology of the disease. One of the most famous of these atherosclerotic animal models is Watanabe heritable hyperlipidemic (WHHL) rabbits. They are deficient of LDL receptors, hence develop spontaneous hypocholesterolemia and atherosclerosis. Previous studies have demonstrated the importance of Fatty acid binding protein-4 (FABP4), a lipid chaperon that plays an important role in atherosclerotic diseases. However, FABP4 expression or role in WHHL rabbits was not investigated yet. Hence, we hypothesis that WHHL rabbits express FABP4 in their aortas and targeting FABP4 acts as a novel target to treat atherosclerosis. **Materials and methods:** Two WHHL rabbits of greater than one year old were sacrificed and aortas were isolated. One of the aorta was flash frozen and other was formalin fixed. Proteins were extracted from frozen section. Western blot was performed to estimate the concentration of FABP4. Immunohistochemistry was performed on the formalin fixed tissue to analyze the expression of FABP4. **Results:** WHHL aortas having noteworthy amount of atherosclerotic plaques expressed FABP4 supporting the importance of FABP4 in cardiovascular diseases. **Conclusion:** WHHL rabbits which are model of atherosclerosis expresses FABP4 in their aortas thus paving the way to use this model to target FABP4 for treating atherosclerosis.

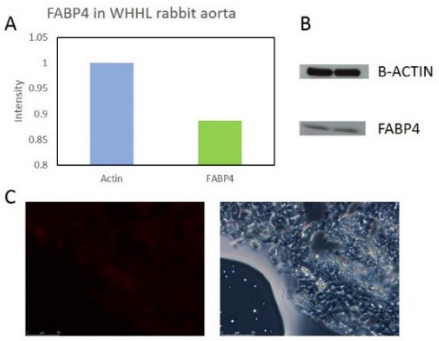

Expression of FABP4 in WHHL rabbit aorta: A and B)-Western blot analysis of FABP4 protein in aortic tissue of WHHL rabbits. C) Immunohistochemistry demonstrating the presence of FABP4 in aortic tissue sections.

P. Prathipati: None. **B. Walton:** None.

623
Activating Liver X Receptors Alters Endothelial Progenitor Cell Differentiation and Enhances the Release of Factors that Reduce Atherosclerosis
Adil Rasheed, Ricky Tsai, Univ of Toronto, Toronto, ON, Canada; Katey J Rayner, Univ of Ottawa Heart Inst, Ottawa, ON, Canada; Carolyn L Cummins, Univ of Toronto, Toronto, ON, Canada

The liver x receptors (LXRα/β) are nuclear receptors that are highly expressed in macrophages and endothelial progenitor cells (EPCs). EPCs are bone marrow (BM) derived cells that facilitate endothelial repair through the secretion of factors. The importance of LXRs in preventing atherosclerosis has been attributed to promoting cholesterol efflux from macrophages. However, a role for EPCs in the LXR response has not been explored. We hypothesized that LXR activation in EPCs contributes to their anti-atherogenic effects by preventing endothelial activation during atherogenesis. In the *Lxr-/-* mice, circulating EPCs were decreased by 27% compared to WT, while myeloid populations were increased. Isolated hematopoietic stem cells treated with LXR agonist (1μM GW3965) *ex vivo* showed a 36% increase in the number of EPC colonies formed, while myeloid colonies were decreased by 25%. GW3965 treatment during EPC differentiation resulted in a 76% decrease in endothelial lineage marker (*Cd144* and *Vegfr2*) expression. To investigate endothelial cell activation, activated human umbilical vein endothelial cells were incubated with the conditioned media (CM) from GW3965-treated WT EPCs, which reduced THP-1 monocyte adhesion by 36% compared to the CM from vehicle treatment. To determine the effects of the EPC-derived CM *in vivo*, *Ldlr-/-* mice were injected with concentrated CM bi-weekly over an 8-week period, which decreased aortic sinus lesion area by 52% compared to the media control injections. Taken together, the loss of LXRs perturbed hematopoietic balance *in vivo*, while the activation of LXRs were associated with

enhanced *ex vivo* EPC formation. Furthermore, LXR activation altered EPC differentiation and secretome resulting in decreased *in vitro* endothelial-monocyte adhesion. When administered to atherosclerotic-prone mice, these secreted factors reduced lesion formation in the aortic sinus. These data suggest that LXRs reduce the development of atherosclerosis in part through the release of EPC-derived factors that can reduce endothelial activation.
A. Rasheed: None. **R. Tsai:** None. **K.J. Rayner:** None. **C.L. Cummins:** None.

624
Interactions Between Adenylate Cyclase Type 9 (ADCY9) and Cholesteryl Ester Transfer Protein (CETP) in Atherosclerosis
Yohann Rautureau, Vanessa Deschambault, Marie-Ève Higgins, Daniel Rivas, Mélanie Mecteau, Pascale Geoffroy, Géraldine Miquel, Kurunradeth Uy, Rocio Sanchez, Audrey Nault, Pierre-Marc Williams, Maria-Laura Suarez, Geneviève Brand, Line Lapointe, Natacha Duquette, Marc-Antoine Gillis, Samaneh Samami, Gaétan Mayer, Philippe Pouliot, Adeline Raignault, Foued Maafi, Mathieu Brodeur, Montreal Heart Inst, Montreal, QC, Canada; Sylvie Lévesque, Marie-Claude Guertin, Montreal Health Innovations Coordinating Ctr, Montreal, QC, Canada; Marie-Pierre Dubé, Éric Thorin, David Rhainds, Éric Rhéaume, Jean-Claude Tardif, Montreal Heart Inst, Montreal, QC, Canada

Pharmacogenomic studies have shown that *ADCY9* genotype determines the effects of the cholesteryl ester transfer protein (CETP) inhibitor dalcetrapib on cardiovascular events, atherosclerosis imaging and body weight variation. The underlying mechanisms responsible for the interactions between ADCY9 and CETP have not yet been determined.
Adcy9-inactivated (*Adcy9*$^{Gt/Gt}$) and wild-type (WT) mice, that were or not transgenic for the CETP gene (CETP^{Gt} and CETP^{WT}), were submitted to an atherogenic protocol (injection of an AAV8 expressing a PCSK9 gain-of-function variant and 0.75% cholesterol diet for 16 weeks). Atherosclerosis, cell adhesion, vasorelaxation, telemetry and adipose tissue MRI were evaluated.
Adcy9$^{Gt/Gt}$ mice had a 65% reduction in aortic atherosclerosis compared to WT (P<0.01). CD68-positive macrophage accumulation and proliferation in plaques were reduced in *Adcy9*$^{Gt/Gt}$ mice compared to WT animals (P<0.05 for both). *Adcy9* inactivation did not change counts of blood monocytes and their subsets. Splenocytes showed reduced adhesion to native aortic endothelium from *Adcy9*$^{Gt/Gt}$ mice (P<0.05 vs WT). Femoral artery endothelial-dependent vasorelaxation was improved in *Adcy9*$^{Gt/Gt}$ mice (versus WT, P<0.01). Selective pharmacological blockade showed that the nitric oxide, cyclooxygenase and endothelial-dependent hyperpolarization pathways all contributed to the improvement of vasodilatation in *Adcy9*$^{Gt/Gt}$ versus WT (P<0.01 for all). *Adcy9*$^{Gt/Gt}$ mice gained more weight than WT with the atherogenic diet, and this was associated with an increase in whole body adipose tissue volume (P<0.05 for both). Feed efficiency was increased in *Adcy9*$^{Gt/Gt}$ compared to WT mice (P<0.05), which was accompanied by improved nocturnal heart rate variability (P=0.0572) and prolonged cardiac RR interval (P<0.05). *Adcy9* inactivation-induced effects on atherosclerosis, endothelium-dependent vasodilation, weight gain and feed efficiency were lost in CETP^{Gt} mice (P>0.05 vs CETP^{WT}).
Adcy9 inactivation protects against atherosclerosis, but only in the absence of CETP activity. This atheroprotection may be explained by decreased macrophage accumulation and proliferation in the arterial wall, improved endothelial function and autonomic tone.
Y. Rautureau: None. **V. Deschambault:** None. **M. Higgins:** None. **D. Rivas:** None. **M. Mecteau:** None. **P. Geoffroy:** None. **G. Miquel:** None. **K. Uy:** None. **R. Sanchez:** None. **A. Nault:** None. **P. Williams:** None. **M. Suarez:** None. **G. Brand:** None. **L. Lapointe:** None. **N. Duquette:** None. **M. Gillis:** None. **S. Samami:** None. **G. Mayer:** None. **P. Pouliot:** None. **A. Raignault:** None. **F. Maafi:** None. **M. Brodeur:** None. **S. Lévesque:** None. **M. Guertin:** None. **M. Dubé:** None. **É. Thorin:** None. **D. Rhainds:** None. **É. Rhéaume:** None. **J. Tardif:** Research Grant; Significant; Amarin, Astra-Zeneca, DalCor, Esperion, Ionis, Merck, Pfizer, Sanofi, Servier. Honoraria; Significant; DalCor, Pfizer, Sanofi, Servier. Other; Modest; Minor Equity interest in DalCor, Author of a pending patent on pharmacogenomics-guided CETP inhibition.

627
Combined Plaque Evaluation by Ultrasound and Microarrays Reveals Bclaf1 as a Novel Regulator of Smooth Muscle Cell Transdifferentiation in Atherosclerosis
Urszula Rykaczewska, Peter Saliba-Gustafsson, Mariette Lengquist, Malin Kronqvist, Kent Lund, Kenneth Caidahl, Josefin Skogsberg, Vladana Vukojevic, Karolinska Inst, Stockholm, Sweden; Jan H Lindeman, Leiden Univ Medical Ctr, Leiden, Netherlands; Gabrielle Paulsson-Berne, Göran K Hansson, Karolinska Inst, Stockholm, Sweden; Nicholas Leeper, Stanford Univ Sch of Med, Stanford, CA; Ewa Ehrenborg, Anton Razuvaev, Ulf Hedin, Ljubica Perisic Matic, Karolinska Inst, Stockholm, Sweden

Objective: Understanding molecular processes behind carotid plaque instability is necessary to develop methods that can identify patients and lesions at risk of stroke. Here, we investigated molecular signatures in human plaques stratified by echogenicity as assessed by duplex ultrasound (US). **Results:** Plaque echogenicity measured by US was correlated to microarray profiles from lesions retrieved at surgery (n=96). Pathway analyses highlighted enrichment of cell apoptosis and proliferation, and BCLAF1 (BCL2 associated factor 1) as the most significantly dysregulated gene (adjusted p<0.0001). BCLAF1 was strongly downregulated in plaques vs. control tissues, positively correlated to markers of cell proliferation and negatively to apoptosis, at both transcriptomic and proteomic level. Immunohistochemistry showed that BCLAF1 was localized in smooth muscle cells (SMCs) nuclei and repressed early during atherogenesis, but reappeared in CD68+ cells in advanced plaques. Proximity ligation assay demonstrated interaction of BCLAF1 with previously reported interaction partners THRAP3 and BCL2, in normal arteries and plaques. *In vitro*, stimulation of SMCs with pro-survival factors EGF, bFGF, PDGFB resulted in induction of BCLAF1, while it was suppressed by macrophage-conditioned medium. Moreover, BCLAF1 silencing in SMCs led to downregulation of BCL2 and SMC markers, and a decrease in proliferation and adhesion (p<0.0001). Transdifferentiation of SMCs using oxLDL, confirmed by CD68 upregulation and MYH11 repression, was accompanied by upregulation of BCLAF1. However, a combination of oxLDL exposure and BCLAF1 silencing, resulted in preserved expression of MYH11 and prevented transdifferentiation. Finally, BCLAF1 expression in CD68+/BCL2+ cells of SMC origin, was verified in plaques from MYH11-lineage tracing atherosclerotic mice.
Conclusions: Carotid plaque echogenicity correlated with enrichment of molecular pathways associated with cell survival and apoptosis and identified BCLAF1, previously not described in atherosclerosis, as the most dysregulated gene. Functionally, BCLAF1 appeared to promote SMC survival by transdifferentiation into macrophage-like phenotype, by interacting with BCL2 and THRAP3.
U. Rykaczewska: None. **P. Saliba-Gustafsson:** None. **M. Lengquist:** None. **M. Kronqvist:** None. **K. Lund:** None. **K. Caidahl:** None. **J. Skogsberg:** None. **V. Vukojevic:** None. **J.H.N. Lindeman:** None. **G. Paulsson-Berne:** None. **G.K. Hansson:** None. **N. Leeper:** None. **E. Ehrenborg:** None. **A. Razuvaev:** None. **U. Hedin:** None. **L. Perisic Matic:** None.

628
Overexpression of ABCA1 in Cultured Endothelial Cells Using Helper-Dependent Adenovirus Enhances ApoAI-Mediated Cholesterol Efflux and has Anti-Inflammatory Effects
Alexis Stamatikos, Nagadhara Dronadula, Univ of Washington, Seattle, WA; Philip Ng, Donna Palmer, Baylor Coll of Med, Houston, TX; Ethan Knight, Bradley Wacker, Chongren Tang, Francis Kim, David Dichek, Univ of Washington, Seattle, WA

Background: ABCA1 removes cholesterol from vascular wall cells via apoAI-mediated efflux, generating HDL that transports cholesterol to the liver for excretion. This process of reverse cholesterol transport is atheroprotective; therefore, strategies that increase vascular wall ABCA1 may prevent or reverse atherosclerosis. Cholesterol efflux mediated by ABCA1 and apoAI can also have anti-inflammatory effects; however, excess depletion of cellular cholesterol can cause cell stress and apoptosis. We tested whether transducing endothelial cells (EC) with a helper-dependent adenoviral vector that expresses ABCA1 (HDAdABCA1) enhances apoAI-mediated cholesterol efflux and reduces inflammatory markers without causing cellular toxicity.
Methods: We cloned rabbit ABCA1, constructed HDAdABCA1, transduced bovine aortic EC (BAEC) with either HDAdABCA1 or empty vector (HDAdNull). We measured ABCA1 protein by immunoblotting and apoAI-mediated cholesterol efflux by loading EC with ^{3}[H] cholesterol, then adding apoAI protein to serum-free medium. We assessed EC phenotype using MTT (metabolic activity), BrdU (proliferation), wound-healing assay (migration), and flow cytometry (apoptosis). We measured ICAM-1, VCAM-1, IL-6, and TNFα mRNA in transduced EC by qRT-PCR both under basal conditions and after serum-starvation, addition of apoAI, and LPS challenge.
Results: We observed a ~3-fold increase in ABCA1 protein in EC transduced with HDAdABCA1 and a ~2-fold increase in apoAI-mediated cholesterol efflux ($P<0.01$ for both). This level of ABCA1 overexpression did not alter EC metabolic activity, proliferation, migration, or apoptosis. Under basal conditions, HDAdABCA1 had no effect on inflammatory markers. However, after serum starvation and addition of apoAI, HDAdABCA1-transduced EC had reduced expression of inflammatory markers both before and after LPS treatment.
Conclusions: HDAdABCA1 increases EC ABCA1 expression and enhances apoAI-mediated cholesterol efflux, but does not cause toxicity or increase inflammatory markers. In contrast, ABCA1 overexpression appears to have anti-inflammatory effects. Future studies will test if HDAdABCA1 decreases lipid rafts, and whether overexpression of ABCA1 in EC in vivo is atheroprotective.
A. Stamatikos: None. **N. Dronadula:** None. **P. Ng:** None. **D. Palmer:** None. **E. Knight:** None. **B. Wacker:** None. **C. Tang:** None. **F. Kim:** None. **D. Dichek:** None.

629
The (Pro)renin Receptor Regulates Scavenger Receptor CD36 Protein Degradation and Functions
Yuan Sun, Liwei Ren, Shenzhen Univ, Shenzhen, China; A.H.Jan Danser, Erasmus Medical Ctr, Rotterdam, Netherlands; Xifeng Lu, Shenzhen Univ, Shenzhen, China

Background: Accumulation of oxidized lipids in monocyte-derived macrophages results in foam cell formation and induces chronic inflammation in the vascular wall, thus contributing to the onset and progression of atherosclerosis. Scavenger receptor CD36 is the most important clearance receptor for ox-LDL, and has been implicated in triggering inflammatory responses in macrophages by ox-LDL. Genetically deleting CD36 reduced foam cell formation and lesion size in ApoE$^{-/-}$ mice. Additionally, circulating macrophages isolated from patients that are deficient of CD36 show much less ox-LDL uptake and accumulation than those from normal subjects. Recently, proprotein convertase subtilisin/kexin type 9 (PCSK9) has been identified as a regulator of CD36 protein degradation. Interestingly, we found that inhibiting the hepatic (pro)renin receptor [(P)RR] dramatically increased plasma PCSK9 levels in C57BL/6J mice. Thus, we wondered if the (P)RR could regulate CD36 protein degradation and functions by increasing PCSK9 levels.
Methods and Results: We inhibited hepatic (P)RR expression in PCSK9$^{-/-}$ mice and wildtype mice, using GalNAc-modified anti-sense oligos targeting the (P)RR. Hepatic (P)RR inhibition reduced hepatic CD36 protein abundance by ~40% in WT mice, without affecting CD36 transcriptional levels. Unexpectedly, inhibiting hepatic (P)RR in PCSK9$^{-/-}$ mice showed a similar reduction in hepatic CD36 protein abundance, suggesting that such reduction in CD36 is unlikely to be mediated by increased plasma PCSK9 levels. To clarify this, we exogenously expressed CD36 in HEK293T cells and studied whether silencing the (P)RR could directly affect CD36 protein abundance. Indeed, silencing the (P)RR reduced exogenously expressed CD36 by almost 50%, confirming that the (P)RR directly controls CD36 degradation. Functional studies revealed that inhibiting/deleting the (P)RR attenuated fatty acid uptake in differentiated 3T3-L1 adipocytes, and ox-LDL uptake in circulating mouse macrophages in a CD36-dependent manner.
Conclusion: The (P)RR acts as a post-transcriptional regulator of CD36, and this occurs in a PCSK9-independent manner. Macrophagic (P)RR may play a role in the development of atherosclerosis by interacting with CD36.
Y. Sun: None. **L. Ren:** None. **A. Danser:** None. **X. Lu:** None.

630
Pcsk9 Deficiency Reduces Atherosclerosis, Apolipoprotein B Secretion, Lipogenesis and Endothelial Dysfunction
hua Sun, UTHealth, Houston, TX; Ronald M Krauss, Children's Hosp Oakland Res Inst, Oakland, CA; Jeffrey T Chang, **Ba-bie Teng**, UTHealth, Houston, TX

Objective: Proprotein convertase subtilisin kexin type 9 (PCSK9) interacts directly with cytoplasmic apolipoprotein B (apoB) and prevents its degradation via the autophagosome/lysosome pathway. This process affects VLDL and LDL production and influences atherogenesis. Here, we investigated the molecular machinery by which PCSK9 modulates autophagy and affects atherogenesis.
Approach and Results: We backcrossed *Pcsk9-/-* mice with atherosclerosis prone LDb (*Ldlr-/-Apobec1-/-)* mice to generate LTp (*Ldlr-/-Apobec1-/-Pcsk9-/-*). Deletion of PCSK9 resulted in decreased hepatic apoB secretion, increased autophagic flux and autophagy signaling, and decreased plasma levels of IDL and LDL particles. The LDLs from LTp mice (LTp-LDL) were less atherogenic and contained less cholesteryl ester and phospholipids than LDb-LDL. Deficiency of PCSK9 affected SREBP-1c lipogenesis pathway. Moreover LTp-LDL induced lower endothelial expression of the genes encoding *TLR2, Lox-1, ICAM-1, CCL2, CCL7, IL-6, IL-1β, Beclin-1, p62*, and *TRAF6*. Collectively, these effects were associated with substantially less atherosclerosis development (> 4-fold) in LTp mice.
Conclusions: The absence of PCSK9 in *Ldlr-/-Apobec1-/-* mice results in decreased lipid and apoB levels, less atherogenic LDLs, and marked reduction of atherosclerosis. The effect on atherogenesis may be mediated in part by the effects of modified LDLs on endothelial cell receptors, and proinflammatory and autophagy molecules. These findings suggest that there may be clinical benefits of PCSK9 inhibition due to mechanisms unrelated to increased LDL receptor activity.
H. Sun: None. **R.M. Krauss:** None. **J.T. Chang:** None. **B. Teng:** None.

631
Reduced Liver X Receptor Alpha S198 Phosphorylation in Bone Marrow Protects against Atherosclerosis and Obesity in Mouse Models
Maud Voisin, NYU Sch of Med, New York, NY; Elina Shrestha, NYU Sch of Med, New york, NY; Tessa J Barrett, Claire Rollet, Hye Rim Chang, Rachel Ruoff, Ira J Goldberg, Edward A Fisher, Michael J Garabedian, NYU Sch of Med, New York, NY

Accumulation of cholesterol-loaded macrophages in arterial walls leads to atherosclerosis, the most common cause of cardiovascular disease. Obesity is a major risk factor for atherosclerosis, and both share pathophysiological features. Indeed, high lipid concentrations and inflammation play key roles in the etiology of both diseases, and this is mediated by alterations in macrophage signaling and gene expression. For example, increased intracellular cholesterol in macrophages activates the Liver X Receptor alpha (LXRα), which plays a central role in reverse cholesterol transport by inducing genes involved in cholesterol efflux and transport. LXRα also responds to environmental signals, such as cholesterol overload, via phosphorylation at serine 198 (pS198). LXRα pS198 selectively regulates the expression of genes that promote inflammation, cell movement, and lipoprotein metabolism, which fosters both atherosclerosis and obesity.
However, whether LXRα phosphorylation impacts progression of atherosclerosis or affects adipose tissue has not been determined. To examine a role of LXRα phosphorylation in atherosclerosis and obesity, we developed a LXRα S198 phosphorylation-deficient knock in mouse (S198A). LDLR-/- mice were reconstituted with bone marrow from LXRα WT or S198A mice and placed on a western diet for 16 weeks. Aortic plaques and perigonadal adipose tissue were histologically analyzed and plasma characteristics were measured. Compared to WT, S198A increased anti-atherogenic HDL (69.2 vs 98.8 mg/dL; p=0.0019) and lowered glucose levels (173.2 vs 149.1 mg/dL; p=0.0019), showed a trend toward decreased plaque macrophage content (32.1 vs 28.7 % plaque area; p=0.085), and reduced macrophage recruitment (# entering cells: 16.6 vs 11.1; p=0.0048), plaque macrophage proliferation (36.6 vs 20.1; p<0.0001), and apoptosis (25.4 vs 14.4; p=0.0002). By FACS, the number of inflammatory adipose tissue macrophages (Cd11c+) was reduced in S198A (28.5 vs 21.5% of total F4/80+ cells; p=0.05). We also observed that the adipocytes were smaller in S198A (3570 vs 2471 μm^2; p=0.01), consistent with a lean phenotype. This suggests that reducing LXRα pS198 in bone marrow promotes a healthier metabolic environment for both atherosclerosis and obesity.
M. Voisin: None. **E. Shrestha:** None. **T.J. Barrett:** None. **C. Rollet:** None. **H. Chang:** None. **R. Ruoff:** None. **I.J. Goldberg:** None. **E.A. Fisher:** None. **M.J. Garabedian:** None.

632
Myeloid beta catenin Deficiency Exacerbates Atherosclerosis in Low-density Lipoprotein-receptor Deficient Mice
Fang Wang, Zun Liu, Se-Hyung Park, Taesik Gwag, Weiwei Lu, Murong Ma, Yipeng Sui, Changcheng Zhou, Coll of Med, Lexington, KY

Objective: The Wnt/β-catenin signaling is an ancient and evolutionarily conserved pathway that regulates essential aspects of cell differentiation, proliferation, migration and polarity, and canonical Wnt/β-catenin signaling has also been implicated in the pathogenesis of atherosclerosis. Macrophage is one of the major cell types involved in the initiation and progression of atherosclerosis, but the role of macrophage β-catenin in atherosclerosis remains elusive. This study aims to investigate the impact of β-catenin expression on macrophage functions and atherosclerosis development.
Approaches and Results: To investigate the role of macrophage canonical Wnt/β-catenin signaling in atherogenesis, we generated low-density lipoprotein receptor-deficient ($LDLR^{-/-}$) mice with myeloid-specific β-catenin deficiency. As expected, deletion of β-catenin decreased macrophage adhesion and migration properties in vitro. However, deficiency of β-catenin significantly increased atherosclerosis in $LDLR^{-/-}$ mice without altering the plasma lipid levels. Mechanistic studies revealed that β-catenin can regulate activation of signal transducer and activator of transcription (STAT) pathway in macrophages, and ablation of β-catenin resulted in STAT3 downregulation and STAT1 activation, leading to elevated macrophage inflammatory responses and increased atherosclerosis.
Conclusions: This study demonstrates a critical role of myeloid β-catenin expression in atherosclerosis by modulating macrophage inflammatory responses.
F. Wang: None. **Z. Liu:** None. **S. Park:** None. **T. Gwag:** None. **W. Lu:** None. **M. Ma:** None. **Y. Sui:** None. **C. Zhou:** None.

635
Osteopontin Targeted Theranostic Nanomedicine for Dual-modality Imaging Guided Photodynamic Therapy for Vulnerable Atherosclerotic Plaque
Mengqi Xu, Dept of Cardiology, Chinese PLA General Hosp, Beijing, China; Weisheng GUO, CAS Key Lab for Biomedical Effects of Nanomaterials and Nanosafety, CAS Ctr for Excellence in Nanoscience, Natl Ctr for Nanoscience and Technology of China, Beijing, China; Yabin Wang, Dept of Cardiology, Chinese PLA General Hosp, Beijing, China; Xingjie Liang, CAS Key Lab for Biomedical Effects of Nanomaterials and Nanosafety, CAS Ctr for Excellence in Nanoscience, Natl Ctr for Nanoscience and Technology of China, Beijing, China; Feng Cao, Dept of Cardiology, Chinese PLA General Hosp, Beijing, China

Background: Macrophage infiltration plays a vital role in vulnerable atherosclerotic plaque (VASP) progression. Our previous work has demonstrated that osteopontin (OPN), overexpressed in foamy macrophages, could be a target for VASP detection. Photodynamic therapy (PDT) can kill foamy macrophages selectively via combining photosensitizer and illumination to generate reactive oxygen species (ROS). Herein, we constructed human serum albumin (HSA)-based nanomedicine (ICG/TPZ/HSA-Ce6-OPN) to achieve precise identification of VASP by optical/MR imaging as well as specific therapy against atherosclerosis (AS).
Methods: Nanomedicines (NMs) were prepared by targeting OPN peptide, conjugating MRI contrast agent Ce6-Mn^{2+}, encapsulating fluorescent dye (ICG) and hypoxia-activated drug tirapazamine (TPZ) (A). Characterization, toxicity, sensitivity and therapeutic effect were evaluated *in vitro*. For *in vivo* study, $ApoE^{-/-}$ mice were fed with a high-fat diet and a perivascular cuff was placed around carotid artery to establish VASP model. NMs were intravenously injected to obtain optical/MR imaging signal. The size and vulnerability of plaques were evaluated after 2 weeks administration of NMs.
Results: The transmission electron microscopy image (B), fluorescence (FL) spectra and UV absorption spectra manifested the discoid-shaped NMs were well-prepared (C, D). Good binding specificity were confirmed according to cellular uptake analysis. CCK-8 assay showed excellent bio-compatibility and therapeutic effect during PDT. *In vivo* study revealed the NMs were accumulated in VASP (F, G).
Conclusion: OPN targeted NMs indicates great potentials for precise identification and therapeutic effect on AS. However, PDT is constrained by the limited light-penetration depth in tissue, so plaques in deep-seated arteries can hardly be treated. Thus, further study is required to overcome light-penetration limitation.

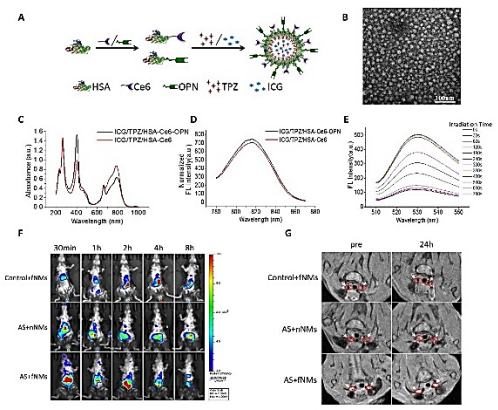

Fig. 1 (C) (D) UV and FL spectra of ICG/TPZ/HSA-Ce6-OPN (fNMs) and ICG/TPZ/HSA-Ce6 (nNMs). (E) ROS generation measured by singlet oxygen sensor green (SOSG) probe.

M. Xu: None. **W. Guo:** None. **Y. Wang:** None. **X. Liang:** None. **F. Cao:** None.

636
Angiotensinogen and Megalin Interaction Contribute to Renal Angiotensin II Production and Hypercholesterolemia-induced Atherosclerosis
Feiming Ye, Chia-Hua Wu, Deborah A Howatt, Univ of Kentucky, Lexington, KY; Adam Mullick, Mark Graham, Ionis Pharmaceuticals, Carlsbad, CA; Craig Vander Kooi, Univ of Kentucky, Lexington, KY; A.H. Jan Danser, Erasmus MC, Rotterdam, Netherlands; Jian-An Wang, Zhejiang Univ, Hangzhou, China; Alan Daugherty, Hong Lu, Univ of Kentucky, Lexington, KY

Objective: Hepatocyte-derived angiotensinogen (AGT) contributes to atherosclerosis through its cleavage to angiotensin II (AngII) by renin and angiotensin-converting enzyme (ACE). Molecular mechanisms of this process and the source of AngII to promote atherosclerosis are unknown. In this study, we used hepatocyte-specific AGT (hepAGT)-/- mice and megalin antisense oligonucleotides (ASO) to determine AGT and megalin interaction and their contributions to renal AngII production and atherosclerosis. **Methods and Results:** Immunostaining of mouse kidney sections demonstrated that AGT, renin, and ACE co-localized with megalin in proximal tubules. Hepatocyte-specific AGT deficiency diminished AGT protein and AngII production in mouse kidney and increased renal renin abundance without changes in plasma AngII concentrations. Inhibition of megalin by administering an ASO eliminated AGT and renin in proximal convoluted tubules and led to profound augmentations of their concentrations in urine, accompanied by 70% reduction of renal, but not plasma, AngII concentrations. To determine whether megalin contributes to atherosclerosis, male LDL receptor -/- mice were fed Western diet and administered two different sequences of megalin ASOs. Megalin inhibition by either ASO resulted in pronounced reductions of atherosclerosis compared to their control groups. These findings were also confirmed in female mice. LDL receptor -/- mice fed Western diet exhibited extensive vacuolization derived from enlarged lysosomes in proximal convoluted tubules. This pathological characteristic was absent in mice with either hepatocyte-specific AGT depletion or megalin inhibition. **Conclusion:** Our study demonstrated that megalin regulates AGT homeostasis, and AngII produced in kidney is a contributor to atherosclerosis through AGT and megalin interaction in proximal tubules.

F. Ye: None. **C. Wu:** None. **D.A. Howatt:** None. **A. Mullick:** Other Research Support; Modest; Ionis Pharmaceuticals employee. **M. Graham:** Other Research Support; Modest; Ionis Pharmaceuticals employee. **C. Vander Kooi:** None. **A.J. Danser:** None. **J. Wang:** None. **A. Daugherty:** None. **H. Lu:** None.

637
Genome-wide Crispr Screen in Primary Macrophages for Identification of a Regulatory Network for Macrophage Efferocytosis
Jianting Shi, Huize Pan, Ira Tabas, **Hanrui Zhang**, Columbia Univ Medical Ctr, New York, NY

Defective macrophage efferocytosis drives important diseases including atherosclerosis, whereas enhancing efferocytosis has potential therapeutic benefits. A systematic approach to identify regulators of efferocytosis in an unbiased manner holds promise for novel molecular mechanisms and targets. This study establishes an experimental framework using a novel CRISPR knockout screen to systematically map the regulatory networks of macrophage efferocytosis. We infected bone marrow-derived macrophages (BMDM) isolated from Cas9 transgenic mice with a pooled, genome-wide lentiviral library with 78,637 gRNAs, and induced efferocytosis by fluorescently-labeled apoptotic Jurkat cells. We used FACS to isolate BMDM that engulfed multiple apoptotic cells (enriched in gRNAs targeting negative regulators) or did not engulf apoptotic cells (enriched in gRNAs targeting positive regulators), and determined gRNA abundance by deep sequencing. The top-ranked 1,000 genes analyzed by two published methods MAGeCK and PBNPA showed substantial overlap (53% for positive regulators, 36% for negative regulators). We recovered many of the known regulators. e.g., *Actr2*, *Actr3* and *Arpc3*, key components of the Arp2/3 complex regulating actin polymerization, were ranked 2, 8 and 4; *Atp6v0b* and *Atp6v0c*, subunits of vacuolar ATPase responsible for acidification of intracellular organelles, were ranked 22 and 27. *Cd36*, a well-known efferocytosis receptor, was ranked 5. The top ranked positive regulators were enriched in GO terms “positive regulation of response to stimulus”, “Fcγ receptor signaling pathway” and “phagocytosis” (FDR-adjusted *P* = 2.19E-14, 1.10E-12 and 4.08E-11, respectively). Individual gRNAs verified a number of top hits from the pooled screen. In summary, we have developed a functional screen that has defined number of genes essential for macrophage efferocytosis. By focusing on a functional phenotype beyond cell viability and growth, we illustrate the versatility of CRISPR screens and provide a general strategy for systematically identifying gene of interest and uncovering novel regulators of complex macrophage functions.

J. Shi: None. **H. Pan:** None. **I. Tabas:** None. **H. Zhang:** None.

638
Delivery of Rapamycin-enriched Nanoparticles to Atherosclerotic Plaques Provides Targeted Regulation of the Macrophage Mtorc1-autophagy Signaling Axis
Xiangyu Zhang, Washington Univ, Saint Louis, MO

Atherosclerotic vascular disease remains the leading cause of death in the United States with the majority of mortality due to coronary artery disease and myocardial infarction. Confirming several prior animal studies, we find the classic mTOR inhibitor, rapamycin, has potent atheroprotective effects in ApoE-null mice. However, an unfavorable system side-effect profile and a poor mechanistic understanding has significantly limited further evaluation of this promising therapy. Our previous work has indicated that macrophage mTORC1 signaling plays a critical role in plaque progression by inhibiting autophagy. We desired to develop a nanoparticle system to enable targeted delivery of rapamycin to plaque macrophages. Utilizing a chemokine receptor type 2 (CCR2)-binding peptide conjugated to tetraazacyclododecane tetraacetic acid (DOTA) and labeled with the fluorochrome Texas Red, we first prepared a nanoparticle system targeting macrophages and suitable for tracing in vivo. We show the specificity of these nanoparticles to macrophages in cell culture and plaque macrophages in vivo. We next loaded these nanoparticles with Rapamycin and show efficient inactivation of

macrophage mTORC1 signaling and corresponding rescue of autophagy inhibition. Although the effects of this nanoparticle system in animal models of atherosclerosis is ongoing, our data support the utility of such targeted therapies in ameliorating the deleterious effects of macrophages in atherosclerosis.
X. Zhang: None.

639
Clinical, Genetic, and Epigenetic Characteristics of Prolonged Postprandial Lipemia
Rafet Al-Tobasei, Marguerite R Irvin, Hemant K Tiwari, Univ of Alabama at Birmingham, Birmingham, AL; Paul N Hopkins, Univ of Utah, Salt Lake City, UT; Jose M Ordovas, Jean Mayer USDA HNRCA at Tufts Univ, Boston, MA; Devin M Absher, Hudson Alpha Inst for Biotechnology, Huntsville, AL; Donna K Arnett, Univ of Kentucky, Lexington, KY; **Stella Aslibekyan**, Univ of Alabama at Birmingham, Birmingham, AL

Postprandial lipemia (PPL), defined as the series of metabolic events occuring after ingestion of fat, plays a key role in atherogenesis. While the plasma lipid response to meals is extremely variable, the determinants of PPL variation remain poorly understood. Using data from the Genetics of Lipid Lowering Drugs and Diet Network (GOLDN, n=1039), we investigated clinical, genetic, and DNA methylation correlates of prolonged PPL. Participants were administered a standardized high-fat milkshake and blood samples were taken at baseline, 3.5, and 6 hours post-meal. A prolonged PPL response was defined as a binary trait: 1 if plasma triglycerides at 6 hours exceeded the level at 3.5 hours, 0 otherwise. Genome-wide sequence and methylation variation was quantified using next generation sequencing and Illumina 450K methylation array in CD4+ T-cells, respectively. Approximately one third (n=312) of GOLDN participants exhibited a prolonged PPL response to the high-fat challenge. Prolonged PPL was significantly associated with increasing age ($P= 1.0x10^{-6}$), waist circumference (P= 0.02), fasting glucose (P=0.006), low-density lipoprotein cholesterol (P= 0.04), and fasting triglycerides ($P= 1.9x10^{-8}$), and inversely associated with high-density lipoprotein cholesterol (P=0.0003). Participants with prolonged PPL were significantly more likely to have prevalent coronary heart disease (P=0.0002) and diabetes mellitus ($P= 1.5x10^{-5}$). No genetic variants were significantly associated with PPL at the genome-wide level, in either single variant or gene-based tests. However, a DNA methylation variant in the *COG5* gene, encoding a component of the oligomeric Golgi complex that has been previously shown to be required for intestinal lipid absorption in a zebrafish model, emerged as the top epigenetic determinant of prolonged PPL response ($P= 2.5x10^{-7}$) in a mixed effects model adjusting for age (linear and quadratic), sex, study site, smoking, alcohol intake, T-cell purity, and familial relationships. Upon successful replication in independent cohorts and/or functional validation, the *COG5* finding can be considered a novel epigenetic target in dyslipidemia, with potential to inform future research efforts and personalized treatment approaches.
R. Al-Tobasei: None. **M.R. Irvin:** None. **H.K. Tiwari:** None. **P.N. Hopkins:** None. **J.M. Ordovas:** None. **D.M. Absher:** None. **D.K. Arnett:** None. **S. Aslibekyan:** None.

643
Atherosclerosis Susceptibility in the Collaborative Cross
Brian J Bennett, USDA-ARS Western Human Nutrition Re, Davis, CA; Alexa Rindy, UC DAvis, Davis, CA; Jody Albright, UNC Nutrition Res Inst, Kannapolis, NC; Phoebe Yam, UC Davis, Davis, CA; Melissa VerHague, UNC Nutrition Res Inst, Kannapolis, NC

Objective—The Collaborative Cross (CC) is a large recombinant inbred mouse population, generated from elaborate intercrosses of C57BL6/J, A/J, NOD/ShiLtJ, NZO/HiLtJ, WSB/EiJ, CAST/EiJ, PWK/PhJ, and 129S1/SvImJ mouse strains, useful for complex trait mapping and systems genetics. The CC population has tremendous genetic diversity, containing approximately 45 million segregating single-nucleotide polymorphisms (SNPs). The purpose of this study was to characterize atherosclerosis susceptibility in an initial cohort of Collaborative Cross strains.
Methods and Results—We obtained 5 females from 20 CC lines available at the University of North Carolina and placed them on a low-fat, synthetic diet (AIN-76) for 2 weeks. Following two weeks of diet, all mice were assessed for plasma cardio-metabolic risk factors. The mice were then randomly assigned to cages and placed on a synthetic high-fat, cholic acid (HFCA) diet that contained 20% fat, 1.25% cholesterol, and 0.5% cholic acid. Aortic root atherosclerosis and cardio-metabolic risk factors were quantitated following 16 weeks of HFCA diet feeding. Atherosclerotic lesion size ranged from completely resistant (strains C004/TauUnc and CC037/TauUnc) to moderate lesion development in a majority of several strains. Notably all mice from strain CC063/Unc died prior to 20 weeks of age, while strain CC028/GeniUnc was highly susceptible to lesion development with an average lesion size of 105,781 ± 17,370 um^2. As expected, strain is a significant contributor to atherosclerosis susceptibility (one way Anova analysis, $p<8.23x10^{-08}$). Similar effects were observed for circulating cholesterol with strains C004/TauUnc and CC037/TauUnc having relatively low circulating total cholesterol after HFCA feeding (187 and 198 mg/dl respectively) to > 500 mg/dl in strains CC006/UNC, CC011/Unc and CC036/Unc. Circulating cholesterol and atherosclerosis were significantly correlated (Spearman rho>0.30, p< 0.007).
Conclusion—These results suggest that selective crosses between various CC strains should yield loci associated with atherosclerosis. High-resolution genome-wide association analysis for atherosclerosis may be feasible when more Collaborative Cross strains become available.
B.J. Bennett: None. **A. Rindy:** None. **J. Albright:** None. **P. Yam:** None. **M. VerHague:** None.

644
Some Perspectives of Preventive Cardiology Development
Tigran Hakob Ghevondyan, L.A. Orbeli Inst of Physiology of Natl Acad of Sciences of Republic of Armenia, Yerevan, Armenia

Background. The role of preventive cardiology becomes more significant in solving heart problems. The analysis of our research results allows making assumptions, promising for prevention of coronary atherosclerosis (CA). **Material and Methods.** The studies were carried out on: hearts of humans died from accidents, from acute myocardial infarction; myocardial biopsies, heart surgical material of patients; hearts of animals; insects flying muscles; placentas of human and animals. The methods were used: autopsy, planimetry of atherosclerotic lesions of aorta and main coronary arteries, heart biopsy, microangio-x-ray, histology, stereology, experimental modeling, measuring of hemodynamic parameters, micromechanography, electron microscopy, cytochemistry, mathematical modeling, statistics. **Aim.** To show that existing data may serve as a basis for further development of new ways to prevent CA. **Results.** Huge differences of myocardial arterial bed (MAB) density exist. The richness of MAB correlates directly with life expectancy of people. In hearts with scant MAB CA develops earlier and atherosclerotic lesions are more severe. Therefore scant MAB is considered as an intracardial risk factor (IRF) for IHD. Large individual differences exist in human hearts also for values for the duration of myocardial fibers oxygen supply. The long time is another IRF for IHD. The density of intraorganic arterial bed in human placentas varies widely. There is a positive correlation between placental arterialization density and newborn weigh. The following morphological multifactorial systemic measurement methods are developed: a) for heart muscle oxygen supply; b) for contractility of cardiomyocyte

using small heart muscle biopsies (patented); c) for gas exchangeability of placenta. The efficiency and exactness of each method were examined. **Conclusion.** The received data allow assuming that atherosclerotic profile of human heart CA will be possible to foretell on the next day of born. In cases of bad prognosis a plan of enrichment of MAB, a plan for spatial improvement of the “capillary - myocardial fiber” system may be composed and undertaken. The received data allow in advanced future to draw up a project of new heart with necessary preset structural parameters.
T.H. Ghevondyan: None.

646
A Simple Multi-Risk-Factor Decision-Making Strategy for Improved Coronary Plaque Burden Increase Prediction: a Patient-Specific 3D FSI Study Using IVUS Follow-up
Dalin Tang, Worcester Polythechnic Inst, Worcester, MA; Liang Wang, Sch of Biological Science and Medical Engineering, Southeast Univ, Nanjing, China; Akiko Maehara, Columbia Univ, The Cardiovascular Res Fndn, New York, NY; David Molony, Habib Samady, Dept of Med, Emory Univ Sch of Med, Atlanta, GA; Zheyang Wu, Worcester Polythechnic Inst, Worcester, MA; Jie Zheng, Mallinckrodt Inst of Radiology, Washington Univ, St. Louis, MO; Gary S. Mintz, Columbia Univ, The Cardiovascular Res Fndn, New York, NY; Don P. Giddons, The Wallace H. Coulter Dept of Biomedical Engineering,, Atlanta, GA

Plaque progression and vulnerability are influenced by many risk factors. Our goal is to find simple methods to combine multiple risk factors for better plaque development predictions. A sample size of 374 intravascular ultrasound (IVUS) slices with matched follow-up was obtained from 9 patients (Mean age 59, 7 m) with informed consent obtained. 3D fluid-structure interaction models were constructed to obtain plaque stress/strain conditions. Four morphological and biomechanical factors (plaque burden (PB), cap thickness (CT), lipid percent (LP) and average plaque wall stress (PWS)) were chosen to predict plaque burden increase defined as PBI = (PB at follow-up) - (PB at baseline). For a given slice Si, the ground truth Y_{PBI} is define as $Y_{PBI}(Si)=1$ if $PBI(Si)>0$; $Y_{PBI}=0$ if $PBI(Si)\leq 0$. For a single predictor W, a threshold value Wc was used to assign the binary prediction outcome: $Y_W(Si)=1$ if $W>Wc$; $Y_W(Si)=0$ if $W\leq Wc$. Wc was chosen to get optimal agreement between Y_W and Y_{PBI}. To use multiple predictors (say, W1, W2, W3) to PBI, a new predictor Combo (W1, W2, W3) was created with its values defined as Combo (W1, W2, W3)=$Y_{W1}+Y_{W2}+Y_{W3}$, where Y_{W1}, Y_{W2} and Y_{W3} were evaluated the same way as before. Combo was then treated as a single predictor and a threshold value was determined to achieve best agreement with Y_{PBI}.
Table 1 summarizes the optimal thresholds and agreement rates for all 15 strategies. Agreement rate using PB alone was 57.5%. PWS was the best single predictor for PBI with agreement rate 62.6%. Combining CT and PWS achieved 66.5% agreement rate, 9% better over PB, which was also obtained by combining 4 risk factors.
The method presented here could be used to combine predictors from different sources (stenosis, cap, lipid, inflammation, macrophage, hemorrhage, stress, strain, flow shear stress, FFR, smoking, diabetes, cholesterol, alcohol, hypertension, pro-rupture genes, etc.) to improve prediction accuracy and help decision-making in clinical practice.

Table 1: The optimal thresholds and agreement rates for PBI prediction using all combinations of PB, CT, LP and PWS. Threshold=optimal threshold; Agreement=Agreement Rate.

Factor	PB	CT	LP	PWS	PB+ CT	PB+ LP	PB+ PWS	CT+LP
Threshold	45%	0.33mm	5%	106.43kPa	1	1	1	1
Agreement	57.5%	61.0%	56.7%	62.6%	64.2%	58.7%	65.4%	63.78%
Factor	CT+PWS	LP+PWS	PB+CT + LP	PB+CT+ PWS	PB+LP + PWS	LP+CT + PWS	PB+CT+ LP+PWS	
Threshold	1	1	1	1	1	1	1	
Agreement	66.5%	64.6%	64.6%	66.5%	65.4%	66.5%	66.5%	

D. Tang: Research Grant; Modest; NIH R01 EB004759, Jiangsu STA BE2016785. **L. Wang:** Research Grant; Modest; NIH R01 EB004759. **A. Maehara:** None. **D. Molony:** None. **H. Samady:** None. **Z. Wu:** None. **J. Zheng:** Research Grant; Modest; NIH R01 EB004759. **G.S. Mintz:** None. **D.P. Giddons:** None.

648
Resident S100β$^+$/Sca1$^+$ Multipotent Vascular Stem Cells Undergo Myogenic and Vasculogenic Differentiation *In Vitro*
Denise Burtenshaw, Emma Fitzpatrick, Dublin City Univ, Dublin, Ireland; Weimin Liu, David Morrow, Eileen M Redmond, Univ of Rochester, Rochester, NY; Paul A Cahill, Dublin City Univ, Dublin, Ireland

Arteriosclerosis is an important age-dependent disease that encompasses atherosclerosis, in-stent restenosis, autologous bypass grafting and transplant arteriosclerosis. Vascular smooth muscle (vSMC)-like accumulation is a key event leading to intimal-medial thickening (IMT), vessel remodelling and an important marker of subclinical disease. Vascular stem cell progeny in addition to de-differentiated SMC and SMC derived from endothelial-mesenchymal transition (EndoMT) are all reported to contribute to IMT as they become activated/dysfunctional, differentiate down vascular and myeloid lineages and subsequently dictate, in-part, vessel remodelling. In this study we examined the multipotent potential of a specialised population of rat adult resident multipotent vascular stem cells (rMVSC) located within the vessel wall and their capability to differentiate down both myogenic (muscle) and vasculogenic (endothelial) lineages when given the appropriate stimulus. Using Sca1-eGFP transgenic mice, *in vivo,* there was a significant increase in the number of Sca1$^+$ cells within the intima of the left carotid artery (LCA) following partial carotid artery ligation-induced injury after 3 days that co-localised with endothelial nitic oxide synthase (eNOS) and CD31$^+$ positive cells, when compared to the sham-operated control vessels and the contralateral right carotid artery (RCA). The number of Sca1-eGFP$^+$ cells significantly increased over time within the adventitial, medial and neointimal layers following ligation-induced injury after 7 and 14 days, respectively. In vitro, S100β/Sca1$^+$ rat MVSCs cultured in vasculogenic inductive media for 7 days underwent differentiation to an endothelial cell phenotype characterised by the appearance of a cobblestone morphology and increased eNOS expression. In contrast, MVSC exposed to media supplemented with TGF-β1 for 7 days underwent myogenic differentiation to SMC. These data suggest that resident S100β/Sca1$^+$ MVSCs are capable of both myogenic and vasculogenic differentiation depending on the inductive stimulus and may contribute in part to intimal medial thickening (IMT) and endothelial regeneration following injury *in vivo.*
D. Burtenshaw: None. **E. Fitzpatrick:** None. **W. Liu:** None. **D. Morrow:** None. **E.M. Redmond:** None. **P.A. Cahill:** None.

649
Skeletal Muscle Satellite Cells Play a Role in Regulating Angiogenesis and Arteriogenesis
Laura M Hansen, Wenxue Liu, Giji Joseph, W. Robert Taylor, Emory Univ, Atlanta, GA

Satellite cells are myogenic stem cells that play a critical role in skeletal muscle repair by proliferating and differentiating into myoblasts to repair muscle fibers. However, their role in reestablishing vascular supply following injury is not well defined. We hypothesized that satellite cells promote vascular growth through paracrine signaling induced following muscle injury or ischemic damage from diseases such as peripheral artery disease. We used a murine model of hind limb ischemia and found that satellite cells increased 3.4 fold ($p<0.01$) in response to this ischemic insult. We used a co-culture system to determine that satellite cells led to a 3.5 fold and 2.8 fold increase in smooth muscle and endothelial cell migration ($p<0.0001$). These results demonstrate the satellite cells produce paracrine factors which drive cell migration required for both angiogenesis and arteriogenesis. To test the potential therapeutic capability,

alginate encapsulated satellite cells were delivered in the hind limb ischemic model. We found the encapsulated cells were viable for up to 2 weeks and mice that received satellite cells had significantly increased perfusion (28%, $p<0.05$) at 2 weeks as measured by Laser Doppler imaging and a 1.9 fold ($p<0.5$) increase in capillaries and small vessels measured by histological staining. To examine the role of satellite cells in a physiological setting and determine if they are critical to robust recovery in our model, we used a Cre-Lox system in which recombination results in the production of diphtheria toxin a (DTA) to deplete Pax7 specific cells. Mice which lacked satellite cells had decreased perfusion by Laser Doppler imaging ($p<0.05$) and capillary density compared animals with intact satellite cells. A cytokine array and genomics analysis show that several factors related to angiogenesis and cell migration are upregulated in satellite cells in response to ischemia. In conclusion, we have found that satellite cells proliferate in response to ischemia, produce factors that drive cell migration, and their delivery or depletion affect vascular growth in vitro. We believe that our studies show that satellite cells play an important role vascular growth and are a novel potential therapy for peripheral artery disease.

L.M. Hansen: Research Grant; Modest; F32HL124974. **W. Liu:** None. **G. Joseph:** None. **W. Taylor:** None.

650

Stem Cell-derived SMCs Are Useful for Vascular Tissue Engineering

Wendou Gu, Xuechong Hong, Alexandra Le Bras, Qingbo Xu, **Yanhua Hu**, Kings Coll London, London, United Kingdom

Objectives: Tissue engineered vascular grafts with long-term patency are in great need in the clinics, for which smooth muscle cells (SMCs) are essential. Recently several laboratories have established methods to obtain SMCs from embryonic stem cells or iPS cells. However, the mechanisms of stem cell differentiation are not fully understood. And also it is hard to obtain a large number of SMCs with higher purity. To solve these issues, we take the advantage of mesenchymal stem cells (MSCs) from human umbilical cord that were cultivated and differentiated in vitro. **Methods:** MSCs from human umbilical cord were cultivated and differentiated to vascular lineages. Signal pathways involved in stem cell differentiation were studied using Western blot, siRNA, PCR, immunoprecipation and transfection. For vascular tissue engineering, stem cell-derived SMCs were applied to decelularized scaffold to create the vessels in a Bioreactor. **Results:** In response to TGFβ1 stimulation, MSCs were abundantly expressing SMC markers including αSMA, SM22, calponin and SMMHC at the gene and protein levels. Functionally, differentiated SMCs displayed a contraction ability in vitro and formed vessels in matrigel plug assay SCID mice. Micro-RNA (miR) array analysis showed the upregulation of miR-503 and the downregulation of miR-222-5p at early time points after TGFβ1 treatment, which was confirmed by TaqMan microRNA assay. Mechanistically, miR-503 was demonstrated to promote SMC differentiation through directly targeting Smad7, a negative regulator of TGFβ1 Smad-related signaling pathways. The expression of miR-503 was Smad4-dependent and Smad4 was enriched at the promoter region of miR-503. In addition, miR-222-5p inhibited SMC differentiation through targeting ROCK2 and αSMA 3'-UTR. Finally, SMCs differentiated from stem cells exhibited the ability to migrate into decellularized mouse aorta and gave rise to vascular graft with smooth muscle layer. **Conclusions:** We established a method to produce a large number of human SMCs from MSCs, which demonstrated the potential of utilizing the cells to generate vascular grafts. And we provide the mechanistic data demonstrating the impact of miRNA-503/222-5p on TGFβ1-mediated signaling in SMC differentiation from stem cells.

W. Gu: None. **X. Hong:** None. **A. Le Bras:** None. **Q. Xu:** None. **Y. Hu:** None.

651

Hedgehog Responsive S100β$^+$/Stem Cell Antigen-1$^+$ Vascular Stem Cells Contribute to Neointimal Formation

Eileen M Redmond, Univ of Rochester, Rochester, NY; Emma Fitzpatrick, Dublin City Univ, Dublin, Ireland; Weimin Liu, Jay-Christian Helt, Univ of Rochester, Rochester, NY; Maryam Alshamrani, Roya Hakimjavadi, Susan Harman, Abidemi Olayinka, Denise Burtenshaw, Eoin Corcoran, Dublin City Univ, Dublin, Ireland; Catriona Lally, Trinity Coll Dublin, Dublin, Ireland; Paul A Cahill, Dublin City Univ, Dublin, Ireland

Intimal medial thickening (IMT) and vascular remodeling are hallmarks of arteriosclerotic disease. However, the origin of neointimal cells and the signaling molecules that dictate their fate and function remains controversial. Herein, we examined whether Hedgehog (Hh) responsive S100β$^+$/Sca1$^+$ stem cells contribute to IMT within carotid arteries of transgenic mice following ligation-induced injury *in vivo* and myogenic differentiation of undifferentiated multipotent S100β$^+$/Sca1$^+$ stem cells *in vitro*. Using Sca1-eGFP and S100β-eGFP transgenic mice, we demonstrated a significant accumulation in the number of eGFP$^+$ cells within the intima and medial layers of injured arteries following ligation concomitant with enhanced expression of Hh signaling components (ptch1 and Gli). Genetic lineage tracing analysis using S100β-eGFP/Cre/ERT2–dTomato transgenic mice to mark S100β$^+$ resident vascular stem cells before injury confirmed that S100β$^+$ progeny that are Sca1$^+$ significantly contribute to IMT, an effect significantly attenuated following treatment with the Hh smoothened inhibitor, cylopamine. In vitro, recombinant SHh (rSHh) treatment of multipotent S100β$^+$/Sca1$^+$ resident stem cells increased Hh target gene Gli expression, decreased telomerase activity and promoted myogenic differentiation and cell growth; effects significantly attenuated following Hh inhibition. In human arteriosclerotic lesions, Hh components were upregulated concomitant with enhanced expression of S100β. Together, these findings suggest that S100β$^+$/Sca1$^+$ stem cells are a major source of neointimal cells contributing to IMT and suggest that this cohort may be a relevant therapeutic target to prevent arteriosclerosis.

E.M. Redmond: None. **E. Fitzpatrick:** None. **W. Liu:** None. **J. Helt:** None. **M. Alshamrani:** None. **R. Hakimjavadi:** None. **S. Harman:** None. **A. Olayinka:** None. **D. Burtenshaw:** None. **E. Corcoran:** None. **C. Lally:** None. **P.A. Cahill:** None.

652

MicroRNA-29b Mediates the Chronic Inflammatory Response in Radiotherapy-induced Vascular Disease

Greg Winski, Suzanne M Eken, Tinna Christersdottir, Karolinska Instt, Stockholm, Sweden; Traimate Sangsuwan, Stockholm Univ, Stockholm, Sweden; Hong Jin, Ekaterina Chernogubova, John Pirault, Changyan Sun, Nancy Simon, Hanna Winter, Per Tornvall, Karolinska Instt, Stockholm, Sweden; Siamak Haghdoost, Stockholm Univ, Stockholm, Sweden; Göran K Hansson, Martin Halle, Lars Maegdefessel, Karolinska Instt, Stockholm, Sweden

Radiotherapy is an established therapeutic method in many different cancer types. Its success raises a new problem, namely radiotherapy-induced vascular disease (vRTx), which typically manifests as coronary disease, heart failure or carotid stenosis. A chronic inflammatory response likely underlies vRTx, involving complex processes, such as vascular smooth muscle cell de-differentiation, oxidative stress, and ECM remodeling. These processes are tightly regulated and thus far difficult to influence therapeutically. In other diseases, a set of microRNAs (miRs) is known to orchestrate these processes. We hypothesized that they similarly could play a role in vRTx and be targets for treatment or prevention of the disease.
We performed qRT-PCR screening of 11 pre-selected miRs, which identified miR-29b as significantly decreased in

irradiated arteries collected from patients undergoing free tissue transfer reconstruction, compared with non-irradiated arteries from the same patient (n=15). In a vascular biology context, miR-29b is known as inhibitor of collagen- and ECM associated mRNA targets, and has been shown to play a detrimental role in aneurysm disease and advanced atherosclerotic lesions.
Consistent with human tissue data, vascular smooth muscle and endothelial cells *in vitro* receiving two radiation doses of 2 Gy, showed decreased miR-29b upon 24 hours after exposure. In these irradiated SMCs, miR-29b induction reduced soluble collagen levels, while inhibition further increased them.
Array-based tissue gene expression analysis showed that Pentraxin-3 (PTX) and dipeptidyl-peptidase 4 (DPP4), both targets of miR-29b and pivotal in inflammation and adverse wound healing, were downregulated in the same patient cohort. Carotid arteries of *Apoe*$^{-/-}$ mice treated with miR-29b mimic, 24h before and 24h after irradiation (14 Gy to the upper chest and neck), displayed a downward trend (non-significant) in *Ptx3* and *Dpp4* gene expression.
Our results suggest that miR-29b overexpression therapy could have a place in the prevention of vRTx. To further strengthen this conclusion, additional *Apoe*$^{-/-}$ mice irradiation experiments are currently ongoing, to further establish PTX3 and DPP4 as mediators of anti-inflammatory and anti-fibrotic strategies.
G. Winski: None. **S.M. Eken:** None. **T. Christersdottir:** None. **T. Sangsuwan:** None. **H. Jin:** None. **E. Chernogubova:** None. **J. Pirault:** None. **C. Sun:** None. **N. Simon:** None. **H. Winter:** None. **P. Tornvall:** None. **S. Haghdoost:** None. **G.K. Hansson:** None. **M. Halle:** None. **L. Maegdefessel:** None.

653
Placental Growth Factor mediates Splenic Sympathetic Overdrive induced by Obesity and induces hypertension
Daniela Carnevale, Sapienza Univ/IRCCS Neuromed, Pozzilli, Italy; Andrea Lori, IRCCS Neuromed, Pozzilli, Italy; Marialuisa Perrotta, SAPIENZA UNIVERSITY, Pozzilli, Italy; Lorenzo Carnevale, Fabio Pallante, Daniele Iodice, Raimondo Carnevale, IRCCS Neuromed, Pozzilli, Italy; Giuseppe Cifelli, IRCCS NEUROMED, Pozzilli, Italy; Giuseppe Lembo, Sapienza Univ/IRCCS Neuromed, Pozzilli, Italy

Obesity is an epidemic condition associated with several cardiovascular comorbidities, as hypertension. Although the molecular mechanisms related to obesity-induced hypertension are not well understood, the sympathetic nervous system (SNS) overactivation typically accompanying obesity has been ascribed as one of the main culprits. Thus far, mechanistic studies focused on the effects of sympathetic overdrive on peripheral resistances. Recent data showing that SNS activation also dictates immune responses involved in hypertension, made us hypothesize whether obesity induced by high fat diet (HFD) could recruit splenic SNS efferent. Thus we subjected WT mice to HFD, as compared to low fat diet (LFD), and monitored the hypertensive response. Blood pressure (BP) started to rise after two months, and hypertensive disease became clearly manifest within 4 months. To gain mechanistic insights responsible for BP increase, we assessed peripheral SNS activation at a time point preceding overt hypertension (i.e. 2 months after HFD). We found elevated circulating noradrenalin levels in HFD mice and, more important, a specific pattern of activated splenic sympathetic overdrive, as recorded by microneurography. WT mice subjected by surgical removal of the left celiac ganglion (CGX) where the splenic nerve originate, before receiving HFD, were protected from hypertension, despite developing obesity the same. The fact that splenectomized mice showed an overlapping response to HFD, supported the conclusion that the sympathetic-immune axis is crucial for HFD-induced hypertension but not for weight regulation. To look for molecular determinants, we analyzed the expression of Placental Growth Factor (PlGF), previously identified as a neuroimmune mediator of other hypertensive challenges. PlGF was significantly overexpressed in the spleen upon HFD, but only when SNS innervation was intact, as CGX mice failed to induce its expression. In the end, PlGF KO mice subjected to HFD, although becoming obese as much as WT did, were protected from hypertension. Overall our results demonstrate that a splenic neuroimmune drive is crucial to allow the onset of hypertensive disease associated with obesity, although having no effect in body weight increase in response to HFD.
D. Carnevale: None. **A. Lori:** None. **M. Perrotta:** None. **L. Carnevale:** None. **F. Pallante:** None. **D. Iodice:** None. **R. Carnevale:** None. **G. Cifelli:** None. **G. Lembo:** None.

654
Isoleukotoxin Promotes Autophagy and Reduces Vascular Cell Adhesion Molecule-1 Expression in Endothelial Cells
Ling-yun Chu, Hsiao-Ling Cheng, Kenneth K. Wu, China Medical Univ, Taichung City, Taiwan

Rapamycin is a widely used autophagy inducer and has been shown to suppress development of atherosclerosis in animal models. However, the side effect is severe including hyperlipidemia. We identified isoleukotoxin, a metabolite of linoleic acid, as an autophagy inducer and hypothesized that it can be used to reduce inflammation of endothelial cells. To test this hypothesis we treated human umbilical vein endothelial cells (HUVECs) with tumor necrosis factor α (TNFα) along with isoleukotoxin. Rapamycin was used as a positive control to induce autophagy. Isoleukotoxin promotes autophagic flux in HUVECs as well as rapamycin. Isoleukotoxin does not inhibit activity of mammalian target of rapamycin complex, while it inhibits activity of the downstream kinase, S6K. Isoleukotoxin modulates TNFα-induced cell adhesion molecules expression in HUVECs with a similar pattern as rapamycin. In this pattern, only vascular cell adhesion molecule-1 (VCAM-1) expression is reduced but not intercellular cell adhesion molecule-1 (ICAM-1). More interestingly, time-course analysis shows that VCAM-1 expression is only reduced after 20 hours treatment, which is different from that of inhibitors of VCAM-1 transcription such as SB202190. By qPCR we confirmed that isoleukotoxin does not inhibit VCAM-1 transcription. To determine whether isoleukotoxin reduces VCAM-1 expression by inhibiting S6K-mediated protein translation, we compared the effect of isoleukotoxin with S6K siRNA. S6K siRNA reduces expression of VCAM-1 slightly and also ICAM-1, which is different from that of isoleukotoxin. After excluding the regulation of transcription and translation, we hypothesize that isoleukotoxin reduces VCAM-1 expression by promoting VCAM-1 degradation via autophagy. This hypothesis is supported by blocking of autophagy and endocytosis. Blocking of autophagy by Atg5 siRNA enhances VCAM-1 expression, suggesting that VCAM-1 may be degraded by autophagy. Blocking of endocytosis by dynasore blocks the effect of isoleukotoxin on VCAM-1 expression, suggesting that VCAM-1 is degraded after endocytosis. Here we propose that isoleukotoxin is an anti-inflammation and a potential therapeutic molecule for inflammatory vascular diseases such as atherosclerosis.
L. Chu: None. **H. Cheng:** None. **K.K. Wu:** None.

655
Notch Inhibition Reverses the Polarization of Pro-Inflammatory (M1) to Anti-Inflammatory-like (M2) Macrophages
Rishabh Dev, Advitiya Mahajan, Neekun Sharma, Chetan P Hans, Univ of Missouri, Columbia, MO

Introduction: Our previous studies demonstrated that loss of Notch1 signaling reduces the incidence of abdominal aortic aneurysm (AAA) by preventing the influx of pro-inflammatory M1 macrophages and that Notch1 deficiency promotes M2-polarization. In the present study, we determined if inhibition of Notch signaling could reverse the

pre-existing pro-inflammatory M1 macrophages to anti-inflammatory M2 phenotype. **Methods and Results:** Raw cells (264.7 murine macrophage cell line) were treated with various concentrations of LPS (5, 10, 100 ng/ml) and IFN-γ (10 ng/ml) for 3h to polarize naïve macrophages into M1-phenotype. After washing, these cells were treated with either vehicle or DAPT (10 ng/ml or 25 ng/ml); a potent Notch inhibitor for 6, 12, 24 or 48h and later used for gene expression studies or functional assays. LPS pretreatment significantly increased the gene expression of M1-genes; *Il6*, *Il12, Cd38, Fpr2* and *iNOS*, whereas the expression of M2 genes; *Egr2* and *c-Myc* was significantly decreased. Replacement of LPS with vehicle alone lowered the expression of *Il6* and *Il12* within 6-12h, but remained significantly higher than basal levels. Expression of *iNOS*, *Cd38* and *Fpr2* remained unchanged in response to vehicle in the LPS-pretreated macrophages. DAPT treatment further reduced the gene expression of *Il6* and *Il12* significantly and *iNOS* moderately as compared to vehicle-treated macrophages. Interestingly, Notch inhibition increased the expression of *Egr2* and *c-Myc* genes at 24 and 48h. Similar trends with regard to M1 and M2 genes were observed in bone marrow derived macrophages from *Apoe*$^{-/-}$ and *WT* mice treated with LPS followed by vehicle or DAPT. Phagocytosis assay showed increased uptake of zymosan bioparticles in the macrophages treated with LPS. Replacement of LPS with vehicle for 24h did not affect the phagocytosis significantly. DAPT treatment decreased phagocytic activity of these macrophages as compared to vehicle-treated macrophages. **Conclusions:** Our data suggest that Notch inhibition reverses the M1-polarized macrophages towards M2-like macrophages. These novel insights in the functions of Notch signaling may have potential implications in chronic inflammatory diseases including AAA and atherosclerosis.

R. Dev: None. **A. Mahajan:** None. **N. Sharma:** None. **C.P. Hans:** None.

660

Elevated Calcium Drives Inflammatory-Driven Angiogenesis

Jocelyne Mulangala, Emma J Akers, Emma L Solly, Peter J Psaltis, Joanne T Tan, Stephen J Nicholls, Christina Bursill, **Belinda A Di Bartolo**, SAHMRI, Adelaide, Australia

Background: Peripheral arterial disease (PAD) is characterised by accelerated arterial calcification and impairment in angiogenesis, both of which can influence cardiovascular clinical outcomes. Studies implicate calcification as a driver of PAD, however, the mechanisms by which calcification modulates angiogenesis remain poorly understood. This study assessed the effect of high calcium on angiogenesis both *in vitro* and *in vivo*. **Methods**: Human Coronary Artery Endothelial Cells (EC) were cultured and treated with calcification medium (CM) ($CaCl_2$ 2.7mM, Na_2PO_4 2.0mM) for 24 h. Angiogenic assays of proliferation, migration and tubulogenesis were conducted, and immunoblotting assessed angiogenic regulatory proteins. *In vivo* studies employed a calcification model with 8-12-week-old male OPG$^{-/-}$ and wildtype (C57BL6/J, control) mice which underwent hind-limb ischaemia (HLI) surgery. Blood flow reperfusion was assessed by Laser Doppler Perfusion Imaging (LDPI). Calcium assay assessed calcium levels in blood serum of the C57BL6/J and OPG$^{-/-}$ mice. **Results**: CM significantly reduced EC tubulogenesis and viability (34% and 58% $p<0.05$) but increased migration ($p<0.0001$) over 24h. There was a significant increase in the protein levels of angiogenic regulators VEGFA ($p<0.0001$) and HIF-1α ($p<0.0001$). CM also significantly increased NF-κB (P65) nuclear protein, a key mediator of inflammatory-driven angiogenesis. qRT-PCR showed upregulation of osteoinductive factor Bone Morphogenetic protein (BMP2), and transcription factor Runx2 mRNA expression, both involved in osteogenesis and calcification. Blood serum calcium levels were significantly increased in OPG deficient mice. LDPI found there was significantly reduced blood-flow reperfusion in OPG$^{-/-}$ mice at days 6 (0.03±0.01 vs 0.32±0.05 $p<0.01$) and day 10 (0.08±0.01 vs 0.35±0.05 $p<0.01$) post HLI induction, compared to controls. **Conclusion**: This is the first demonstration that high-levels of calcium impair ischaemia-driven angiogenesis *in vivo* and cause inflammation in ECs that suppresses tubule formation *in vitro*, despite upregulation of key angiogenic regulators VEGFA and HIF-1α. These findings have implications for the development of therapies that can suppress calcification in PAD.

J. Mulangala: None. **E.J. Akers:** None. **E.L. Solly:** None. **P.J. Psaltis:** None. **J.T.M. Tan:** None. **S.J. Nicholls:** None. **C. Bursill:** None. **B.A. Di Bartolo:** None.

661

Regulation of *CCL2* Expression in Vascular Endothelial Cells by a Long Noncoding RNA

Nadiya Khyzha, Melvin Khor, Univ of Toronto, Toronto, ON, Canada; Ulf Hedin, Dept of Molecular Med and Surgery, Karolinska Inst, Stockholm, Sweden; Lars Maegdefessel, Dept of Med, Karolinska Inst, Stockholm, Sweden; Michael D Wilson, Genetics and Genomy Biology, The Hosp for Sick Children, Toronto, ON, Canada; Jason E Fish, Univ of Toronto, Toronto, ON, Canada

Vascular inflammation is a critical driver of chronic diseases such as atherosclerosis. A network of NF-κB-dependent leukocyte adhesion molecules and chemokines are induced in endothelial cells (ECs) in response to inflammatory mediators. This includes chemokine (C-C motif) ligand 2 (*CCL2*), which contributes to atherosclerosis by recruiting monocytes to the endothelium. Recently, long noncoding RNAs (lncRNAs) have been implicated in regulating gene expression through epigenetic mechanisms, but lncRNAs remain poorly studied in the context of vascular inflammation and NF-kB pathway regulation. LncRNAs are frequently retained in the nucleus where they interact with chromatin remodelling complexes to modulate the expression of neighboring protein-coding genes. Hence, identifying NF-kB-regulated neighboring mRNA-lncRNA pairs in vascular endothelial cells may uncover functional lncRNAs that play a role in fine-tuning the expression of their neighboring inflammatory genes.

The Arraystar human lncRNA microarray V3 was employed to identify differentially expressed lncRNAs and mRNAs in ECs stimulated with the pro-inflammatory cytokine, IL-1β. Neighboring IL-1β-regulated mRNA-lncRNA pairs demonstrated a larger magnitude of mRNA induction than mRNAs lacking a neighboring lncRNA. This phenomenon was associated with shared regulatory elements and localization within the same topologically associated domain. Follow-up analysis was performed on the nuclear-enriched, *lncRNA-CCL2*, which is transcribed through a super-enhancer near *CCL2*. Both *lncRNA-CCL2* and *CCL2* responded to the same inflammatory stimuli. Similar to *CCL2*, *lncRNA-CCL2* transcript was elevated in unstable human atherosclerotic plaques. Knockdown of *lncRNA-CCL2* decreased *CCL2* mRNA levels in multiple EC cell lines, but had no effect on other inflammatory genes or distal *CCL* genes. Hence, our approach has uncovered neighboring IL-1β-regulated mRNA-lncRNA pairs and identified a novel functional lncRNA, *lncRNA-CCL2*.

N. Khyzha: None. **M. Khor:** None. **U. Hedin:** None. **L. Maegdefessel:** None. **M.D. Wilson:** None. **J.E. Fish:** None.

662

Long Intergenic Non-coding RNA Rp11-10j5.1 is a Novel Regulator of Macrophage Activation

Daniel Y Li, Columbia Univ Medical Ctr, New York, NY; Ying Wang, Stanford Univ, Stanford, CA; Hanrui Zhang, Chenyi Xue, Xuan Zhang, Wen Liu, Muredach P Reilly, Columbia Univ Medical Ctr, New York, NY

Background - Genetic discoveries for complex traits suggest roles for recently evolved regulatory elements, such as long intergenic non-coding RNAs (lincRNAs). The goal of the current study was to identify and functionally assess the

contribution of a novel non-conserved, macrophage-enriched lincRNA, RP11-10J5.1, in macrophage inflammatory activation. **Methods and results** - We recently showed from RNA-seq that dozens of lincRNAs were upregulated during primary human macrophage inflammatory activation (LPS/IFN-γ) associated with cardiometabolic diseases including atherosclerosis. Among these differentially expressed (DE) lincRNAs, RP11-10J5.1 is one of the most substantially up-regulated, specifically expressed in human and enriched in macrophages. qRT-PCR confirmed upregulation of RP11-10J5.1 in THP1-derived macrophages (THP-1Φ) and human induced pluripotent stem cell-derived macrophages (IPSDM). Cellular fractionation revealed that RP11-10J5.1 localized almost exclusively in the nuclear fraction. We performed RACE (rapid amplification of cDNA ends) to accurately map the transcription start site and full-length sequence of the three isoforms of RP11-10J5.1. Knock-down (KD) of RP11-10J5.1 isoforms using site-specific antisense oligonucleotides (LNA-ASO) targeting the common exon in LPS/IFN-γ-stimulated HMDM (n=3 subjects) followed by RNA-seq has identified 43 DE genes (21 up, 22 down, fold change > 1.5, FDR < 0.05) that are potential targets of RP11-10J5.1. Validation in four additional subjects confirmed that KD of RP11-10J5.1 attenuated inflammatory-induction of *NTN1* and *IRF4*, key regulators of macrophage apoptosis and inflammatory activation. Conversely, overexpression of RP11-10J5.1 in HMDM enhanced inflammatory upregulation of *NTN1* and *IRF4*, supporting the potential role of RP11-10J5.1 in inducing *NTN1* and *IRF4* expression. Mechanistically, *in vitro* RNA pull-down followed by mass spectrometry analysis has identified interaction of RP11-10J5.1 with a number of candidate proteins that regulate transcription and mRNA splicing. **Conclusion** - These data suggest that lincRNA RP11-10J5.1 is a novel modulator of inflammatory macrophage activation.

D.Y. Li: None. **Y. Wang:** None. **H. Zhang:** None. **C. Xue:** None. **X. Zhang:** None. **W. Liu:** None. **M.P. Reilly:** None.

663

Nuclear RSK1 Induces Pro-Inflammatory Activation of Macrophages through STAT1 Phosphorylation at Ser727

Keishi Nihira, Arda Halu, Lee Lang Ho, Alexander C Mojcher, Hideyuki Higashi, Iwao Yamada, Jiao Qiao, Jianguo Wang, Julius L Decano, Elena Aikawa, Sasha A Singh, Masanori Aikawa, Ctr for Interdisciplinary Cardiovascular Sciences; Brigham and Women's Hosp and Harvard Medical Sch, Boston, MA

OBJECTIVE: Maladaptive inflammatory responses involve macrophage activation by pro-inflammatory cytokines such as IFN-γ. Proteins that undergo nuclear translocation may regulate these processes.

APPROACH and RESULTS: To explore novel key regulators of macrophage activation, we performed quantitative proteomics to monitor protein translocation to the nuclei of human primary macrophages elicited with IFN-γ for 0, 10, 20, 30, or 60 min. Bioinformatics identified RSK1, a ribosomal protein kinase, as one of the candidates. We found that IFN-γ stimulation promotes RSK1 phosphorylation at Ser380. STAT1 is a key mediator of IFN-γ-triggered cellular responses. Mass spectrometry identified RSK1-mediated phosphorylation sites within STAT1, including Ser727. siRNA silencing of RSK1 attenuated STAT1 phosphorylation in IFN-γ-stimulated macrophages. In concert with these results, RSK1 silencing hindered IFN-γ-induced secretion of pro-inflammatory chemokines in human primary macrophages, such as CCL2/MCP-1, CCL7/MCP-3, and CCL8/MCP-2.

CONCLUSION: We discovered that RSK1 nuclear translocation triggers STAT1 phosphorylation, resulting in pro-inflammatory activation of macrophages (Figure), a novel role for a ribosomal protein-associated kinase in nuclear signaling and inflammation.

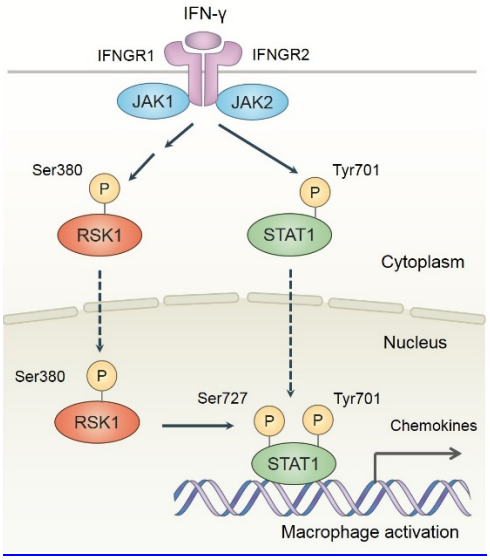

K. Nihira: None. **A. Halu:** None. **L. Lang Ho:** None. **A.C. Mojcher:** None. **H. Higashi:** None. **I. Yamada:** None. **J. Qiao:** None. **J. Wang:** None. **J.L. Decano:** None. **E. Aikawa:** None. **S.A. Singh:** None. **M. Aikawa:** Research Grant; Significant; Kowa Company, Ltd.

664

Regulation of Angiogenesis and Associated Inflammation by Antioxidant Glutathione in Smooth Muscle Cells

Bandana Shrestha, Louisiana Health Science Ctr - Shreverport, Shreveport, LA

Peripheral artery blockage due to formation of atherosclerotic plaques in PVD (Peripheral Vascular Diseases) causes loss of blood flow to peripheral limbs leading to pathogenic consequences, necrosis and in severe cases amputation of the limb. Angiogenesis, the development of new collateral blood vessels is necessary to compensate for this loss of blood flow and prevent pathogenesis resulting from blockage. However, PVD patients, to their detriment, often see decreased angiogenesis and lack of adequate compensatory neo-vascularization along with decreased circulating antioxidant levels. Angiogenesis requires a specific balance of Reactive Oxygen Species(ROS) and neutralizing antioxidants including Glutathione (GSH). Interestingly, our mouse models of PVD with femoral artery ligation (FAL) show a contradictory increase in angiogenesis with a slight decrease in GSH (~80% GSH, Gclm HET mice) compared to WT (100% GSH), not seen with severely decreased GSH in Gclm KO mice (~20% GSH). This suggests that the balance of ROS and antioxidants can be adjusted to a favorable outcome. This led us to hypothesize that a slight decrease in GSH is beneficial and provides “necessary” inflammation to kick-start angiogenesis. To investigate this hypothesis, we performed mRNA-seq analysis on Smooth Muscle Cells (SMCs), an important component of blood vessels known to promote angiogenesis. SMCs were isolated from Gclm WT/HET/KO mice and subjected to hypoxia/re-oxygenation (HR) to mimic blood flow blockage and reperfusion *in-vivo*. Our hypothesis was confirmed with an increased inflammatory gene expression profile in HET SMCs compared to WT and KO. Results show that slight decrease in antioxidant GSH leads to significant increases in the IL-8, NF-kB, fMLP, MAPK kinase and Notch related signaling pathways, all of which positively influence inflammation associated angiogenesis. Our study suggests that a slight increase in oxidative stress leads to an “appropriate” increase in inflammation and provides adequate environment for accelerated angiogenesis and subsequent tissue perfusion.

B. Shrestha: None.

665
Perivascular Adipose Tissue near Aortic Arch is a Major Site for Atheroprotective IgM Producing B-1 Cells
Prasad Srikakulapu, Aditi Upadhye, John Davy, Coleen A McNamara, Univ of Virginia, Charlottesville, VA

Background: Perivascular adipose tissue (PVAT) regulates artery physiology and pathology, such as promoting atherosclerosis development through local production of inflammatory cytokines. The phenotype of PVAT is region-specific and PVAT composed of brown adipose tissue (near the aortic arch and thoracic aorta) and white adipose tissue (near the abdominal aorta). B-1 cells limit adipose tissue inflammation and atherosclerosis through the production of IgM antibodies. PVAT harbors high numbers of B cells. Id3 is a basic helix-loop-helix protein and important for B cell development. B cell-specific Id3 deficiency ($Id3^{BKO}$) increases B-1b cell numbers and provides atheroprotection. However, the location and regulation of IgM producing B-1 cells in the PVAT are unknown.
Methods and Results: Flow cytometry analysis of PVAT of normal chow diet fed young $ApoE^{-/-}$ mice (n=5) demonstrated that the abundant $CD19^{+}$ B cells (per gram fat) harbored in PVAT around aortic arch ($2.7 \pm 0.69 \times 10^5$ cells) compared to PVAT near the thoracic ($0.9 \pm 0.29 \times 10^5$ cells) and abdominal aorta ($1.1 \pm 0.51 \times 10^5$ cells). Interestingly, a large proportion (40%) of these B cells are belong to the $CD19^{hi}$ $B220^{low}$ B-1 subset in PVAT near aortic arch. CXCL13 is a chemokine, which is important for B-1 cell recruitment to omental fat. Real time-PCR data confirmed that high numbers of B-1 cell recruitment to PVAT near aortic arch is due to high expression of CXCL13 in the PVAT near the aortic arch compared to PVAT near thoracic aorta and abdominal aorta. Moreover, Flow cytometry and ELISPOT data in normal chow fed young $ApoE^{-/-}$ mice with $Id3^{BKO}$ demonstrated that $Id3^{BKO}$ increased B-1b cells ($Id3^{BKO}$: $1.2 \pm 0.16 \times 10^3$; $Id3^{WT}$: $0.4 \pm 0.06 \times 10^3$; p-value: <0.01; n=6 mice/group) and IgM secreting cells ($Id3^{BKO}$: $2.0 \pm 0.42 \times 10^3$; $Id3^{WT}$: $0.78 \pm 0.23 \times 10^3$; p-value: <0.05; n=6 mice/group) respectively in PVAT near aortic arch compared to $Id3^{WT}$ control mice.
Conclusion: Results provide the first evidence that atheroprotective B-1 cell profile in PVAT is region-specific and identify Id3 and CXCL13 as regulators of aortic arch PVAT B-1b cell numbers and IgM production.
P. Srikakulapu: None. **A. Upadhye:** None. **J. Davy:** None. **C.A. McNamara:** None.

666
Klotho Suppresses the Protein Kinase R-mediated Inflammatory Response to Soluble Matrilin-2 in Human Aortic Valve Interstitial Cells
Erlinda The, Lihua Ao, Yufeng Zhai, Peijian Zhang, David A. Fullerton, Xianzhong Meng, Univ of Colorado-Denver, Aurora, CO

Calcific aortic valve disease (CAVD) is a chronic, progressive inflammatory disease. Soluble extracellular matrix (ECM) proteins can function as damage-associated molecular patterns (DAMPs) and may play a role in the progression of CAVD. Matrilin-2 is an ECM protein and has been found to up-regulate the pro-osteogenic activity in human aortic valve interstitial cells (AVICs). Klotho is an anti-aging protein that is recently found to have an anti-inflammatory effect. The impact of matrilin-2 and Klotho on AVICs inflammatory response is unclear. This study is to test the hypothesis that matrilin-2 induces the inflammatory response in human AVICs and to explore the anti-inflammatory potential of Klotho for suppression AVIC inflammation. Methods and Results: Human AVICs isolated from normal valves were treated with recombinant matrilin-2 (2.0 µg/ml). Matrilin-2 caused NF-κB-dependent increase in the levels of ICAM-1, MCP-1 and IL-6. In addition, matrilin-2 induced rapid activation of PKR through Toll-like receptor (TLR) 2 and 4. Treatment with PKR inhibitors, 2-AP or C13H8N4OS, prior to matrilin-2 stimulation, abrogated NF-κB phosphorylation and intranuclear translocation. Inhibition of PKR abolished the production of inflammatory mediators induced by matrilin-2 in human AVICs. Further experiments using recombinant Klotho revealed that Klotho (0.5 µg/ml) suppressed the activation of PKR and NF-κB, and markedly reduced the production of inflammatory mediators in human AVICs exposed to matrilin-2. Conclusion: This study demonstrates that soluble matrilin-2 induces the inflammatory response in human AVICs through a TLR-PKR-NF-κB signaling cascade and that Klotho is capable of suppressing human AVICs inflammatory response to a soluble ECM protein. The novel findings of this study indicate that soluble ECM proteins may fuel the progression of CAVD by inducing aortic valve inflammation and that Klotho has the potential for suppression of such inflammation.
E. The: None. **L. Ao:** None. **Y. Zhai:** None. **P. Zhang:** None. **D. Fullerton:** None. **X. Meng:** None.

667
Endothelial Cell "Memory": Rapid Recall of Chemokines After Prior Exposure to Inflammatory Stimuli
Nicole M Valenzuela, UCLA Immunogenetics Ctr, Los Angeles, CA

Background: Surprisingly little has been studied on the capacity of cytokine-primed endothelial cells (EC) to respond upon secondary challenge. The principal hypothesis is that EC store and rapidly recall chemokines after upon secondary challenge.
Methods: Confluent primary human aortic (AEC), dermal microvascular (DMVEC), umbilical vein (UVEC), and renal glomerular (RGEC) endothelial cells were pre-exposed to TNFα or IL-1β (10ng/mL, 18hr), allowed to rest (4-24hr), and re-challenged with the secretagogues PMA or histamine. The repertoire of rapidly recalled soluble mediators was determined by ELISA, and cell surface P-selectin by cell-based ELISA. Total P-selectin content was measured by Western Blot.
Results: Priming with TNFα or IL-1β overnight increased IL-8 secretion by all EC. 4hr after removal of TNFα or IL-1β, IL-8 was still in all supernatants. After 7hr rest, IL-8 was detectable from RGEC but undetectable in other EC. After 24hr, IL-8 was undetectable in the supernatants from all EC. Secondary challenge with secretagogues 24hr after removal of TNFα or IL-1β stimulated rapid secretion of IL-8, but not from unprimed endothelium. P-selectin was rapidly externalized at the cell surface of unprimed cells after 20min exposure to PMA or 10min Histamine. TNFα-primed EC exhibited significantly lower P-selectin induction, mirrored by profoundly reduced total intracellular P-selectin expression. mRNA expression of LAMP3 (CD63, a tetraspanin critical for P-selectin sorting to Weibel-Palade bodies) was highest in microvascular EC and lowest in larger vessel EC. LAMP3 might be important for controlling WPb content as well as durability of exocytosis upon type 1 activation and sorting of newly synthesized type II mediators to WPb for rapid recall.
Conclusions: The data confirm that prior exposure of EC to inflammatory stimuli evokes storage of IL-8 that can be rapidly secreted upon exposure to a second stimulus. Moreover, constitutive expression of P-selectin is suppressed by TNFα exposure, but not IL-1β. Thus, EC exhibit a chronic inflammatory phenotype after cytokines have been encountered and removed, due to storage of chemokines within Weibel-Palade bodies or other granules.
N.M. Valenzuela: Research Grant; Significant; ISHLT Career Development Award.

668
Myeloid Pfkfb3 Deficiency Protect Mice from Hypoxia Induced Pulmonary Hypertension
Lina Wang, Yapeng Cao, Qiuhua Yang, Jiean Xu, Peking Univ, Beijing, China; Zhiping Liu, Yuqing Huo, Augusta Univ, Augusta, GA

Background: Pulmonary hypertension is a progressive disease and perivascular inflammation is found in all types of pulmonary hypertension patients. Macrophage are innate inflammatory cells and the number of macrophages are significantly increased in the lungs of PAH patients. Glycolysis is the main pathway to generate energy and intermediate products for macrophage activation. However, the effect of macrophage glycolysis on the development of pulmonary hypertension remains unknown. As PFKFB3 is a critical regulator in glycolysis, we investigated the effect of macrophage glycolysis on pulmonary hypertension using myeloid PFKFB3 specific deficiency mice and hypoxia induced pulmonary hypertension model.
Results: In mouse and rat hypoxia induced pulmonary hypertension models, we found that PFKFB3 was upregulated in macrophages. PFKFB3 myeloid specific depletion protected mice from the formation of pulmonary hypertension. Knockdown of PFKFB3 in macrophages suppressed the expression of growth factors and inflammatory cytokines in whole lung tissue. Also, we found that PFKFB3 knockdown decreased the numbers of perivascular macrophages and interstitial macrophages using immunostaining and FACS. The number of alveolar macrophages showed no significant difference, while the expression of growth factors and inflammatory cytokines were decreased in alveolar macrophage when PFKFB3 was depleted.
Conclusions: PFKFB3 depletion in macrophage decreases the number of perivascular macrophages and interstitial macrophages in the lung, and suppresses the expression of growth factors and inflammatory cytokines in alveolar macrophage, thus protecting mice from the formation of pulmonary hypertension.
L. Wang: None. **Y. Cao:** None. **Q. Yang:** None. **J. Xu:** None. **Z. Liu:** None. **Y. Huo:** None.

669
Apabetalone (rvx-208) Decreases Risk of Major Adverse Cardiovascular Events in Diabetes Mellitus Patients with Cvd by Attenuating Monocyte Adhesion to Endothelial Cells
Laura Tsujikawa, Ewelina Kulikowski, Cyrus Calosing, Sylwia Wasiak, Dean Gilham, Christopher Halliday, Resverlogix Corp., Calgary, AB, Canada; Jan Johansson, Mike Sweeney, Resverlogix Inc., San Francisco, CA; **Norman Wong**, Resverlogix Corp., Calgary, AB, Canada

Apabetalone (RVX-208, 200 mg/d) given orally to patients with diabetes mellitus (DM) and CVD leads to a 57% relative risk reduction in major adverse cardiovascular events (MACE). Potential actions of RVX-208, an inhibitor (BETi) of bromodomain extra-terminal (BET) proteins that are epigenetic readers of acetylated lysine residues within histones, in lowering MACE is explored by testing its effect on genes mediating monocyte adhesion to endothelial cells in response to high glucose (HG) and the dietary metabolite trimethyl-amine oxide (TMAO). Cultured THP-1 monocytes, HUVEC endothelial cells and primary human hepatocytes (PHH) were exposed to varying concentrations of glucose and TMAO. Results showed that HG (25.6 mM) induced Very Late Antigen-4 (VLA-4) mRNA, a gene mediating THP-1 adhesion by 1.3-fold and RVX-208 suppressed it >50%. Similarly, BETi blocked TMAO induction of VLA-4 mRNA by >50% in THP-1. In HUVECs RVX-208 abrogated HG induction of E-selectin and MYD88 mRNA by 2- and 1.3-fold, respectively and lowered TMAO induction of these mRNAs by >50%. Microbiome processing of dietary phospholipids followed by hepatic flavin mono-oxygenase-3 (FMO3) metabolism yields TMAO. In PHH exposed for 24 hrs to RVX-208, FMO3 mRNA was lower by 40% but it also suppressed a transcriptional regulator of FMO3, farnesoid X receptor (FXR). BETi suppressed both FXR mRNA and protein within 6 hrs by >80% suggesting a direct effect of BETi on the gene encoding FXR. Furthermore, ChiP data showed that BRD4, a BET protein, dissociated immediately from FXR gene upon exposure to RVX-208. Since BRD4 guides a complex containing RNA pol II along actively transcribed genes containing histones that are highly acetylated, the dissociation of BRD4 from FXR DNA would halt transcription of this gene. In summary, Apabetalone inhibits HG and TMAO enhanced adhesion of THP-1 to HUVECs a process that mimics a step in the pathogenesis of CVD. RVX-208 suppresses genes underlying cellular adhesion; VLA-4 in THP-1 and both E-selectin plus MYD88 in HUVECs. BETi blocks not only activity of TMAO but also its production by inhibiting FXR expression, a regulator of FMO3 gene transcription. The rapid actions of BETi in dissociating BRD4 from FXR DNA suggests a direct effect of RVX-208 on transcription of this gene.
L. Tsujikawa: Employment; Significant; Resverlogix Corp.. Ownership Interest; Significant; Resverlogix Corp. **E. Kulikowski:** Employment; Significant; Resverlogix Corp.. Ownership Interest; Significant; Resverlogix Corp. **C. Calosing:** Employment; Significant; Resverlogix Corp.. Ownership Interest; Significant; Resverlogix Corp. **S. Wasiak:** Employment; Significant; Resverlogix Corp.. Ownership Interest; Significant; Resverlogix Corp. **D. Gilham:** Employment; Significant; Resverlogix Corp.. Ownership Interest; Significant; Resverlogix Corp. **C. Halliday:** Employment; Significant; Resverlogix Corp.. Ownership Interest; Significant; Resverlogix Corp. **J. Johansson:** Employment; Significant; Resverlogix Corp.. Ownership Interest; Significant; Resverlogix Corp. **M. Sweeney:** Employment; Significant; Resverlogix Corp.. Ownership Interest; Significant; Resverlogix Corp. **N. Wong:** Employment; Significant; Resverlogix Corp.. Ownership Interest; Significant; Resverlogix Corp.

670
Smooth Muscle Cell-Specific (SMC) Expression of a Constitutively Active TGF-β Receptor 1 Variant Prevents Aortopathy in SMC TGF-β Receptor 2 Deleted Mice
Stoyan N Angelov, Jie Hong Hu, Jay Zhu, David A Dichek, Univ of Washington, Seattle, WA

Background: Abnormal smooth muscle cell (SMC) TGF-β signaling is implicated in the pathogenesis of thoracic aortic aneurysms and dissections (TAAD); however, the mechanisms through which altered TGF-β signaling causes TAAD are poorly understood. In particular, whether elevated SMC TGF-β signaling *per se* is sufficient to cause aortopathy is unknown. To begin to answer this question, we generated mice in which SMC-targeted constitutive TGF-β signaling can be activated postnatally. To determine whether this strategy activates biologically significant TGF-β signaling in SMC, we tested whether it could prevent aortopathy in mice with SMC-specific loss of TGF-β signaling due to SMC-specific deletion of TGF-β receptor 2 (TBR2). **Methods:** We obtained mice with a floxed-stop TGF-β receptor 1 allele that is active independently of ligand binding (TBR1-CA), and is expressed only after tamoxifen-induced Cre excision. We bred this allele into the *Tgfbr2*$^{flox/flox}$ background. Via matings with Acta2-*Cre*^{ERT2} mice, we generated 3 groups: 1) wt TBR2, no TBR1-CA expression (negative control); 2) SMC-TBR2 null, no TBR1-CA expression (positive control); and 3) SMC-TBR2 null, SMC-TBR1-CA (experimental). Aortas were examined grossly, sectioned, stained, and subjected to computer-assisted planimetry. **Results:** Aortic intramural hematoma was present in 0 of 9 Group 1 mice (0%), 2 of 5 Group 2 mice (40%), and 0 of 10 Group 3 mice (0%; *P*=0.09 vs Group 2). Prussian blue staining (evidence of past aortic intramural hemorrhage) was present in histologic sections of thoracic aortas of 0 of 9 Group 1 mice (0%), 3 of 4 Group 2 mice (75%), and 0 of 7 Group 3 mice (0%; *P*=0.02 vs Group 2). Aortic medial area (mm^2) was 0.123 for Group 1 mice (n = 9), 0.161 for Group 2 mice (n = 5), and 0.135 for Group 3

mice (n = 5; *P*=0.09 vs Group 2). **Conclusions:** A conditional TBR1-CA allele, when expressed in mouse aortic SMC, appears to prevent or reduce aortopathy caused by SMC-specific loss of TBR2. This result confirms that aortopathy in SMC-TBR2 null mice is due to loss of TGF-β signaling and suggests that the conditional TBR1-CA allele will be a useful tool for uncovering the consequences of elevated SMC TGF-β signaling and for probing whether other mouse aortopathies are caused by elevated or depressed SMC TGF-β signaling.
S.N. Angelov: None. **J.H. Hu:** None. **J. Zhu:** None. **D.A. Dichek:** None.

671
Looking with the Poiseuille's Glasses - a Proposal of a Novel Hypothetical Method to Increase the Dimensions of the Coronary Arteries when Required
Mark C Arokiaraj, Pondicherry Inst Medical Science, Pondicherry, India

Background: The purpose was to develop a novel hypothetical method to increase the dimensions of coronary arteries. **Methods:** In the long-term observation, the coronary sizes were dilated in three unexpected scenarios. The coronary artery sizes were observed in patients with mitral stenosis patients (n=12) by angiogram. The coronaries of patients with patent ductus arteriosus who underwent surgical/coil closure in the past (n=7) were examined by echocardiogram. These patients also had normal aortic and left ventricular dimensions, and all had surgeries/coil closure more than four years prior to this observation. Patients with renal failure on long-term dialysis through peripheral arterio-venous fistula without left ventricular hypertrophy (n=13) were studied by echocardiography for coronary dimensions. Normal age and sex-matched coronary sizes served as controls in the study. All these observations were made over a period of 10 years. **Results:** The sizes of coronaries in patients with mitral stenosis were greater than 22% (± 4) of the normal. The coronary sizes were 32% (±4) higher than normal in patients with patent ductus arteriosus without left ventricular or aortic dilatation. Patients with renal failure on hemodialysis without left ventricular hypertrophy had coronary sizes 28% (±5) higher than similarly sized ventricles. Reducing the diastolic blood pressures, the increase in coronary angulation by sine (θ) function, and increase in the coronary length and diameters can be achieved by observing the differential equations of Poiseuille's. A hypothetical model to increase the coronary sizes could be developed based on the analysis of the differential equations. The proposed method is creating a peripheral arterio-venous fistula, which can be closed later by a percutaneous method/surgery. The closure time needs to be determined by experimental studies. The other methods could be a continuous exercise program or usage of beta-blockers. **Conclusion:** A novel hypothetical method of peripheral arterialvenous fistula formation could potentially increase the size of the coronaries. Further experiments need to be performed to observe the results.
M.C. Arokiaraj: None.

672
SUMOylation of Vps34 by SUMO1 Promotes Phenotypic Switching of Vascular Smooth Muscle Cells by Activating Autophagy in Pulmonary Arterial Hypertension
Yufeng Yao, Hui Li, Yong Li, Changqing Hu, Bo Tang, Zhenkun Hu, Xingwen Da, Qixue Song, Yubing Yu, Huazhong Univ of Science and Technology, Wuhan, China; **Qiuyun Chen**, Qing K Wang, Cleveland Clinic, Cleveland, OH

Pulmonary arterial hypertension (PAH) is a life-threatening disease without effective therapies. PAH is associated with a progressive increase in pulmonary vascular resistance and irreversible pulmonary vascular remodeling. SUMO1 (small ubiquitin-related modifier 1) can bind to target proteins and lead to protein SUMOylation, an important post-translational modification mechanism with a key role in many diseases. However, the contribution of SUMO1 to PAH remains to be fully characterized. In this study, we explored the role of SUMO1 in the dedifferentiation of vascular smooth muscle cells (VSMCs) involved in hypoxia-induced pulmonary vascular remodeling and PAH. In a mouse model of hypoxic PAH, SUMO1 expression was significantly increased, which was associated with activation of autophagy (increased LC3b and decreased p62), dedifferentiation of VSMCs (reduced α-SMA, SM22 and SM-MHC), and pulmonary vascular remodeling. Overexpression of SUMO1 significantly increased VSMC proliferation, migration, hypoxia-induced VSMC dedifferentiation, and autophagy, but these effects were abolished by inhibition of autophagy by 3-MA. Mechanistically, SUMO1 promotes Vps34 SUMOylation and the assembly of the Beclin-1-Vps34-Atg14 complex, thereby inducing autophagy, whereas Vps34 mutation K840R reduces Vps34 SUMOylation and inhibits VSMC dedifferentiation. In conclusion, our data uncovers an important role of SUMO1 in VSMCs proliferation, migration, activation of autophagy, and phenotypic switching (dedifferentiation) involved in pulmonary vascular remodeling and PAH. Targeting of the SUMO1-Vps34-autophagy signaling axis may be exploited to develop therapeutic strategies to treat PAH.
Y. Yao: Research Grant; Modest; National Natural Science Foundation of China. **H. Li:** Research Grant; Modest; National Natural Science Foundation of China. **Y. Li:** Research Grant; Modest; National Natural Science Foundation of China. **C. Hu:** Research Grant; Modest; National Natural Science Foundation of China. **B. Tang:** Research Grant; Modest; National Natural Science Foundation of China. **Z. Hu:** Research Grant; Modest; National Natural Science Foundation of China. **X. Da:** Research Grant; Modest; National Natural Science Foundation of China. **Q. Song:** Research Grant; Modest; National Natural Science Foundation of China. **Y. Yu:** Research Grant; Modest; National Natural Science Foundation of China. **Q. Chen:** Research Grant; Significant; NIH. **Q.K. Wang:** Research Grant; Significant; NIH.

673
Discovering and Dissecting the Function of Conserved NF-κB Binding Events in the Human Genome
Azad Alizada, Hosptial for Sick Children, Toronto, ON, Canada; Nadiya Khyzha, Melvin Khor, Toronto General Hosp Res Inst, Toronto, ON, Canada; Lina Antounians, Liangxi Wang, Hosp for Sick Children, Toronto, ON, Canada; Alejandra Medina-Rivera, Univ Nacional Autonoma de Mexico, Juriquilla, Mexico; Minggao Liang, Huayun Hou, Michael D Wilson, Hosp for Sick Children, Toronto, ON, Canada; **Jason E Fish**, Toronto General Hosp Res Inst, Toronto, ON, Canada

The nuclear factor kappa-light-chain-enhancer of activated B cells (NF-κB) transcription factor plays a prominent role in inflammation and contributes to the development of atherosclerosis. Genome-wide DNA binding assays of the human NF-κB subunit RELA (p65) have revealed tens of thousands of NF-κB binding sites and hundreds of target genes. However, the function of individual RELA binding sites and the extent to which NF-κB occupancy and function is conserved across mammals are not well understood. To better understand the function of NF-κB we characterized the genome-wide binding of RELA in primary vascular endothelial cells (ECs) isolated from the aortas of human, mouse and cow. ECs were stimulated acutely with the pro-inflammatory cytokine tumor necrosis factor alpha (TNFA) and we profiled RELA occupancy, open chromatin, select histone modifications, and RNA expression. We found ~5000 RELA binding events conserved across all three species and these highly conserved human binding events were enriched for genes controlling vascular development, apoptosis, and pro-inflammatory responses. Approximately 2000 of these highly conserved RELA binding events were also shared across multiple human cell types, revealing a conserved

core of robustly bound NF-κB sites. These NF-κB binding sites were also prominent components of ~40 inflammation-induced super-enhancers (SE) common to several tissues. To gain insight into the function of individual conserved NF-κB binding sites we focused on the inflammation-induced SE proximal to the monocyte recruiting chemokine *CCL2*, which we detected as a SE in all three species and across multiple cell types. We tested the functional significance of six conserved RELA binding sites comprising this SE using CRISPR/Cas9 genome editing. We found that only deletion of the most proximal upstream RELA binding site could abolish the induction of *CCL2* upon TNFA treatment. This site also contains a disease associated variant that can modulate *CCL2* induction. Overall, our comparative genomics assessment of NF-κB binding gives new insight into NF-κB biology and the function of conserved transcription factor binding events within mammalian super-enhancers.

A. Alizada: None. **N. Khyzha:** None. **M. Khor:** None. **L. Antounians:** None. **L. Wang:** None. **A. Medina-Rivera:** None. **M. Liang:** None. **H. Hou:** None. **M.D. Wilson:** None. **J.E. Fish:** None.

674

Vesselin Controls Vascular Morphogenesis by Activating Small Gtpases in Endothelial Cells

Yanling Wang, Zhengqiang He, Hao Duan, Menggui Huang, Yi Fan, **Yanqing A Gong**, Univ of Pennsylvania, Philadelphia, PA

Vascularization is a fundamental process in development, wound healing, and the progression of cardiovascular diseases. Formation of new blood vessels with functional and structural integrity is crucial for organ growth as well as post-injury tissue repair and regeneration. Although vascular sprouting and outgrowth, *i.e.*, angiogenesis, has been extensively studied, the underlying mechanisms for vessel formation remain largely unexplored. Here we reveal a critical role of phosphatidylinositol 4,5-bisphosphate (PIP2) for vessel formation in endothelial cells (ECs). Moreover, by using mass spectrometry, our identified Tbc1d2b as a novel PIP2-binding protein in vessel-formatting ECs. Considering its critical function in vessel formation, we name this protein “vesselin”. We showed that vesselin preferentially localizes to blood vessels in various human tissues, and that its siRNA-mediated knockdown inhibits EC tube formation, supporting its major role in vessel formation. Remarkably, injection of inhibitory vesselin morpholino into the embryos blocks blood vessel formation and zebrafish development. Vesselin contains PH (pleckstrin homology) and TBC (Tre2/Bub2/Cdc16) domains, which are known to bind phosphatidylinositols and display GTPase-activating protein (GAP) activities towards Rab GTPases, respectively. Consistently, we found by mass spectrometry that vesselin interacts with the small GTPase Rab13 and small GTPase Rac1. Finally, our further mechanistic studies showed that vesselin interacts with Rac1 and Rab13 during EC vessel formation, and regulates their activity in a PIP2-dependent manner. Thus, we uncover a previously unidentified regulatory system for EC vessel formation, providing molecular resolution of vascular morphogenesis. Targeting vesselin may provide new therapeutic strategies in cardiovascular diseases.

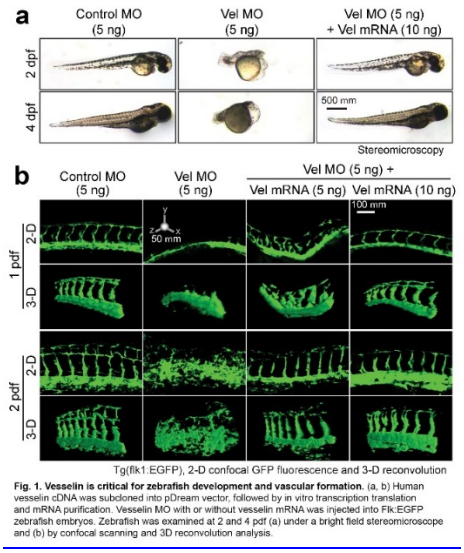

Fig. 1. Vesselin is critical for zebrafish development and vascular formation. (a, b) Human vesselin cDNA was subcloned into pDream vector, followed by in vitro transcription translation and mRNA purification. Vesselin MO with or without vesselin mRNA was injected into Flk:EGFP zebrafish embryos. Zebrafish was examined at 2 and 4 pdf (a) under a bright field stereomicroscope and (b) by confocal scanning and 3D reconvolution analysis.

Y. Wang: None. **Z. He:** None. **H. Duan:** None. **M. Huang:** None. **Y. Fan:** None. **Y.A. Gong:** None.

This research has received full or partial funding support from the American Heart Association.

675

Biomechanical Alterations of Endothelial Cells That Affect Infection by *Listeria Monocytogenes*

Effie Bastounis, Yi-Ting Yeh, Julie Theriot, Stanford Univ, Stanford, CA

Endothelial cells (ECs) line the inner lumen of vessels forming a protective barrier against spread of a variety of insults, including bacterial infections. ECs display remarkable phenotypic heterogeneity in part due to the different mechanical stimuli transmitted from their extracellular environment, including variations in subendothelial stiffness and shear flow. Although EC response to mechanical signals has been studied extensively, how bacterial uptake occurs in ECs residing on varying stiffness environments was hitherto largely unknown. We exploited *Listeria monocytogenes* (Lm), an intracellular bacterial pathogen, to determine the biophysical relationships between ECs, their subendothelial stiffness matrix and bacterial infection. We found that adhesion of Lm onto ECs increases with increasing subendothelial stiffness in a focal adhesion kinase (FAK)-dependent manner and that FAK activity is critical for uptake of Lm by ECs. We also found that the amount of vimentin exposed at the apical surface of host ECs is reduced when FAK activity is decreased, which leads to reduced *Lm* uptake by ECs. Our results identify a novel pathway wherein increased subendothelial stiffness sensed by ECs leads to enhanced FAK activity and host surface vimentin, that in turn increases Lm uptake. We envision that by uncovering the molecular details of vascular infection and gaining mechanistic insight into how mechanics affect infection of the vasculature, we could lay important groundwork for the development of novel therapeutic interventions against bacterial infections.

E. Bastounis: None. **Y. Yeh:** None. **J. Theriot:** None.

This research has received full or partial funding support from the American Heart Association.

676
Hypoxia Upregulates NADPH Oxidase 4-Mediated Hydrogen Peroxide Release by a HIF-Independent Mechanism in Human Endothelial Cells
Coy Brunssen, Alexander Arsov, David M. Poitz, Claudia Eickholt, Anja Hofmann, Heike Langbein, Melanie Brux, Felix Engelmann, Claudia Goettsch, Winfried Goettsch, Antje Augstein, Stefan R. Bornstein, Ruth H. Strasser, Georg Breier, Henning Morawietz, Univ of Technology Dresden, Dresden, Germany

NADPH oxidases are important sources of reactive oxygen species in the vascular wall. Recent evidence supports a vasoprotective role of H_2O_2 produced by the main endothelial isoform Nox4. The impact of hypoxia on NOX4 expression in human endothelial cells and the underlying mechanism remains to be elucidated. In this study, we show that NOX4 mRNA and protein expression was upregulated by hypoxia (1 % O_2) in human umbilical vein endothelial cells (HUVEC). Correspondingly, H_2O_2 production was 2-fold elevated in HUVEC after hypoxia. In contrast to rotenone and oxypurinol, lentiviral downregulation via shNOX4 abolished the elevated hypoxic hydrogen peroxide levels to normoxic values. Hypoxia stabilized the hypoxia-inducible factor (HIF)-1α protein in endothelial cells. Furthermore, VEGF promoter activity and a control promoter containing 3 hypoxia-responsive elements (HRE) were induced by hypoxia. NOX4 promoter deletions up to -119/+239 had an increased basal activity compared to control vector. A full-length and a terminally deleted NOX4 promoter construct missing a putative HRE showed a comparable activity under hypoxic and normoxic conditions, suggesting that NOX4 is not induced on the transcriptional level by hypoxia in endothelial cells. In addition, stabilization of HIF-1α protein under normoxic conditions using DMOG did not change NOX4 mRNA expression in HUVEC. Furthermore, overexpression of HIF-1α did not alter NOX4 promoter activity. Blockade of active transcription by actinomycin D revealed an increased stability of the NOX4 mRNA under hypoxic conditions. In conclusion, this study demonstrates an HIF-independent upregulation of NOX4 as major source of endothelial hydrogen peroxide generation in response to hypoxia. Our data support as a novel mechanism an increased NOX4 mRNA stability under hypoxic conditions in human endothelial cells.

C. Brunssen: None. **A. Arsov:** None. **D.M. Poitz:** None. **C. Eickholt:** None. **A. Hofmann:** None. **H. Langbein:** None. **M. Brux:** None. **F. Engelmann:** None. **C. Goettsch:** None. **W. Goettsch:** None. **A. Augstein:** None. **S.R. Bornstein:** None. **R.H. Strasser:** None. **G. Breier:** None. **H. Morawietz:** None.

677
Genetic Depletion of the Long Non-coding RNA H19 in Mice Protects from Elastase-induced Abdominal Aortic Aneurysms
Ekaterina Chernogubova, Karolinska Inst, Stockholm, Sweden; Albert Busch, Yuhuang Li, Klinikum rechts der Isar, Technical Univ, Munich, Germany; Hong Jin, Greg Winski, Karolinska Inst, Stockholm, Sweden; Patrick Hofmann, Reinier A. Boon, Inst for Cardiovascular Regeneration, Goethe Univ, Frankfurt, Germany; Alexandra Bäcklund, Lars Maegdefessel, Karolinska Inst, Stockholm, Sweden

Long noncoding RNAs (lncRNAs) have been shown as crucial molecular regulators in various biological processes and diseases. Recently we demonstrated that lncRNA H19 is highly upregulated during abdominal aortic aneurysm (AAA) development and progression in murine models (Angiotensin II in ApoE-/- mice; porcine pancreatic elastase model (PPE) in C57BL/6 mice). Experimental H19 knock-down using specific antisense LNA oligonucleotides showed a significant reduction in AAA growth in both models. Aim of this current study was to utilize genetically mutated H19-depleted mice (H19-/-) vs. wildtype littermate controls, to assess their behavior upon experimental AAA induction using PPE. In addition, we studied the proliferation rates of smooth muscle cells, originating from either H19-/- or H19+/+ mice in a kinetic live-cell imaging system. H19-/- on a C57BL/6J background were exposed to PPE. The aortic diameter in H19-/- mice was compared to WT littermate controls (upon PPE-AAA induction) at baseline, and then consecutively at days 7, 14, and 28. Primary mouse aortic smooth muscle cells were isolated from wild type or H19-depleted aortas, and cultured and monitored in the IncuCyte live cell imaging system for 48 hours, in an effort to study their proliferation rate. H19-/- mice upon PPE-AAA induction displayed significantly lower diameters throughout the study compared to WT controls. Primary aortic smooth muscle cells from H19-depleted mice showed greatly increased proliferation rates (based on cell confluency detection) in our kinetic live-cell imaging system in comparison to WT control cells. In conclusion, our study in H19-depleted mice supports our previously presented efforts, that H19 is an important contributor to experimental AAA development and progression. Further mechanistic studies will have to reveal the molecular properties of this long non-coding RNA in smooth muscle cell survival and proliferation.

E. Chernogubova: None. **A. Busch:** None. **Y. Li:** None. **H. Jin:** None. **G. Winski:** None. **P. Hofmann:** None. **R.A. Boon:** None. **A. Bäcklund:** None. **L. Maegdefessel:** None.

678
microRNA 146a Reduces Activity of Matrix-Metalloproteinases in the Context of Arterial Stiffness
Angelika Dannert, Isabel N Schellinger, Joanna Jakubiczka-Smorag, Karin Mattern, Anne Petzold, Gerd Hasenfuss, Uwe Raaz, Univ Medical Ctr Göttingen, Göttingen, Germany

Background: Arterial stiffness is part of arterial aging and strongly associated with increased risk for cardiovascular events. Unfortunately, until today there is no treatment available effectively counteracting arterial stiffening. One key feature of arterial stiffening is elastin fragmentation. Breakdown of elastin is mediated by matrix metalloproteinases (MMPs), in particular MMP-2 and MMP-9 play a pivotal role in this process. Non-coding micro RNAs (miRs) were found to effectively regulate gene expression, consequentially representing potential therapeutic targets. We hypothesize that miR146a inhibits MMP-2 and MMP-9, thus leading to decreased elastin fragmentation in the vascular extracellular matrix.
Methods and Results: RNA Sequencing found miR146a to be upregulated in a stiffness-dependent manner *in vitro* and in an age dependent manner *in vivo*. Since both MMP-2 and MMP-9 are predicted targets of miR146a, we transfected aortic smooth muscle cells with constructs either increasing (mimicking construct) or decreasing (inhibitory anti-sense construct) effective miR146a levels and evaluated the effect on MMP-2 and MMP-9 expression and activity *in vitro*. qRT-PCR analysis demonstrated significantly de-repressed MMP-2 and MMP-9 levels upon transfection with inhibitor constructs, while mimic constructs further repressed the expression of MMP-2 and MMP-9. Overall MMP activity was significantly altered accordingly after transfection with the respective constructs as determined by a fluorimetric MMP Activity Assay. MMP-2 activity could be specifically assessed using Zymography. After transfection with miR146a inhibitor, both active MMP-2 as well as pro-MMP-2 activity were found to be significantly increased.
Conclusion: Our study provides first evidence that miR146a reduces the levels and activity of MMP-2 and MMP-9 in vascular smooth muscle cells. We conclude that miR146a might have protective function on the integrity of the elastin network in the arterial media. We therefore consider miR146a a potential drug target in the context of elastin fragmentation and arterial stiffness, thus potentially alleviating the development of aortic aneurysm.

A. Dannert: None. **I.N. Schellinger:** None. **J. Jakubiczka-Smorag:** None. **K. Mattern:** None. **A. Petzold:** None. **G. Hasenfuss:** None. **U. Raaz:** None.

679
Pdgf/snail-mediated Endothelial Plasticity Drives Non-productive Neovascularization and Impedes Tissue Repair After Myocardial Infarction
Yi Fan, Menggui Huang, Fan Yang, Hao Duan, Univ of Pennsylvania, Philadelphia, PA

Ischemic heart disease is the most common cause of death in the Western world, largely due to myocardial infarction (MI). After MI, formation of new blood vessels, *i.e.*, neovascularization, is crucial for ischemic tissue reperfusion, repair and regeneration. However, the newly formed vasculatures in infarcted tissue are characterized by functional and structural abnormalities, which compromise vascular delivery function and impede cardiac recovery after MI. Likewise, aberrant non-productive neovascularization, albeit previously under-appreciated, represents a promising therapeutic target for post-MI treatment. Here we reveal that mesenchymal transformation-mediated endothelial cell (EC) plasticity induces aberrant post-ischemic neovascularization. In contrast to the old concept implicating that ECs undergo endothelial mesenchymal transitions to generate fibroblasts *de novo* in infarcted cardiac tissue, we suggest that ECs acquire mesenchymal phenotypes including high proliferation and motility to generate excessive abnormal vasculatures after MI. By utilizing genetic EC lineage tracing and single-cell RNAseq technologies with a mouse MI model induced by ligation of left anterior descending coronary artery, our transcriptome analysis uncovers that ECs undergo mesenchymal transformation in infarcted tissues. Moreover, exposure of cardiac ECs to ischemic microenvironment *in vitro* induces EC expression of mesenchymal genes including S100A4, ACTA2, and CDH2, and interestingly, EC functions including tube formation and uptake of ac-LDL are retained, suggesting EC mesenchymal transformation without lineage transition. Furthermore, we identify a PDGF/Snail-mediated axis that controls EC transformation under hypoxia. Notably, genetic ablation of PDGF receptor-β in ECs promotes blood perfusion and tissue repair after hindlimb ischemia and MI in mice. These findings identify a novel cellular mechanism controlling non-productive neovascularization after ischemia, and suggest that targeting EC plasticity may offer promising therapeutic opportunities for normalization of aberrant neovasculature and improvement of tissue repair in ischemic heart diseases.
Y. Fan: None. **M. Huang:** None. **F. Yang:** None. **H. Duan:** None.

680
Specific Deletion of SHP-1 in Smooth Muscle Cells Restores PDGF Action in Diabetes
Stéphanie Robillard, Farah Lizotte, **Pedro Miguel Geraldes**, Univ of Sherbrooke, Sherbrooke, QC, Canada

Introduction - Ischemia due to narrowing of the femoral artery and distal vessels is also a major cause of peripheral arterial disease and morbidity affecting patients with diabetes. Our laboratory has previously shown that hyperglycemia reduced platelet-derived growth factor (PDGF) activity in ischemic muscle of diabetic mice, which was associated with increased SHP-1 expression, a protein tyrosine phosphatase. The objective of this study is to evaluate the impact of SHP-1 deletion in smooth muscle cells both in vitro and in vivo. **Methods -** Non-diabetic (NDM) and 3 months diabetic (DM) mice with deletion of SHP-1 specifically in smooth muscle cells (SMC) were used. Ligation of the femoral artery was performed and blood flow reperfusion was measured by laser Doppler for 4 weeks. Primary SMC were exposed to normal (5.6mM; NG) or high glucose concentrations (25mM; HG) for 48h, in normoxia (20% oxygen) or hypoxia (1%) for the last 24h in presence of PDGF, a pro-angiogenic factor. **Results -** Blood flow was recovered to 47% in DM mice compared to 80% in NDM mice. Specific SMC deletion of SHP-1 enhanced reperfusion in NDM and DM mice up to 78% and 67%, respectively. In culture, PDGF-induced proliferation, migration, and Akt phosphorylation were reduced by 69%, 50% and 40%, respectively in SMC exposed to HG+hypoxia. Inhibition of PDGF actions was associated with increased SHP-1 phosphatase activity (40%) and enhanced interaction of SHP-1 with the PDGF receptor-β (5.6-fold). Overexpression of the dominant negative form of SHP-1 restored PDGF-induced proliferation and migration as well as Akt and ERK phosphorylation in SMC exposed to HG+hypoxia. **Conclusion -** High glucose level induced SHP-1 activity and caused inhibition of PDGF pro-angiogenic actions in SMC, whereas the deletion of SHP-1 specifically in SMC restored blood flow reperfusion in diabetes.
S. Robillard: None. **F. Lizotte:** None. **P.M. Geraldes:** None.

681
Enhanced Notch3 Signaling Contributes to Pulmonary Emphysema in a Murine Model of Marfan Syndrome
Zhibo Liu, Matthew Fitzgerald, Trevor Meisinger, Rishi Batra, B. Timothy Baxter, Wanfen Xiong, Dept of Surgery, Univ of Nebraska Medical Ctr, Omaha, NE

Marfan syndrome (MFS) is a heritable disorder of connective tissue, caused by mutations in fibrillin-1 gene. Pulmonary emphysema is one of the most common manifestations in MFS. However, the pathogenesis and molecular mechanism of pulmonary emphysema in MFS patients is underexplored. Notch signaling is essential for lung development. It has been shown that constitutive Notch3 activation inhibited the differentiation of distal lung progenitors into alveolar cells. Upregulation of Notch3 promoted endothelial cell death. As our objective, we investigated whether Notch3 signaling plays a role in pulmonary emphysema in MFS. By using a murine model of MFS, mgR/mgR mice, we found the pulmonary emphysematous-appearing alveolar patterns in the lung of mgR/mgR mice by Verhoeff-Van Gieson connective tissue staining and H&E staining. Lungs in mgR/mgR mice had decreased septation in terminal alveoli compared to wild type controls. Western blot analysis demonstrated that Notch3 levels were increased in the lung of mgR/mgR mice compared to wild type controls. This is associated with decreased expression of vascular endothelia growth factor (VEGF) and increased matrix metalloproteinase (MMP) -2 and MMP-9 production in the lung of mgR/mgR mice. To confirm that the increased Notch3 signaling in mgR/mgR mice were responsible to structure alternations in the lung of mgR/mgR mice, mice were treated with N-[N-(3,5-difluorophenacetyl)-L-alanyl]-S-phenylglucine t-butyl ester (DAPT), a *γ* -secretase inhibitor of Notch signaling. DAPT treatment was able to restore the normal lung structure in mice with MFS. This study indicates that Notch3 crosstalk with VEGF signaling pathways in the lung contribute to pulmonary emphysema in mgR/mgR mice. The results may have the potential to lead to novel strategies to prevent and treat pulmonary manifestations in patients with MFS.
Z. Liu: None. **M. Fitzgerald:** None. **T. Meisinger:** None. **R. Batra:** None. **B. Baxter:** None. **W. Xiong:** None.

685
Sterol Regulatory Element-Binding Protein 2-Mediated Endothelial-to-Mesenchymal Transition Contributes to Pulmonary Fibrosis
Marcy Martin, Jiao Zhang, UC San Diego, La Jolla, CA; Yifei Miao, City of Hope, Duarte, CA; Jian Kang, UC San Diego, La Jolla, CA; Hsi-Yuan Huang, Natl Chiao Tung Univ, Hsin-Chu, Taiwan; Ming He, Jianjie Dong, Simon Wong, UC San Diego, La Jolla, CA; Hsien-Da Huang, Natl Chiao Tung Univ, Hsin-Chu, Taiwan; Zhen Chen, City of Hope, Duarte, CA; James S Hagood, John Y-J Shyy, UC San Diego, La Jolla, CA

Objective: Idiopathic pulmonary fibrosis (IPF) is a progressive interstitial lung disease with a median survival rate of 3-5 years. The clinical presentation of IPF relies on

the formation of fibroblastic foci, areas of active myofibroblasts depositing extracellular matrix resulting in stiff and dilated alveoli. Whereas therapeutics targeting fibroblast proliferation have made little clinical progress, the role of endothelial cell (EC) dysfunction in pulmonary fibrosis has been overlooked. Having previously identified that sterol regulatory element-binding protein 2 (SREBP2) is a key mediator of innate immune and redox responses in ECs, we postulate that SREBP2 plays a role in promoting EC dysfunction contributing to pulmonary fibrosis. **Approach and Results:** RNA-sequencing demonstrated that SREBP2 overexpression in ECs led to the induction of TGF, Wnt, and cytoskeleton remodeling gene ontology pathways. SREBP2 regulation of these pathways indicated mesenchymal cell differentiation, which alluded to the promotion of endothelial-to-mesenchymal transition (EndoMT). SREBP2 overexpression in cultured ECs led to increased expression of mesenchymal genes such as snai1 family transcriptional repressor 1 (snai1), α-smooth muscle actin (αSMA), vimentin, and neural cadherin (N-cad). Furthermore, SREBP2 was found to directly bind to the promoter regions and transactivate these mesenchymal genes in ECs. Furthermore, a myofibroblast-like phenotypic switch in ECs was evident, including increased proliferation, stress fiber formation, and ECM deposition. Pulmonary fibrosis mouse models using bleomycin demonstrated exacerbated lung vascular remodeling and increased EndoMT in endothelial-specific SREBP2 overexpression transgenic (EC-SREBP2-Tg) mice when compared to wildtype littermates. Additionally, SREBP2 was found to be markedly increased in lung specimens from IPF patients. **Conclusions:** SREBP2 promotes EndoMT through direct transactivation of mesenchymal genes (i.e., snai1, αSMA, vimentin, and N-Cad). Pathogenic factors activating SREBP2 specifically in ECs increased EndoMT and exacerbated pulmonary fibrosis *in vivo*. This suggests that targeting SREBP2 may be a potential therapeutic in pulmonary fibrosis.

M. Martin: None. **J. Zhang:** None. **Y. Miao:** None. **J. Kang:** None. **H. Huang:** None. **M. He:** None. **J. Dong:** None. **S. Wong:** None. **H. Huang:** None. **Z. Chen:** None. **J.S. Hagood:** None. **J.Y. Shyy:** None.

686

The Impact of Tobacco Smoke on Level of Endothelial Dysfunction Markers in Patients with Essential Hypertension

Valery Podzolkov, Anna Bragina, Natalia Druzhina, I.M. Sechenov First Moscow State Medical Univ, Moscow, Russian Federation; Leila Mohammadi, Univ of California, San Francisco, CA; **Natalia Murashko**, I.M. Sechenov First Moscow State Medical Univ, Moscow, Russian Federation

Objectives: to study the markers of endothelial dysfunction (ED): metabolites of Nitric Oxide (NO), endothelin1 (E1), homocysteine (HC), Von Willebrand factor (vWF), tissue plasminogen activator (tPA) in plasma of tobacco smokers and nonsmokers with essential hypertension (EH).
Material and methods: 124 hypertensive were recruited: 45 men and 79 women, with the mean age of 51,4±6,5 yrs and average duration of EH for 8,5±7,6 yrs. The control group included 25 healthy subjects (10 men and 15 women) with mean age of 48,2±7,8 yrs. Plasma NOx levels were determined by spectrometry, E1, HC, Wf, tPA levels by enzyme immunoassay. The results of study were analyzed by using Statistica 10.0.
Results: to determine the effects of smoking on level of ED markers, we divided our subjects to subgroups: hypertensive smoker (35%), hypertensive nonsmokers (65%), smokers without hypertension (38%) and healthy nonsmokers (62%). In hypertensive smokers, in comparison to nonsmokers, we found a significant induction in NOx level (48,2±18,8 umol/l and 40,3±21,2 umol/l respectively, p<0,05), E1 (1,2±0,16 and 0,6±0,2 fmol/l respectively, p<0,05), HC (25,7±6,04 and 16,2±6,5 umol/l, respectively, p<0,05), vWF (1,3±0,8 and 1,1±0,6 mg/dl, respectively, p<0,05) and tPA (13,05±6,2 and 8,5±6,2 umol/l respectively, p<0,05). The NOx level correlated with smoking (r=0,46, p<0,05), HC level with smoking (r=0,4, p<0,05), and vWF level with the risk level of SCORE (r=0,43, p<0,05). In a controled group, the smokers, turned out to have significantly higher level of HC (20,7±5,3 and 17,2±4,7 umol.l, respectively, p<0,05), vWF (1,3±0,8 and 0,8±0,6 mg/dl, respectively, p<0,05) and tPA (11,1±6,5 and 6,6±5,2 umol/l, respectively, p<0,05). The changes in NOx and E-1 level were not significant.
Conclusion: we observed an increase in level of ED markers in smokers with EH and of the control group. That confirms an important influence of smoking not only on development, but also progression of ED.

V. Podzolkov: None. **A. Bragina:** None. **N. Druzhina:** None. **L. Mohammadi:** None. **N. Murashko:** None.

687

CaMKII in Mitochondria of Smooth Muscle Cells Controls Mitochondrial Mobility, Migration and Neointimal Hyperplasia

Emily K Nguyen, Olha Koval, Isabella Grumbach, Univ of Iowa, Iowa City, IA

Objective: To define the mechanisms by which mitochondria control VSMC migration and impact neointimal hyperplasia. **Approach and Results**: The multifunctional Ca^{2+}/calmodulin-dependent kinase II (CaMKII) in the mitochondrial matrix of VSMC drove a feed-forward circuit with the mitochondrial Ca^{2+} uniporter (MCU) to promote matrix Ca^{2+} influx. MCU was necessary for the activation of mitochondrial CaMKII (mtCaMKII), whereas mtCaMKII phosphorylated MCU at the regulatory site S92 that promotes Ca^{2+} entry. mtCaMKII was necessary and sufficient for PDGF-induced mitochondrial Ca^{2+} uptake. This effect was dependent on MCU. mtCaMKII and MCU inhibition abrogated VSMC migration and mitochondrial translocation to the leading edge. Overexpression of WT MCU, but not MCU S92A mutant in $MCU^{-/-}$ VSMC rescued migration and mitochondrial mobility. The outer mitochondrial membrane GTPase Miro-1 promotes mitochondrial mobility, but arrests it in subcellular domains of high Ca^{2+} concentrations. In $Miro\text{-}1^{-/-}$ VSMC, mitochondrial mobility and VSMC migration were abolished, overexpression of mtCaMKII nor a CaMKII inhibitory peptide in mitochondria (mtCaMKIIN) had no effect. Consistently, inhibition of mtCaMKII increased and prolonged cytosolic Ca^{2+} transients. MtCaMKII inhibition diminished phosphorylation of focal adhesion kinase and myosin light chain, leading to reduced focal adhesion turnover and cytoskeletal remodeling. In a transgenic model of selective mitochondrial CaMKII inhibition in VSMC, neointimal hyperplasia was significantly reduced after vascular injury.
Conclusions: These findings identify mitochondrial CaMKII as a key regulator of mitochondrial Ca^{2+} uptake via MCU, thereby controlling mitochondrial translocation and VSMC migration following vascular injury.

E.K. Nguyen: None. **O. Koval:** None. **I. Grumbach:** None.

688

Differential Matricellular Protein (CCN) Expression in Atherosclerotic and Aneurysmal Smooth Muscle Cells

Monica Polcz, Vanderbilt Univ. Medical Ctr, Nashville, TN; Nathan Airhart, West Virginia Univ, Morgantown, WV; Monique Marshall, John Curci, Vanderbilt Univ. Medical Ctr, Nashville, TN

Introduction: Recent evidence implicates reduced activity of CCN3 as a mediator of MMP production and aortic wall degeneration in the process of model aortic aneurysm. We have previously shown that AAA-derived VSMC have increased elastolytic activity. We hypothesized that there would be differential CCN expression and production by VSMC derived from human AAA or derived from human atherosclerotic plaque.
Results: Early passage cell lines of VSMC lineage as confirmed by flow cytometry were analyzed by Illumina expression array. The VSMC were derived from infrarenal aneurysm (AAA, n=22) or atherosclerotic plaque (Pl, n=29). There were no differences in expression of CCN1, 2, 5 or 6

(Fig A) between the two cell types. Expression of CCN3 was significantly reduced in AAA compared to PI, CCN4 was significantly greater in AAA than in PI-derived VSMC. Western blot of cellular extracts from these cells (n=3 each) confirms qualitatively greater CCN3 in PI vs AAA VSMC, while no appreciable difference was seen in the production of CCN4 (Fig B). Production of CCN1, 2 and 6 are qualitatively similar and there may be slightly lower CCN5 production in PI vs AAA-derived VSMC (Data not shown). Matricellular protein expression show distinct patterns between Plaque-derived and AAA-derived VSMC and may be related to the enhanced elastolytic activity of cells in AAA.

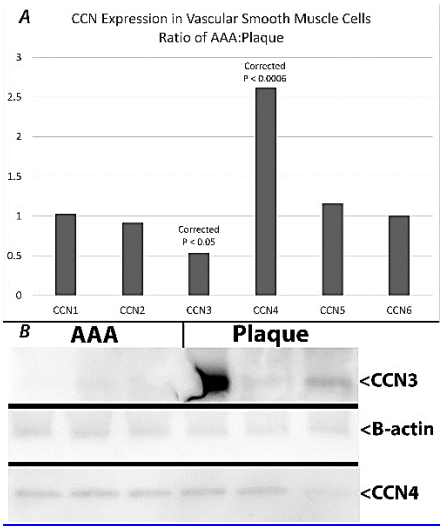

M. Polcz: None. **N. Airhart:** None. **M. Marshall:** None. **J. Curci:** None.

690
Endothelial-Specific Krüppel-Like Factor 2 Inactivation Promotes Endothelial Dysfunction in the Setting of Uremia
Keith L Saum, Begoña Campos-Naciff, Univ of Cincinnati, Cincinnati, OH; Diego Celdran-Bonafonte, Prabir Roy-Chaudhury, Univ of Arizona, Tucson, AZ; A. Phillip Owens III, A. Phillip Owens III, Univ of Cincinnati, Cincinnati, OH

Background: Uremic solutes that accumulate in end-stage renal disease (ESRD) contribute to endothelial dysfunction and subsequent cardiovascular disease in ESRD patients. However, the specific mechanisms which mediate uremia-induced endothelial dysfunction in ESRD are not understood. Kruppel-like factors (KLFs) are important regulators of endothelial homeostasis which may be affected by the uremic milieu. In this study, we examined the role and regulation of endothelial KLF2 in mediating endothelial dysfunction in the setting of uremia. **Methods and Results**: First, we assessed the impact of the uremic milieu on endothelial gene expression utilizing serum from uremic and non-uremic pigs with chronic renal insufficiency. We demonstrate that KLF2 expression was dose-dependently decreased with uremic serum in human umbilical vein endothelial cells (HUVECS) versus normal serum which was reversed by prolonged serum dialysis or the application of laminar shear stress. Carboxymethyl-lysine (CML) modified albumin, a uremic advanced glycation end-product (AGE), also inhibited KLF2 expression. This effect was completely abrogated by receptor for AGE (RAGE) siRNA, as well as by a constitutively active form of IκBα, implicating a role for RAGE activation and the NF-κB signaling pathway. KLF2 suppression also promoted endothelial dysfunction in vitro, as adenoviral overexpression of KLF2 inhibited reactive oxygen species production and leukocyte adhesion in HUVECs treated with uremic serum or CML-AGE. For in vivo translation, we utilized high-frequency ultrasound and quantified flow-mediated dilation of the femoral artery in endothelial-specific KLF2 conditional knockout (cKO) mice after 5 minutes of hindlimb ischemia and demonstrated a 50% reduction in vasodilation in KLF2 cKO mice compared to controls. The lack of femoral artery vasodilation in KLF2 cKO mice was also accompanied by attenuated return of wall shear stress to baseline independent of blood velocity. **Conclusions**: Collectively, these observations implicate loss of endothelial KLF2 as mediator of endothelial dysfunction in the setting of uremia and suggest that elevating KLF2 expression may be a novel strategy for prevention and treatment of cardiovascular disease in ESRD.

K.L. Saum: None. **B. Campos-Naciff:** None. **D. Celdran-Bonafonte:** None. **P. Roy-Chaudhury:** None. **A. Owens III:** None. **A. Owens III:** None.

691
Mir-146a as a Modulator and Pathomechanistic Target of Vascular Calcification
Isabel N Schellinger, Giriprakash Chodisetti, Karin Mattern, Sabine Maamari, Anne Petzold, Joanna Jakubiczka, Gerd Hasenfuss, **Uwe Raaz**, Univ Heart Ctr Goettingen, Goettingen, Germany

Background: Arterial stiffness, which may develop due to vascular calcification, is a significant pathophysiological factor associated with arterial aging or diseases such as type-2 diabetes or end stage renal disease. With no effective therapy clinically available to date, molecular and epigenetic mechanisms of ectopic calcification in conduit arteries are receiving increasing attention to identify targets for therapeutical interference. Here we show that miR-146a may serve as a therapeutic candidate to counteract vascular calcification. **Methods:** Ectopic calcification was assessed in human aortic smooth muscle cells (AoSMCs) using Alizarin red and Von kossa stainings. The total calcium content in hydroxyapatite crystals was assessed using QuantiChrom™ calcium assay kit. The mRNA expression levels of BMP2, MSX2 and SORT1 were assessed by TaqMan real-time PCR. **Results:** The endogenous expression of miR-146a was significantly decreased and simultaneously ectopic calcium deposition was significantly increased in AoSMCs exposed to osteogenic stimulation. However, overexpression of miR-146a in AoSMCs cultured in vitro reduced the ectopic calcium deposits. Simultaneously, mRNA expression levels of osteogenic markers and drivers of calcification, such as BMP2, MSX2 and SORT1 - all predicted miR-146a target genes - were significantly reduced. Conversely, significantly increased calcium deposits were observed when miR-146a was inhibited in these cells in similar culture conditions with upregulated BMP2, MSX2 and SORT1 mRNA expression levels. **Conclusion:** The results suggest that miR-146a may serve as a modulator of AoSMC calcification and miR-146a supplementation may qualify as a therapeutic intervention to counteract vascular calcification due to aging, type-2 diabetes or end stage renal disease.

I.N. Schellinger: None. **G. Chodisetti:** None. **K. Mattern:** None. **S. Maamari:** None. **A. Petzold:** None. **J. Jakubiczka:** None. **G. Hasenfuss:** None. **U. Raaz:** None.

692
Development of the Gene Therapy With CRE Decoy ODN to Prevent Vascular Intimal Hyperplasia
Daiki Uchida, Yukihiro Saito, Satoshi Hirata, Nobuyoshi Azuma, Asahikawa Medical Univ, Asahikawa, Japan

《Background》 Intimal hyperplasia (IH) is the main cause of vein graft stenosis or failure after bypass surgery. However, in the previous study, no therapeutic targets for the treatment of IH have been identified. Our recent research have been reported that the inhibition of Cyclic adenosine monophosphate response-element (CRE) binding protein (CREB) activation is a key role for vein graft IH. 《Objective 》 In consideration of future clinical application, we focused on decoy oligodeoxynucleotide (ODN) transfection as gene therapy strategy for suppressing IH. The goal of the present study is to identify whether the CRE decoy ODN had the therapeutic efficacy for suppressing IH. 《Methods》 We developed phosphorothioate CRE decoy ODN and checked

binding ability to a CRE sequence using CREB transcription assay . We chose a decoy ODN having high first-binding ability and transfected it to vascular smooth muscle cell(VSMC) in vitro. Proliferation was assessed using MTS assay and migration was assessed using a modified Boyden-chamber assay. We examined CRE activity using Luciferase reporter gene assay. We checked expression of mRNAs using qRT-PCR. In wire-injury mouse model(C57BL6,n=6), CRE decoy ODN was transfected to injured vessel wall using ultrasound-sonoporation method in vivo. 《Results》 CREB transcription factor assay showed CRE decoy had about 80 folds binding ability of control decoy in IC50 value (vs.control,n=5). Transfer of CRE decoy ODN resulted in significantly downregulated CRE activity(vs.control,P<.01,n=12) and inhibited VSMC proliferation (vs.control,P<.01,n=12) and migration (vs.control,P<.01,n=5). In a wire-injury mouse model, histopathological analysis revealed that transfer of the CRE decoy ODN significantly repressed IH whereas intensive IH was observed in the control group. In this vessel tissue, Levels of mRNA CCNA2 and Bcl2 were significantly lower in CRE decoy group than in control group(n=6,P<.01,respectively). CRE-activated gene expression was strongly repressed. 《Conclusions》 The present result suggested that CRE decoy ODN inhibiting CREB function provide an effective therapeutic approach to suppressing IH.

D. Uchida: Research Grant; Modest; MEXT KAKENHI Grant. **Y. Saito:** None. **S. Hirata:** None. **N. Azuma:** None.

693

RNA Stability Protein ILF3 Mediates IL-19 Induced Angiogenesis

Christine N Vrakas, Allison B Herman, Mitali Ray, Gavin Landesberg, Sheri E Kelemen, Rosario Scalia, Michael V Autieri, Lewis Katz SOM at Temple Univ, Philadelphia, PA

Angiogenesis is a physiological process vital for growth, development and wound healing but is also a promising therapeutic target for the treatment of ischemic cardiovascular disease. Presently, there is nothing known regarding the role of, the RNA binding protein, Interleukin Enhancer-binding Factor 3 (ILF3) in angiogenesis. RNA binding proteins play crucial roles in cellular processes, specifically, post-transcriptional control of RNAs through mRNA stabilization. We hypothesized that ILF3 plays an essential role in angiogenesis through the stabilization of pro-angiogenic mRNA transcripts. Using immunohistochemistry we identified abundant ILF3 expression in $CD31^+$ vessels of hypoxic porcine cardiac tissue exposed to ischemic myocardial infarction. Using both western blotting and qRT-PCR, we found that pro-angiogenic stimuli, IL-19 and VEGF, induce ILF3 expression in cultured human coronary artery endothelial cells (hEC). Angiogenic proliferation, migration and tube formation are all significantly reduced in hEC when ILF3 is knocked down using siRNA. Importantly, these angiogenic assays are significantly increased when ILF3 is overexpressed in hEC using adenovirus. Using ILF3 siRNA in addition to VEGF stimulation in hEC, several angiogenic factors including CXCL1, IL-8, and HGF are decreased at the transcript and protein level. However, these angiogenic factors are increased when hEC are infected with AdILF3 and stimulated with VEGF. Through immunohistochemistry we found that ILF3 translocates from the nucleus to the cytoplasm of hEC stimulated with VEGF or IL-19 at various time points, suggesting a role in mRNA stability. Using the transcription inhibitor actinomycin D, we found that ILF3 stabilizes pro-angiogenic transcripts including VEGF, CXCL1, and IL-8 in hEC. Together these data suggest that in endothelial cells, the RNA stability protein, ILF3, plays a novel and central role in angiogenesis. We believe that ILF3 is impacting functional angiogenesis through cytokine-inducible mRNA stabilization of pro-angiogenic transcripts.

C.N. Vrakas: None. **A.B. Herman:** None. **M. Ray:** None. **G. Landesberg:** None. **S.E. Kelemen:** None. **R. Scalia:** None. **M.V. Autieri:** None.

694

Smooth Muscle Cell TBR2 Deletion in Mice Decreases Nitric Oxide Bioavailability

Jay Zhu, Univ of Washington, Seattle, WA; Fatos I Yildirim, Istanbul Univ, Istanbul, Turkey; Stoyan N Angelov, Hao Wei, Univ of Washington, Seattle, WA; Frank V Brozovich, Mayo Clinic, Rochester, MN; Francys Kim, David Dichek, Univ of Washington, Seattle, WA

Background: Abnormal smooth muscle cell (SMC) TGF-β signaling is thought to cause both syndromic and nonsyndromic thoracic aortic aneurysms and dissections (TAAD). However, the mechanisms by which altered SMC TGF-β signaling causes TAAD are poorly understood. To investigate the roles of SMC TGF-β signaling in maintaining normal aortic physiology, we generated mice with SMC-specific deletion of the type II TGF-β receptor (TBR2). SMC-TBR2-deficient mice have thickened aortic medias. When evaluated with tension myography, aortas of SMC-TBR2-deficient mice have a hypercontractile response to phenylephrine (PE) and impaired relaxation to acetylcholine (ACh). We investigated the cellular and molecular basis of these vasomotor abnormalities.
Methods & Results: Tension myography showed that SMC-TBR2-deficient aortas were also hypercontractile to K^+; yet hypercontractility was less than with PE suggesting mechanisms other than increased SMC contractile proteins. Accordingly, immunoblots revealed no increase in smooth muscle myosin heavy chain and alpha actin in SMC-TBR2-deficient aortas. To test the role of endothelium in the hypercontractile response, we compared PE responses in WT and SMC-TBR2-deficient aortas with and without endothelial denudation. Endothelial denudation blunted the difference in contractility to PE, demonstrating that hypercontractility in SMC-TBR2-deficient aortas depends on the presence of endothelium ($p<0.05$ by ANOVA for interaction of PE and endothelium; n=9-10). eNOS deficiency was not responsible for hypercontractility to PE and impaired relaxation to ACh, as SMC-TBR2-deficient aortas had normal levels of eNOS protein. However, SMC-TBR2-deficient aortas had decreased phosphorylation of vasodilator-associated phosphoprotein, an indicator of nitric oxide bioavailability, (64% reduction; $p<0.0001$; n=8).
Conclusion: Loss of physiologic SMC TGF-β signaling causes aortic hypercontractility and deficient endothelium-dependent relaxation by impairment of endothelial function that includes decreased nitric oxide bioavailability. We speculate that endothelial dysfunction may contribute to the pathogenesis of TAAD associated with abnormal TGF-β signaling.

J. Zhu: Research Grant; Significant; NIH T32 Cardiovascular Training Grant: T32HL007828. **F.I. Yildirim:** None. **S.N. Angelov:** None. **H. Wei:** None. **F.V. Brozovich:** None. **F. Kim:** None. **D. Dichek:** Research Grant; Significant; NIH funding: R01HL116612.

695

Rage-mDia1 Mediates Vascular Remodeling in Angiotensin Ii Induced Thoracic Aortic Aneurysm

Maximilian Kreibich, Samiat Awosanya, Joseph E Bavaria, **Emanuela Branchetti**, Univ Pennsylvania, Philadelphia, PA

Background. The Receptor for Advanced Glycation End Products (RAGE), when activated, induces irreversible vascular tissue injury by promoting pro-oxidative and pro-inflammatory signaling pathways. RAGE signal transduction requires the engagement of RAGE cytoplasmic domain with the formin Diaphanous 1 (mDia1) and results in the release of soluble RAGE in the circulation. We have previously demonstrated that the RAGE/sRAGE axis is involved in the development and progression of thoracic aortic aneurysm (TAA) in humans and mice. Elevated levels of sRAGE are

found in aneurysmal patients and in mouse models of TAA. In addition, RAGE inhibition counteracts aortic dilatation and the release of sRAGE in the circulation. We hypothesize that RAGE induced vascular remodeling in TAA is mediated by mDia1. **Methods.** AngII infusion (1000 ng/Kg/min) was performed in C57BL6 male mice, fed with hypercolesterolaemic diet. Mice were treated for 4 weeks with losartan or with a RAGE antagonist (RAP). Ascending aortas of treated animals were harvested at day 28 post-infusion. Aortic dilatation and degeneration were assessed by echocardiography and histology. Immunofluorescence and Real Time PCR were performed to evaluate the expression of RAGE, mDia1, extracellular matrix proteins (ECM) and pro-inflammatory genes. **Results.** AngII infusion induces ascending aorta dilatation and medial thickening characterized by a substantial ECM deposition. RAGE and mDia1 expression is significantly increased in the aneurysmal aorta of mice chronically infused with AngII together with up-regulation of pro-inflammatory molecules (IL-6, MCP-1, IL1beta, TLR4, CCR2) and markers of extracellular matrix remodeling (Col1, Col3, MMP-2 and MMP12). Inhibition of RAGE dampens mDia1 expression and significantly reduces medial pro-inflammatory and pro-fibrotic signals while counteracting aneurysm formation. **Conclusion.** Formin mDia1 is involved in RAGE mediated TAA formation. Strategies that block RAGE-mDia1 interaction may unveil novel therapeutic approaches for the treatment of TAA.

M. Kreibich: None. **S. Awosanya:** None. **J.E. Bavaria:** None. **E. Branchetti:** None.

696

Transgelin in Aortic Abdominal Aneurysm and its Potential Link in Electronic Cigarette Vapor Mediated Cardiovascular Disease

Abhijit Ghosh, Will Krause, Seth Kasten, Andrew Abdallah, Anirudh Hirve, Univ Michigan Sch Med, Ann Arbor, MI; Angela Pechota, Michigan State Univ, East Lansing, MI; Laura Durham, Veronica Dunivant, Jonathan L Eliason, Univ Michigan Sch Med, Ann Arbor, MI

Introduction:
The E-cigarette form of smoking (e-cig) has rapidly increased. Potential adverse cardiovascular effects are unknown. We sought to determine if e-cig use affects Transgelin (TAGLN), an actin binding protein with multiple important cell-signaling and regulatory actions noted to be targeted by autoantibodies in AAA.
Methods: Human aortas and serum from abdominal aortic aneurysm (AAA) (n=26) and non-AAA (n=15), and rat aortas from elastase-perfused (EP) or saline-perfused (SP) animals (n=3 each group) were analyzed for aortic transgelin (TAGLN) and alpha smooth muscle actin (α-sma) content, serum TAGLN content and/or serum anti-TAGLN antibodies (AB). Rats exposed to e-cig vapor (EV) 90 min/day for 4 or 8 weeks , or room air (RA) (n=6 per group), and rats undergoing aortic low-dose topical elastase (LDTE) to induce inflammation followed by EV or RA x 100 days (n=6 per group), were also analyzed. Aortas were assessed by Western blot for TAGLN and actin content, while serum studies used Elisa to detect circulating TAGLN, or anti-TAGLN antibodies.
Results: Western blots revealed loss of TAGLN and α-sma in the aortas of AAA compared to control tissues. In rat AAA we observed loss of TAGLN and diminished levels of α-sma in EP compared to SP control aortas. Serum from AAA patients had increased anti-TAGLN antibodies (*P*=0.085, 45% more in AAA) and circulating TAGLN (P=0.008) compared to controls. LDTE EV rat aortas had less TAGLN (*P*=0.002) and α-sma (*P*=0.008) compared to RA rats throughout the aorta. LDTE + EV rat serum had high levels of anti-TAGLN antibodies (P=0.027) and circulating TAGLN (P=0.007) compared to RA rats.
Conclusion: These results show that AAA is associated with decreased aortic TAGLN in humans and rats in the region of the aneurysm. EV exposure alone, and especially following LDTE results in marked reduction of TAGLN throughout all segments of the aorta. Human AAA patients and EV rats with LDTE also exhibit elevation of circulating TAGLN and anti-TAGLN antibodies. These results suggest an autoimmune mechanism for TAGLN targeting in the aorta when AAA is present or e-cig vapor exposure occurs, and that e-cig use may result in cardiovascular risk.

A. Ghosh: None. **W. Krause:** None. **S. Kasten:** None. **A. Abdallah:** None. **A. Hirve:** None. **A. Pechota:** None. **L. Durham:** None. **V. Dunivant:** None. **J.L. Eliason:** None.

698

Functional Analysis of Smad3 Deficiency in VSMCs Derived From Crispr/cas9-modified Human Induced Pluripotent Stem Cells

Jian Gong, Ping Qiu, Eugene Chen, Bo Yang, Univ of Michigan, Ann Arbor, MI

Introduction: Transcription factor Smad3 plays key roles in both TGF-β signaling transduction and vascular smooth muscle cells(VSMCs) differentiation. SMAD3 gene mutations cause aneurysms-osteoarthritis syndrome(AOS), an autosomal dominant genetic disease with high rate occurrence of thoracic aortic aneurysm(TAA) and early-onset osteoarthritis. The production of patient-derived hiPSCs and genomic-modified ihPSCs by using Crispr/Cas9 technique provide a promise for in vitro disease modeling of SMAD3 mutation in VSMCs as well as drug screening for potential therapeutic targets.
Hypothesis: We hypothesis that introducing SMAD3 mutations into hIPSCs that mimic the identified genotypic alteration in AOS patients could recapture the phenotypic defects of differentiation, contractibility and extracellular matrix(ECM) of VSMCs derived from hIPSCs-differentiated neural crest stem cells(NCSCs), the embryonic origin of VSMCs for both aorta root and ascending aorta.
Method: hIPSCs were generated from non-TAA patients' peripheral blood mononuclear cells by overexpression of Yamanaka factors. The indel mutation targeting SMAD3 exon5 were induced by using Crispr/Cas9 technique, which form frameshift mutation close to one in identified AOS patients. Selected cell clones of genomic modified hIPSCs were differentiated into NCSCs-derived VSMCs. Comparing analysis of VSMCs function were proceed in both hIPSCs lines with or without SMAD3 mutation.
Result: We generated a homozygote with SMAD3 frameshift mutation. It contains a 7-base pair deletion(c.633_639delGATGTCC), which is similar with a pathogenic Smad3 mutation (c.652 delA). This mutation leads to a premature stop codon and remove the Smad3 protein. The qRCR and WB result showed that the expression of ACTA2 decreased in the differentiated SMC with SMAD3 mutation. Also, the expression of elastin, collagen type III were significantly down-regulated in the SMAD3 mutation cell line while the MMP9 was up-regulated.
Conclusion: SMAD3 mutation may cause defects of differentiation, contractibility and ECM synthesis of VSMCs derived from NCSC.

J. Gong: None. **P. Qiu:** None. **E. Chen:** None. **B. Yang:** None.

699

Endothelial Mineralocorticoid Receptor and Neutrophils Mediate Aldo plus Salt-Induced Abdominal Aortic Aneurysm

Shu Liu, Yu Zhong, **Zhenheng Guo**, Ming Gong, Univ of Kentucky, Lexington, KY

Background—We recently reported that administration of mice with Aldo or deoxycorticosterone acetate (DOCA) plus salt induces abdominal aortic aneurysm (AAA) and treatment of mice with mineralocorticoid receptor (MR) blockers abolished Aldo plus salt-induced AAA. However, the mechanism by which Aldo plus salt induces AAA is largely unknown. Methods—A tamoxifen inducible EC (EC)-specific MR knockout mouse model (iECMRKO) was developed. ECMRKO mice, and control mice were administered with

Aldo or DOCA plus sat salt to induce AAA. C57BL/6 mice were injected with anti-mouse polymorphonuclear (PMN) leukocytes antibody to deplete neutrophils. The aortic internal and external diameter, the aortic dilation rate, and the incidence of AAA were determined. Results—Selective genetic deletion of MR from ECs, protects mice from Aldo or DOCA plus salt-induced AAA. EC-specific MR deletion had little effect on Aldo plus salt-induced sodium retention, hypertension, and renal fibrosis, but largely suppressed aortic elastin degradation, matrix metallopeptidase (MMP) 2 and MMP9 upregulation, macrophage and neutrophil infiltration. Surprisingly, neutrophil, but not macrophage, was observed in aorta from control mice, but not iECMRKO mice, indicating that neutrophils but not macrophages is involved in the early processes of Aldo plus salt-induced and endothelia MR-mediated AAA development. Treatment of C57BL/6 mice with of anti- PMN antibody selectively suppressed DOCA plus salt-induced circulating Ly6G-postive neutrophils, but not CD4-postive leukocytes, protected mice from DOCA plus salt-induced AAA. Aldo-induced endothelial adhesion molecule (E-selectin, P-selectin, ICAMP1, and VCAM-1) and proinflammatory cytokine (IL-6 and MCP-1) mRNA expressions were abolished in cultured MR-deficient ECs. Aldo plus salt-induced ICAM-1 but not VCAM-1 protein upregulation was abolished in aorta from ECMRKO mice. Conclusions—Our results demonstrate a significant role of endothelial MR, in Aldo plus salt-induced AAA. Moreover, our results also reveal a provocative mechanism by which ICAM-1, but not VCAM-1, and neutrophils, but not macrophages, mediates the early processes of Aldo plus salt-induced and endothelia MR-mediated AAA development.

S. Liu: None. **Y. Zhong:** None. **Z. Guo:** None. **M. Gong:** None.

700

Adipocyte-Specific Calpain-2 Deficiency Attenuates Obesity-accelerated Abdominal Aortic Aneurysms in Mice

Aida Javidan, Weihua Jiang, Jessica J. Moorleghen, Venkateswaran Subramanian, Univ of Kentucky, Lexington, KY

Background and Objective: Recent clinical studies demonstrated that abdominal adiposity is associated with increased risk of abdominal aortic aneurysm (AAA) development. Calpains are non-lysosomal calcium dependent cysteine proteases that are highly expressed in human and experimental AAAs. Using a pharmacological inhibitor and genetically deficient mice, we identified that calpain-2 (a major ubiquitous isoform) plays a critical role in Angiotensin II (AngII)-induced AAA formation in obese mice. In addition, we demonstrated that calpain inhibition strongly suppressed adipose tissue inflammation in obese mice. The purpose of this study was to determine the role of adipocyte-specific calpain-2 on obesity-accelerated AAA. **Methods and Results:** Calpain-2 floxed mice that were hemizygous for Adiponectin Cre (Cre+/0) were produced by breeding male Cre+/0 to female calpain-2 floxed mice. Littermates that were homozygous for the floxed calpain-2 gene, but without the Cre transgene (Cre0/0), were used as control mice. Western blot analyses showed that calpain-2 protein is depleted in various fat tissues including periaortic adipose, from Cre+/0 mice, while not influencing abundance in aorta and other tissues. Male Cre+/0 and Cre0/0 mice were fed a high fat diet (60% Kcal) for 20 weeks. After 16 weeks of diet feeding, mice (n=20-22) were infused with either saline or AngII (1,000 ng/kg/min) by osmotic minipumps for 4 weeks. Depletion of calpain-2 in adipocytes had no effect on high fat diet-induced body weight gain, fat mass, glucose and insulin tolerance. Interestingly, adipocyte-specific calpain-2 depletion significantly attenuated AngII-induced expansion of ex-vivo maximal diameter of abdominal aortas in obese mice (Saline- Cre0/0: 0.95 ± 0.03; Cre+/0: 0.98 ± 0.02 mm; AngII - Cre0/0: 1.95 ± 0.20; Cre+/0: 1.25 ± 0.08 mm P<0.001). In addition, calpain-2 depletion also reduced the incidence of AngII-induced AAAs in mice (Cre0/0: 76% versus Cre+/0: 27%). **Conclusion:** These findings suggest that adipocyte-derived calpain-2 plays a critical role in AngII-induced AAA development in diet-induced obese mice.

A. Javidan: None. **W. Jiang:** None. **J. Moorleghen:** None. **V. Subramanian:** None.

This research has received full or partial funding support from the American Heart Association.

705

Nudt6 Inhibition Limits Smooth Muscle Cell Apoptosis and Abdominal Aortic Aneurysm Progression

Hong Jin, Hanna Winter, Ekaterina Chernogubova, Yuhuang Li, Greg Winski, Alexandra Bäcklund, Lars Maegdefessel, Karolinska Inst, Solna, Sweden

Abdominal Aortic Aneurysm (AAA) is a highly lethal disease, of which diagnosis and treatment is still a major burden. Natural Antisense Transcripts (NAT) are known to inhibit key transcripts by antisense targeting. Their contribution to the development and progression of aneurysm disease has not been studied to date. The aim of this study was to investigate the role of the NAT Nudix Hydrolase 6 (Nudt6) and its antisense target Fibroblast growth factor (Fgf2) in AAA disease, by modulating NUDT6 *in vivo* in Angiotensin II (AngII)-induced experimental AAA *via* sonoporation (microbubble procedure) as well as *in vitro* in primary mouse aortic smooth muscle cells (mAoSMCs) via transfection. Further, primary mAoSMCs were observed using the IncuCyte imaging system to monitor changes in dynamic processes like proliferation and apoptosis. FGF2 is known to be a potent mitogen of smooth muscle cell (SMC) proliferation; a process being drastically diminished in AAA progression. By inhibiting Nudt6 with GapmeR *in vivo* we could observe smaller aortic diameters, increased both Fgf2 expression and SMCs survival by immunohistochemistry. *In vitro*, proliferation was increased in Nudt6 inhibited AngII-stimulated primary mouse aortic SMCs. Overexpression of Nudt6 did not have a significant effect on proliferation. Nudt6 and Fgf2 gene expression are inversely correlated and experience a switch of expression patterns during AngII stimulation over a longer period of time if primary SMCs are transfected with Nudt6 inhibitor and treated with AngII. All findings suggest a beneficial effect of Nudt6 inhibition in experimental AAA. In the future, it could be used as a potential therapeutic target in AAA by increasing SMC survival rates.

H. Jin: None. **H. Winter:** None. **E. Chernogubova:** None. **Y. Li:** None. **G. Winski:** None. **A. Bäcklund:** None. **L. Maegdefessel:** None.

706

Effect of Intraluminal Thrombus on the Transcriptome of the Tunica Media and Adventitia in Abdominal Aortic Aneurysms

Moritz Lindquist Liljeqvist, Rebecka Hultgren, Christina Villard, Malin Kronqvist, Per Eriksson, Joy Roy, Karolinska Instt, Stockholm, Sweden

OBJECTIVE: Most clinically significant abdominal aortic aneurysms (AAA) contain an intraluminal thrombus (ILT), the role of which in the AAAs progression to rupture remains unclear. Our objective was to describe the tunica-specific coding and non-coding transcriptome of ILT-covered and -free AAA vessel wall. METHODS: Aortic tissue samples from 76 patients with AAA and 13 transplant donors (controls) were collected from our biobank and analyzed with Affymetrix HTA 2.0 microarrays. For 34 patients, a comparison between ILT-covered and -free vessel wall could be made. All samples were divided into intimal/medial and adventitial wall layers. Differential expression and orthogonal partial least squares discriminant analysis (OPLS-DA) were performed with R. Gene set enrichment analysis (GSEA) was performed for annotated transcripts against the Molecular Signatures Database hallmark gene sets. RESULTS: 4691 and 164 genes, before and after correction for multiple comparisons, respectively, were differentially

expressed in the ILT-covered vs ILT-free media of AAAs with TGFB2 being the most downregulated and IL3RA the most upregulated gene. The corresponding numbers for adventitia were 926 and 0. Epithelial mesenchymal transition, angiogenesis, hypoxia and notch signalling gene sets were upregulated, whereas TNF-alpha signalling was downregulated, in the ILT-covered compared with ILT-free tunica media. In the AAA vs Ctrl comparisons, both ILT-covered and -free AAA media showed a strong upregulation of apoptosis and inflammatory pathways, such as allograft rejection. Using OPLS-DA, significant separation could be made between ILT-covered and -free AAA media, but not adventitia. CONCLUSIONS: The presence of an ILT is associated with the expression of genes related to epithelial mesenchymal transition, angiogenesis and hypoxia in the underlying tunica media of AAAs.

M. Lindquist Liljeqvist: None. **R. Hultgren:** None. **C. Villard:** None. **M. Kronqvist:** None. **P. Eriksson:** None. **J. Roy:** None.

707

Vascular Smooth Muscle Cell Tfeb Deletion Promotes Abdominal Aortic Aneurysms

Haocheng Lu, Yanbo Fan, Wenying Liang, Wenting Hu, Wenhao Xiong, Ziyi Chang, Minerva Garcia-Barrio, Jifeng Zhang, Yuqing Chen, Univ of Michigan, Ann Arbor, MI

Rationale: Abdominal aortic aneurysm (AAA) is a vascular disease with a very high mortality rate in the case of rupture. Vascular smooth muscle cells (VSMCs) are crucial to maintaining vascular integrity and function. Transcription Factor EB (TFEB) is a master regulator of autophagy and lysosomal biogenesis in a variety of cell types via inducing the transcription of a coordinated lysosomal regulatory gene network. TFEB shows anti-inflammatory and anti-atherosclerotic effects in vascular endothelial cells and macrophages. However, the role of TFEB in vascular disease remains to be further explored.
Objectives: To investigate the role of VSMC TFEB in AAA.
Methods and Results: We found that TFEB was down-regulated in human aortic aneurysmal lesion compared with the non-lesion area by QRT-PCR and immunostaining. In human aortic smooth muscle cells (HASMCs), TFEB mRNA and protein abundance were decreased upon treatment with pro-inflammatory factors while adenovirus-mediated TFEB overexpression potently inhibits inflammation, apoptosis (caspase 3 cleavage and Annexin V staining) and matrix metalloproteinase activity (zymography). A consistent phenotype was observed in the TFEB knockdown HASMCs. Mechanistically, TFEB activates the PI3K-Akt pathway, and PI3K inhibitors (wortmannin and LY294002) abolished the anti-apoptotic effect of TFEB in HASMCs. Utilizing VSMC-specific TFEB deficiency mice (floxed-TFEB/myh11-ERT2 cre+), we determined the effect of TFEB on AAA formation in vivo. In the mouse aneurysm model induced by the combination of angiotensin II and 3-aminopropionitrile infusion, TFEB VSMC-deletion significantly increases aneurysm formation, rupture, and mortality (n =13-14 for each group, $p< 0.01$).
Conclusions: Our data reveal a critical protective role of TFEB in VSMC homeostasis, suggesting TFEB to be a potential target to treat aortic aneurysm.

H. Lu: None. **Y. Fan:** None. **W. Liang:** None. **W. Hu:** None. **W. Xiong:** None. **Z. Chang:** None. **M. Garcia-Barrio:** None. **J. Zhang:** None. **Y. Chen:** None.

This research has received full or partial funding support from the American Heart Association.

708

Using Global Proteomics and Network Science to Explore Therapeutic Targets for Abdominal Aortic Aneurysm (AAA)

Stephanie Morgan, Lang Ho Lee, Arda Halu, Hideyuki Higashi, CICS Brigham Womens Hosp, Boston, MA; Alan Daugherty, Univ of Kentucky Coll of Med, Lexington, KY; Elena Aikawa, Sasha Singh, Masanori Aikawa, CICS Brigham Womens Hosp, Boston, MA

OBJECTIVE: To understand mechanisms critical to aneurysm development and identify potential therapeutic targets, we performed global proteomics and network analysis in mouse models of AAA.
METHODS and RESULTS: AAAs were produced by luminal perfusion of the infrarenal aorta of C57BL/6 (wild-type) mice with elastase or subcutaneous infusion of angiotensin II (AngII) in Apoe-/- and Ldlr-/- mice (on congenic C57BL/6 background). Aortas were harvested at two intervals corresponding to developing or end-point aneurysm phenotypes that are specific to each model (n=3 for each procedure, interval, and genotype). Aortas were dissected into 8 segments spanning the arch to infrarenal portion, resulting in combined 288 aortic segments for label-free proteomics. Proteins were classified as significantly correlated to aneurysm according to their fold-change over control. Additional correlations were derived from a high-dimensional data analysis tool ("Xina"), developed in our laboratory, which enables clustering of proteins according to model, genotype, aortic region, and interval. Using our criteria, we identified lists of 159 proteins in the Apoe-/- and 158 proteins in the Ldlr-/- mice (AngII infused), and 173 proteins in wild-type mice (elastase perfused). Network analysis of these protein lists reveal commonalities between the models to include protein pathways related to protein translation, immune function, platelet activation, and extracellular matrix organization. Pathways enriched following AngII infusion included phagosome function and platelet aggregation, while pathways enriched in the elastase model included apoptosis, smooth muscle cell contraction, and Fc gamma R-mediated phagocytosis.
CONCLUSION: Identification of pathways and proteins shared among these models may present master regulators of aneurysmal events and identify therapeutic targets. Conversely, identifying aneurysmal events unique to each model will provide valuable information regarding the model(s) chosen for use in a study and help contextualize model-specific findings.

S. Morgan: None. **L. Lee:** None. **A. Halu:** None. **H. Higashi:** Employment; Significant; Kowa Company, LTD. **A. Daugherty:** None. **E. Aikawa:** None. **S. Singh:** None. **M. Aikawa:** Research Grant; Significant; Kowa Company, LTD.

709

Computational Seal Zone Mechanics - Predicting EVAR Failures

Luka Pocivavsek, Univ of Pittsburgh Medical Ctr, Pittsburgh, PA; Christopher Skelly, Ross Milner, The Univ of Chicago, Chicago, IL

Introduction: Endovascular aortic stent-graft technology (EVAR) radically altered aortic aneurysm repair from a maximally invasive procedure to a minimally invasive approach. While the overall principle of the repair remained the same, the surgeon ceded control of graft/aorta coupling with EVAR from the time-honored surgical approach of suturing, which creates a mechanical kinematic coupling constraint at the graft/aorta interface. In EVAR, the coupling condition is replaced by contact mechanics between the outer graft surface and the aorta. We hypothesize that proximal endograft failure is linked to the complex contact mechanics occurring at the graft/aorta interface. **Methods**: We performed a detailed geometric/finite element analysis (FEA) of an abdominal aortic aneurysm in a patient who presented with a ruptured juxta-renal AAA. We used the pre and post-operative CTA imaging to perform FEA and defined the stent graft (SG)/aortic wall interactions using a fully integrated cohesive zone model (CZM) (see figure 1). **Results**: Three degrees of adhesion strength were studied, corresponding to F~0.1, 10, and 1000 Newton. In the case of the two weaker adhesion strengths, the SG and neck separated at local points along the interface. These areas of

separation (interfacial failure) corresponded to zones of high stress (~ 10MPa) within the aortic wall. This points to a new physical model of aortic/SG stability, where local elastic deformation energy in the neck (G) competes with aortic/SG adhesion energy (gamma~Gc) giving rise to the criterion for seal failure: G>Gc . **Conclusions**: The energy balance of deformation of the aortic neck with stent graft adhesion strength provides a key new parameter in evaluating future EVAR repairs. Non-linear neck geometries give rise to complex non-linear stress distributions that can greatly impact the stability of a repair. We provide a computational methodology in which this can be systematically studied for any given patient anatomy.

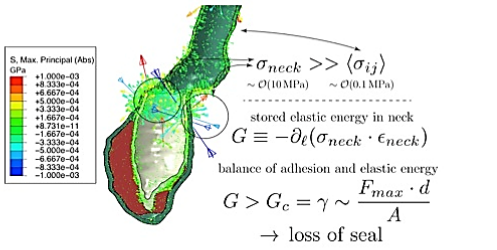

Figure 1: Representative image of finite element analysis showing cross-sectional cut across the system: aorta (green), SG (grey), inter luminal thrombus (red). The vectors correspond to the element based maximal principle stresses (positive – tensile, negative – compressive). As shown, the average stress in the aortic wall around the neck seal zone is nearly ten times that of the normal proximal aorta at systolic pressures. Analysis is based upon the balance of stored elastic energy per unit of adhesive interfacial length in the aortic wall (G) and the adhesion energy (gamma), which is proportional to the maximal displacement force (F), length of neck (d), and area of contact (A). When the available stored elastic energy becomes greater than the adhesive strength of the interface between aorta and SG, the condition of interfacial failure leading to loss of seal exist.

L. Pocivavsek: None. **C. Skelly:** Other; Modest; Inside Ultrasound, Maji Therapeutics, Springer. **R. Milner:** Consultant/Advisory Board; Modest; Medtronic, WL Gore.

710
Deficiency of IL12p40 Promotes Angiotensin II-Induced Abdominal Aortic Aneurysm
Neekun Sharma, Anthony Belenchia, Rishabh Dev, Ryan Toedebusch, Annayya Aroor, Lakshmi Pulakat, Chetan Hans, Univ of Missouri, Columbia, MO

Introduction: Abdominal aortic aneurysm (AAA) is caused by the immune and inflammatory cell accumulation of the aortic wall, leading to enhanced inflammation and aneurysm formation. Our recent studies demonstrate that inhibition of Notch signaling attenuates AAA formation by shifting the macrophage balance towards anti-inflammatory (M2) phenotype. Using IL12p40 knockout (KO) mice, we investigated the direct effects of M2-like macrophages in the development of AAA.
Methods and Results: Male (8-10 week-old) wild-type (WT) and IL12p40-KO mice (n=10) on C57BL/6 background were infused with angiotensin-II (AngII, 1,000 ng/kg/min) by implanting osmotic pumps subcutaneously for 28 days. Comparable increase in mean, systolic and diastolic arterial blood pressure was observed between WT and IL12p40-KO mice in response to AngII. Unexpectedly, AngII significantly increased the AAA-associated mortality (2/10) and luminal expansion (7/10) in IL12p40-KO mice as determined by transabdominal ultrasound. In addition, IL12p40-deficiency significantly increased aortic stiffness in the abdominal aortas in response to AngII than WT as measured by pulse wave velocity (PWV) and atomic force microscopy (AFM). Macroscopic and histological examination also showed that IL12p40-KO mice exhibited severe abdominal aortic lesion formation and increased maximal aortic width compared to WT mice. Increased elastin fragmentation and collagen deposition was detected in aorta of AngII-infused IL12p40-KO mice compared to AngII-infused WT mice. Further, there was no significant change in the total cholesterol, triglycerides and HDL-cholesterol levels in the serum of WT and IL12p40-KO mice treated with AngII. Importantly, bone marrow derived macrophages (BMDM) from IL12p40-KO mice showed increased mRNA expression of M2-markers (TGF-β1 and IL10) and decreased expression of M1-markers (iNOS and TNF-α) at basal level compared to WT BMDM.
Conclusions: IL12p40 deficiency may promote the development of AAA, in part, by facilitating recruitment of M2-like macrophages and potentiating aortic-stiffness and fibrosis mediated by TGF-β1 and IL10. In summary, optimal M1/M2 balance rather than predominance of M2-phenotype may be prerequisite to prevent AAA formation.
N. Sharma: None. **A. Belenchia:** None. **R. Dev:** None. **R. Toedebusch:** None. **A. Aroor:** None. **L. Pulakat:** None. **C. Hans:** None.

711
Gut Bacteria Influences the Growth of Abdominal Aortic Aneurysms in Mice
Ian Stines, Sanjiv Hyoju, Olga Zaborina, John Alverdy, Trissa Babrowski, Univ of Chicago, Chicago, IL

Objectives: The goal of this study was to determine if highly collagenolytic bacteria introduced to the gut microbiome induces abdominal aortic aneurysm in mice.
Methods: C57BL/6 mice received a prolonged 4-day course of preoperative antibiotics (oral clindamycin and subcutaneous cefoxitin) and received pre- and postoperative enemas containing either 10% glycerol solution (control) or a freshly prepared bacterial suspension with a highly collagenolytic strain of *Serratia marcescens* (S2). All mice underwent laparotomy, aortic crush injury with forceps, and application of either 0.9% sodium chloride (control) or 10% calcium chloride to the periadventitial aortic space. Aortic diameter was measured on initial exposure and on sacrifice on postoperative day 21. Groups were compared using a series of Student's T-test.
Results: On postoperative day 21, the difference in aortic diameter for mice treated with periadventitial sodium chloride and glycerol enema was minimal (control 1, n=6, 0.03 mm ± 0.30). In mice treated with periadventitial calcium chloride and glycerol enema, fusiform aneurysm was reliably produced compared to control 1 (control 2, n=6, 0.53 mm ± 0.30, $p \leq 0.05$). In mice treated with periadventitial sodium chloride and S2 enema, fusiform aneurysm was reliably produced with a significant difference in diameter compared to control 1 (n=8, 0.63 mm ± 0.30, $p \leq 0.05$). In mice treated with periadventitial calcium chloride and S2 enema, fusiform aneurysm was reliably produced with a significant difference in diameter compared to control 1 (n=8, 0.59 mm ± 0.30, $p \leq 0.05$). There was no significant difference between the 2 treatment groups.
Conclusions: The introduction of highly collagenolytic *Serratia marcescens* to the gut microbiome of mice in addition to aortic crush injury reliably produces fusiform aortic aneurysm in this model. Further investigation is required to elucidate the mechanism of aneurysm formation.

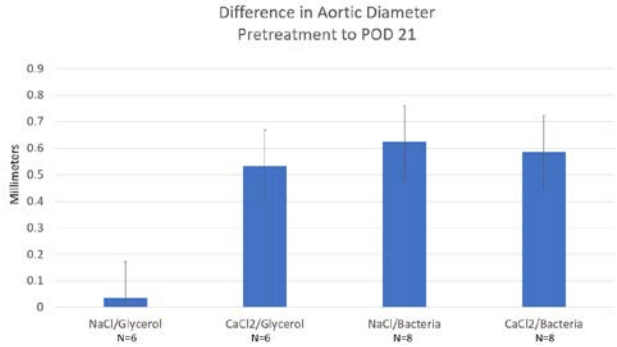

I. Stines: None. **S. Hyoju:** None. **O. Zaborina:** None. **J. Alverdy:** None. **T. Babrowski:** None.

712
Elastin Derived Peptides Augments Abdominal Aortic Aneurysm Formation
Jane Stubbe, Nelly Bjørnes, Tu Quyen Pham, Anne Katrine Kurtzhals, Silke Griepke Dam Nielsen , Univ of Southern Denmark, Odense C, Denmark; Lars Melholt Rasmussen, Jes Sanddal Lindholt, Ctr for Individualized Med in Arterial Diseases, Odense Univ Hosp, Odense C, Denmark

Abdominal aortic aneurysm AAA is a chronic dilatation of the abdominal aorta. It is a potentially life threatening disease as it develops asymptomatic and is often first discovered at the time of rupture. One key element in AAA formation is degradation of the elastin fibers in the aortic wall. When elastin is degraded small bioactive elastin derived peptides (EDPs) are released into the circulation. These EDPs affect vascular smooth muscle cells in the aortic wall and attract monocytes to the aortic wall resulting in further degradation of elastin. We hypothesize that the level of circulating elastin derived peptides (EDPs) augments AAA expansion and that inhibition of circulating EDPs will inhibit AAA expansion. We tested the hypothesis in an elastase induced aneurysm murine model by applying synthetic EDPs or scrambles peptides and measure the AAA size. In addition, EDP-neutralizing antibody or control IgG was given to angiotensin II induced AAA in ApoE-/- mice and AAA size was determined 28 days later. Fourteen days after elastase infusion the abdominal aortic diameter was significantly increased in the EDP treated group when compared to the scramble peptid treated control group (1.33±0.07 vs. 1.13±0.06 mm, n=17-19, p<0.05). Inhibition of circulating EDPs by EDP neutralizing antibodies when compared to IgG controls showed a clear trend toward decreased AAA expansion based on outer aortic diameter (1.4 ±0.1 vs. 2.2 ±0.4 mm, n=8-9, p=0.059) and wet weights of the abdominal aorta (median: 9.2 vs. 22.1 mg, n=7-9, p=0.07) 28 days after angiotensin II infusion in ApoE-/- mice. In the aneurysmal wall of the mice treated with elastin neutralizing antibody, there was less ruptured elastin, and there was significantly fewer infiltrating of CD45 positive cells, while CD206 positive anti-inflammatory M2 macrophages were significantly augmented when compared to IgG treated controls (n=7-9).In conclusion, EDPs augment abdominal aortic aneurysms. Thus, inhibition of circulating EDPs shows great potential against AAA expansion.

J. Stubbe: None. **N. Bjørnes:** None. **T. Pham:** None. **A. Kurtzhals:** None. **S. Griepke Dam Nielsen :** None. **L. Melholt Rasmussen:** None. **J. Sanddal Lindholt:** None.

713
Angiotensin 1-7 Suppresses Experimental Abdominal Aortic Aneurysms
Baohui Xu, Gang Li, Hongping Deng, Anna Cabot, Stanford Univ Sch of Med, Stanford, CA; Xiaofeng Chen, Whenzhou Medical Univ Taizhou Hosp, Linhai, China; Hai Yuan, Xuejun Wu, Shandong Province Hosp, Jinan, China; Sara A Michie, Ronald L Dalman, Stanford Univ Sch of Med, Stanford, CA

Objectives: Abdominal aortic aneurysm (AAA) is a chronic inflammatory disease, the pathogenesis of which remains incompletely defined. We and others have demonstrated the critical role of angiotensin (Ang) II and its receptor AT1 in experimental AAAs. Although Ang 1-7 and its receptor Mas counteract many AT1 functions, the role of the Ang 1-7/Mas pathway has not been studied in AAAs. This study evaluated the influences of Ang 1-7 and Mas on experimental AAAs. **Methods:** AAAs were created in male C57BL/6J mice via porcine pancreatic elastase (PPE) infusion. Mice were treated with Ang 1-7 (0.5 mg/kg/day via s.c) or vehicle starting immediately prior to, or 4 days following, PPE infusion. Additional mice were co-treated with Ang 1-7 and the Mas receptor antagonist A779 (0.5 mg/kg/day) beginning immediately prior to PPE infusion. Influences on AAAs were evaluated by serial ultrasound imaging and histology. **Results:** Figure summarizes major results. In ultrasound imaging, at 14 days Ang 1-7 treatment initiated immediately following aneurysm creation substantially suppressed aortic enlargement as compared to vehicle treatment. Histologically, Ang 1-7 treatment was associated with attenuation of aortic medial elastin and smooth muscle cell depletion, mural macrophage, $CD4^+$, $CD8^+$ T and B cell density and neoangiogenesis. Co-treatment with Ang 1-7 receptor Mas antagonist A779 “rescued” the aneurysm phenotype. Additionally, Ang 1-7 treatment initiated even 4 days following AAA creation was still effective in limiting further aneurysmal enlargement and pathologic evolution. **Conclusions:** Ang 1-7 treatment, initiated either at, or up to 4 days following, AAA initiation limits further progression of experimental AAAs. This inhibitory effect seems likely related to activation of the Mas receptor. These results suggest that either Ang 1-7 or alternative Mas receptor agonists may have clinical utility in suppressing progression of early AAA disease.

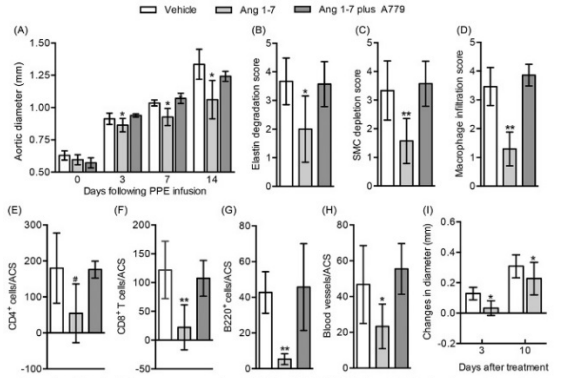

Figure. Angiotensin 1-7 suppresses experimental AAAs. Male C57BL/6J mice at 10-12 wks of age underwent intra-aortic PPE infusion and received subcutaneous injection of Ang 1-7 alone or with A779 (either 0.5 mg/kg/day) beginning immediately prior to PPE infusion (A-H) or 4 days thereafter (I) for 14 days (A-H) or 10 days (I). (**A**) Aortic diameter measured via ultrasonography. (**B-H**) Quantification of medial elastin degradation (B) and SMC depletion (C), CD68+ macrophages (D), CD4+ T cells (E), CD8+ T cells (F), and CD31+ neovessels). (I) Influence on futher aneurysm enlargement in mice with existing AAAs. All data: mean and SD. ACS: aortic cross-section. Two-way ANOVA followed by two sample test, *P<0.05 compared to vehicle treatment (A & I). Mann-Whitney test, 0.05<#P<0.1, *P<0.05 and **P<0.01 compared to vehicle treatment (B-H). n=7-9 mice per group.

B. Xu: None. **G. Li:** None. **H. Deng:** None. **A. Cabot:** None. **X. Chen:** None. **H. Yuan:** None. **X. Wu:** None. **S.A. Michie:** None. **R.L. Dalman:** None.

714
Does the Sickle Trait Portend Increased Cardiovascular Risks?
Derick Okwan-Duodu, Raymundo A Quintana, Giji Joseph, Laura Hansen, Wenxue Liu, Hassan Sellak, Emory Univ, Atlanta, GA; David Archer, Emory Univ, atlanta, GA; W Robert Taylor, Emory Univ, Atlanta, GA

Objectives: Despite the increased incidence and worse outcomes of cardiovascular diseases among African-Americans compared to the general population, the contribution of sickle cell trait (AS) to this racial disparity remains unknown. We aimed to delineate the impact of AS on the pathogenesis of cardiovascular diseases alone, and in the setting of other risk factors. **Methods**: We compared multiple cardiovascular endpoints between AS and wild-type genotype (AA) using the humanized Townes sickle cell mouse model. To determine whether AS modifies a pre-existing cardiovascular risk factor, diabetes was induced in a cohort of mice using streptozotocin (STZ). Hind limb ischemia model was employed to evaluate collateral vessel formation, and perfusion recovery was characterized with LASER Doppler perfusion imaging (LDPI). The running wheel assay assessed spontaneous motor function after ischemia. Angiotensin II (Ang II) and L-NAME were used to evaluate hypertensive response. Experimental stroke was induced by unilateral common carotid artery ligation and daily 15 min exposure to 7.5% oxygen for 3 days, and the infarct size was quantified as the ratio of the infarcted area to the total area of the uninjured contralateral hemisphere. PCSK9 gain-of-function mutation in the setting of Ang II and high-fat diet was used to evaluate atherosclerosis development. **Results**: 4 groups of mice were studied: AA, AS, AA-STZ and AS-STZ. The formation of collateral vessels was equivalent between the AA and AS (day 28, AA: 80 ±

6%, AS: 85 ± 5%, p=0.8), and in the setting of diabetes (39 ± 5% AA-STZ; 36 ± 4% AS-STZ). Systolic blood pressure at baseline (110 ± 4 mmHg vs 112 ± 5 mmHg), and in response to Ang II (148 ± 4 mmHg vs 142 ± 5 mmHg) and L-NAME (135 ± 3mmHg vs 138 ± 5 mmHg) were equivalent. Mortality from stroke was equivalent between AA and AS. After 1 month of PCKS9 gain-of-function mutation/high-fat diet, AA and AS demonstrated similar lipid profiles. Mortality and infarct volume after stroke induction were identical between AA and AS. **Conclusions**: All major indices of cardiovascular outcomes were similar between AA and AS, even in the presence of diabetes. These various experimental models suggest that the sickle trait likely does not contribute significantly to the poor cardiovascular outcomes seen in the African-American population.
D. Okwan-Duodu: None. **R.A. Quintana:** None. **G. Joseph:** None. **L. Hansen:** None. **W. Liu:** None. **H. Sellak:** None. **D. Archer:** None. **W. Taylor:** None.

715
Peripheral Artery Disease in Patients with End Stage Renal Disease: Nationwide Trends in Management and Outcomes
Ahmed Al-Ogaili, Ali Ayoub, Luis Paz, Christian Torres, Harry Fuentes, John H Stroger Hosp of Cook County, Chicago, IL; Alfonso Tafur, Vascular Med, Northshore Univ Healthsystem, Evanston, IL

Background: Patients with end stage renal disease (ESRD) are at high risk for peripheral artery disease (PAD). We sought to determine the national prevalence of PAD, trends in management and outcomes among this high risk population. **Methods:** We queried the 2003-2014 National Inpatient Sample databases to identify PAD related admissions (claudication and critical limb ischemia) among patients with ESRD using ICD-9 codes. Temporal trends in treatment options, and in-hospital mortality were analyzed. Multivariate logistic regression was used to assess predictors of major amputation. **Results:** Among 9 million ESRD patient admissions, 357,949 (3.9%) had PAD related diagnosis. Patients were mainly white (39%), men (58%), with mean age of 65.6 years. The prevalence of PAD slightly decreased from 4.3% in 2003 to 3.9% in 2014 (P trend < 0.001). Utilization of percutaneous transluminal angioplasty (PTA) increased by 142% (10.6% to 25.7%), whereas, open bypass use decreased by 51% (14.1% to 6.9%) during the study period (P trend < 0.001). Moreover, the total number of major amputations was 65,669. There was a notable decline in its usage from 25.9% to 15.3% (adjusted odds ratio [OR] per year: 0.96; 95% confidence interval: 0.95-0.98, P<0.001). Revascularization appeared to reduce the risk of amputation (OR 0.49, P<0.001). On the contrary, hypertension (OR 2.5, P<0.001), heart failure (OR 1.5, P<0.001), and black race (OR 1.5, P<0.001) were independent predictors of amputation. Overall in-hospital mortality rate was 6.3%, with no statistically significant trend throughout the years. **Conclusion:** PAD is a common disease in ESRD patients. Among therapeutic options, a significant increase in less invasive endovascular revascularization methods and a decline in open bypass surgeries were noted. Despite the significant drop in amputation rates, racial disparities persist, with black patients having higher odds of major amputation.

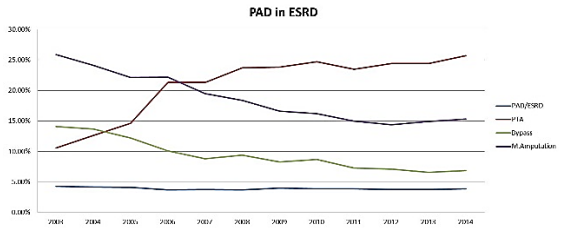

A. Al-Ogaili: None. **A. Ayoub:** None. **L. Paz:** None. **C. Torres:** None. **H. Fuentes:** None. **A. Tafur:** None.

716
Generation of ɣ-secretase Inhibitor-loaded PLGA-Fe_3O_4-Magnetic Nanoparticles
Roa Bashmail, Niamh Mckenna, Ciaran O'Shea, Roya Hakimjavadi, Claire Molony, Dorota Kozlowska, Paul A Cahill, Dublin City Univ, Dublin, Ireland

Cardiovascular disease (CVD) is the number one killer in Ireland and the wider EU. A hallmark of the disease is the obstruction to blood flow due to the build-up of vascular smooth muscle (SMCs)-like cells within the vessel wall. While polymer-coated DES have significantly reduced the incident of in-stent restenosis, current DESs lack the fundamental capacity for (i) adjustment of the drug dose and release kinetics and the (ii) ability to replenish the stent with a new drug on depletion. This limitation can be overcome by a strategy combining magnetic targeting via a uniform field-induced magnetization effect and a biocompatible magnetic nanoparticle (MNP) formulation designed for efficient entrapment and delivery of specific drugs that target the resident vascular stem cell source of the SMC. Magnetic nanoparticles (MNP's) containing magnetite (Fe3O4) were fabricated, polymer coated with poly (DL-lactide-co-glycolide) polyvinyl alcohol [PLGA-PVA] and loaded with a ɣ-secretase inhibitor (GSI) of Notch signalling, DAPT using an oil in water emulsification technique. The free GSI's and GSI-loaded MNP's were assessed for drug release, the efficacy at controlling mesenchymal stem cell (MSC) growth (proliferation and apoptosis) and inhibiting myogenic differentiation under magnetic and non-magnetic conditions. The DAPT-loaded MNPs had an average hydrodynamic diameter of 351 d.nm Up to 40% of drug was released from MNPs within 48 h rising to 65% after 1 week under magnetic conditions. The Notch ligand, Jagged1 increased Hey1 mRNA levels and promoted myogenic differentiation of MSCs in vitro by increasing SMC differentiation markers, myosin heavy chain 11 (Myh11) and calponin1 (CNN1) expression, respectively. This effect was significantly attenuated following treatment of cells with MNP's loaded with DAPT when compared to unloaded MNP's. Notch GSI - loaded magnetic nanoparticles are functional at targeting vascular stem cells in vitro.
R. Bashmail: None. **N. Mckenna:** None. **C. O'Shea:** None. **R. Hakimjavadi:** None. **C. Molony:** None. **D. Kozlowska:** None. **P.A. Cahill:** None.

717
Sequential Inflow Occlusion and Walking Capacity in Large Animal Model of PAD
Luke P Brewster, Walker Upchurch, Emory Univ Hosp; Atlanta VAMC, Decatur, GA

Introduction: Peripheral artery disease (PAD) affects over 8 million Americans over 40 years of age. PAD patients are heavily burdened by pain and walking dysfunction. Treatment paradigms for PAD are evolving, but optimal medical therapy, risk factor modification, and supervised exercise therapy (SET) are the first line therapies for these persons. SET improves walking time and may improve skeletal muscle perfusion. However, the mechanisms by which SET and other treatments are not well understood. Translational models of PAD may be useful in developing novel therapeutics for PAD patients. Objective: The objective of this work is to introduce a large animal (porcine) model of PAD that includes sequential occlusion of inflow that can be used on patient-like treadmills for SET or quantification of walking distance and dysfunction. Methods: Two female Yorkshire swine were accommodated to our treadmill one week prior to procedure. On day 0, swine underwent endovascular placement of a covered stent (GORE® VIABAHN® endoprosthesis) into the right external iliac artery followed by placement of a vascular plug (AMPLATZER, St. Jude Medical) inside this stent was used in the initial procedure. In order to mimic the common presentation of PAD patients having one leg more severely ischemic than the other, we performed a sequential occlusion of the

ipsilateral internal iliac artery and contralateral external iliac artery one week later. Vascular flow were quantified by arteriogram, a modified ankle brachial index, and duplex ultrasound. Animals were walked weekly on a large animal treadmill with a 3.5 KM/HR pace and 10 degree incline until failure (pigs would slide to end of treadmill). Results: There were no technical failures or complications. One and three weeks after the initial procedure, pigs walked 40% and 45% of pre-procedural maximal walking time. There was sustained depression of the blood pressure ratio of ischemic hindlimb to unaffected forelimb (hindlimb index or HLI), which was significantly inhibited out to 6 weeks (*HLI of 0.4-0.63*). Conclusion: We have created a pilot model of PAD that can be used for both SET testing and quantifying maximal walking time/distance. This model may be useful in testing novel therapeutics and validating promising mechanistic findings from small animals.
L.P. Brewster: None. **W. Upchurch:** None.

718
Loss of Epsins Attenuates Thrombosis by Protecting Thrombomodulin From Endocytosis and Degradation
Hong Chen, Harvard Medical Sch, Boston, MA

Sepsis is caused by a deleterious host response to infection, which is primarily responsible for further injury of host tissue and cause of organ dysfunction. Despite significant progress, the pathophysiology of sepsis and the underlying regulatory mechanisms are still not fully understood. We previously established that endothelial epsins play a pivotal role in mediating post-developmental endothelial activation and vascular remodeling through the regulated internalization of activated VEGFR2. Given the importance of endothelial activation and vascular remodeling during sepsis and that both Tissure factor (TF) and Thrombomodulin (TM) activities are potentially modulated by internalization, we investigated the potential role for epsins during sepsis. In this study, we uncover a novel and protective role for epsin deficiency against the development of LPS-induced sepsis. We show that epsin-deficiency upregulates TM surface protein expression by preventing its internalization and subsequent degradation under chronic inflammatory conditions such as that induced by LPS exposure. Sustained surface TM activity subsequently impaired the heightened TF expression and activation that usually occurs in response to LPS. Whether epsin loss protects against or restores normal host coagulopathy after LPS challenge remains to be determined; but, given the cyclic nature of the coagulation pathway, an induced protection of TM after LPS induction will likely also provide restorative and future therapeutic benefits.
H. Chen: None.

This research has received full or partial funding support from the American Heart Association.

719
Radiotracer Imaging of Lower Extremity Skeletal Muscle Perfusion is Significantly Correlated With Exercise Tolerance
Ting-Heng Chou, Mitchel R Stacy, Yale Univ Sch of Med, New Haven, CT

Introduction: Exercise therapy is a proven treatment for peripheral artery disease (PAD) that is now reimbursable by the US Centers for Medicare and Medicaid Services. Traditional methods for detecting responses to exercise in PAD have been peak walking time and the distance walked until onset of claudication, as well as the ankle-brachial index and quality of life questionnaires. However, a quantitative approach for assessing regional perfusion responses to exercise programs does not exist, thus hindering the ability to monitor physiological responses to exercise therapy. Therefore, we investigated if radiotracer-based perfusion imaging of the lower extremities could be utilized as a non-invasive correlate to exercise tolerance for future application in evaluating PAD patients undergoing exercise therapy. Methods & Results: Patients (n=24) underwent single-photon emission computed tomography (SPECT)/CT imaging of the calves after a standard Bruce protocol treadmill stress test, as well as under resting conditions (Fig. 1A). Average SPECT image intensity values were normalized to injected radiotracer dose and patient body weight to generate standardized uptake values (SUVs) within CT-defined muscle groups of the calf (gastrocnemius, soleus, anterior tibias; Fig. 1B). Perfusion reserve was calculated as the percent change of SUV from the rest to stress condition for each muscle group. SPECT/CT-derived measures of perfusion reserve in the soleus and anterior tibialis muscle groups were significantly correlated with peak METs during treadmill stress testing (Fig. 1C). Conclusion: Lower extremity SPECT/CT perfusion imaging is significantly correlated with exercise tolerance and therefore may offer a novel non-invasive tool for physiologically characterizing responders and non-responders to structured exercise therapy in the setting of PAD.

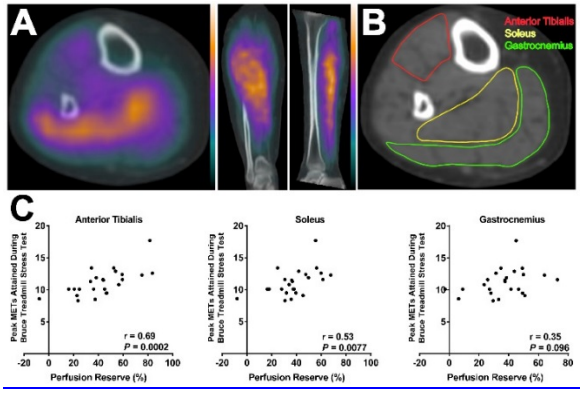

T. Chou: None. **M.R. Stacy:** None.

721
The Exercise Pressor Response to Lower Extremity Dynamic Exercise is Accompanied by an Abnormal Change in Total Peripheral Resistance in Peripheral Arterial Disease Subjects
Marcos T Kuroki, Dept of General Surgery, Penn State Health Milton S. Hershey Medical Ctr, Hershey, PA; Danielle J Kim, Jian Cui, Zhaohui Gao, Cheryl Blaha, Urs A Leuenberger, Lawrence I Sinoway, Penn State Heart and Vascular Inst, Penn State Coll of Med, Hershey, PA

Patients with peripheral arterial disease (PAD) have an exaggerated pressor response to dynamic exercise of the affected limb. We tested the hypothesis that this response is mediated by an increase in total peripheral resistance (TPR). We measured heart rate, blood pressure, stroke volume, cardiac output (CO), and total peripheral resistance (TPR) during exercise in 9 subjects with PAD and 9 age matched controls using continuous finger arterial pressure monitoring (Finometer). Finometer derived values were adjusted to values obtained by echocardiography, and brachial pressure at baseline. The average age and ABI was 65 ± 7 and 1.06 ± 0.07 in controls, and 66 ± 7 and 0.64 ± 0.08 in PAD. Participants performed dynamic plantar flexion at progressive workloads of 2 to 12kg (increased by 1kg/min until onset of fatigue/pain) using their symptomatic leg or leg with lower ABI. Those who reached 12kg continued exercise at a constant load until onset of fatigue/pain or a maximum of 4 minutes. Participants were then asked to perform an isometric handgrip exercise at 30% of maximum voluntary contraction (MVC) until fatigue. Results are shown in Table 1. There were no differences in hemodynamic parameters at baseline. The average weight at end of plantar flexion was 12.0 ± 0.2 and 9.2 ± 2.5 kg ($p<0.0001$) for control and PAD. Perceived exertion (Borg scale) and pain (NPRS scale) at end of exercise was 15 ± 2 and 0, and 15 ± 2 and 6 ± 3 in

control and PAD. Plantar flexion elicited a significantly higher rise in blood pressure in PAD compared to control. TPR decreased in controls, but slightly increased in PAD. In contrast, isometric handgrip elicited a similar pressor response, as well as changes in CO and TPR in both groups. We conclude that the exaggerated pressor response in PAD is mediated by an abnormal response in TPR, which counteracts the normal vasodilatory response to dynamic leg exercise seen in controls. This response appears to be specific to dynamic plantar flexion exercise in PAD.

Table 1: Baseline hemodynamics and response to exercise in PAD and Control

	Baseline				Plantar Flexion (% Change)			Handgrip (% Change)		
	Control	PAD	p		Control	PAD	p	Control	PAD	p
HR (bpm)	63.1 ± 1.4	65.6 ± 1.4	0.2266	HR (%Δ)	13.38 ± 1.73	13.95 ± 1.76	0.8178	**17.76 ± 1.90**	**11.67 ± 2.01**	**0.0326**
SBP (mmHg)	132.2 ± 3.4	133.1 ± 3.5	0.8583	SBP (%Δ)	**9.81 ± 2.98**	**19.97 ± 3.04**	**0.0210**	28.18 ± 3.31	26.49 ± 3.52	0.7285
DBP (mmHg)	68.6 ± 1.6	67.1 ± 1.7	0.5239	DBP (%Δ)	**9.67 ± 2.45**	**18.91 ± 2.50**	**0.0113**	28.15 ± 3.12	23.50 ± 3.32	0.3125
MAP (mmHg)	89.6 ± 1.6	89.1 ± 1.6	0.8096	MAP (%Δ)	**6.71 ± 2.32**	**15.40 ± 2.37**	**0.0117**	31.90 ± 3.21	27.06 ± 3.41	0.3060
SV (mL)	93.4 ± 5.0	83.3 ± 5.3	0.1751	SV (%Δ)	6.21 ± 1.66	1.29 ± 1.73	0.0459	-3.08 ± 2.23	-1.70 ± 2.37	0.6733
CO (L/min)	5.83 ± 0.28	5.17 ± 0.29	0.1027	CO (%Δ)	21.77 ± 2.85	15.37 ± 2.97	0.1269	15.35 ± 3.21	9.58 ± 3.42	0.2245
TPR (dyn.s/cm5)	1279 ± 67	1414 ± 70	0.1695	TPR (%Δ)	**-7.67 ± 2.55**	**4.42 ± 2.66**	**0.0020**	16.12 ± 4.28	18.49 ± 4.55	0.7052

M.T. Kuroki: None. **D.J.K. Kim:** None. **J. Cui:** None. **Z. Gao:** None. **C. Blaha:** None. **U.A. Leuenberger:** None. **L.I. Sinoway:** None.

722
Evaluation of Peripheral Calcium Score as a Measure of Peripheral Artery Disease Severity
Sujin Lee, Kanika Kalra, Benjamin Redpath, Brent Little, Adam Bernheim, Luke Brewster, Leslee Shaw, Emory Univ Sch of Med, Atlanta, GA; Shipra Arya, Stanford Univ Sch of Med, Palo Alto, CA

The current gold standard for diagnosing PAD is Ankle Brachial Index (ABI). However, vascular calcification can falsely elevate ABI. No studies have compared the diagnostic value of peripheral calcium score (PCS) in lower extremity arteries with ABI.
Primary aim of this study was to describe the association of PCS with continuous ABI values and categories of ABI in a retrospective cohort design. We identified 50 patients who underwent CTA and ABI measurements [ABI categories for PAD severity: severe (<0.5), moderate (0.5-0.9), normal (0.9-1.4), noncompressible (>1.4)]. We evaluated CTAs imaged from abdominal aorta through lower extremities and determined total calcium volume of plaques with density >130 HU and area >1mm^2 from infrarenal abdominal aorta to the foot using TeraRecon by two independent readers (Intra class correlation 99%). We explored the association between ABI and PCS in SAS using multiple linear regression and analysis of covariance adjusting for age, race, smoking status, hypertension, hyperlipidemia, type II diabetes, and chronic kidney disease.
We found that ABI was inversely associated with PCS in linear regression (p<0.01, Figure 1A). Differences in mean PCS were statistically significant across ABI categories [F(3,29)= 5.03, p=0.01, Figure 1B]. Across subgroups, the mean PCS was significantly different for ABIs <0.5 and 0.5-0.9 (p=0.02), <0.5 and >1.4 (p<0.001), 0.5-0.9 and >1.4 (p=0.04), 0.9-1.4 and >1.4 (p=0.05). Proportion of tibial calcium to overall PCS was much lower in ABI<0.5: 0.0003 vs ABI>1.4: 0.357 (p=0.02).
Mean PCS may be a valid measure of PAD severity and percentage of tibial calcium may help quantify PAD burden in non-compressible vessels. Our study serves as proof of concept for a comprehensive PCS system to diagnose and evaluate PAD severity, particularly in high-risk subpopulations where non-invasive studies may be unreliable.

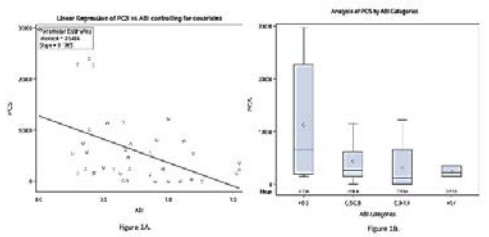

S. Lee: None. **K. Kalra:** None. **B. Redpath:** None. **B. Little:** None. **A. Bernheim:** None. **L. Brewster:** None. **L. Shaw:** None. **S. Arya:** None.

723
A Nitric Oxide-donor Based Vasodilatory Therapy Mitigates Hypoxia-induced Brain Injury on a Zebrafish Model of Hypoxic Ischemic Encephalopathy
Hui-Jen Lin, Ya-Qi Yang, Natl Chiao Tung Univ, Hsinchu, Taiwan; Wei-Tien Chang, Natl Taiwan Univ Hosp and Coll of Med, Taiwan, Taiwan; **Ian Liau**, Natl Chiao Tung Univ, Hsinchu, Taiwan

Hypoxic ischemic encephalopathy (HIE), a brain injury caused by cerebral hypoxia due to perinatal asphyxia, has high mortality, high morbidity and severe sequelae, but therapeutic options remain limited. Cerebral vasoconstriction has been known to contribute to neuronal damage of HIE. Here we report a zebrafish model of brain injury induced by hypoxia and reoxygenation to mimic HIE, and explore the therapeutic potential of a vasodilatory agent to mitigate neuronal damage. Larval zebrafish (6 dpf) were immersed in a hypoxic medium (dissolved O2 below 0.2 ppm) for 15 min to induce brain injury, and then a normoxic medium to mimic resuscitation. The vascular width, blood flow and cerebral cell death were assessed with confocal imaging on transgenic fish that express fluorescent proteins in endothelium, red blood cells (RBCs) and cranial motor neurons, respectively. Neurological function was determined with a modified scoring system based on the movement, coordination and response of zebrafish to stimuli. Larvae survived from the hypoxic assault were categorized according to the severity of impaired cerebral hemodynamics. The *serious* group was featured with greater cerebral vasoconstriction (32% vs. 6%) and lower blood flow (82 vs. 728 RBCs/min) relative to the *moderate* group. These two groups showed notably different outcome measured 2 d post hypoxia with the serious group having a significantly higher cerebral cell death (34% vs. 4%), a lower neurological score (2.5 vs. 6) and survival rate (60% vs. 89%) relative to the moderate group. The strong correlation between the post-hypoxia cerebral hemodynamics and the outcome indicates that a vasodilatory therapy might be a strategy to ameliorate hypoxia induced brain injury. A treatment of s-nitrosoglutathione (GSNO, 15 μM), a nitric oxide donor, effectively alleviated vasoconstriction (7.4% vs. 14.3%), improved the neurological score (3.5 vs. 2.5) and increased the survival rate (63% vs. 54%) relative to the untreated control. In conclusion, a zebrafish model of HIE has been developed. We show that cerebral vasoconstriction may contribute the brain injury associated with HIE, and vasodilatory therapies possess a potential for the remedy of HIE.
H. Lin: None. **Y. Yang:** None. **W. Chang:** None. **I. Liau:** None.

724
Improved Carotid Stenoses Quantification on Novel 4D/3D-Doppler Ultrasonography Indexing to the Common Carotid Artery
Roland Richard Macharzina, Sascha Kocher, Fabian Hoffmann, Aljoscha Rastan, Nian Fan, Franz-Josef Neumann, Thomas Zeller, Univ Heart Ctr Freiburg Bad Krozingen, Bad Krozingen, Germany

Objective Accuracy of internal carotid artery stenosis (ICAS) quantification depends on the method of stenosis measurement, impacting therapeutic decisions and outcomes. The NASCET-method references the stenotic to the distal ICAS lumen, the ECST-method to the local outer and the common carotid artery (CC) method to the CC-diameter. Direct morphometric stenosis measurement with four-dimensionally guided three-dimensional ultrasonography (4D/3DC-US) demonstrated good validity for the commonly used NASCET-method. The NASCET-definition has clinically relevant drawbacks. Our purpose was

to investigate the validity of the ECST- and CC-method. **Approach** 4D/3DC-US percent-stenosis measures of 103 stenoses (80 patients) were compared to quantitative catheter angiography and duplex-ultrasonography (DUS) in a blinded fashion. **Results** The 4D/3DC-US versus angiography intermethod standard deviation of differences (SDD, n = 103) was lower for the CC (5.7%) compared to the NASCET- (8.1%, p <0.001) and ECST-method (9.1%, p <0.001). Additionally, it was lower than the NASCET angiography interrater SDD of 52 stenoses (SDD 7.2%, p = 0.047) and non-inferior for the ECST-method (p = 0.065). Interobserver analysis of equivalent grading methods showed no differences for the SDDs between angiography and 4D/3DC-US observers (p >0.076). Binary comparison to angiography showed equal Kappa values >0.7 and an accuracy >85% for the NASCET- and CC-method, higher than for the ECST-method. Binary accuracy of ICAS grading did not differ from DUS for all methods. **Conclusion** The new 4D/3DC-US CC-method is an accurate and well reproducible alternative to the NASCET- and ECST-method and offers perspectives for clinical application.

R.R. Macharzina: None. **S. Kocher:** None. **F. Hoffmann:** None. **A. Rastan:** None. **N. Fan:** None. **F. Neumann:** None. **T. Zeller:** None.

726

Intermittent Pneumatic Compression during Hemodialysis to improve Quality of Life in Patients with Peripheral Artery Disease and End Stage Renal Disease

Luis H Paz Rios, Ahmed Al-Ogaili, **Christian Torres**, Muhammad T Ayub, Juan Del Cid Fratti, Ahmed A Kolkailah, Ali Ayoub, John H. Stroger, Jr. Hosp Of Cook County, Chicago, IL; Iva Golemi, Northshore Univ HealthSystem, Evanston, IL; Harry E Fuentes, Peter Hart, Christine Acob, John H. Stroger, Jr. Hosp Of Cook County, Chicago, IL; Alfonso J Tafur, Northshore Univ HealthSystem, Chicago, IL

Peripheral artery disease (PAD) is a prevalent global problem with increased mortality. Affects about one in four patients with end stage renal disease (ESRD). Intermittent pneumatic compression (IPC) has shown improvement of lower extremity hemodynamics and symptoms and may be implemented during hemodialysis (HD).

We designed a trial to test the utility of IPC in the ESRD population by assessing improvement in quality of life (QOL) and functional limitation from PAD-related symptoms. We aim to present our design and initial results.

Methods: This is a prospective single cohort study for paired analysis undergoing recruitment of outpatients at the HD unit of John H. Stroger, Jr. Hospital of Cook County. A sample size of 78 yields a power of 80% and alpha of 0.05, assuming an average peak walking time of five minutes and 25% improvement after supervised exercise. PAD is confirmed by ankle-brachial index (ABI) and demographics collected. A baseline Six-minute Walk Test (6MWT), Peripheral Artery Questionnaire (PAQ) and Walking Impairment Questionnaire (WIQ) are administered and will be compared with their performance post intervention. The IPC device (Bio Arterial Plus) will be used for intervention during each HD for two months average. We present continuous variables as mean±SD and categorical variables as percentage.

Results: From 10 recruited patients in the first month, 60% are men, age 54.6±13.1 years, the majority Hispanic (80%). 70% of ABI were abnormal, all due to non-compressible PAD (1.44±0.20). All patients have HTN, 50% diabetes, 20% hyperlipidemia, 10% had a stroke and 10% revascularization for PAD. At baseline 6MWT, distance walked was 357.7±59.5 m, with 600±52.5 total steps and fatigue as main symptom (30%) and no typical claudication. QOL questionnaires showed WIQ walking distance 68.58±18.04, WIQ walking speed 72.5±26.36, and WIQ stair climbing 50.04±30.04 points; PAQ physical limitation 61±21.4, PAQ symptoms 62.79±18.7, PAQ satisfaction 68.67±27.9, PAQ quality of life 64±13.04, and PAQ social limitation 70±23.13 points.

Conclusion: Non-compressible PAD is prevalent in ESRD, and QOL seems significantly compromised from it. Our trial will provide insight of an alternative therapy, and optimize the time in HD even further.

L.H. Paz Rios: Other Research Support; Modest; Research supplies. **A. Al-Ogaili:** None. **C. Torres:** None. **M.T. Ayub:** None. **J. Del Cid Fratti:** None. **A.A. Kolkailah:** None. **A. Ayoub:** None. **I. Golemi:** None. **H.E. Fuentes:** None. **P. Hart:** None. **C. Acob:** None. **A.J. Tafur:** Other Research Support; Modest; Research supplies.

728

The Neutrophil-to-lymphocyte Ratio is Associated With Amputation Free Survival in Critical Limb Ischemia

Femke C van Rhijn-Brouwer, Hendrik Gremmels, Ian D van Koeverden, Martin Teraa, Gerard Pasterkamp, Gert J de Borst, Joost O Fledderus, Marianne C Verhaar, Univ Medical Ctr Utrecht, Utrecht, Netherlands

Introduction: Inflammation plays a key role in ischemic cardiovascular disease. The neutrophil-to-lymphocyte ratio (NLR) is an inexpensive marker for inflammation and correlates with outcomes in critical limb ischemia (CLI). Previous studies have suffered from low power due to low event rates, and show only limited adjustment for confounders. We examined in a prospective cohort whether the peripheral blood (PB) NLR predicts amputation-free-survival (AFS) and has additional predictive power over established risk factors. We also studied bone-marrow (BM) composition and plasma cytokines to elucidate the etiology of NLR alterations.

Methods and results: Data from CLI patients in the JUVENTAS Trial and ATHERO-EXPRESS registry were pooled (N=351). Median follow-up was 3.16 years during which 128 events (amputation or death) occurred. In patients that experienced an event, the PB NLR was elevated (Event: 4.2 (SD 2.8) vs No event: 3.0 (SD 1.9) p=<0.001), the neutrophil count was higher (6.3 (SD 2.5) vs 5.5 (SD2.3) p=0.0003), and the lymphocyte count was lower (1.7 (SD 0.8) vs 2.1 (SD 0.8) p<0.001).

Cox regression showed that the hazard ratio (HR) for AFS was 1.6 (CI: 1.4-1.9), $p=2*10^{-8}$. In a model adjusting for age, sex, diabetes mellitus, BMI, smoking, and GFR the NLR significantly predicted AFS, HR 1.4 (CI 1.2-1.7) p=0.0003. In a sub study in the JUVENTAS cohort, the PB NLR correlated with the BM NLR, but the BM NLR did not correlate with AFS. Additionally, the NLR correlated strongly with the inflammatory cytokines IL-6, IL-8, and CRP.

Discussion and conclusion: These results show that the NLR is an independent predictor of AFS in CLI. While most studies analyzed the NLR as a binary value, here we show a continuous correlation between the NLR and AFS, even when corrected for major confounders. We show that blood NLR is reflected in BM and correlates with inflammatory cytokines, indicating that our incidental measurements may reflect chronic inflammation-driven alterations in BM.

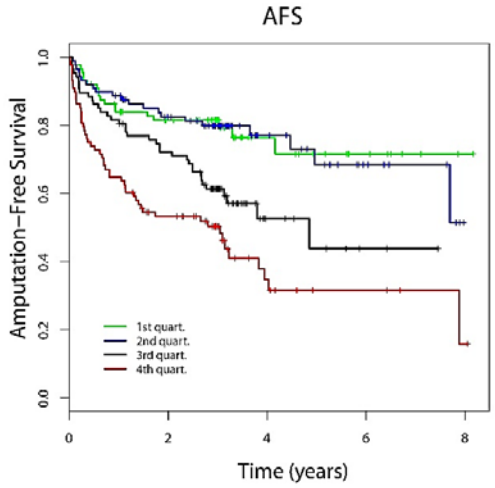

F.C.C. van Rhijn-Brouwer: None. **H. Gremmels:** None. **I.D. van Koeverden:** None. **M. Teraa:** None. **G. Pasterkamp:** None. **G.J. de Borst:** None. **J.O. Fledderus:** None. **M.C. Verhaar:** None.

729
Ultrasound Ultrafast Imaging of the Carotid Artery Pulse Wave Velocity: is the Surrogate of Regional Artery Stiffness?
Lingyun Fang, Dan Zhang, **Jing Wang**, Union Hosp, Wuhan, China

Aims: Cardiovascular diseases (CVDs) are the leading causes of death among the worldwide. Increased Arterial stiffness could be a robust predictor for coronary heart disease and stroke. Pulsed wave velocity(PWV) is “the most hallowed and still probably the best” measure of arterial stiffness and closely related to the processing of arteriosclerosis. A new ultrasound-based technique, Ultrasound Ultrafast imaging system own a high frame rate over than 2000 frames per second, and could quickly obtain the PWV propagate along the carotid artery wall. The objective of this paper is to detect the carotid artery PWV of elder subjects in vivo, to determine the feasibility and accuracy to assess artery stiffness by Ultrasound Ultrafast imaging. **Methods:** Ultrasound Ultrafast imaging was performed to obtain the velocity propagate along the left common carotid arteries of fifty-nine (n = 59) healthy volunteers. Including the PWV at the beginning of the systole and at the ending of the systole($_{BS}$PWV, $_{ES}$PWV), the mean PWV(mPWV) were calculated. E-Tracking technology in measuring artery elasticity modulus (PWVβ)and cardio-ankle vascular index(CAVI) were calculated in all subjects. The correlation between parameters from Ultrafast imaging and elastic modulus from e-tracking, CAVI were analyzed. Indicate artery elasticity and the impact of modifying factors such as BMI, age and hypertension. **Results**: (1) The success rate of the $_{BS}$PWV,$_{ES}$PWV were 94.2% and 90.8%,which required a median overall duration of 73s. (2) BMI, age and hypertension were also positively correlated with mPWV ; mPWV were significant positively correlated with PWVβ and CAVI(r=0.68,P<0.01,r=0.48,P<0.05) (3) The mPWV have a good repeatability and conformity. Interobserver and intraobserver variabilities were 4.2% and 3.6 % respectively. **Conclusion:** The elasticity of carotid artery is the important components of the global arterial elasticity. The decreased elasticity of carotid artery occurs with the ageing and global artery stiffness increased. The Ultrasound Ultrafast imaging is a reliable method to assess the carotid artery stiffness. The technique provides a new, convenient, accurate method for early detection of local artery elasticity.

L. Fang: None. **D. Zhang:** None. **J. Wang:** None.

731
Biophysical Properties of Nanofibrillar Scaffolds Modulate Endothelial Cell Survival in the Ischemic Hind Limb
Guang Yang, Maureen Wanjare, Karina Nakayama, Ngan Huang, Stanford Univ, Palo Alto, CA

Research Background & Objectives: Endothelial cells (ECs) are a promising cell type for the treatment of peripheral arterial disease (PAD). We previously showed that anisotropic nanofibrillar scaffolds augment the angiogenic function of ECs. Here we reported the effect of nanofibril size and crosslinking on EC survival and function to optimize the biophysical properties of scaffolds for treatment of PAD.
Methods: Aligned nanofibrillar collagen scaffolds of varying fibril diameters and stiffness were prepared by altering the ionic strength (IS) of monomeric collagen and then crosslinked at varying levels of 1-ethyl-3-(3-dimethylaminopropyl)carbodiimide hydrochloride (EDC). Scaffolds were characterized for surface topography and nanofibril diameter by atomic force microscopy (AFM). Primary human ECs seeded onto the scaffolds were assessed for migration and survival under hypoxia. The regenerative potential of EC-seeded scaffolds was examined in a mouse hind limb ischemia (HLI) model.
Results: Scaffold formulation with varying ionic strength (IS) resulted in different fibril diameter regardless of the degree of crosslinking (**Figure 1A**: ~100 nm in low IS group vs. ~200 nm in high IS groups). When cultured under hypoxia, ECs seeded on high IS scaffold crosslinked by 1xEDC exhibited improved survival compared to those on low IS. Accordingly, the high IS 1xEDC scaffold was selectively tested in a mouse HLI model for cell survival and blood perfusion restoration. Bioluminescently-tagged ECs were seeded onto high IS 1xEDC scaffold or a randomly oriented fibrillar scaffold (20 mm of each). Non-invasive bioluminescence imaging for quantification of viable cells demonstrated markedly higher cell survival on aligned nanofibrillar scaffold than on randomly oriented scaffold (**Figure 1B, C**).
Significance: Aligned nanofibrillar scaffolds that improve survival and angiogenesis of ECs provide a viable clinical strategy for the therapeutic neovascularization.

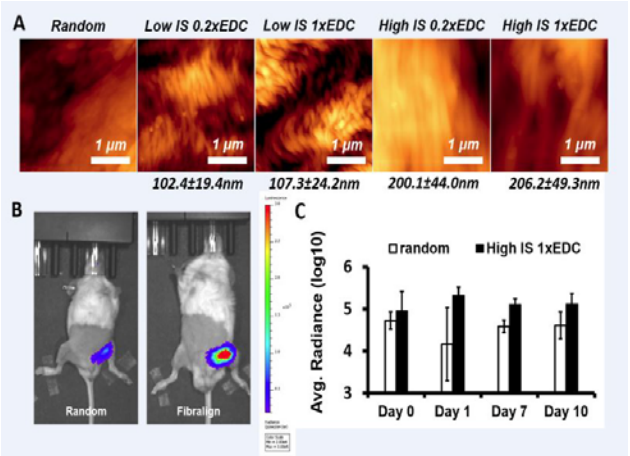

Figure 1. A: The ionic strength (IS) of the starting collagen material influences the fibril diameter. B: Representative heat map of bioluminescent intensity at the site of ischemia. C: Quantified bioluminescent signal that indicates cell retention/survival at the time of ischemia (n=6).

G. Yang: None. **M. Wanjare:** None. **K. Nakayama:** None. **N. Huang:** None.